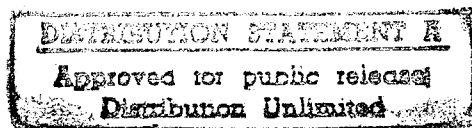


NASA Conference Publication 2079

*index all papers
rel to skin*

*Note:
Do not include 4
1-ep 5/1*

Graphite/Polyimide Composites



Proceedings of a technical symposium
held at Langley Research Center
Hampton, Virginia
February 28 - March 1, 1979

19960228 022

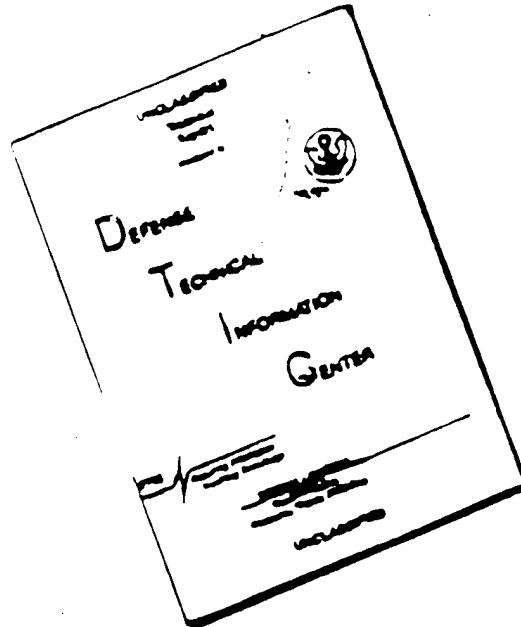
NASA

DTIC QUALITY INSPECTED 1

PLASTEC

330-130
330-130

DISCLAIMER NOTICE



THIS DOCUMENT IS BEST
QUALITY AVAILABLE. THE COPY
FURNISHED TO DTIC CONTAINED
A SIGNIFICANT NUMBER OF
PAGES WHICH DO NOT
REPRODUCE LEGIBLY.

Add 428025 -

NASA Conference Publication 2079

428052

Graphite/Polyimide Composites

H. Benson Dexter and John G. Davis, Jr., *Editors*
Langley Research Center

Proceedings of a technical symposium
held at Langley Research Center
Hampton, Virginia
February 28 - March 1, 1979



National Aeronautics
and Space Administration

Scientific and Technical
Information Branch

1979

PREFACE

The proceedings of the CASTS Project Technical Symposium held at Langley Research Center on February 28 - March 1, 1979 are reported in this NASA Conference Publication.

The purpose of the symposium was to provide early dissemination of new technology generated by NASA specifically related to graphite/polyimide composites for advanced space transportation systems. The technology reported in this symposium resulted from both in-house and contract efforts sponsored primarily by the Composites for Advanced Space Transportation Systems (CASTS) Project. In addition, an industry assessment of the state-of-the-art of graphite/polyimide composites was discussed by panelists representing five aerospace companies.

The topics covered by session were

- I. Fabrication
- II. Adhesives
- III. Test Methods
- IV. Structural Integrity
- V. Design and Analysis
- VI. Advanced Technology Developments
- VII. Recent High Temperature Polymer Research at NASA
- VIII. Gr/PI State-of-the-Art Panel Discussion

Certain materials are identified in this publication in order to specify procedures adequately. In no case does such identification imply recommendation or endorsement of the product by NASA, nor does it imply that the materials are necessarily the only ones or the best ones available for the purpose. In many cases equivalent materials are available and would probably produce equivalent results.

H. Benson Dexter
Symposium Chairman

CONTENTS

PREFACE	iii
1. WELCOME ADDRESS R. R. Heldenfels	1
2. COMPOSITES FOR ADVANCED SPACE TRANSPORTATION SYSTEMS - (CASTS) John G. Davis, Jr.	5

SESSION I - FABRICATION Chairman: Edward L. Hoffman

3. LaRC FABRICATION DEVELOPMENT Robert M. Baucom	330.14	19
4. DEVELOPMENT OF FABRICATION TECHNIQUES FOR NR150B2-S5X GRAPHITE/POLYIMIDE HIGH TEMPERATURE COMPOSITES W. G. Scheck, C. W. Smith, and E. Harrison	330.15	39
5. DEVELOPMENT AND DEMONSTRATION OF MANUFACTURING PROCESSES FOR FABRICATING GRAPHITE/PMR-15 POLYIMIDE STRUCTURAL ELEMENTS C. H. Sheppard, J. T. Hoggatt, and W. A. Symonds	330.16	61
6. LARC-160 FABRICATION DEVELOPMENT J. Devereaux Leahy	330.17	85
7. INTERIM RESULTS OF THERMID 600 ENGINEERING DEVELOPMENT Richard D. Hoffman	330.18	107
8. FABRICATION OF STRUCTURAL ELEMENTS Fred J. Darms, Jr.	330.19	111

SESSION II - ADHESIVES Chairman: Norman J. Johnston

9. POLYIMIDE ADHESIVE BONDING Donald Progar	330.20	123
10. ADHESIVES FOR BONDING RSI TILE TO Gr/PI STRUCTURE FOR ADVANCED SPACE TRANSPORTATION SYSTEMS Kenneth E. Smith, Charles L. Hamermesh, and Peter A. Hogensen	330.21	139
11. NR-150 ADHESIVE DEVELOPMENT Philip S. Blatz and Hugh H. Gibbs	330.22	149
12. DEVELOPMENT OF LARC-13 ADHESIVE SYSTEMS John T. Hoggatt	330.23	163

SESSION III - TEST METHODS
Chairman: H. Benson Dexter

13. GRAPHITE/POLYIMIDE TENSION TESTS AT ELEVATED AND CRYOGENIC
TEMPERATURES 33024 (175)
Andrew J. Chapman
14. SANDWICH BEAM COMPRESSIVE TEST METHOD . 33025 (189)
Mark J. Stuart
15. APPLICATION OF THE IITRI COMPRESSION TEST FIXTURE AT 33026
ELEVATED TEMPERATURE (201)
Charles J. Camarda
16. RAIL SHEAR TEST METHOD 33027 (221)
Ramon Garcia and Robert R. McWithey

SESSION IV - STRUCTURAL INTEGRITY
Chairman: Walter Illg

17. EFFECTS OF LOW-VELOCITY IMPACT ON Gr/Pi COMPRESSION LAMINATES (239)
Ramon Garcia and Marvin D. Rhodes 33028
18. PRELIMINARY BOLTED-JOINT DATA 33029 (249)
Gregory R. Wichorek
19. FATIGUE AND FRACTURE 33030 (259)
Walter Illg and Richard A. Everett, Jr.

SESSION V - DESIGN AND ANALYSIS
Chairman: Sidney C. Dixon

20. MECHANICAL PROPERTY DEGRADATION OF GRAPHITE/POLYIMIDE COMPOSITES
AFTER EXPOSURE TO MOISTURE OR SHUTTLE ORBITER FLUIDS 273
W. Barry Lisagor 33031
21. MECHANICAL AND THERMOPHYSICAL PROPERTIES OF GRAPHITE/POLYIMIDE
COMPOSITE MATERIALS 289
Donald R. Rummeler and Ronald K. Clark 33032
22. ANALYSIS METHODS AND PRELIMINARY DESIGN STUDY 303
C. L. Blackburn and J. C. Robinson 33033
23. DESIGN CONSIDERATIONS FOR COMPRESSION PANELS AT ELEVATED
TEMPERATURE 319
Robert R. McWithey, Charles J. Camarda, and Gerald G. Weaver 33034

SESSION VI - ADVANCED TECHNOLOGY DEVELOPMENTS

Chairman: Darrel R. Tenney

24. GLASS POLYIMIDE HONEYCOMB CORES FOR ADVANCED SPACE TRANSPORTATION
SYSTEMS 33035 (339)
Jay Brentjes
25. DEVELOPMENT OF HYBRID POLYIMIDE COMPOSITES 33036 (349)
Milan G. Maximovich
26. HPLC FOR QUALITY CONTROL OF POLYIMIDES 33037 (361)
Philip R. Young and George F. Sykes
27. QUALITY ASSURANCE OF PMR-15 33038 (375)
A. B. Hunter

SESSION VII - RECENT HIGH TEMPERATURE POLYMER RESEARCH AT NASA

Chairman: John G. Davis, Jr.

28. RECENT DEVELOPMENTS IN PMR POLYIMIDES AT NASA LEWIS 33039 (391)
T. T. Serafini
29. HIGH TEMPERATURE POLYMER RESEARCH AT NASA LANGLEY 33040 (413)
Terry L. St. Clair

SESSION VIII - GRAPHITE/POLYIMIDE STATE-OF-THE-ART

PANEL DISCUSSION

Moderator: H. Benson Dexter

30. William G. Scheck 431
31. Morton Kushner 435
32. William H. Morita 441
33. Robert C. Curley 445
34. Clayton A. May 451

WELCOME ADDRESS

R. R. Heldenfels
Director for Structures
NASA Langley Research Center

Good morning! Welcome to the Langley Research Center. We are pleased that you came to this technical symposium on graphite/polyimide composites sponsored by the CASTS Project. This is the first comprehensive technical report presented at the Langley Research Center on the state of technology for a particular composite material. We have been interested in graphite/polyimide for years and have developed an extensive data base. Graphite polyimide is, in our opinion, the composite material of greatest potential for elevated temperature applications. We will share our data with you in two days of presentations and conclude this meeting with a panel discussion. Our schedule includes time for your participation after each talk and during the panel discussion. Therefore we both welcome and solicit your comments, questions, and suggestions as we go along. In that way we can have an effective, two-way exchange of information.

APPLICATION OPPORTUNITIES FOR GRAPHITE/POLYIMIDE COMPOSITES

Graphite/polyimides have been developed to a stage where they are very attractive for a variety of structures that operate at elevated temperature. In such applications they can have significantly less mass than comparable structures of metals or graphite/epoxy composites.

Figure 1 shows the time-temperature capabilities of graphite/polyimide in general terms. For example, at the far left, satisfactory structural performance can be obtained at 700 to 756 K (800° to 900°F) for about one minute, and at the far right satisfactory performance at 450 to 506 K (350° to 450° F) can be sustained for about 100,000 hours.

Also indicated on the chart is the expected service life required in several applications, which could benefit from graphite/polyimide structures, such as:

1. Missiles for a single flight of a few minutes.
2. Space Shuttle Orbiter for a design life of 125 flights.
3. Jet engine parts for exposures up to several thousand hours.
4. Structures for an advanced fighter for 10,000 hours service.
5. Structures for a supersonic transport for 50,000 hours service.

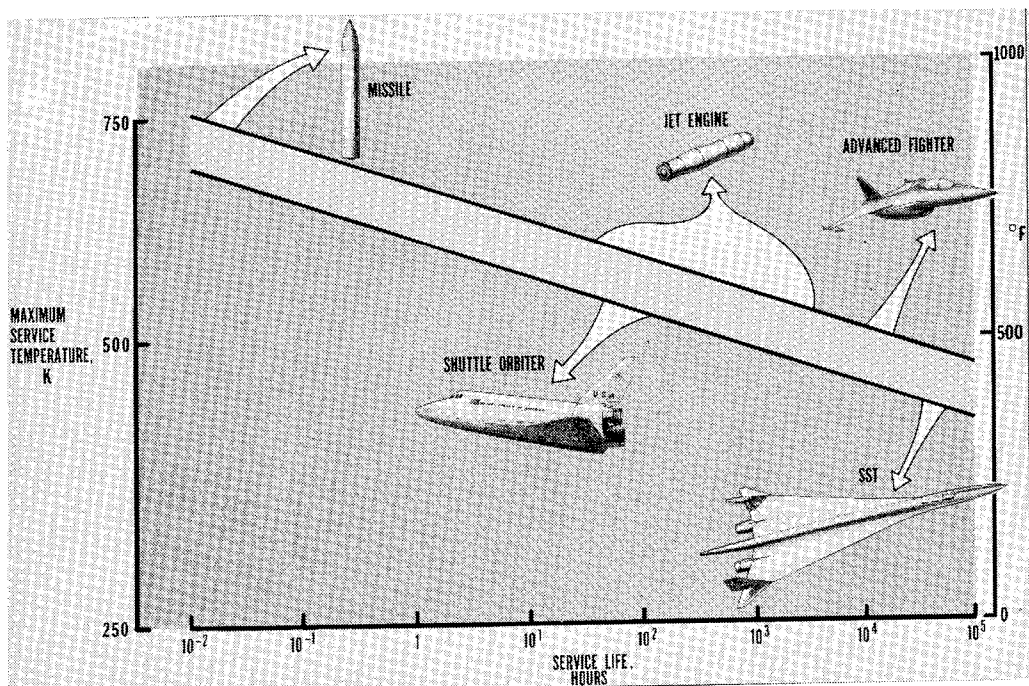


Figure 1

TECHNOLOGY BASE FOR GR/PI SYMPOSIUM

The data base to be presented in this symposium resulted from several research programs, some of which have been in progress for many years. These sources are listed on figure 2. The research and technology base programs at Langley and Lewis have made continuing contributions to graphite/polyimide composites technology. The Supersonic Cruise Research (SCR) program, that began in 1973, has contributed substantial advances in Gr/PI technology since Gr/PI composites can provide large weight reductions in supersonic transports.

The major Gr/PI contributions, however, have come from the CAST Project which was planned in 1974 to generate the technology needed for application of resin-matrix composites to space transportation systems. That program will be described in detail by the next speaker. The original plan included the design, construction, and ground tests of a shuttle component. The aft body flap of the Shuttle Orbiter was the component subsequently selected. However, the present budget does not provide funding for a component demonstration and cuts short the technology readiness activities required for such a demonstration.

Some Gr/PI activity in the Air Force Materials Laboratory composite program, jointly sponsored by the CASTS Project, will be presented, too.

- NASA LANGLEY R & T BASE PROGRAMS
- NASA LEWIS R & T BASE PROGRAMS
- NASA LANGLEY AND LEWIS SUPERSONIC CRUISE RESearch PROGRAM (SCR)
- ★ NASA LANGLEY CASTS PROJECT
(COMPOSITES FOR ADVANCED SPACE TRANSPORTATION SYSTEMS)
- AFML ADVANCED COMPOSITES APPLICATION PROGRAM

Figure 2

ORGANIZATIONS PROVIDING AUTHORS AND/OR PANELISTS

The organizations shown on figure 3 have provided the authors, panelists, or both that will speak during this symposium. They have worked hard to generate their technical data and present it effectively. I want to thank them and their organizations for their excellent support of this symposium. The speakers and panelists, and you, the audience, represent major aerospace companies, subcontractors, materials suppliers, government laboratories, and universities. Together you make this meeting an assemblage of most of our nation's experts on Gr/PI. If you in the audience and the speakers will share your experiences and plans for Gr/PI development and application we can leave this meeting with an accurate, up-to-date assessment of the potential applications and remaining problems in Gr/PI technology. So please speak up with your comments, suggestions, and advice as we go along.

Thank you for coming and for your participation. We are pleased that you are here and hope that these two days will be interesting, informative, and productive.

GOVERNMENT

NASA LANGLEY RESEARCH CENTER

NASA LEWIS RESEARCH CENTER

INDUSTRY

BOEING AEROSPACE

DOUGLAS AIRCRAFT

E. I. DUPONT de NEMOURS

GENERAL DYNAMICS

HERCULES

HEXCEL

LOCKHEED MISSILES AND SPACE

MCDONNELL DOUGLAS ASTRONAUTICS

ROCKWELL INTERNATIONAL/SPACE

STANFORD RESEARCH INSTITUTE

Figure 3

COMPOSITES FOR ADVANCED SPACE TRANSPORTATION SYSTEMS - (CASTS)

John G. Davis, Jr.
NASA Langley Research Center

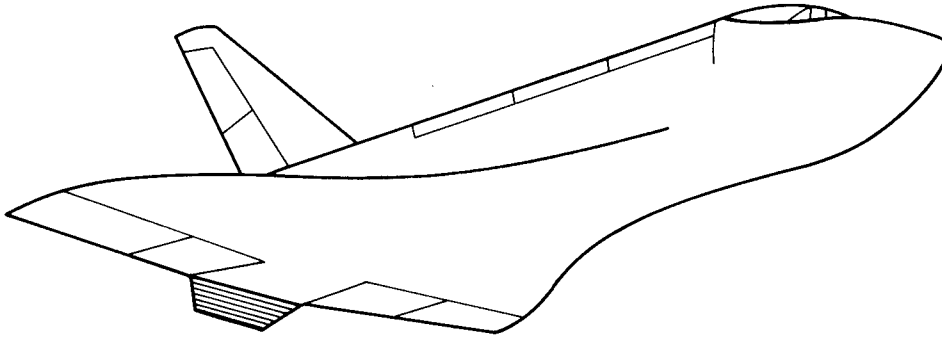
EXPANDED ABSTRACT

The CASTS Project was initiated in 1975 to develop graphite fiber/polyimide matrix (Gr/PI) composite structures with 589K (600°F) operational capability for aerospace vehicles. NASA Langley Research Center in-house and contract efforts are being utilized to achieve the objective of approximately twenty-five percent reduction in structural mass compared to conventional metallic construction. Both near term and far term research efforts are included. Near term tasks included in the original project plan were: screening composites and adhesives for 589K (600°F) service, developing fabrication procedures and specifications, developing design allowables test methods and data, design and test of structural elements and construction of a full scale aft body flap for the Space Shuttle Orbiter Vehicle for ground testing. Reductions in funding for fiscal years 1980 through 1983 have eliminated significant amounts of the effort planned to develop design allowables data and construction of the full scale aft body flap. Utilization of a segment of the body flap or other structural components to demonstrate the Gr/PI technology is currently under consideration. Far term tasks include research efforts directed at new materials, manufacturing procedures and design/analysis methodology.

Four Gr/PI composites and three PI adhesives with 589K (600°F) service potential for periods ranging from 125 to 500 hours have been identified using interlaminar shear, flexure and lap shear strength test data. An adhesive formulation suitable for bonding reusable surface insulation (RSI) tiles to 589K (600°F) Gr/PI substructure has been developed. The capability to fabricate and nondestructively inspect laminates, hat section shaped stiffeners, honeycomb sandwich panels, and chopped fiber moldings has been demonstrated utilizing one of the Gr/PI composites. Test methods for measuring design allowables at 117K (-250°F), RT and 589K (600°F) have been demonstrated. The effects of moisture, temperature, thermal cycling and shuttle fluids on the thermal, physical and mechanical properties of Gr/PI is underway and preliminary data obtained to date have not uncovered any environmental degradation problems that would preclude the use of Gr/PI in advanced space transportation systems.

COMPOSITES FOR ADVANCED SPACE TRANSPORTATION SYSTEMS

By 1974 Gr/PI composites had been identified as one of the most promising technology areas for reducing the structural mass and improving the performance of future space transportation systems. As a result, the CASTS Project was initiated in 1975 to develop Gr/PI composite structures with 589 K (600° F) operational capability for application to aerospace vehicles. A twenty-five percent reduction in structural mass compared to conventional metallic structure was selected as a major goal. Achievement of the goal was to be demonstrated by designing, fabricating and ground testing a structural component for the Space Shuttle Orbiter Vehicle. Reductions in funding for fiscal years 1980 through 1983 do not permit construction of a full scale component and the feasibility of utilizing a segment of an aft body flap to demonstrate the technology is under consideration.



OBJECTIVE: 589K (600° F) GRAPHITE/POLYIMIDE STRUCTURES
FOR ADVANCED SPACE TRANSPORTATION SYSTEMS

Figure 1

COMPOSITE AFT BODY FLAP FOR SPACE SHUTTLE

Figure 2 shows the aft body flap for the Space Shuttle Orbiter Vehicle, which was selected for the technology demonstration component, and lists estimated weights for baseline aluminum and Gr/PI composite designs. The vertical tail and elevons on the Orbiter were also evaluated for technology demonstration. Selection of the body flap was made on basis of the degree of technology advancement, risk, costs and potential ease of retrofit. The flap is 6.4 x 2.1 m (21 x 7 ft) in size and, based on a preliminary design in reference 1, the use of Gr/PI composites is predicated to yield approximately 27 percent reduction in weight compared to the baseline aluminum design. Both designs require the use of significant amounts of reusable surface insulation (RSI) since the outer surface of the flap reaches temperatures of 1728 K (2650° F). In the baseline design, the aluminum is not permitted to exceed 450 K (350° F) whereas the Gr/PI structure is designed to withstand 589 K (600° F). Attachment of the RSI to either type of structure is accomplished by adhesive bonding.

The aft body flap also serves as a focal point in the technology development and serves as a guide to insure that all required technical disciplines are being worked in the CASTS Project.

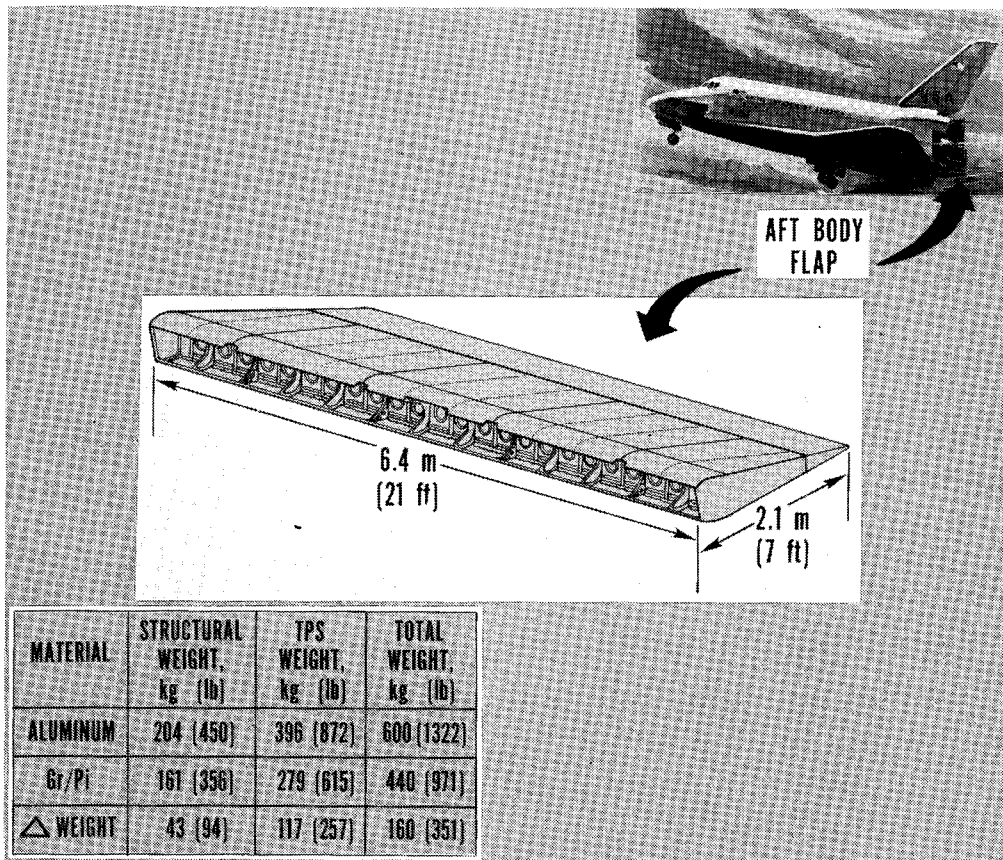


Figure 2

CASTS PROJECT

Figure 3 is a logic chart for the CASTS Project and shows the major in-house and contract tasks. Gr/PI composites and PI adhesives were screened to determine the most promising candidates for subsequent development of fabrication procedures and specifications. Test results on Gr/NR150B2, Gr/PMR-15, Gr/LARC160 and Gr/THERMID 600 indicated that development of fabrication procedures was warranted. Effort has been directed at extending the currently accepted test methods for determining design allowables properties of Gr/Ep to include Gr/PI composites between 117 K (-250° F) and 589 K (600° F). The original project plan included development of a set of design allowables data for the two most promising composites. Development of repair technology for manufacturing and/or service induced flaws or damage and procedures and specifications for adhesively bonding Gr/PI composites structures are planned. An adhesive for attaching reuseable surface insulation (RSI) to 589 K (600° F) Gr/PI composites has been identified. Effort is underway to extend the current capability to design and analyze Gr/Ep composite structures to include Gr/PI structures that operate between 117 K (-250° F) and 589 K (600° F). Many of the test specimens and structural elements that will be tested in-house are being fabricated under contract. The original project plan included a major contract effort to design, fabricate and ground test a Gr/PI composite aft body flap to demonstrate the technology. Due to funding cuts, the feasibility of demonstrating the technology by constructing a segment of the aft body flap is being considered. Items funded to date under advanced technology development include research on PI adhesives, hybrid PI matrix composites, and glass/PI honeycomb core.

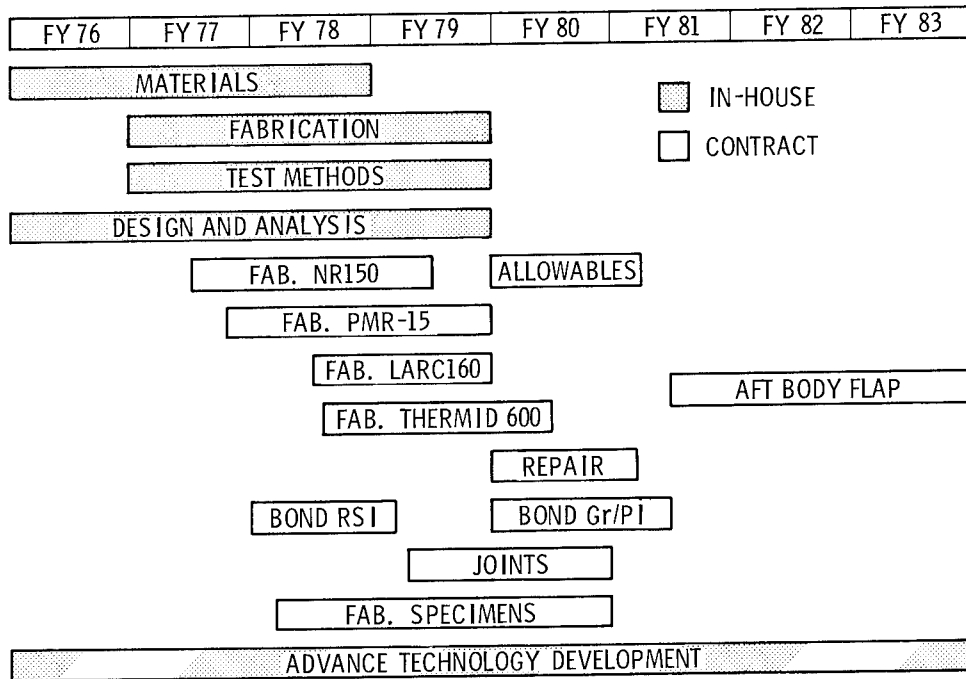


Figure 3

CASTS - CRITERIA FOR MATERIALS SELECTION

Selection of Gr/PI composites that would be subjected to extensive fabrication development effort was based on four criteria which are listed in figure 4. The intent of these criteria was to limit the choice to Gr/PI composites that are suitable for application to advanced space transportation systems and that could be fabricated into large size structural components with existing aerospace industry facilities. Structural materials used on the Space Shuttle Orbiter must be capable of supporting design loads after exposure to a thermal environment equivalent to 125 flights. Future systems will probably be required to withstand exposure times in excess of 125 hours. The CASTS Project schedule required that only materials which have the potential to be made commercially available in the near future be selected. In order to insure that the Gr/PI composites could be fabricated into large structural components using existing aerospace industry facilities, limits of 2.07 mPa (300 psi) and 5.6 K/minute (10° F/minute) were set on the maximum lamination pressure and heat up rate, respectively, that could be used to cure the composites being evaluated.

The criteria listed in figure 4 were also used to select adhesives for bonding Gr/PI structural components.

- 589K (600⁰F) SERVICE CAPABILITY FOR 125-500 HOURS
- POTENTIAL FOR NEAR TERM COMMERCIAL AVAILABILITY
- LAMINATION PRESSURE LESS THAN 2.07 MPa (300 psi)
- HEAT UP RATE LESS THAN 5.6K/MIN. (10⁰F/MIN.)

Figure 4

MATERIALS EVALUATED FOR ELEVATED TEMPERATURE SERVICE

Fourteen matrix materials, six adhesives and five graphite fibers which are listed in figure 5 have been evaluated for elevated temperature service. Matrix materials and graphite fibers were evaluated on the basis of the performance of flexure and interlaminar shear specimens that had been exposed to atmospheric pressure air maintained at 505 K (450° F), 533 K (500° F), 561 K (550° F) or 589 K (600° F) for periods up to 500 hours. Four matrix materials, NR150B2, PMR-15, LARC-160 and THERMID 600, and two graphite fibers, CELION and AS4, meet the selection criteria.

Performance of the five structural adhesives was evaluated on the basis of lap shear and flat wise tensile test results. FM-34, LARC 13 and NR150B2 meet the selection criteria. RTV560-SQX adhesive was evaluated for bonding RSI to 589 K (600° F) Gr/PI substructure and the results indicate adequate performance. References 2 and 3 report test results on the adhesives.

MATRIX

NR 150B2	PMR-15-II	NR150A/R	PPQ
PMR-15	HR 600	P13N	X5230
LARC-160	F 178	S703	
THERMID 600	K 601	S710	

ADHESIVE

FM-34
LARC 13
NR 150B2G
~~PPQ~~
~~A380~~
RTV 560-SQX

FIBER

~~HTS1~~
~~MODMOR-II~~
~~HTS 2~~
CELION
AS4

Figure 5

GRAPHITE/POLYIMIDE FLEXURE STRENGTH¹

Figure 6 lists flexure strength test results for four Gr/PI composites that were fabricated with either NR150B2, PMR-15, LARC-160 or THERMID 600 polyimide matrix materials. Most specimens were machined from laminates that were fabricated near the beginning of the CASTS Project and the reinforcing fiber was HTS1. The exception is one set of CELION/PMR-15 specimens which were fabricated after all HTS1/PMR-15 laminates had been used for other tests. Specimens in the as fabricated condition were tested at room temperature. Specimens that contained NR150B2 or THERMID 600 matrix material were exposed 500 hours at 589 K (600° F) and then tested at 589 K. Specimens that contained PMR-15 and LARC-160 were exposed 125 hours at 589 K (600° F) and then tested at 589 K. Tests were conducted in accordance with ASTM standard D790 utilizing a 32-to-1 span-to-depth ratio. Specimens tested at 589 K were maintained at the test temperature for 15 minutes prior to the initiation of loading.

The effect of exposure and elevated temperature is reduction in flexure strength for each of the Gr/PI composites and ranges from approximately 20 to 35 percent compared to the as fabricated specimens.

<u>MATERIAL</u>	<u>EXPOSURE</u>	<u>TEST TEMPERATURE, K</u>	<u>STRENGTH MPa (ksi)</u>
HTS/NR150B2	AS-FABRICATED	294	1430 (207)
HTS/NR150B2	500 hr AT 589K	589	1140 (165)
HTS/PMR-15	AS-FABRICATED	294	1430 (208)
CELION/PMR-15	125 hr AT 589K	589	970 (160)
HTS/LARC-160	AS-FABRICATED	294	2130 (309)
HTS/LARC-160	125 hr AT 589K	589	1370 (199)
HTS/THERMID 600	AS-FABRICATED	294	1280 (185)
HTS/THERMID 600	500 hr AT 589K	589	1040 (151)

Figure 6

¹Unidirectional laminates

GRAPHITE/POLYIMIDE INTERLAMINAR SHEAR STRENGTH²

Figure 7 lists interlaminar shear strength test results for the same materials, exposure conditions and test temperatures that are listed in figure 6. Interlaminar shear specimens were tested in accordance with ASTM standard D2344 utilizing a 4-to-1 span to depth ratio. Specimens tested at 589 K (600° F) were maintained at the test temperature 15 minutes prior to the initiation of loading.

The effect of exposure and elevated temperature is a reduction of approximately 50 percent in strength compared to the as fabricated specimens tested at room temperature.

Based on the data shown in figures 5 and 6, Gr/PI composites utilizing NR150B2 or THERMID 600 polyimide matrix materials appear to be capable of 589 K (600° F) service for 500 hours in aerospace vehicle structures. Data on PMR-15 and LARC-160 polyimide matrix composites indicate 125 hour service capability at 589 K (600° F).

<u>MATERIAL</u>	<u>EXPOSURE</u>	<u>TEST TEMPERATURE, K</u>	<u>STRENGTH, MPa (ksi)</u>
HTS/NR150B2	AS-FABRICATED	294	70 (10.2)
HTS/NR150B2	500 hr AT 589K	589	34 (5.0)
HTS/PMR-15	AS-FABRICATED	294	111 (16.1)
CELION/PMR-15	125 hr AT 589K	589	59 (8.5)
HTS/LARC 160	AS-FABRICATED	294	96 (13.9)
HTS/LARC 160	125 hr AT 589K	589	48 (6.9)
HTS/THERMID 600	AS-FABRICATED	294	83 (12.1)
HTS/THERMID 600	500 hr AT 589K	589	41 (6.0)

Figure 7

²Unidirectional laminates

CASTS - FABRICATION DEVELOPMENT COMPONENTS

Development of fabrication procedures and specifications for Gr/PI composites utilizing NR150B2, PMR-15, LARC-160 and THERMID 600 polyimide matrix materials is underway. Prepreg specifications, cure and post cure cycles, manufacturing methods applicable for building full scale structural components and nondestructive inspection procedures are included in the effort. Items shown in figure 8 will be built to demonstrate the fabrication technology. Flat laminates up to 3.18 mm (.125 in.) thick and .6 x 1.2 m (2 x 4 ft) in area, chopped fiber moldings, honeycomb core sandwich panels, skin-stringer panels and a built-up component such as a body flap segment will be fabricated utilizing each of the four matrix materials. Mechanical fasteners, secondary bonding and cocuring are being evaluated for fabricating joints in Gr/PI structures.

Both in-house and contract efforts are being used to develop fabrication technology. The in-house effort is focused on PMR-15 and LARC-160 Gr/PI composites and reference 4 reports the accomplishments. Separate contracts were awarded to develop fabrication procedures for each of the four Gr/PI composites. References 5 through 8 report on the contract effort.

The capability to fabricate structural components has been demonstrated with the Gr/PMR-15 composite.

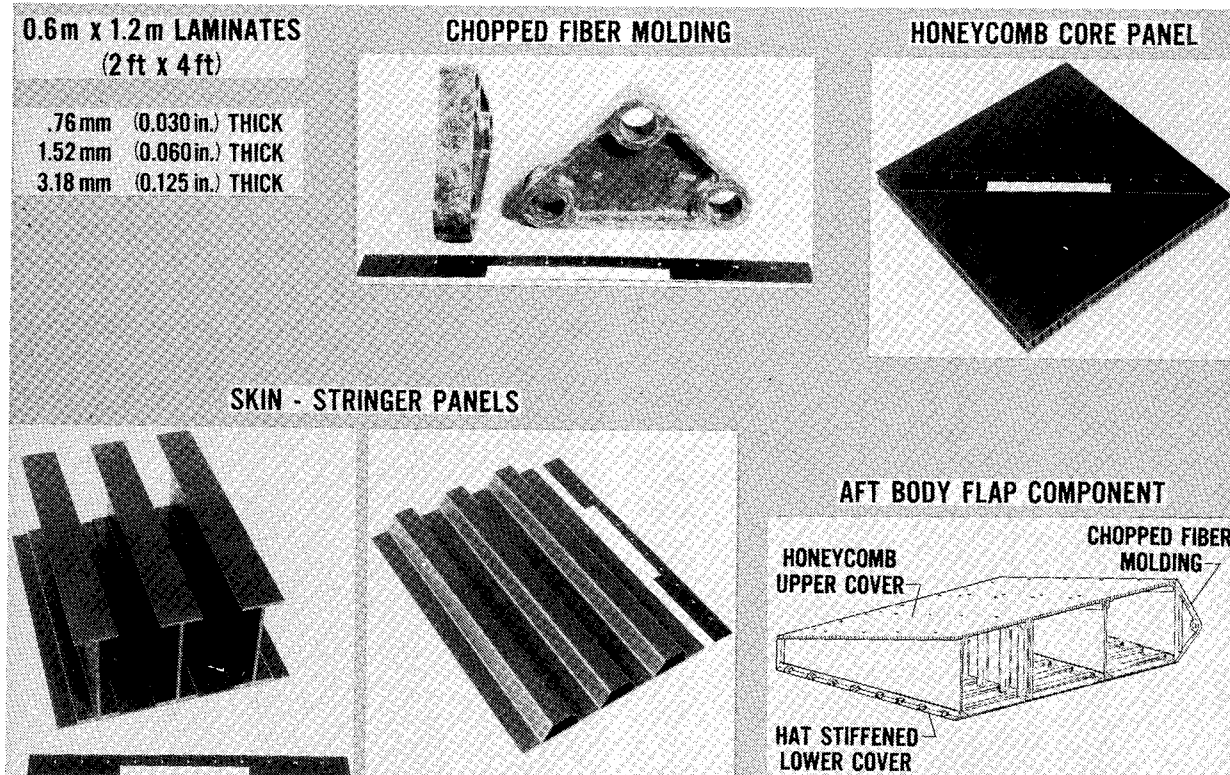


Figure 8

GRAPHITE/POLYIMIDE DESIGN ALLOWABLES FOR CASTS

Figure 9 lists the specimen types, data, environments and laminate configurations included in the Gr/PI design allowables effort. Determining the adequacy of test methods currently used on graphite/epoxy composites (Gr/Ep) to measure the properties of Gr/PI between 117 K and 589 K (-250° F and 600° F) and obtaining preliminary data are major objectives. Tension, compression, shear, bolt bearing, fatigue and fracture test methods and effects of moisture, thermal cycling, and shuttle fluids are reported in references 9 through 17. Based on the information reported in references 9 through 17, the test methods currently used on Gr/Ep composites can be used to measure the design allowables properties of Gr/PI between 117 K and 589 K (-250° F to 600° F). However, attention must be given to details associated with instrumentation and load introduction which are discussed in the references. Moisture and elevated temperature produce significant reductions in interlaminar shear and compression strength but do not preclude the use of Gr/PI in advanced space transportation systems.

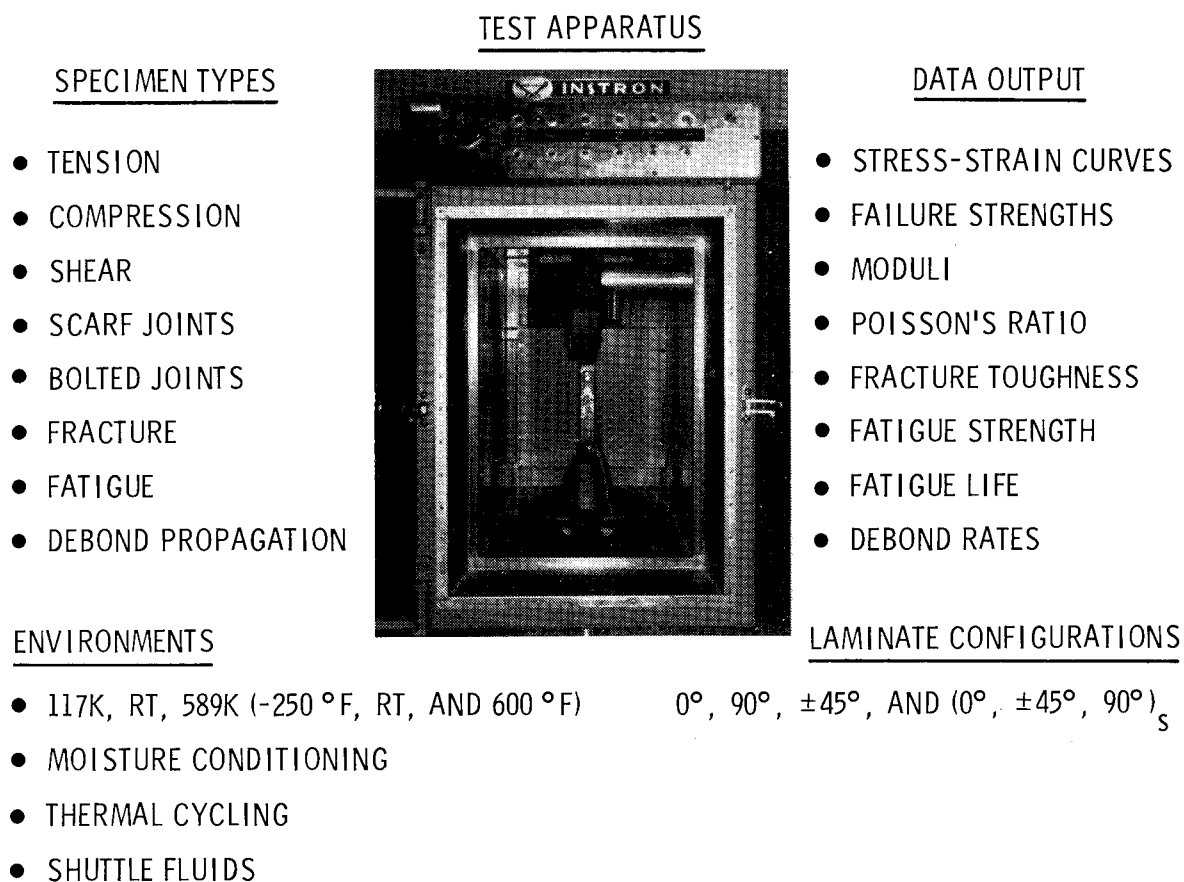


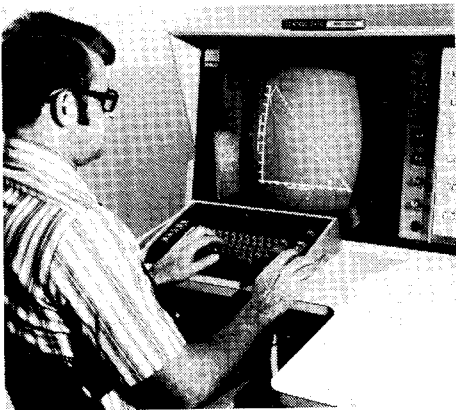
Figure 9

DESIGN AND ANALYSIS OF GRAPHITE/POLYIMIDE STRUCTURES

Extension of the current capability to design and analyze Gr/Ep structures to include Gr/PI structures that operate between 117 K and 589 K (-250°F and 600°F) is underway. The technical areas are depicted in figure 10 and include improving computer programs, design and test of compression and shear panels, design and test of joints representative of the types required for an aft body flap, and preliminary design of an aft body flap. Computer program modifications that account for temperature effects and orthotropic material behavior and preliminary design of a Gr/PI aft body flap are reported in reference 1. Reference 18 provides a status report on the design and test of skin-stringer and sandwich compression panels.

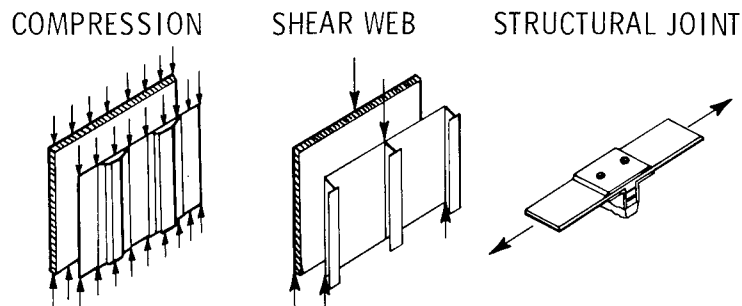
Thus far the effort has not uncovered any problem that would preclude the use of Gr/PI structures in advanced space transportation systems.

COMPUTER PROGRAM MODIFICATIONS



- SPAR
- VIPASA
- POP

STRUCTURAL TEST COMPONENTS



FULL-SCALE AFT BODY FLAP

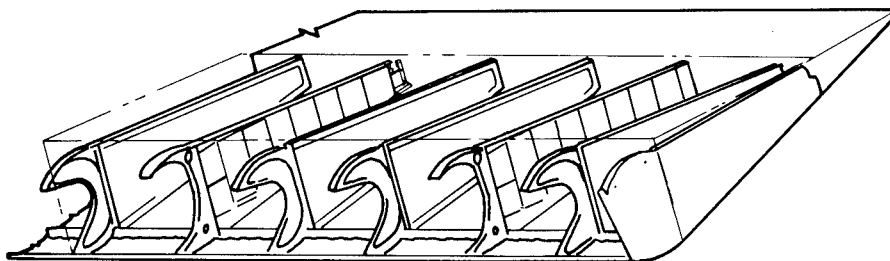


Figure 10

SUMMARY

Four Gr/PI composites and three PI adhesives with 589 K (600° F) service potential for periods ranging from 125 to 500 hours have been identified using interlaminar shear, flexure and lap shear strength test data. An adhesive formulation suitable for bonding reusable surface insulation (RSI) tiles to 589 K (600° F) Gr/PI substructure has been developed. Test methods for measuring design allowables at 117 K (-250° F), RT and 589 K (600° F) have been demonstrated. The capability to fabricate and nondestructively inspect laminates, hat section shaped stiffeners, honeycomb sandwich panels, and chopped fiber moldings has been demonstrated utilizing Gr/PMR-15 composite. Investigation on the effects of moisture, temperature, thermal cycling and shuttle fluids on the thermal, physical and mechanical properties of Gr/PI is underway and preliminary data obtained to date have not uncovered any environmental degradation problems that would preclude the use of Gr/PI in advanced space transportation systems.

- Gr/Pi COMPOSITES AND ADHESIVES WITH THE POTENTIAL FOR APPLICATION TO 589K (600°F) AEROSPACE STRUCTURES HAVE BEEN IDENTIFIED
- TEST METHODS FOR DETERMINING DESIGN ALLOWABLES OVER THE TEMPERATURE RANGE 117K TO 589K (-250°F TO 600°F) HAVE BEEN VERIFIED
- THE CAPABILITY TO FABRICATE STRUCTURAL COMPONENTS HAS BEEN DEMONSTRATED WITH ONE Gr/Pi COMPOSITE
- NO TECHNICAL ROAD BLOCKS TO BUILDING A Gr/Pi COMPOSITE BODY FLAP HAVE BEEN IDENTIFIED

Figure 11

REFERENCES

1. Blackburn, C. L.; and Robinson, J. C.: Analysis Methods and Preliminary Design Study. Graphite/Polyimide Composites, NASA CP-2079, 1979. (Paper no. 22 of this compilation.)
2. Progar, Donald: Polyimide Adhesive Bonding. Graphite/Polyimide Composites, NASA CP-2079, 1979. (Paper no. 9 of this compilation.)
3. Smith, Kenneth E.; Hamermesh, Charles L.; and Hogenson, Peter A.: Adhesives for Bonding RSI Tile to Gr/Pi Structure for Advanced Space Transportation Systems. Graphite/Polyimide Composites, NASA CP-2079, 1979. (Paper no. 10 of this compilation.)
4. Baucom, Robert M.: LaRC Fabrication Development. Graphite/Polyimide Composites, NASA CP-2079, 1979. (Paper no. 3 of this compilation.)
5. Scheck, W. G.; Smith, C. W.; and Harrison, E.: Development of Fabrication Techniques for NR150B2-S5X Graphite/Polyimide High Temperature Composites. Graphite/Polyimide Composites, NASA CP-2079, 1979. (Paper no. 4 of this compilation.)
6. Hoggatt, John T.: Development of LaRC-13 Adhesive Systems. Graphite/Polyimide Composites, NASA CP-2079, 1979. (Paper no. 12 of this compilation.)
7. Leahy, J. Devereaux: LaRC-160 Fabrication Development. Graphite/Polyimide Composites, NASA CP-2079, 1979. (Paper no. 6 of this compilation.)
8. Hoffman, Richard D.: Interim Results of THERMID 600 Engineering Development. Graphite/Polyimide Composites, NASA CP-2079, 1979. (Paper no. 7 of this compilation.)
9. Chapman, Andrew J.: Graphite/Polyimide Tension Tests at Elevated and Cryogenic Temperatures. Graphite/Polyimide Composites, NASA CP-2079, 1979. (Paper no. 13 of this compilation.)
10. Shuart, Mark J.: Sandwich Beam Compressive Test Method. Graphite/Polyimide Composites, NASA CP-2079, 1979. (Paper no. 14 of this compilation.)
11. Camarda, Charles J.: Application of the IITRI Compression Test Fixture at Elevated Temperature. Graphite/Polyimide Composites, NASA CP-2079, 1979. (Paper no. 15 of this compilation.)
12. Garcia, Ramon; and McWithey, Robert R.: Rail Shear Test Method. Graphite/Polyimide Composites, NASA CP-2079, 1979. (Paper no. 16 of this compilation.)

13. Garcia, Romon; and Rhodes, Marvin D.: Effects of Low-Velocity Impact on Gr/Pi Compression Laminates. Graphite/Polyimide Composites, NASA CP-2079, 1979. (Paper no. 17 of this compilation.)
14. Wichorek, Gregory R.: Preliminary Bolted-Joint Data. Graphite/Polyimide Composites, NASA CP-2079, 1979. (Paper no. 18 of this compilation.)
15. Illg, Walter; and Everett, Richard A., Jr.: Fatigue and Fracture. Graphite/Polyimide Composites, NASA CP-2079, 1979. (Paper no. 19 of this compilation.)
16. Lisagor, W. Barry: Mechanical Property Degradation of Graphite/Polyimide Composites After Exposure to Moisture or Shuttle Orbiter Fluids. Graphite/Polyimide Composites, NASA CP-2079, 1979. (Paper no. 20 of this compilation.)
17. Rummeler, Donald R.; and Clark, Ronald K.: Mechanical and Thermophysical Properties of Graphite/Polyimide Composite Materials. Graphite/Polyimide Composites, NASA CP-2079, 1979. (Paper no. 21 of this compilation.)
18. McWithey, Robert R.; Camarda, Charles J.; and Weaver, Gerald G.: Design Considerations for Compression Panels at Elevated Temperature. Graphite/Polyimide Composites, NASA CP-2079, 1979. (Paper no. 23 of this compilation.)

LaRC FABRICATION DEVELOPMENT

3

Robert M. Baucom
NASA Langley Research Center

EXPANDED ABSTRACT

The NASA Langley Research Center is conducting studies directed toward the goal of manufacturing graphite fiber/polyimide matrix (Gr/PI) composite structures with 589 K (600° F) operational capability for application to aerospace vehicles. The fabrication of structures from Gr/PI requires a thorough understanding of the characteristics of Gr/PI prepreg materials and the development of processing techniques for conversion of the prepreg into structures. After fabrication, the structures must be nondestructively evaluated and subjected to mechanical test to verify manufacturing procedures.

This paper reports on the interim results of in-house efforts in support of the Supersonic Cruise Research (SCR) Program to develop fabrication procedures for the manufacture of Gr/PI wing panels for the NASA YF-12 airplane. In addition, manufacturing procedures are outlined for the fabrication of structures in support of the CASTS Project. The results of studies directed toward the development of Gr/PI prepreg manufacturing capability, assembly, of structural elements from prepreg, final processing of Gr/PI structural shapes, and techniques for verification of structural integrity are presented herein.

YF-12 Gr/PI WING PANEL DEVELOPMENT

The YF-12 is a NASA high performance airplane capable of sustained flight at Mach 3 or above. The panel chosen as a Gr/PI fabrication feasibility component for this airplane is an upper surface wing panel located between the engine and fuselage. In this area the wing surface is aerodynamically heated to temperatures up to 524 K (485°F) during flight at speeds near Mach 3. The current production panel for this location is a blade stiffened titanium wing panel which is loaded primarily in shear. HTS1/PMR-15 and Celion 6000/LARC-160 are two of the primary materials being investigated in-house for manufacture of composite wing panels. Key accomplishments in the fabrication of two wing panel configurations with Gr/PI are given hereinafter.

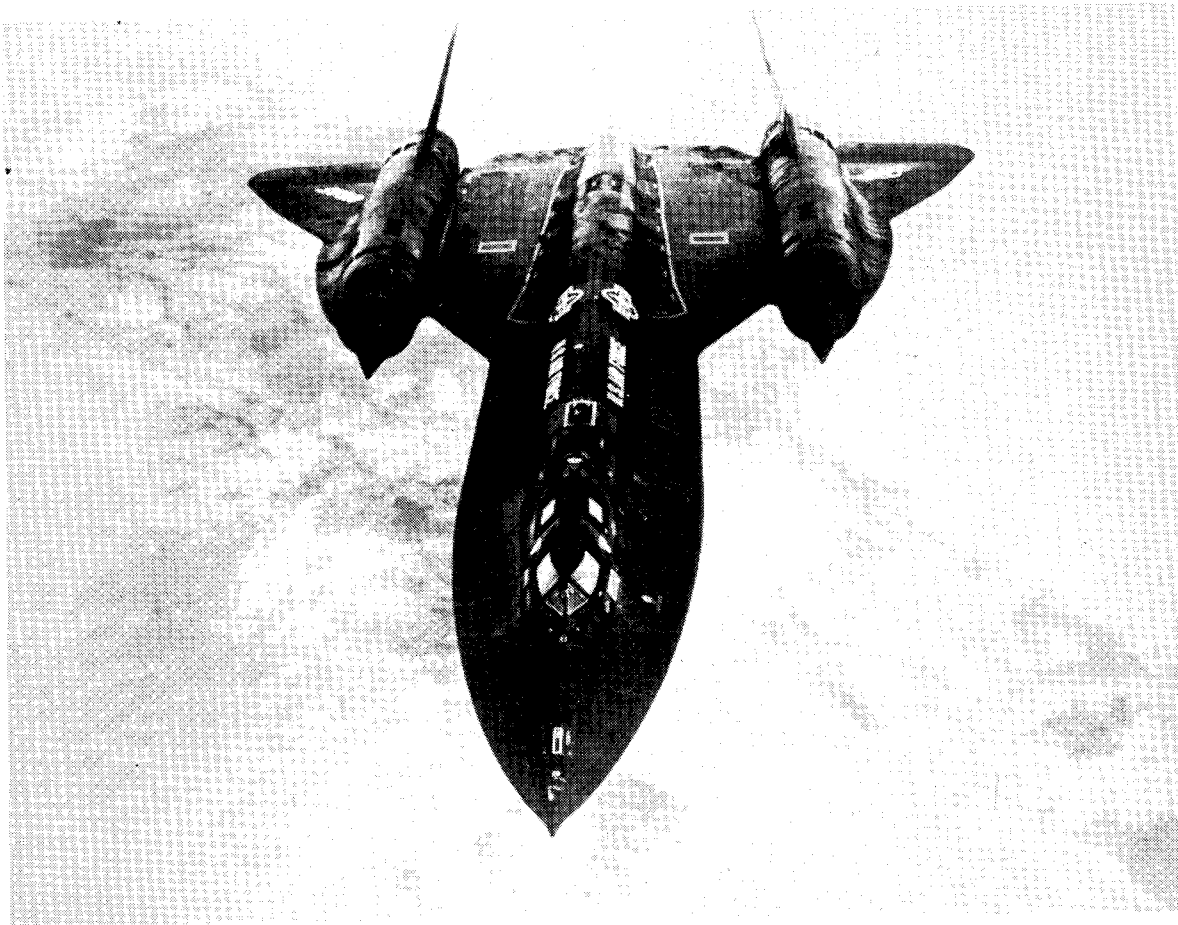


Figure 1

GRAPHITE/POLYIMIDE YF-12 WING PANEL CONFIGURATIONS

The configurations for the NASA LaRC honeycomb stiffened and hat stiffened Gr/PI YF-12 wing panels are presented below. The outer face sheets and inner face sheets of the honeycomb panels are composed of 9 plies and 6 plies, respectively, of HTS1/PMR-15. The fiberglass/polyimide honeycomb material is 25.40 mm (1.00 in) thick and has a density of 93 kg/m^3 (5.8 lbm/ft^3). Spacer shims made from HTS1/PMR-15 are bonded to the panel flanges for correct fit to the airplane wing substructure. The outer and inner face sheets, honeycomb, and spacer shims are bonded together with LARC-13, an in-house developed polyimide adhesive.

The hat stiffened panel shown on the right is currently being fabricated with Celion 6000/LARC-160. The face sheet for this panel is 10 plies thick. The corrugated hat-stiffeners are 4 plies thick with an additional 5 plies of unidirectional Celion 6000/LARC-160 reinforcement in the caps. A sub scale prototype of this panel has been successfully fabricated to date and the fabrication of the full-scale panels is currently underway.

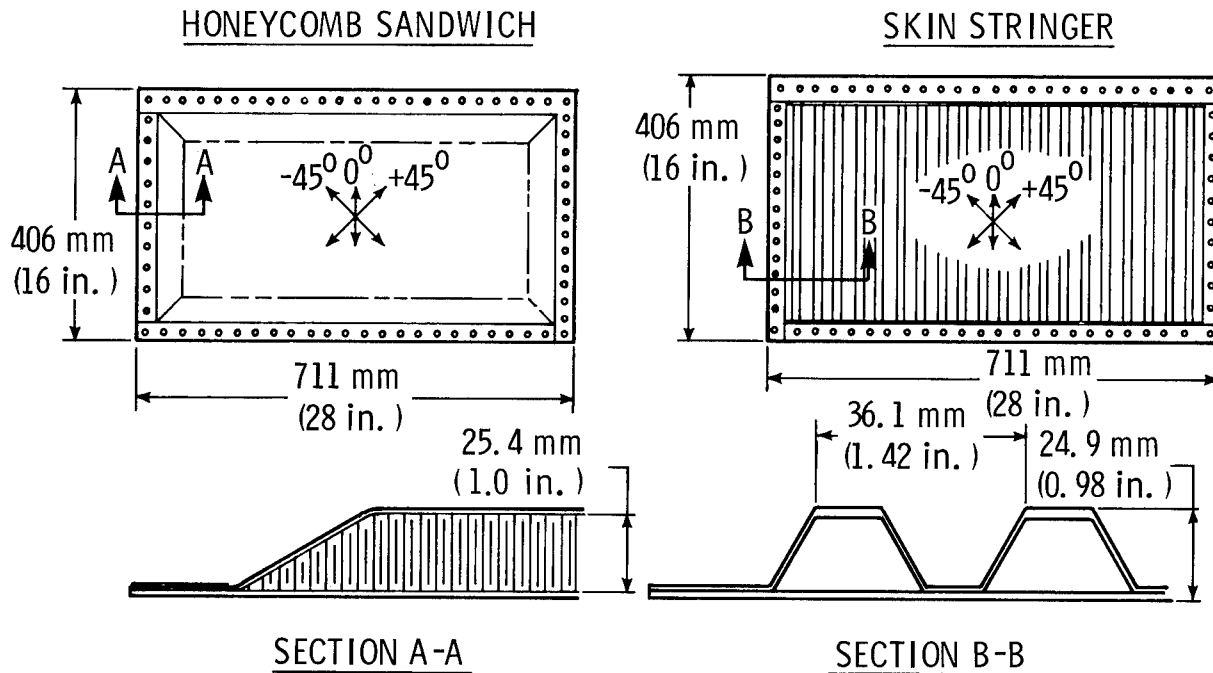


Figure 2

PRECOMPACTION VACUUM BAG SCHEMATIC FOR NASA PMR-15 YF-12 WING PANEL

The Gr/PI material is precompacted prior to cure in order to remove the excess solvent and resin. The prepreg is first laid up into the proper laminate orientation. It is then weighed to the nearest 0.1 g and perforated teflon coated fiberglass release cloth is placed on the top and bottom of the laminate. Bleeder paper is then applied to each side of the assembly. A thin film of nylon is applied to an aluminum caul plate and the laminate assembly is placed on the nylon. A 3.05 mm (0.12 in) thick mild steel upper caul sheet is then placed on top of the laminate to provide a smooth upper mold surface during precompaction. Two layers of bleeder paper are placed onto the steel caul plate and the assembly is vacuum bagged with a .100 mm (.004 in) thick film of nylon. The seal between the vacuum bag and the aluminum caul plate is provided with a conventional low temperature polybutadiene strip sealant. The assembly is then placed under vacuum to ascertain the integrity of the vacuum bag and seals.

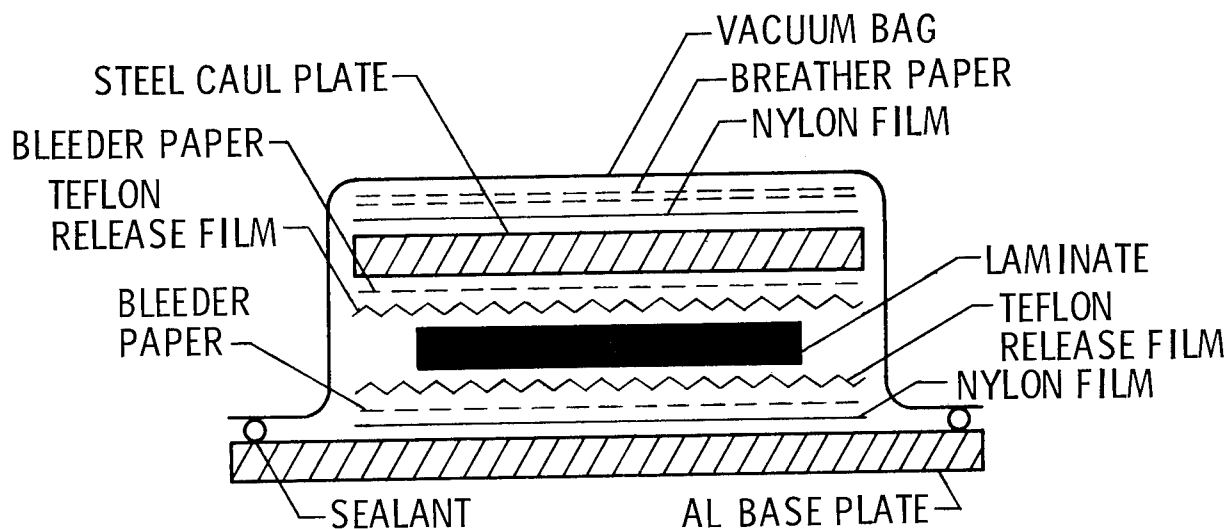


Figure 3

NASA PMR-15 PRECOMPACTION CYCLE FOR YF-12 PANEL

After the vacuum bagged laminate is installed in the autoclave, the assembly is checked for leaks. If no leaks are detected a vacuum of 34 kPa (5 psi) is applied to the laminate and the temperature is increased at a rate of 2.8 K (5° F)/min. After reaching 477 K (400° F) the temperature is held for one hour at a vacuum level of 34 kPa (5 psi). The vacuum is then released and the laminate is cooled down at a rate of 2.8 K (5° F)/min. until the laminate reaches 338 K (150° F). The assembly is removed from the autoclave and the laminate is weighed to determine the percentage of resin remaining. The laminate is visually examined for fiber movement, gaps between tows, and resin rich or starved areas. It is then placed in a sealed polyethylene bag and stored until final curing.

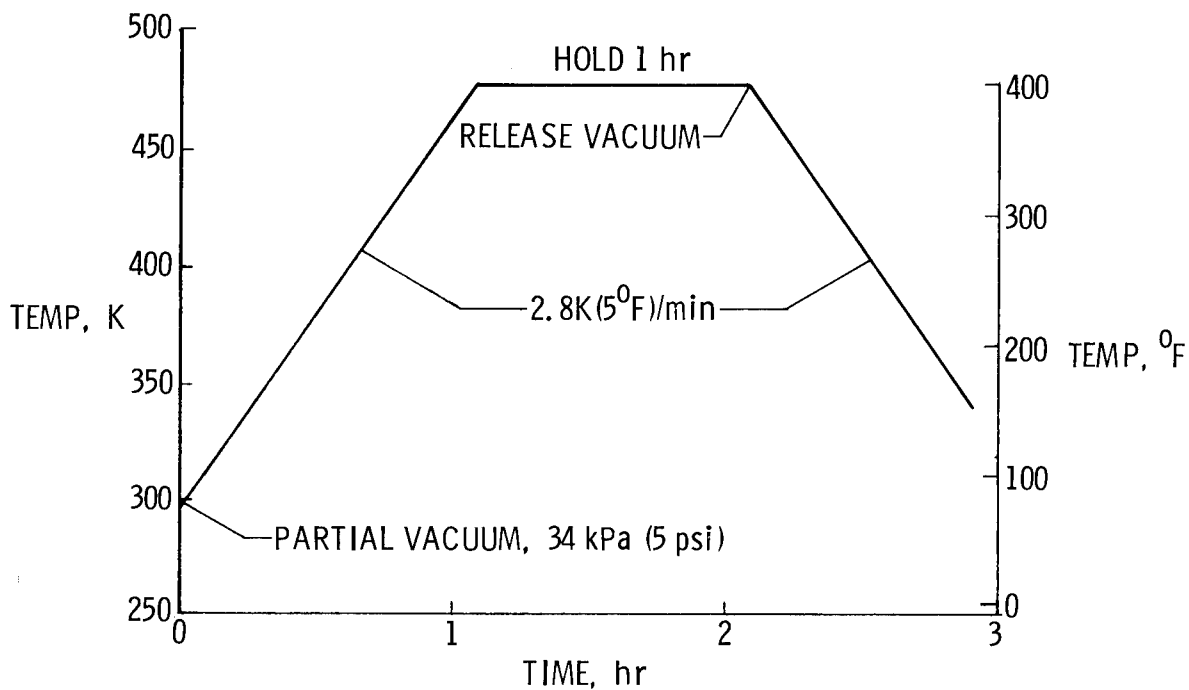


Figure 4

CURE VACUUM BAG SCHEMATIC FOR NASA PMR-15 YF-12 PANEL

The vacuum bag assembly for final laminate curing for the Gr/PI cover sheets and spacers is shown in this figure. Teflon coated style 104 fiberglass release cloth is placed on the top and bottom of the previously pre-compacted laminate. Style 181 fiberglass bleeder cloth is then placed on each side of the laminate. A sheet of polyimide film is placed on the steel caul plate and the laminate is placed on the film. This assembly is then covered with vacuum bagging materials in the following order: Teflon coated style 104 fiberglass release cloth, polyimide film, 5.1 mm (0.2 in) thick upper steel caul plate, two plies of style 1044 fiberglass breather cloth, and one layer of polyimide film. The .152 mm (.006 in) thick annealed aluminum vacuum bag is then installed over the assembly with an inner seal of uncured silicone and an outer seal of polybutadiene sealer. A vacuum is applied to the assembly to check for leaks and proper vacuum bag "pull-down".

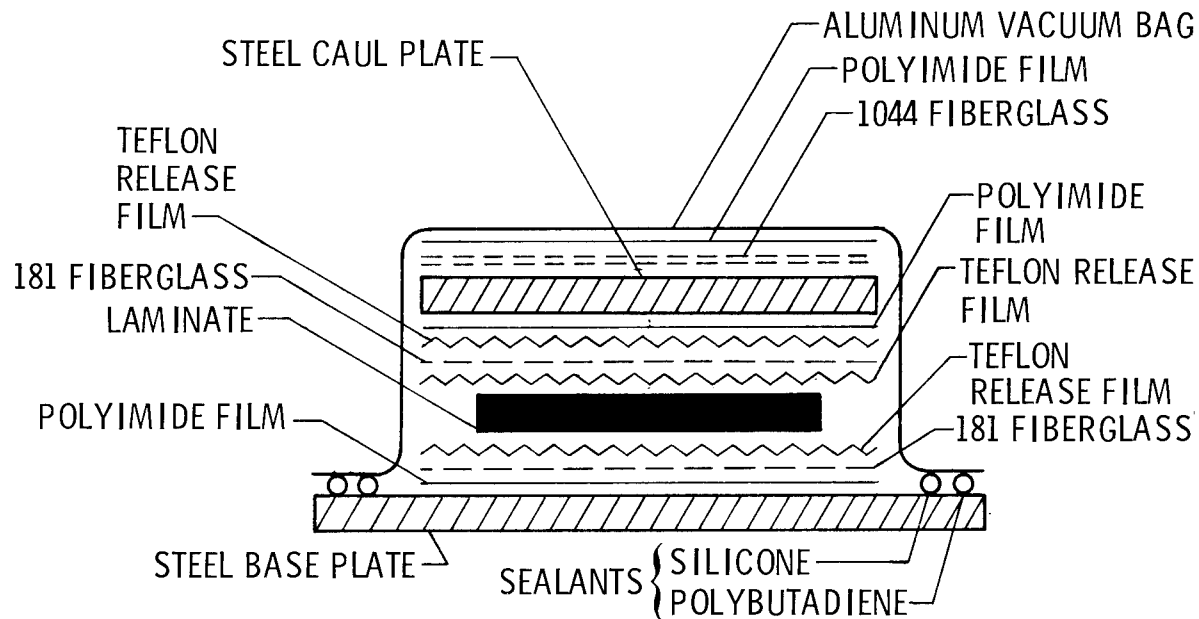


Figure 5

NASA PMR-15 CURE CYCLE FOR YF-12 PANEL

The bagged Gr/PI laminate is placed in the autoclave and the vacuum lines and thermocouples are connected to the assembly. A full vacuum and 207 kPa (30 psi) of positive autoclave pressure is applied to the laminate. The temperature is increased at a rate of 5 K (9° F)/min until the laminate reaches 589 K (600° F). During this heat-up, the autoclave pressure is increased to 3.4 MPa (500 psi) and the vacuum is released when the laminate temperature reaches 505 K (450° F). After a hold at 589 K (600 °F) for one hour the autoclave pressure and temperature are decreased at 34 kPa (5 psi)/min and 2.7 K (4° F)/min, respectively. This slow depressurization and temperature reduction rate is employed to minimize **micro-cracking in the** laminate during cool down. After the laminate temperature reaches 338 K (150° F), the autoclave is turned off and the vacuum bag assembly is removed. The laminate is removed from the vacuum bag, weighed and subjected to ultrasonic C-scan inspection. If no anomalies are detected, the laminate is placed in a polyethylene bag for storage.

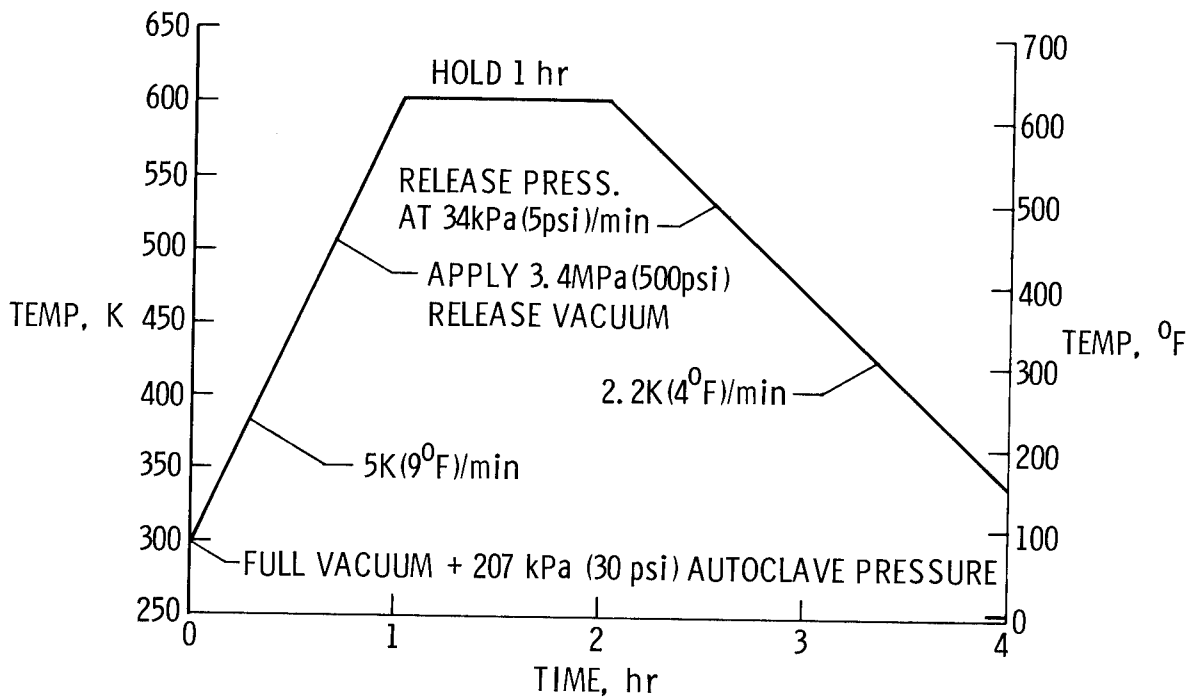


Figure 6

AUTOCLAVE ASSEMBLY FOR BONDING Gr/PI FY-12 WING PANEL

The adherend surfaces of the Gr/PI wing panel upper and lower covers are prepared for bonding by sanding the adherend surfaces with 600 grit sandpaper. These surfaces are then thoroughly wiped with methyl ethyl ketone. The adherend surfaces are then primed by applying LARC-13, an in-house formulated polyimide adhesive. This primer coating is dried by placing the Gr/PI covers in an air circulating oven maintained at 422 K (300° F) for thirty minutes. The polyimide film adhesive, LARC-13 coated style 104 fiberglass, is then placed on the adherend surfaces of the upper and lower wing panel covers. The covers are then placed on the honeycomb core; the assembly is vacuum bagged and placed in the autoclave. A partial vacuum of 34 kPa (5 psi) and 207 kPa (30 psi) positive autoclave pressure are applied to the assembly and the temperature is increased to 589 K (600° F). The temperature is decreased to 338 K (150° F) under vacuum and pressure. The fully cured assembly is removed and subjected to NDE to verify structural integrity. The wing panel is trimmed and the appropriate mounting holes are drilled.

BONDING PROCEDURE

- DULL SURFACES
- PRIME WITH LARC-13, DRY AT 422K (300°F) FOR 30 min
- ASSEMBLE
- APPLY 34 kPa (5 psi) VACUUM, 238 kPa (35 psi) AUTOCLAVE PRESSURE
- HEAT TO 589K (600°F), HOLD 1 HOUR
- COOL UNDER PRESSURE AND VACUUM

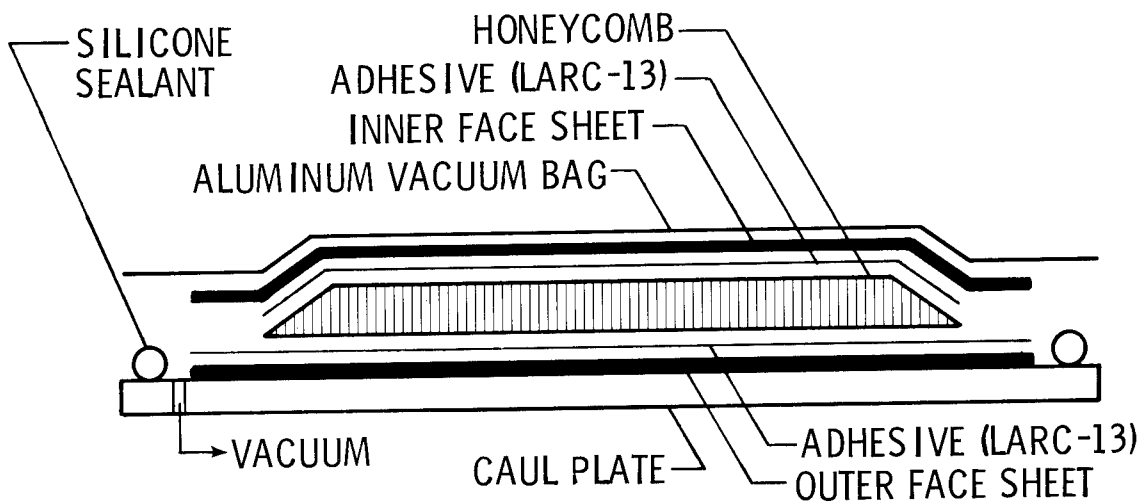


Figure 7

HTS1/PMR-15 YF-12 WING PANEL

This figure shows one of the ten (10) Gr/PI YF-12 honeycomb core wing panels that have been fabricated at Langley. These panels weigh approximately 1.9 kg (4.2 lbm) after the final machining operations. This compares to 3.9 kg (8.5 lbm) for the production titanium wing panels. These panels are currently being subjected to a variety of ground tests including exposures up to 10,000 hours at 533 K (500° F), thermal cycling up to 3,000 cycles between 219 K (-65° F) and 533 K (500° F), and destructive shear testing.

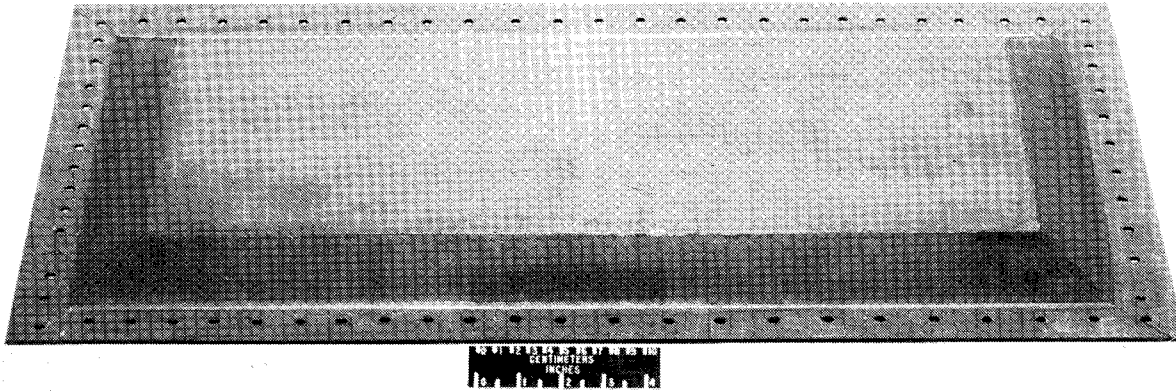


Figure 8

PREPREG DEVELOPMENT

The requirement for prepreg material for the CASTS in-house fabrication development studies resulted in the establishment of the capability for production of high quality graphite/polyimide prepreg. During this period several fiber/resin combinations were manufactured and evaluated. HTS1, HTS2, Modmor II, Celion 6000 and 3000, Thornel 300 and Type AS fibers have been evaluated in PMR-15, LARC-160, and NR150B2 resin systems. PMR-15 and LARC-160 prepregging resins are formulated in-house and NR150B2 is procured commercially. Prepreg from various combinations of these fibers and resins is produced in our drum winding facility. Prepreg sheets up to 1.9 x 1.5 m (75 x 58 in) in size can be produced with this equipment.

- FIBERS

- HTS 1
- HTS 2
- CELION 6000

- RESINS

- PMR-15
- NR150-B2
- LARC-160

- PREPREG

- DRUM WOUND SHEETS 1.9 x 1.5 m (75 x 58 in.)

Figure 9

DRUM WINDING MACHINE FOR PREPREG MANUFACTURE

A conventional filament winding machine was utilized for the in-house manufacture of graphite/polyimide. The drum diameter and length is approximately 610 mm (24 in) and 1470 mm (58 in), respectively. The graphite fiber tow is fed from a self tensioning creel at the rear of the machine. During winding, resin is pumped into the fiber tow through a hollow stem brush which forces the resin into the tow bundle for complete wetting. Typical drum rotational speed, tow spacing, and resin flow are 10 rpm, 2.0 tow/cm (5.6 tows/in), and 24 grams/min in the fabrication of .15 mm (0.006 in) per ply prepreg. After the sheet of prepreg is wound onto the drum, a bank of radiant heat lamps are positioned to drive off the excess solvent. The prepreg is then covered with a .025 mm (.001 in) thick sheet of teflon and removed from the drum. The resultant sheet of prepreg is 1.9 m (75 in) long and up to 1.5 m (58 in) wide. The sheets are placed in a freezer maintained at 291 K (0° F) for storage.

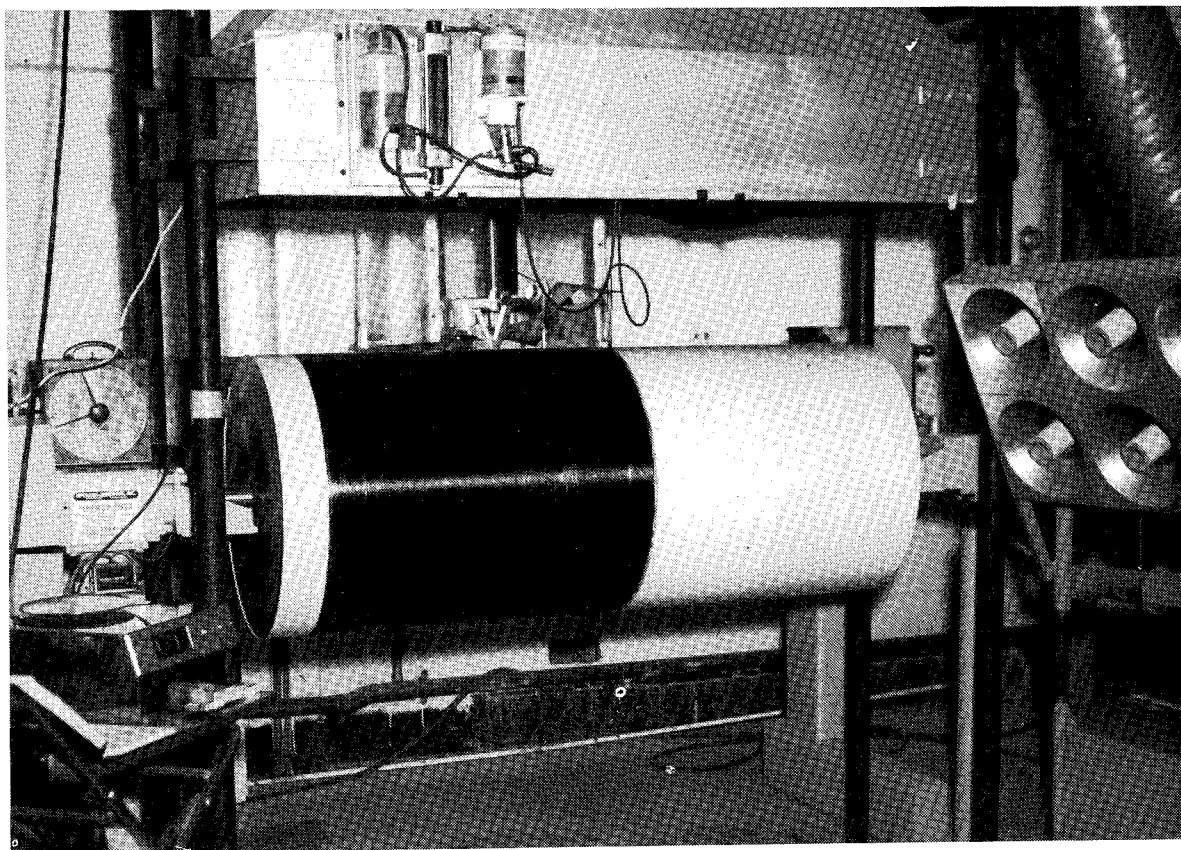


Figure 10

GR/PI PREPREG PRODUCTION EXPERIENCE

Since the prepreg facility was placed in operation five years ago, approximately 818 kg (1800 lbs) of graphite/polyimide prepreg, with various fiber/resin combinations have been produced. Some of the early prepreg work was performed with the NR150B2 resin system. Due to difficulty experienced in curing graphite/NR150B2 laminates, the production of NR150B2 resin-based prepreg was stopped after making a total of approximately 70 kg (150 lbm). Graphite/PMR-15 prepreg was then placed in production to supply material for the CASTS Project. A total of 580 kg (1277 lbm) of graphite/PMR-15 has been produced to date. The HTS1/PMR-15 system has been produced in the largest quantity with a total of 299 kg (658 lbm). HTS2/PMR-15 and Celion 6000/PMR-15 have been produced in quantities of 99 kg (218 lbm) and 281 kg (619 lbm). Recently the LARC-160 resin system has been utilized in the manufacture of graphite/LARC-160. Research quantities of HTS2/LARC-160, Celion 3000/LARC-160, and type AS/LARC-160 have been manufactured and a total of 78 kg (172 lbm) of Celion 6000/LARC-160 has been prepregged for laminate fabrication in support of the CASTS Project.

RESIN/FIBER

LaRC PRODUCTION, kg (lb)

HTS 1/PMR-15

298 (658)

HTS 2 /PMR-15

99 (218)

CELION 6000/PMR-15

281 (619)

HTS 1/NR150 B2

68 (150)

CELION 6000/LARC-160

78 (172)

TOTAL

824 (1817)

Figure 11

VACUUM BAG SCHEMATIC FOR PMR-15 AND LARC-160 AUTOCLAVE CURE

In order to insure that the fabrication procedures could be used to manufacture full scale structures in existing aerospace industry facilities, limits of 2.1 MPa (300 psi) and 6 K (10° F)/min were imposed on the maximum pressure and heat up rate that could be used. Figures 13 through 15 provide detailed information on the bagging and cure cycles used to fabricate PMR-15 and LARC-160 laminates in support of the CASTS Project.

A total envelope vacuum bag is utilized for curing PMR-15 and LARC-160 laminates in-house. Vacuum bag materials are applied symmetrically to the laminate in the following order: Porous Teflon release film, fiberglass bleeder plies, non-porous polyimide film, steel caul sheet, fiberglass breather plies and polyimide film vacuum bag. The two vacuum bag halves are sealed with a high temperature uncured silicone sealant strip and the assembly is checked for vacuum leaks. If no leaks are detected, the assembly is installed in the autoclave for final curing.

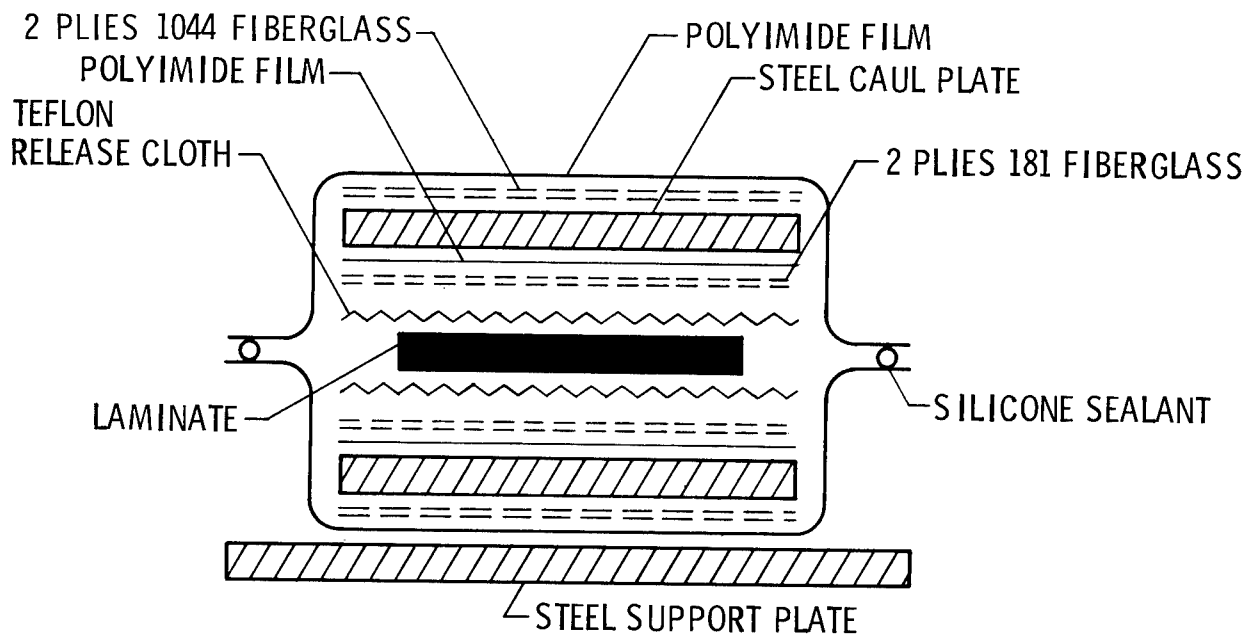


Figure 12

CURE CYCLE FOR PMR-15

After the laminate is installed in the autoclave a partial vacuum of approximately 17 kPa (2.5 psi) is applied and the temperature is increased at the rate of 5.6 K (10° F)/min until the laminate reaches 522 K (480° F). After a ten minute hold at this temperature a full vacuum is applied to the laminate. After an additional ten minute hold at 522 K (480° F) the autoclave pressure is increased to 2.1 MPa (300 psi). This pressure and vacuum level are maintained and the temperature is increased to 603 K (625° F) at a rate of 5.6 K (10° F)/min after a total hold time at 522 K (480° F) of 30 minutes. The laminate is held at 603 K (625° F) for three hours and cooled down under pressure and vacuum at a rate of 2.8 K (5° F)/min until the laminate reaches 338 K (150° F). The pressure and vacuum are released and the laminate is removed from the autoclave.

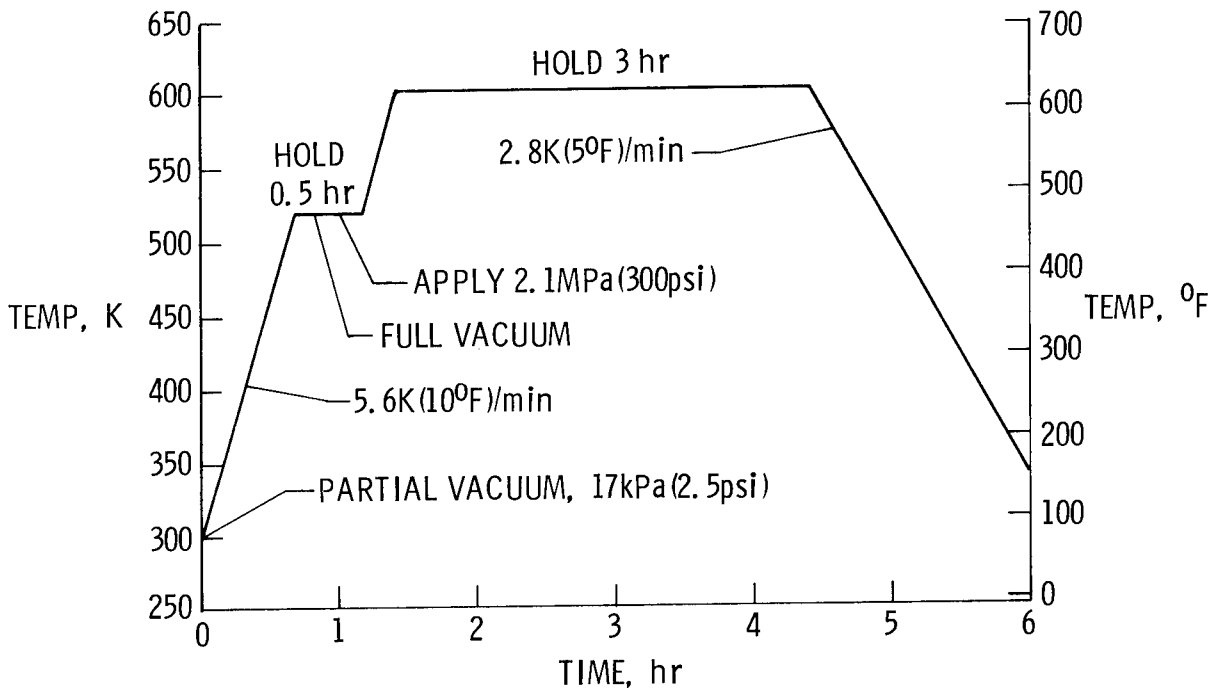


Figure 13

CURE CYCLE FOR LARC-160

Care must be exercised in the cure of LARC-160 to preclude the removal of an excessive amount of the resin during solvent removal and imidization. A partial vacuum of 10 kPa (1.5 psi) is applied to the laminate and the temperature is increased to 366 K (200° F). The laminate is held at this temperature for 15 minutes to allow most of the solvent to be removed. The temperature is then increased to 435 K (325° F) and held for one hour to allow the laminate to imidize and to remove the imidization by-products. The laminate is then heated to 603 K (625° F) and held for two hours. During the heat-up to 603 K (625° F), a full vacuum and 1.4 MPa (200 psi) are applied to the laminate when the laminate temperature reaches 546 K (525° F). After the two hour hold at 603 K (625° F) the temperature is decreased to 338 K (150° F), the pressure and vacuum are released and the laminate is removed from the autoclave.

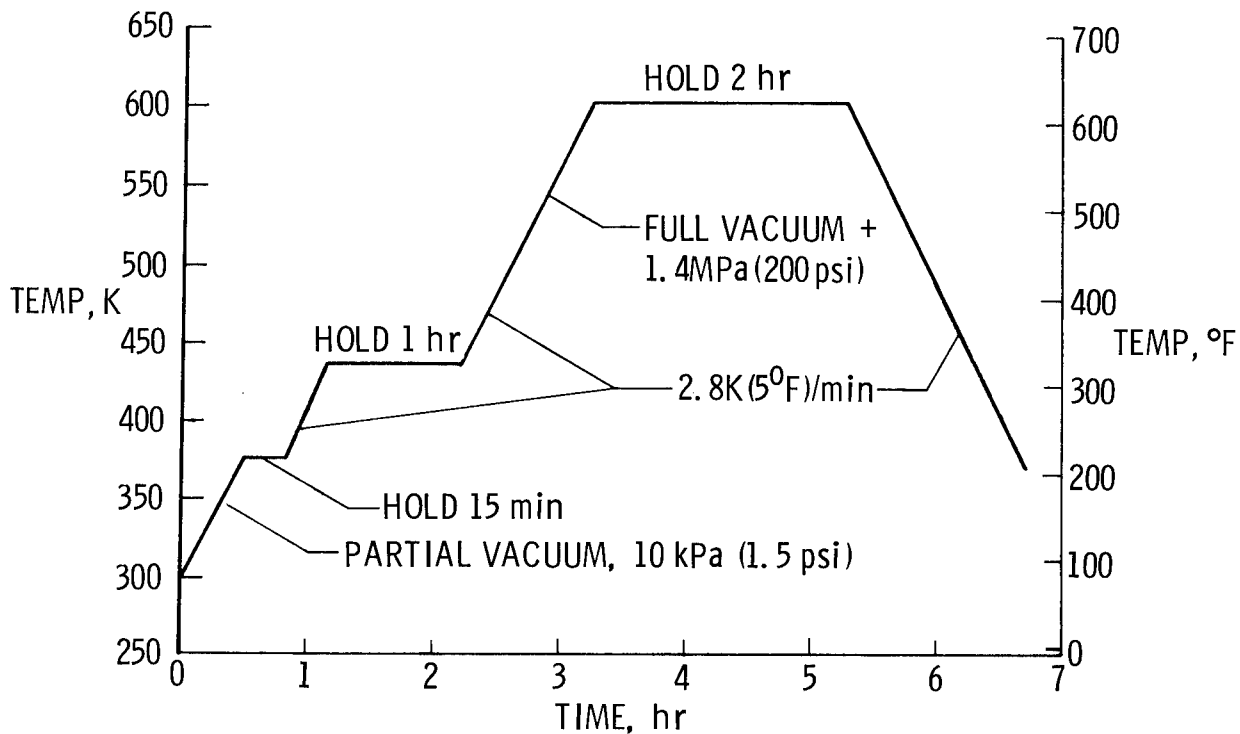


Figure 14

INSPECTION TECHNIQUES

After the laminates are fabricated they are subjected to ultrasonic C-scan inspection to determine if there are voids or delaminations in the laminates. The ultrasonic C-scan record shown in the upper left of this figure represents an acceptable laminate for further processing. The photomicrograph of this laminate shown in the upper right verifies the integrity of the laminate as indicated by the C-scan. Conversely, a poor quality laminate is indicated in the C-scan in the lower left. The photomicrograph in the lower right substantiates this finding as shown by the void areas in the cross-section.

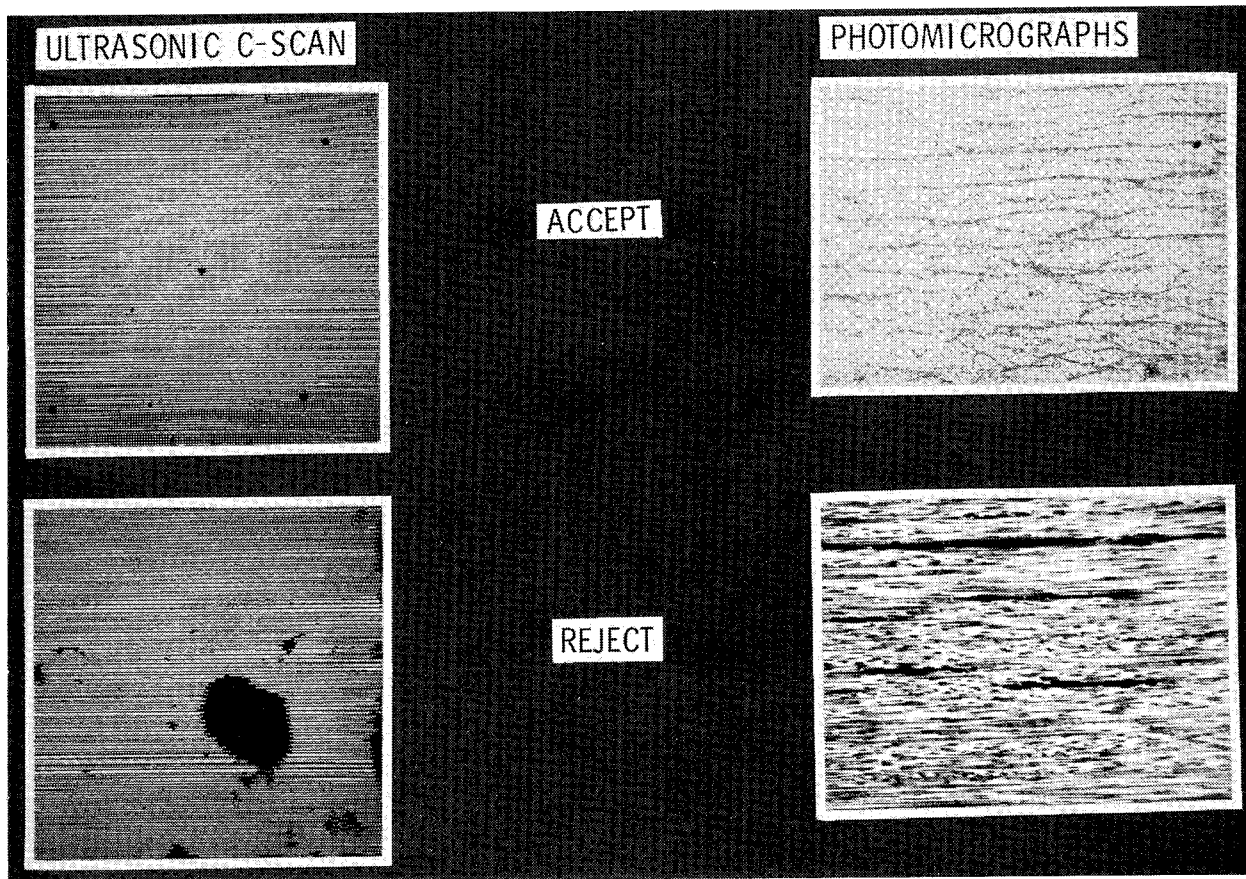


Figure 15

FABRICATION DEMONSTRATION ARTICLES

A 16 ply isotropic laminate is shown in the upper left photograph. The laminate is 660 mm (26 in) wide and 1270 mm (50 in) long. The honeycomb stiffened panel was fabricated with 8 ply isotropic skins and fiberglass/polyimide honeycomb core bonded with FM-34 polyimide adhesive and is also 660 mm (26 in) wide and 1270 mm (50 in) long. The hat-stiffened panel shown on the upper right is 152 mm (6 in) wide and 305 mm (12 in) long. The hat stiffener is bonded to the face sheet with FM-34 polyimide adhesive. A 12.7 mm (0.5 in) thick by 152 mm (6 in) square laminate is shown in the lower right photograph.

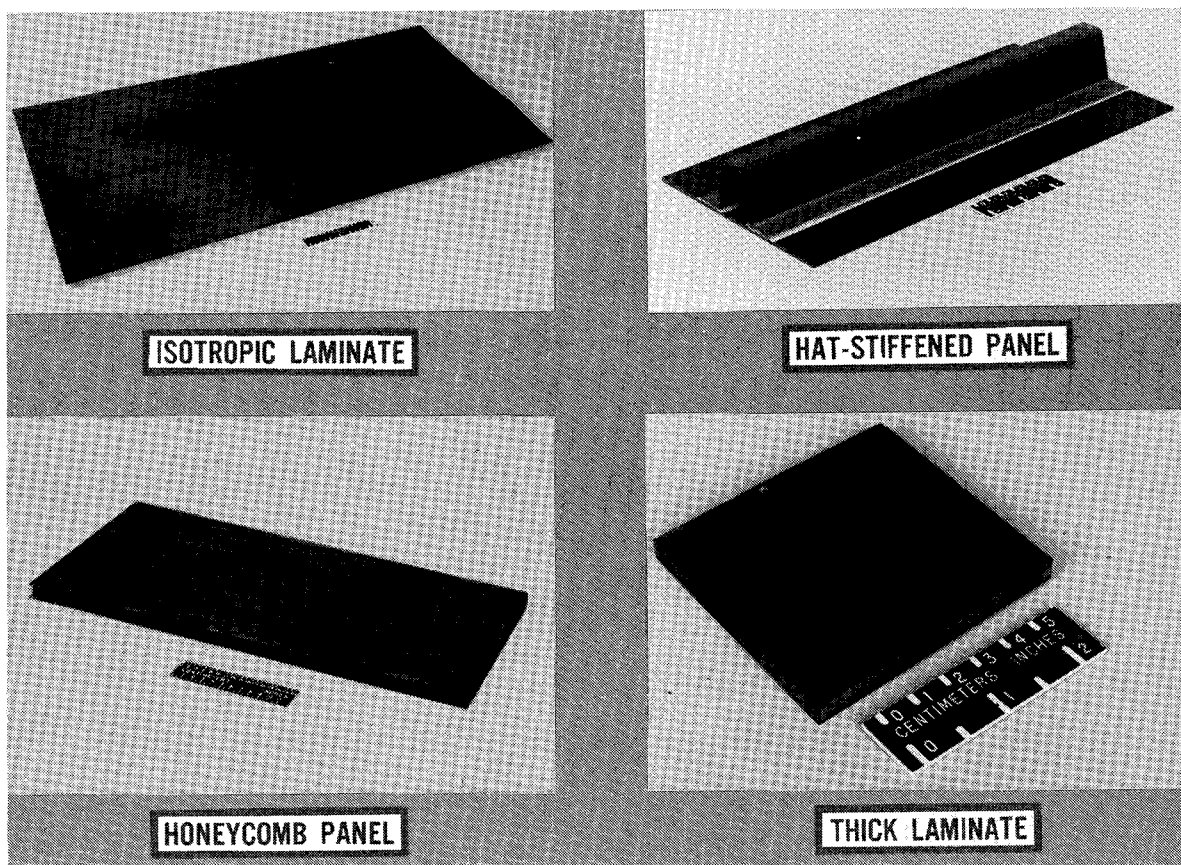


Figure 16

MANUFACTURING DEMONSTRATION ARTICLE

This component is approximately 254 mm (10 in) high in the front tapering to 102 mm (4 in) in the rear. The width and length are 406 mm (16 in) and 610 mm (24 in) respectively. The covers and ribs for this article were made by curing 4 ply skins and bonding them to 12.7 mm (0.5 in) thick fiberglass/honeycomb core material with FM-34 polyimide adhesive. The covers were then bonded to the tapered ribs with the same adhesive.

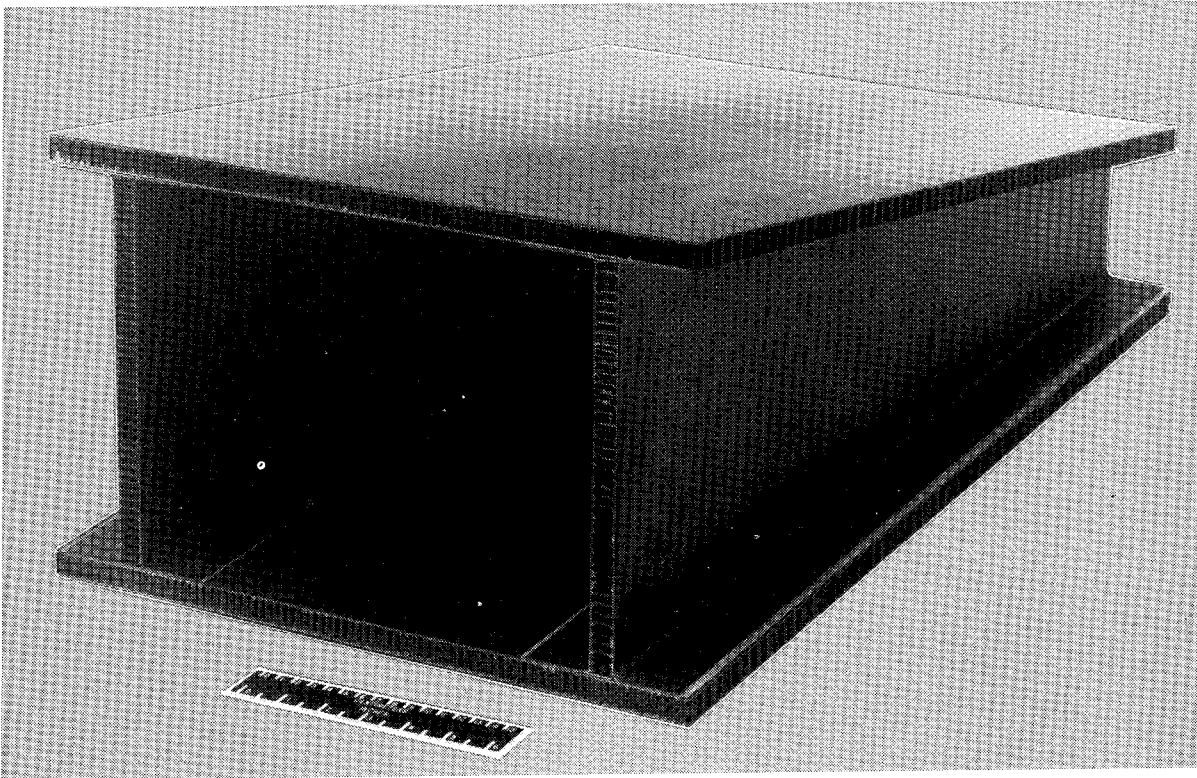


Figure 17

SUMMARY

An in-house capability for prepregging graphite fiber reinforced PMR-15, LARC-160, and NRL50B2 has been established to support the SCR Program and CASTS Project. Cure cycles have been successfully developed for vendor supplied and in-house manufactured graphite/PMR-15 and graphite/LARC-160 prepreg. A total of 10 graphite/polyimide honeycomb stiffened panels and a prototype hat stiffened panel subcomponent have been successfully fabricated. A wide variety of CASTS manufacturing feasibility components have been fabricated including laminates up to .6 m by 1.2 m (2 ft by 4 ft) and up to 12.7 mm (0.5 in) thick. Structural articles that have been fabricated in support of the CASTS Project include hat-stiffened panels, honeycomb stiffened panels and a manufacturing demonstration component. Non-destructive evaluation procedures have been established for all laminates and articles fabricated.

- IN-HOUSE PREPREGGING CAPABILITY ESTABLISHED
- CURE CYCLES DEVELOPED FOR PMR-15 AND LARC-160
SYSTEMS
- Gr/PI YF-12 WING PANELS SUCCESSFULLY FABRICATED
AND EVALUATED
- CASTS MANUFACTURING FEASIBILITY COMPONENTS
FABRICATED
- NDE TECHNIQUES ESTABLISHED FOR STRUCTURAL
ARTICLES

Figure 18

DEVELOPMENT OF FABRICATION TECHNIQUES FOR
NR150B2-S5X GRAPHITE/POLYIMIDE HIGH TEMPERATURE COMPOSITES

W. G. Scheck, C. W. Smith, and E. Harrison
General Dynamics, Convair Division

EXPANDED ABSTRACT

Under sponsorship of NASA-LRC Contract NAS1-14784 entitled: "Develop and Demonstrate Manufacturing Processes for Fabricating Graphite Filament Reinforced Polyimide Composite Structural Elements," General Dynamics Convair is developing fabrication techniques for NR150B2-S5X graphite/polyimide composites. This presentation covers the development of fabrication, tooling, and quality assurance techniques used for the NR150B2-S5X composites. Detailed processing information and preliminary mechanical property data is presented. Long term aging data is also presented.

PROGRAM OBJECTIVE

This broad objective is divided into many integral parts. To begin with, the resin is to be characterized to the point that the aerospace manufacturer has confidence he is receiving the same material each time. Material processing techniques are to be developed and reported in such detail that anyone with the right facilities can reproduce the initial work. In order to demonstrate that the fabrication techniques that are developed are applicable to actual detail parts, simple I-beams, hat stiffeners, and honeycomb panels will be fabricated and tested. Following this a typical section of the Space Shuttle body flap will be fabricated as a manufacturing demonstration article.

Development and demonstration of fabrication processes for graphite composites based on NR150B2-S5X polyimide resin which are applicable to fabrication of large size structures

Figure 1

PROGRAM TASKS

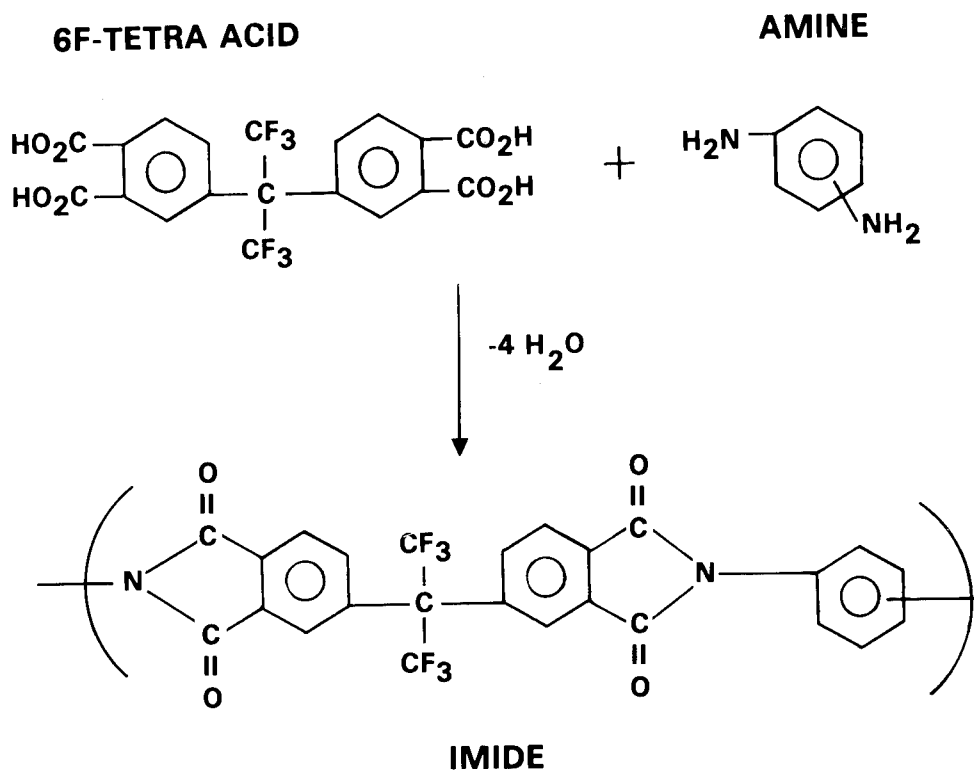
The subject program was separated into four sub-tasks with the principal effort being made toward resin characterization and development of processing techniques. A secondary objective was the fabrication and testing of various honeycomb or stiffened panel subelements followed by fabrication of a demonstration article representing a section of the Space Shuttle body flap. The material and process specification will be distributed to several material suppliers prior to finalizing it and publishing it in the final report.

- Resin characterization, flat laminate process development, and establishment of nondestructive inspection techniques
- Honeycomb panel, stiffened panel, and preliminary design data development
- Material and process specifications
- Demonstration component fabrication

Figure 2

DUPONT'S NR150B2-S5X

This figure shows the theoretical formation of NR150B-2 or NR150B2-S5X resin during the curing and postcuring process. Unfortunately, many things occur between the making of the resin and the final prepreg product that most of the aerospace community receives from their material suppliers. Our results to date have indicated a wide variation from the proposed chemical reaction such as the formation of amides, imide salts and some formation of the imide before we have even started processing the material. Additional work needs to be conducted to fully understand this polyimide resin.



H.H. Gibbs & C.V. Breder Am. Chem. Soc. Prepr. 15(1), 775(1974)

H.H. Gibbs Sci. Adv. Mat'r & Proc. Eng. Series (SAMPE) 21, 592 (1976)

Figure 3

RESIN CHARACTERIZATION

One of the primary objectives of this program was to fingerprint or characterize the selected resin system. We have conducted numerous chemical tests of as-received resin, film and prepreg and have not been able to pinpoint a good or bad lot of material. We have resorted to fabricating a small laminate followed by C-scan and mechanical property testing. If the C-scan is good the mechanical properties will be good. Additional work is required in this area to develop more sensitive test methods or better quality control of the resin and the resulting prepreg material.

- Infrared
- Acid content of resin, film, or prepreg
- High pressure liquid chromatography (HPLC)
- Amine content of resin, film, and prepreg
- Volatile content
- Results
- All methods investigated have either shown no difference between a good and bad lot of material or results were so inconsistent that no credibility could be drawn because of material variation or the test methods used were not reliable
- Solution: Fabricate quality assurance laminate using optimized process and conduct nondestructive testing and mechanical property testing

Figure 4

PROCESS DEVELOPMENT

Early in the program the NR150B2-S5X resin solution was selected over the NR150B-2 solution because of the potential of an ortho diester forming when ethyl alcohol is present as a solvent. The presence of the ortho ester would change processing techniques significantly. Previous studies at Convair, as well as elsewhere, have shown that certain graphite fibers oxidize at high temperatures and are unsuitable for long term high temperature applications. We conducted a study on fiber stability and selected Modmor II with Celion 6000 as a second choice. When Modmor went out of business Celion 6000 was selected for the program. We used dielectric monitoring for establishing our precompaction, cure and postcure studies. We determined that a high temperature postcure was required which required the development of special metallic bagging techniques and bulk graphite tooling concepts.

- Selected NR150B2-S5X over NR150B-2 resin matrix
NR150B2-S5X has only NMP solvent
NR150B-2 has 2/3 NMP and 1/3 ethanol
- Originally selected Modmor-II graphite fiber but later changed to C-6000 graphite fiber with NR150B-2 finish
- Used dielectric monitoring to establish cure and postcure cycles
- Established precompaction, cure, and postcure cycles for both NR150B2-S5X and NR150B-2 resin solutions
- Established tooling and high temperature bagging concepts

Figure 5

PRELIMINARY GRAPHITE/POLYIMIDE C-6000/NR150B2-S5X
PREPREG SPECIFICATION

The preliminary material specification shown is the one that Convair currently uses to buy all of their NR150B2-S5X graphite/polyimide prepreg for the CASTS Project and others. This preliminary specification has been accepted and quoted to by two material suppliers, Fiberite and U. S. Polymeric. At the completion of this program, a much more detailed specification will be written including processing requirements and minimum mechanical properties requirements.

- Celion 6000 fiber strength 2,748 MN/m² (400 ksi) minimum
- Celion 6000 fiber modulus 2,198 X 10³ MN/m² (32 X 10³ ksi) minimum
- NR150B-2 sizing on Celion 6000 fiber
- .0127 cm/ply (5 ± 0.3 mils/ply) cured thickness
- Areal weight of prepreg 145 ± 10 gms/m²
- Resin content 32 ± 2% by weight
- Maximum volatiles 14% by weight at 204 C (400 F)
- Percent flow at 177 C (350 F) 10 to 20%
- Drape — bend around 0.318 cm (0.125 in.) diameter mandrel without fiber separation
- General good quality workmanship

Figure 6

PRECOMPACTION BAGGING SEQUENCE FOR NR150B2-S5X

Standard materials for debulking or precompaction such as glass cloth, cork dams and teflon coated glass are used. The one unique difference is that a layer of Celgard 4500 is placed between the bleeder and the breather. This material allows volatiles through, but no resin. Upon completion of the precompaction cycle, little if any further resin bleed occurs during the subsequent cure and postcure cycles.

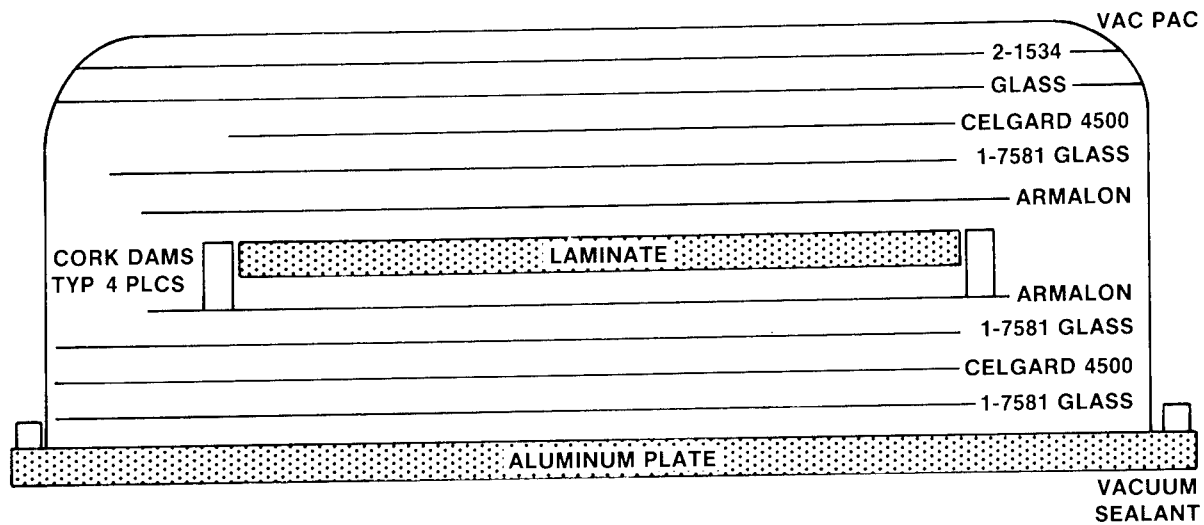


Figure 7

PRECOMPACTION CYCLE FOR NR150B2-S5X

The precompaction cycle is conducted under vacuum bag pressure and can be heated either in an oven or an autoclave. The prepreg material to be precompacted is heated to approximately 135C (275F) at a rate of 2C (3F) per minute. It is held at 135C (275F) for ninety minutes and then cooled to 66C (150F) at a rate of 2C (3F) per minute. The purpose of the precompaction cycle is to debulk the prepreg and remove 7 to 9% of the volatile solvent.

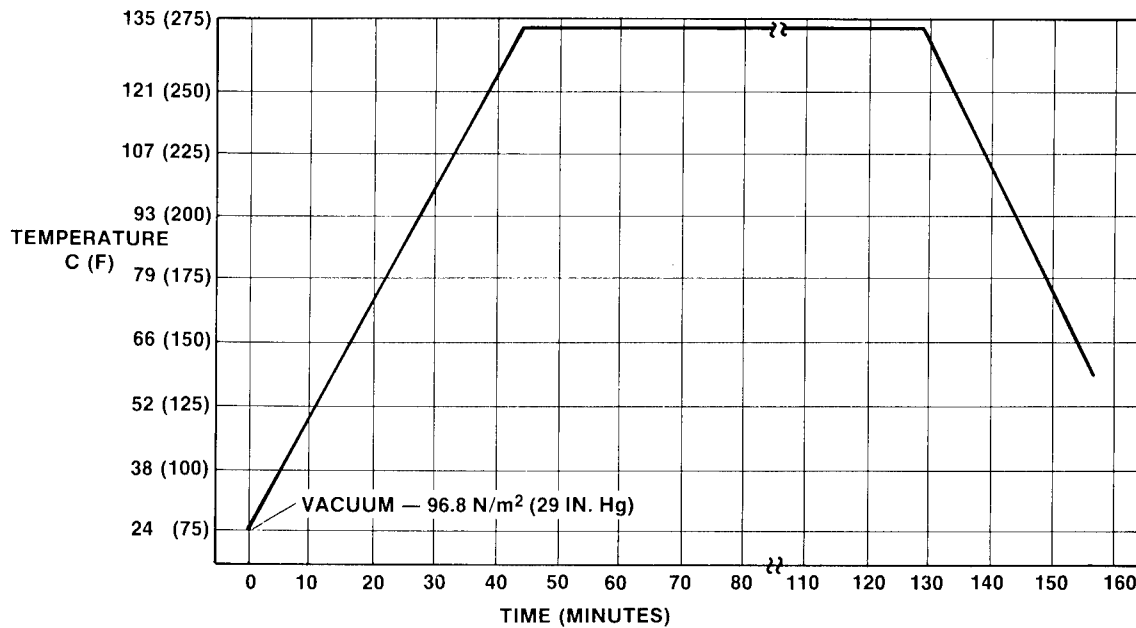


Figure 8

CURE BAGGING SEQUENCE FOR NR150B2-S5X

Normal bagging procedures are used with the exception of a double vacuum bag seal and the bagging material is VAC-ALLOY instead of nylon film. An inner silicone seal A-800 is required because the cure temperature reaches 203C (400F) and the normal sealing material, zinc chromate, will not withstand this temperature for the length of the cure. On the other hand, the silicone sealing material is not flexible enough to seal at lower temperatures thus requiring both sealing materials.

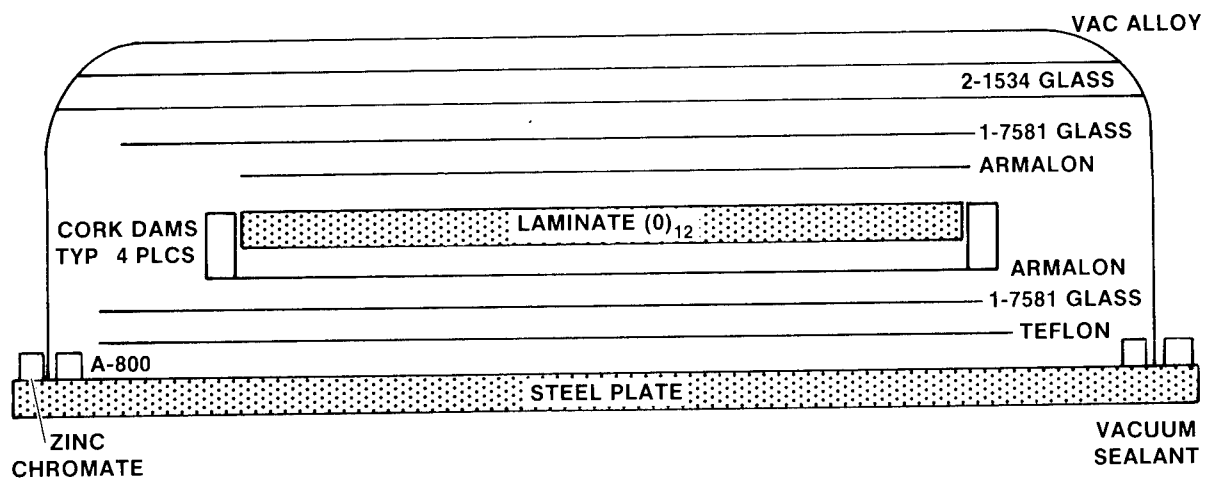


Figure 9

CURE CYCLE FOR NR150B2-S5X

Vacuum pressure is applied at room temperature and the part is heated to 149C (300F) at a rate of 2.5C (4.5F) per minute. At 149C (300F) 1379 kn/m^2 (200 psig) pressure is applied. A dwell time of 25 minutes has been inserted into the cure cycle thus allowing plenty of time for the pressure to be applied in the autoclave. The part is then heated to a final cure temperature of 204C (400F) and held there for two hours and cooled under pressure to 66C (150F).

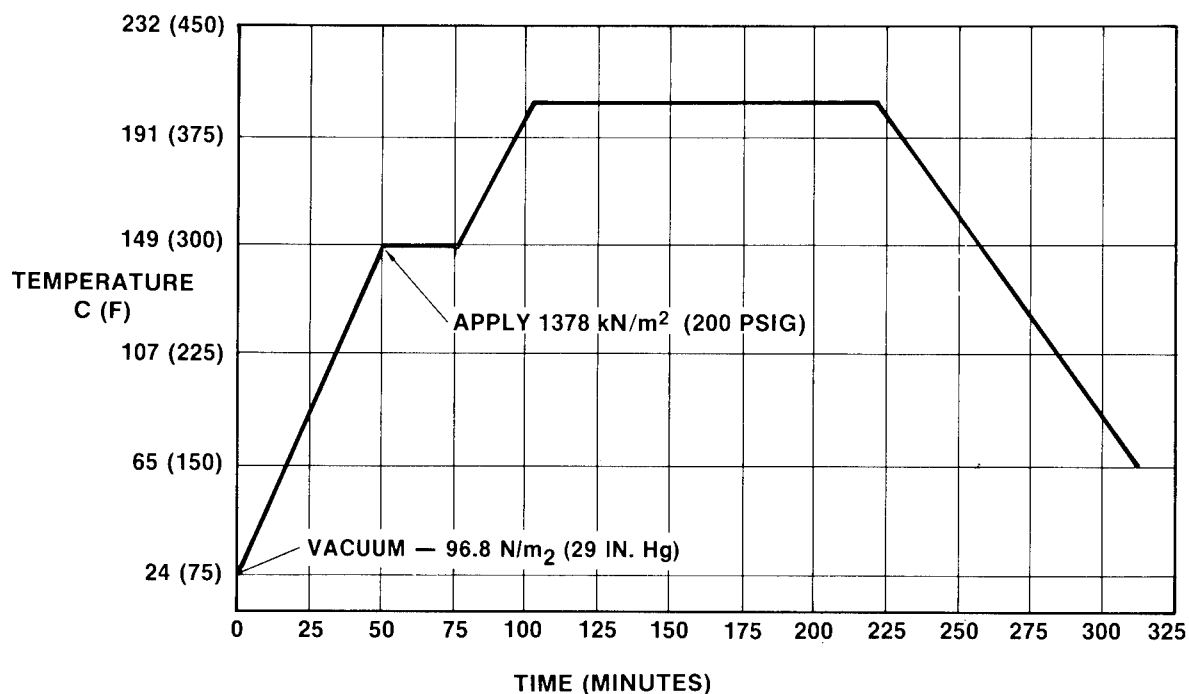


Figure 10

POSTCURE BAGGING SEQUENCE FOR NR150B2-S5X

The bagging procedures used for the postcure are identical to the cure bagging sequence. In the fabrication of flat laminates we do change bleeder and vacuum bags, but its really not necessary in that no bleeding of the resin occurs during the cure cycle. In the fabrication of actual detail parts the cure and postcure cycle will be combined into a single cycle. Also, the bleeder on the tool side of the part may not be necessary since we get no further bleeding during the cure or postcure cycle.

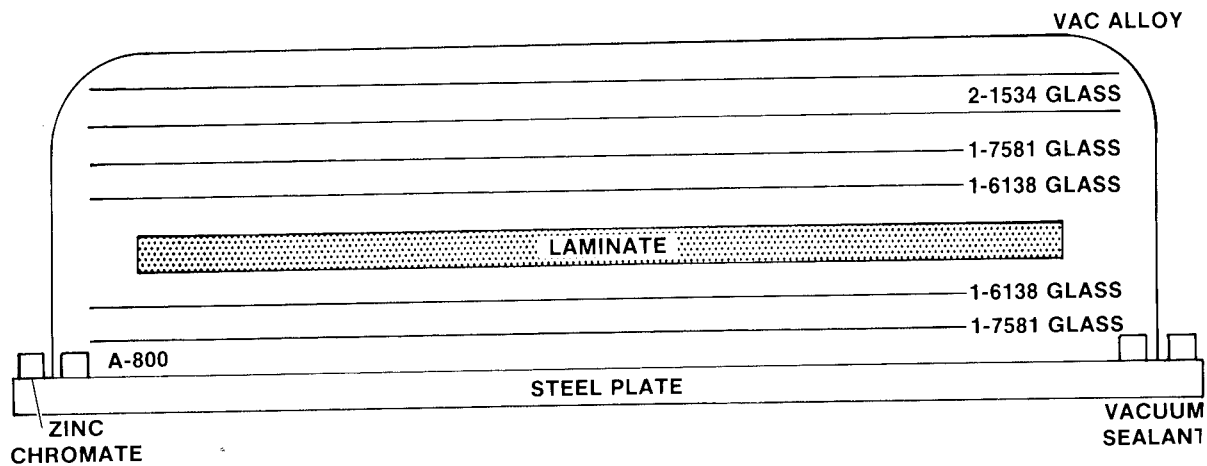


Figure 11

POSTCURE CYCLE FOR NR150B2-S5X

Vacuum pressure 96.8 N/m^2 (29 in. Hg) and 1378 kN/m^2 (200 psig) is applied at room temperature and the part is heated at 3°C (6°F) per minute to 191°C (375°F). From 191°C (375°F) to 302°C (575°F) the part is heated at 0.6°C (1°F) per minute. From 302°C (575°F) to the final postcure temperature of 399°C (750°F) the heat-up rate is 0.3°C (0.5°F) per minute. The reason for the slow heat-up rates from 191°C (375°F) is that the laminate is extremely dense but still has about 2% volatiles remaining. The volatiles actually have to diffuse through the resin. If the heat-up rate is too fast the part will delaminate and have to be scrapped.

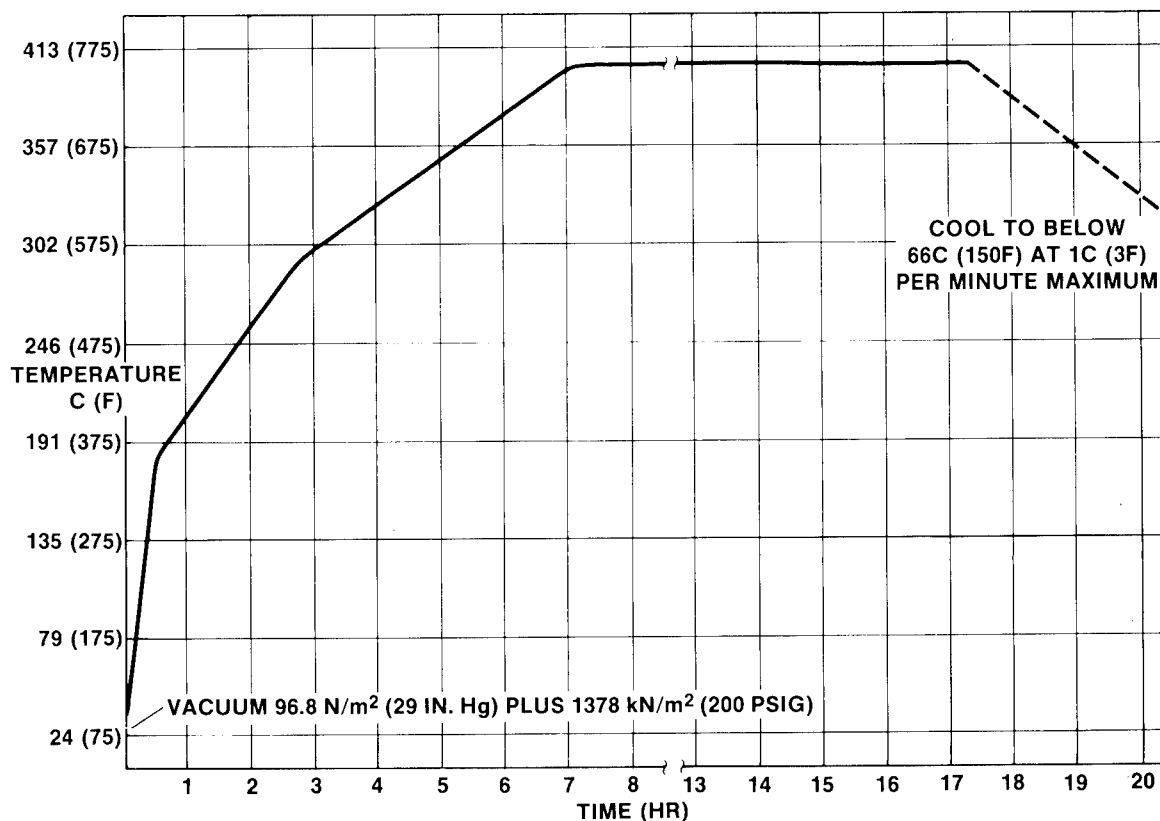


Figure 12

ULTRASONIC C-SCANS FOR LAMINATE C-176

The laminate shown here is a 30 mm (12 in.) by 30 mm (12 in.) 12 ply unidirectional NR150B2-S5X laminate. We have selected 5MHz as the frequency that Convair inspects all polyimide parts. This was done after evaluating many different frequencies and gains. Panel 176 is considered an excellent part with a very low void content. The little white spots are air bubbles on the surface of the panel.

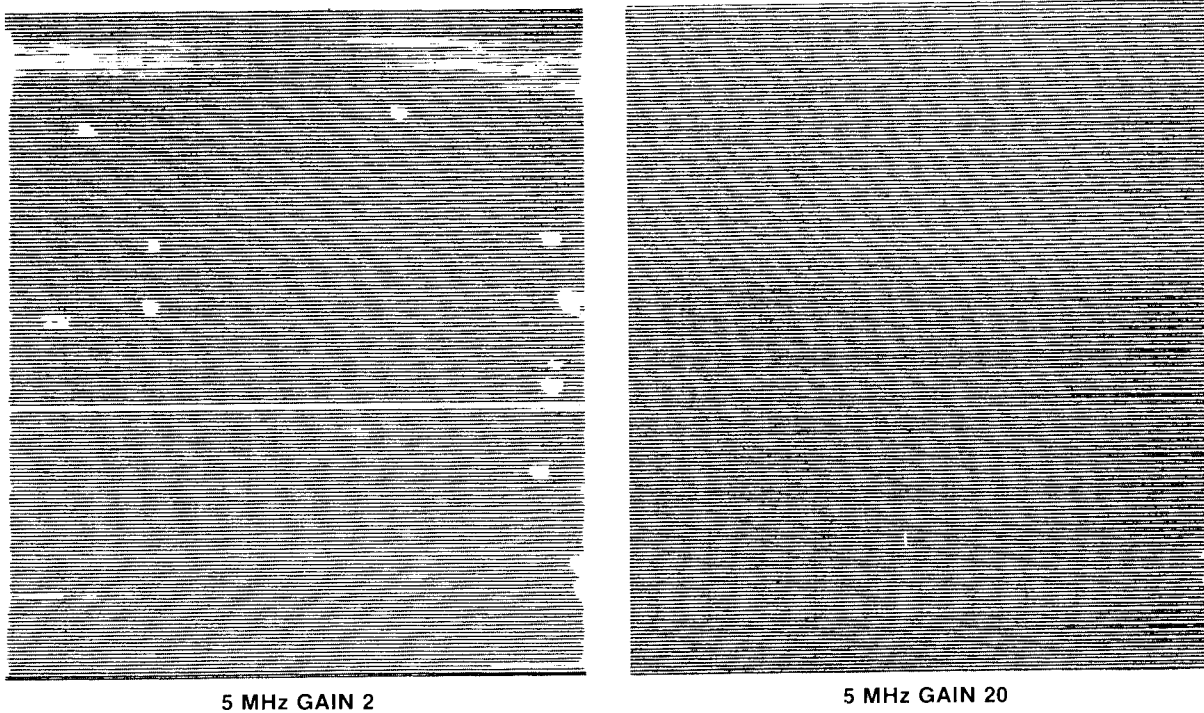


Figure 13

C-6000/NR150B2-S5X LAMINATE PROPERTIES-EPOXY SIZING

Convair has evaluated both the epoxy and polyimide sizing on Celeon 6000 fiber. The epoxy sizing in this limited study appears to give the higher flexural properties initially at 316C (600F). Tests are scheduled in the near future to determine if the finish on the fiber has an effect on the long term aging of the composite at elevated temperatures. The test data presented here represents material from three different lots of material.

		Laminates				
		<u>C-176</u>	<u>C-193B</u>	<u>C-200A</u>	<u>C-193C*</u>	<u>C-200B*</u>
Flexural strength	24C (75F)	2,205 (321)	1,880 (273)	1,905 (276)	1,632 (237)	1,940 (281)
MN/m ² (ksi)	316C (600F)	1,424 (207)	1,345 (195)	1,412 (205)	1,385 (201)	1,545 (224)
Specific gravity		1.62	1.63	1.64	1.63	1.64
Fiber volume %		70.0	68.6	69	68.6	69
Resin content %		23.6	25.9	25.4	25.9	25.4
Void content %		<1	<1	<1	<1	<1

*Tested by NASA-LRC

Figure 14

C-6000/NR150B2-S5X LAMINATE PROPERTIES
POLYIMIDE SIZING

The important fact about the data presented in this table is the somewhat higher fiber volume than is usually found in epoxy composites. However, even with this higher fiber volume the interlaminar shear strength is still acceptable. The effects of voids is readily seen by comparing laminate C-233 against any other laminate test data presented in this table. The laminates were made from 3 different lots of material from two different suppliers.

		Laminates			
		<u>C-228</u>	<u>C-233</u>	<u>C-239</u>	<u>C-503</u>
Flexural strength	24C (75F)	1,820 (264)	1,874 (272)	2,005 (291)	2,150 (312)
MN/m ² (ksi)	316C (600F)	1,240 (180)	1,137 (165)	1,247 (181)	1,474 (214)
Short beam shear	24C (75F)	—	88.8 (12.9)	82.6 (12.0)	84.0 (12.2)
Strength MN/m ² (ksi)	316C (600F)	—	36.5 (5.3)	41.3 (6.0)	55.0 (8.04)
Fiber volume	%	68.1	66.0	71.8	—
Resin content	%	24.9	25.3	21.9	—
Void content	%	2.6	<6	<2	—
Specific gravity		1.59	1.59	1.61	—

Figure 15

C-6000/NR150B-2 LAMINATE PROPERTIES

The NR150B-2 laminates were cured using the same cure cycle used for the NR150B2-S5X laminates. The flexural strengths at 316C (600F) are as much as 25% lower for the NR150B-2 composites compared to the NR150B2-S5X composites. This can be attributed to perhaps a non-optimized cure cycle for the NR150B-2 system and a lower fiber volume when compared to the NR150B2-S5X system.

		Laminates					
		<u>C-175</u>	<u>C-178</u>	<u>C-196</u>	<u>C-199</u>	<u>C-216</u>	<u>C-217</u>
Flexural strength	24C (75F)	1,910 (278)	1,755 (255)	1,722 (250)	1,690 (245)	1,960 (284)	1,855 (269)
MN/m ² (ksi)	316C (600F)	1,030 (150)	1,020 (148)	1,096 (159)	1,020 (148)	1,248 (181)	1,096 (159)
Short beam shear	24C (75F)	—	—	86 (12.4)	82 (11.9)	107 (15.5)	102 (14.8)
Strength MN/m ² (ksi)	316C (600F)	—	—	46 (6.6)	46 (6.6)	47 (6.8)	52 (7.5)
Specific gravity		1.63	1.66	1.61	1.59	1.62	1.64
Fiber volume %		61.2	—	67.3	64.9	65.1	63.3
Resin content %		32.6	—	27.1	28.7	29.0	30.6
Void content %		<1	—	<1	<1	<1	<1
Fiber finish		Epoxy	Polyimide	Epoxy	Polyimide	Epoxy	Polyimide

Figure 16

HEAT AGING TEST RESULTS FOR C-6000/NR150B2-S5X UNIDIRECTIONAL LAMINATES

Specimens from 3 different laminates were heat-aged at 316C (600F) in an air circulating oven for periods up to 1000 hours. All laminates were fabricated using the standard cure and postcure cycles and with prepreg that had fibers with a polyimide finish. There were no significant effects on strength through 500 hours of aging at 316C (600F). From 500 to 1000 hours a straight line has been drawn between test data points. If more specimens had been available, additional test points between 500 and 1000 hours could have been obtained and the drop-off in strength could have been more accurately determined.

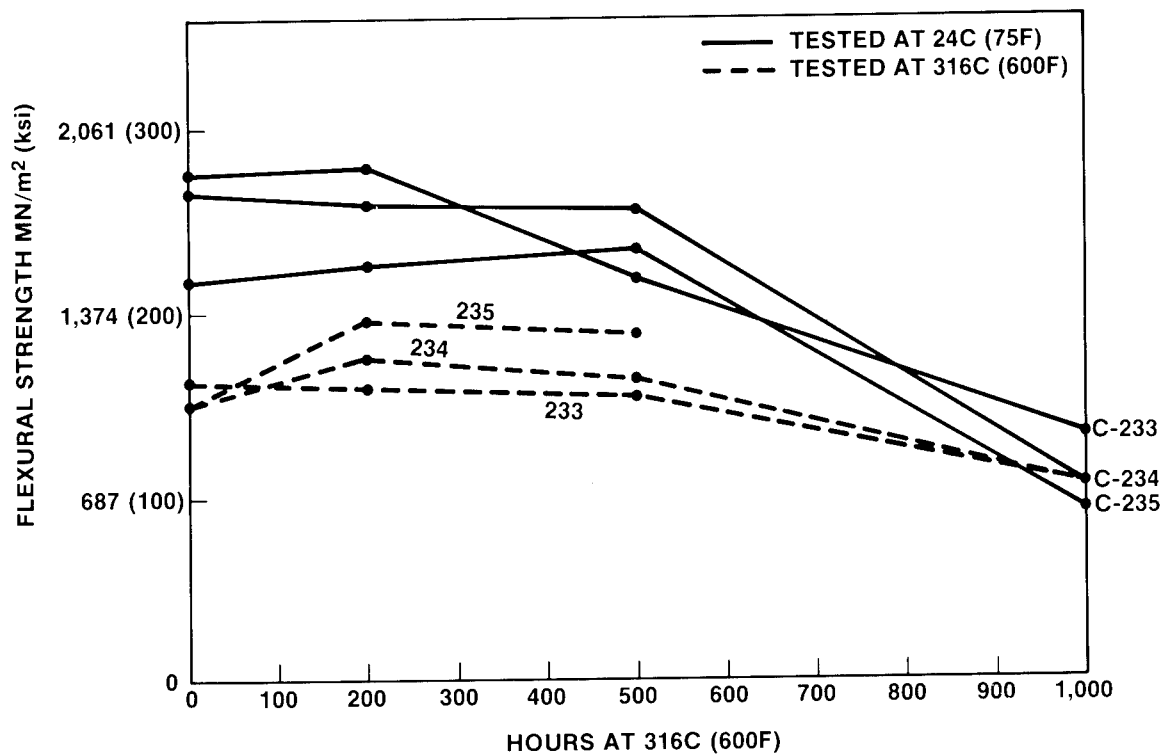


Figure 17

BULK GRAPHITE TOOL

General Dynamics, Convair, has selected bulk graphite as the baseline tooling material. It has a thermal expansion similar to that of the composite thus ensuring dimensional control. It is lighter and less costly than its steel counterpart and has excellent thermal transfer properties. This concept has been proven to be cost effective and acceptable from a tooling viewpoint on a number of programs.

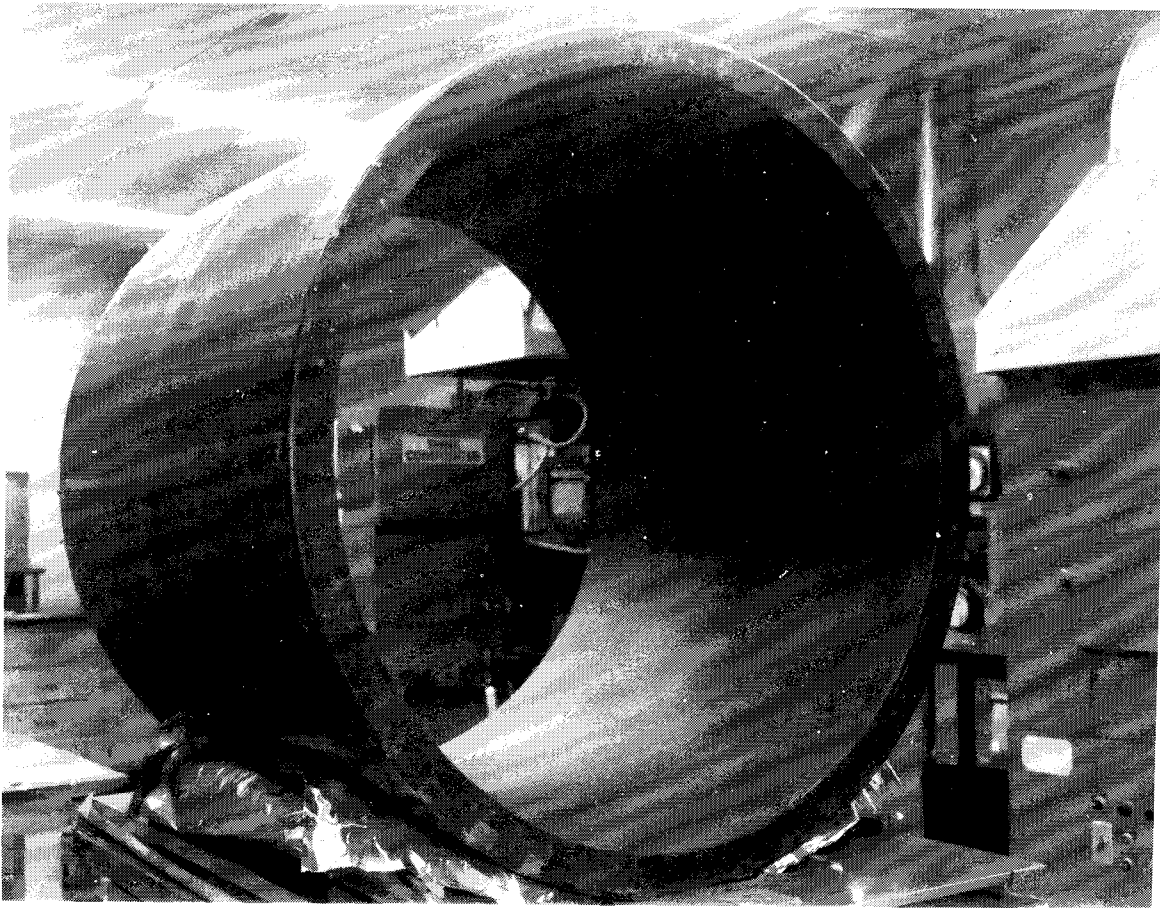


Figure 18

PROPOSED AFT BODY FLAP COMPONENT

The proposed component is a simulated section of the aft body flap and is approximately 121.9 cm (48 in.) by 106.7 cm (42 in.) with a depth which varies from 30.5 cm (12 in.) to 10.2 cm (4 in.). The component is a slight modification of a component to be built by Rockwell out of the LARC-160 polyimide system. The demonstration part involves all of the technology previously developed in separate tasks throughout the program.

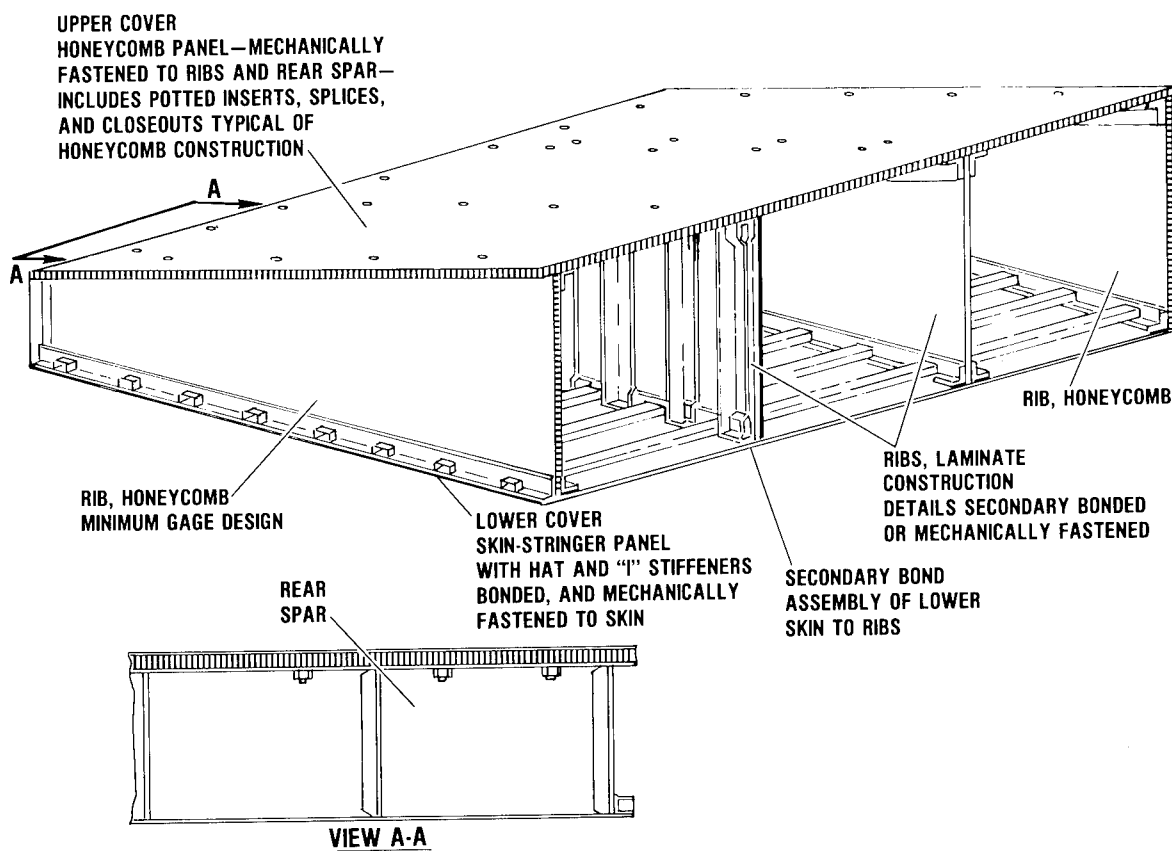


Figure 19

C-6000/NR150B2-S5X FABRICATION STATUS

This viewgraph presents the current status of the program as of February 1979. The basic processing has been developed, preliminary NDT and prepreg specifications have been written, and outstanding mechanical properties at both room and 316C (600F) have been generated. In the near future large panels, hats, and I-beams will be fabricated and tested.

- o DEVELOPED CURE AND POSTCURE CYCLES FOR BOTH NR150B2 AND NR150B2-S5X
- o DEVELOPED NDT STANDARDS
- o ESTABLISHED PREPREG PARAMETERS
- o ESTABLISHED TOOLING CONCEPTS
- o DEMONSTRATED SUPERIOR MECHANICAL AND AGING PROPERTIES
- o PRESENTLY FABRICATING LARGE PANELS, HATS, AND I-BEAMS
- o NEED ANALYTICAL METHOD FOR INDUSTRY WIDE QUALITY ASSURANCE OF RESIN/PREPREG

Figure 20

DEVELOPMENT AND DEMONSTRATION OF MANUFACTURING PROCESSES FOR FABRICATING
GRAPHITE/PMR-15 POLYIMIDE STRUCTURAL ELEMENTS

C. H. Sheppard, J. T. Hoggatt, and W. A. Symonds
Boeing Aerospace

EXPANDED ABSTRACT

Under NASA Contract NAS1-15009, Boeing initiated a study to develop and demonstrate the processing requirements for graphite/PMR-15 polyimide composites. The goal of the program was to demonstrate the structural integrity of polyimide composite structural elements at temperatures up to 589K (600°F). The program consisted of 8 major tasks: quality assurance development, materials and process development, specification verification, flat panel fabrication, stiffened panel fabrication, honeycomb panel fabrication, chopped fiber moldings, and demonstration component fabrication. All phases of the program were successfully completed and the technology demonstrated by delivering to NASA Langley Research Center a 762mm (30 in) segment of the Space Shuttle aft body flap.

Materials, processing and quality assurance documents were prepared from experimentally derived data. Structural elements consisting of flat panels, corrugated stiffeners, I-beams, hat stiffeners, honeycomb panels, and chopped fiber moldings were made and tested. Property data from 219K (-65°F) to 589K (600°F) were obtained. All elements were made in a production environment. The size of each element was sufficient to insure production capability and structural component applicability. Problems associated with adhesive bonding, laminate and structural element analysis, material variability, and test methods were addressed.

The program demonstrated that graphite/PMR-15 polyimide composites are suitable for structural application at 589K (600°F).

OBJECTIVES

The program objective was to demonstrate that commercially available graphite/PMR-15 prepreg could be manufactured into useful structural hardware using a low-pressure [1.4 MPa (200 psi)] autoclave process.(Figure 1) During the course of the program, the commercially available graphite/PMR-15 was found to vary between lots of material. An additional effort was then started to determine the reasons for this material variability and in turn develop a manufacturing process and accept/reject criteria for the prepreg system. The program was originally divided into eight tasks (A thru H) with a ninth task (J) being added. Following is a description of the work performed during the program by task.

ORIGINAL PROGRAM

- **DEVELOP PROCESSES & Q. A. CONTROLS FOR FABRICATION OF GRAPHITE/PMR-15 STRUCTURES**
- **DEMONSTRATE PROCESSES AND CONTROLS THROUGH FABRICATION OF MAJOR COMPOSITE STRUCTURAL ELEMENTS**

VARIABILITY PROGRAM

- **DEVELOP MANUFACTURING PROCESS FOR STABLE PMR-15 RESIN**
- **DEVELOP ACCEPT/REJECT CRITERIA FOR PREPREG SYSTEM**

Figure 1

NAS1-15009 GRAPHITE/PMR-15

PHASE 1

The original program objectives were divided into two separate phases: (1) development of material and process specifications and Q. A. controls for the fabrication of the graphite/PMR-15 structures, and (2) demonstration of the adequacy of those processes and controls thru fabrication of major composite structural elements. The three tasks addressed in Phase 1 are shown in Figure 2.

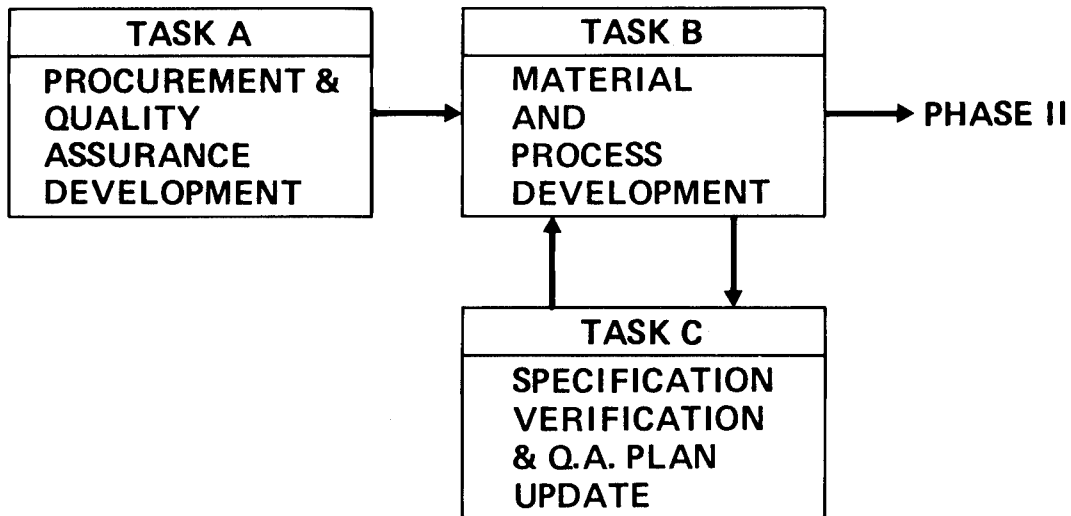


Figure 2

TASK A - PROCUREMENT & QUALITY ASSURANCE DEVELOPMENT

The objective of this task was to obtain and document quality assurance criteria for the graphite/PMR-15 prepreg. This included the accept/reject criteria for raw materials, processes for evaluating prepreg, and processes for final composite elements. The results of this effort were four documents (i. e., Material Specification, Process Specification, Quality Assurance Document, and NDI Test Plan). Also included in this effort was obtaining chemical data on numerous lots of graphite/PMR-15 prepreg. (Figure 3)

OBJECTIVE: PROVIDE QUALITY ASSURANCE CRITERIA FOR RAW MATERIALS, PROCESSES, AND FINAL COMPOSITE ELEMENTS AND DOCUMENT THE FINDINGS

RESULTS:

- **MATERIAL SPECIFICATION PREPARED (REVISION FORTHCOMING)**
- **PROCESS SPECIFICATION PREPARED (REVISION POSSIBLE)**
- **NDI SPECIFICATION PREPARED**
- **QUALITY ASSURANCE DOCUMENT PREPARED**
- **ALL SPECIFICATIONS VERIFIED IN PRODUCTION SHOPS**
- **NDI CRITERIA SUBSTANTIATED WITH NASA STANDARDS AND VERIFIED WITH PROPERTY DATA**

Figure 3

TASK B - MATERIAL PROCESS & SPECIFICATION DEVELOPMENT

The objective for this task was to develop autoclave processes for the fabrication of graphite/polyimide structural elements and to establish accept/reject criteria for their acceptance. During this effort, flat laminates of different dimensions and fiber orientations were fabricated and tested. Further work developed specific layup and fabrication techniques for various structural elements. Among the elements for which processes were developed are honeycomb sandwich panels and I-stiffener sections. (Figure 4)

**OBJECTIVE: TO DEVELOP PROCESSES FOR THE FABRICATION OF
POLYIMIDE/GRAPHITE STRUCTURAL ELEMENTS AND TO
ESTABLISH ACCEPT/REJECT CRITERIA FOR QUALITY
ASSURANCE**

**RESULTS: PROCESSES AND TOOLING REQUIREMENTS ESTABLISHED
FOR:**

- **LARGE-AREA FLAT MULTIDIRECTIONAL LAMINATES**
 - $t = .125''$
 - **UNIDIRECTIONAL**
 - ± 45
 - **PSEUDO-ISOTROPIC**
 - $[0 - 90]_s$
- **HONEYCOMB SANDWICH**
 - **COCURED**
 - **SECONDARILY BONDED**
 - **METALLIC CORE**
 - **NON-METALLIC CORE**
- **I-BEAM & STIFFENED PANELS**
 - **COCURED**
 - **SECONDARILY BONDED**

Figure 4

TASK B - MATERIAL PROCESS & SPECIFICATION DEVELOPMENT (CONTINUED)

In addition to the I-stiffened sections, hat-stiffened stringer panels were also fabricated. A processing document was prepared using the data obtained from this task. The results of this task could be summarized below. (Figure 5)

- o Selection of proper tooling.
- o Large-area laminates and sandwich and corrugated panel processes were developed and refined.
- o Cure and postcure cycles were evaluated.
- o Graphite fiber thermal stability assessed.
- o High temperature adhesives evaluated.

RESULTS: (CONTINUED)

- CORRUGATED PANELS (LARGE AREA)
 - COCURED
 - SECONDARILY BONDED
- HAT-STIFFNERS
- CHOPPED FIBER MOLDINGS
- MATERIAL VARIATIONS STUDIED
- CURE CYCLES/POST CURE CYCLES EVALUATED
- GRAPHITE REINFORCEMENT THERMAL STABILITY ASSESSED
- HIGH TEMPERATURE ADHESIVES ASSESSED
 - FM-34/BR-34
 - LARC-13
 - A7F

Figure 5

TASK C - PROCESS VERIFICATION

The objective of this task was to substantiate the structural integrity of the composite elements fabricated using the processes developed in Task B. All structural elements evaluated demonstrated satisfactory structural integrity and their properties are satisfactory for quality flight hardware. All structural elements were demonstrated on designs containing more plies than anticipated which permits maximum design flexibility. (Figure 6)

- **OBJECTIVE: TO SUBSTANTIATE STRUCTURAL INTEGRITY OF COMPOSITE ELEMENTS FABRICATED USING ESTABLISHED SPECIFICATIONS**
- **RESULTS:**
 - **ALL ELEMENTS EVALUATED DEMONSTRATED SATISFACTORY STRUCTURAL INTEGRITY AND PROPERTIES FOR FLIGHT QUALITY HARDWARE:**
 - **FLAT PANELS**
 - **I-BEAM STIFFENED PANELS**
 - **HAT-STIFFENED PANELS**
 - **CORRUGATED STIFFENED PANELS**
 - **CHOPPED FIBER MOLDINGS**
 - **HONEYCOMB PANELS**
 - **ALL STRUCTURAL ELEMENTS DEMONSTRATED WERE ON "HEAVY-WEIGHT" DESIGNS, PERMITTING MAXIMUM DESIGN FLEXIBILITY**

Figure 6

TASK C - SUMMARY MECHANICAL PROPERTY DATA GRAPHITE/PMR-15 FLAT LAMINATES

Among the elements evaluated were flat laminates with 0-degree fiber orientation. Figure 7 is a summary of the flexural and shear strength versus temperature and showing the effect of a 125 hr/589K (600°F) age.

At 589K (600°F) the flexure and short-beam shear strength were approximately 50% of their RT values. The modest increase in strength in flexure and shear after aging for 125 hrs at 589K (600°F) is probably due to a slight advancement of the PMR-15 resin after the aging cycle.

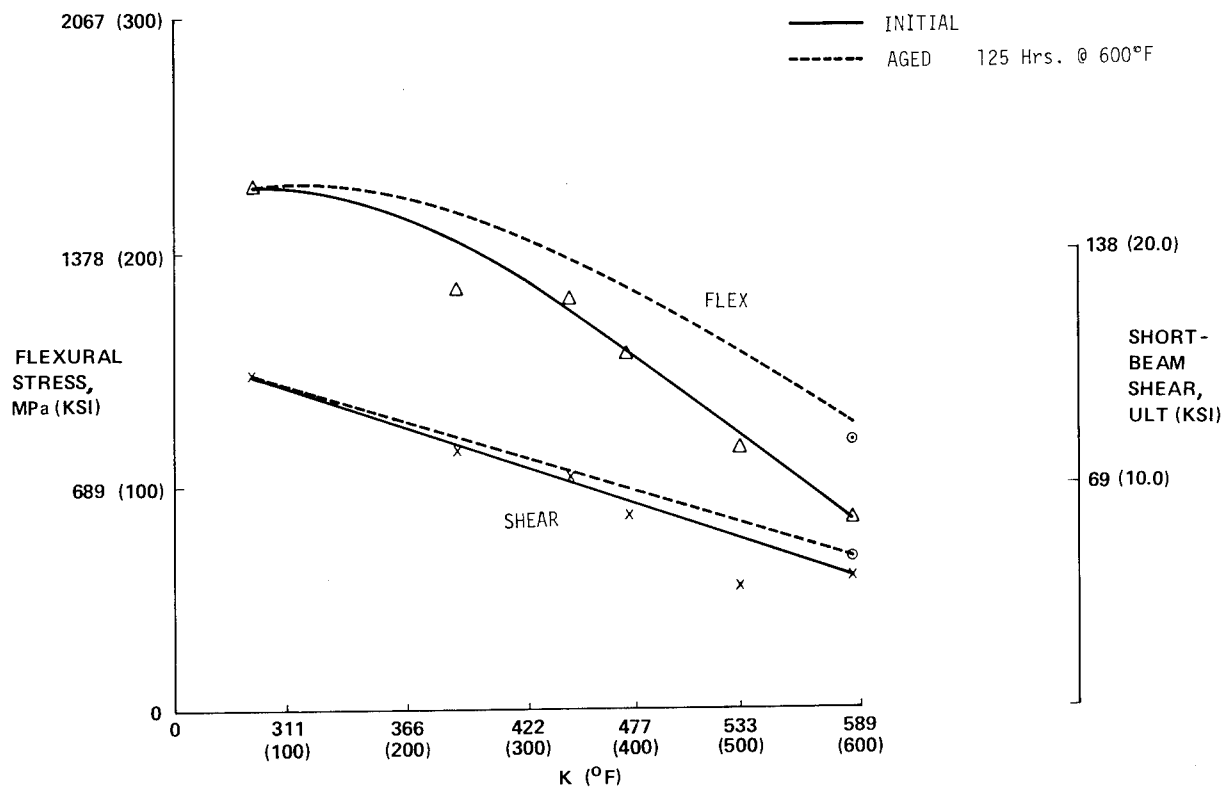


Figure 7

TASK C - SUMMARY PROPERTY DATA GRAPHITE/PMR-15 STRUCTURAL
FLAT LAMINATES

Tensile and compressive properties were obtained from flat laminates at RT and 589K (600°F). The tensile strength and modulus at 589K (600°F) were approximately 20% lower than at RT, and the compressive strength and modulus were about 50% lower over the same temperature range. (Figure 8).

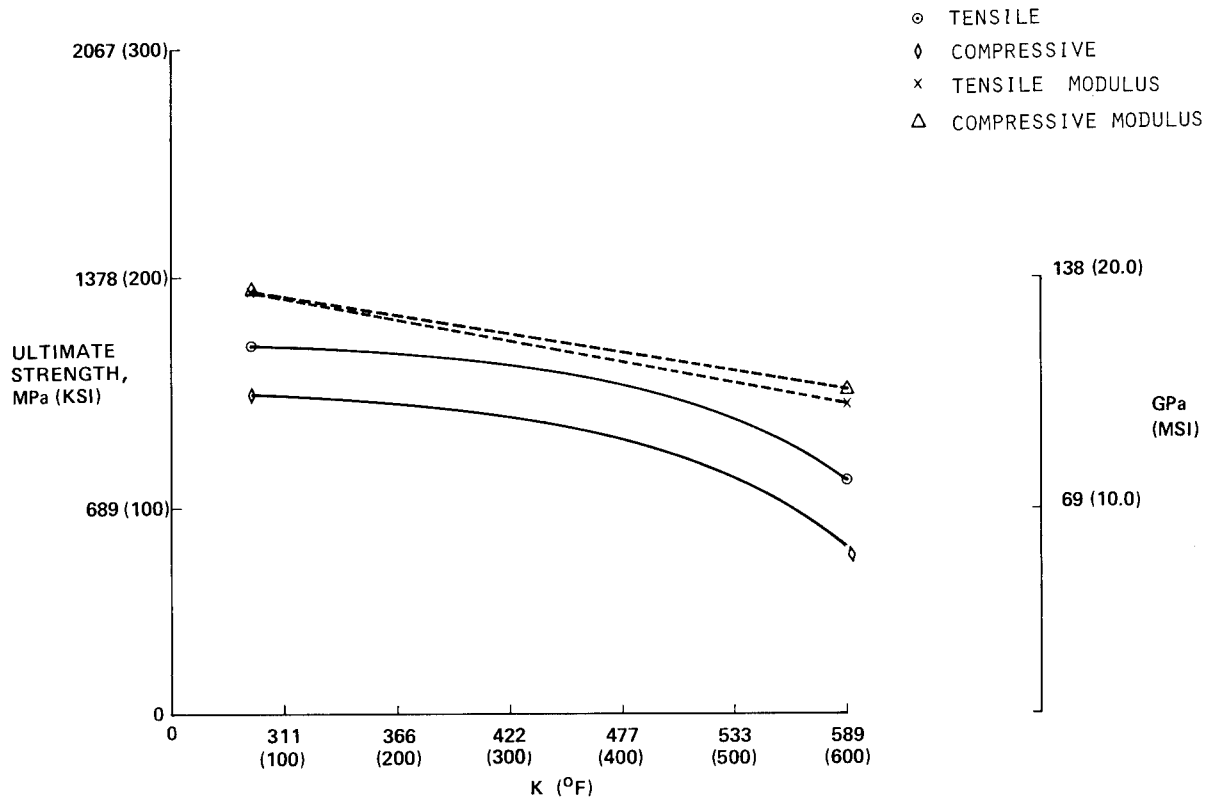


Figure 8

TASK C - HONEYCOMB PANELS

Secondary bonded honeycomb sandwich panels using 12 ply \pm 45 orientation skins, HRH 327 polyimide fiberglass honeycomb core, and two adhesive systems were evaluated at RT and 589K (600°F). The A7F adhesive system demonstrated somewhat lower flatwise tensile strengths at RT and 589K (600°F) than that obtained for FM-34 in this application. However, FM-34 has limited application because of the problem of removing condensation products from large-area bonds.

	A7F	FM 34
● FLATWISE TENSILE MPa (PSI)		
AMBIENT	3.02 (439)	3.48 (505)
589K (600°F)	1.38 (200)	2.82 (410)
589K (600°F) AGED	1.01 (146)	—
● EDGEWISE COMPRESSION MPa (KSI)		
AMBIENT	123 (17.9)	—
589K (600°F)	32 (4.7)	—
589K (600°F) AGED	66 (9.7)	—

Figure 9

TASK C - GRAPHITE/PMR-15 STIFFENED PANEL DATA

The final structural elements evaluated during this task were hat-stiffened flat panels and I-stiffeners. The data obtained was compressive buckling strength at two temperatures. (Figure 10) The buckling strength at 589K (600°F) was substantially reduced from the RT values for each panel design. After 125 hours of aging at 589K (600°F) the buckling strength at 589K (600°F) increased substantially which indicates that the panels were not fully post-cured.

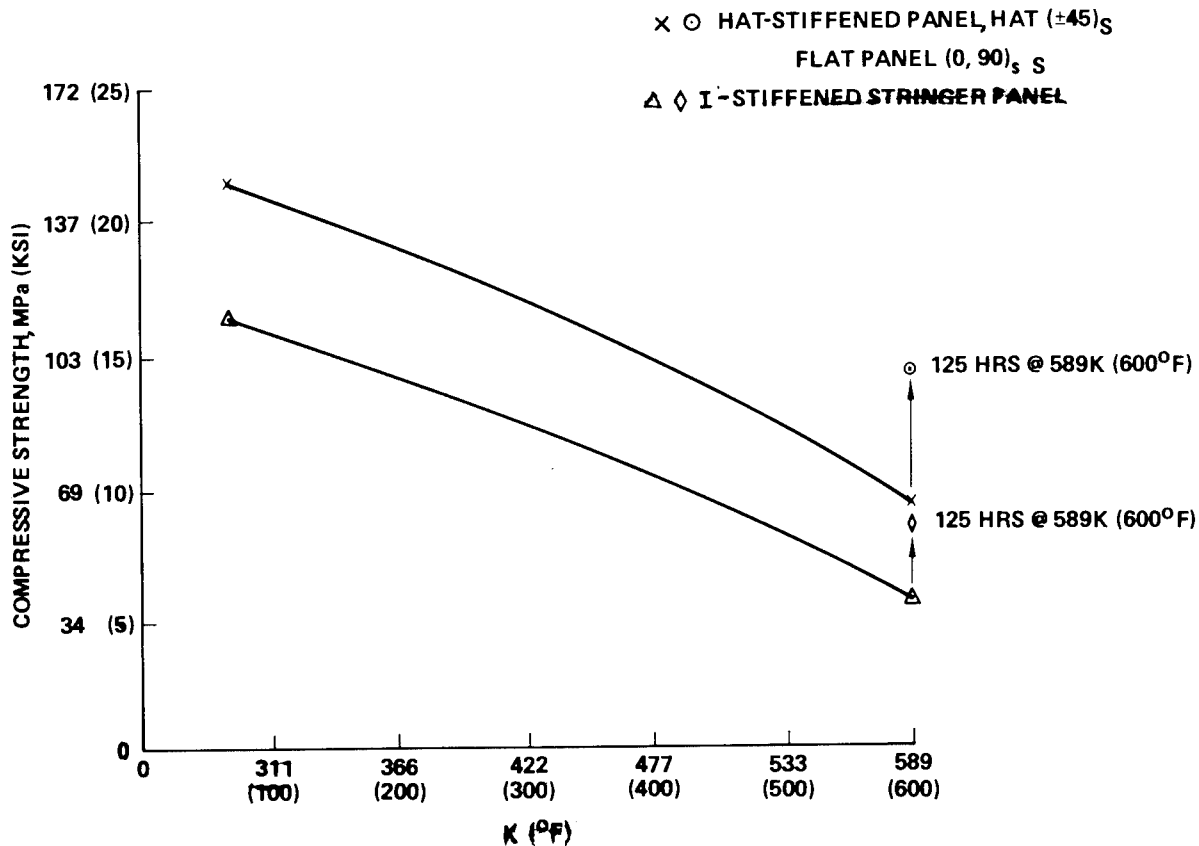


Figure 10

PHASE II

The final phase of the program was divided into five tasks. (Figure 11) The fabrication of different structural elements and a demonstration component was accomplished in these tasks. The structural elements fabricated included large-area flat panels, structural elements, sandwich panels and chopped fiber molded parts. The hardware fabrication was accomplished by tasks D-H and are described hereafter.

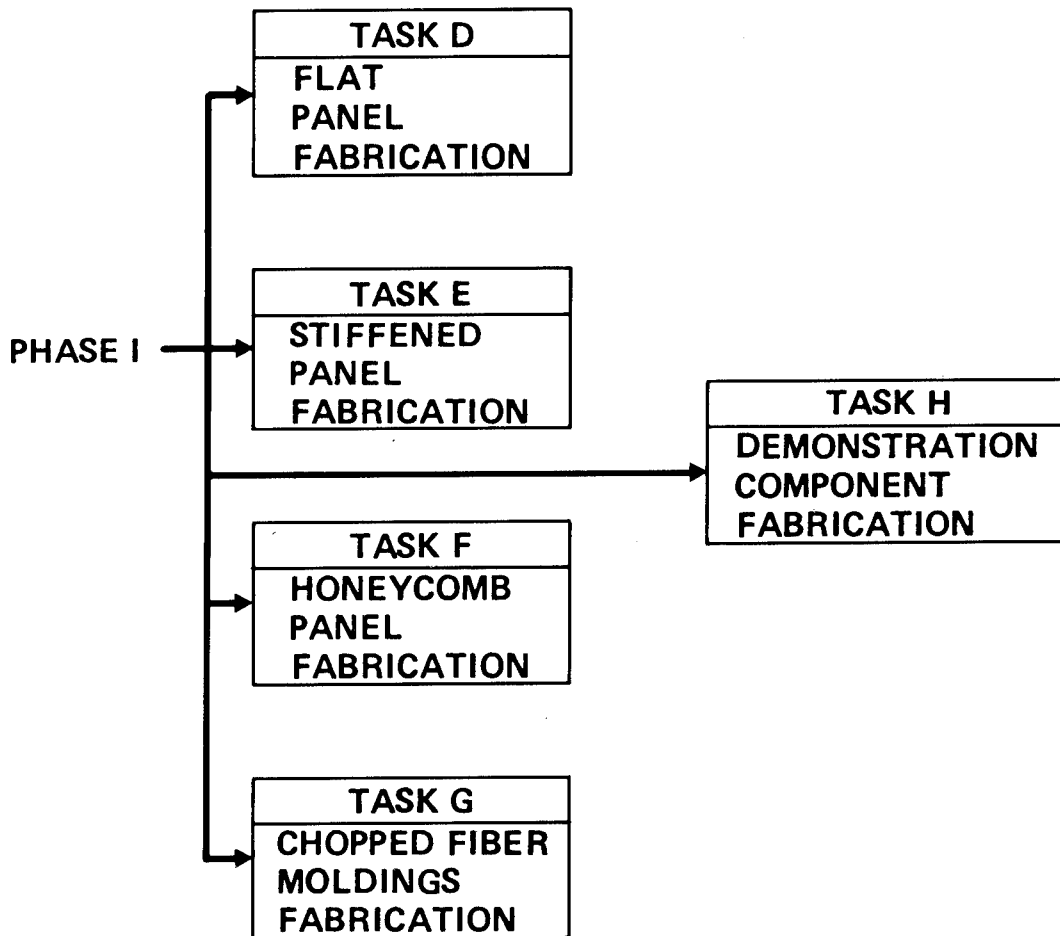


Figure 11

TASK D - FLAT PANEL FABRICATION

During this task, three flat panels 0.6m x 1.2m were fabricated, one at 0.76mm thick, one at 1.52mm, and the last at 3.2mm. (Figure 12) For convenience in the manufacture of the large fabrication demonstration articles, panels up to 1.2m x 2.4m were also fabricated.

- **PANEL SIZES: 2 FT x 4 FT**

- **PANEL ORIENTATIONS:**
 - 1) 6 PLY (0, +45, -45)_{2T}
 - 2) 12 PLY (0, +45, -45)_{4T}
 - 3) 24 PLY (0, +45, -45)_{8T}

- **COMMENTS: PANELS UP TO 4' x 8' SUCCESSFULLY FABRICATED**

Figure 12

TASK D - PHOTOGRAPH OF FLAT PANEL

During this task 0.6m (2 ft.) x 1.2m (4 ft.) panels were fabricated. The panel shown on Figure 13 is 12 plies thick in a $(0, +45, -45)_4T$ orientation.

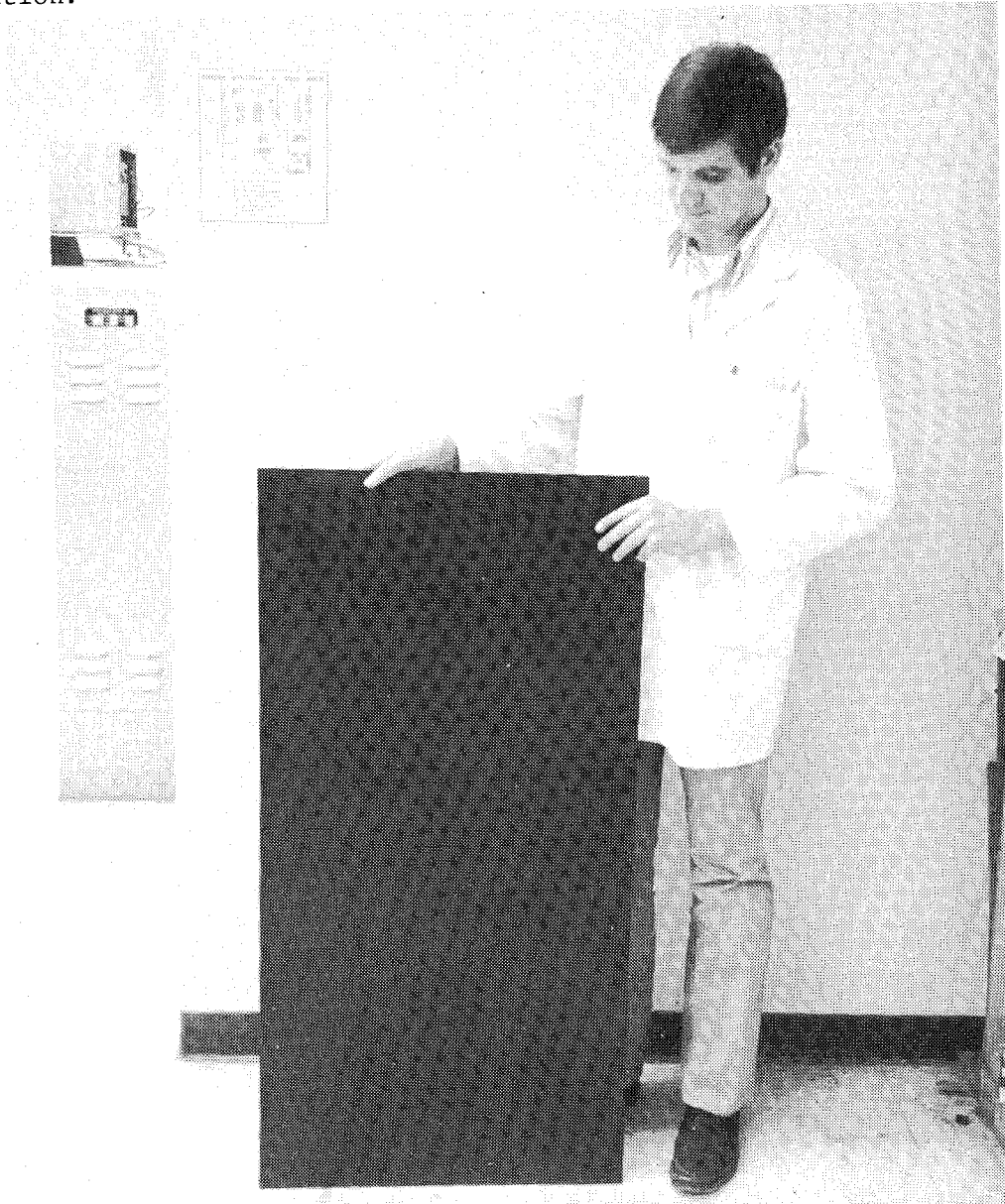


Figure 13

TASK E - STIFFENED PANEL FABRICATION

During this task, a total of 21 stringer panels were fabricated. Two different sizes were made: 18 of the panels were 229mm X 305mm and 3 were 254mm X 1270mm. The panel configurations are summarized below. (Figure 14)

- **PANEL SIZES: 18 STIFFENED PANELS**
 - 9 EA CORRUGATION-STIFFENED PANELS - 9 IN x 12 IN
 - 9 EA I-STIFFENED PANELS - 9 IN x 12 IN
 - 3 EA CORRUGATION-STIFFENED PANELS - 10 IN x 50 IN
- **PANEL CONFIGURATIONS:**

CORRUGATIONS	8 PLY (± 45) _{4T}	- 9 EA 9 IN x 12 IN
	24 PLY (0, ± 45 , 90) _{6T}	- 9 EA 9 IN x 12 IN
	8 PLY (± 45) _{4T}	- 3 EA 10 IN x 50 IN
	8 PLY (0, ± 45 , 90) _{2T}	- 3 EA 10 IN x 50 IN
I BEAMS	12 PLY (± 45) _{6T}	WEBBS
	12 PLY (0, 90) _{6T}	CAPS
	24 PLY (0, ± 45 , 90) _{6T}	FLAT PANELS
- **COMMENTS:**
 - PANELS COCURED AND SECONDARILY BONDED (FM 34 ADHESIVE), AND MECHANICALLY FASTENED
 - CORRUGATIONS UP TO 1' x 4' SUCCESSFULLY FABRICATED
 - I-BEAMS 3-FT LONG SUCCESSFULLY FABRICATED

Figure 14

TASK E - I-STIFFENED PANEL

An example of the I-stiffened stringer panel is in Figure 15.

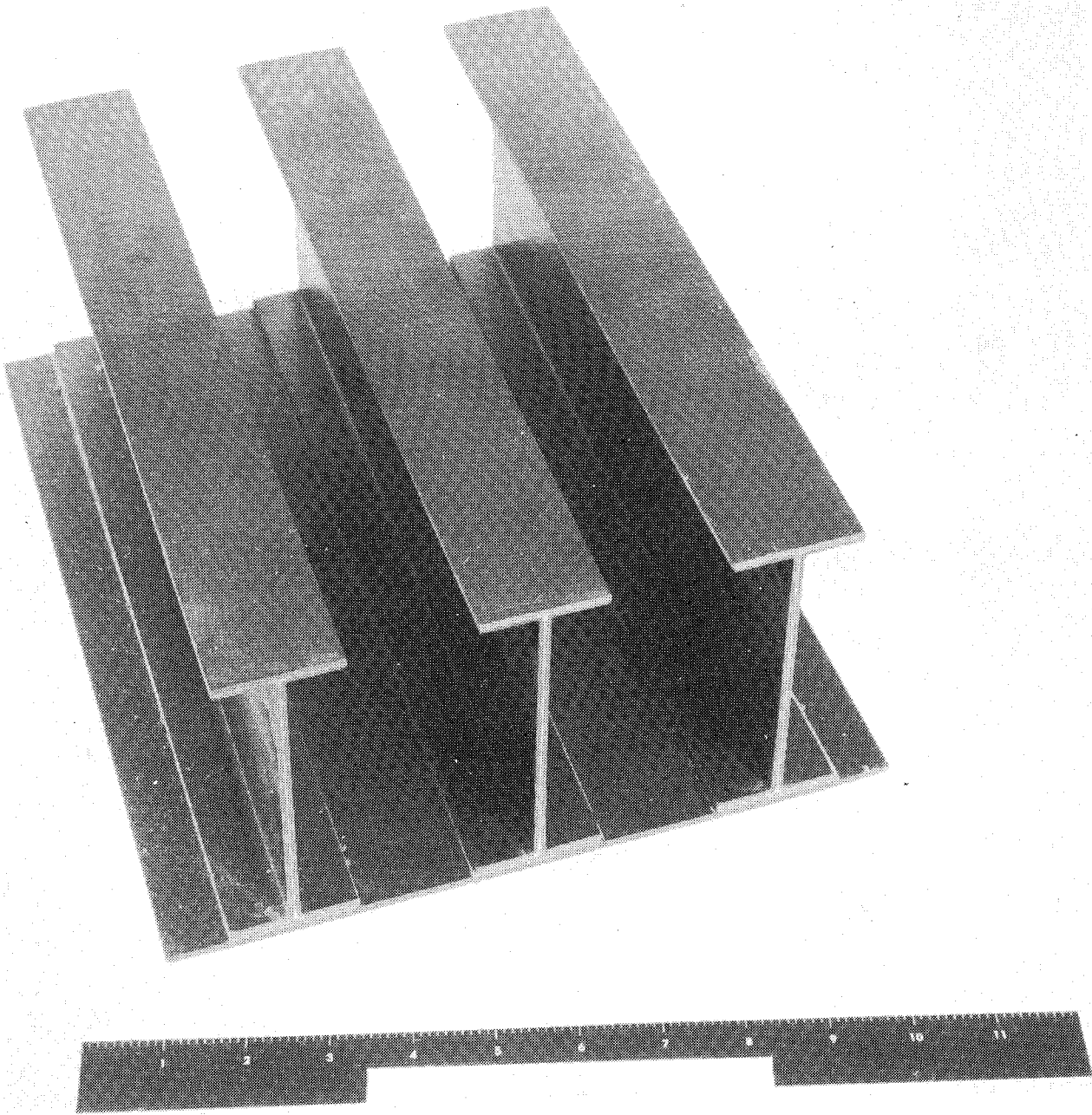


Figure 15

TASK E - HAT-STIFFENED PANEL

An example of the multiple hat-stiffened stringer panel is in Figure 16.

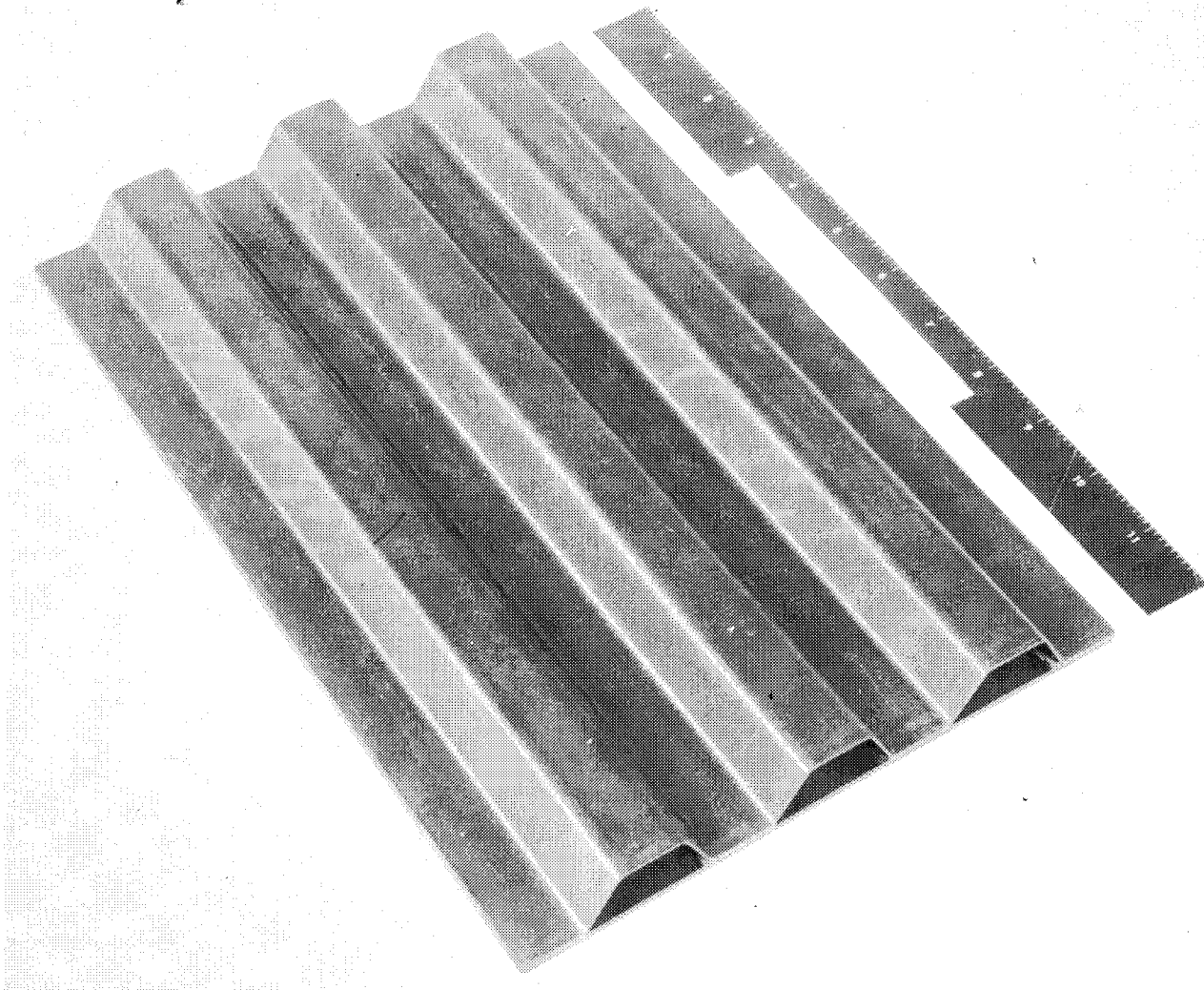


Figure 16

TASK E - LARGE-AREA HAT-STIFFENED PANEL

An example of the larger area multiple hat-stiffened stringer panel bonded with FM-34 adhesive is in Figure 17.

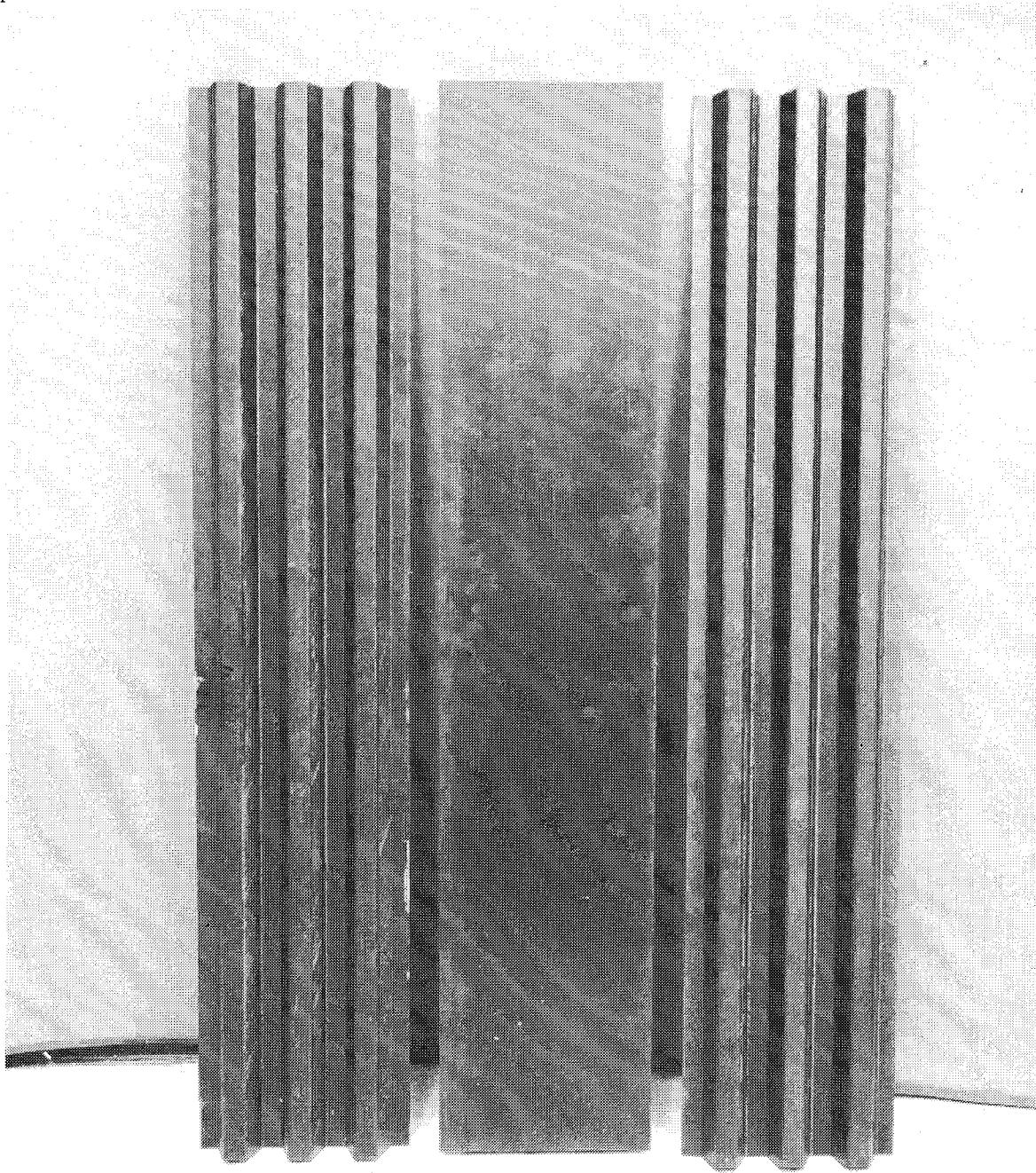


Figure 17

TASK F - HONEYCOMB PANEL

During this task, six graphite honeycomb sandwich panels were fabricated using the secondary bonding manufacturing process. The adhesive used was FM-34. Five of the six sandwiches were fabricated in one panel (i.e., 305mm X 1295mm) as a prelude to the demonstration component. The sixth sandwich was fabricated as a small sandwich (305mm X 305mm) the same as the Task C sandwich. (Figure 18)

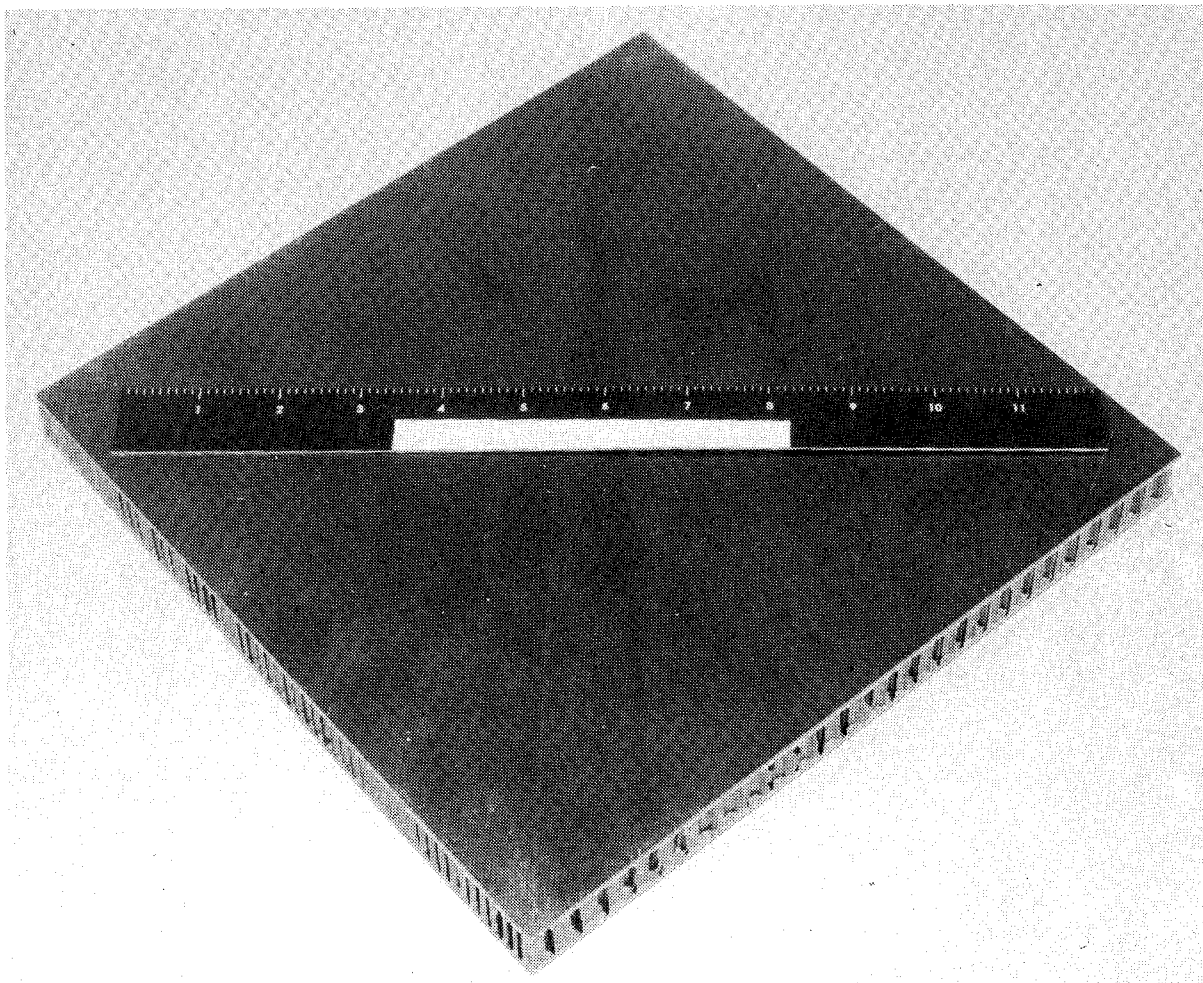


Figure 18

TASK G - CHOPPED FIBER MOLDED FITTINGS

During this task, six graphite molded parts were fabricated using a NASA designed mold and PMR-15 chopped graphite molding compound.
(Figure 19)

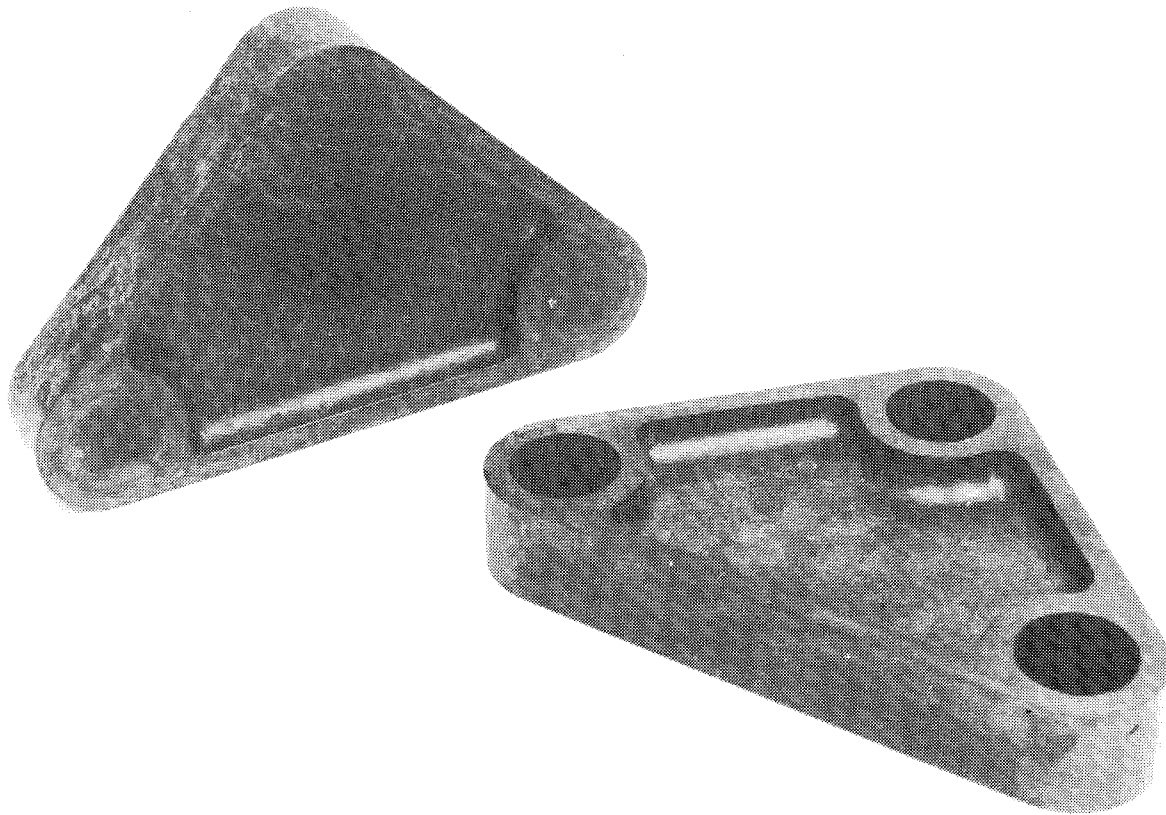


Figure 19

TASK H - DEMONSTRATION COMPONENT

During this task, a 762mm section of a simulated aft body flap was fabricated. The purpose of this component was to demonstrate the adaptability of the established processes for PMR-15 to large scale hardware fabrication and to assess high temperature assembly requirements. The component mass was approximately 36.4 kg (80 lbm). (Figure 20)

- **COMPONENT DESCRIPTION:** 30" SEGMENT REPRESENTING THE FULL SCALE AFT BODY FLAP OF THE SPACE SHUTTLE
- **PURPOSE:** TO DEMONSTRATE THE ADAPTABILITY OF THE ESTABLISHED PROCESSES FOR PMR-15 TO LARGE SCALE HARDWARE FABRICATION AND TO ASSESS HIGH TEMPERATURE ASSEMBLY REQUIREMENTS
- **COMPONENT MASS:** 80 LBM

Figure 20

TASK H - PHOTOGRAPH OF DEMONSTRATION COMPONENT

The large scale demonstration component is shown in Figure 21. Details of the hat-stiffened skins and the honeycomb-stiffened ribs can be seen in this view. This piece of hardware was fabricated to demonstrate that the manufacture of the different structural elements of Tasks D thru F could be adapted to large scale components. Following is a list of the technology utilized in the demonstration component.

1. Large-area bonding
2. Large-area flat laminates
3. Stiffened panel technology
4. Mechanical attachments
5. Honeycomb sandwich technology
6. Bonded attachments and clips

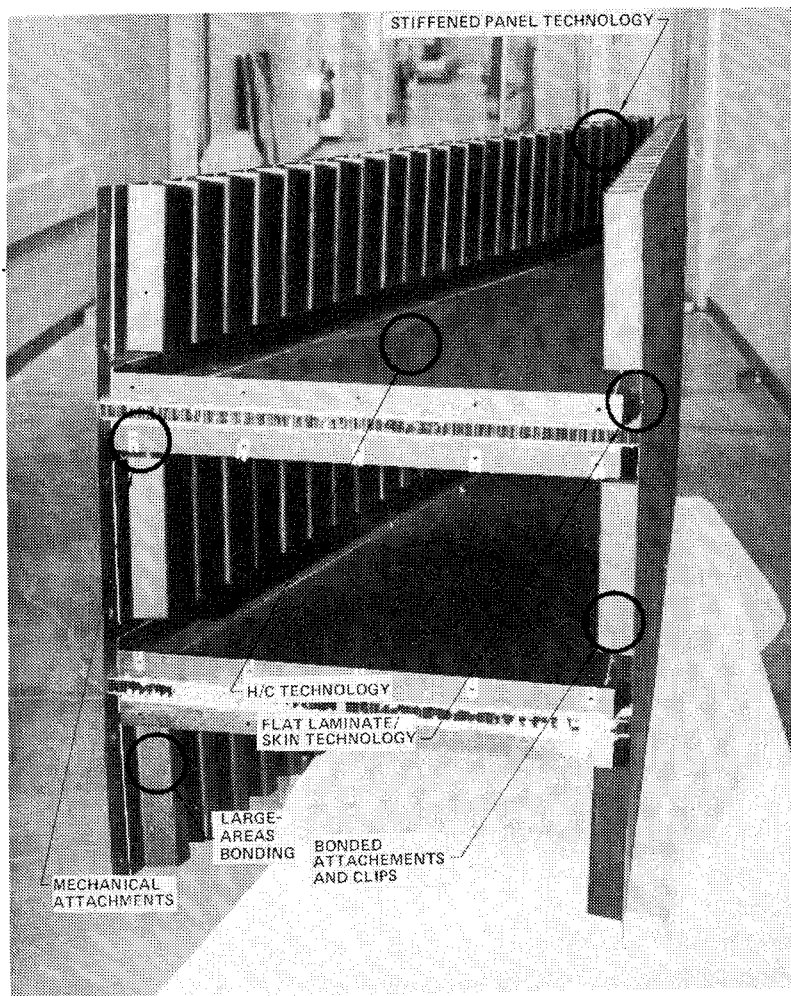


Figure 21

TASK J - PMR-15 VARIABILITY

The current effort on Task J of the program is directed to eliminating the material variability observed during the course of the program. To date the effort has identified the causes to be in manufacture of the monomers and/or resin and the aging characteristics of the mixed resin. The work needed to be accomplished is the determination of conditions of manufacture and/or storage of the monomers, resin and prepreg, revising the appropriate documents and demonstrating the reproducibility of the system. (Figure 22)

OBJECTIVE

TO IDENTIFY CAUSES FOR PREPREG VARIATION

WORK ACCOMPLISHED TO DATE:

- **IDENTIFIED CAUSES OF VARIABILITY**
 - **MANUFACTURE OF MONOMERS AND/OR RESIN**
 - **MONOMER & RESIN ADVANCEMENT WITH AGE**

WORK TO BE DONE:

- **DEVELOP MANUFACTURING & STORAGE CONDITIONS OF MONOMERS, RESIN, PREPREG**
- **DEMONSTRATE REPRODUCIBILITY OF PREPREG**
- **REVISE APPROPRIATE DOCUMENTS**

Figure 22

CONCLUSIONS

During the course of the program processes were developed, documented and demonstrated using the graphite/PMR-15 prepreg system. The property data obtained using the PMR-15 system is promising enough to warrant obtaining more detailed properties and then fabricating flight hardware. (Figure 23)

- **MANUFACTURING PROCESSES FOR PMR-15/GRAPHITE COMPOSITES HAVE BEEN ESTABLISHED AND DEMONSTRATED**
- **THE STRUCTURAL INTEGRITY OF KEY ELEMENTS HAS BEEN VERIFIED**
- **LARGE SCALE FABRICATION CAPABILITY HAS BEEN DEMONSTRATED**
- **SPECIFICATION AND NDI DOCUMENTATION HAS BEEN PREPARED AND SUBSTANTIATED**
- **NO SERIOUS PROBLEMS IDENTIFIED**
- **PMR-15/GRAPHITE COMPOSITES SUITABLE FOR SPACE SHUTTLE HARDWARE CONSIDERATION**

Figure 23

J. Devereaux Leahy
Rockwell International
Space Systems Group

EXPANDED ABSTRACT

Project CASTS, Composites for Advanced Space Transportation Systems, has been established to develop and demonstrate the technology required to achieve Gr/PI structural components with 316C (600F) operational capability.

Under this project, research and development programs are currently underway to develop and demonstrate processes for fabricating graphite/polyimide structural elements that have applications for manufacturing components for advanced space transportation systems. The primary objective of these studies is the development of fabrication processes viable for scale up to fabricating large structures and quality assurance programs necessary for quality control of material and non-destructive inspection (NDI) of structures. Structural element fabrication in these studies includes the manufacture of flat laminates, honeycomb panels, skin stringer panels, chopped fiber moldings, and others.

This paper reports on the scope and status of the fabrication development program on the third candidate graphite/polyimide material, utilizing the LARC-160 polyimide system. The results of initial chemical characterization studies on resin monomer constituents and intermediate esters are discussed, in particular, the problem of identifying the nadic ester endcapper material and establishing specifications to ensure material reproducibility. Progress on the process development task, including prestaging, cure, and postcure studies on flat laminates is reported. In addition, the design and processing of hat and "I" section stiffeners is reviewed. Initial efforts on the development of standards for non-destructive C-scan inspection for the various types of structures is discussed. Finally, the approach to qualifying the developed processes is outlined along with other ancillary studies in progress.

PROGRAM SCOPE/SCHEDULE

PHASE 1 - PROCESS DEVELOPMENT

Task (a) - Quality Assurance program including characterization of Celion/LARC-160 materials to derive a procurement and Q/C specification, a process specification, and a specification for NDI of fabricated components.

Task (b) - Develop processes for fabricating laminates, hat and "I" stiffeners, honeycomb core panels, and chopped fiber moldings.

Task (c) - Qualify processes by specimen fabrication and test.

PHASE 2 - DEMONSTRATION COMPONENTS

Task (d) through (g) - Fabricate and NDI structural elements utilizing the processes developed in Task (b).

Task (h) - Fabricate a representative component of the Space Shuttle aft body flap incorporating the various types of structures outlined in Task (b).

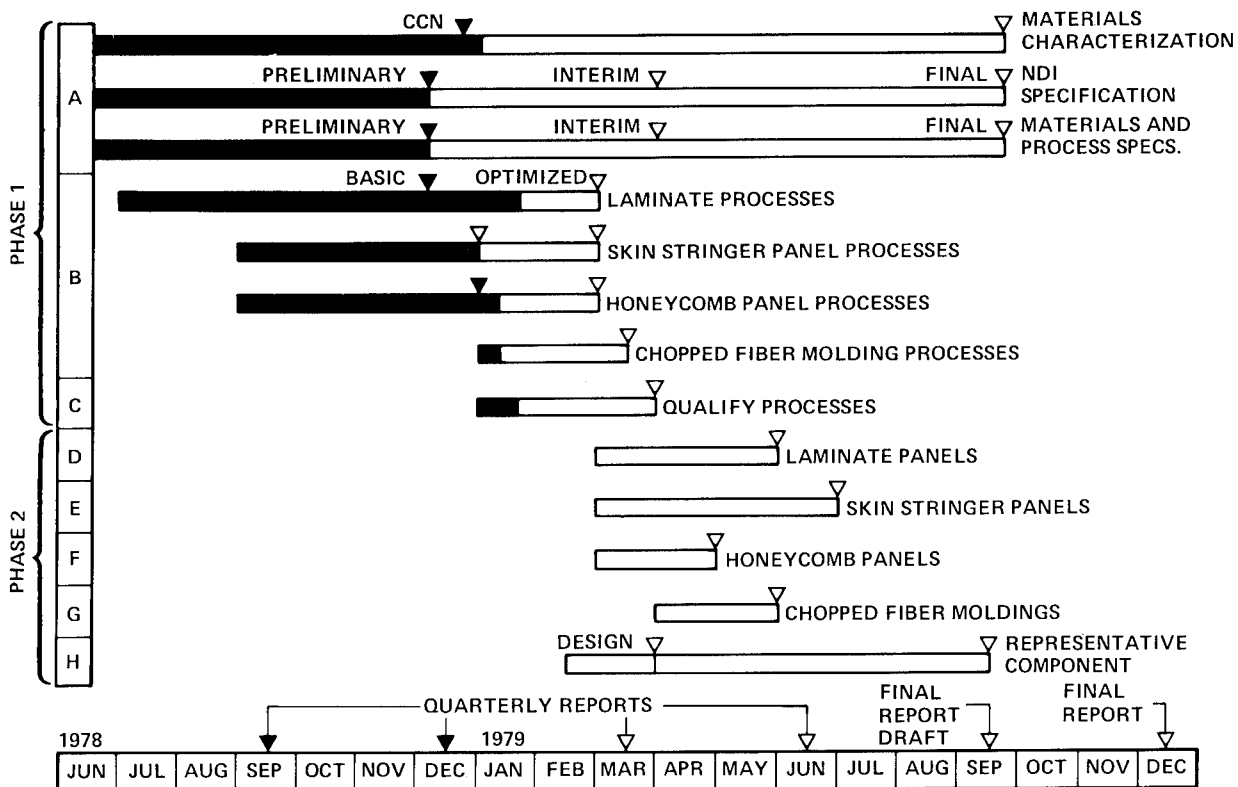


Figure 1

MATERIALS CHARACTERIZATION - LOGIC

The 316C (600F) polyimide material candidates and their various structural/environmental applications are highly sophisticated in nature, and unlike epoxy matrix composites, no extensive commercial application of polyimides has occurred. It has, therefore, become evident that the task of establishing formulation procedures and quality control standards for resin and prepreg manufacture is extremely complex. The burden of responsibility for providing graphite/polyimide prepregs with consistent batch-to-batch properties will ultimately rest on the prepreggers. Rockwell International has, therefore, taken steps to include the prepreg supplier as a contributing member of its development program team.

Since the extent to which chemical characterization must be carried out to ensure consistent prepreg quality cannot be defined at this time, a series of analytical steps tied in with the resin/prepreg production sequence is felt to be in order.

Gas chromatography (GC), mass spectrometry (MS), differential scanning calorimetry (DSC), and infrared spectroscopy (IR) can all be used for quick checks of monomer quality. High pressure liquid chromatography (HPLC) is being investigated as a more accurate finger-printing tool, and may ultimately result in the ability to reject or adjust a resin formulation during its processing.

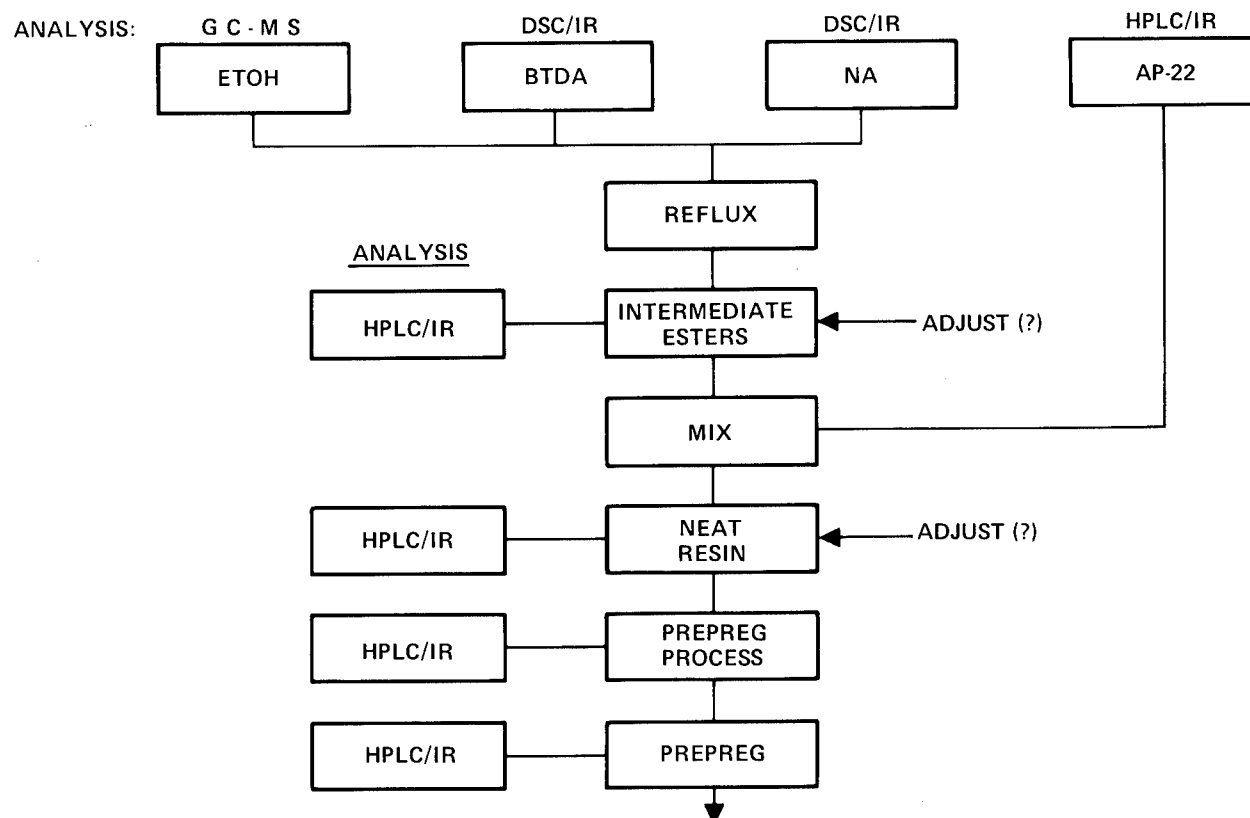


Figure 2

REPRODUCIBILITY OF ESTER SYNTHESIS

Approach: Prepare pure ester standards to be used for "fingerprinting," i.e., identification and quantification of the major components of intermediate esters, neat resin, and prepreg resin extract.

Status: Preliminary standards were established by reacting monomers with methanol and ethanol using a water/acetonitrile solvent gradient at pH=2 and 254 nm ultraviolet detection. The intermediate BTDA ester components were then separated and identified using the same procedure. It is believed the nadic ester comes off at approximately 13 minutes elution time with other components and is "hidden" in that peak.

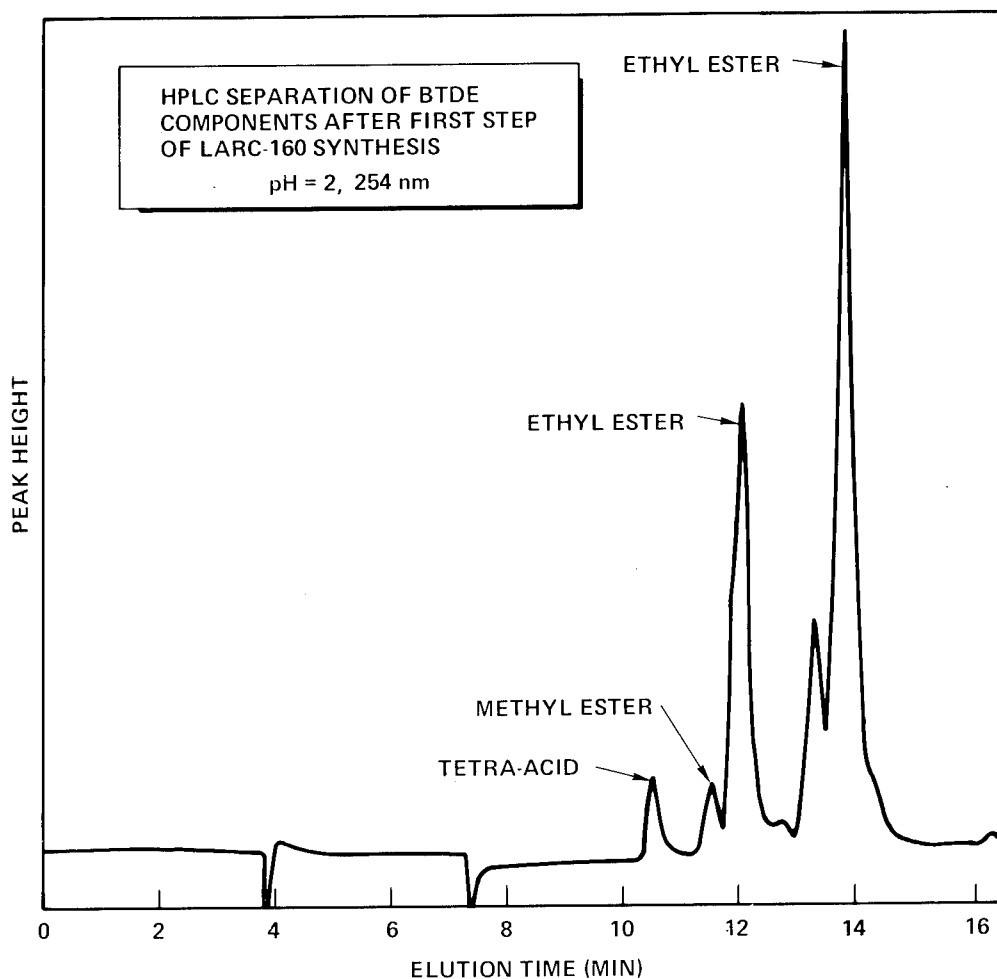


Figure 3

DETECTION OF NADIC ESTER (NE) ENDCAPPER

Approach: Separation by HPLC and detection at lower wave length in the ultraviolet.

Status: Using a water/acetonitrile solvent gradient at pH=7 with 200 nm ultraviolet detection the BTDA esters come off more rapidly and the nadic ethyl ester peak becomes visible.

Future efforts will include the further identification and quantification of chemical components at various formulation stages.

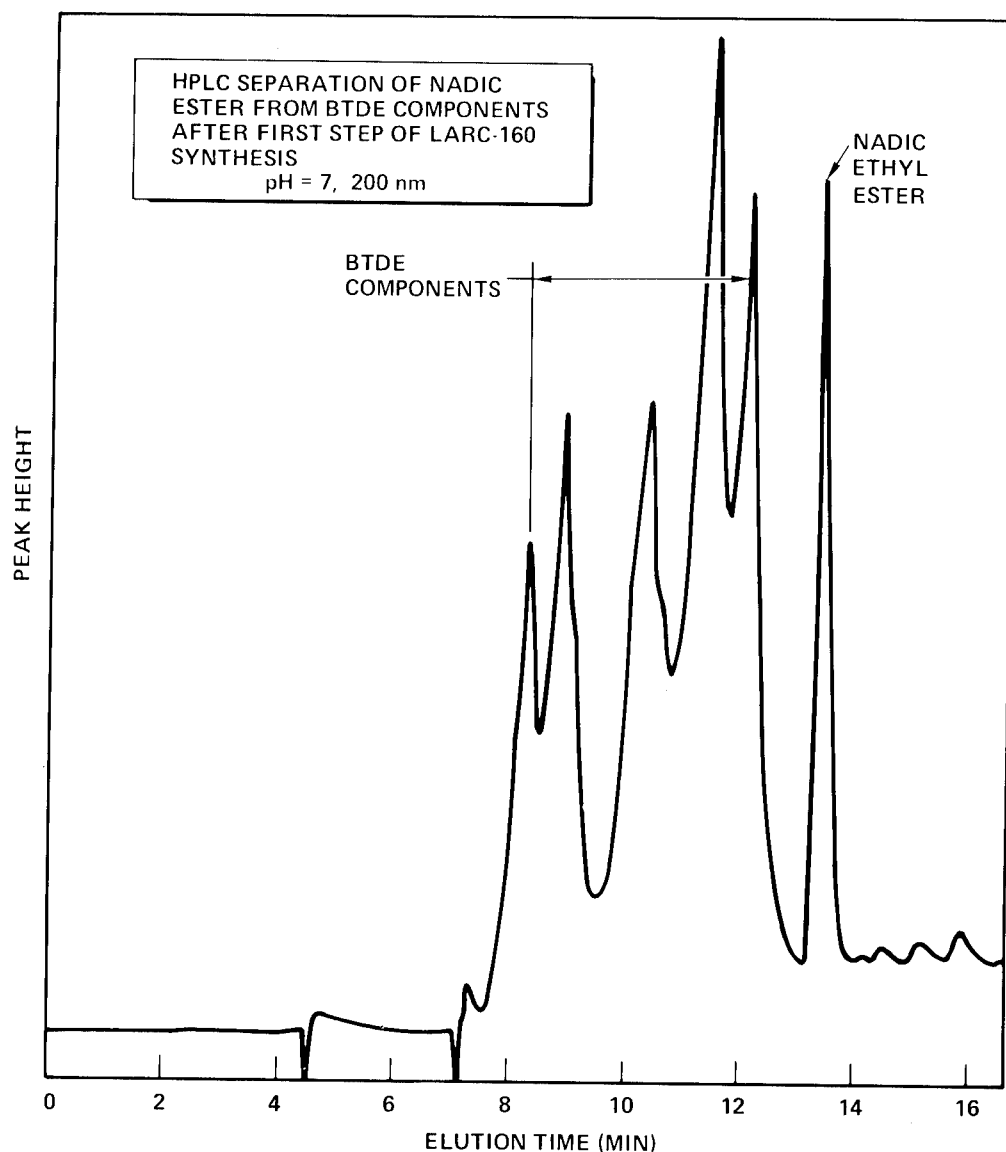


Figure 4

MATERIAL QUALIFICATION/CHARACTERIZATION

Since the ultimate determination and control of material quality will fall to the prepregger, Rockwell International conducted written and in-person surveys of a number of U.S. prepreg suppliers prior to selecting one to be the prime initial supplier for the LARC-160 program. Factors considered included experience with polyimide resins, expertise of personnel, adequacy of production facilities and controls and current or planned acquisition of chemical analysis equipment suitable for polyimide characterization.

The initial four 10-pound lots of prepreg were produced from four separate 50 pound batches of resin, 50 pounds being the smallest production batch of resin feasible. The object of this procedure was to eliminate the introduction of possible variables due to scale-up from laboratory to production quantities and also to obtain an indication of batch-to-batch consistency.

Status: Problem Areas/Resolution

- Low fiber tensile strength, $<2620 \text{ MN/m}^2$ (380 ksi), resulted in low flex properties / Changed to stronger fiber, 3240 MN/m^2 (470 ksi), 6K fiber.
- 6K fiber prepreg - spreading produces tape which is inferior to 3K fiber tape with regard to gaps, alignment, and edge waviness / Prepregger will correct with improved process control.
- NR-150B2 fiber sizing causes fuzzing and possible fiber damage / Fiber producer seeking improved sizing methods.
- Fiber splicing - Use of cellulose-acetate can create voids in composite/ polyimide adhesives being investigated.

• PURPOSE

- DEMONSTRATE RESIN AND PREPREG PRODUCTION BATCH REPEATABILITY

• PROCEDURE

- FOUR -- 22.5 KG (50 LB) BATCHES OF RESIN PREPARED
- FOUR -- 1.35 KG (3 LB) AND FOUR 3.15 KG (7 LB) BATCHES OF 15.24 CM (6 INCHES) WIDE PREPREG TAPE PRODUCED
 - MATERIAL PRODUCED IN STEP BY STEP SEQUENCE TO DEMONSTRATE BATCH TO BATCH CONSISTENCY
 - MINIMUM GAUGE, 0.064 MM (2.5 MILS)/PLY, TAPE -- HIGH QUALITY
 - SPECIMENS TAKEN FOR CHEMICAL ANALYSIS AT MONOMER, INTERMEDIATE ESTER AND NEAT RESIN STAGES
 - PREPREG PROCESSING DATA COLLECTED FOR CORRELATION OF BATCH-TO-BATCH RESULTS

Figure 5

EFFECT OF RESIN FORMULATION/PROCESS VARIABLES

In order to further define the effect of variables in both materials and processes on resin and prepreg and pave the way to development of quality assurance specifications which will maximize consistency of quality in composites, a program is underway to selectively vary resin formulation and compare the properties of resultant batches.

Coordination between Rockwell International, the prepreg supplier, and NASA LaRC resulted in the selection of 13 batches which will be varied as shown below. Analysis will be performed at various processing points as noted.

PREPREG BATCH 1.35 KG (3 LB) EA	FORMULATION VARIABLES		PROCESS VARIABLES		ANALYSES						
	CONC. AP-22	CONC. ANHYDRIDES	COOK TIME	REFLUX TIME	NA	BTDA	AP-22	INT. ESTER	RESIN	PREPREG EXTRACT	LAM
STANDARD					✓	✓	✓	✓	✓	✓	✓
1	+2%	STD	STD	STD	✓	✓	✓	✓	✓	✓	✓
2	-2%	↑	↑	↑				✓	✓	✓	✓
3	+5%	↑	↑	↑				✓	✓	✓	✓
4	-5%	↓	↓	↓				✓	✓	✓	✓
5	+10%	↓	↓	↓				✓	✓	✓	✓
6	-10%	STD	STD	STD				✓	✓	✓	✓
7	STD	NA (+5%)	STD	STD				✓	✓	✓	✓
8	↑	BTDA (STD)	↑	↑				✓	✓	✓	✓
9	↓	NA (-5%)	↓	↓				✓	✓	✓	✓
10	STD	BTDA (STD)	STD	STD				✓	✓	✓	✓
		NA (STD)						✓	✓	✓	✓
		BTDA (+5%)						✓	✓	✓	✓
		NA (STD)						✓	✓	✓	✓
		BTDA (-5%)						✓	✓	✓	✓
11	STD	STD	EXTENDED	STD				✓	✓	✓	✓
12	STD	STD	INTERMED.	STD				✓	✓	✓	✓
13	STD	STD	STD	6 HR				✓	✓	✓	✓

Figure 6

RESIN REPEATABILITY/PREPREG PROCESSING, STORAGE AND OUT-TIME

The resin batch formulation which produces the optimum properties in the variable investigation will be checked for repeatability by producing five separate resin/prepreg batches. Specimens from three of these batches will also be given a prepreg storage and out-time evaluation over a period of six months.

If satisfactory repeatability is demonstrated, a single 4.5 kg (10 lb) prepreg batch will be produced. The neat resin in the "pot" will be sampled during processing and compared with resin extracted from composites made from prepreg produced at the same point. This study may identify prepreg quality variations due to resin cook-time.

● RESIN FORMULATION REPEATABILITY/PREPREG STORAGE AND OUT-TIME EVALUATION

PREPREG BATCH 1.35 KG (3 LB) EA	FORMULATION & PROCESS	ANALYSES				STORAGE & OUT-TIME EVALUATION					
		INT. ESTER	RESIN	PREPREG- EXTRACT	LAM.	1 MO. STORAGE	3 MO. STORAGE	6 MO. STORAGE	OUT-TIME 1 MO. MAT'L	OUT-TIME 3 MO. MAT'L	OUT-TIME 6 MO. MAT'L
1	OPTIMUM- PER VARIABLES STUDY	✓	✓	✓	✓						
2		✓	✓	✓	✓						
3		✓	✓	✓	✓						
4		✓	✓	✓	✓						
5		✓	✓	✓	✓						
1				✓	✓	✓			✓		
3				✓	✓		✓			✓	
5				✓	✓			✓			✓

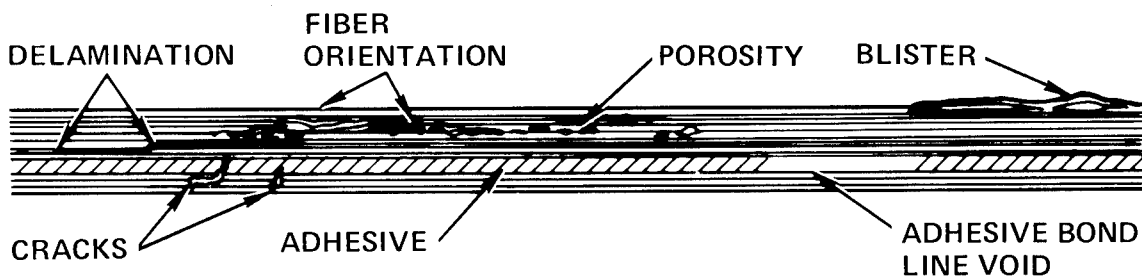
● PREPREGGING TIME/TEMPERATURE ANALYSIS

PREPREG BATCH 4.5 KG (10 LB)	FORMULATION & PROCESS	NEAT RESIN ANALYSES		PREPREG ANALYSES	
		INT. ESTER	POT TIME	RESIN EXTRACT	LAMINATE
1	OPTIMUM- PER VARIABLES STUDY	✓	✓ -START	✓	✓
			✓	✓	✓
			✓	✓	✓
			✓	✓	✓
			✓ -FINISH	✓	✓

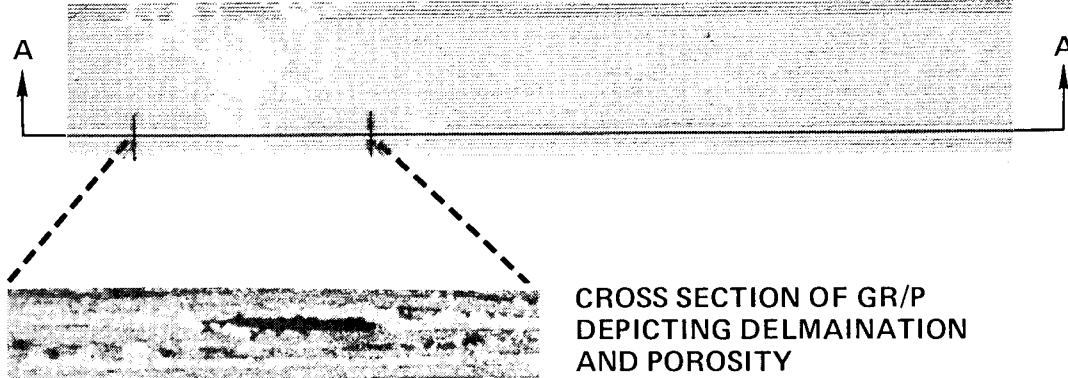
Figure 7

NON-DESTRUCTIVE EVALUATION (NDE)

Ultrasonic, C-scan inspection has been utilized for some time for the non-destructive detection of anomalies in composite structures. All specimens, panels, and assemblies produced in the course of the LARC-160 development program are being C-scanned in accordance with standards agreed upon by Rockwell International and NASA LaRC. Radiography will be used where inspection of radii, fillets, corners, etc., is required. Since this is the initial development program on Celion/LARC-160 polyimide material, no acceptance criteria has been established to cover the various types of defects shown below.



U/S TECHNIQUE I ULTRASONIC C-SCAN OF GR/P-8 PLY



ANOMALIES DETECTABLE WITH NONDESTRUCTIVE EVALUATION

Figure 8

ESTABLISHING C-SCAN STANDARDS

In order to establish a sensitivity for producing C-scans which would indicate acceptable quality, NASA LaRC produced six reference standards and scanned them at three different sensitivities.

The standards and scans were then sent to Rockwell, where they were scanned with the instrumentation adjusted to duplicate the NASA C-scans for each standard at each of the three sensitivities, gain settings of 30, 50, and 82. These were labeled "A," "B," and "C" respectively as shown below. Three of the six standards were retained by Rockwell and the others returned to NASA.

The "A" sensitivity setting has been agreed upon as the standard against which LARC-160 laminate composites will be evaluated and which will be utilized to establish standards for other types of structural assemblies.

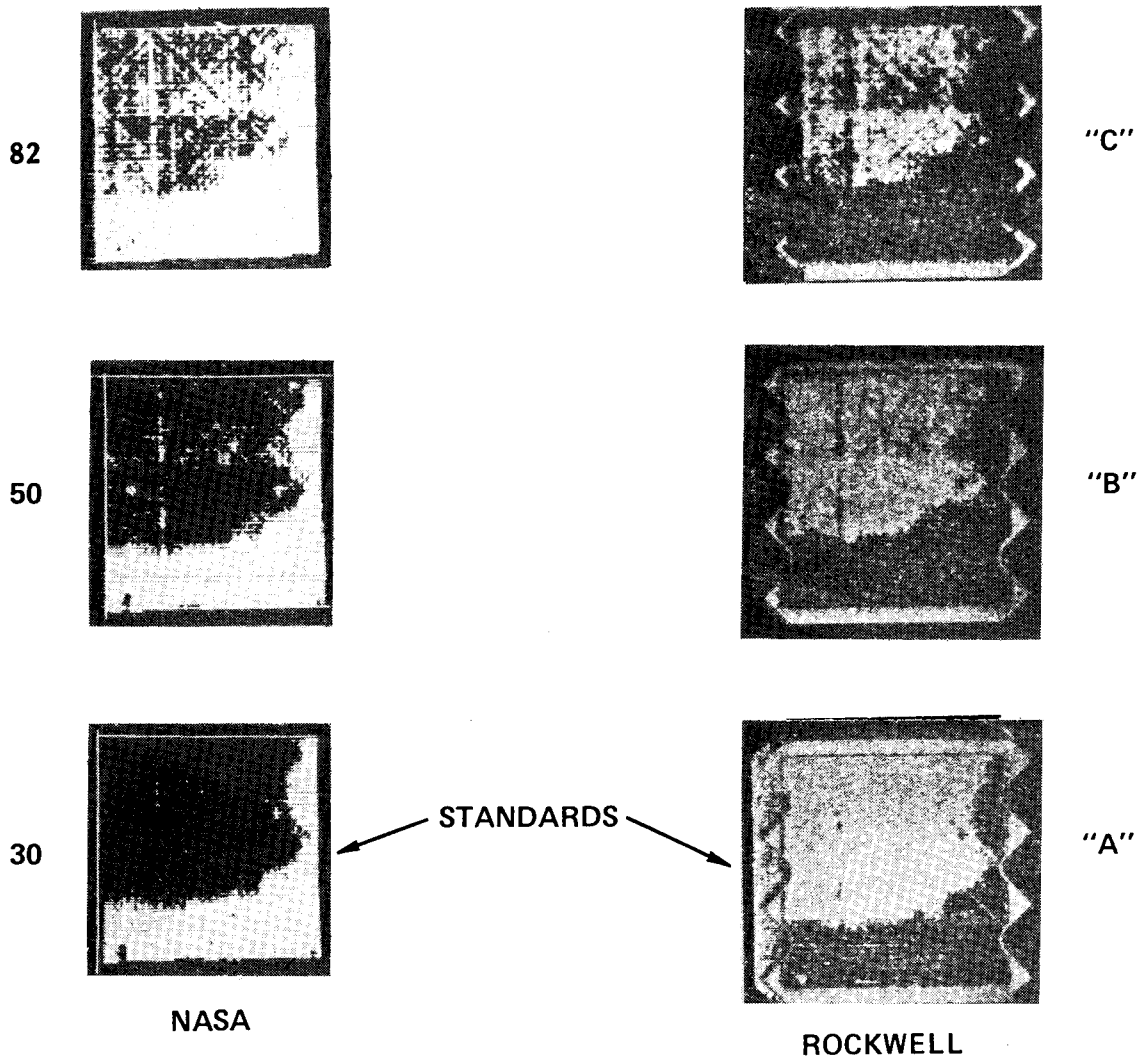


Figure 9

C-SCAN INSPECTION OF COMPLEX SHAPES

To establish correlation between C-scans of composite structures and the type and location of defects in the structure, photomicrographs can be employed. As shown in the figure below, an 8-ply graphite/polyimide "Pi" joint was first C-scanned at the "A" sensitivity and then cut open for photomicrograph inspection of the voids observed in the C-scan. Such standards are being established and utilized as the program progresses.

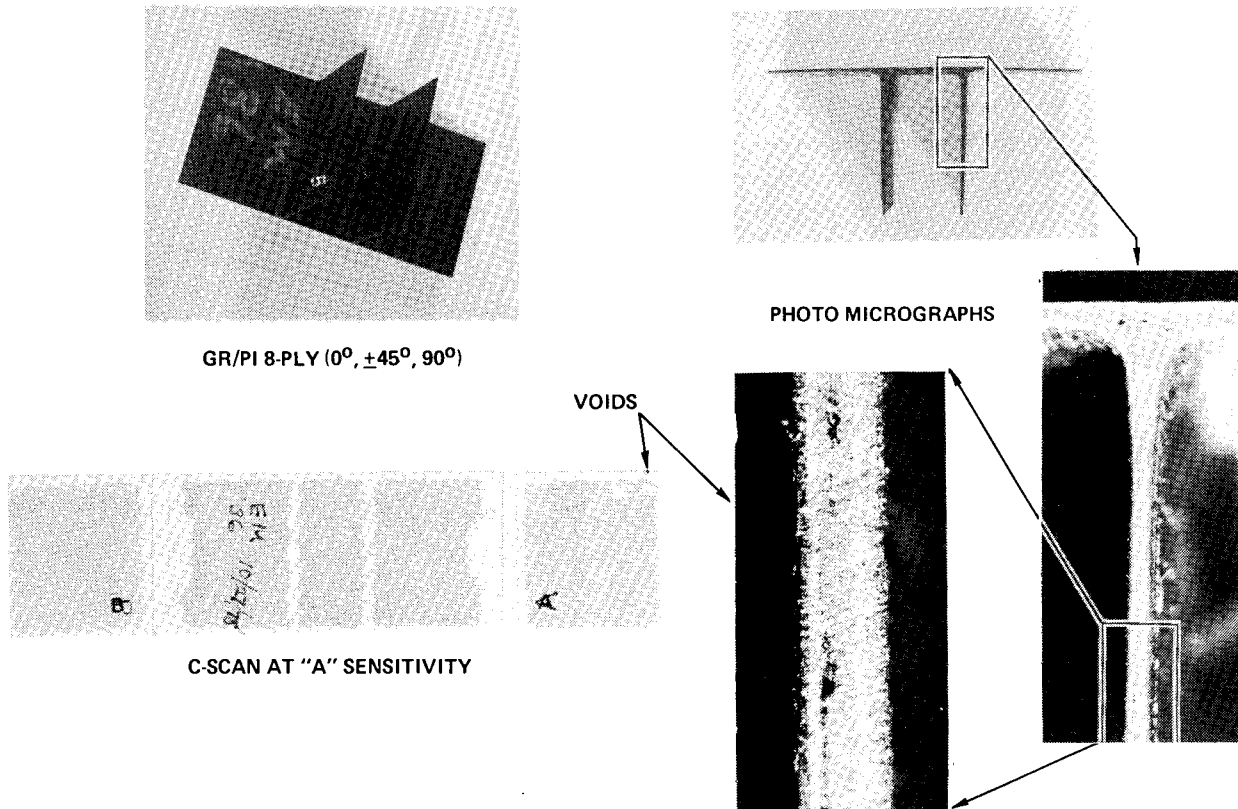


Figure 10

PROCESS DEVELOPMENT - TASK (b)

Objective

- Utilize basic (NASA) cure cycle as basis for processing study.
- Develop processes and tooling suitable for scale-up to production of large flat and complex components.
- Establish NDE C-scan standards and test procedures.

Approach

- Establish processing limits for autoclave curing.
 - o Staging - comparison of in situ versus pre-impregnating
 - o Minimum cure pressure and temperature
 - o T_g - Effect of cure versus postcure
 - o Laminate thickness - maximum
 - o Optimum heat-rise rate
 - o Optimum temperature/pressure application point
 - o Compare perforated and non-perforated tooling requirements

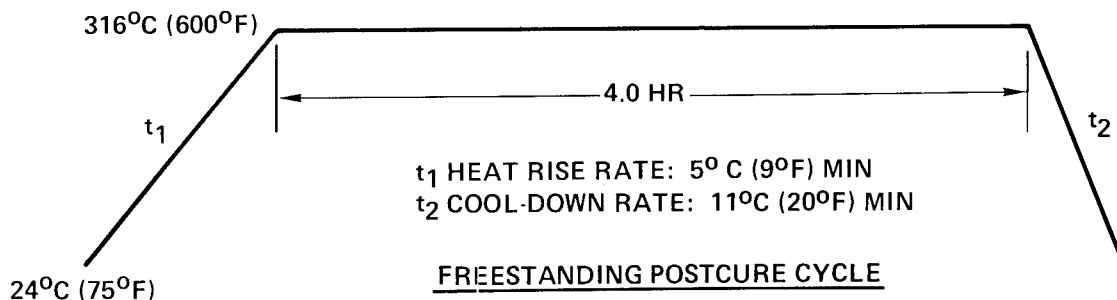
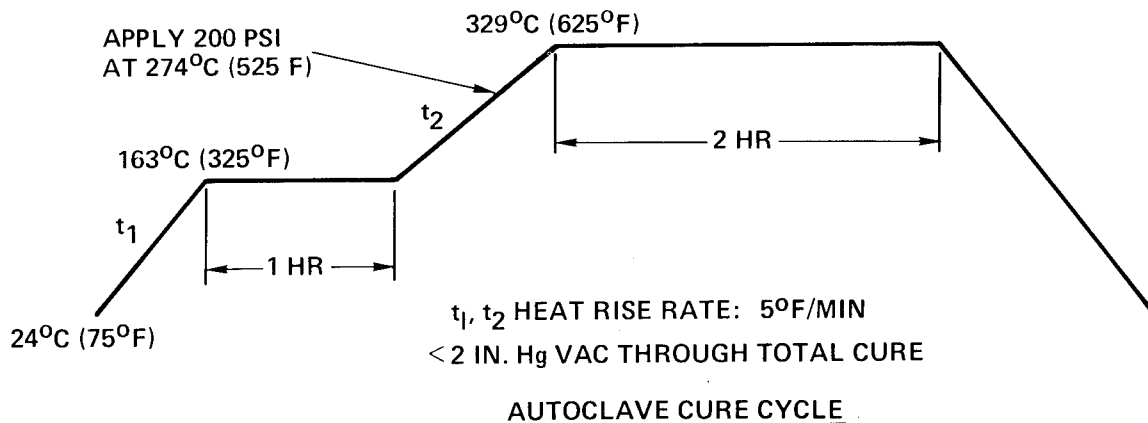


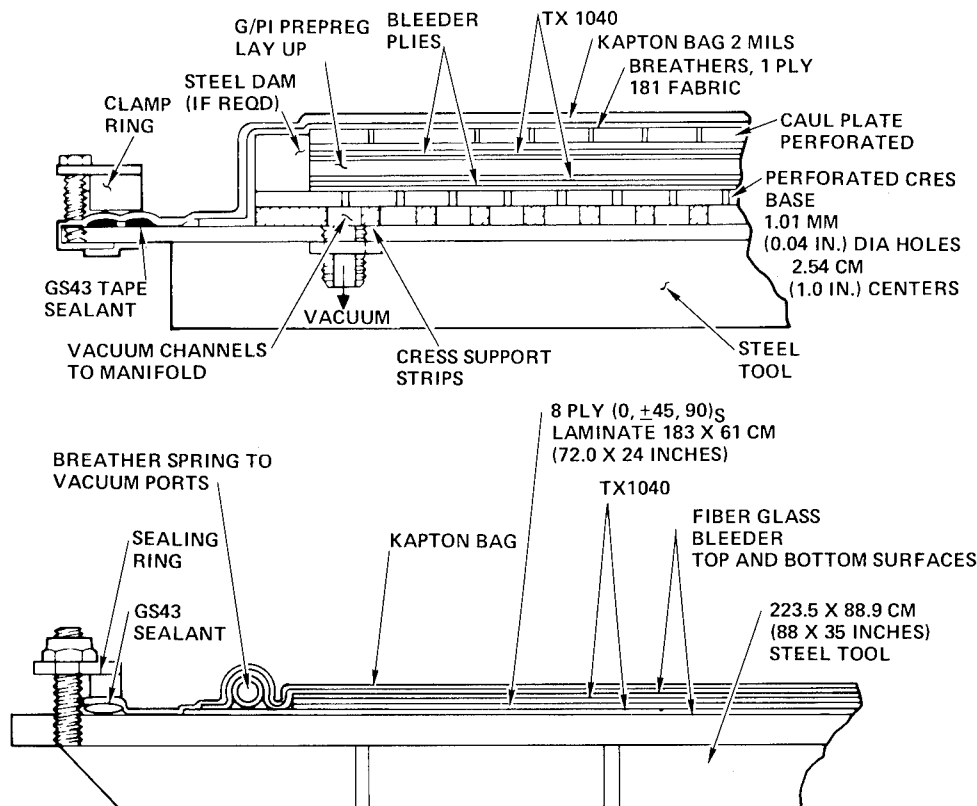
Figure 11

FLAT LAMINATE PROCESS DEVELOPMENT

Target Properties

- Physical
 - o <2% voids; 55-62% fiber volume; T_g , >340C (644F)
 - o NDE C-scan > 99% defect free at NASA - "A" sensitivity
- Mechanical
 - o Flexural strength; >1572 MN/m² (228 ksi) @ room temperature and >938 MN/m² (136 ksi) @ 316C (600F)
 - o Short beam shear strength: >103 MN/m² (15 ksi) @ room temperature and >7 ksi @ 316C (600F)

While the use of a perforated tool and caul plate greatly enhances the achievement of high quality laminates by permitting uniform volatile removal, the use of non-perforated tooling for large production parts is desirable. One alternative is the use of a peripheral spring manifold around the part, as shown below, to which vacuum is applied through ports in both ends of the tool. This approach is being studied along with pre-imidization of the material for partial removal of volatiles.

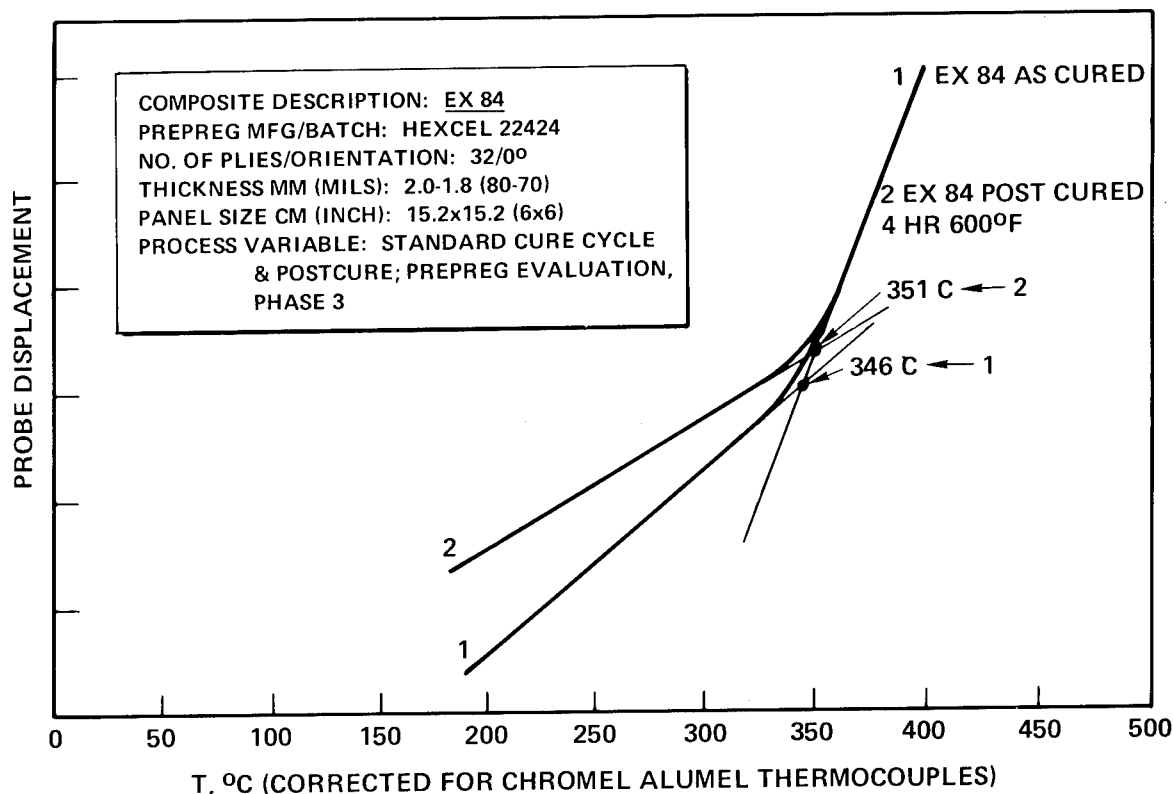


FLAT LAMINATE LAYUP DETAILS WITH PERFORATED (TOP) AND NON-PERFORATED TOOLING

Figure 12

RESULTS OF LAMINATE PROCESS STUDIES

- Perforated tool/caul plate produced quality laminates in 45.7 cm (18 in) X 55.9 cm (22 in) panels up to 2.54 mm (0.10 in) thick - Excellent C-scans
 - o Some problems in meeting target fiber volume - spread of 58 to 68%
- Processing limits
 - o Staging limits not fully determined: 163C (325F) for 60 to 120 minutes or 177C (350F) for 45 to 75 minutes produced equivalent high quality laminates in terms of C-scan and physical/mechanical properties.
 - o Pressure: 0.69 MN/m^2 (100 psi) to 1.38 MN/m^2 (200 psi) produced acceptable laminates - variations in staging time/temperature could reduce pressure required to $<0.69 \text{ MN/m}^2$ (100 psi).
 - o Cure Temperature: 274C (525F) minimum demonstrated - good C-scans and mechanical properties.
 - o Cure versus Postcure: 4 hour postcure (freestanding @ 316C (600F)) yields a higher Tg than "as cured" laminates. (See figure below)
 - o Laminate Thickness: Maximum (0, + 45, 90)_s stacks were produced in nominal thicknesses up to 12.7 mm (0.50 in) with some voids - pre-imidizing being studied to resolve this problem.
 - o When large flat panels 89 X 208 cm (35 X 82 in) were fabricated, a caul plate was required to produce a smooth, wrinkle-free top surface.



TMA/Tg-TYPICAL RESULTS

Figure 13

STIFFENED PANEL DESIGN REQUIREMENTS

Test panel design requirements were as follows:

- Panel Design Load: 0.525 N/m^2 (3000 lb/in) nominal
(2800 lb - 3200 lb/in)
- Panel Failure Mode: 122 cm (48 in) long panels - Euler buckling
30.5 cm (12 in) long panels - local crippling or buckling
- Panel Skin: 8 Ply isotropic layup $(0, \pm 45, 90)_s$
- Stringers: 3 minimum
- Panel Dimensions and Fabrication Concepts:
 - o 22.9 cm (9 in) wide X 30.5 cm (12 in) long panels
 - (9) Hat stiffened - 3 each, bonded, bolted, cocured
 - (9) "I" stiffened - 3 each, bonded, bolted, cocured
 - o 22.9 cm (9 in) wide X 122 cm (48 in) long
 - (3) of best configuration from those built and tested above

The design cross section for the hat-section stringer panel is shown below.

NOTE: ELEMENT IS
30.5 CM (12.0
INCHES) LONG

COMPOSITE 60% FIBER VOL, 0.145 MM (5.7 MIL)/PLY:
A. SKIN - 8-PLY ISOTROPIC $(0, \pm 45, 90)_s$

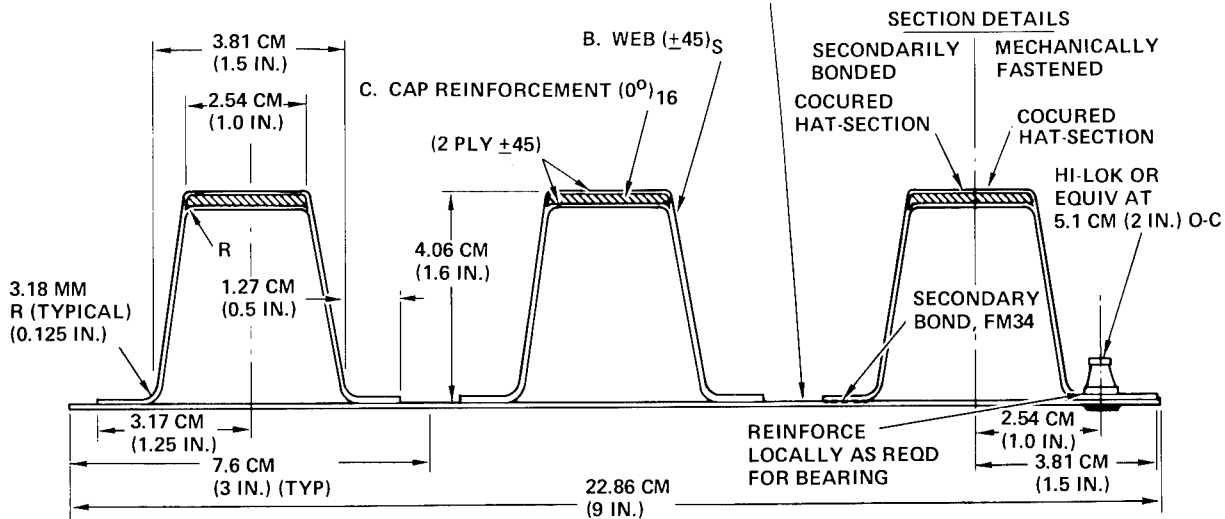


Figure 14

"I" STRINGER DESIGN

Based on the design requirements described previously, the "I" stringer stiffened panel cross section design is as shown below. Following the fabrication and testing of the 22.9 cm (9 in) wide by 30.5 cm (12 in) long panels, one type/construction panel will be selected and a 22.9 cm (9 in) wide by 122 cm (48 in) long panel fabricated for testing.

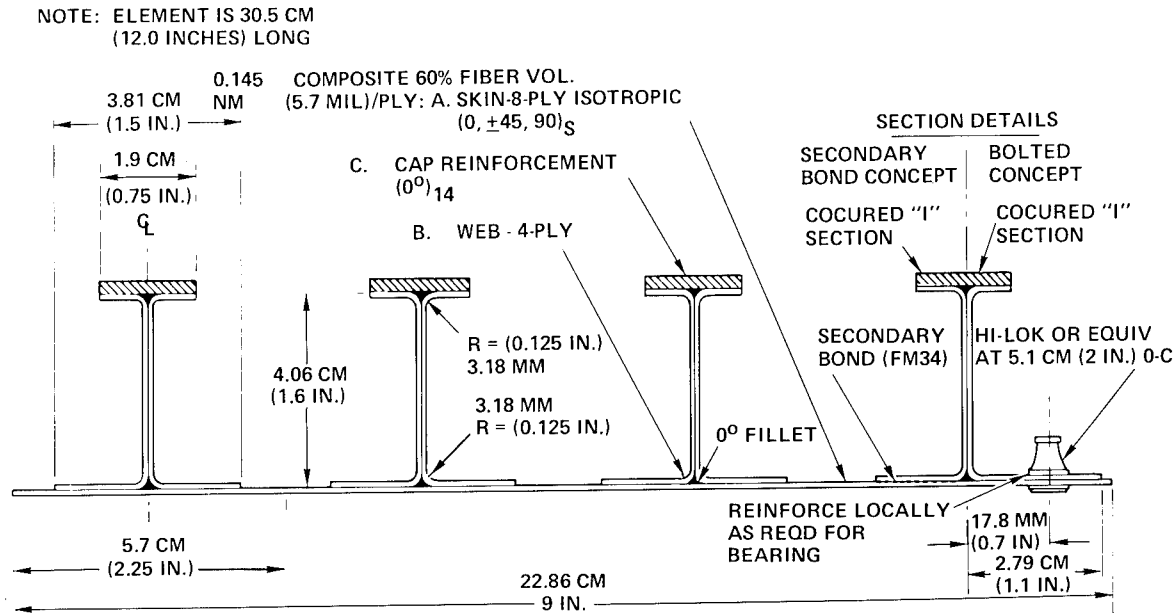
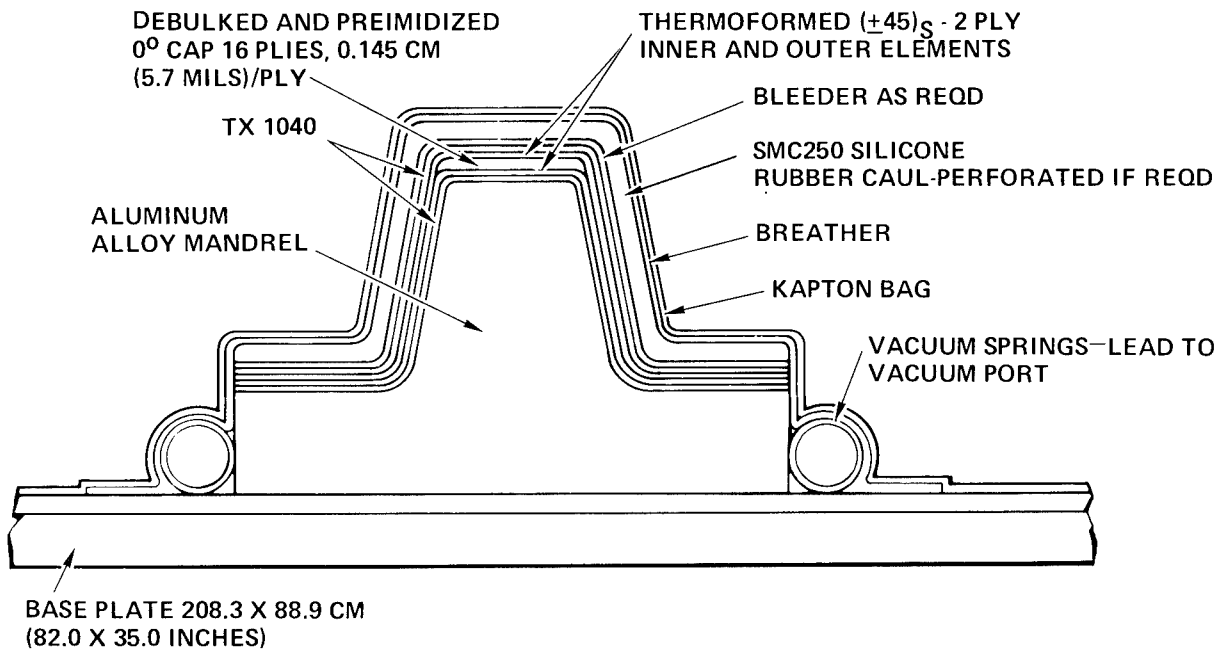


Figure 15

HAT-SECTION STRINGER-LAYUP AND TOOLING APPROACH

- Tooling
 - o Aluminum mandrel
 - o SMC 250 silicone rubber caul
 - o Vacuum manifold spring
- Process
 - o Webs and flanges fabricated utilizing vacuum bag debulking and thermoforming techniques
 - o Cap element debulked, bled, and pre-imidized to remove volatiles to <2% level, reduce resin content to $\approx 33\%$ and debulk to near net thickness.
 - o Parts staged to the standard time-imidizing temperature cycle, but maximum cure temperature will be 287C (550F) to prevent thermal degradation of rubber caul.
 - o Used standard postcure cycle.



HAT-SECTION STRINGER-TOOLING/LAYUP DETAILS

Figure 16

CO-CURED HAT STIFFENED SKIN/STRINGER ELEMENTS

- Results

- o Two approaches were used on the 0° cap preforms. One was merely staged at 93C (200F), the other staged at 93C (200F) and imidized at 163C (325F). Both were of excellent appearing quality and well consolidated. Final thickness ranges of the preforms were 2.49 to 2.79 mm (98 to 110 mils). The staged preform was more pliable and had some tack while the imidized preform was rigid.
- o The stiffener shown below was excellent in appearance. The silicone rubber caul plate afforded uniform pressure distribution to the preformed laminate parts on the tool during cure, resulting in a smooth, wrinkle-free surface.
- o NDE C-scans at "A" sensitivity webs/flanges 100% void free/caps - 95% - some voids and porosity.

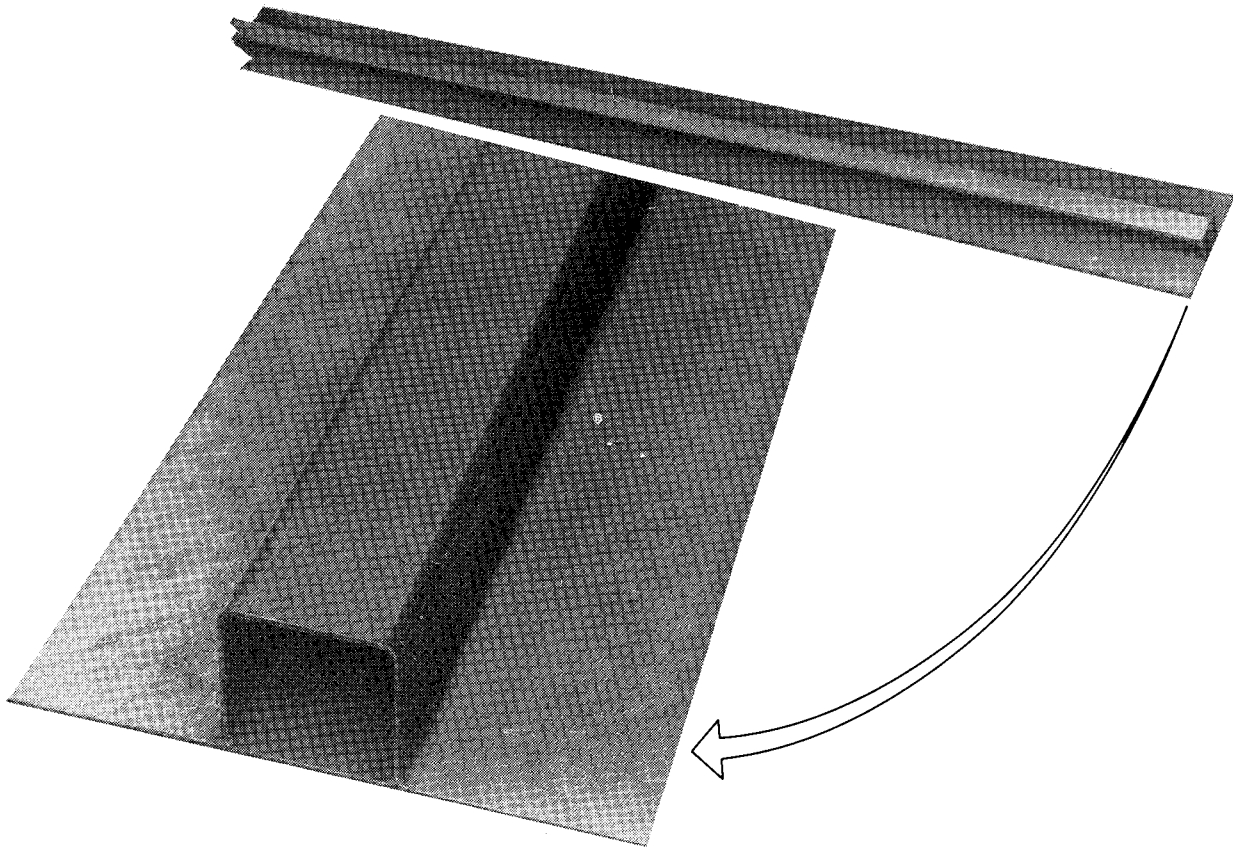


Figure 17

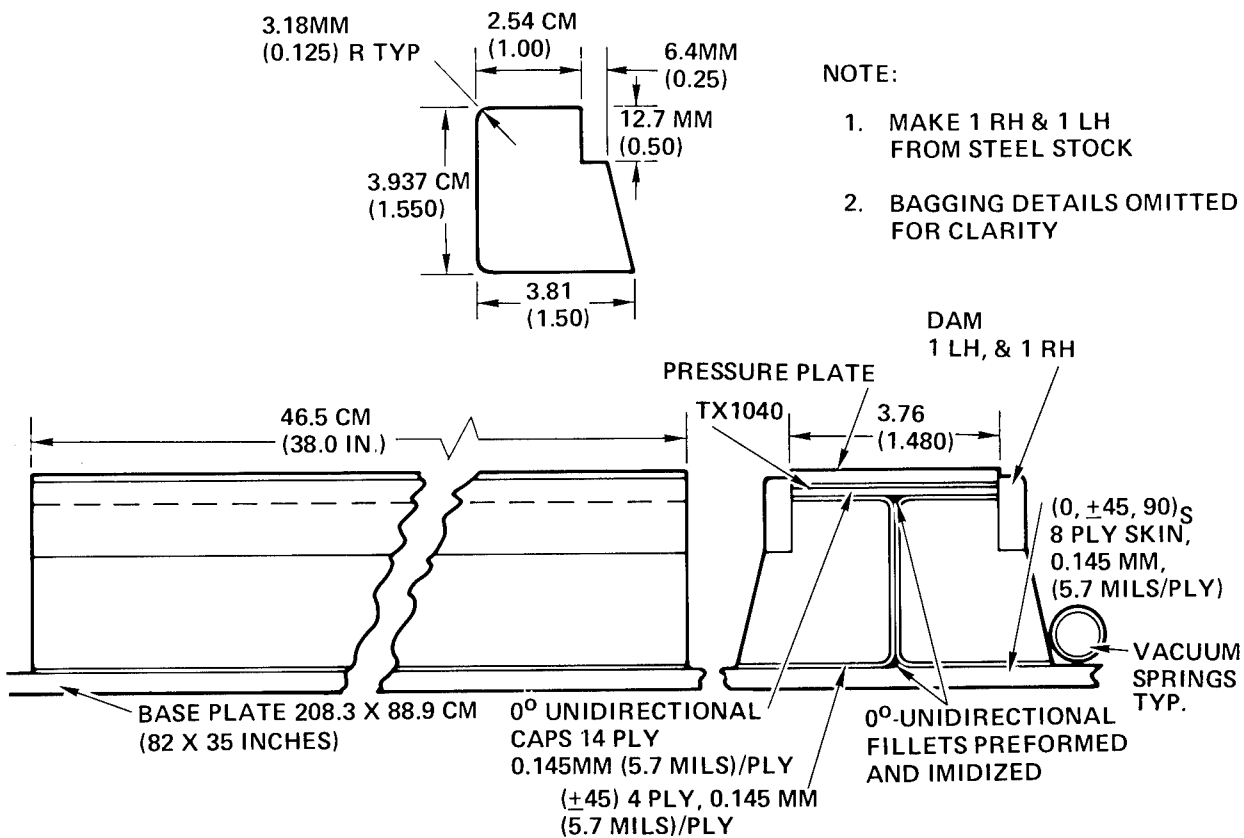
"I" SECTION STRINGER-LAYUP AND TOOLING APPROACH

- Tooling

- o Steel, right and left hand mandrels utilized to obtain comparison with aluminum used for hat section mandrel.
- o Peripheral vacuum manifold spring

- Layup/Processing

- o Prebleed, debulk, and imidize 0° cap and fillets - to produce stable preform and remove excess volatiles.
- o Thermoform $(+45)_s$ webs and flanges and pre-imidize on tool to remove excess volatiles which might otherwise be trapped.
- o Use standard cure, postcure cycles.



"I" STIFFENER TOOLING/LAYUP DETAILS

Figure 18

OTHER PROCESS DEVELOPMENT EFFORTS

Investigations on adhesive bonding materials (FM 34 and LARC 13) and techniques, mechanical attachments and chopped fiber molding compounds are currently underway as outlined below.

- ADHESIVE BONDING
 - SANDWICH PANELS
 - LAP SHEAR
 - CO CURE
- MECHANICAL ATTACHMENT
 - SANDWICH INSERTS
 - COMPOSITE TO COMPOSITE
- CHOPPED MOLDING COMPOUNDS
 - 3 RESIN CONTENTS
 - VARY STAGING PROCESSES
- TEST ALL ABOVE AT RT, AND 316 C (600 F) AND AFTER 125 HOURS AGING AT 316 C (600 F)

Figure 19

PROCESS QUALIFICATION TASK (c)

To qualify the processes developed for the specified structural elements, develop preliminary structural design data and finalize procedures for the fabrication and NDE inspection of demonstration components, a series of qualification specimens are being fabricated and tested. Appropriate shear, flex, tensile, compressive, and other properties noted below are being determined for a representative number of specimens.

The initial results of tensile testing on laminate specimens are as follows:

$$\begin{aligned} F^{TU} &= 1710 \text{ MN/m}^2 (248 \text{ ksi}), (0) \\ &614 \text{ MN/m}^2 (89 \text{ ksi}), (0, \pm 45, 90)_S \\ &176 \text{ MN/m}^2 (25.5 \text{ ksi}), (\pm 45)_S \end{aligned}$$

● PURPOSE

● QUALIFY PROCESSES

● DEVELOP MECHANICAL PROPERTY DATA

F_{ISU} : (0)

F_{FU}, E_F : (0)

$F_{TU}, E_T, \epsilon_{TU}, \nu_T$: (0), (90), (± 45)_S, (0, $\pm 45, 90$)_S

F_{CU}, E_C, E_{CU} : (0), (90), (± 45)_S, (0, $\pm 45, 90$)_S

● TESTS TO BE PERFORMED AT -270°F, RT, 400°F AND 600°F AND AFTER EXPOSURE TO 600°F, 125 HRS

● NDE - C-SCAN TEST ALL PARTS

● STATUS & RESULTS

● FLAT LAMINATE STOCK COMPLETE FOR MECHANICAL PROPERTIES

● NDI C SCAN = 99 TO 100% SOUND TRANSMISSION

● TESTING INITIATED

● HAT STRINGER TEST PANELS BEING FABRICATED

● "I" STRINGER PROTOTYPE TEST PARTS BEING AUTOCLAVE MOLDED

Figure 20

INTERIM RESULTS OF THERMID 600 ENGINEERING DEVELOPMENT

7

Richard D. Hoffman
Hercules Incorporated/Bacchus

EXPANDED ABSTRACT

The team of Hercules Incorporated/Aerospace Division (prime), Hughes Aircraft Company/Aerospace Group, and Northrop Corporation/Aircraft Group is engaged in a program of Thermid 600 Engineering Development on AFML/MB (WPAFB) contract No. F33615-78-C-5167. Thermid 600 is an acetylene terminated polyimide which was developed on previous AFML contracts.

The program will develop and evaluate Thermid 600 as a matrix material for advanced composite structure applications in harsh environments. The 23-month program will be divided into three phases. Phase I, Process Development, will consist of the prepreg work needed to develop a versatile and reproducible prepreg and fabrication work needed to develop laminate and structural shape processing methods. Phase II, Composite Characterization, will consist of advanced composite design guide tests needed to generate a design data base. The processes developed in the first phase will be used for the fabrication of test specimens. Phase III, Producibility, Manufacturing and Test of Structural Elements, will use processing methods developed in the first phase and the data generated in the second phase to design selected structural elements for the material. The elements will be manufactured and tested to demonstrate their producibility and performance.

The current effort underway is Phase I, Task 1, Prepreg Development. This task involved the use of reactive diluents in resin mixture studies with neat resin screening, prepreg process scaleup and selection of final candidate for Task 2.

COMMERCIALLY AVAILABLE FORMS OF THERMID 600

The Phase I, Task 1 program objectives are to define a prepreg process for Thermid 600 prepreps and to increase the melt flow time of Thermid 600 (T-600) through the use of reactive diluents. Two of the commercially available forms of T-600 are shown in Figure 1. Both of these forms are being evaluated on this program.

The imidized form of T-600 has the advantage of producing no volatiles due to cure reactions but is only soluble in high-boiling solvents like (1) methyl, (2) pyrrolidinone (NMP). The amic acid form of T-600 yields water of imidization on cure but is soluble in low-boiling ketone solvents. Both forms of T-600 are dry powders at room temperature (RT) and require solvent retention in the prepreps for **handleability**. A lower boiling solvent is desirable in the prepreg as it can be removed in the autoclave at a temperature which advances the T-600 to a lesser extent.

The Aerospace Group of Hughes Aircraft Company developed the original synthesis for T-600 (formerly called HR 600).

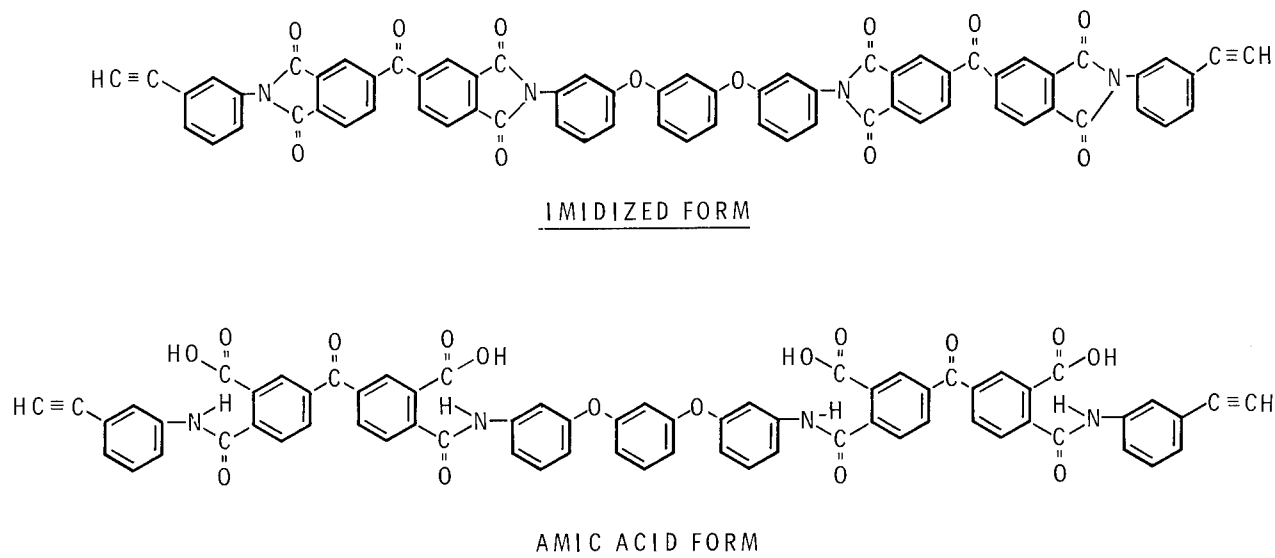


Figure 1

REACTIVE DILUENTS AND THEIR CONSTITUENTS

Hughes personnel subsequently synthesized the acetylene terminated reactive diluents shown in Figure 2. In this program, various mixtures of these diluents were evaluated to: a. Decrease the temperature at which a liquid melt is achieved; and b. Increase the gel time of the liquid melt. These two parameters serve to increase the flow time of a laminate during an autoclave cure cycle. Mixtures of structure VIII with T-600 at 30/70 weight ratios melt 50°C lower than T-600 alone and yield a 3 minute flow time prior to gel. Incorporation of structure IV into T-600 during the synthesis of the T-600 by partial replacement of the benzophenone tetracarboxylic dianhydride can achieve a liquid melt at 175°C and a gel time of 5 minutes.

Prepreg trials of both forms of T-600 mixed with various reactive diluents revealed that only the amic acid form of T-600 yields a prepreg with sufficient handleability to be useful in the manufacture of structures.

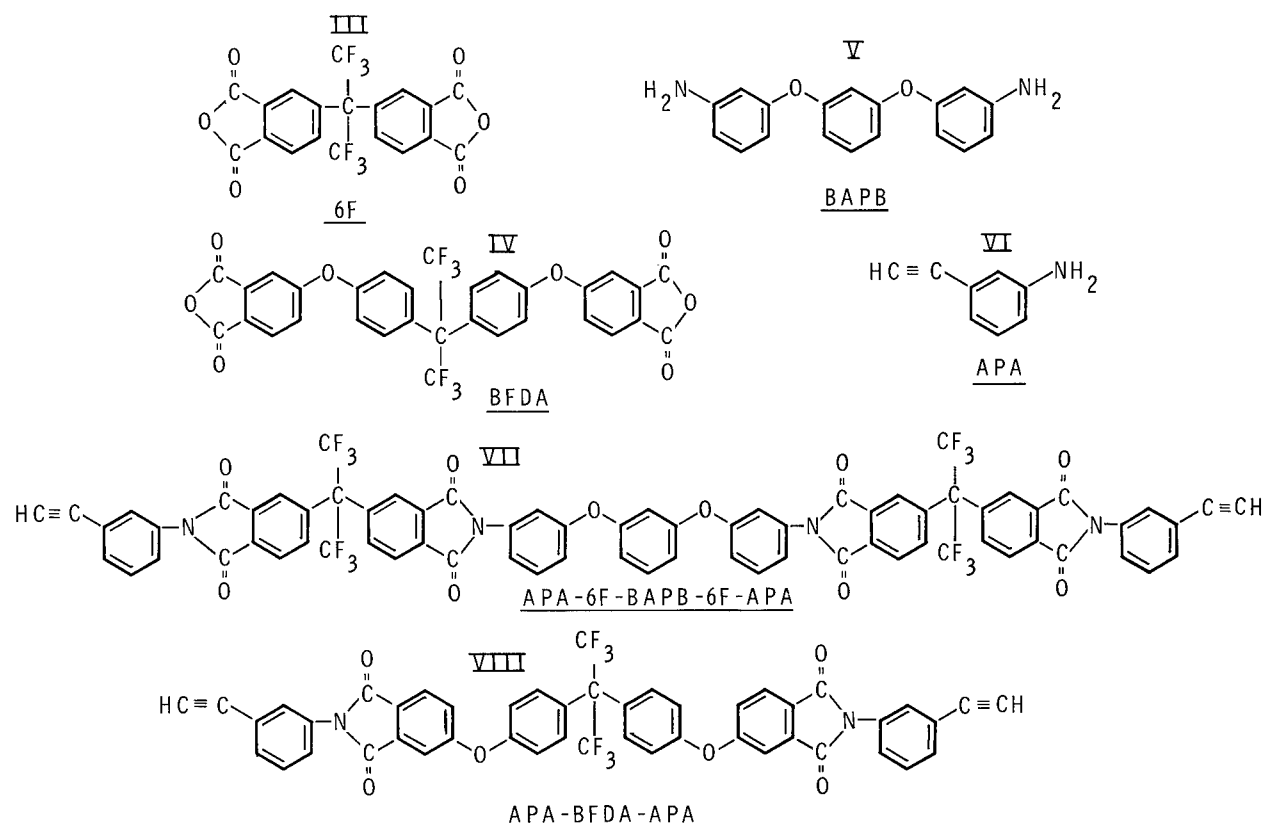


Figure 2

THERMID 600 (AMIC ACID FORM)/GRAPHITE LAMINATE CURE CYCLE

The autoclave cure cycle used for flat panels was recommended by the T-600 manufacturer and is shown in figure 3. Laminates were prepared from the amic acid form of T-600 plus diluent prepregs using this cure cycle. The postcure cycle used was:

1.4° K/min rise (2.5° F/min) to 505° K (450° F), hold for 1 hour;
rise at 0.56° K/min (1° F/min) to 589° K (600° F), hold for 4 hours;
rise at 0.56° K/min (1° F/min) to 644° K (700° F), hold for 8 hours;
cool at 1.12° K/min (2° F/min) to 366° K (200° F), and remove.

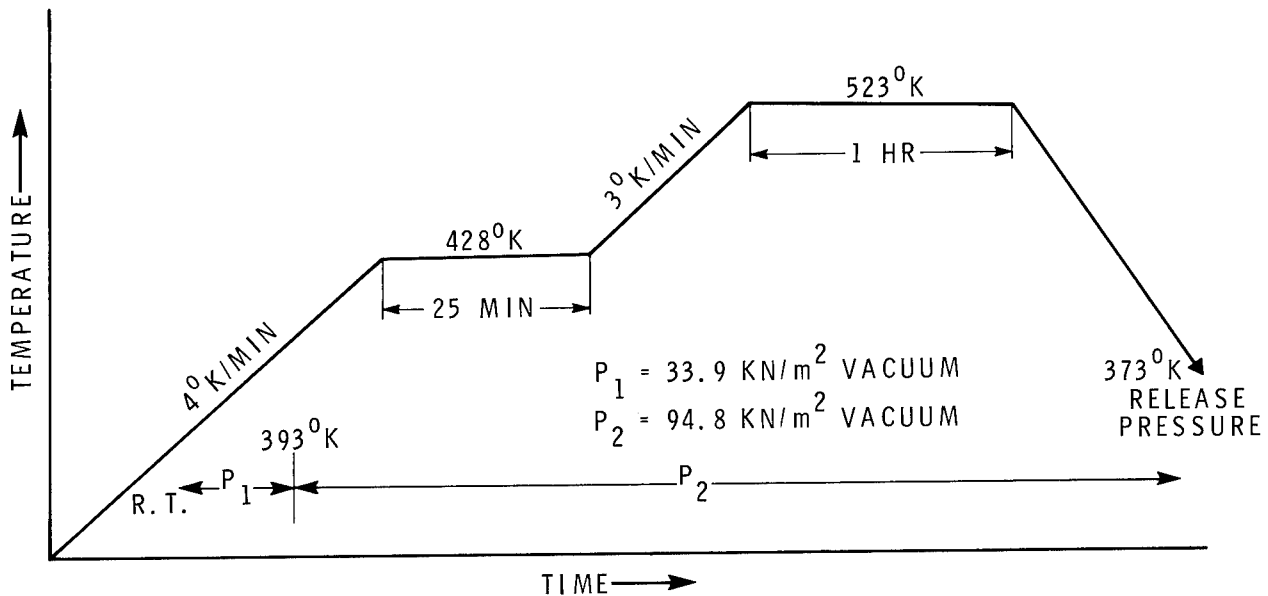


Figure 3

FABRICATION OF STRUCTURAL ELEMENTS

Fred J. Darms, Jr.
Rockwell International Corporation

EXPANDED ABSTRACT

NASA Contract NAS1-15183, "Design, Fabrication and Test of Graphite/Polyimide Specimens and Structural Elements" is part of the Composites for Advanced Space Transportation Systems (CASTS) program. It was established to assist in the development of a data base for 315C (600F) graphite/polyimides through the performance of specific tasks, assigned as requirements are defined. To date, the major effort has been directed toward the fabrication and delivery of fracture, fatigue, bolted joint, bonded joint and honeycomb sandwich specimens. Production has concentrated on graphite reinforced composites with PMR-15 matrices, although a number of specimens using NR-150B2 matrices are required.

This paper describes the laminate fabrication procedures and quality assurance ultrasonic c-scan results used for deliverable specimens on Contract NAS1-15183. These procedures are the result of processing eleven lots of graphite/PMR-15 prepreg tape materials and two lots of graphite/NR-150B2. Early processing difficulties with NR-150B2 composites have been corrected, permitting the fabrication of quality specimens from either of the two currently prescribed matrix materials. The quality of all deliverable specimens is measured by the control of fiber content, glass transition temperature, and void content, as well as laminate ultrasonic c-scan data.

PROGRAM SCOPE

Contract NAS1-15183 has concentrated on the production and delivery of Celion/PMR-15 and Celion/NR-150B2 test specimens. The scope of current task assignments is indicated by the summation of specimen requirements. This summation shows a total of 1967 specimens have been defined to date. All specimens listed are scheduled for NASA tests. Approximately 500 Celion/PMR-15 specimens have been delivered. Production of NR-150B2 specimens has recently been initiated after early processing difficulties. To date 106 kg (235 pounds) of Celion/PMR-15 have been used in producing specimens ranging in thickness from 0.053 to 0.254 cm (0.021 to 0.100 inch). This volume of material represents eleven (11) lots from a single vendor. The Celion/NR-150B2 processes are based on the use of 4.5 kg (10 pounds) of material in two (2) lots. All secondary bonds have used FM-34 adhesive with BR-34 primer. Some LARC-13 adhesive bonds are currently scheduled.

<u>SPECIMEN TYPE</u>	<u>CELION/PMR-15</u>	<u>CELION/NR-150B2</u>
FRACTURE	343	100
FATIGUE	282	282
BOLTED JOINT	55	55
BONDED JOINT		
SCARF	50	50
ANGLE LAP	220	-
HONEYCOMB SANDWICH	24	-
DEBOND	58	58
MOISTURE	-	390
TOTAL SPECIMENS	<u>1032</u>	<u>935</u>

Figure 1

SCARF JOINT SPECIMENS

The scarf joint represents one type of bonded joint specimen that has been produced under Contract NAS1-15183. These specimens use eight ply quasi-isotropic graphite/polyimide laminates for adherends and were fabricated with either a 20:1 or 40:1 taper in the scarf joint. Adherends are aligned to minimize local discontinuity stresses. The adhesive used was FM-34 with a BR-34 primer on bonded surfaces. Glass/polyimide tabs were bonded to the ends of specimens to provide for testing machine grips.



Figure 2

HONEYCOMB SANDWICH SPECIMENS

Six honeycomb sandwich specimens have been delivered to NASA. The skins were eight ply quasi-isotropic Celion/PMR-15 having a total thickness of 0.053 cm (0.021 inch). This thickness was achieved using Celion 3000 graphite/polyimide to produce a ply gage of less than 0.008 cm (0.003 inch). The HRH-327-3/8-4 honeycomb core was bonded to the face sheets with FM-34 adhesive after being filled along the load application edges with a 30/1 ratio of milled glass fiber/BR-34. Glass cloth/PMR-15 bonded at the specimen ends for load induction incorporated scalloped doublers. Finally, stainless steel strips were located at the load application ends for alignment of the test fixture to produce a pinned end fixity.

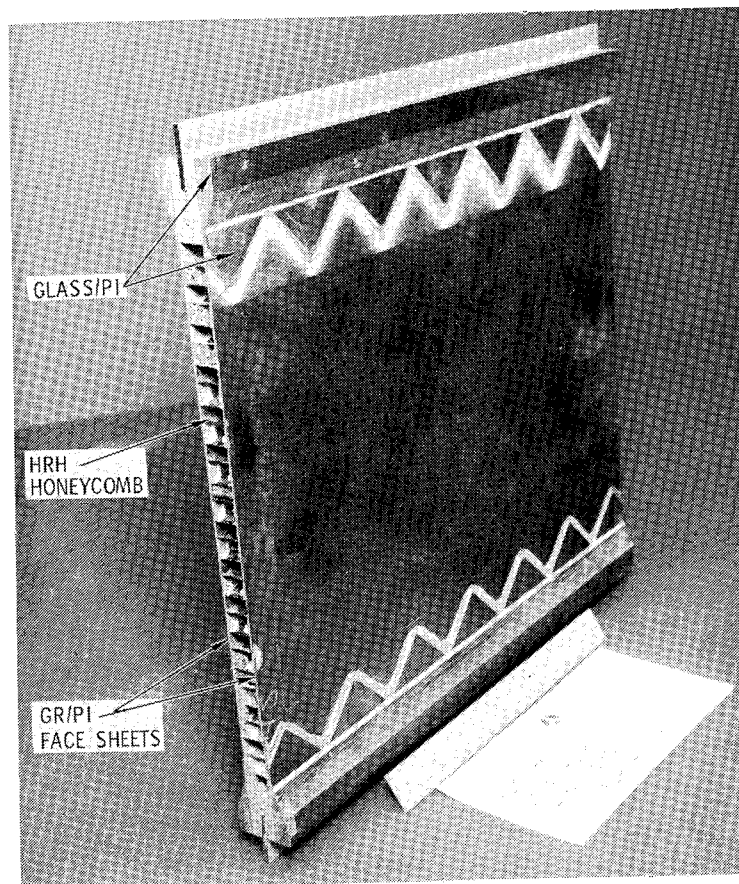


Figure 3

ADDITIONAL SPECIMEN FORMS

Three other types of graphite/polyimide specimens are being used by NASA for fracture, bolted joint and fatigue tests. The largest of these specimens is 41.9 by 10.0 cm (16.5 by 3.95 inches). Circular holes or slots are ultrasonically drilled in a majority of these specimens to provide a fracture initiation point on quasi-isotropic, ± 45 and other laminate orientations.

The second specimen form is 17.8 cm (7.0 inch) long and of various widths. The center hole of the five hole pattern is reinforced on both sides of the sixteen ply quasi-isotropic laminate with glass cloth/PMR-15 doublers. The secondary bond of these doublers is accomplished with epoxy to provide room temperature data.

The third specimen is fabricated from an eight ply quasi-isotropic laminate. A four hole pattern at each end provides for test fixture attachment. A hole is also positioned in the center of the test section.

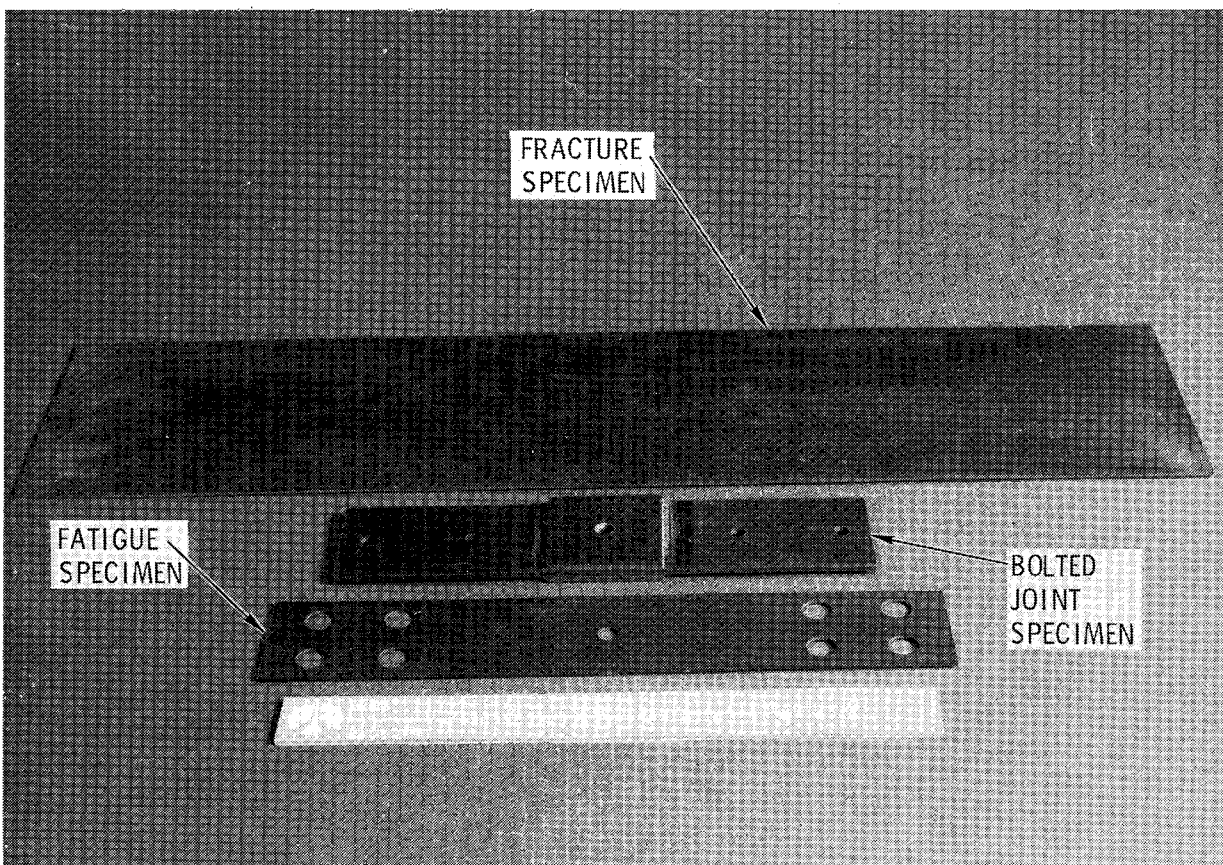


Figure 4

KEY ISSUES

The purpose of the Contract NAS1-15183 program is to produce test specimens that will provide reasonable and consistent data for the interpretation of the effects of design and material variables. This objective can only be accomplished with the production of high quality laminates from which the specimens are machined. The key issues involved in the production of these laminates have been defined. They encompass material control, process control and the techniques used to evaluate laminate quality. This paper will focus on the laminating process used to produce graphite/PMR-15 and graphite/NR-150B2 specimens and the types of c-scan defects noted during the processing of more than 110 kg (242 lb) of material.

MATERIAL CONTROL

- FIBER AREAL DENSITY
- RESIN SOLIDS PERCENT
- VOLATILES CONTENT

PROCESS CONTROL



- AUTOMATIC AUTOCLAVE CONTROL
- CONTINUOUS PRESSURE, TEMPERATURE & VACUUM RECORDING

LAMINATE QUALITY



- FIBER & VOID CONTENT
- THICKNESS
- GLASS TRANSITION TEMPERATURE
- ULTRASONIC C-SCAN TO NASA STANDARDS

Figure 5

CELION/PMR-15 PROCESS

A two-step process is used to cure graphite/PMR-15 laminates. The staging step is performed in an oven at a vacuum of 3.4×10^4 Pag (10 inches of Hg). The laminate is bagged with bleeder paper top and bottom, vacuum is drawn and the temperature increased at a constant rate to 210C (410F) in two hours. The hold time is regulated to give the proper fiber content based on the batch of material and laminate thickness. After the hold time, the temperature is reduced in one hour to 66C (150F) at a uniform rate. Vacuum is released at this temperature.

Final cure is achieved in an autoclave after rebagging the laminate and applying glass cloth bleeder plies. Full vacuum and 10.3×10^5 Pag (150 psig) pressure is applied. The temperature is increased to 249C (480F) at a uniform rate over a two and one-quarter hour time period. Pressure is increased to 13.8×10^5 Pag (200 psig) and the temperature held for 40 minutes. After the hold time, the temperature is increased to 329C (625F) in 45 minutes. Finally, the temperature is held at 329C (625F) for three hours before decreasing the temperature to 66C (150F) and releasing pressure and vacuum.

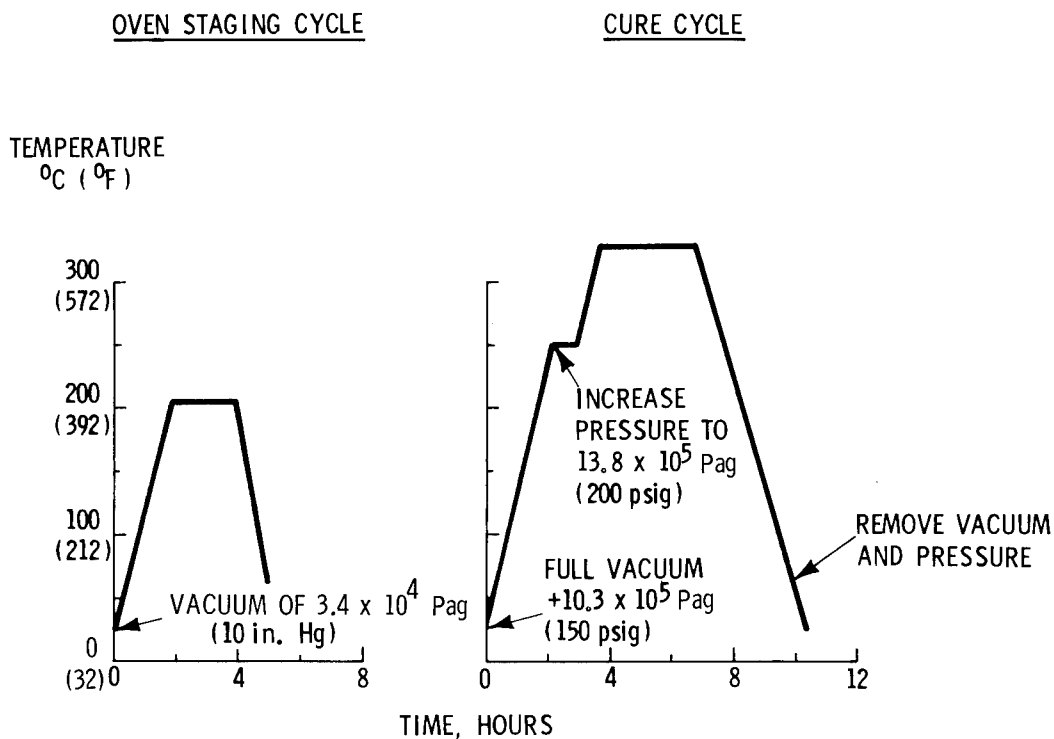


Figure 6

CELION/NR-150B2 PROCESS

The graphite/NR-150B2 laminates are cured in a two-step process, designated the cure and post cure processes. The cure process, which is accomplished in an autoclave, is primarily a zero resin loss procedure using material with a resin content that has been gaged to produce a laminate fiber volume of 60 ± 2 percent. Resin flow is restricted using cell-guard material separated from the laminate by teflon coated cloth. The purpose of this material is to contain the resin solids while permitting the escape of volatiles.

The post cure step may be accomplished in either an autoclave or a press with a heated platen. Glass cloth breather plies are used on each side of the laminate. For press cure, the vacuum is not required. The maximum pressure for either post cure process is 13.8×10^5 Pag (200 psig).

TEMPERATURE
°C (°F)

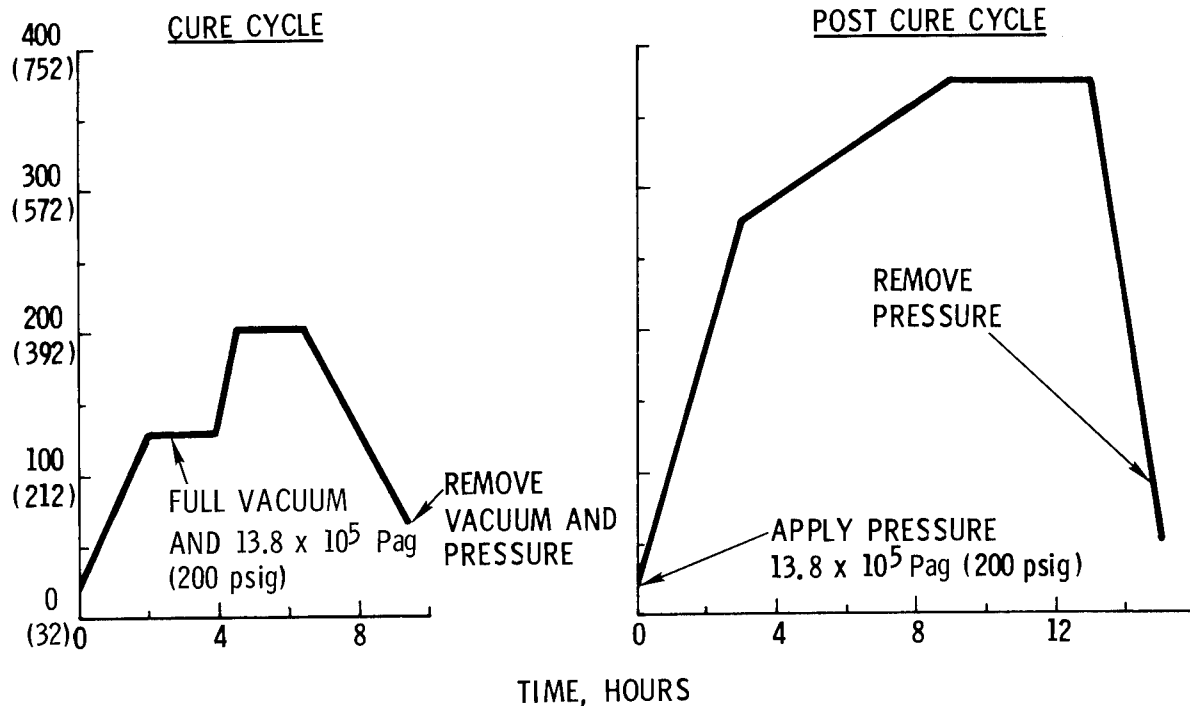
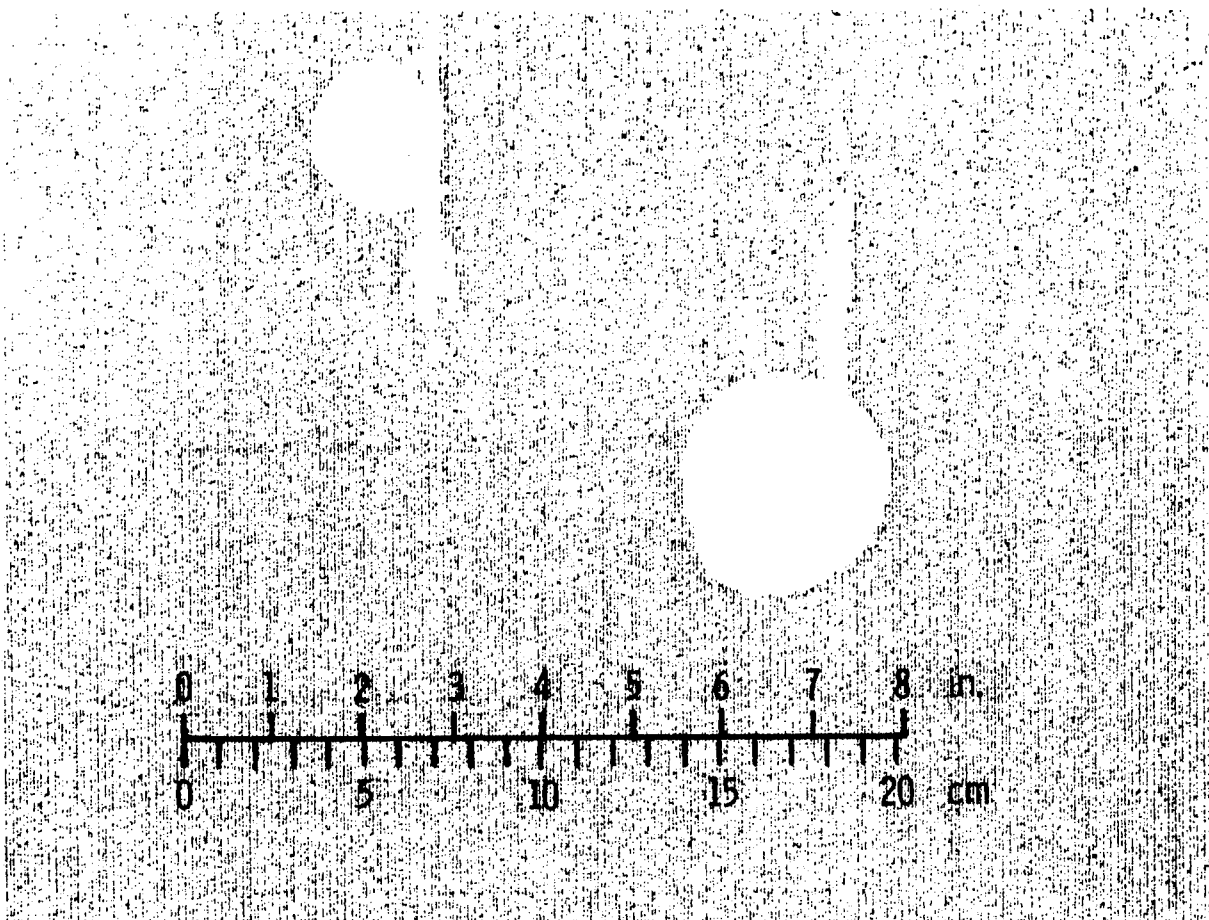


Figure 7

LARGE DELAMINATION TYPE DEFECTS

The large delamination defects were prevalent in early graphite/PMR-15 production laminates. This defect is characterized by a nearly circular delamination, usually near the center of the laminate thickness. A tail is often attached to the circular portion. This tail parallels the fiber direction of the layer(s) adjacent to the defect. Defect diameters to 10 cm have been noted.

The cause of the defect is now known. However, the defect was not noted in laminates after the staging temperature was increased from 205C (400F) to 210C (410F). The disappearance of this defect and the emergence of a short linear defect as the common form may mean that the large delamination is a low temperature version of the short linear defect.



PANEL CP8C-37

(0/45/90/-45)_S

Figure 8

EFFECT OF THIN PREPREG EDGES

The defects in laminates produced by thin and split prepreg tape edges are viewed by ultrasonic c-scan as a series of linear voids. These linear voids are spaced at the tape width in each lamina. The problem is most severe at lamina crossover points where two adjacent layers accentuate the dryness of the material edge.

Trimming of the prepreg tape edges by 1.27 to 2.54 cm (0.5 to 1.0 inch) produced good c-scan quality laminates; but increased the prepreg scrap rate. Cure without caul plates consolidated the laminate and produced good c-scans at the sacrifice of thickness uniformity.

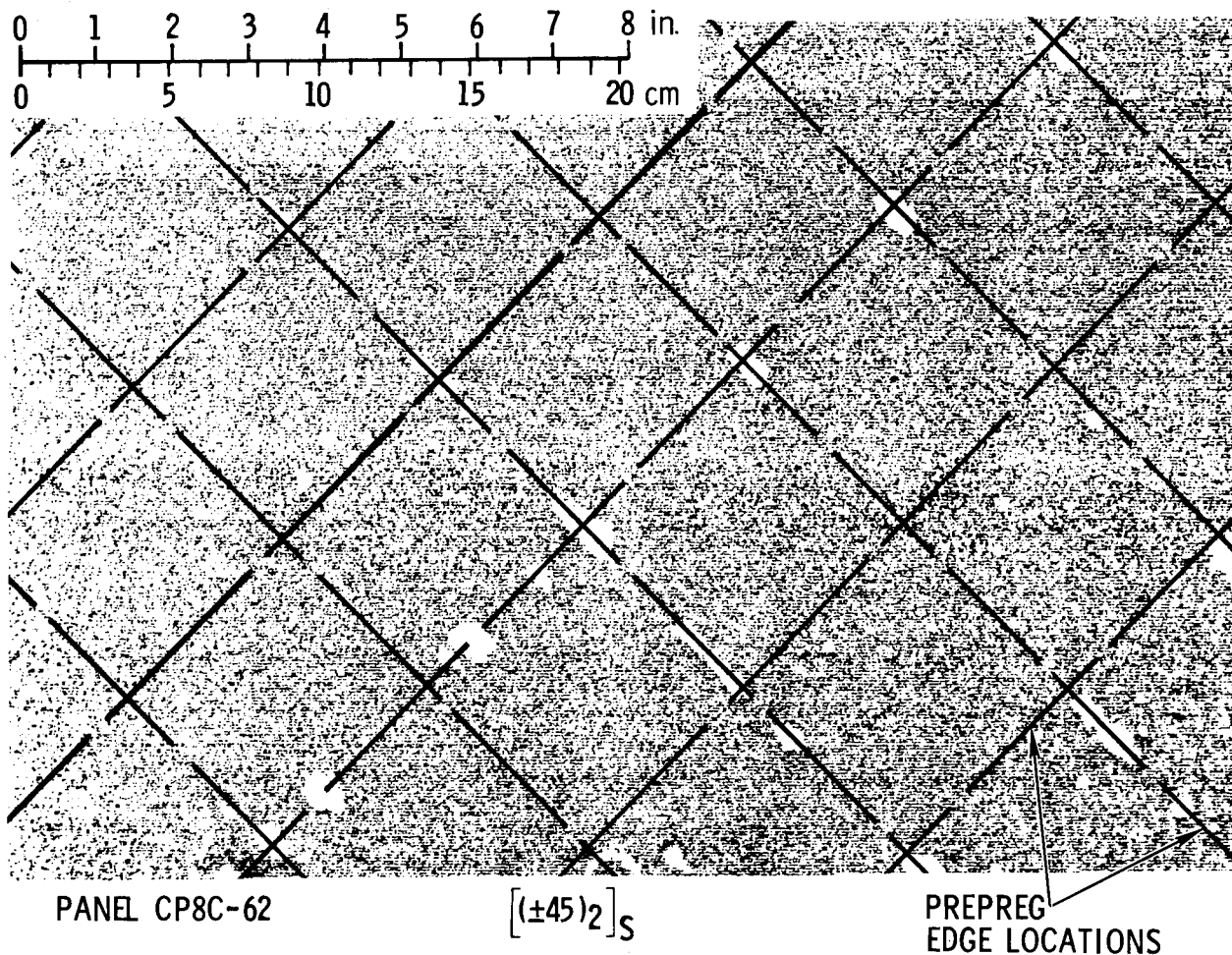


Figure 9

TYPICAL DEFECTS ASSOCIATED WITH TOW SPLICES

The presence of tow splices in the prepreg tape appears to produce random linear voids in the ultrasonic c-scan data. These defects are typically 2.54 cm (1.0 inch) long by 0.32 cm (1/8 inch) wide. The anomaly sometimes is associated with a surface blemish.

Increased surveillance during cutting of prepreg tape has resulted in the reduction of the incidence of this type of defect. The need to perform this inspection, however, does impact laminate layup time.

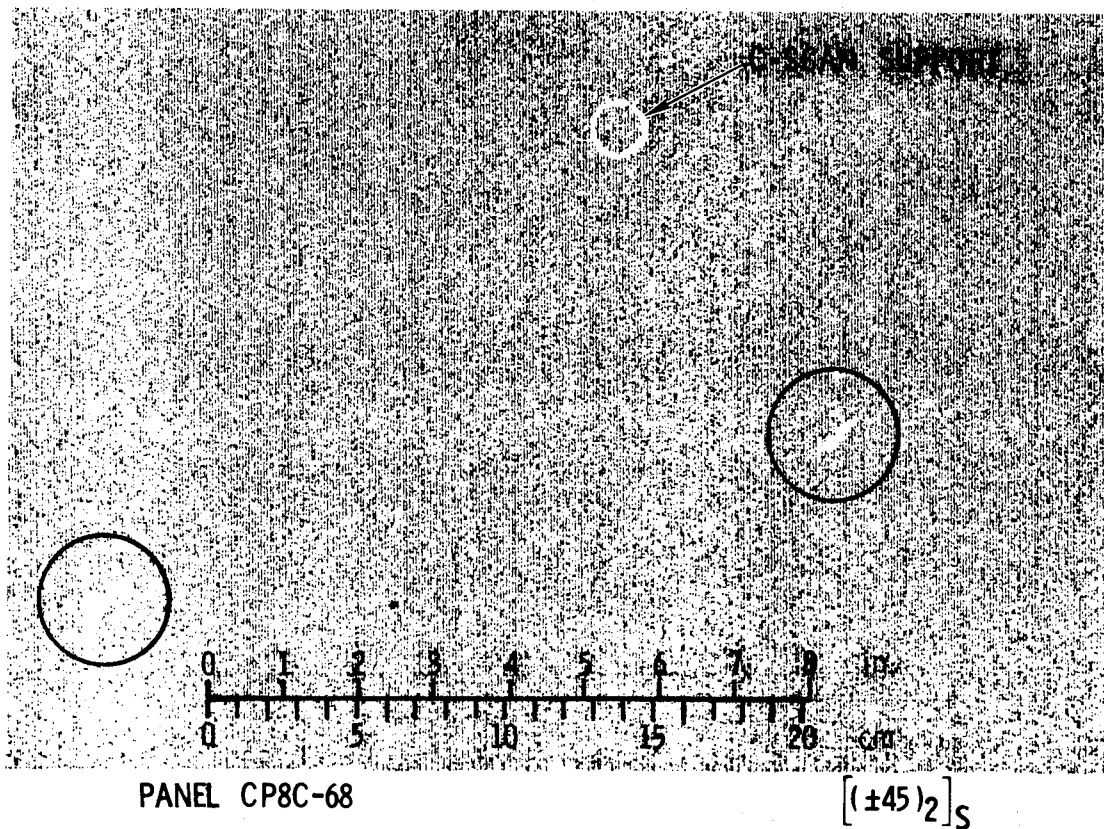


Figure 10

C-SCAN DEFECTS CAUSED BY TOW SPLICES

Two types of tow splices have been experienced in vendor supplied prepreg tape. One is produced by the fiber manufacturer and one occurs because of tow splicing during the prepreg operations. The fiber manufacturer's splice is of the order of 1.3 cm long and uses "airplane cement." They have not defined the chemical composition. The prepreg supplier's splice is from 5 to 10 cm long and is made with cellulose acetate. The materials in both splices are considered undesirable from the standpoint of quality polyimide laminate production since low temperature volatilization and dry areas can be expected. Current fabrication policy is to remove these splices when located by either visual methods or by vendor's tags.

In one instance a crossing pattern of splices was found. It was created by a splice in each of the two outer layers of a production laminate. This pattern was visible in the cured laminate and also appeared in the ultrasonic c-scan.

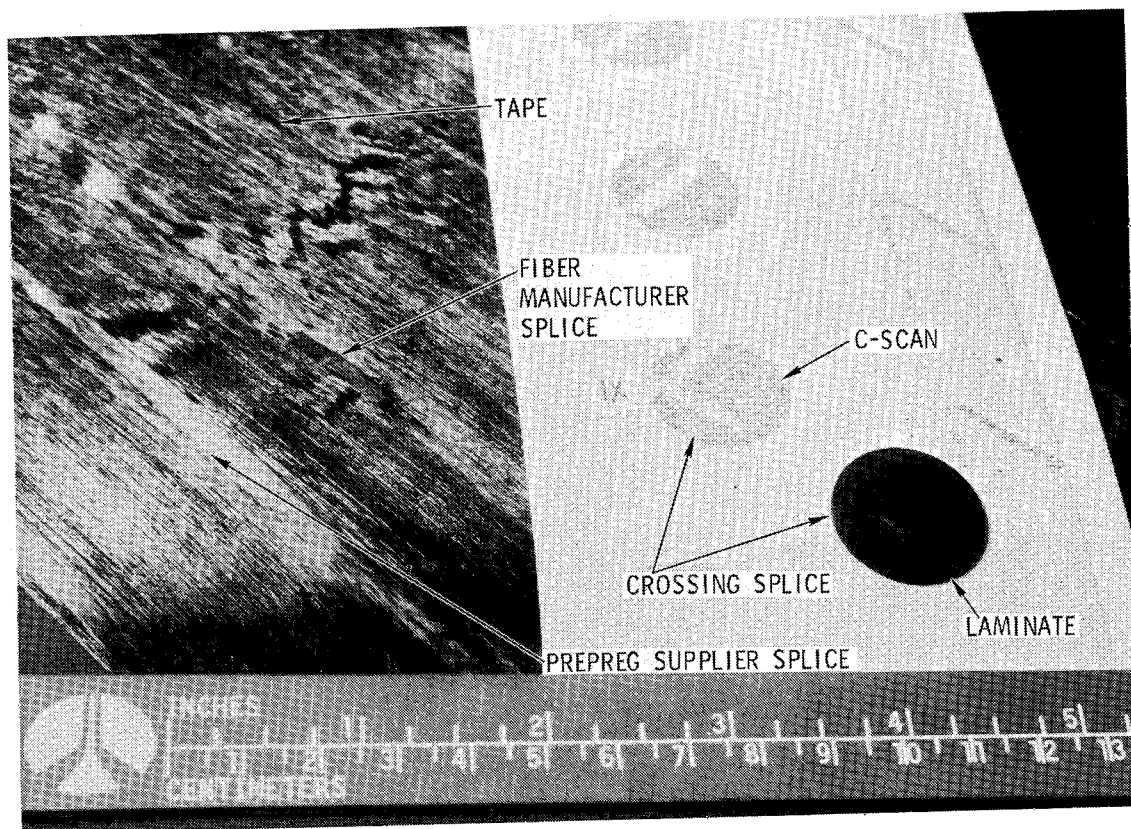


Figure 11

POLYIMIDE ADHESIVE BONDING

Donald Progar
NASA Langley Research Center

EXPANDED ABSTRACT

Little published literature is available on the bonding of high performance, high temperature composites for use at 589K (600°F). The purpose of this study was to screen and select adhesive systems which could be used to bond composite-to-composite, composite-to-titanium and honeycomb sandwich structures with operational capability at 589K for a minimum of 125 hours. Selection of candidate adhesives was based on previous experience and reported data on high temperature metal-to-metal bonding. The adhesives initially selected for screening were American Cyanamid's FM-34 and FM-34B-18, NASA Langley Research Center's LARC-13, polyphenylquinoxaline (PPQ), Dupont's NR056X and Rhodia's Nolimid A380.

Evaluations were based on mechanical property tests such as lap shear and flatwise tensile and on processability. Quasi-isotropic Celion 6000/PMR-15 composite adherend was used to construct lap shear and flatwise tensile specimens. Hexcel's HRH-327-3/16-6.0 glass-polyimide honeycomb core was also utilized in the flatwise tensile specimens. The screening program included room temperature and 589K mechanical property tests for as-fabricated specimens and thermally aged (125 hr/589K) or moisture aged (24-hour water boil and 30-day 95 percent relative humidity/344K) specimens. Numerous processing variations were also studied that led to selected cure cycles for each adhesive. Shear specimens having either 12 mm (0.5 in.) or 75 mm (3 in.) overlaps were used to determine the effect of bond size on processability and lap shear properties.

The data indicate that processing of FM-34, FM-34B-18, LARC-13 and NR056X can be achieved using a cure compatible with the composite adherend. No significant differences in mechanical properties were observed among the three adhesive systems and all three are suitable candidates for 589K/125 hour service.

CANDIDATE ADHESIVES

The adhesives initially chosen for screening are listed in Figure 1. Selection was based on previous experience and literature reports on high temperature metal-to-metal bonding (ref. 1-6). FM-34, NR056X and Nolimid A380 are condensation-type polyimides; LARC-13 is an addition-type polyimide.

FM-34 adhesive tape consists of a polyamic acid (polyimide prepolymer) filled with aluminum powder and supported on style 112 glass cloth containing a Volan A finish. FM-34B-18 is a formulation of FM-34 without arsenic additives. Bloomingdale Department of the American Cyanamid Company manufactures FM-34 and FM-34B-18.

LARC-13 adhesive was developed at the Langley Research Center and is made from benzophenone tetracarboxylic dianhydride (BTDA), m,m'-methylene dianiline (m,m'-MDA) and nadic anhydride (NA) in dimethylformamide (DMF) (ref. 3).

NR056X, developed by Dupont under NASA contract NAS1-14620, is an adhesive version of the NR150 polymer family. Dupont supplies the resin as a monomeric solution of 6F tetraacid, p-phenylene diamine (PPD) and oxydianiline (ODA) in diglyme (ref. 5).

Nolimid A380 was supplied by Rhodia but has since been discontinued, and therefore, was dropped from the program. PPQ had a processing temperature which exceeded the temperature limitation of the composite adherend and was also dropped from the program.

ADHESIVE	SUPPLIER	PRIMER	DESCRIPTION
FM-34	AM. CYAN.	BR-34	COND. PI, AI, 112-VOLAN A, ARSENIC
FM-34B-18	AM. CYAN.	BR-34B-18	COND. PI, AI, 112-VOLANA, NO ARSENIC
LARC-13	LaRC	LARC-13	} ADDN. PI, AI, 112-A1100 BTDA; m, m'-MDA; NA (DMF)
LARC-13	LaRC	BR-34	
NR056X	DU PONT	NR056X	COND. PI, AI, 112-A1100 3:1 PPD:ODA; 6F (DIGLYME)
NOLIMID A380	RHODIA	605	COND. PI, AI, 112, ARSENIC AB MONOMER
PPQ	LaRC	PPQ	THERMOPLASTIC, 112-A1100 m-PBB, TABP (1:1 mCRESOL:XYLENE)

Figure 1

PROCESSING CYCLES

Processing cycles for each adhesive had to be developed which would be compatible with Celion 6000/PMR-15 composite adherend of $(0,+45^\circ,90^\circ-45^\circ)_s$ orientation. The maximum processing temperature was dictated by the thermal limit of the composite, 616K (650°F). The cure and postcure cycle for FM-34 which provided the best results is given in Figure 2. Vacuum and 1.38MPa (200 psi) were maintained throughout the cure cycle. Cool-down rate was not greater than 5.6K/min (10°F/min) and specimens were postcured in a forced-air oven. Pressure during bonding of flatwise tensile specimens was limited to 0.34MPa (50 psi) to preclude crushing or damaging the glass-polyimide honeycomb core. The processing cycle for LARC-13 was determined empirically by varying the bonding parameters. The best processing cycle of those investigated is given in Figure 2. The processing cycle developed for NR056X adhesive was a modification of that suggested by Dupont (ref. 5) and is shown in Figure 2. The higher pressure, 2.07MPa (300 psi), and the higher cure and postcure temperatures used to bond 2.79 mm (0.11 in.) thick unidirectional HTS/PMR-15 adherends produced lap shear strength values comparable to Dupont's unidirectional graphite/NR150B2 test results. As with the other two adhesives, vacuum was maintained throughout the cure cycle. Although various bonding parameters were investigated during the program, the final processing cycles that were used were not optimized and only represent the best of those studied.

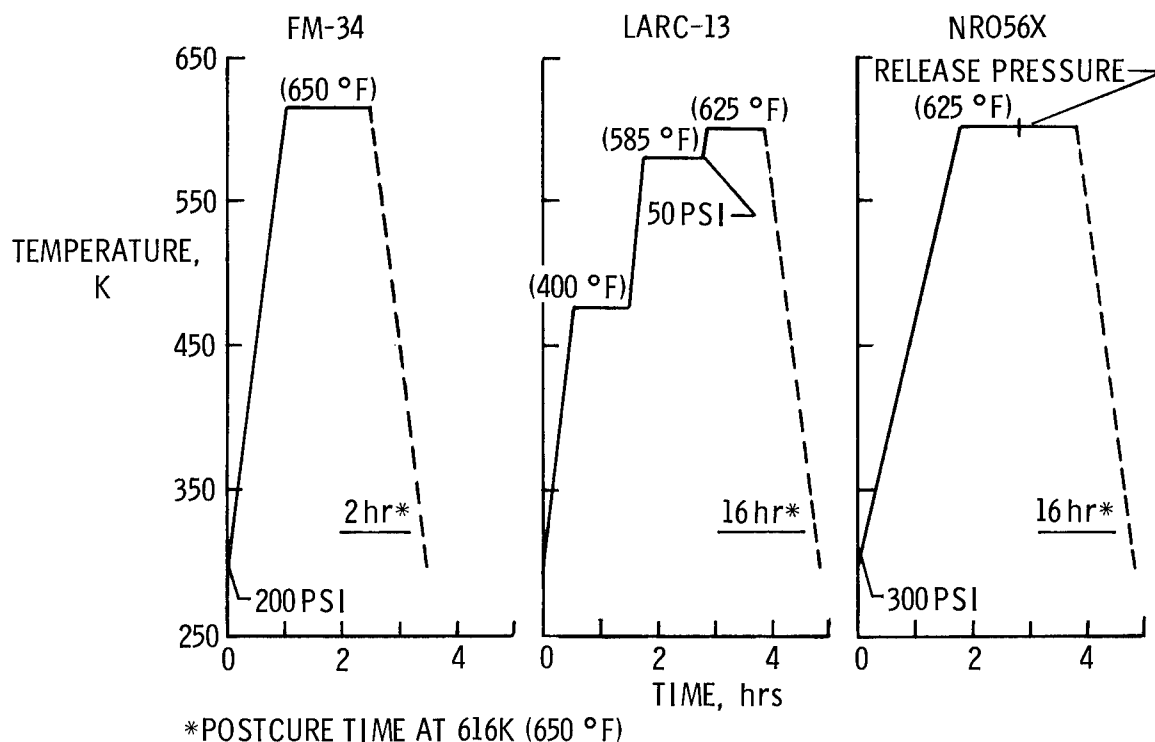


Figure 2

LAP SHEAR SPECIMEN AND TEST PROCEDURE

Composite lap shear test specimen configuration was adapted from ASTM D-1002. The specimen consists of two 25 mm (1.0 in.) wide by 65 mm (4.0 in.) long adherends bonded with a 12 mm (0.5 in.) overlap (Figure 3). Room temperature (RT) and 589K tests were conducted on an Instron Universal Testing Instrument. Specimens were heated in a clamshell quartz-lamp oven to 589K and held 10 minutes before testing.

The Celion 6000/PMR-15 composite adherends were fabricated in-house and were 1.143 ± 0.127 mm (0.045 ± 0.005 in.) thick. The quality of the composite was determined by ultrasonic inspection.

Test results are not reported for the composite-to-titanium lap shear specimens since the data were similar to those obtained for the composite-to-composite bonds.

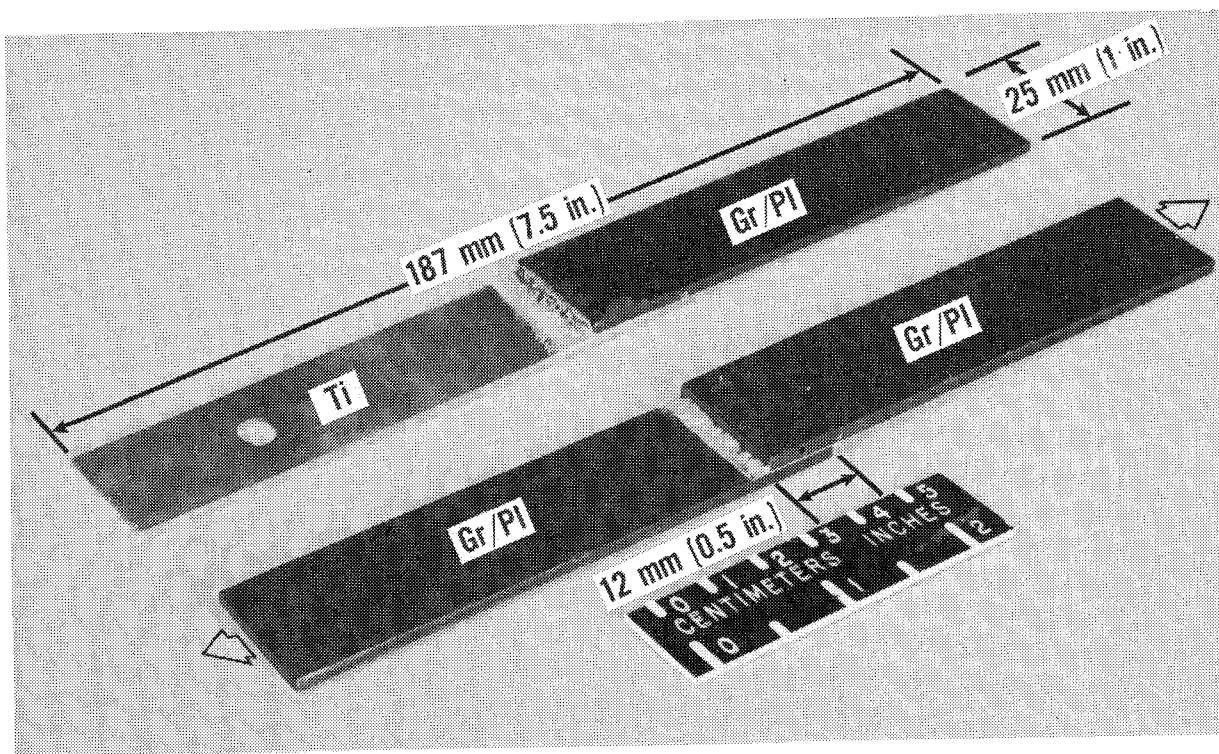


Figure 3

FAILED LAP SHEAR SPECIMENS

Typical surfaces of failed lap shear specimens tested at RT and 589K are shown in figure 4. Failures at RT were 70-100 percent shear in the first ply (zero orientation) of the composite. At 589K failures were 100 percent cohesive.

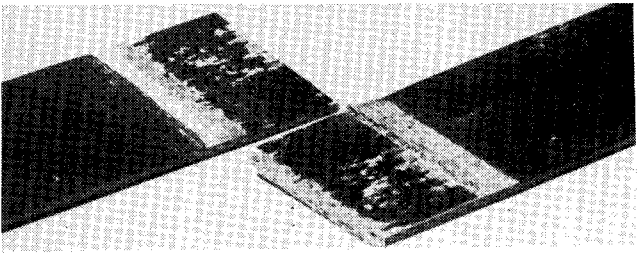
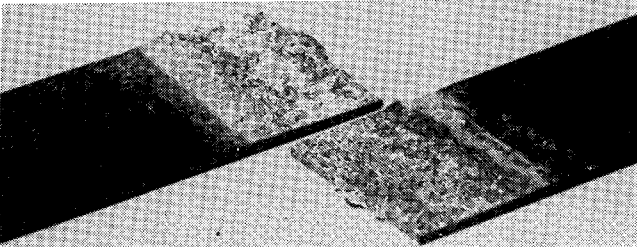
SURFACE	TEST TEMPERATURE	FAILURE MODE
	ROOM	70 - 100% COMPOSITE FAILURE
	589K (600 °F)	100% COHESIVE

Figure 4

LAP SHEAR STRENGTH OF FM-34 ADHESIVES

Concern for materials containing toxic or possible carcinogenic substances led to a study comparing lap shear strength of FM-34 (with arsenic compound) and FM-34B-18 (without arsenic compound). Tests were conducted at RT and 589K on unaged specimens and specimens aged at 589K for 125 hours. Each bar in figure 5 represents the average of four (4) test values. No significant differences were observed in the lap shear strengths of the two adhesives for the test temperatures or exposure conditions investigated.

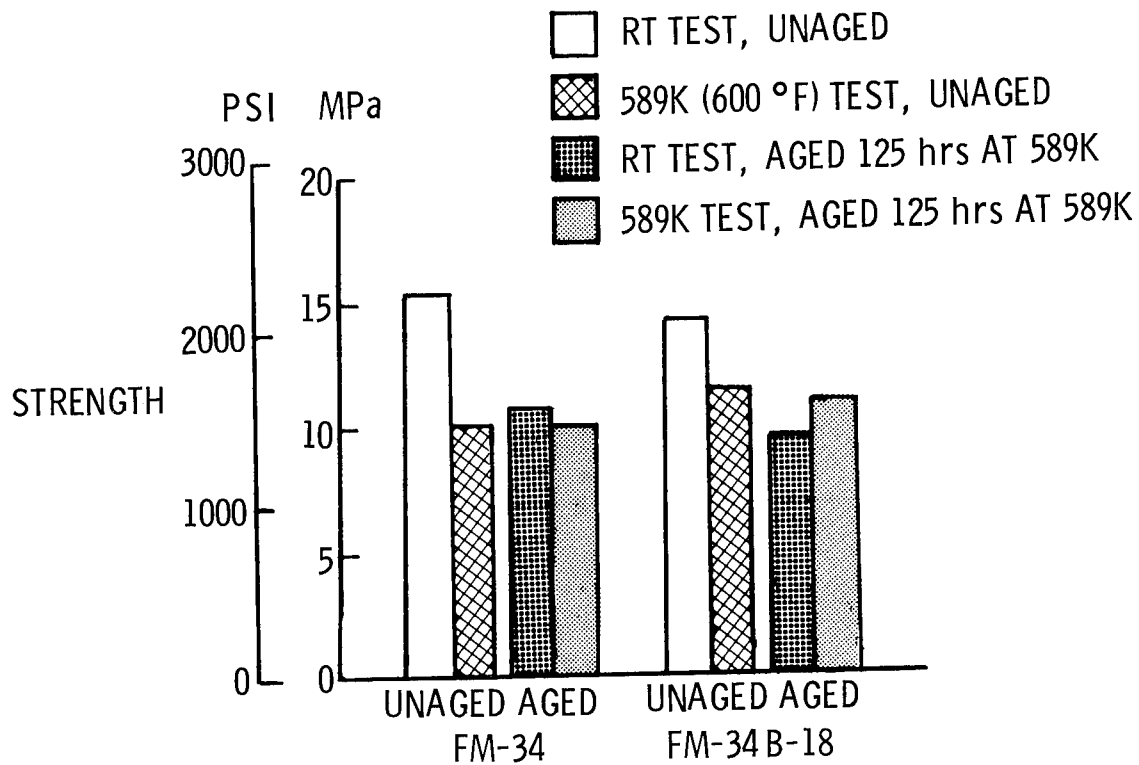


Figure 5

LAP SHEAR STRENGTH OF LARC-13 ADHESIVE

The use of a more protective primer coating (such as BR-34) instead of LARC-13 solution containing aluminum powder on the Celion 6000/PMR-15 composite adherend would be expected to improve the long-term aging (125 hours) of the composite adherend and the bonded joint. As shown in figure 6, the lap shear strength values of unaged specimens at RT and 589K are about the same for both systems. When BR-34, the primer for FM-34, was used in conjunction with LARC-13 adhesive, an improvement in the lap shear strengths for specimens aged 125 hours at 589K was realized. A 58 percent increase in the RT strengths and a 34 percent increase in the 589K values were observed.

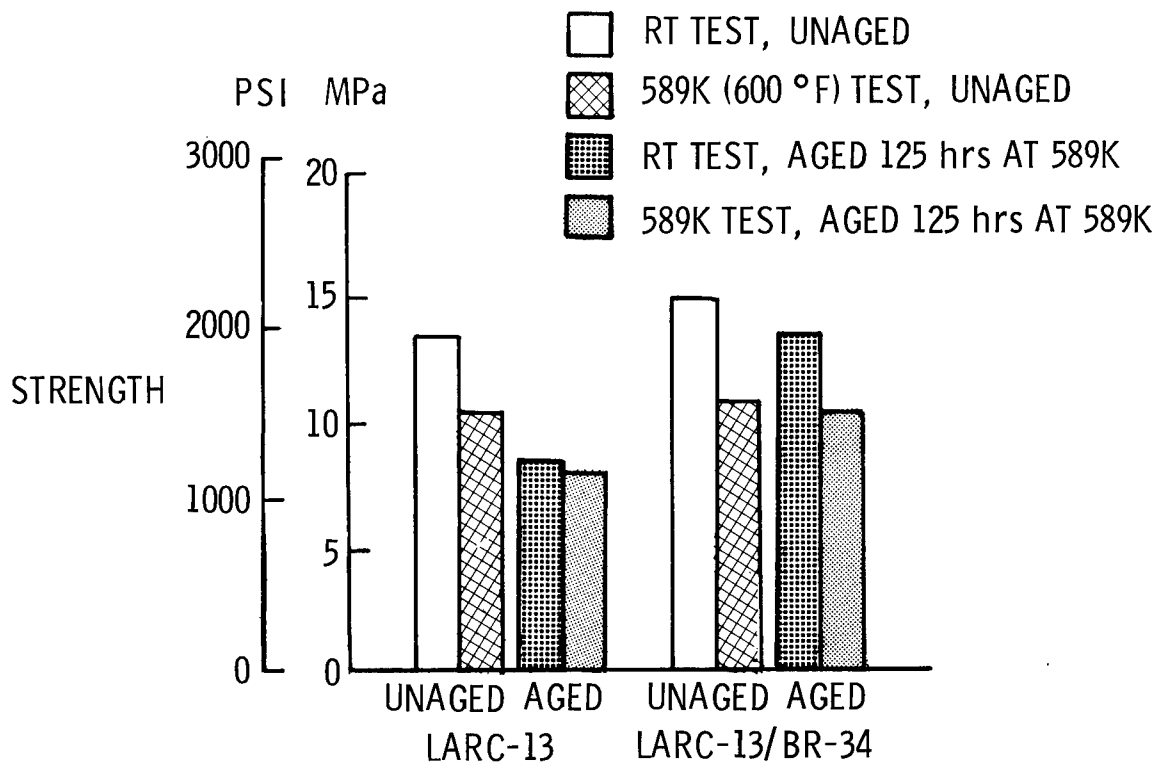


Figure 6

COMPARISON OF LAP SHEAR STRENGTHS

Lap shear strengths of composite-to-composite specimens bonded with FM-34B-18, LARC-13/BR-34 and NRO56X are compared in figure 7. Elevated temperature shear values for FM-34B-18 and LARC-13/BR-34 adhesives were similar. More variation was seen in the RT shear values of these two materials after exposure to 589K for 125 hours but since the failures were in the composite, the test was not indicative of the adhesive's true strength but of possible variability in composite properties. The 589K shear values of NRO56X unaged and aged specimens were lower than those of the other two adhesives.

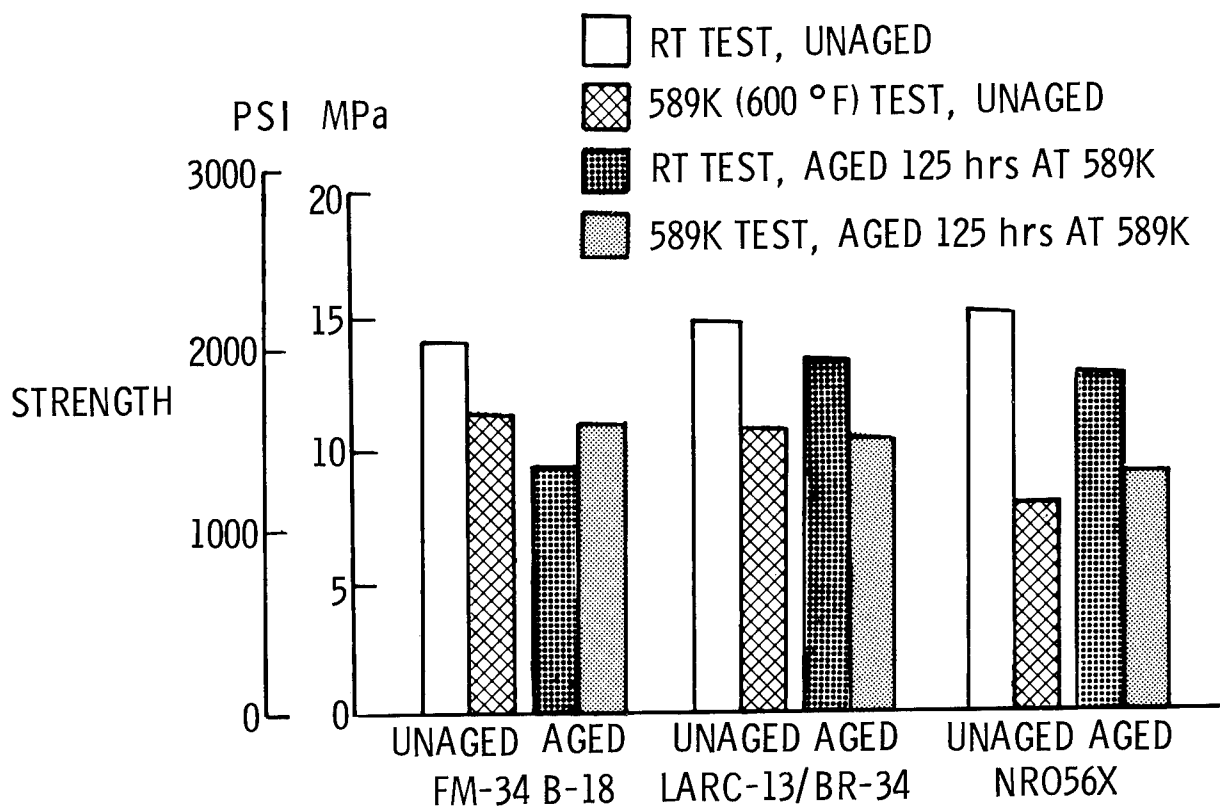


Figure 7

EFFECT OF MOISTURE ON 589K (600°F) LAP SHEAR STRENGTH

To determine the effect of moisture on joint strength, lap shear specimens were exposed to a 24 hour water boil and to 95 percent relative humidity (R.H.) at 344K (160°F) for 30 days. For the former, specimens were immersed for 24 hours in boiling distilled water, then tested within 10 minutes after removal from the water. Thirty day humidity exposures were conducted in a temperature-humidity controlled bell-jar. Specimens were then removed and stored in a zip-loc plastic bag containing a damp paper towel for approximately 30 minutes before testing.

In the grips of the test instrument, they were heated to 589K in approximately four (4) minutes, then failed four (4) minutes after load application. A high heat-up rate was used in order to retain as much of the moisture as possible during the test. The high heat-up rate caused some blistering of the composite adherend.

As was observed throughout the study, all joint failures from the elevated temperature tests were cohesive. No significant differences between FM-34 and LARC-13 were observed for the as-fabricated and water boil exposures (figure 8). FM-34 specimens exposed for 30 days to 95 percent R. H. and 344K decreased from 10.6MPa (1530 psi) to 7.6MPa (1100 psi), a 28 percent decrease. LARC-13/BR-34, for the same exposure, decreased from 9.2MPa (1340 psi) to 8.3MPa (1200 psi), a 10 percent decrease.

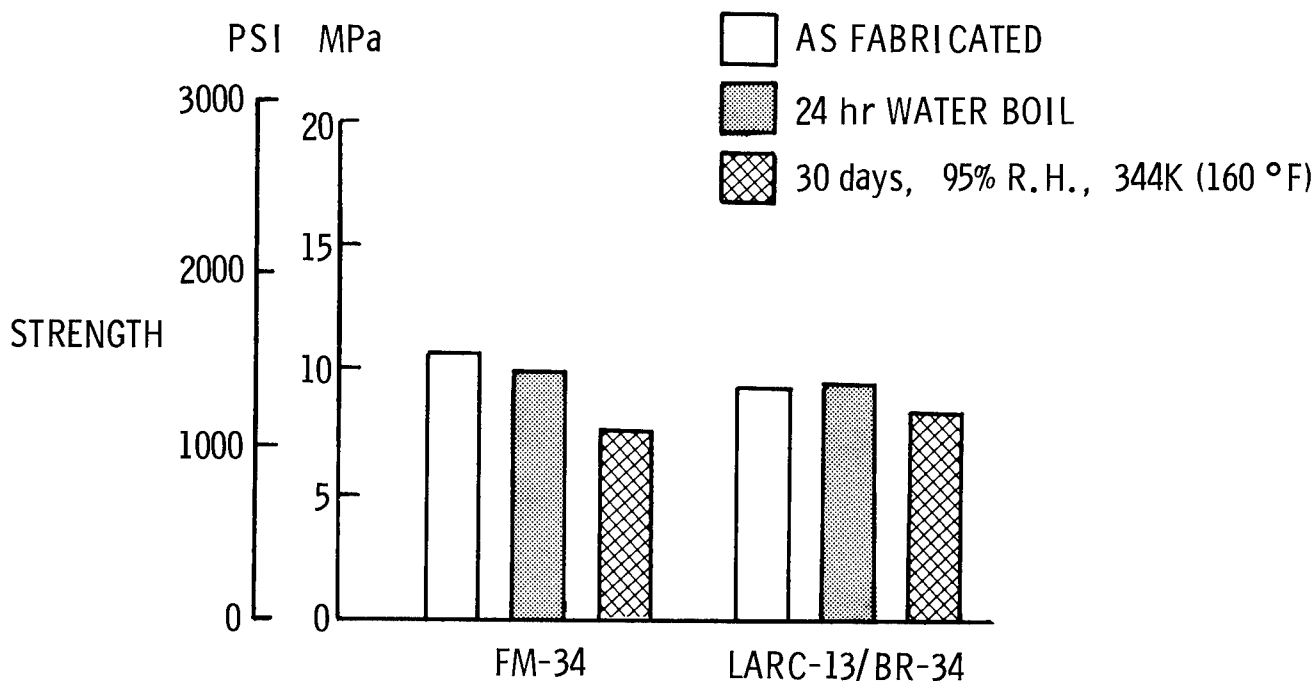


Figure 8

BOND AREA SCALE-UP

The data given in figures 5-8 were obtained from 12 mm (0.5 in.) overlap specimens fabricated and cut as shown in figure 9. The data given in figure 10 were obtained from specimens with a 75 mm (3 in.) overlap, fabricated and cut as shown in figure 9. The 75 mm overlap specimen was used to simulate the maximum area that would ultimately be employed in bonding face sheet to stringers in the shuttle aft body flap.

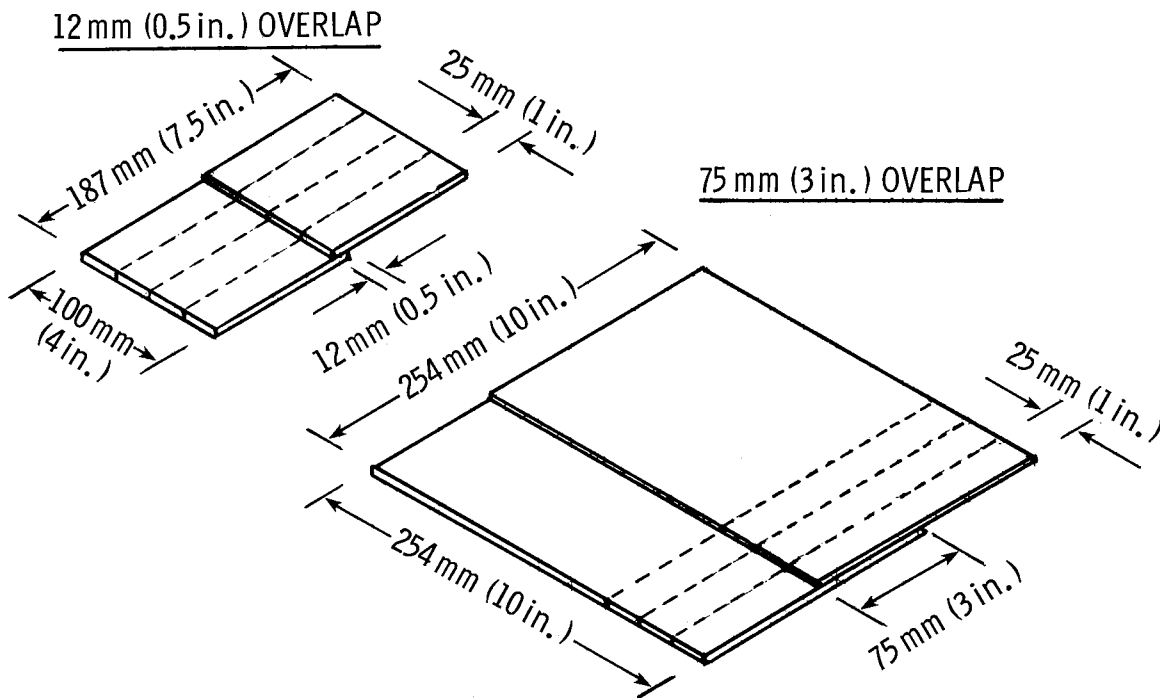


Figure 9

LAP SHEAR STRENGTH OF 75 mm (3 in.) OVERLAP SPECIMENS

Lap shear strengths for 75 mm (3 in.) overlap specimens tested at RT and 589K (600°F) are shown in figure 10. RT tests produced shear failures in the composite first ply (zero direction ply) so no significant differences in shear strengths were observed. Specimens tested at 589K failed primarily cohesively with FM-34 approximately 15 percent lower than either LARC-13/BR-34 or NR056X.

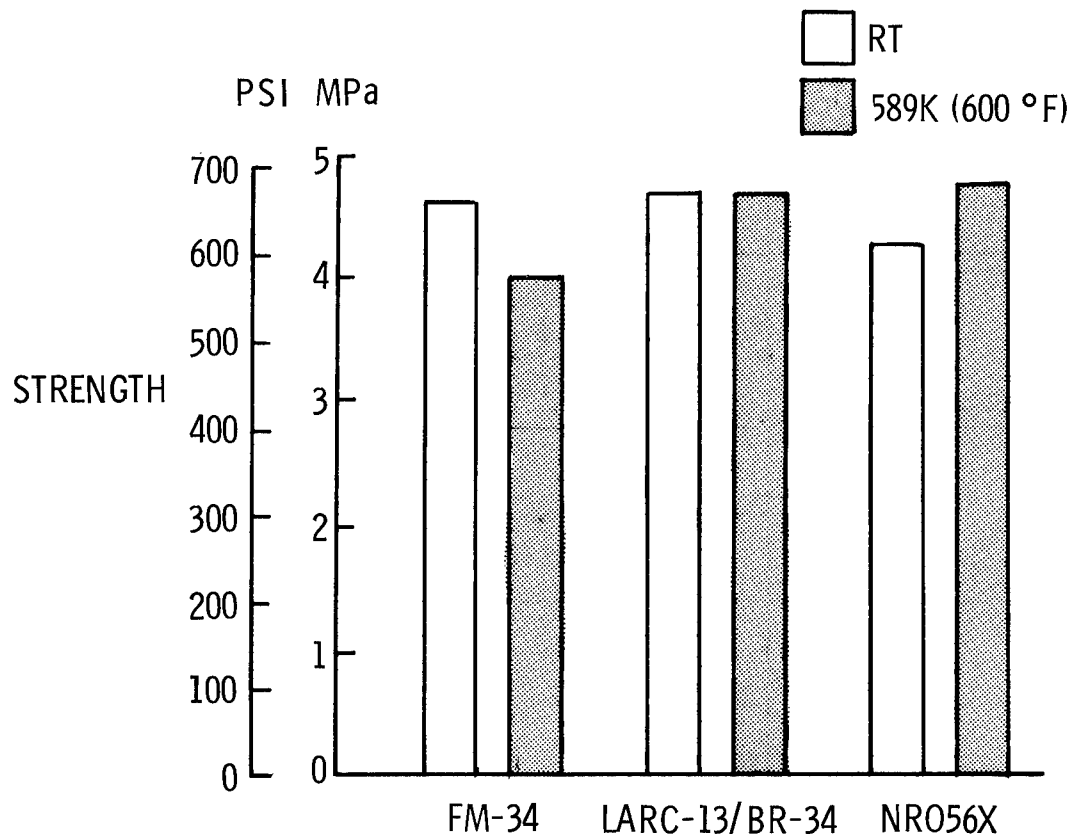


Figure 10

FLATWISE TENSILE TEST

For the flatwise tensile test 75 mm (3 in.) square specimens (figure 11) were cut from a 330 mm (13 in.) square sandwich structure which had been fabricated in-house from Celion 6000/PMR-15 quasi-isotropic face sheets, the adhesive under evaluation, and Hexel's HRH-327-3/16-6.0 perforated glass-polyimide honeycomb core. Stainless steel blocks were bonded to the face sheets with HT-424 adhesive (American Cyanamid Company). Aged specimens were bonded to the steel blocks after they had been exposed for 125 hours at 589K. Perforations were made by drilling through each cell of the core with a pointed metal rod.

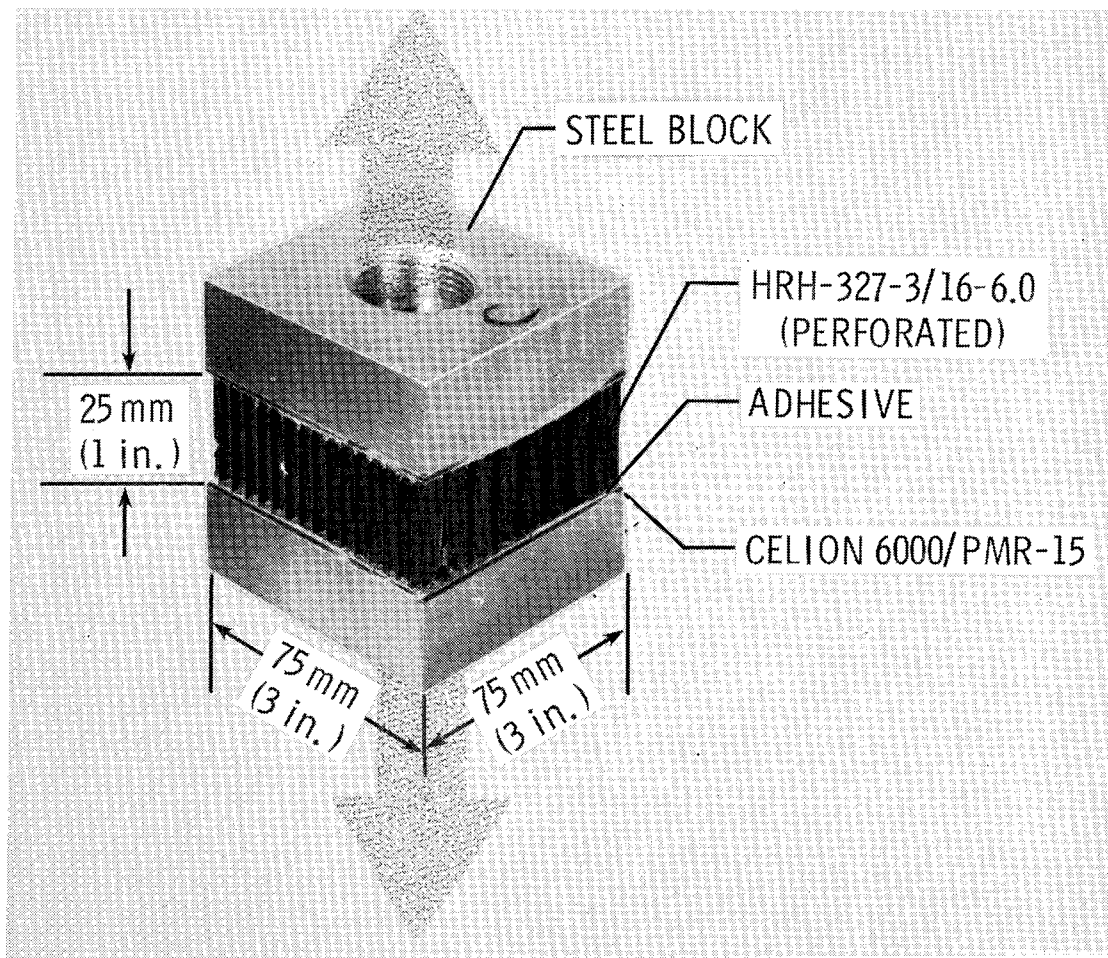


Figure 11

FAILED FLATWISE TENSILE SPECIMEN

The failed specimen shown in figure 12 is typical of those obtained in this study. Failure occurred between the core edges and the face sheet with adhesive being retained on both surfaces. As evident in figure 12, polyimide adhesives do not provide the fillet that epoxy adhesives provide; consequently, the specimens have little bonded area in the core cells for mechanical interlocking.

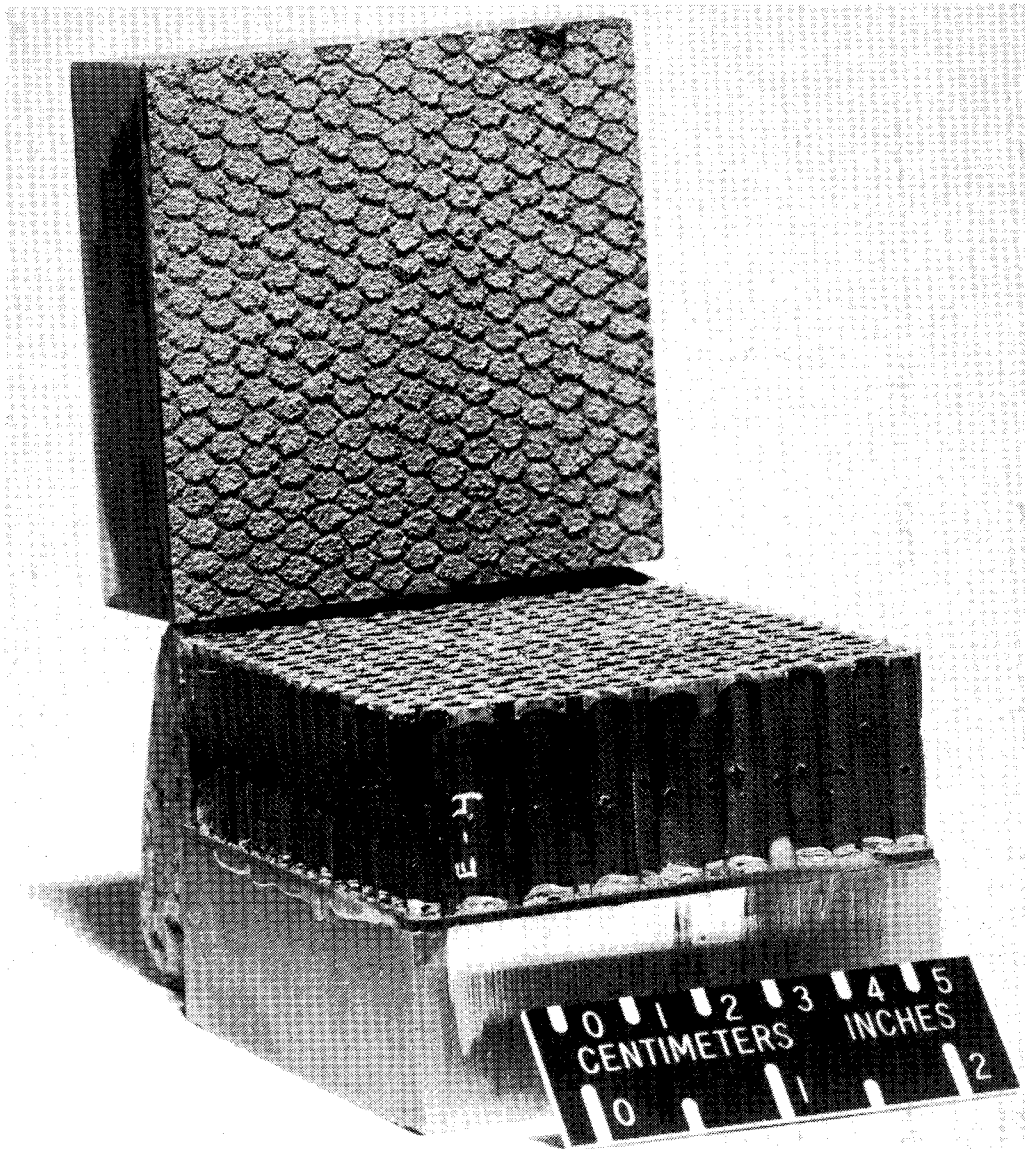


Figure 12

FLATWISE TENSILE STRENGTHS

Flatwise tensile strengths obtained at RT and 589K on unaged specimens and specimens aged at 589K for 125 hours are shown in figure 13.

Each bar in figure 13 represents the average of three (3) test values. No discernable difference is evident for the three adhesive systems at the test temperatures and exposure conditions investigated.

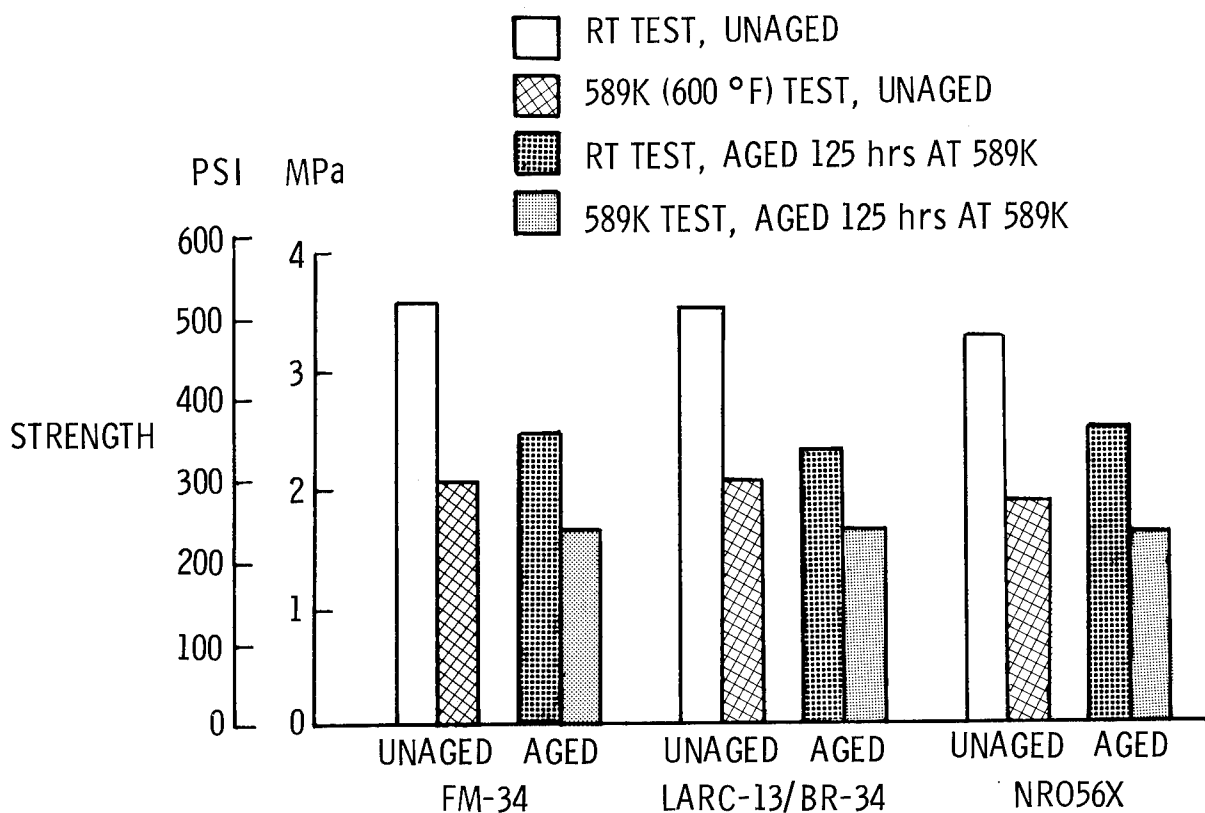


Figure 13

CONCLUSIONS

The adhesive evaluation was based on lap shear and flatwise tensile tests and adhesive processability. Of the five (5) adhesive systems initially selected for screening, only three, FM-34, LARC-13/BR-34 and NR056X, were evaluated in depth. For each adhesive system, processing cycles were developed which were compatible with the composite used in the investigation, quasi-isotropic Celion 6000/PMR-15. Cure temperatures to 602-616K (625-650^UF) and postcures of 616K for up to 16 hours were employed. Although various bonding parameters were investigated during the program, the final processing cycles that were used were not optimized and only represent the best of those studied.

The lap shear and flatwise tensile tests on unaged specimens and on specimens aged 125 hours at 589K did not clearly discriminate between the three adhesive systems. In general, good retention of initial shear and flatwise tensile strengths after 125 hours at 589K was shown for all three adhesives. Therefore, all three, FM-34, LARC-13/BR-34 and NR056X appear to be suitable candidates for bonding composite-to-composite and honeycomb sandwich structures for 125 hour service at 589K.

High temperature adhesives are still in an emerging state of development. This is evidenced by the present concern with adhesives containing toxic substances as well as the fact that adhesives such as Nolimid A380 are being dropped from the market while others such as LARC-13 and NR056X are being introduced and developed.

- CANDIDATE ADHESIVES CAN BE PROCESSED USING A CURE COMPATIBLE WITH THE COMPOSITE ADHEREND
- FM-34, LARC-13, AND NR056X ADHESIVE SYSTEMS ARE SUITABLE CANDIDATES FOR 589K (600 °F) SERVICE FOR 125 HOURS
- HIGH TEMPERATURE ADHESIVES ARE IN AN EMERGING STATE OF DEVELOPMENT

Figure 14

REFERENCES

1. American Cyanamid Co. Inc., Technical Bulletin, FM-34 Adhesive Film, Jan. 25, 1968.
2. Pike, R. A.; Novak, R. C.; and DeCrescente, M. A.: An Evaluation of FM-34 Polyimide Adhesive. 30th Conference, Reinforced Plastics/Composites Institute, Soc. Plastics Industry, Inc., Feb. 1975, Proc., Sec. 18-G pp. 1-10.
3. St. Clair, A. K.; and St. Clair, T. L.: Structure-Property Relationships of Isomeric Addition Polyimides Containing Nadimide End Groups. Polymer Eng. and Sci., vol. 16, no. 5, 1976, pp. 314-317.
4. Darmory, F. P.: Nolimid A380 Extreme High Temperature Polyimide Adhesive. 5th National SAMPE Technical Conference, Oct. 9-11, 1973.
5. Blatz, P. S.: NR-150 Polyimide Precursor Adhesive Solution Developed. Adhesives Age, vol. 21, no. 9, Sept. 1978, pp. 39-44.
6. Hergenrother, P. M.; and Progar, D. J.: High Temperature Composite Bonding With PPQ. Adhesives Age, vol. 20, no. 12, Dec. 1977, pp. 38-43.

ADHESIVES FOR BONDING RSI TILE TO GR/PI STRUCTURE
FOR ADVANCED SPACE TRANSPORTATION SYSTEMS

Kenneth E. Smith, Charles L. Hamermesh, and Peter A. Hogenson
Rockwell International Corporation

EXPANDED ABSTRACT

The aluminum structure of the present Orbiter has an operating temperature of 177C (350F). It is protected from excess temperatures by fused silica RSI (Reusable Surface Insulation) tiles bonded to the skin through an intermediary felt SIP (Strain Isolation Pad). Consideration is being given to future use of Gr/Pi composites as a replacement for aluminum in selected components to promote weight reduction. The full weight-saving advantages of Gr/Pi can only be realized if the structure is permitted to attain temperatures approaching the design allowable of 316C (600F). This would be accomplished by the use of thinner tiles and, possibly, by elimination of the SIP. A major obstacle to achieving maximum temperature operation is the adhesive used in bonding the tiles to the SIP or substrate. The RTV silicones now being used are ideal except that their maximum operating temperature appears to be 260C (500F) or less. This places a corresponding limit on bondline temperatures and will result in greater-than-optimum tile thickness and weight when used with Gr/Pi structure.

This paper reports on the results of the preliminary phase of a program, just completed, to develop an adhesive having improved high-temperature capability while retaining the ideal processing characteristics of RTV silicones. After evaluating several possibilities, mixtures of RTV with glass resins were selected as most promising. While results are not conclusive, tests of the final mixture evaluated, designated RA59, indicated capability of performing as a tile bonding agent to temperatures approaching 370C (700F) during repeated cycling.

Additional work remains to optimize the mixture, fully determine its characteristics, develop processing and quality control, and to qualify the final product as a flight article.

METHOD OF ATTACHING RSI TILES TO THE ORBITER SKIN

The aluminum outer skin of the Orbiter has a maximum allowable operating temperature of 177C. It receives passive thermal protection from excess temperatures during launch and reentry by Reusable Surface Insulation (RSI) tiles bonded to the skin as shown in Figure 1. These tiles are low density fused silica, protected by a ceramic coating, and have very low coefficients of thermal conductivity, k , and expansion, α . Tiles are fragile and must be isolated from the movement of the aluminum structure as it responds to stresses induced by mechanical and thermal conditions encountered during flight.

Isolation of the tiles is provided by means of the Strain Isolation Pad (SIP) which is installed between the outer skin and the tiles. The SIP is a needled felt consisting of aramid fiber which effectively decouples the tiles from strain and dimensional discontinuities of the skin while providing sufficient positioning constraint.

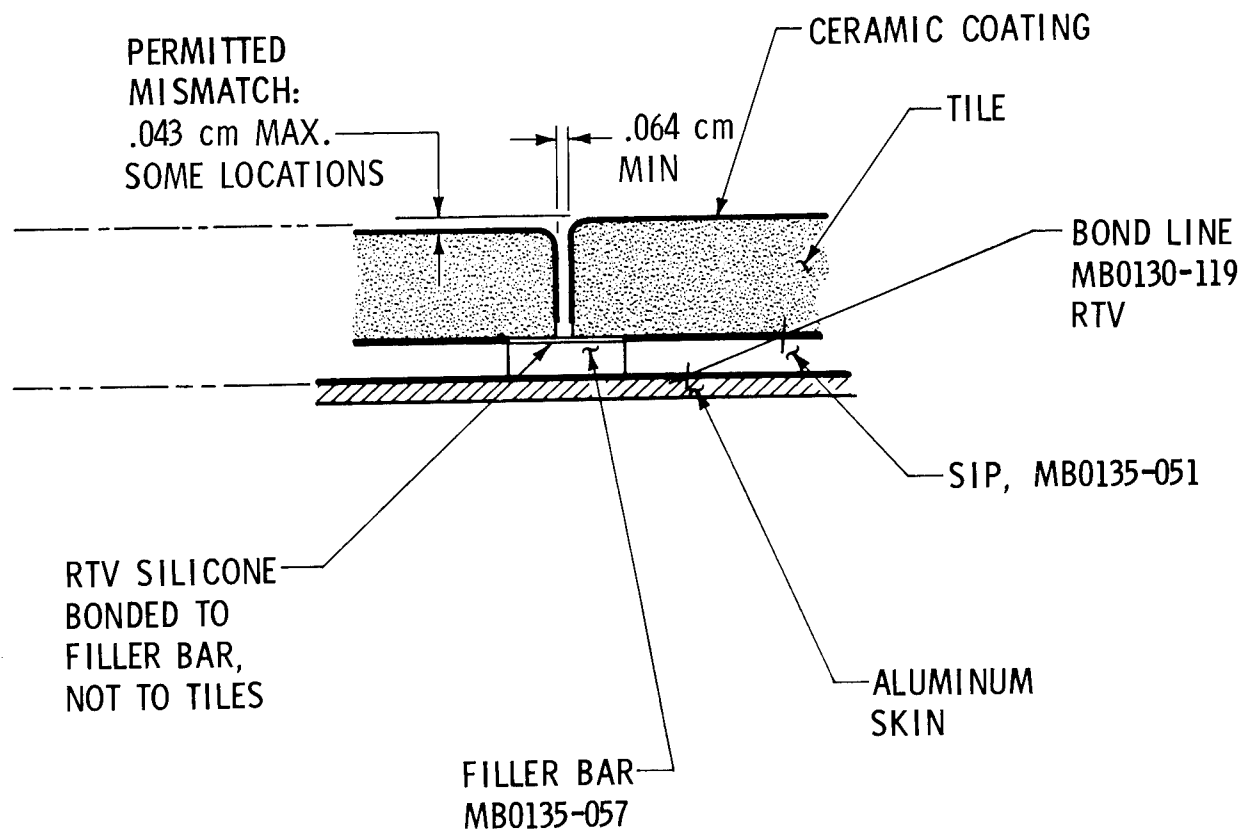


Figure 1

APPLYING TILES TO UNDERSIDE OF ORBITER 102

Tile installation on the Orbiter is an extremely complex operation which will not be described here except to mention the bonding sequence. First, a lattice of filler bars is installed over a given area as shown in Figure 2. Filler bars are of SIP material and form the thermal barrier at the base of the spaces between adjacent tiles. The lattice is bonded to the skin but not to the tiles. SIP pads are bonded to the tiles and, in turn, bonded to the skin. Bonding of groups of tiles is accomplished using a holding fixture to position the tiles properly within the filler bar lattice. In the end product there are two adhesive layers separated by the SIP. The outer bondline is, of course, discontinuous at the filler bars.

The possibility of using Gr/Pi composites for selected Orbiter components requires reconsideration of the mechanisms of tile attachment. In order to take full advantage of the weight saving potential of composites, the service temperature must be increased to values approaching 316C, normally assumed as the maximum for Gr/Pi materials. This would permit the use of thinner tiles. Also, the possibility is offered of eliminating the SIP since the α mismatch between tiles and structure is greatly reduced.

In any case, from the standpoint of bonding, bondline design temperature must be equal to or greater than that of the composite substrate.

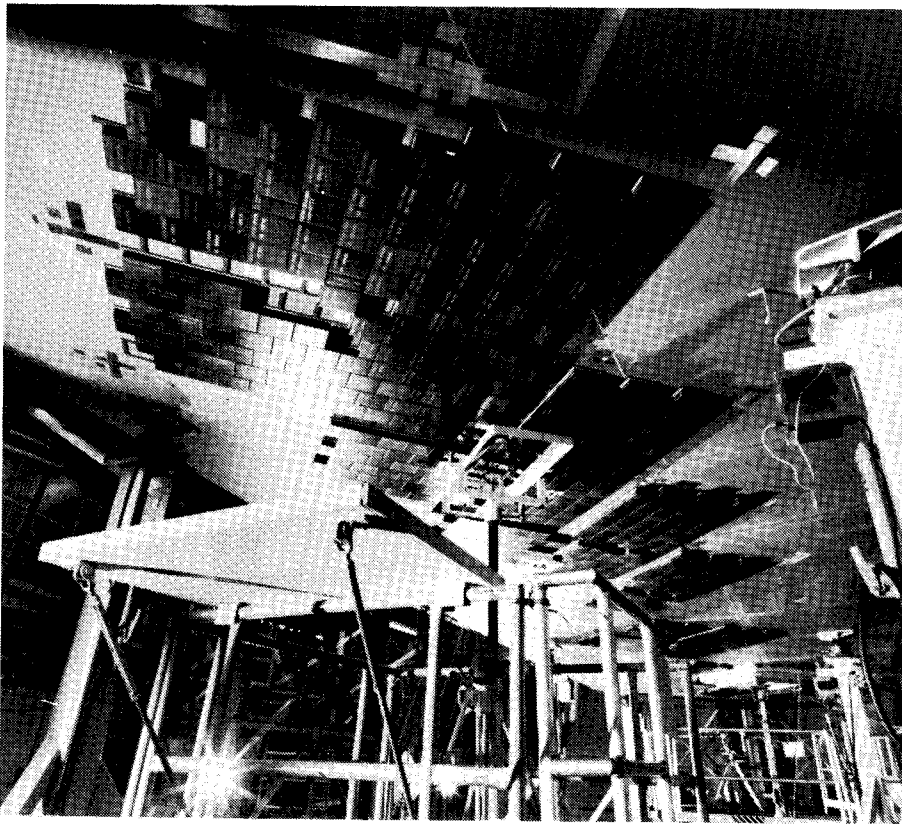


Figure 2

SQS MOLECULAR STRUCTURE

In developing new adhesive for bonding RSI tiles, a goal of 370C (700F) was set. This is well above the maximum operating temperature of 260C (500F) for RTV silicones. In addition to high temperature, the adhesive must be compatible with the tiles at cold soak temperatures in the order of -157C (-250F) or lower, where shrinkage of the adhesive may tend to drive the tile to failure. This could be a problem if the adhesive is unconstrained by the Gr/Pi substrate as in the case where SIP is used.

Other requirements involve processing and environmental factors. Obviously, the adhesive must not be absorbent nor degrade in the presence of moisture. It must be capable of withstanding the full range of Orbiter environment. For acceptable processing it must be nontoxic and obtain an acceptable level of cure at room temperature.

Early work by Rockwell International on solvent activation of polyphenyl-quinoxaline films was somewhat promising but abandoned due to toxicity of the solvents needed. All other candidate materials such as polyimides, polybenzimidazoles, and sesquisiloxane (SQS) had shortcomings which made them similarly unacceptable. No material was found which, by itself, approached the desirable features of the RTV silicones.

Figure 3 compares the molecular structure of RTV silicone with that of SQS. The end groups in the SQS used in the program were either methyl or phenyl.



RTV - SILICONE

GLASS RESIN - SESQUISILOXANE

Figure 3

COMPARISON OF FWT TEST SPECIMEN FAILURES

SQS is a silicone polymer of a type known as "glass resin" due to its glasslike appearance. It is too brittle for use as a bonding agent; however, it has acceptable processing and other characteristics. It was found to form a compatible mixture with RTV, the mixture giving promise of higher temperature performance while retaining other desirable characteristics of the RTV.

Laboratory tests of various mixtures were made primarily using lap shear methods. It was found that optimum performance occurred at about 20 to 30 percent glass resin in RTV. Mixtures were made by first dissolving glass resin granules in acetone then mixing with RTV. Solvent was allowed to evaporate at room temperature often with the aid of a bell jar. The normal RTV catalyst, dibutyltin dilaurate, was then added and the mixture used immediately for bonding. The final mixture selected for testing, 25 percent glass resin (GR) in RTV, was designated RA59.

Once near-optimum mixtures were obtained both lap shear and flatwise (FWT) tensile tests were made with tile coupons in an Instron at temperatures up to 370C. It was found that RA59 lap shear strengths exceeded RTV by two- to fourfold at this temperature; however, the sample size was small. Strengths were only in the order of 24 psi; however, this should be adequate for a tile bonding agent provided consistency can be obtained.

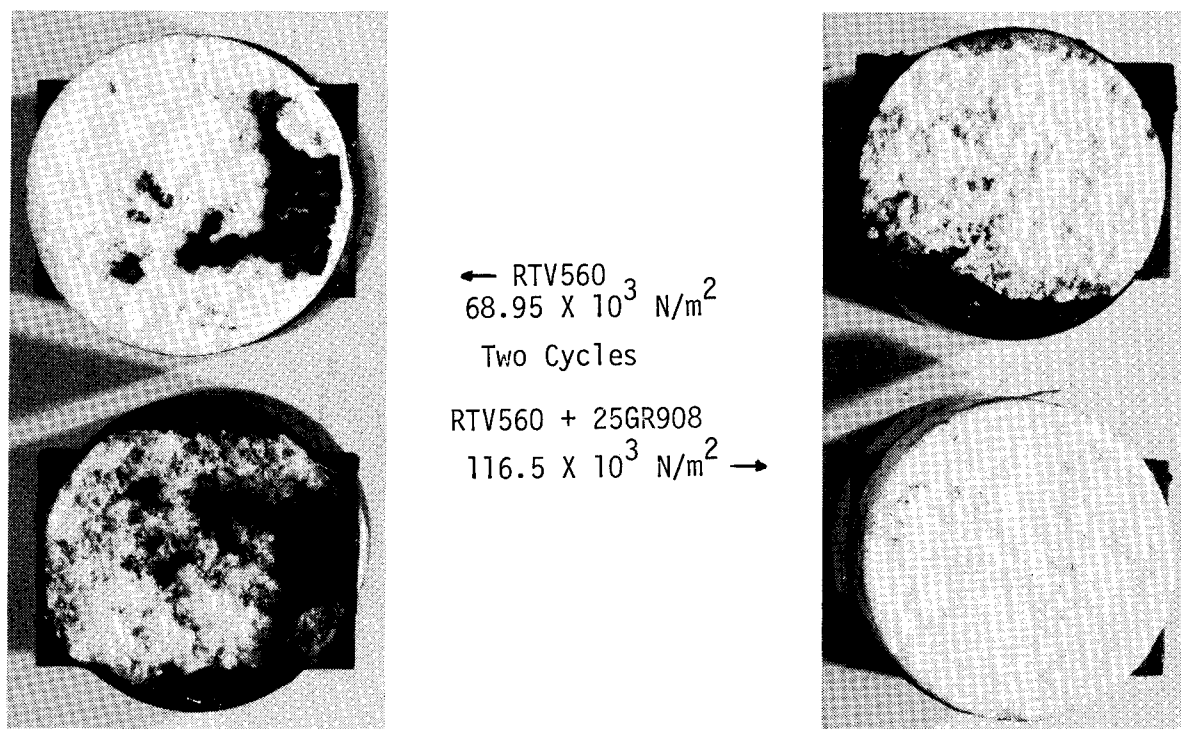


Figure 4

SHEAR STRENGTH VERSUS TEMPERATURE EXPOSURE

Up to this point, three different glass resins were being considered. However, a single GR component was selected for all future work as having the best shelf life and resulting in a more consistent mixture.

Quality of mixture varied considerably from batch to batch. Some batches remained lumpy and would often separate when allowed to stand. At other times they would harden prematurely. This was not traceable to individual batches of either mixture component. The problem was alleviated in part by limiting the evaporation rate. However, some batches of mixture still were of poor quality. This problem was never resolved completely and requires further investigation.

Most testing was done by the lap shear method which is much simpler than FWT testing. Steel "finger specimens" per FTMS MMM-A-132 were primed with SE 4155 and bonded with RA59 using 0.010-inch wire for thickness control. Bonding pressure was applied by drawing a slight vacuum on the assembled specimens. RTV specimens were prepared concurrently. Figure 5 gives the results of this study which shows a direct correlation between room temperature lap shear strength and exposure time at 370C of up to eight hours. Cohesive failure (failure within the adhesive) occurred in all specimens.

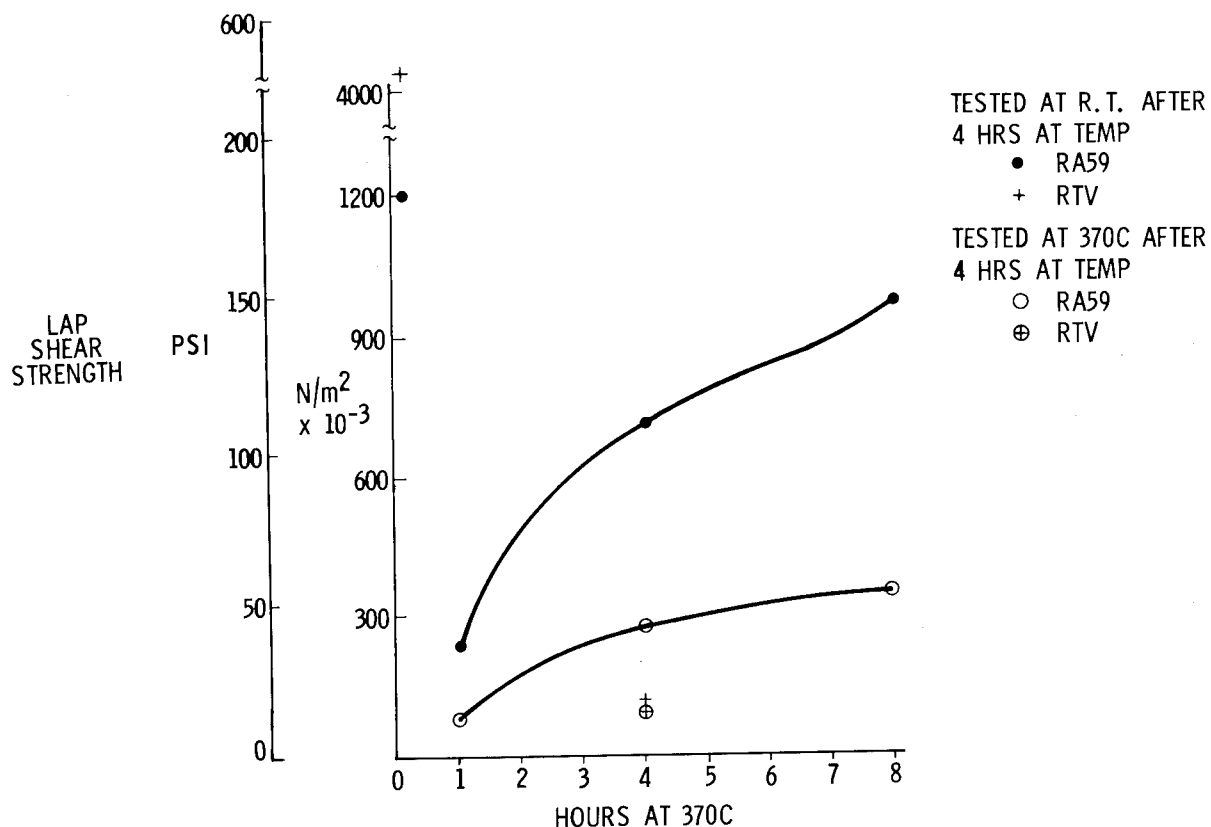


Figure 5

EFFECT OF TEMPERATURE EXPOSURE

Thermo-physical property tests indicated that molecular changes occurred within RA59 at temperatures as low as 140C. A group of lap shear specimens was prepared for testing after exposure to temperatures below 370C in order to determine if low temperature post cure could provide high temperature stability. The same batch of RA59 and processing parameters used for the 370C study were used for these specimens. Testing was performed at room temperature and at 149C, 316C, and 370C with prior conditioning for four hours at those temperatures. Two different batches were tested.

Results of these groups of tests are shown in Figure 6. The upper group of data points shows lap shear strength at room temperature after a four hour exposure at the temperatures indicated.

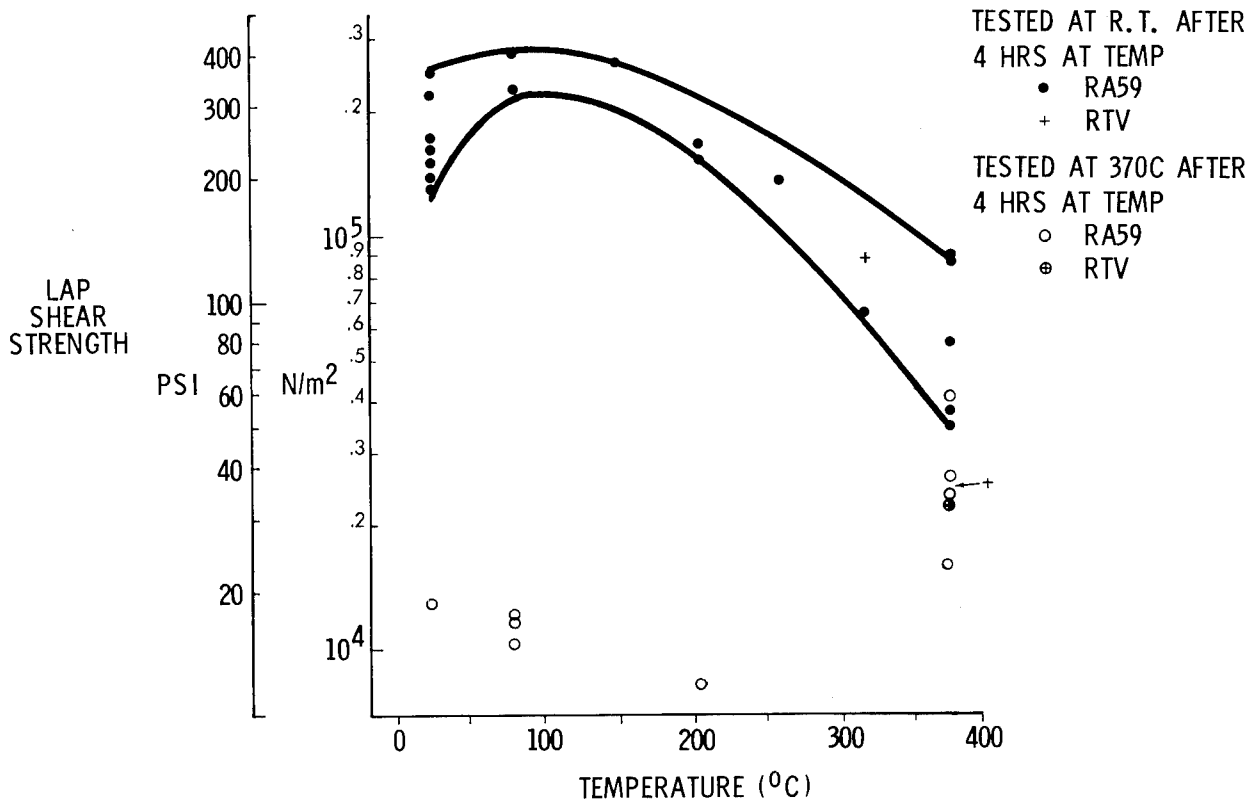
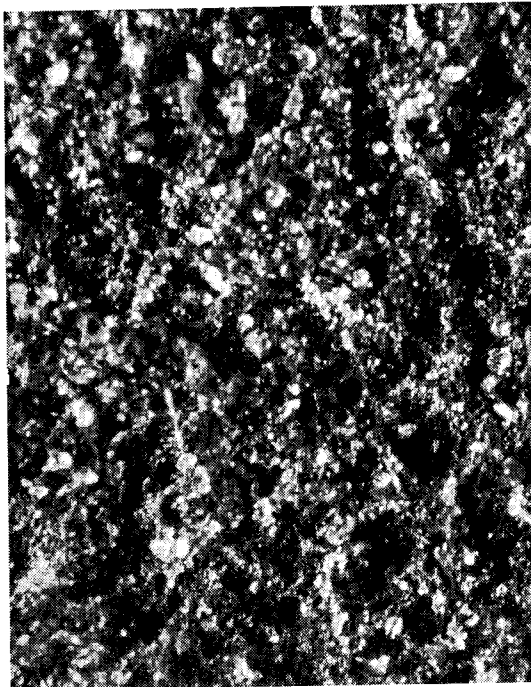


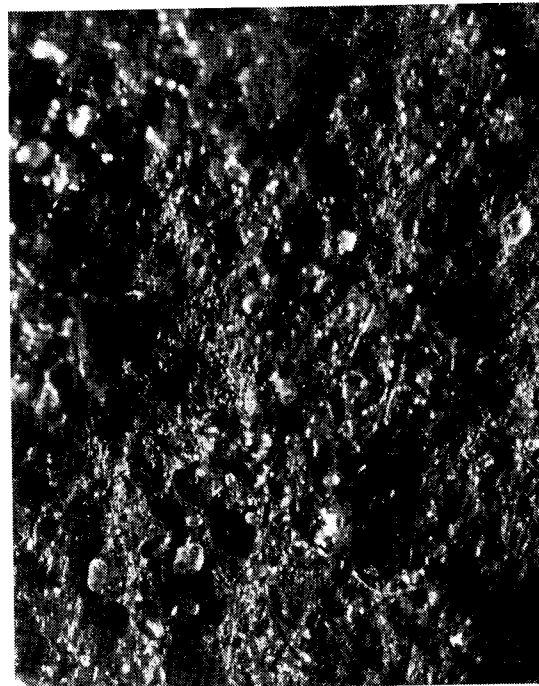
Figure 6

20X MICROPHOTOGRAPHS SHOWING THE EFFECT
OF TEMPERATURE EXPOSURE ON GLASS RESIN SOLUTION

In comparing the adhesive surface of failed lap shear specimens, it was noted that the surface was granular for those specimens which had not been exposed to elevated temperatures while specimens exposed to 370C had a uniform rubber-like appearance as shown in Figure 7. Microscopic examination of specimens which had not been exposed to elevated temperature revealed a heavy concentration of small shiny glass-like globules dispersed over the surface. From specimens made at the same time with the same adhesive mix but post-cured at 370C, the globules were smaller and significantly fewer. It was apparent that the form and mode of dispersion of the glass resin in the RTV matrix was changed by application of heat.



ROOM TEMPERATURE



AFTER ONE-HALF HOUR AT 370C

Figure 7

FLATWISE TENSILE TESTS AFTER 4 HOURS AT TEMPERATURE

Limited flatwise tensile testing was conducted to compare RA59 with RTV. Data in Figure 8 indicate a significant potential performance improvement of RA59. However, the sample size was too small for results to be conclusive.

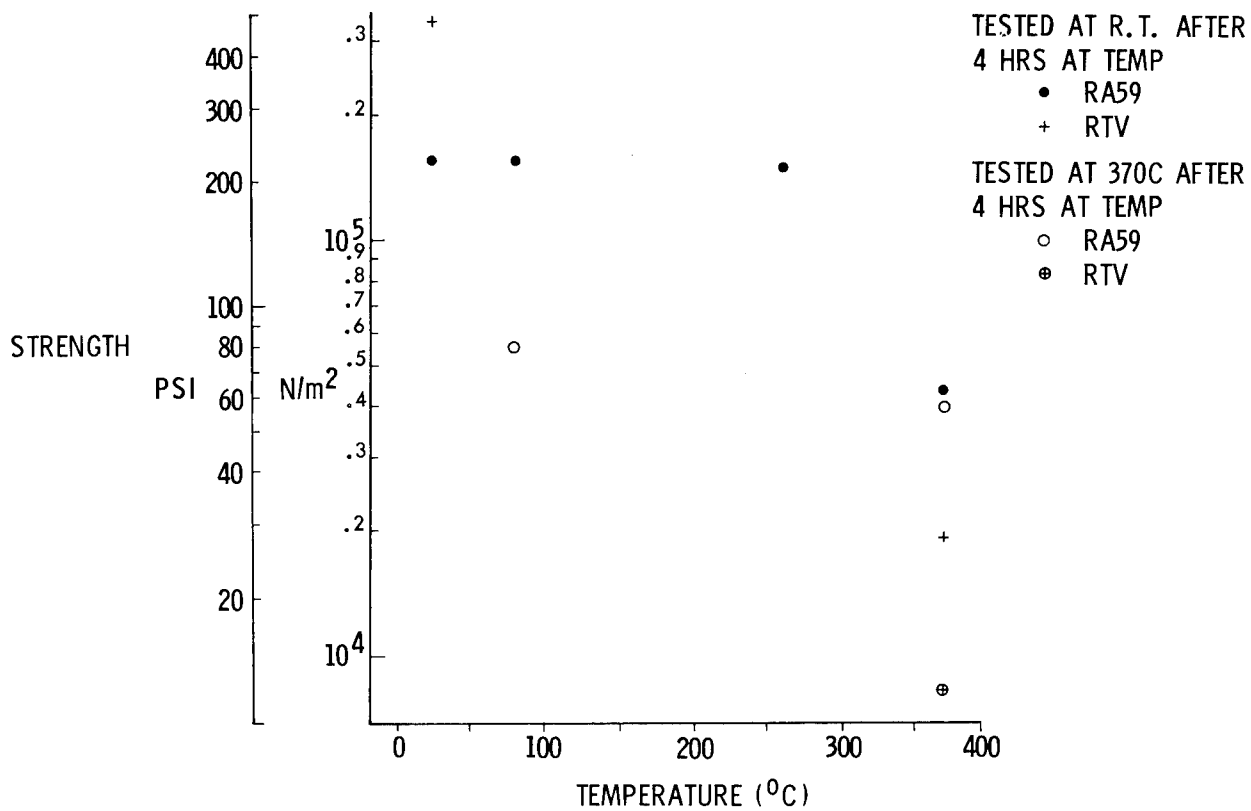


Figure 8

TGA CURVES FOR RA59 PREPARED AT DIFFERENT WEIGHT PERCENTAGES OF CURING AGENT

Dynamic weight loss measurements for RA59, prepared for different catalyst percentages, are shown in Figure 9. Weight loss increases with increased catalyst. However, as expected, the curves are generally similar to that for RTV with decomposition occurring around 370C. The absolute service ceiling could be expected to be below this value.

In conclusion, we believe that glass resin/RTV silicone mixtures may offer significant potential as a class of RSI tile adhesives capable of operating in the temperature range exceeding 260C and approaching 370C. This could permit Gr/Pi composites to operate to full design temperature with resultant maximum weight savings in the thermal protection system. Additional work in testing, chemical characterization, and quality control is needed, however, before their potential as a flight article can be finally determined.

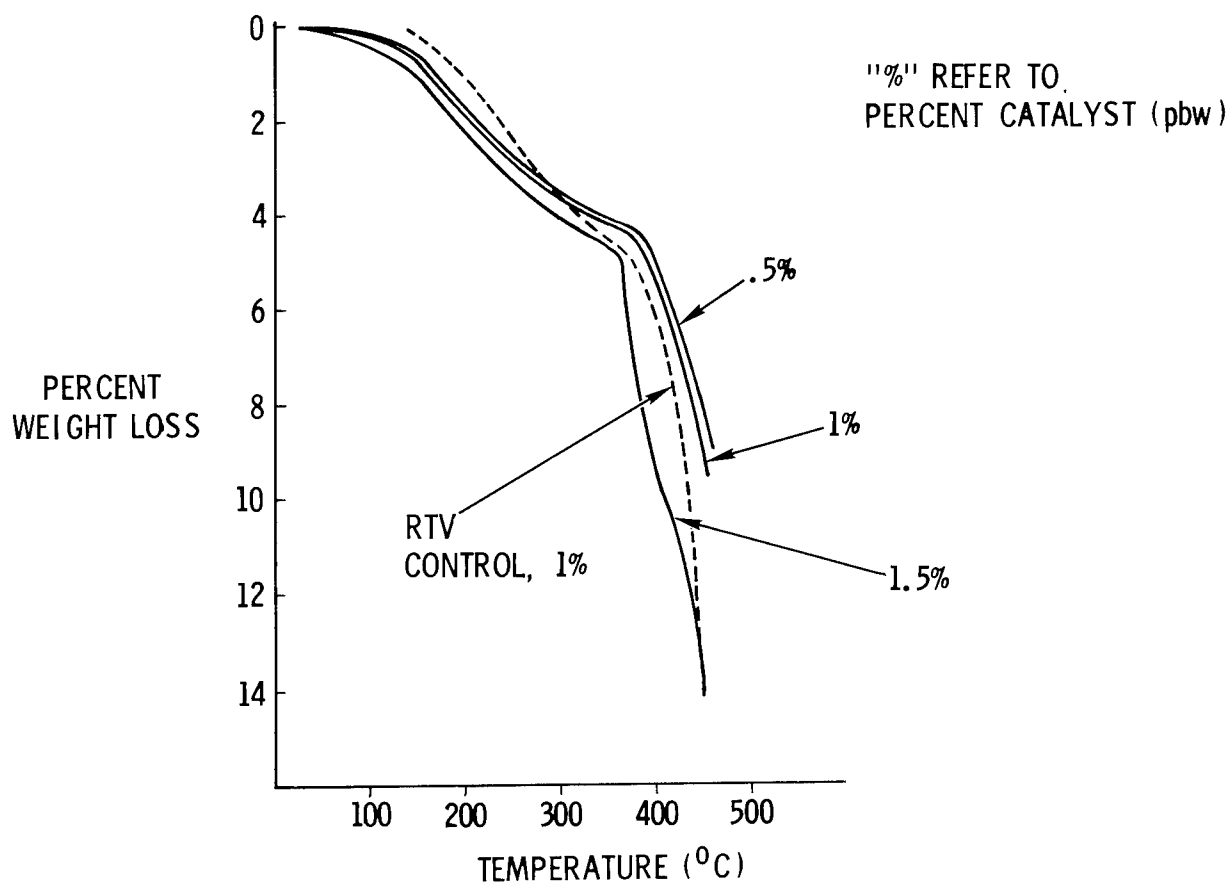


Figure 9

Philip S. Blatz and Hugh H. Gibbs
E. I. du Pont de Nemours & Co., Inc.

EXPANDED ABSTRACT

A new polyimide precursor adhesive solution, code-named NR-056X, has been developed. It reproducibly gives low void, high strength bond lines at both room temperature and 589 K (600°F) using either titanium or graphite/polyimide composite adherends having 12.7 mm (1/2 in.) overlaps.

Lap shear samples prepared using this new adhesive and composite adherends based on graphite/NR-150B2 have been shown to have a high degree of resistance to such adverse environments as air at 589 K (600°F), high humidity, methyl ethyl ketone and jet fuel. Bond line toughness was illustrated by the complete resistance to cracking in the wedge-crack propagation test.

Although the adhesive has not yet been shown to be suitable for wide area metal to metal bonding, the available evidence indicates that wide area composite to composite or composite to metal bonding should be feasible.

DEFICIENCIES OF HIGH TEMPERATURE ADHESIVES

State-of-the-art high temperature adhesives are known to result in brittle, high void bond lines with inconsistent strength levels and relatively poor long term thermal-oxidative stability. Such adhesives are also known to possess relatively poor wide area bonding capability.

- HIGH VOID BOND LINES
- BRITTLENESS
- THERMAL — OXIDATIVE INSTABILITY
- INCONSISTENCY
- LACK OF WIDE AREA BONDING CAPABILITY

Figure 1

OBJECTIVES

In addition to overcoming the deficiencies of other types of high temperature adhesives, the principle objective of this program was to modify the existing NR-150B2G so that the processability would be enhanced without any sacrifice in toughness, stability, environmental resistance and strength up to at least 589 K (600°F). One way of making it easier to obtain high quality, low void bond lines would be to change the formulation in such a way that there was improved resin flow at lower volatiles levels. A further objective was to demonstrate the feasibility of wide area bonding.

TO CHEMICALLY MODIFY NR-150B2G ADHESIVE SOLUTION TO OBTAIN:

- IMPROVED RESIN FLOW AT LOWER VOLATILES LEVELS
- ACCEPTABLE BOND STRENGTHS AT R.T. AND 589 K (600°F)
- EQUIVALENT TOUGHNESS
- EQUIVALENT ENVIRONMENTAL RESISTANCE
- IMPROVED CONSISTENCY
- WIDE AREA BONDING CAPABILITY

Figure 2

NR-150 ADHESIVE SOLUTIONS
STATE-OF-THE-ART

All NR-150 adhesive solutions are based on 6FTA. At the beginning of this study, two adhesive solutions were known. The 6FTA/ODA combination in NMP is useful to 533 K (500°F), whereas the more rigid PPD/MPD diamine system, also in NMP, increases the softening temperature well beyond 616 K (650°F). The purpose of this study was to develop an improved formulation using the existing monomers, combined with optimum proportions in an improved solvent system which would result in consistent high strength levels at 589 K (600°F).

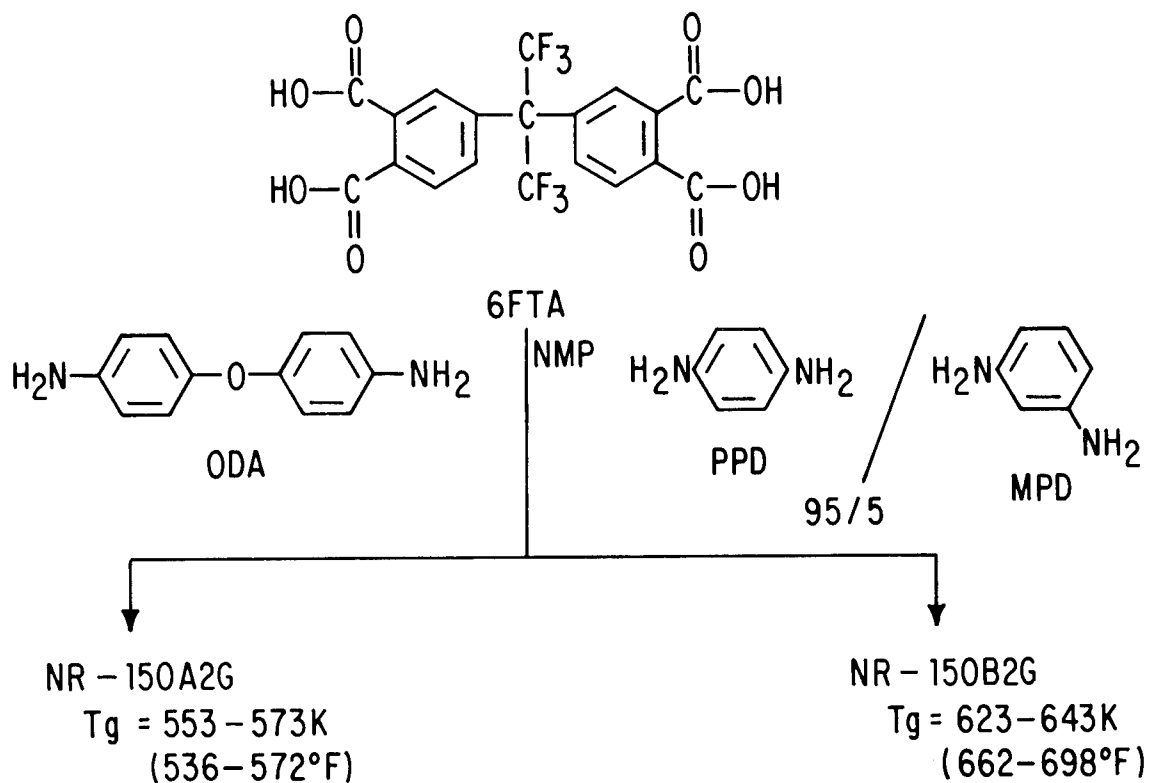


Figure 3

KEY FEATURES OF POLYIMIDES FROM NR-150

Polyimides based on 6FTA are amorphous, linear and **ultra-high in molecular weight**. The net result of these three features is an unusually high degree of toughness. Since the polyimides are thermoplastic, the application of pressure above the T_g can result in low void bond lines. The optimum balance of processing vs properties are achieved through T_g control using the two different diamine systems. The unprecedented thermal-oxidative stability comes from the "all aromatic" nature of the polymer chain. Our goal was to maintain all of these key features in the new and improved adhesive formulation.

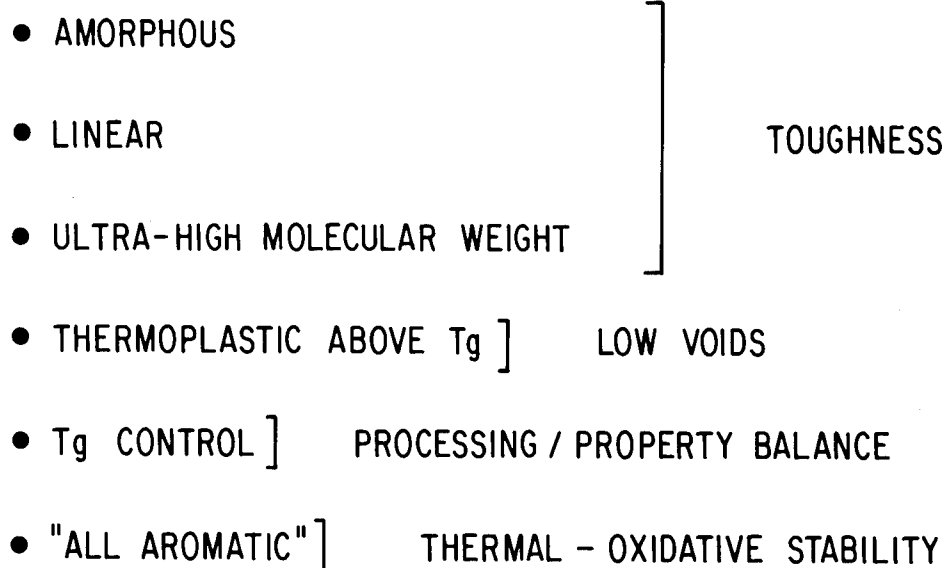


Figure 4

FORMULATION STUDIES

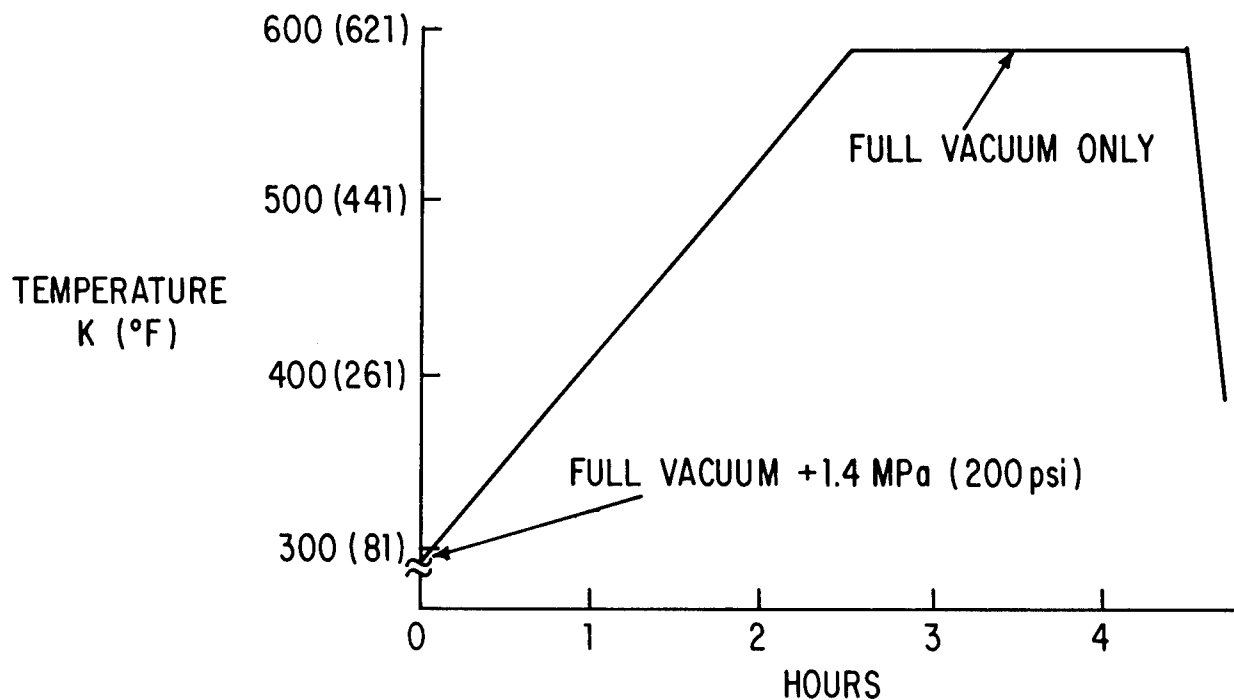
Studies indicated that imbalanced systems tended to be too brittle, hence, stoichiometric proportions of 6FTA and diamines were preferred. For greater ease of processing at 589 K (600°F), the 75/25 PPD/ODA combination was found to be optimum. The use of diglyme in place of NMP resulted in more facile devolatilization, thus making it easier to prepare consistently high quality bond lines. The use of a 65 weight percent loading of aluminum powder filler also resulted in a further incremental improvement in processability.

<u>VARIABLE INVESTIGATED</u>	<u>CONCLUSION</u>
MONOMER IMBALANCE	PREFER STOICHIOMETRIC PROPORTIONS
COPOLYIMIDES	PREFER 75/25 PPD / ODA
SOLVENT	PREFER DIGLYME
FILLER	USED 65 wt. % ALUMINUM POWDER

Figure 5

TYPICAL MOLDING CYCLE

Most samples were molded and post-cured according to the cycle described below. The maximum final molding temperature of 589 K (600°F) was called for by NASA. Had higher final molding temperatures been allowed, even better results might have been obtained.



POST-CURE (FREE STANDING): 16 hrs at 589K (600°F)

Figure 6

PREFERRED COMPOSITION

The preferred formulation to evolve from this study is based on 6FTA/PPD/ODA in the molar ratios 1.00/0.75/0.25. The solution contains 48 weight percent cured resin solids in diglyme and has a viscosity of 6.0 Pa.s (60 poises) and has been code-named NR-056X. The addition of 65 weight percent aluminum powder filler is recommended when NR-056X is used as an adhesive.

CODE - NR-056X

SOLVENT - DIGLYME

% CURED RESIN SOLIDS - 48

SOLUTION VISCOSITY - 6.0 Pa.s (60 poises)

MONOMER MOLAR RATIOS - 1.00 / 0.75 / 0.25
6FTA / PPD / ODA

RECOMMENDATION - 65 wt. % ALUMINUM POWDER FILLER
SHOULD BE ADDED BEFORE USE

Figure 7

LAP SHEAR STRENGTH PERFORMANCE
OF ALUMINUM FILLED NR-056X SOLUTION

The NASA lap shear strength goal levels of 20.7 MPa (3000 psi) at room temperature and 13.8 MPa (2000 psi) at 589 K (600°F) were exceeded using both Ti-6Al-4V and composite (graphite/NR-150B2) adherends.

TEST TEMP.	SUBSTRATE		NASA GOAL LEVEL
	6/4 TITANIUM	COMPOSITE- GRAPHITE / NR-150B2	
R. T.	24.1 MPa (3500 psi)	23.4 MPa (3400 psi)	20.7 MPa (3000psi)
589 K (600°F)	15.1 MPa (2200 psi)	15.1 MPa (2200 psi)	13.8 MPa (2000 psi)

Figure 8

ENVIRONMENTAL EXPOSURE TESTS

In all of the environmental exposure tests run on samples made with composite (graphite/NR-150B2) adherends, the bond line was stronger than the composite. Solvent resistance was excellent as judged by no effect from a 90-day exposure to either JP-4 jet fuel or methyl ethyl ketone. Due to the flammability of JP-4 and methyl ethyl ketone, no high temperature testing was carried out.

ADHERENDS: GRAPHITE FIBER / NR - 150B2

ADHESIVE: NR - 056X

FILLER: ALUMINUM POWDER (65wt.%)

EXPOSURE CONDITION	% DECREASE IN BOND STRENGTH	
	R.T.	589 K (600°F)
500 HOURS IN AIR AT 589K (600°F)	9*	17*
30 DAYS IN 95% RH AT 322K (120°F)	24*	40*
30 DAYS IN MEK AT R.T.	NONE	NOT TESTED
30 DAYS IN JP-4 AT R.T.	NONE	NOT TESTED

*FAILURE OCCURRED WITHIN COMPOSITE ADHEREND

Figure 9

WEDGE-CRACK PROPAGATION TEST

The high level of toughness of the polyimide derived from NR-056X was illustrated by the lack of crack growth in the wedge-crack propagation test run at 589 K (600°F) on bonds based on composite (graphite/NR-150B2) adherends.

ADHERENDS: GRAPHITE FIBER / NR-150B2

ADHESIVE: NR-056X

FILLER: ALUMINUM POWDER (65 wt.%)

TEST TEMPERATURE: 589K (600°F)

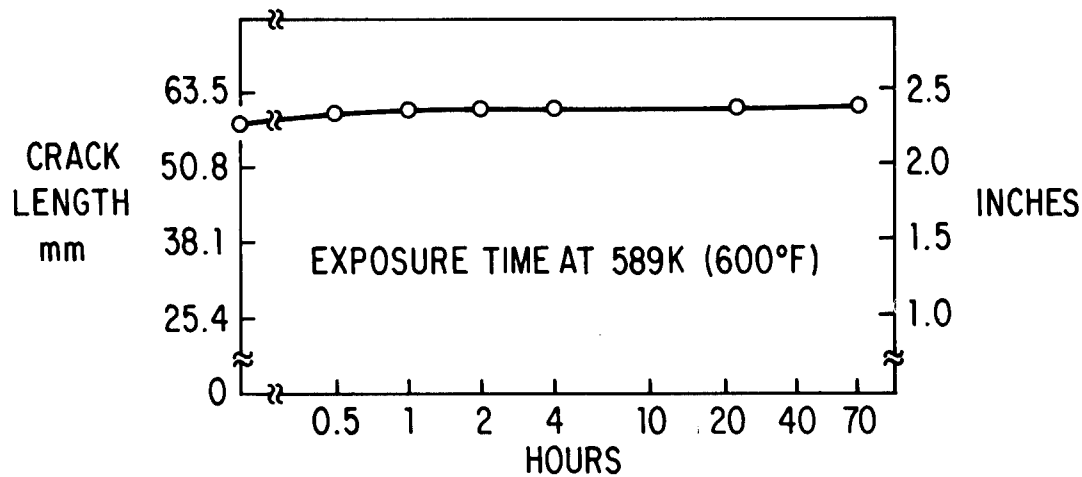


Figure 10

WIDE AREA COMPOSITE TO COMPOSITE BONDING

Promising results were obtained in the bonding of moderately wide area composite adherends. Improved lap shear strengths in the center section of the sandwich construction could undoubtedly be obtained through further optimization of molding and post-cure cycles. Somewhat higher final molding temperatures should be particularly effective in promoting the complete devolatilization of the interior of the bond line.

ADHERENDS: GRAPHITE FIBER / NR-150B2

ADHESIVE: NR-056X

FILLER: ALUMINUM POWDER (65 wt. %)

FINAL MOLDING TEMPERATURE: 589K (600°F)

FINAL POST-CURE TEMPERATURE: 616K (650°F)

PANEL SIZE: 0.124m X 0.124m (6" X 6")

LAP SHEAR STRENGTH, MPa (psi)

OUTSIDE		INSIDE	
R.T.	589K (600°F)	R.T.	589K (600°F)
16.9 (2400)	17.8 (2600)	9.65 (1400)	4.53 (660)

T_g = 585K (594°F)

Figure 11

CONCLUSIONS

NR-056X offers relatively simple autoclave bonding and post-cure cycles. Tough, moisture and solvent resistant, low void bond lines can be reproducibly obtained in standard lap shear specimens which have high bond strengths up to at least 589 K (600°F). Evidence indicates that wide area composite to composite or composite to metal bonding should be feasible.

NR - 056X OFFERS:

- SIMPLE AUTOCLAVE BONDING AND POST-CURE CYCLES
- LOW VOID BOND LINES
- HIGH BOND STRENGTH UP TO 589 K (600°F)
- TOUGH BONDS
- RESISTANCE TO MOISTURE, MEK AND JP-4
- REPRODUCIBILITY
- PROBABLE WIDE AREA COMPOSITE TO COMPOSITE OR COMPOSITE TO METAL BONDABILITY

Figure 12

DEVELOPMENT OF LARC-13 ADHESIVE SYSTEMS

John T. Hoggatt
Boeing Aerospace Company

EXPANDED ABSTRACT

The Boeing Company has been actively engaged in the development and evaluation of high temperature adhesive systems. These studies on NASA contracts and IR&D evaluate various adhesive formulations and effects of various environments upon different titanium bond surface treatments. Initial data show LARC-13 to possess good 589K (600°F) stability as compared to other high temperature stable systems.

OBJECTIVES

The primary objectives (Figure 1) of the NASA program are, (1) to improve the physical/chemical properties of LARC-13 in adhesive applications to 600°F, (2) optimization of LARC-13 adhesive formulations and bonding parameters, and (3) identification of compatible titanium and composite surface preparation techniques.

- **PHYSICAL/CHEMICAL IMPROVEMENT OF LARC-13 FOR 589K (600°F) ADHESIVE APPLICATIONS**
- **OPTIMIZATION OF LARC-13 ADHESIVE FORMULATION AND BONDING PARAMETERS**
- **IDENTIFICATION OF COMPATIBLE TITANIUM AND COMPOSITE SURFACE PREPARATION TECHNIQUES**

Figure 1

PHYSICAL/CHEMICAL MODIFICATIONS

Physical/chemical modifications (Figure 2) include increasing the thermal stability in incorporation of additional aromatic structure through addition of 3,3' metaphenylene diamine (3,3' MPD) and 3,5 diaminobenzamidobenzene (3,5 DABAB). Increased adhesive toughness will be promoted by introduction of amide-imide copolymer resin. This modification significantly increases bond properties. A third modification will involve addition of fillers such as aluminum powder to also increase filleting and control flow during cure.

- INCREASE THERMAL STABILITY BY INCORPORATION OF
ADDITIONAL AROMATIC STRUCTURE
3,3' MPD AND 3,5 DABAB
- INCREASE VISCOSITY BY INTRODUCTION OF COPOLYMER
— AMIDE— IMIDE RESIN
- ENHANCE FILLETING AND CONTROL FLOW BY MODIFICATION
OF FILLER, FILLER LEVEL AND CARRIER

Figure 2

SUMMARY LARC-13
LAP SHEAR DATA

The Table in Figure 3 illustrates the lap shear properties of LARC-13 using 6Al-4V Titanium and PMR-15 composite substrates. As seen, initial values on titanium are around 4,500 psi with initial 600°F value at 2,400 psi. Composite shear specimens start at about 2,200 psi and maintain 1,200 psi shear after 125 hours exposure at 600°F tested at 600°F.

	TI/TI	PMR-15/PMR-15
AMBIENT MPa(Psi)	30.9 (4480)	15.2 (2,200)
589K (600°F) (30 MINUTES)	16.5 (2400)	12.4 (1,805)
589K (600°F) (125 HOURS)	—	8.3 (1,205)

Figure 3

ADHESIVE PROGRAM REVIEW

Boeing is also executing a second contract with NASA Langley to develop high temperature stable adhesive systems (including LARC-13) for extended 450°F service. The adhesive system includes substrate surface preparation, primer and adhesive formulation (Figure 4).

This work will ultimately support Supersonic Cruise Aircraft Research (SCAR). Titanium wedge specimens along with lap-shear and T-peel are tested initially and after 120°F/95% relative humidity. Long term +450°F aging tests are also scheduled. Comparison of this data with two LARC-13 formulation modifications on the NASA LARC-13 development will be performed.

- SCAR
 - TITANIUM WEDGE SPECIMENS
 - 322K(120°F) 95% REL HUMIDITY
 - 505K(450°F)
- LARC 13
 - LAP SHEAR PANELS TITANIUM AND PMR-15 GRAPHITE COMPOSITE
 - TI/TI
 - GRAPHITE/GRAPHITE
 - COMPARISON OF LARC 13 WITH TWO MODIFICATIONS
- SUMMARY
 - THREE SURFACE PREPARATION

Figure 4

Ti/Ti CRACK EXTENSION DATA
322K (120°F), 95% RH (CHROMIC ACID ANODIZED)

The following series of Figures illustrate the effects of various environments upon different titanium surface treatments using three different adhesives including LARC-13. Figure 5 illustrates the effect of 120°F/95% RH on the crack extension values on titanium bonds with chromic acid anodized surface treatment. Three adhesive systems shown are; BR34/FM34, LARC-13, and NR150B2. All three systems are comparable in crack extension exposed to this environment.

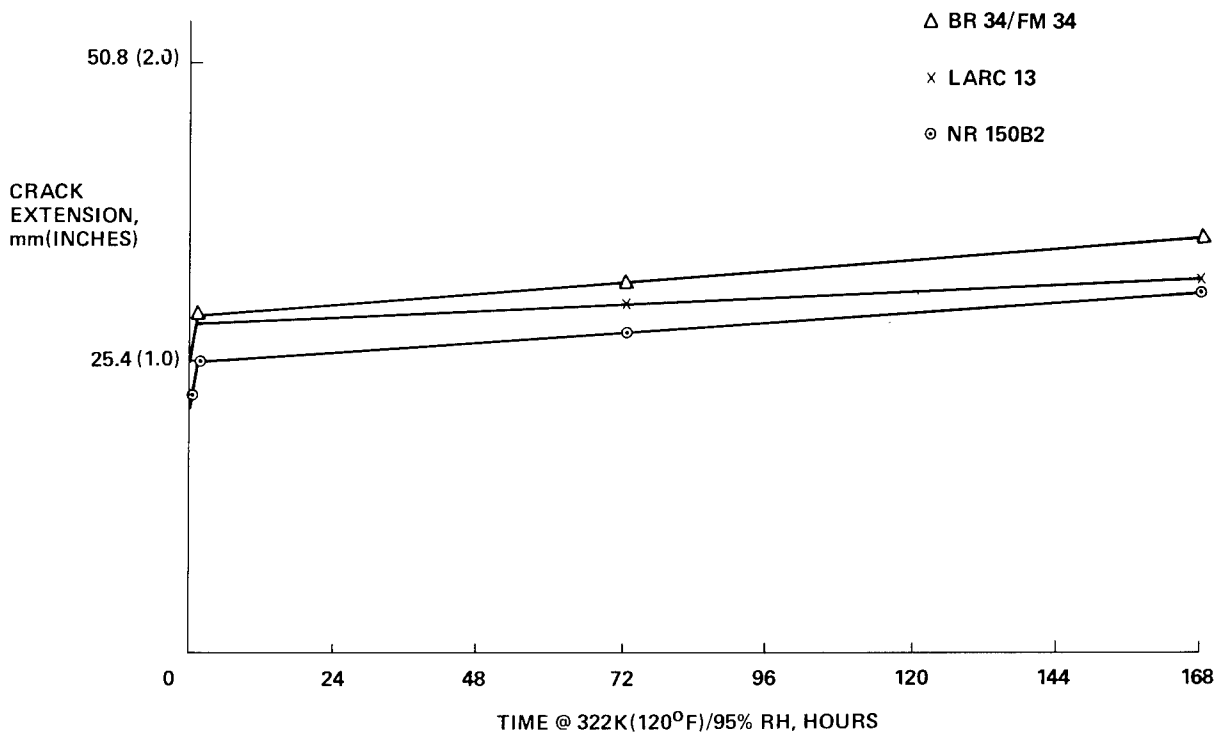


Figure 5

Ti/Ti CRACK EXTENSION DATA
505K (450°F) (CHROMIC ACID ANODIZED)

Figure 6 shows these three adhesive systems on titanium substrate (chromic acid anodized) exposed to continuous 450°F. LARC-13 is slightly more resistant to crack extension than FM34. NR150B2 is slightly more resistant to crack extension than either LARC-13 or FM34.

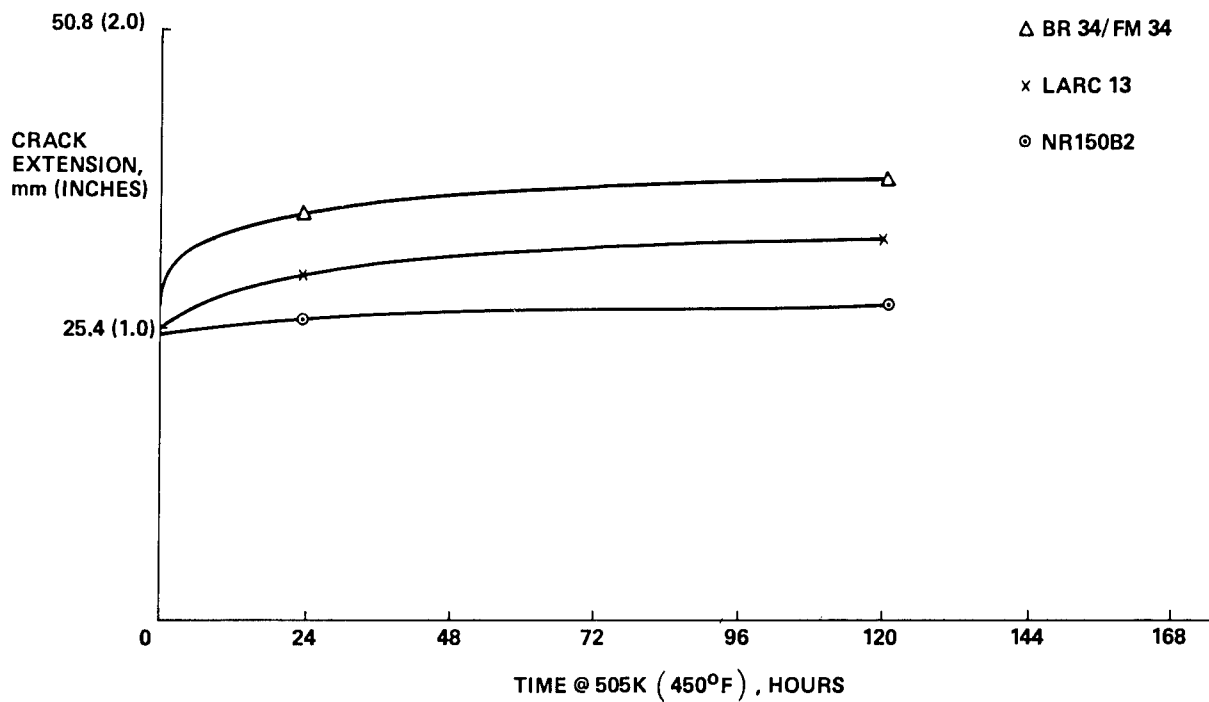


Figure 6

Ti/Ti CRACK EXTENSION
322K (120°F), 95% RH (PHOSPHORIC ACID ANODIZED)

Figure 7 shows the effect of 120°F/95% RH environment upon phosphoric acid anodized titanium bonded with LARC-13, BR34/FM34, and NR150B2. In this series of tests, LARC-13 is slightly more resistant to crack extension than the other two systems. Crack extension between phosphoric acid anodized and chromic acid anodized was very similar using these three adhesive systems. In all cases, the crack extends from about 1.2 to 1.4 inches.

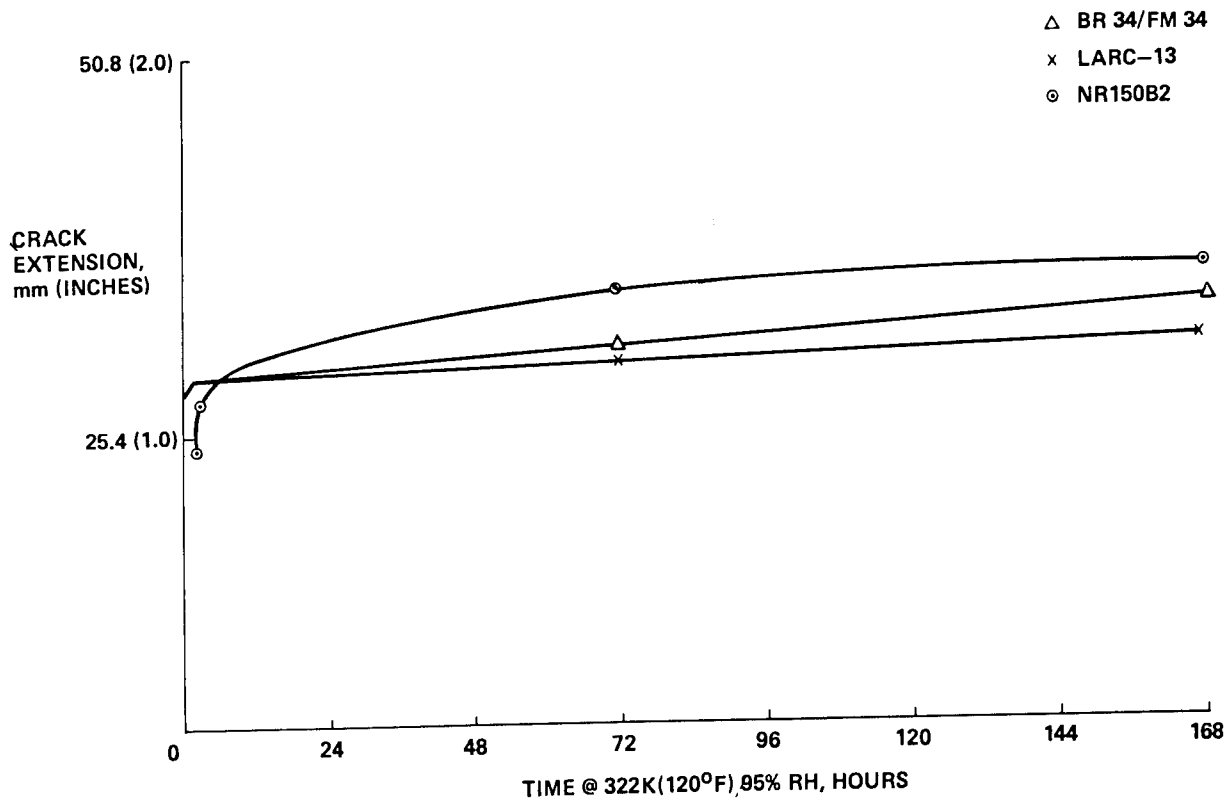


Figure 7

Ti/Ti CRACK EXTENSION
505K (450°F) (PHOSPHORIC ACID ANODIZED)

The results of 450°F aging on titanium crack extension specimens are presented in Figure 8 (phosphoric acid anodized bonded with BR34/FM34, LARC-13, and NR150B2). Here, LARC-13 is slightly inferior to both FM34 and NR150B2 although, for all systems, the crack growth is essentially zero from 4 hours to 120 hours.

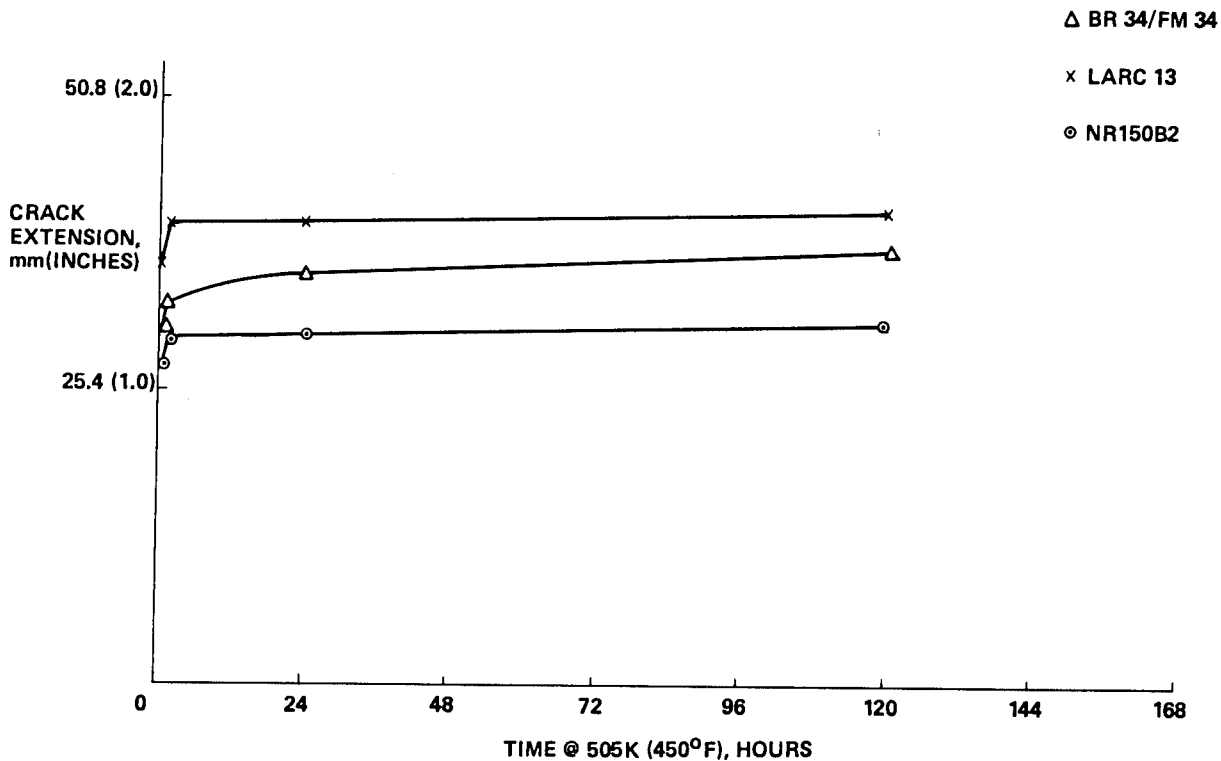


Figure 8

Ti/Ti CRACK EXTENSION
322K (120°F), 95% RH PHOSPHATE FLUORIDE (PICATINNY)

Figure 9 illustrates the effects of 120°F/95% RH environment upon titanium crack extension specimens treated with the Picatinny method for phosphate fluoride. FM34 exhibited the least effect of this environment while LARC-13 and NR150B2 both had the crack extend to almost 2 inches.

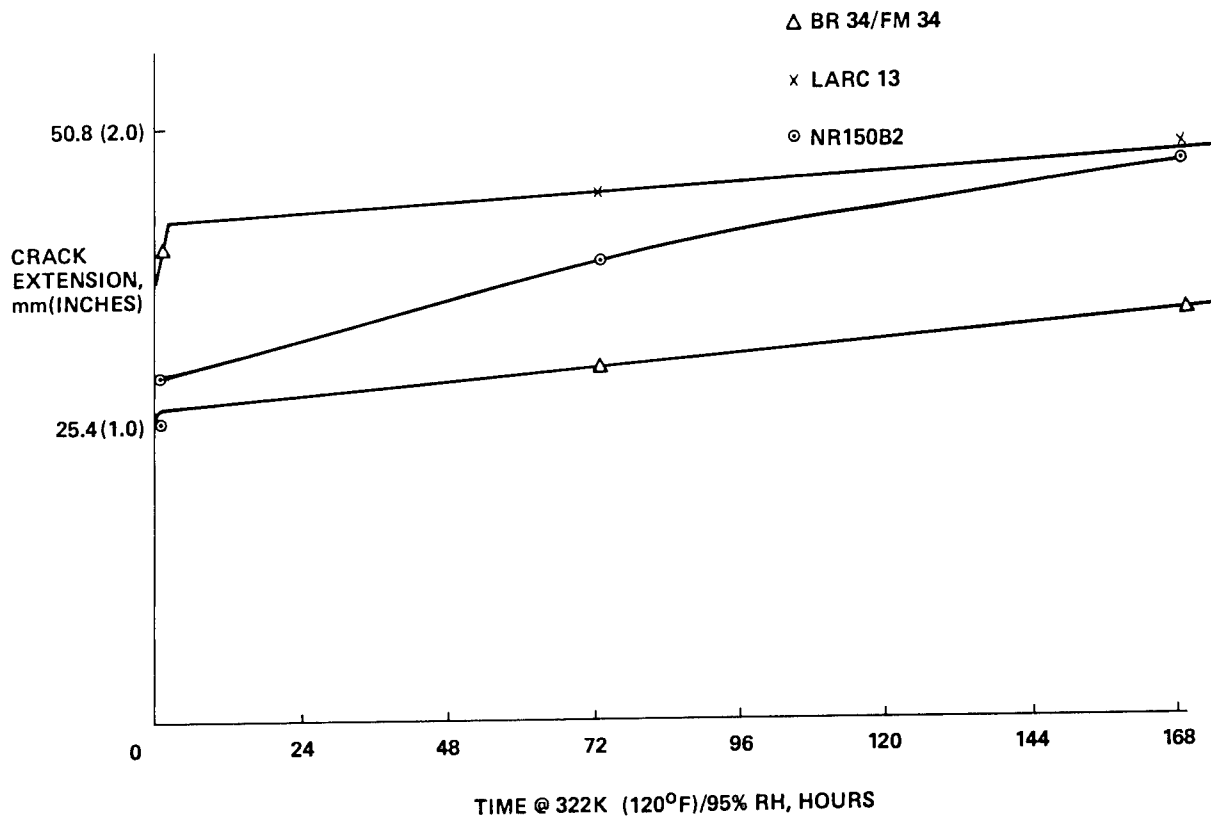


Figure 9

Ti/Ti CRACK EXTENSION
505K (450°F) PHOSPHATE FLUORIDE (PICATINNY)

The effect of 450°F upon phosphate fluoride (Picatinny Method) treated titanium wedge specimens is shown in Figure 10. Again, LARC-13 exhibits greater crack extension than either FM34 or NR150B2 at 2 inches compared to about 1.4 inches. In all three systems, crack growth is nearly stopped at 24 hours exposure.

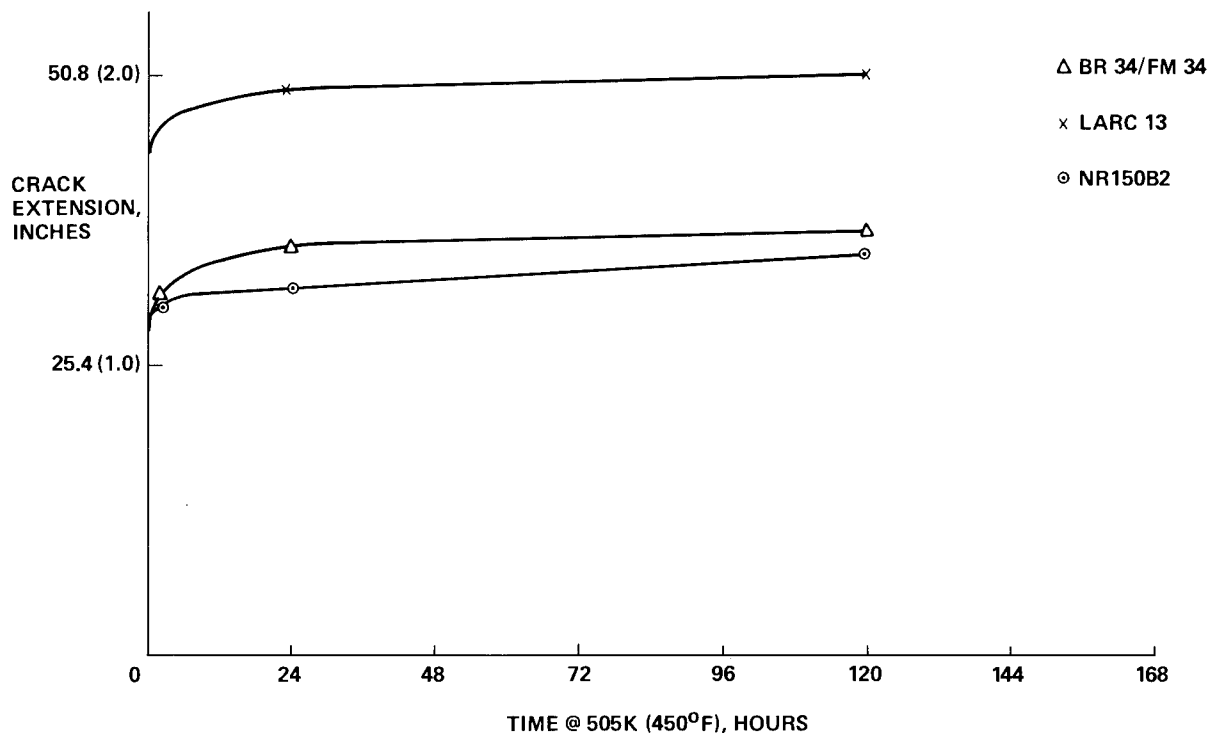


Figure 10

SUMMARY
LARC-13 ADHESIVE DEVELOPMENT

The development of LARC-13 adhesive formulations is a valuable contribution to polyimide bonding technology. This system offers the potential of producing structures of metal-to-metal and honeycomb sandwich with large area bonds in both titanium and polyimide composites because of the high flow and low volatile evolution characteristics. The resulting pay-off from LARC-13 adhesive bonding is a major structural design alternative to titanium superplastic forming and brazing in future high performance aircraft and space applications.

GRAPHITE/POLYIMIDE TENSION TESTS
AT ELEVATED AND CRYOGENIC TEMPERATURES

Andrew J. Chapman
NASA Langley Research Center

EXPANDED ABSTRACT

Graphite/polyimide composites are being considered for use in aerospace structures which may experience temperatures as-high-as 589 K (600° F) and as-low-as 117 K (-250° F). Consequently, the mechanical properties required for designing flightworthy structures must be characterized at these temperatures of intended use. Although resin-matrix structural composites have been broadly characterized at normal ambient temperatures, only limited experience is available for characterizing these materials at temperatures as-high-as 589 K (600° F).

Interim results for characterizing tension properties of graphite/polyimide laminates are reported in this paper. Existing test procedures for resin-matrix composites were evaluated for use through the extreme temperature range indicated above. Of particular concern was the performance of resistance strain gages at the elevated temperatures and tests were carried out to compare their performance against that of a capacitive strain gage. Limited design data are reported for graphite/polyimide laminates which are being produced through the CASTS Project.

OBJECTIVES

The focus of this task is to evaluate test procedures for characterizing tension properties of graphite/polyimide composites at temperatures from 117 K (-250° F) to 589 K (600° F). Test techniques used to characterize resin-matrix composites at room temperature were modified with the addition of a temperature chamber and high-temperature strain gages. While evaluating test techniques, preliminary design properties were obtained for graphite/polyimide laminates produced through the CASTS Project.

- EVALUATE TEST PROCEDURES FOR CHARACTERIZING TENSION PROPERTIES OF GRAPHITE/ POLYIMIDE COMPOSITES AT TEMPERATURES FROM 117 K (-250° F) TO 589 K (600° F)
- OBTAIN PRELIMINARY DESIGN PROPERTIES FOR GRAPHITE/ POLYIMIDE AT 117 K (-250° F), ROOM TEMPERATURE, AND 589 K (600° F)

Figure 1

TEST SPECIMEN CONFIGURATION

The test configuration was a modified IITRI tension specimen similar to that described in the USAF Advanced Composites Design Guide. This specimen has a constant width gage section and long tapered tabs for transferring load uniformly into the specimen. The tabs are graphite/polyimide laminates, usually cut from the same panel as the specimen, and are bonded to the specimen using a polyimide adhesive.

High temperature strain gages were bonded to the specimen surface near the center of the gage section along the longitudinal and transverse axes using a polyimide adhesive. The resistance gages are standard products advertised for use at temperatures to 672 K (750° F) for short times. The concerns in using these gages for obtaining design properties include accuracy and repeatability at high temperature and durability of adhesive bonds.

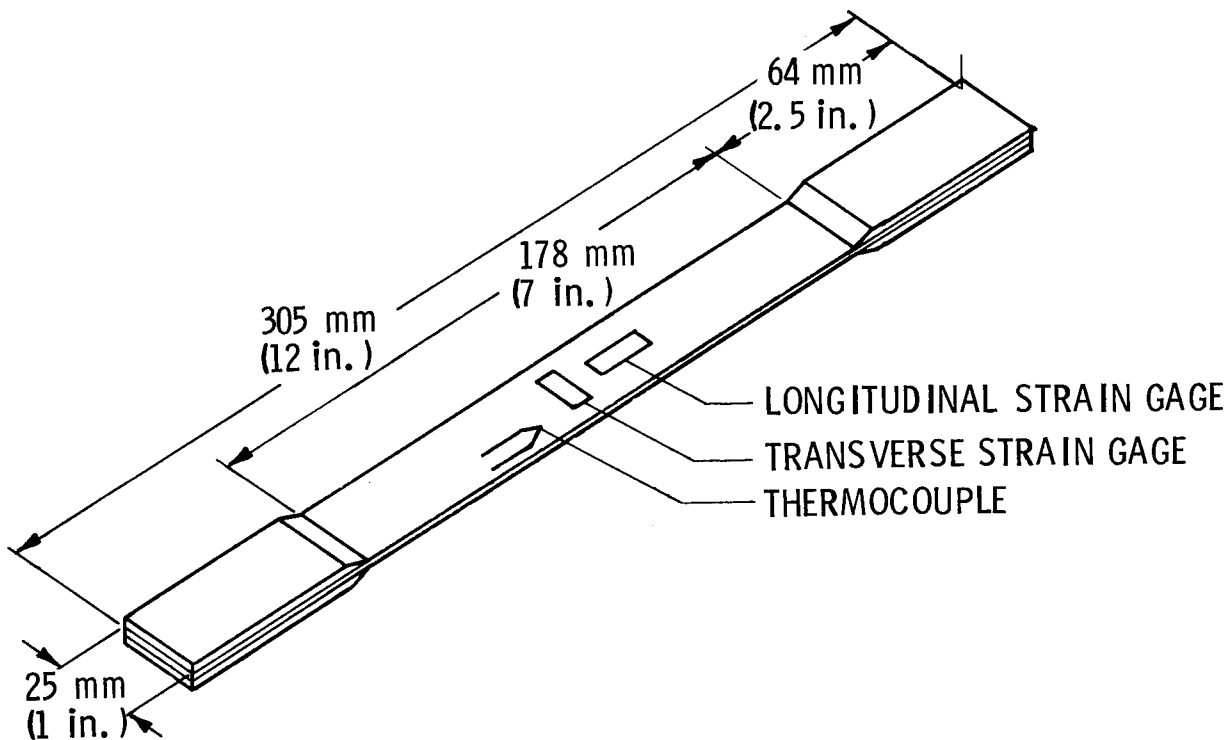


Figure 2

TEST APPARATUS

Specimens were tested in a conventional load machine such as the mechanically actuated machine shown in figure 3. Test temperatures, both cryogenic and elevated, were produced in the chamber which mounted between the test machine columns and completely enclosed the specimen and grips. Temperatures as-high-as 589 K (600° F) were produced by electrical resistance heaters. Temperatures as-low-as 117 K (-250° F) were produced by controlled liquid nitrogen flow and evaporation in the chamber. The chamber control system maintained specimen temperature (as measured by an attached thermocouple) within ± 3 K ($\pm 5^\circ$ F) of the selected temperature. The chamber atmosphere was circulated continuously to maintain a uniform temperature on the specimen and the grips.

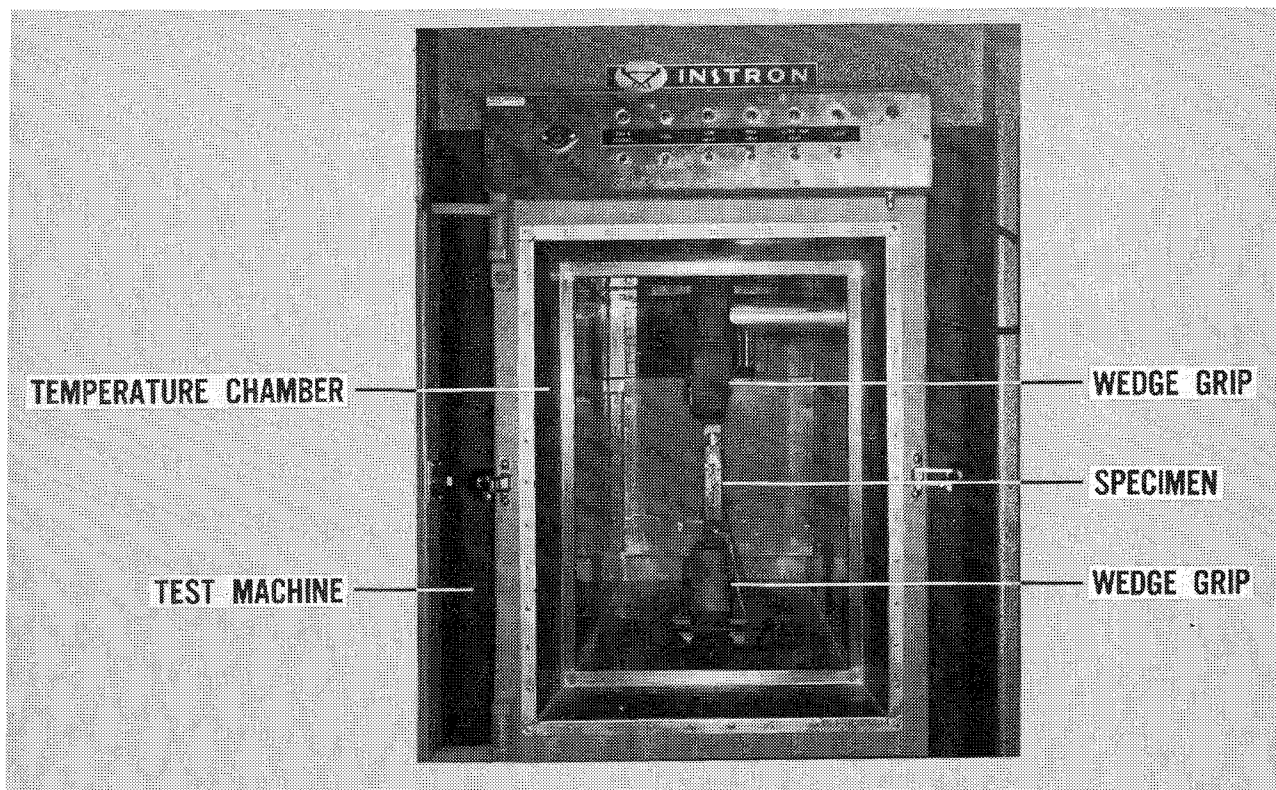


Figure 3

CAPACITIVE STRAIN GAGE

A capacitive strain gage was used as a standard to evaluate performance of the resistance gages at the elevated temperatures. The capacitive gage has been shown to be accurate at temperatures as high as 1089 K (1500° F). The gage attachment strips are bonded to the specimen adjacent to the resistance gage, the distance between the attachment strips defines the gage length. Specimen strain displaces the concentric rings which form a capacitor. The resulting change in capacitance modulates a carrier voltage, producing an output voltage proportional to specimen strain. Capacitive and resistance gage outputs are recorded digitally together with other test parameters. The capacitive sensor is assembled around a longitudinal rod which compensates for thermally induced strains if the rod and specimen have closely matched coefficients of expansion.

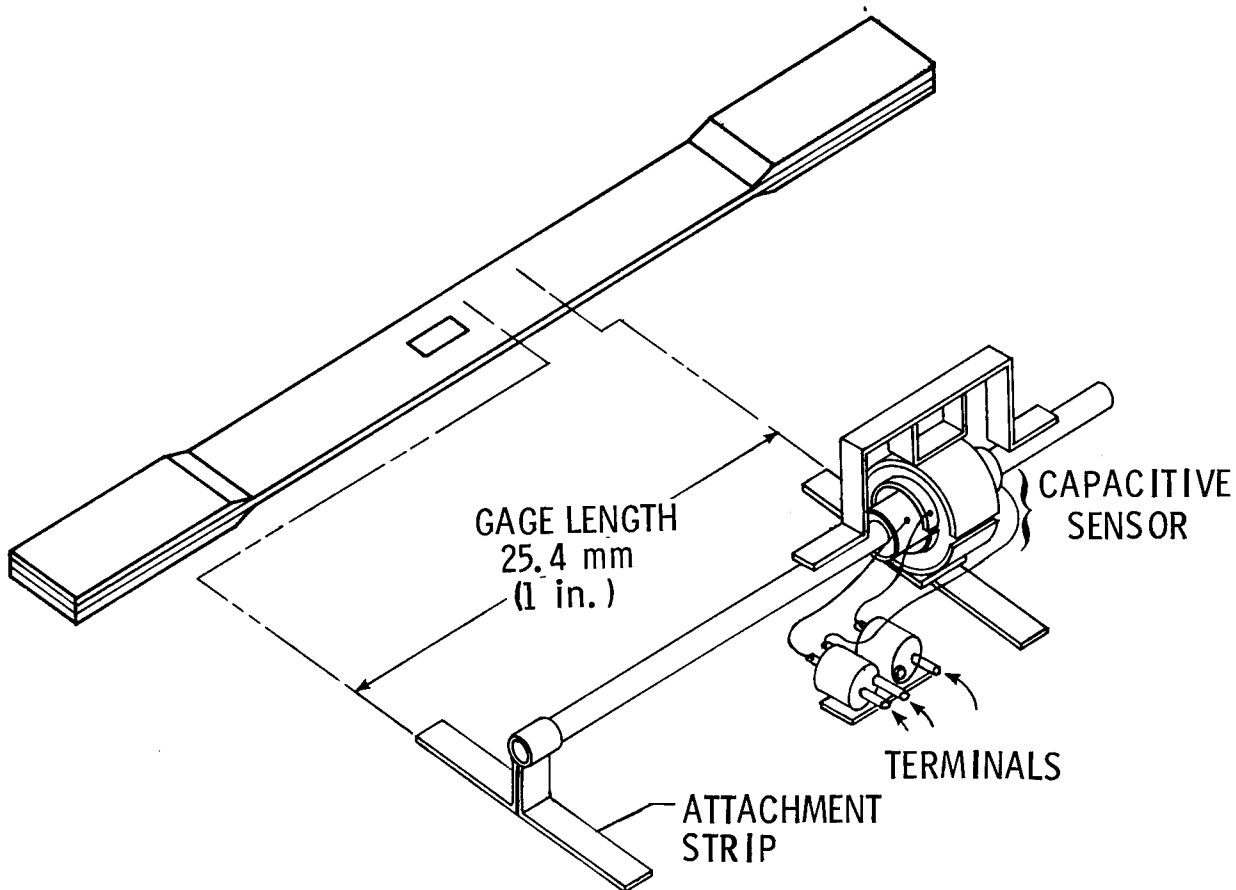


Figure 4

CAPACITIVE AND RESISTANCE STRAIN GAGE PERFORMANCE

Capacitive and resistance strain gage performance was compared by testing instrumented specimens at various temperatures up to 589 K (600° F). During each test, specimens were loaded to a strain level of approximately .004, well within the proportional limit for the laminates tested. Specimens were not tested to failure because of the high cost of the capacitive strain gage. The stress-strain curves for a quasi-isotropic laminate of HTS/PMR-15 show very good agreement for back-to-back resistance gages and the capacitive gage, both at room temperature and at 589 K (600° F).

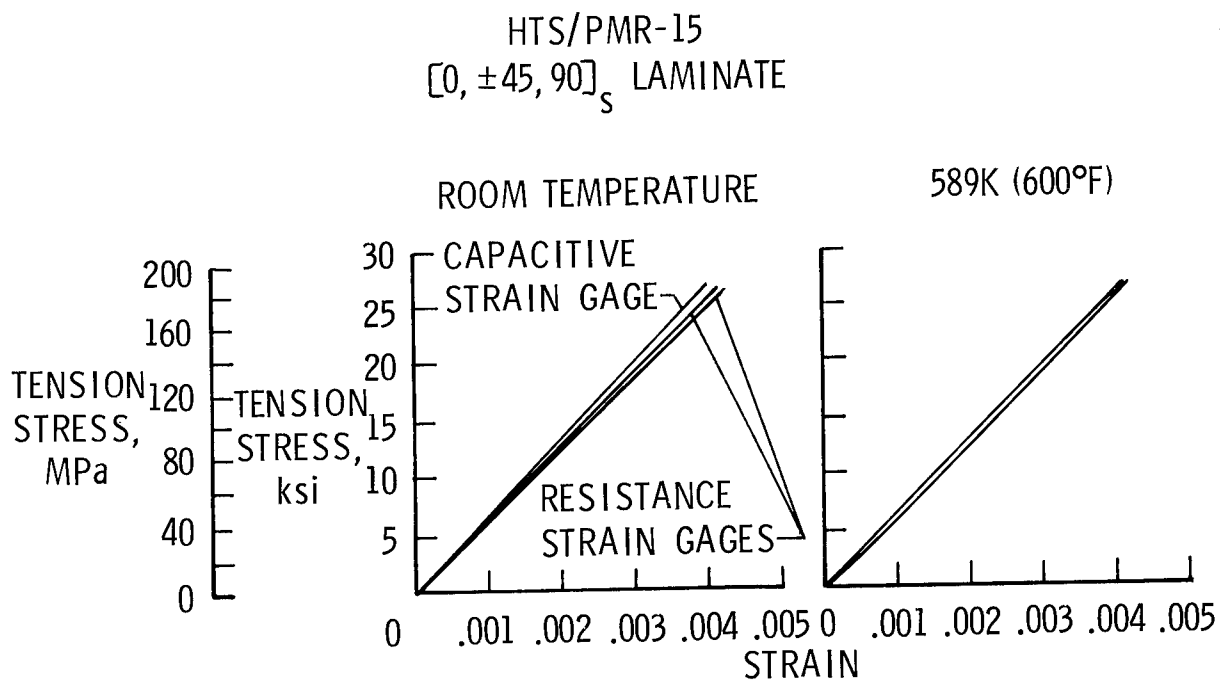


Figure 5

EFFECT OF TEMPERATURE ON TENSION MODULUS

Tension modulus values obtained from capacitive and resistance strain gage indications are shown as a function of test temperature. Modulus was obtained by a least square fit to the linear portion of the stress-strain curves. Resistance strain gage indications were corrected for gage factor variation with temperature. Modulus values from the back-to-back resistance gages and the capacitive gage agree closely at each temperature. The modulus for this quasi-isotropic laminate was nearly constant throughout the temperature range from room temperature to 589 K (600° F).

The close agreement between resistance and capacitive strain gages during repeated tests throughout the temperature range has demonstrated accurate and repeatable performance for the resistance gages at temperatures as-high-as 589 K (600° F).

HTS1/PMR-15 $[0, \pm 45, 90]_S$

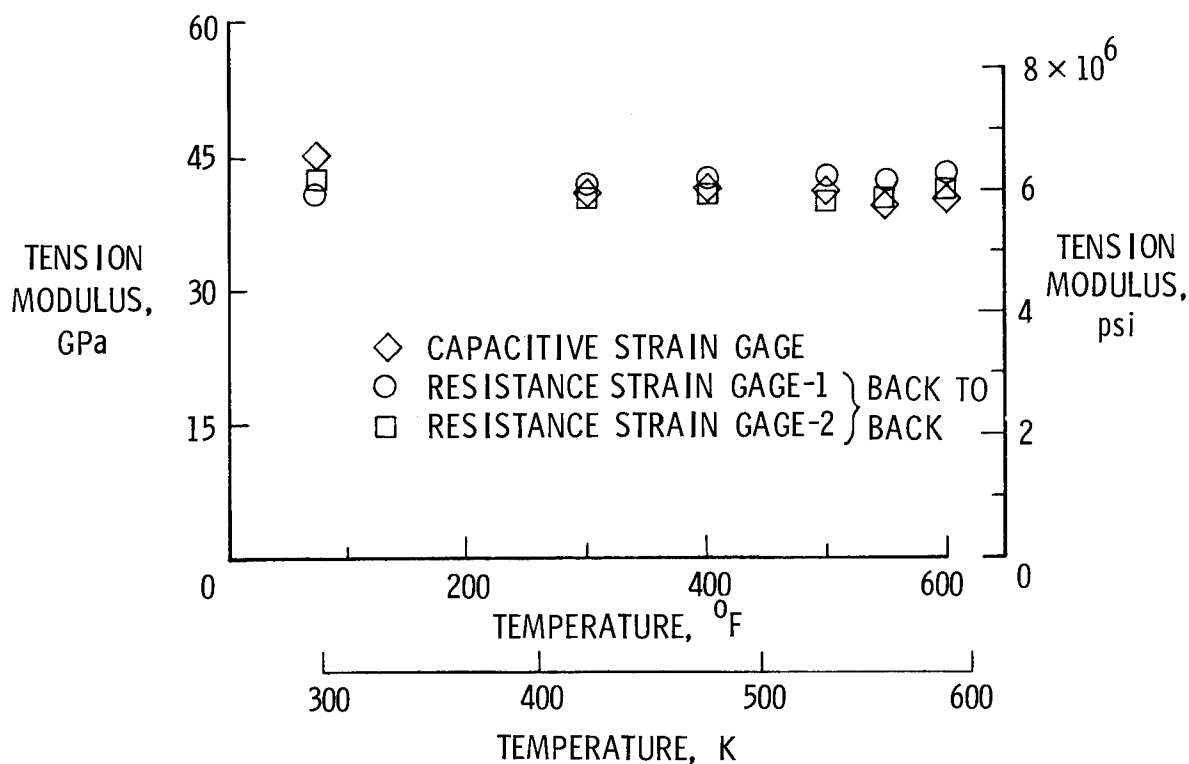


Figure 6

EFFECT OF TEMPERATURE ON TENSION MODULUS

TYPICAL DESIGN DATA

The test procedures described are being used to characterize tension properties of various graphite/polyimide materials as they are produced through the CASTS Project. Some typical test results are shown in figure 7. Unidirectional, quasi-isotropic, and forty-five degree laminates of HTS1/NR150B2 were tested at temperatures of 117 K (-250° F), room-temperature, and 589 K (600° F). Modulus values of fiber-dominated unidirectional and quasi-isotropic laminates varied only slightly throughout the test temperature range. Modulus values of the resin dominated forty-five degree laminates decreased somewhat with increasing temperature. For each laminate, agreement among tests at each temperature was good in most cases, further demonstrating repeatable results for the resistance gages over the test temperature range.

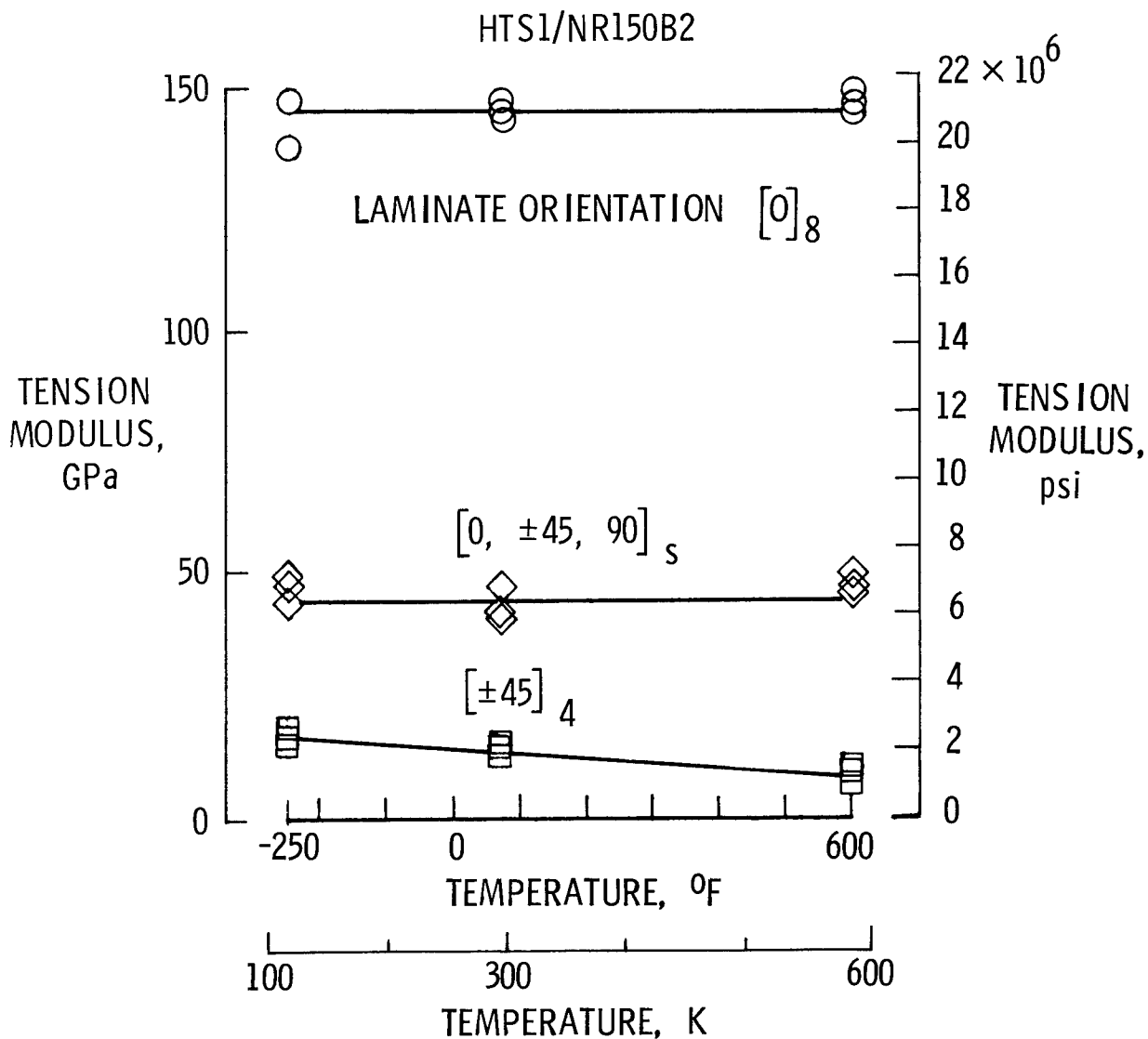


Figure 7

EFFECT OF TEMPERATURE ON TENSION STRENGTH

TYPICAL DESIGN DATA

Ultimate tensile strength of the HTS1/NR150B2 laminates is shown in figure 8. For the uniaxial laminate, ultimate strength values show somewhat more scatter than modulus values in the previous figure. For the quasi-isotropic and forty-five degree laminates, agreement of ultimate strength values at each temperature is very good and these values are nearly constant with temperature.

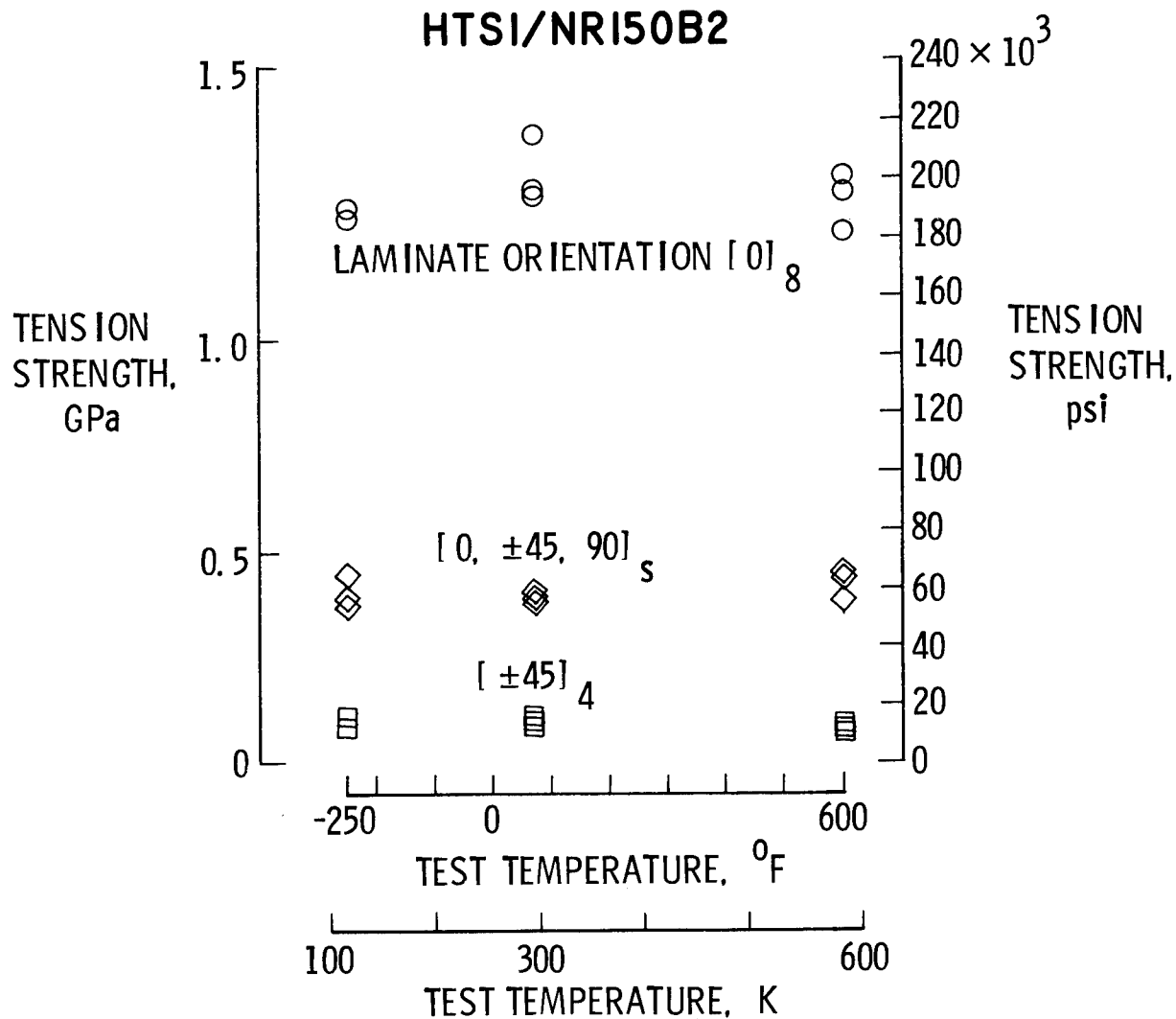


Figure 8

FAILED TENSION SPECIMENS

Failure modes are shown for a quasi-isotropic laminate tested at 117 K (-250° F), room temperature, and 589 K (600° F). For these tests, failure occurred very near the center of the specimen. The tension test procedures used for these tests usually produced failure within the gage area and well away from the tabs.

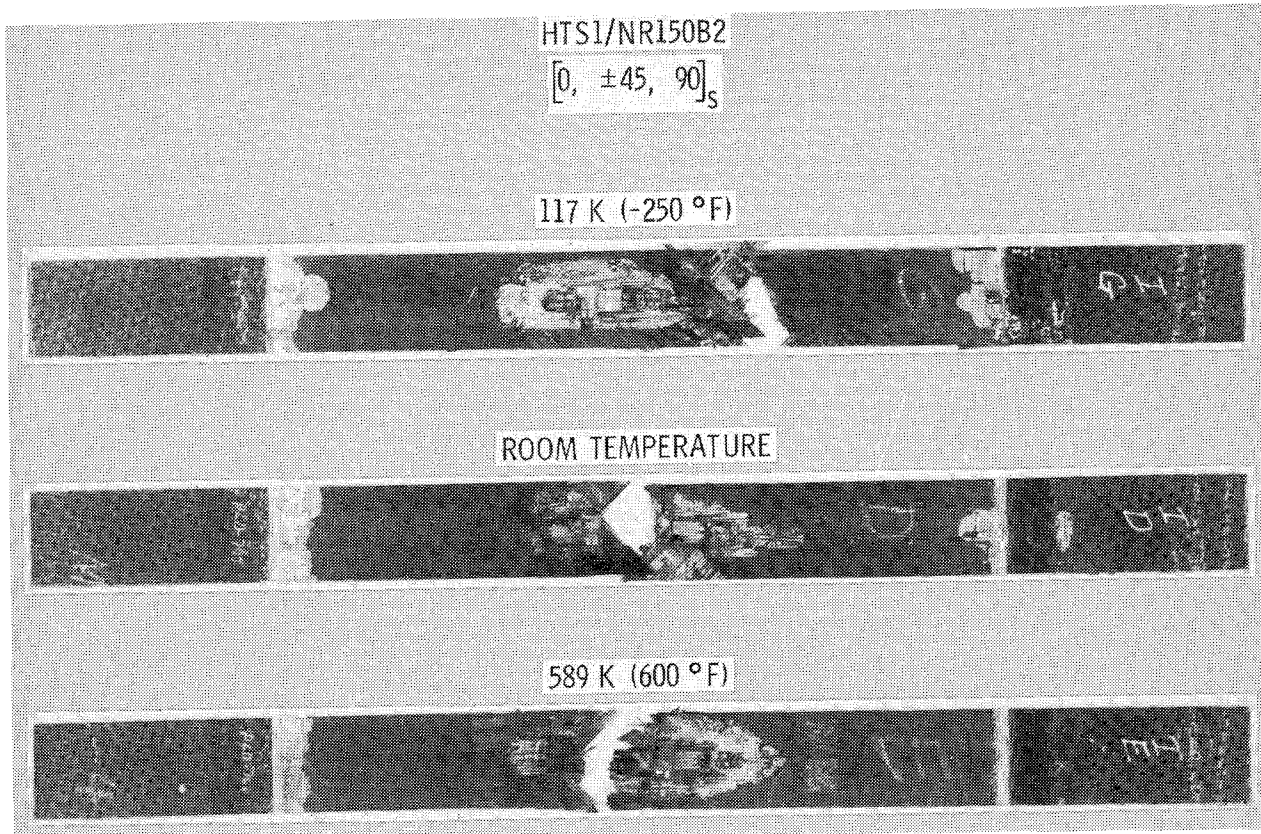


Figure 9

DETERMINATION OF SHEAR MODULUS FROM TENSION TESTS

Tension tests of plus and minus forty-five degree laminates may be used to obtain in-plane shear-modulus values, G_{12} , for the unidirectional lamina. Longitudinal and transverse strains, together with longitudinal tensile stress, are related by the expression derived by Rosen and Petit to obtain the longitudinal shear modulus.

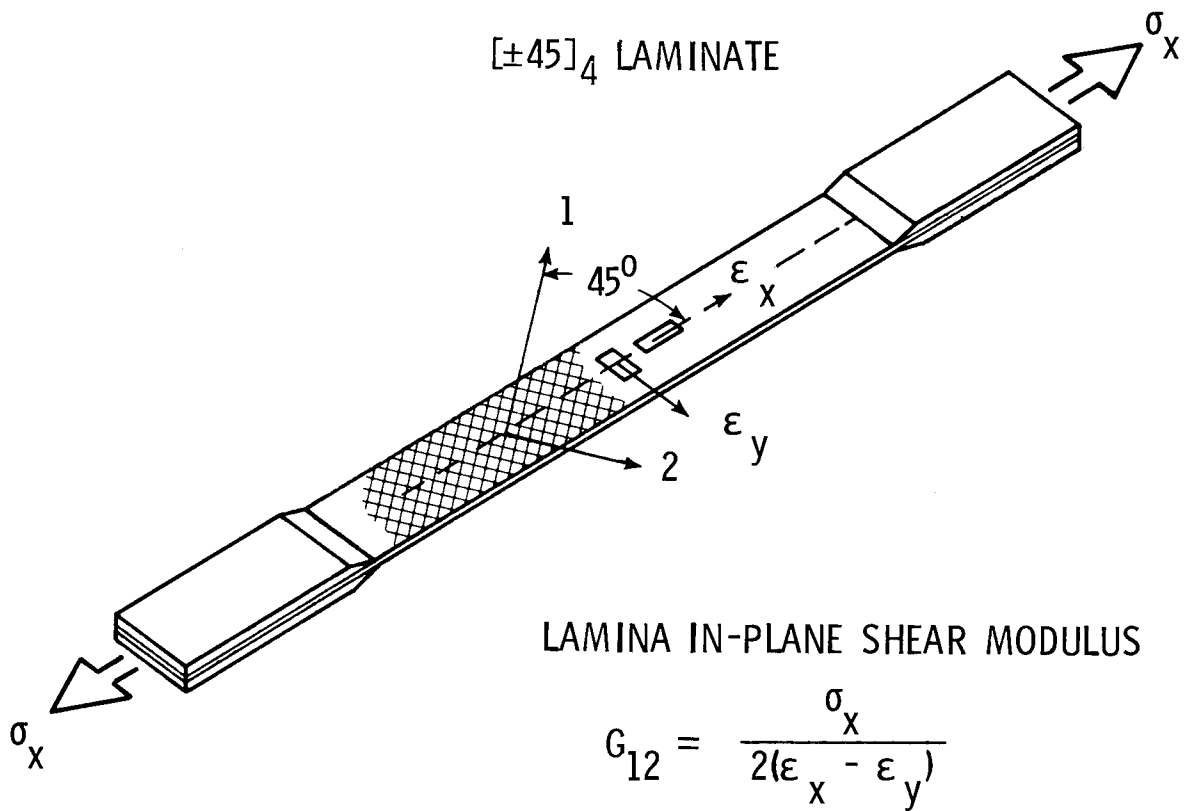


Figure 10

EFFECT OF TEMPERATURE ON SHEAR MODULUS

Lamina shear modulus, G_{12} , is shown as a function of test temperature in figure 11. Shear modulus values are within a range expected for a unidirectional lamina, and decrease with increasing temperatures as expected for a resin sensitive property. These results illustrate that tension tests can be used to supplement the more difficult shear tests (such as the rail-shear method) to characterize lamina shear modulus.

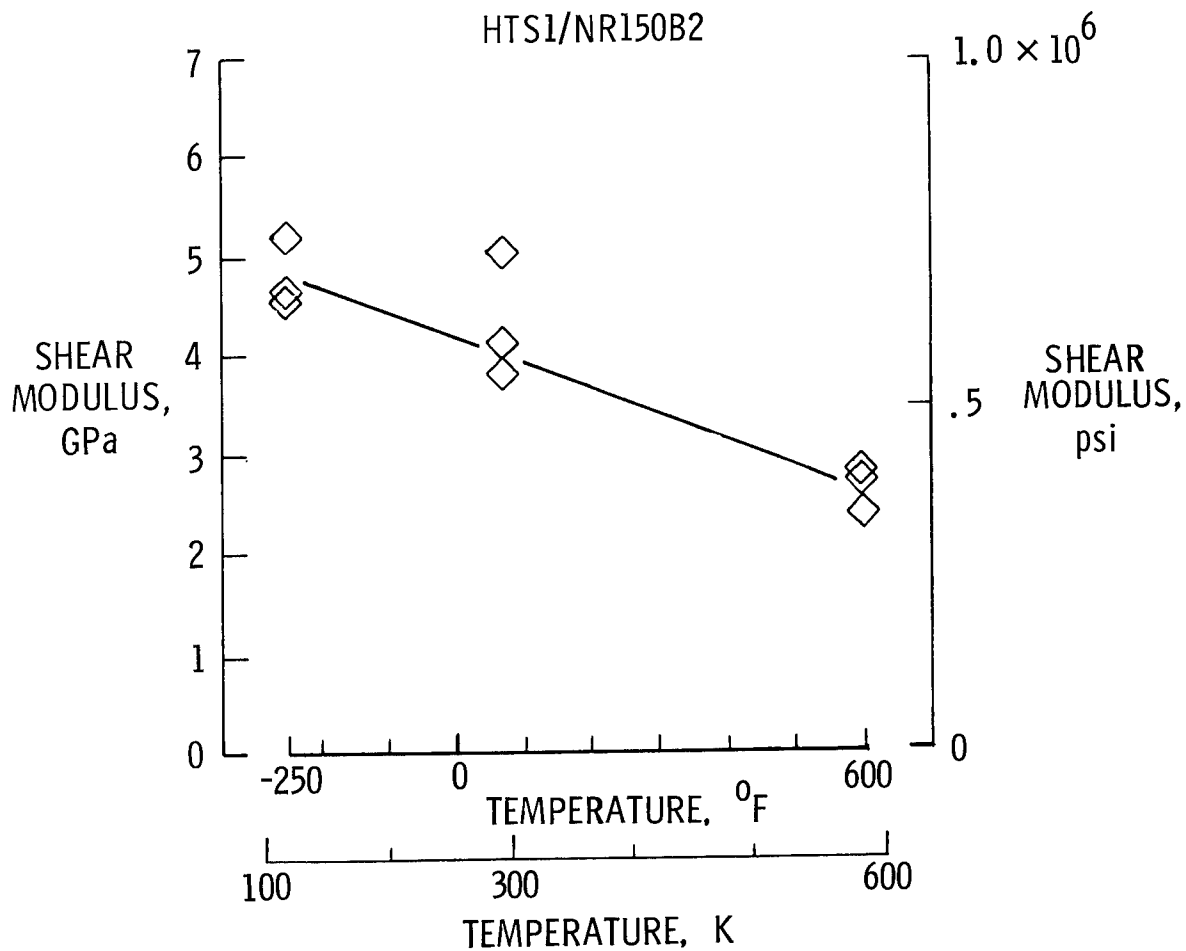


Figure 11

CONCLUDING REMARKS

Tension properties of graphite/polyimide laminates have been obtained at temperatures from 117 K (-250° F) to 589 K (600° F) by modifying existing test procedures for resin-matrix composites. Throughout this temperature range, resistance strain gages provided accurate and repeatable results, suitable for characterizing mechanical properties. Preliminary tension design properties of graphite/polyimide laminates produced through the CASTS Project were obtained at temperatures of 117 K (-250° F), room temperature, and 589 K (600° F).

Mark J. Stuart
NASA Langley Research Center

EXPANDED ABSTRACT

Many test methods have been used for obtaining compressive design data for composite materials. However, few evaluations of such current test methods have been documented. The sandwich beam in four-point bending has been widely used to obtain room temperature compressive data for composites although any effects from the honeycomb core on composite mechanical properties have not been determined. Further, this test method has not been used over a temperature range such as 117 K (-250° F) to 589 K (600° F).

This program showed that the sandwich beam in four-point bending could be used to obtain reliable compressive elastic constants for graphite/polyimide laminates although some difficulties were encountered measuring composite compressive strengths. Data were obtained for ultimate stress, ultimate strain, Young's modulus, and Poisson's ratio values in 117 K, room temperature, and 589 K test environments for the HTS1/PMR-15 material system. A total of 36 compressive tests on $[0]_8$, $[90]_8$, $[(+45)_2]_S$, and $[0/+45/90]_S$ laminates were performed. Also, 24 tensile tests on the same laminate orientations were performed to obtain input to the analytical portion of this program. A portion of the beam test section was analyzed using a linear elastic finite element computer program to predict the stress state in the graphite/polyimide composite. Specifically, the influence of the honeycomb core on this stress state was analytically determined.

SANDWICH BEAM AND CONSTITUENTS

The sandwich beam has been a widely used test specimen (ref. 1 - 3). For this program (ref. 4) each beam was fabricated using a composite top cover, a metal bottom cover, and a metal honeycomb core (figure 1). The assembled specimen measured nominally 559 mm (22 in) long, 25 mm (1.0 in) wide, and 43 mm (1.7 in) high. Different density honeycomb cores were used along the length of the beam. In the beam test section a low density, 98 kg/m^3 (6 lb/ft^3), core was used to minimize any influence from the honeycomb on composite mechanical properties. The remainder of the beam used a higher density core to support the transverse (through the beam thickness) shear load in this region.

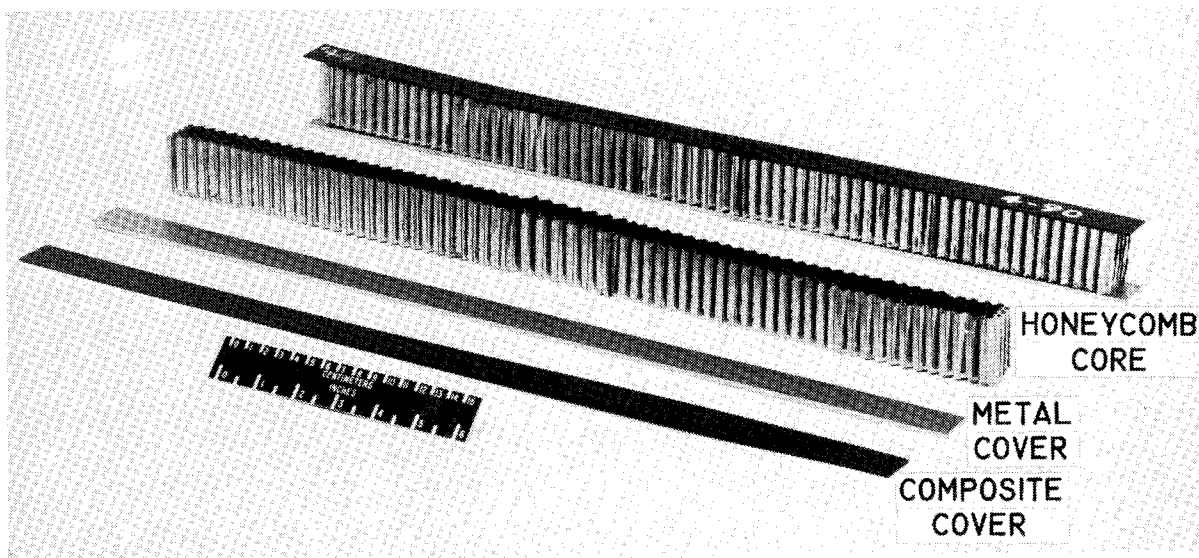


Figure 1

CONSTITUENT TEST SPECIMENS

Constituents of the sandwich beam were tested to obtain input properties for the finite element analysis. Figure 2 shows typical test specimens. The honeycomb used in the beam test section was tested in compression to obtain elastic properties which were neither available from the literature nor available from the manufacturer. Specifically, Young's modulus parallel to the honeycomb ribbon direction, Young's modulus perpendicular to the ribbon direction, and inplane Poisson's ratio data were obtained. Graphite/polyimide specimens were tested in tension to obtain Young's modulus and Poisson's ratio input data. An assumption in the computer analysis was that composite elastic properties were the same in tension and compression. Hence, these tensile elastic constants were used to model composite compressive behavior.

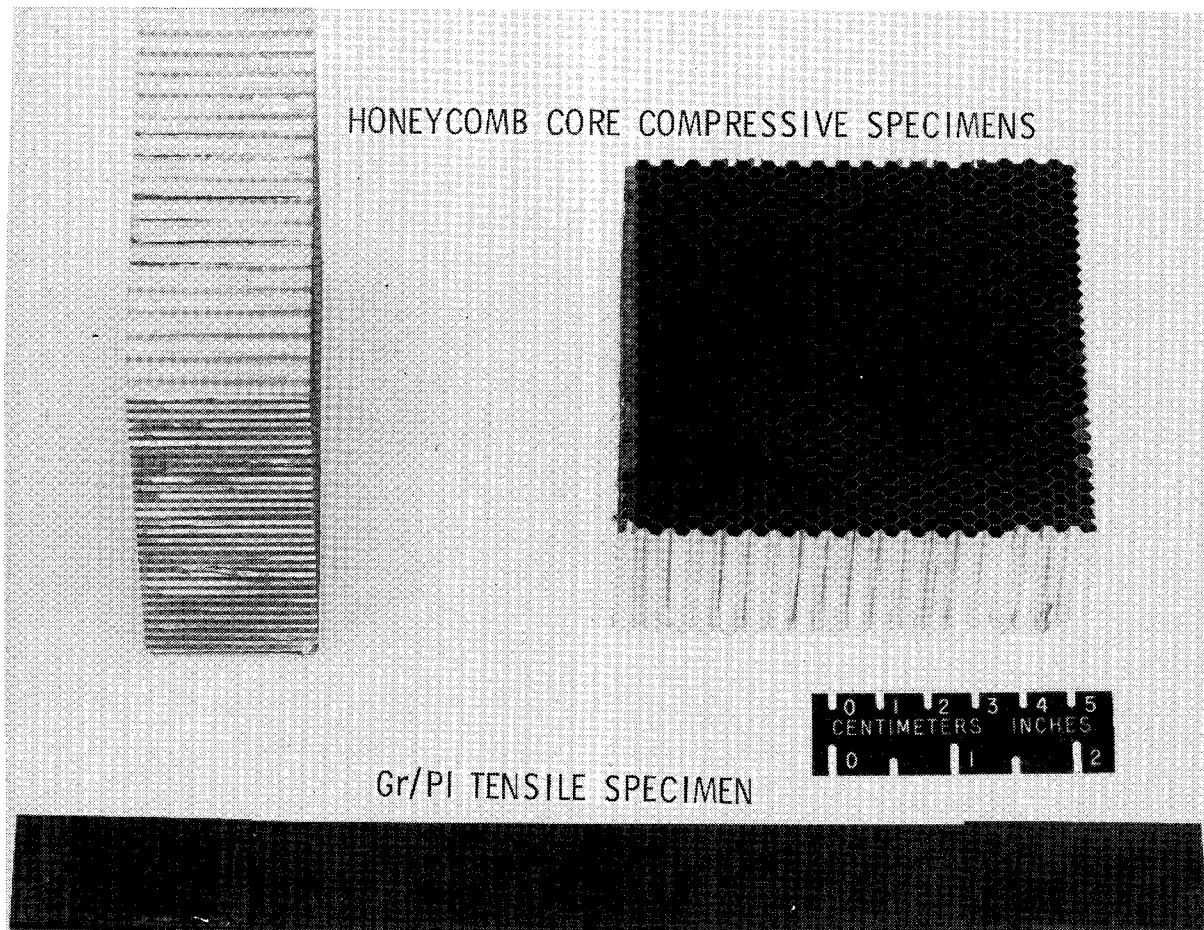


Figure 2

SANDWICH BEAM TEST APPARATUS

A sandwich beam loaded in four-point bending is pictured in figure 3. Load was introduced to the test apparatus through the load platen and applied to the beam specimen at the two points on the top cover. The beam was supported at the two points on the bottom cover. Each of these four points used a 25 mm (1.0 in) diameter rod ground flat to distribute the load over a 625 mm^2 (1.0 in^2) area. Thin load pads were used at the points of load application to minimize any local stress concentrations due to loading. Strain data were obtained from gages located in the center of the top cover.

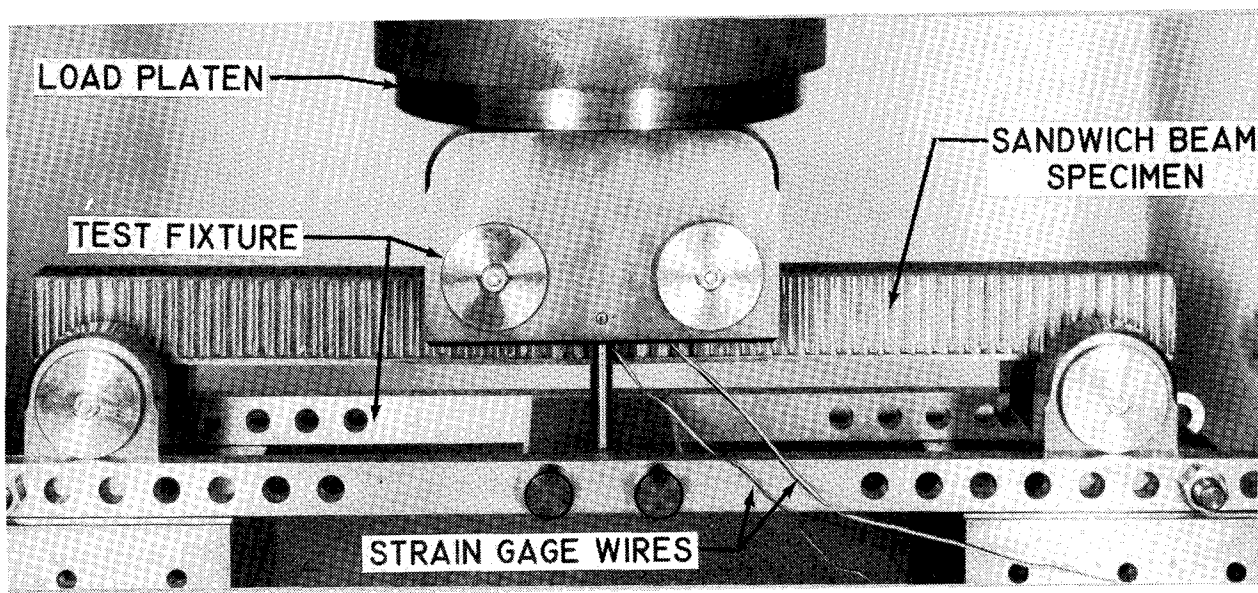


Figure 3

TYPICAL FAILURE OF $[0/\pm 45/90]_s$ LAMINATE

Figure 4 is a close-up view of the test section for a failed quasi-isotropic beam specimen. This location of failure was typical for the $[90_8]$, $[(+45)_2]_s$, and $[0/\pm 45/90]_s$ specimens tested at room temperature. As seen in the figure, the failure of this laminate was due to fiber crushing accompanied by ply delamination. The $[0_8]$ specimens tested at room temperature failed at the point of load application. This location of failure was caused by the high bearing stresses associated with $[0_8]$ laminates. Also, all specimens tested at 117 K (-250° F) failed at the point of load application. These failures may have been caused by material degradation.

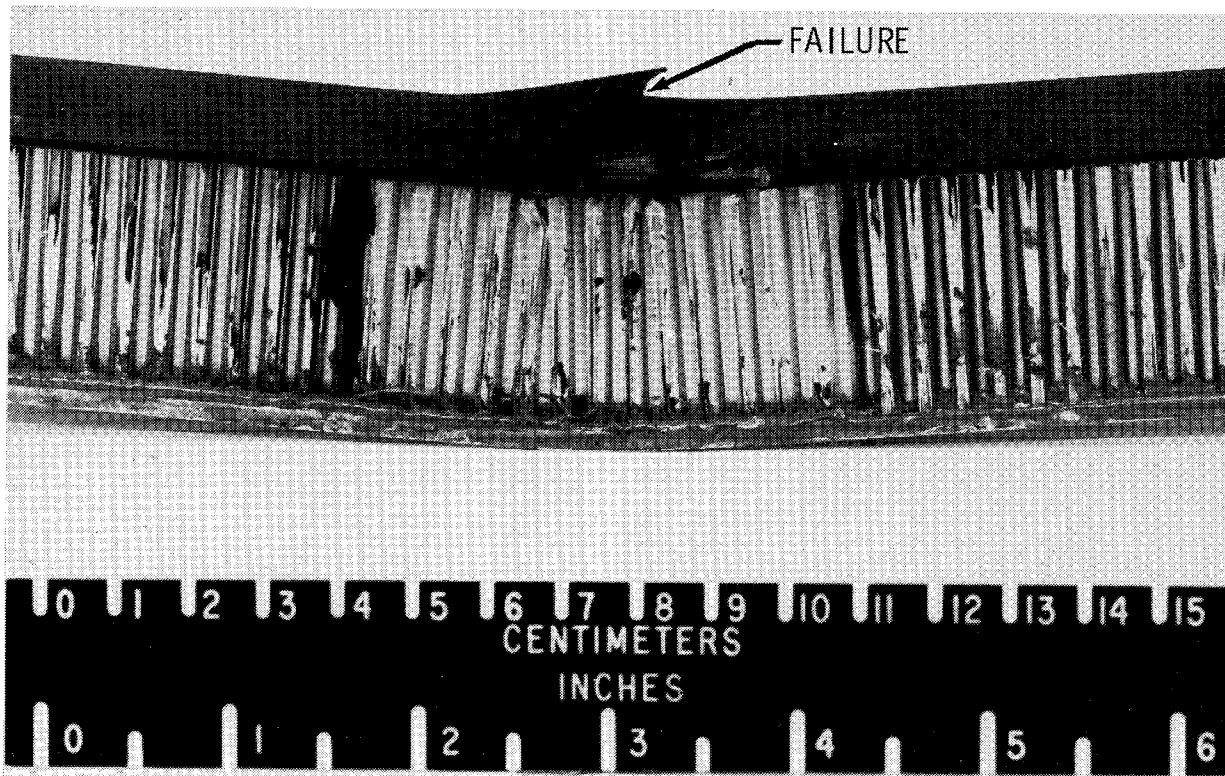


Figure 4

COMPRESSIVE STRESS-STRAIN BEHAVIOR FOR $[0/+45/90]_S$ HTS1/PMR-15

Compressive stress-strain data were obtained at 117 K (-250° F), room temperature, and 589 K (600° F) for all laminates in this study. Data for a $[0/+45/90]_S$ laminate are shown in figure 5. These data indicated a slight difference in Young's modulus at the different test temperatures. Young's modulus is discussed in more detail in a subsequent figure. Although the specimen tested at 117 K failed at the point of load application, the ultimate stress at 117 K was approximately the same as the ultimate stress at room temperature. However, the ultimate stress at 589 K was 49 percent lower than that at room temperature in this figure. All specimens tested at 589 K failed at stresses that were more than 30 percent lower than the corresponding room temperature ultimate stresses. The failures at 589 K were caused by debonding between the composite cover and the honeycomb core. The shear strength of the adhesive between the top cover and the core was not sufficient to carry the shear stresses developed at this interface. Although some modifications were made to minimize this problem, the debond failures were not completely eliminated from the program.

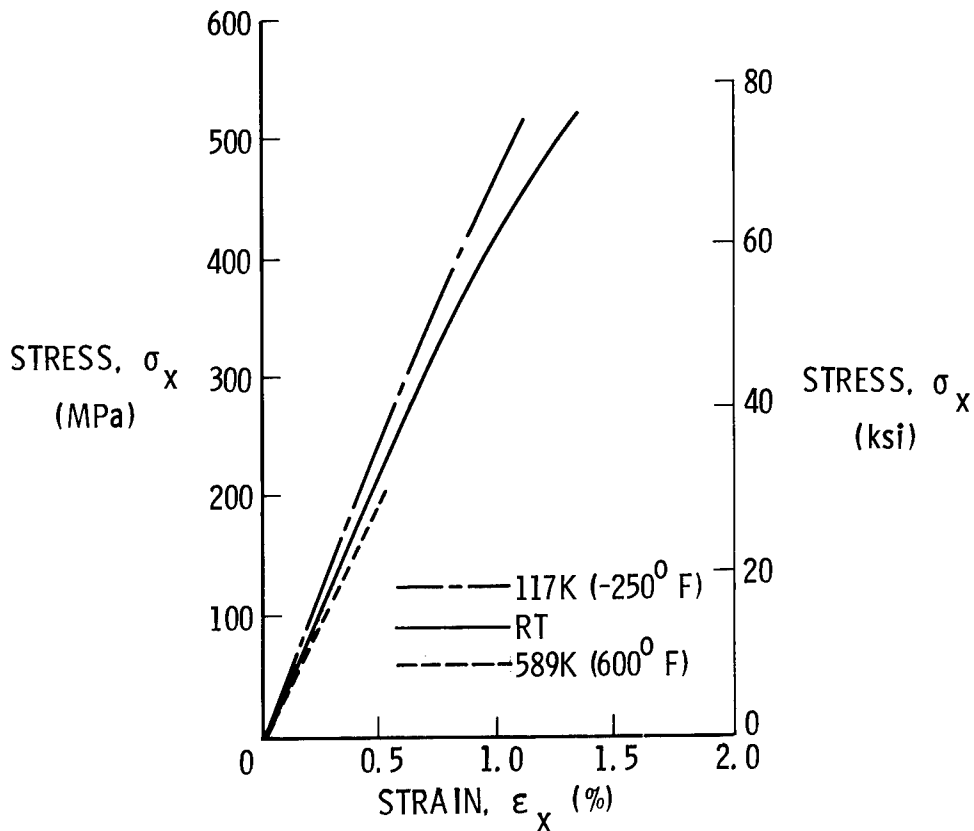


Figure 5

COMPRESSIVE YOUNG'S MODULUS FOR HTS1/PMR-15 LAMINATES

Figure 6 shows the effects of temperature on Young's modulus for all the laminate orientations investigated in this study. Except for $[0_8]$ and $[90_8]$ specimens tested at 589 K (600°F) and 117 K (-250°F), respectively, each data point represents the average of three tests; the exceptions use two tests for each point. Scatter for each data point is also indicated in the figure. Young's modulus for the $[0_8]$ laminate was not affected by temperature although unexplainable scatter appeared in the 117 K data. Young's modulus for the $[0/ \pm 45/ 90]_s$ laminate was approximately the same at 117 K and room temperature but was 15 percent lower at 589 K. This trend indicated some effect from temperature on the modulus of this laminate at 589 K. Since the $[0_8]$ and $[0/ \pm 45/ 90]_s$ configurations are fiber-dominated laminates, temperature was not expected to affect modulus values. Young's modulus values for the $[(+45)_2]_s$ and $[90_8]$ orientations were significantly affected by temperature. For both laminates the values of Young's modulus at 117 K and at 589 K were more than 35 percent higher and more than 15 percent lower, respectively, than the room temperature value. Since $[(+45)_2]_s$ and $[90_8]$ orientations are considered matrix-dominated laminates, these effects from temperature were expected.

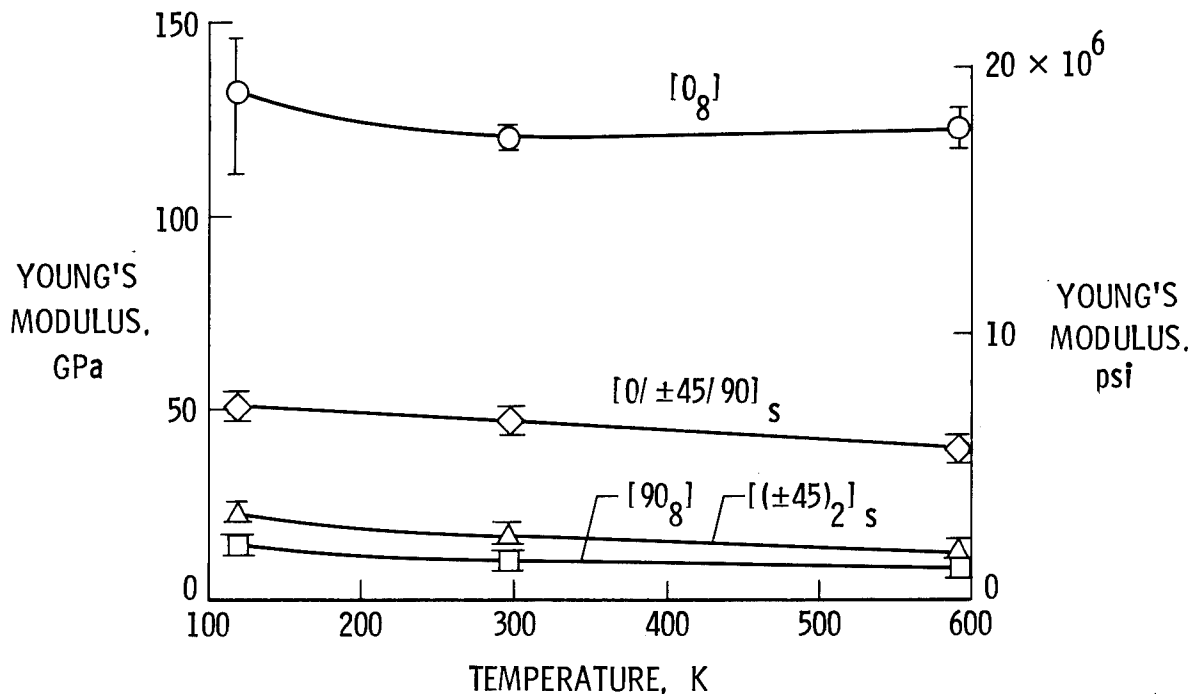


Figure 6

COMPRESSIVE POISSON'S RATIO FOR HTS1/PMR-15 LAMINATES

The effects of temperature on Poisson's ratio for each laminate orientation are shown in figure 7. As expected for the fiber-dominated laminates the values of Poisson's ratio for the $[0_8]$ and $[0/\pm 45/90]_s$ configurations did not appear to be affected by temperature. Any differences were within the experimental scatter of the data. The value of Poisson's ratio for the $[(+45)_2]_s$ orientation was 10 percent lower at 117 K and 10 percent higher at 589 K than the room temperature value. For the $[90_8]$ orientation Poisson's ratio was more than 35 percent higher at 117 K than the room temperature value and appeared to remain constant from room temperature to 589 K. Because of its order of magnitude, Poisson's ratio for the $[90_8]$ laminate was difficult to accurately measure at room temperature and at 589 K.

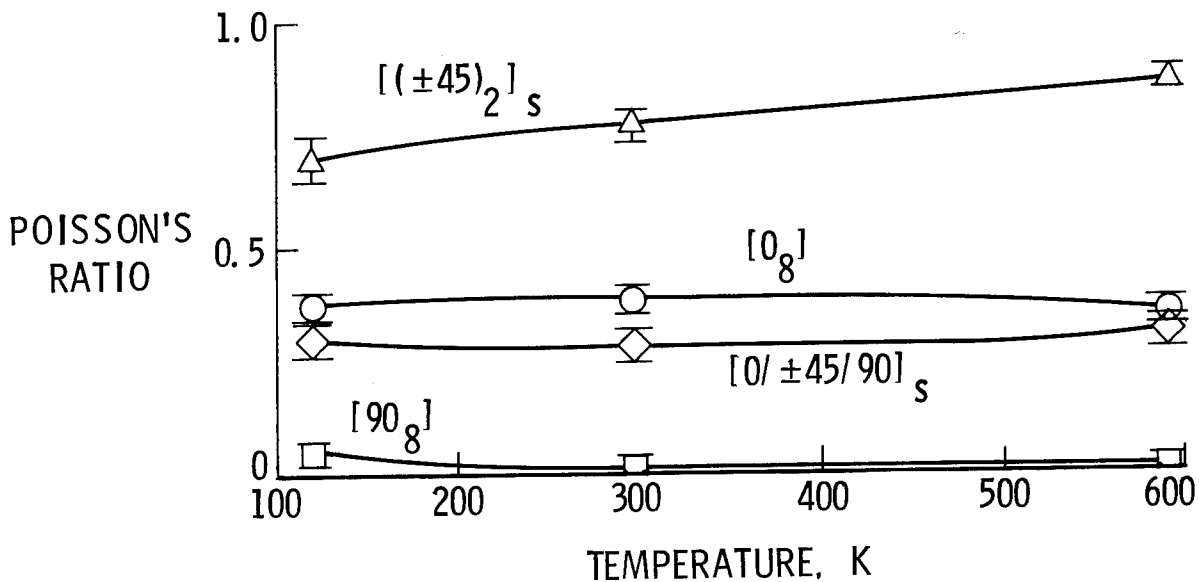


Figure 7

DIAGRAM OF FINITE ELEMENT MODEL FOR SANDWICH BEAM

The three-dimensional finite element model for a portion of the beam test section is illustrated in figure 8. A linear, elastic analysis was used. The composite top cover and the honeycomb core were assumed to be homogeneous, orthotropic materials. The model consisted of 750 elements and 1248 nodes with each node having three translational degrees of freedom, u , v , and w . Three-dimensional brick elements were used to model both the top cover and the honeycomb core; two-dimensional plate elements were used to model the bottom cover. As seen in the figure, many elements were located at the composite-honeycomb interface. The influence of the honeycomb on the stress state in the top cover occurred in this region. The measure of this influence was the magnitude of the y -direction normal stress in the top cover and is discussed in the next figure.

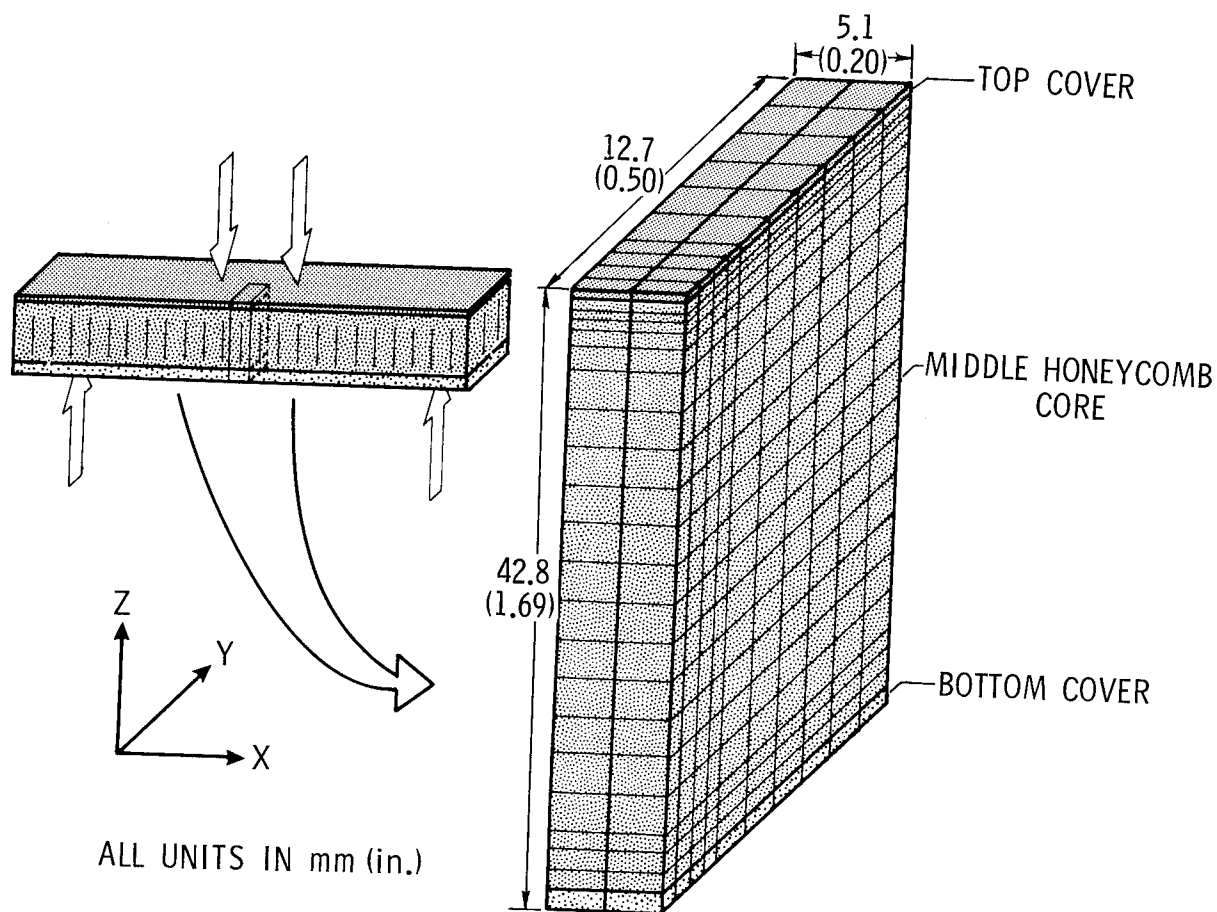


Figure 8

FINITE ELEMENT RESULTS FOR BIAXIAL STRESS EFFECTS
IN TOP COVER OF SANDWICH BEAM

Figure 9 summarizes the results of the analytical portion of this program. The equation in the figure represented the extensional strain in the test section of the top cover. If the effects of the honeycomb core on the stress state in the top cover were negligible, the shaded term in the equation, $\bar{\nu}_{xy} \frac{\bar{\sigma}_y}{\bar{\sigma}_x}$, should be much smaller than unity. As seen in the table,

this term was at least three orders of magnitude smaller than one for all the composite top cover cases.

A check case for a beam specimen with 2024-T3 top and bottom covers was also experimentally and analytically investigated. Young's modulus and Poisson's ratio obtained from beam specimens were the same as those reported in the literature (ref. 5). As seen in the table of analytical results (figure 9), the effects of the honeycomb were predicted to be negligible. Hence, the finite element analysis indicated that a uniform, uniaxial compressive stress state exists in the test section of the beam top cover.

$$\epsilon_x^0 = \frac{\bar{\sigma}_x}{E_x} \left(1 - \bar{\nu}_{xy} \frac{\bar{\sigma}_y}{\bar{\sigma}_x} \right)$$

TOP COVER	MATERIAL SYSTEM	$-\bar{\nu}_{xy} \frac{\bar{\sigma}_y}{\bar{\sigma}_x}$
$[0_8]$	Gr/ PI	0.0001
$[90_8]$	Gr/ PI	0.0001
$[(\pm 45)_2]_s$	Gr/ PI	0.0005
$[0 / \pm 45 / 90]_s$	Gr/ PI	0.0001
2024 - T3	ALUMINUM	0.0099

Figure 9

CONCLUDING REMARKS

The sandwich beam in four-point bending has been examined as a compressive test method for graphite/polyimide composites. Preliminary compressive elastic constants were obtained from laminates tested at 117 K (-250° F), room temperature, and 589 K (600° F). These data indicated that test temperature had minimal effect on Young's modulus and Poisson's ratio for $[0_8]$ and $[0/+45/90]_s$ laminates but had considerable effect on the corresponding properties for $[90_8]$ and $[(+45)_2]_s$ laminates. Compressive strength data did not appear to be reliable for many tests. Failures occurred at the points of load application for $[0_8]$ room temperature specimens and for all 117 K specimens. Also, failures for all 589 K specimens were caused by debonding between the composite cover and the honeycomb core. The finite element analysis did indicate that a uniform, uniaxial compressive stress state existed in the test section of the beam top cover. The influence of the honeycomb core on the stress state in the test section was found to be negligible. Hence, this test method can be used to obtain reliable elastic properties for composites.

REFERENCES

1. Advanced Composite Airframe Structures. First Monthly Progress Report for AF Contract F 33615-68-C-1301, Grumman Aircraft Corporation, March 1967.
2. Waddoups, M. E.: Characterization and Design of Composite Materials. Composite Materials Workshop, S. W. Tsai, J. C. Halpin, and N. J. Pagano, eds., Technomic Publishing Co., Inc., 1968, pp. 254-308.
3. Herakovich, C. T.; and Davis, J. G., Jr.; and Viswanathan, C. N.: Tensile and Compressive Behavior of Borsic/Aluminum. Composite Materials: Testing and Design (Fourth Conference) ASTM STP 617, American Society for Testing and Materials, 1977, pp. 344-357.
4. Shuart, M. J.; and Herakovich, C. T.: An Evaluation of the Sandwich Beam in Four-Point Bending as a Compressive Test Method for Composites. NASA TM 78783, September 1978.
5. Lyman, Taylor, ed.: Metals Handbook. Vol. 1. 8th ed. American Society for Metals, 1961.

APPLICATION OF THE IITRI
COMPRESSION TEST FIXTURE AT ELEVATED TEMPERATURE

15

Charles J. Camarda
NASA Langley Research Center

EXPANDED ABSTRACT

Graphite/polyimide composite materials have potentially attractive properties for use in elevated temperature applications up to 589K(600°F) (ref. 1), but have yet to be sufficiently characterized at elevated temperatures. The designer, in order to use a material system properly, must have a reliable experimental characterization of the response of the material to various loadings such as compression; however, the characterization of composite materials is considerably more complex than metals because of the heterogeneous and anisotropic nature of composite lamina.

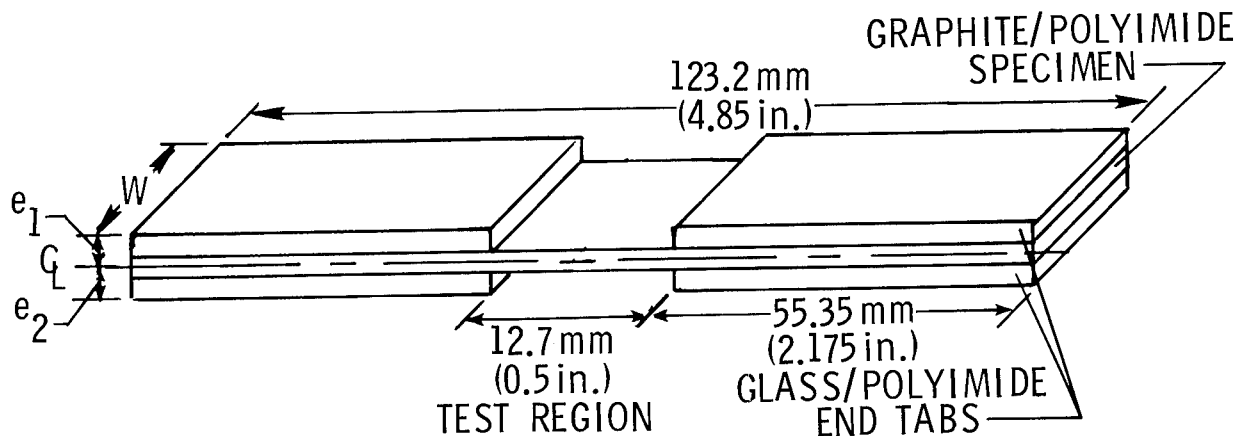
There have been numerous attempts to develop a reliable compressive test technique to determine moduli and ultimate strains of composite materials. A good historical account of compressive test techniques for composites and their associated problems is presented in references 2 to 4. Various specific test techniques ranging from block compression tests of composites to fully supported laminate tests are given in references 5 to 11; each technique exhibits deficiencies in meeting one or more of the criteria for acceptable compression allowables testing or is not readily adaptable to elevated temperature application. The most successful compression technique to date has been the sandwich beam flexure method. However, sandwich beam flexure specimens are relatively large and expensive, requiring a large amount of composite material for fabrication. Also, the low adhesive shear strengths at elevated temperature of bonding agents used to join the laminates to the sandwich core could cause premature specimen failure outside the test region. The standard IITRI test fixture (refs. 2 and 3) does not require expensive test specimens and meets most of the criteria for a successful compression allowables test.

The purpose of the present paper is to describe an application of the IITRI compression test fixture at elevated temperature (589K (600°F)) and to present compressive moduli and ultimate strains of HTS/PMR-15 graphite/polyimide material. Considerable care was taken in specimen fabrication to minimize back-to-back strain variations due to specimen bending. The effects of specimen width and temperature were studied for various laminate orientations. The IITRI specimen was analyzed using three-dimensional finite elements to determine the magnitude and location of stress concentrations to assess their potential effects on measured moduli and ultimate strains. Stress concentrations are of concern since end constraints, free-edge effects, and thermal effects add to the three-dimensional nature of stresses in a specimen as noted in references 12 to 18.

IITRI SPECIMEN CONFIGURATION

End tabs of $[0, 90]_s$ laminates of 7576/CpI-2237 glass/polyimide material were bonded to 123 x 88.9 mm (4.85 x 3.50 in.) graphite/polyimide specimen blanks. The end tabs were primed and assembled with FM-34 film adhesive in a bonding fixture and enclosed in a vacuum bag. The assembly was positioned on a platen press, a vacuum (710 mm Hg (28 in. Hg)) was drawn, and the press was closed to contact the specimen with minimal pressure to allow uniform heating. The specimen was heated to 405K (270°F) at which point a pressure of 0.689 MPa (100 psi) was applied. The temperature was then raised to 589K (600°F) and held for two hours after which the specimen was allowed to cool in the water-cooled platens to room temperature and the pressure was released.

Specimens were machined to specified dimensions maintaining tolerances within ± 0.076 mm (± 0.003 in.). In an effort to obtain parallel surfaces to minimize bending of the specimen during testing, tab surfaces were ground to tolerances of ± 0.051 mm (0.002 in.), maintaining the eccentricity $e_1 - e_2$ (see figure) to within ± 0.076 (0.003 in.). The ends were ground to tolerances of ± 0.076 mm (± 0.003 in.). However, variation in specimen tolerance and the cost of machining the specimens to the tolerances described above were not addressed in this study.



FABRICATION DETAILS:

- END TABS BONDED TO 123.2 X 88.9 mm (4.85 X 3.5 in.) SPECIMEN BLANKS
- FM-34 ADHESIVE
- ALL DIMENSIONAL TOLERANCES (INCLUDING $e_1 - e_2$) WERE WITHIN ± 0.08 mm (± 0.003 in.)

Figure 1

TEST MATRIX

A total of seventy-nine HTS/PMR-15 specimens of various laminate orientations and widths were tested both at room temperature and 589K (600°F) as shown in the figure. The $[0]$ (15 and 16 ply) and $[0, \pm 45, 90]_{2s}$ laminate orientations were fabricated from HTS1/PMR-15 material and the $[90]_{20}$ and $[\pm 45]_{5s}$ laminate orientations were fabricated from HTS2/PMR-15. About three replicate tests were made for each width and temperature investigated. Several titanium specimens were also tested to qualify the test technique at elevated temperature and to insure proper load alignment and friction-free elevated temperature testing.

LAMINATE ORIENTATION	MATERIAL	TEST TEMPERATURE	NUMBER OF SPECIMENS			
			WIDTH			
			6.35 mm (0.25 in.)	12.7 mm (0.5 in.)	19.1 mm (0.75 in.)	25.4 mm (1.0 in.)
$[0]_{15}$	HTS1/PMR-15	ROOM TEMP.	4	4	-	-
		589K(600°F)	4	3	-	-
$[0]_{16}$		ROOM TEMP.	-	-	3	3
		589K(600°F)	-	-	1	3
$[0, \pm 45, 90]_{2s}$		ROOM TEMP.	3	3	3	3
		589K(600°F)	-	4	2	3
$[\pm 45]_{5s}$	HTS2/PMR-15	ROOM TEMP.	3	3	3	3
		589K(600°F)	1	2	1	3
$[90]_{20}$		ROOM TEMP.	-	2	3	3
		589K(600°F)	-	-	3	3

Figure 2

IITRI TEST APPARATUS

The IITRI test fixture consists of two massive end blocks and two trapezoidal wedge collets which grip the specimens and fit in slots machined in the end blocks. Compressive load is transferred to the specimen from the testing machine primarily by shear through the specimen end tabs. The trapezoidal wedge collets were modified to accommodate various width specimens. The collets were tightened to a uniform clamping pressure of 45.8 MPa (6640 psi) at each end tab and end loading pins were included in each collet to prevent specimen slippage early in the load cycle and to support the specimen if the tabs should shear off at elevated temperature. Lateral alinement of the fixture was insured by a guidance system of two parallel roller bushings in the upper half of the fixture and two hardened alinement pins in the lower half. Considerable effort was required to aline the fixture and specimen to minimize bending strains. The faces of the end blocks were alined with a tolerance of ± 0.076 mm (± 0.003 in.). Once proper alinement was accomplished, consistent results were obtained without requiring any further realinement.

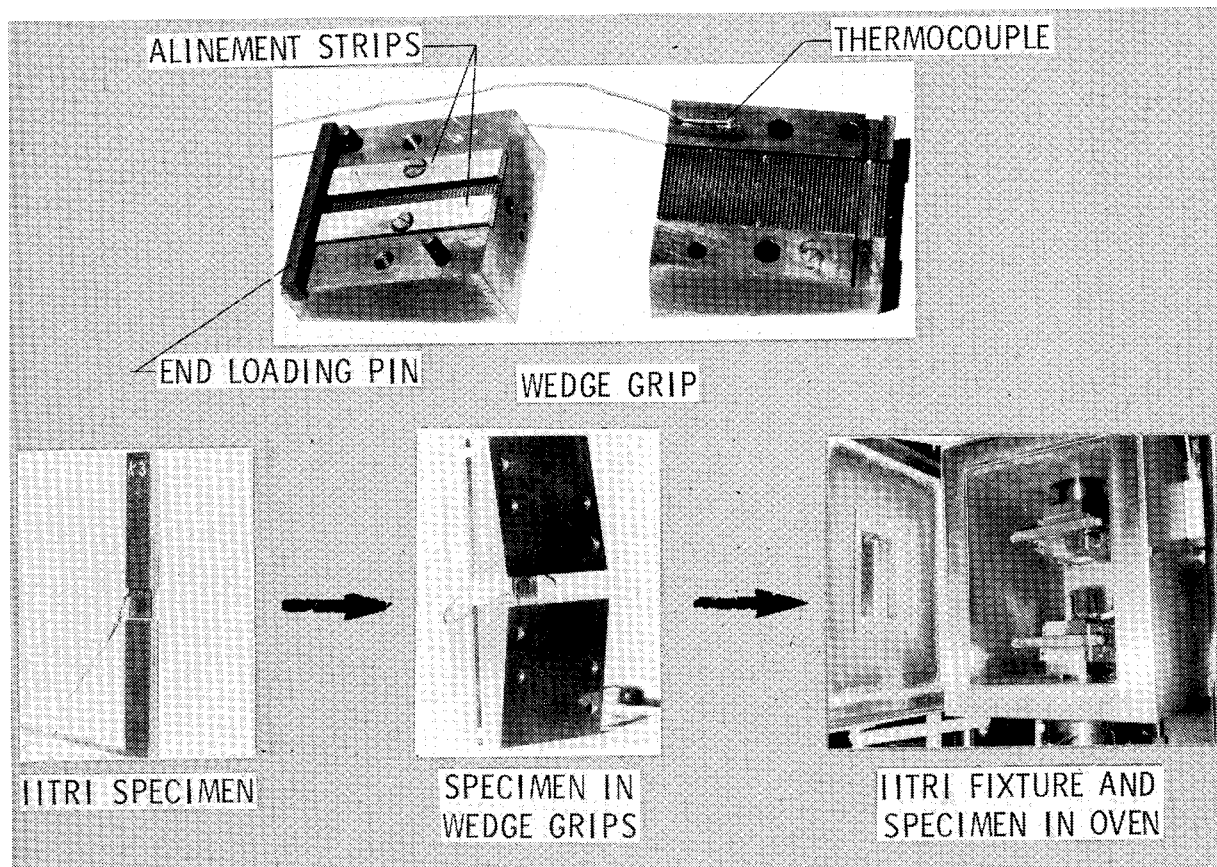


Figure 3

IITRI COMPRESSION TEST FIXTURE AND SPECIMEN IN OVEN

To overcome potential difficulties such as thermal gradients which could occur using the thin wafer-type heaters suggested in reference 2, the entire test fixture, as shown in the figure, was inserted inside an environmental chamber and aligned. To minimize thermal distortion all components of the test fixture and supporting rods except the alignment pins were fabricated from heat-treated 17-4 stainless steel. The alignment pins were solid AISI C-1060 steel hardened to Rockwell 60C. Strip heaters were used to accelerate heat-up of the massive end blocks and reduce test time. The strip heaters and environmental chamber were individually controlled to maintain a uniform temperature for the fixture and specimen. Thermocouples bonded to the specimen, wedge collets, and grips were used to measure temperature uniformity. The alignment pins were coated with a high-temperature lubricant to reduce frictional forces at elevated temperature.

The specimen was bolted into the wedge collets and placed in the bottom grip as shown in the figure and the specimen was allowed to expand freely as the temperature increased. Once the desired steady-state temperature condition was reached, the apparent thermal strains were zeroed out and the specimen was tested.

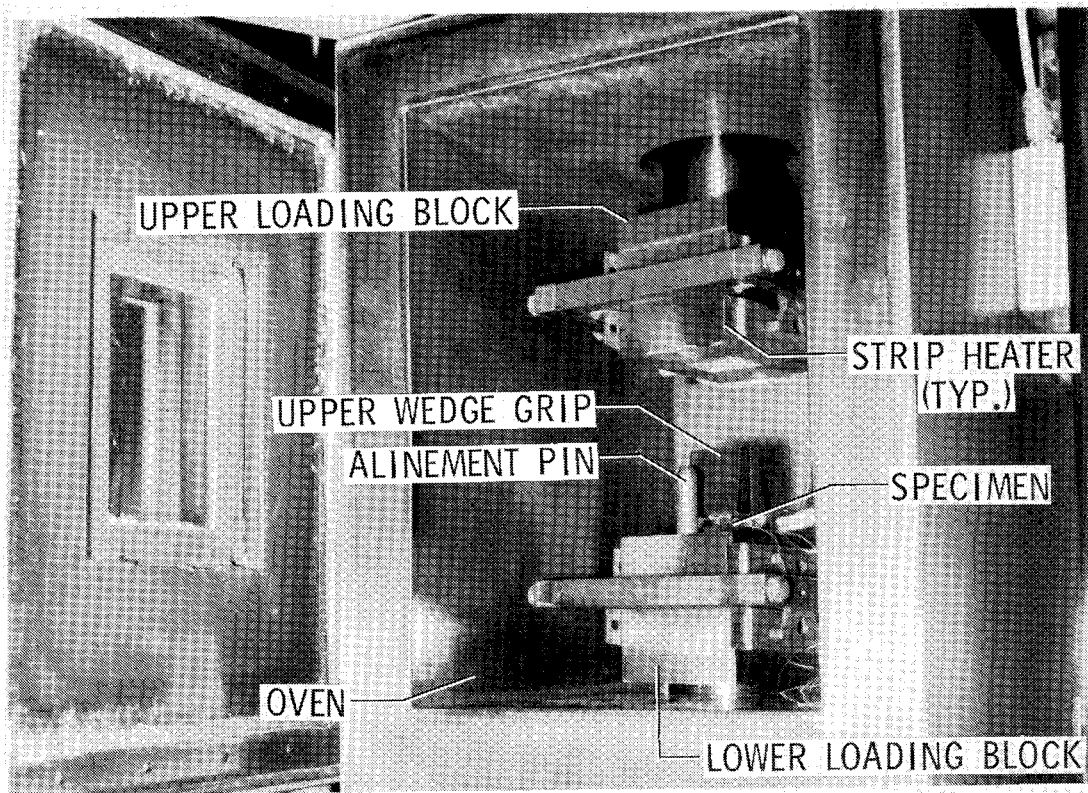


Figure 4

BACK-TO-BACK STRAIN VARIATION

At least one specimen of each series of replicate tests had a self-temperature-compensation high-temperature Micro-Measurements strain rosette, WK-06-030 WR-130 (0.76 mm (0.03 in.) in length) on one face to obtain Poisson's ratio and a single gage, WK-06-062 AP-350 (1.58 mm (0.062 in.) in length) on the opposite face to measure bending strains during testing in order to define proper load alinement. All other specimens had back-to-back single strain gages. Back-to-back strain variations were low even in the nonlinear portion of the stress-strain curve as shown in the figure for the $[\pm 45]_{5s}$ laminate for both room and elevated temperature. The average variation of back-to-back strains for all tests was below 8 percent with minimum and maximum variations of 0 and 18 percent respectively, indicating proper load alinement and negligible specimen bending.

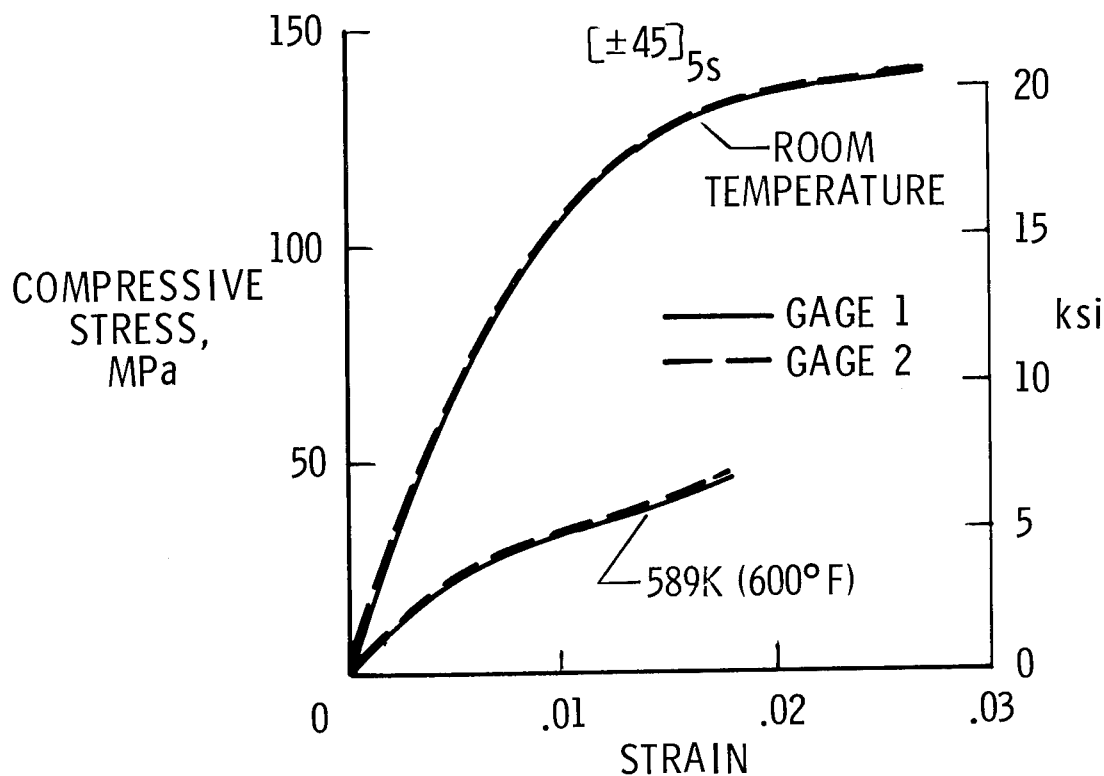


Figure 5

SCATTER OF DATA FROM REPLICATE TESTS

Scatter in each series of replicate tests was evaluated by a statistical analysis of test data. After each series of replicate tests were completed a data reduction program averaged the longitudinal strains in the back-to-back gages of the individual tests and used a regression analysis to determine the coefficients of a best fit (in a least squares sense) of a third order polynomial relating stress and strain to all the data in the series as indicated in the figure. The resulting polynomials were differentiated to calculate tangent modulus-vs-strain curves. The third order polynomial curve produced a good fit of the experimental data.

To assess the magnitude of scatter of experimental points about the regression equation, the standard error of estimate, which is a measure of the mean deviation of the data points from the regression line, was calculated for each series of replicate tests. Scatter of the $[\pm 45]_5$ laminates was representative of the average for all of the tests and as shown by the shaded region in the figure was relatively low. The average standard error of estimate for all four replicate series of the $[\pm 45]_5$ laminate at room temperature was only 2.56 MPa (371 psi) for an average ultimate strength of 136 MPa (19,700 psi).

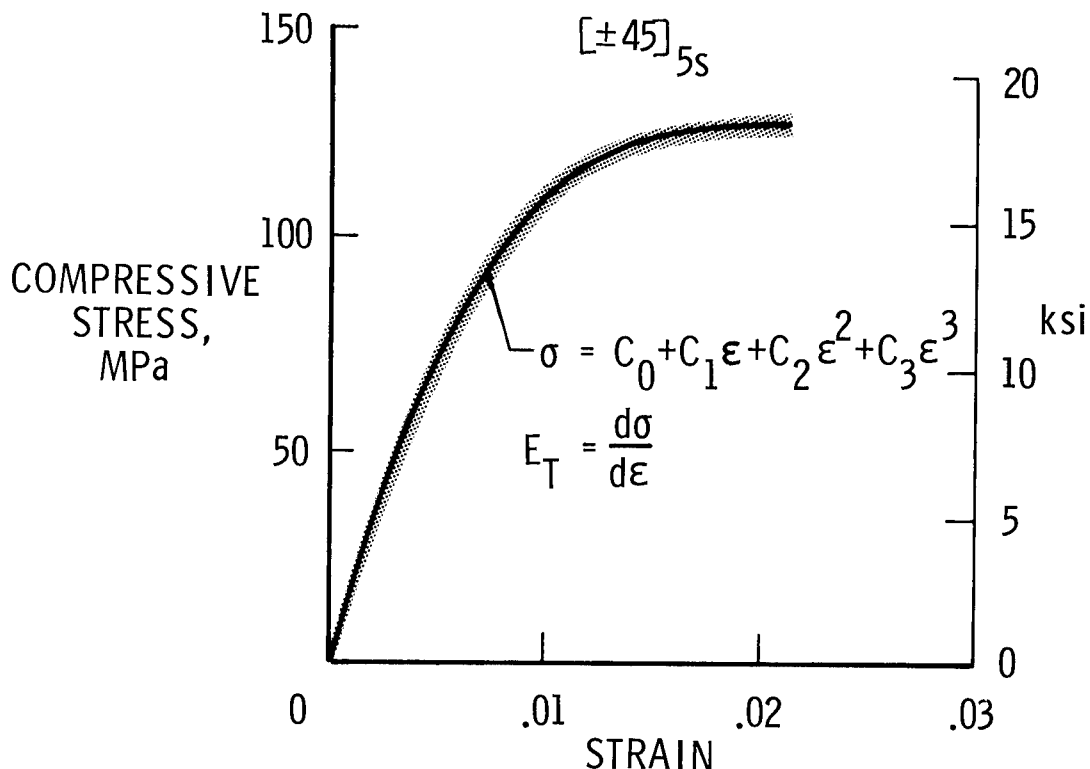


Figure 6

ROOM TEMPERATURE BEHAVIOR OF FILAMENT-CONTROLLED LAMINATES

The unidirectional and quasi-isotropic laminates exhibited a nonlinear behavior at both room and elevated temperature. Average ultimate strain of both laminates was approximately 0.0093. The tangent modulus of the 6.4 mm (0.25 in.) width unidirectional specimens, shown in the figure, decreased by over 30 percent before failure. Results were similar to sandwich beam flexure tests of the same material reported in reference 4. Because of the nonlinear behavior of even the filament controlled laminates, design moduli should not be based on initial values but rather on values corresponding to operating stress or strain levels. A list of tangent moduli at various strain levels at room and elevated temperature is presented in Appendix A. The X's in the tangent modulus curve are tangent modulus values calculated in the following manner: a delta-strain ($\Delta\epsilon$) region was chosen over which all results of the replicate tests were fitted by means of least squares using a straight line fit; hence, the tangent modulus in each $\Delta\epsilon$ region was the slope of each particular straight line. As shown in the figure this technique for calculating tangent modulus-vs-strain agreed well with the curve obtained by differentiating the third order polynomial relating stress to strain.

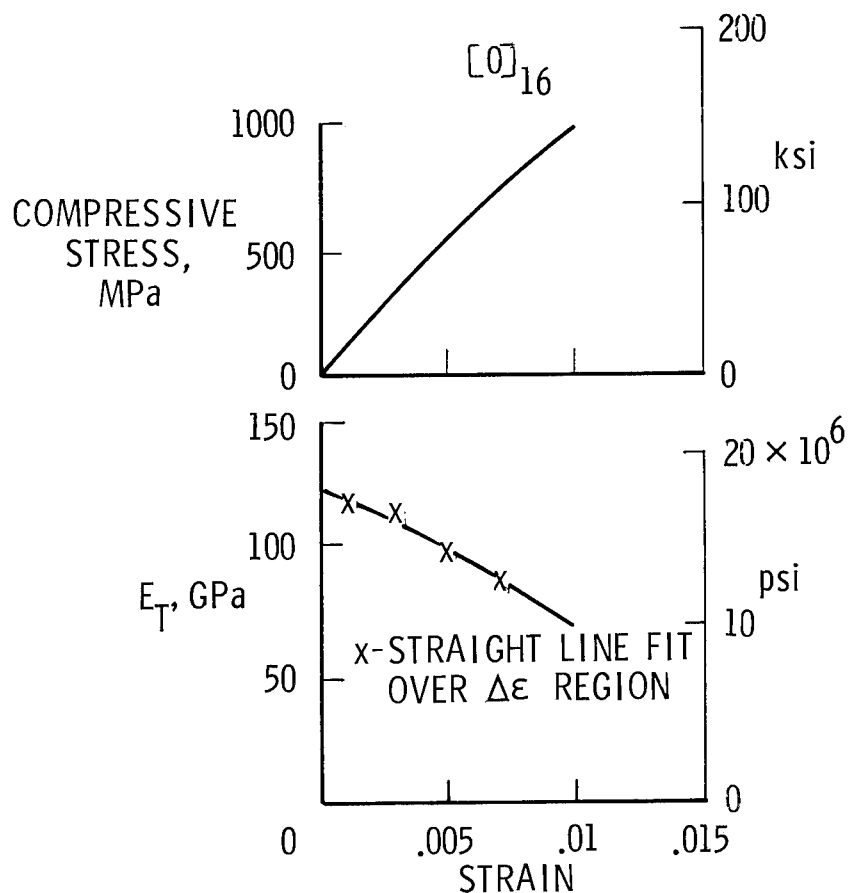


Figure 7

ROOM TEMPERATURE BEHAVIOR OF MATRIX-CONTROLLED LAMINATES

The behavior of the matrix controlled specimens ($[90]_{20}$ and $[\pm 45]_{5s}$ laminate orientations) was more nonlinear than the filament-controlled ones, as would be expected. Average ultimate strain of the $[90]_{20}$ specimens was 0.026 as compared to 0.02 for the $[\pm 45]_{5s}$ specimens. A tangent modulus of approximately 15 GPa (2.2×10^6 psi) at a strain of 0.002 for the $[\pm 45]_{5s}$ specimens reduces to zero at a strain of 0.018 as shown in the figure. The $[\pm 45]_{5s}$ laminate results were more nonlinear than the $[90]_{20}$ laminate. Tangent modulus values at various strain levels at room and elevated temperature are tabulated in Appendix A for both laminates.

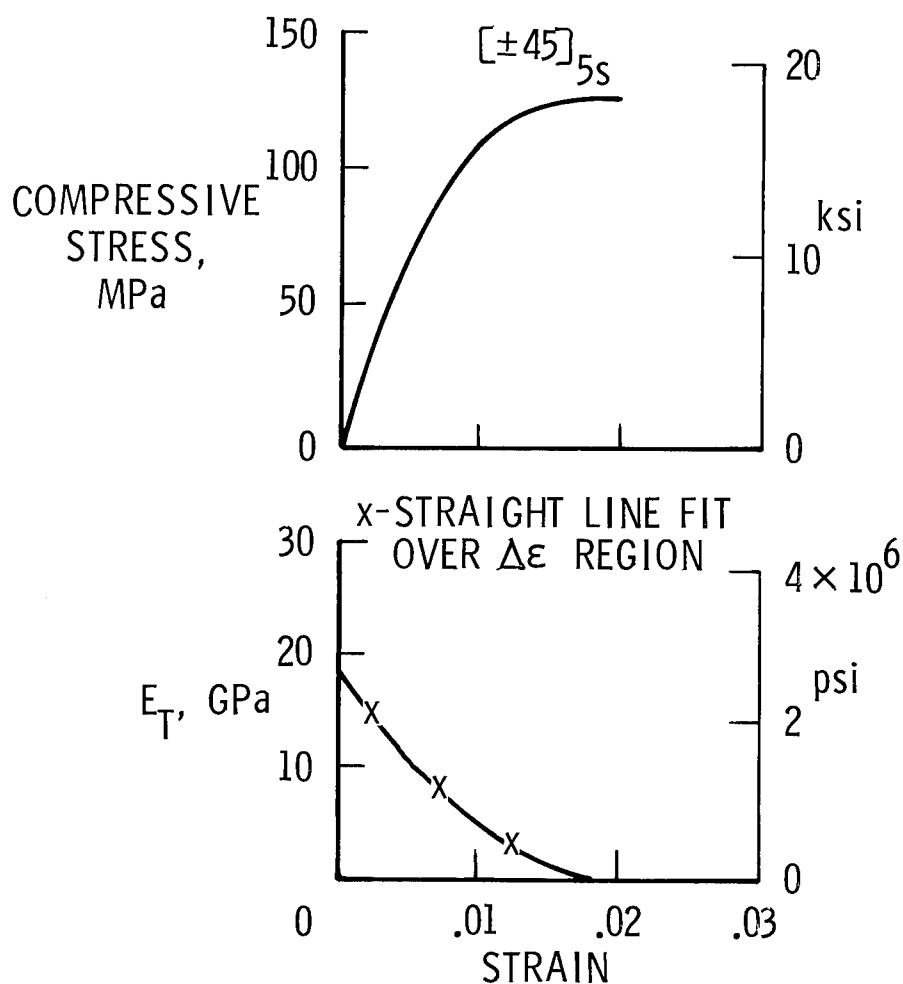


Figure 8

EFFECT OF SPECIMEN WIDTH AND TEMPERATURE ON FILAMENT-CONTROLLED LAMINATES

Specimen width had a negligible effect on average material properties; variation in ultimate strength with specimen width was of the same order as the magnitude of scatter of replicate tests. Ultimate unidirectional compressive strengths decreased by approximately 46 percent at 589K (600°F) from room temperature values of 0.97 GPa (140 ksi).

An interesting feature of unidirectional HTS1/PMR-15 is that measured average initial modulus values of approximately 130 GPa (18.9×10^6 psi) at 589K (600°F) were 20 percent higher than room temperature values. Although this increase in stiffness at elevated temperature is abnormal it was not caused by extraneous frictional loads and was repeatable. Temperature had very little effect on initial modulus of the quasi-isotropic laminate but strengths at 589K (600°F) were 20 percent lower than an average room temperature value of 0.38 GPa (55 ksi).

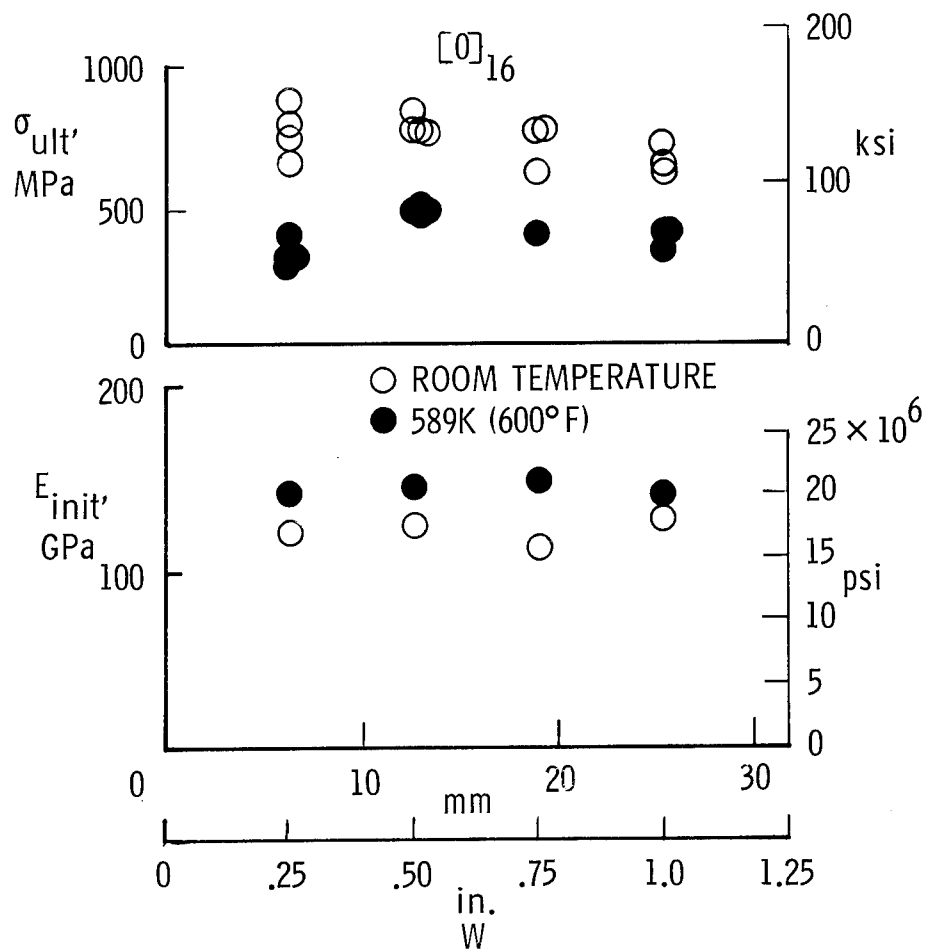


Figure 9

EFFECT OF SPECIMEN WIDTH AND TEMPERATURE ON MATRIX-CONTROLLED LAMINATES

The room temperature ultimate strength of $[\pm 45]_{5s}$ specimens tends to increase with increasing width as shown in the figure. The initial modulus and strength of the $[\pm 45]_{5s}$ laminate orientation at 589K (600°F) decreased from room temperature values of 16 GPa (2.2×10^6 psi) and 120 MPa (18 ksi) by 57 and 53 percent, respectively. Initial modulus values of 8.3 GPa (1.2×10^6 psi) of the $[90]_{20}$ laminate orientation were lower than the $[\pm 45]_{5s}$ laminate orientation, as expected, and dropped to 5.2 GPa (0.75×10^6 psi) at 589K (600°F). Ultimate strengths of this laminate were higher than those of the $[\pm 45]_{5s}$ laminate orientation and dropped from 190 MPa (28 ksi) at room temperature to 69 MPa (10 ksi) at elevated temperature.

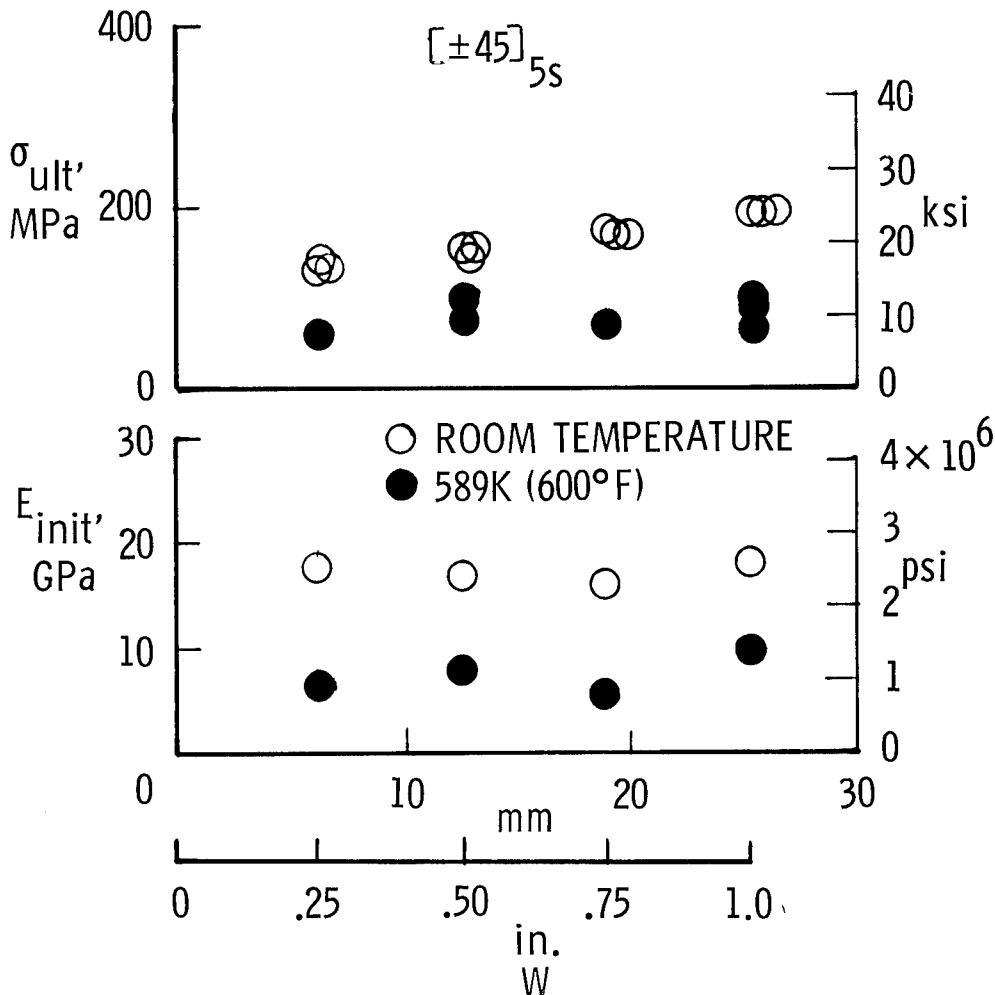


Figure 10

FAILURE MODES OF LAMINATES

Most of the unidirectional specimens failed near the tab region as shown in the figure. The fractured surface in the majority of cases was at right angles to the direction of load indicating shear failure through the fibers and matrix as described in reference 19. In some cases, however, the fractured surface was inclined at an angle. Both types of failures were noted in reference 11. The quasi-isotropic laminates failed in the center of the specimen throughout the thickness of the laminate by matrix cracking along the fiber direction of each lamina. The $[90]_{20}$ specimens failed in the center of the test region at an angle to the load indicating a shear type of failure. Failure surfaces angled from the center of the specimen toward the end tabs.

The modes of failure of the above mentioned laminates did not vary at elevated temperature. The failure mode of the $[\pm 45]_{5s}$ specimens did, however, change with temperature. Most of the room temperature $[\pm 45]_{5s}$ specimens failed near the tab region in the upper two layers by delamination as shown in the figure. However, at 589K (600°F) most of the $[\pm 45]_{5s}$ specimens failed by cracks which extended through the specimen thickness from the center to regions near the tabs. No change in failure mode of any specimens occurred as the specimen width was varied.

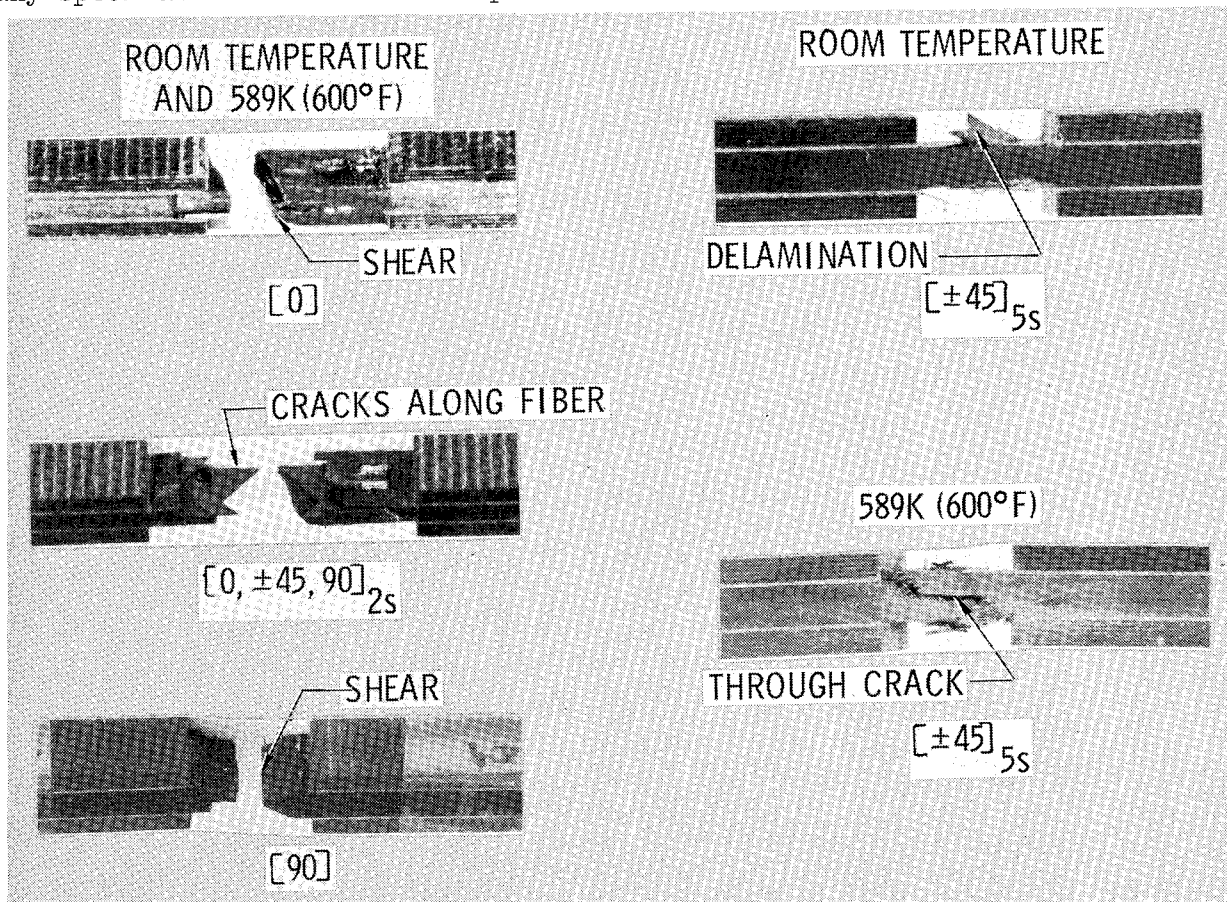


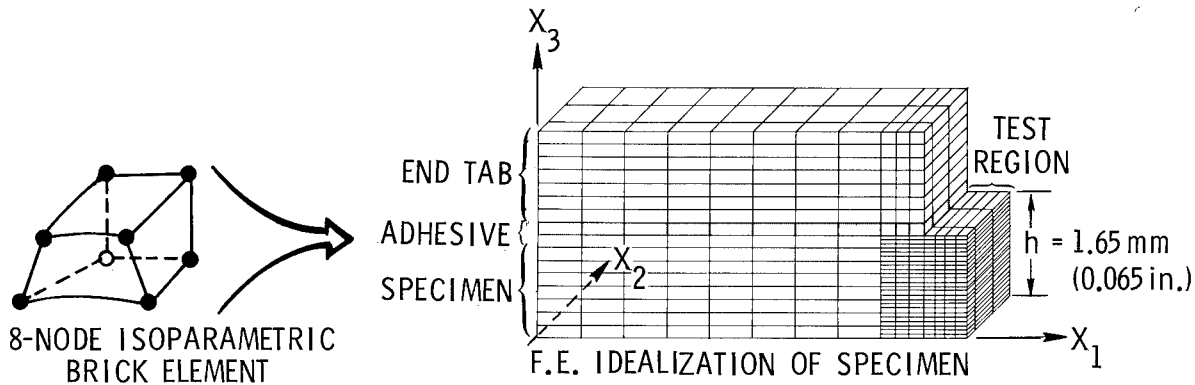
Figure 11

THREE-DIMENSIONAL FINITE ELEMENT IDEALIZATION OF IITRI COMPRESSION SPECIMEN

To fully understand the effects of end loading conditions such as tab shear, fixture clamping, and end pin (axial), and to investigate thermal effects produced by a uniform increase in specimen temperature, the IITRI specimen, including end tabs and adhesive, was analyzed using finite elements.

Because of symmetry only one-eighth of the specimen was modeled. The analysis is based on 8-node orthotropic isoparametric brick elements using the ATLAS integrated structural analysis and design system (ref. 20). The finite-element model represents a 16-layer balanced symmetric laminate specimen, 7-layer glass-polyimide end tabs having a $[0, 90]_S$ laminate orientation, and one layer of FM-34 polyimide adhesive. Each lamina was modeled macroscopically by one element (0.2057 mm (0.0081 in.) thick) in the thickness direction in the coarse grid region and by three elements (0.0686 mm (0.0027 in.) thick) in the thickness direction in the fine grid region located in the test section of the specimen and partially under the tabs. It was assumed that the specimen was free of residual stress at room temperature. Additional information for the finite element model is given in the figure.

The classical tension problem of references 14 and 16 was analyzed as a checkout of the modeling techniques and the ATLAS 3-D elements, and results of the present study agreed well with the published results.



- ONE-EIGHTH OF SPECIMEN MODELED DUE TO SYMMETRY
- EACH LAMINA MODELED MACROSCOPICALLY BY ORTHOTROPIC ELEMENTS
- 3 ELEMENTS IN THICKNESS DIRECTION PER LAMINA IN TEST REGION
- 1008 ELEMENTS, 4100 D.O.F.

Figure 12

ANALYTICAL RESULTS OF A $[\pm 45]_{4S}$ LAMINATE SUBJECTED TO A TAB SHEAR LOAD

Although all six components of stress were calculated in each lamina of all of the laminates tested only results for normal stresses in the fiber direction of the $[\pm 45]_{5S}$ specimens are presented for selected lamina. In an effort to save modeling time the finite element analysis assumed a 16 ply balanced symmetric laminate specimen ($[\pm 45]_{4S}$). This difference in analytical and experimental laminate thicknesses was considered to have a negligible effect on the comparison of analytical and experimental results. The stresses are centroidal, and the stresses labeled σ' are in the material coordinate system of each individual lamina, and are presented in the form of stress contour plots as shown in the figure.

Results indicate that in the gage area the specimen stresses are uniform and similar to lamination theory values of -757 MPa (-110 ksi). Therefore the test method should predict accurate modulus values. However, stress concentrations exist in the upper layer near the tab ($x_3/h = 0.91$) and in the center of the specimen ($x_3/h = 0.02$) in the middle of the test section which probably result in conservative ultimate strength values. The actual value of the stress concentrations are -1590 MPa (-230 ksi) at $x_3/h = 0.91$ near the end tab and -1170 MPa (-170 ksi) at $x_3/h = 0.02$ in the center of the test region. The region of predicted peak compressive stress agrees with the location of failure for this laminate and the test condition described earlier.

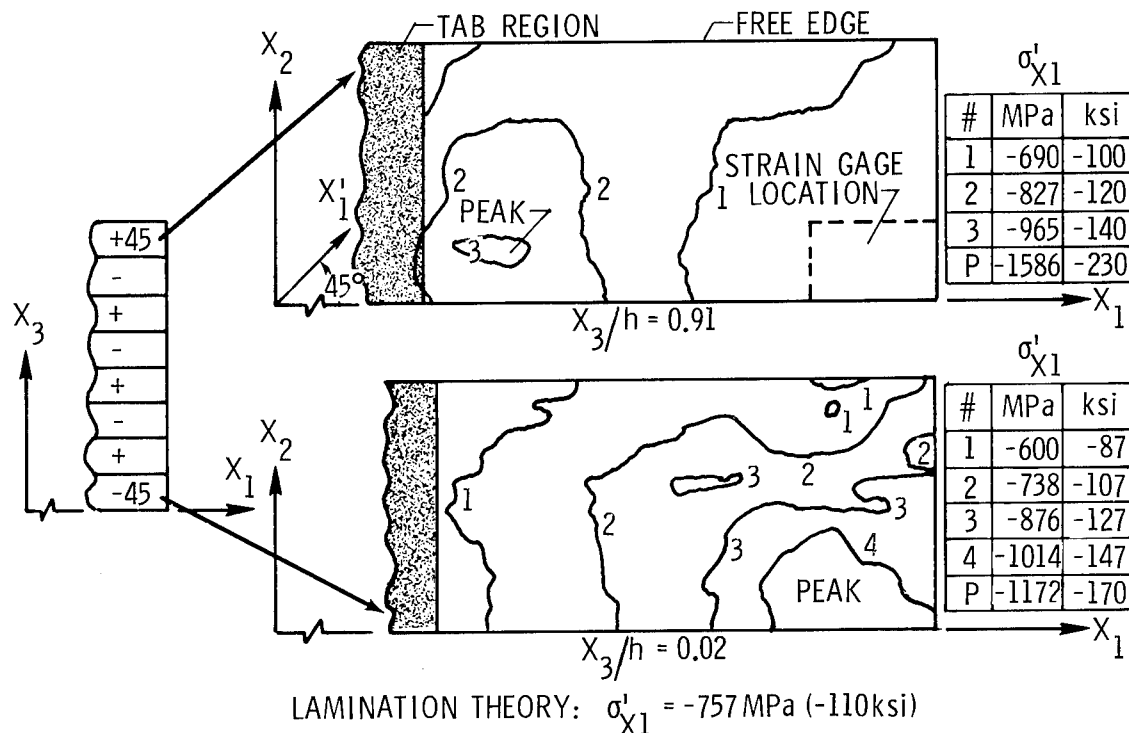


Figure 13

ANALYTICAL RESULTS OF A $[\pm 45]_{4S}$ LAMINATE
SUBJECTED TO A UNIFORM INCREASE IN TEMPERATURE TO
589K (600°F)

Compressive stresses in the fiber direction of selected lamina of a $[\pm 45]_{4S}$ laminate subject to only a uniform increase in temperature of 589K (600°F) are shown in the figure. An interesting result of this load case is the normal tensile stresses in the fiber direction of the top layer and the compressive stresses in the middle layer. These stresses are a result of a combination of the following: coefficient of thermal expansion mismatch between the end tabs and the specimen, free-edge effects, and lamina-to-lamina material property variation. Peak stresses for the combined mechanical and thermal load case occur in the same regions as in the mechanical load case and actual values were obtained from computer listings. Because of the nature of the stress distribution at elevated temperature the location of peak compressive stresses for the combined mechanical and thermal problem changes from the room temperature location. At elevated temperatures stress concentrations near the tabs at $x_3/h = 0.91$ are reduced from room temperature values of -1590 MPa (-230 ksi) to -1260 MPa (-182 ksi) and stress concentrations near the center of the test region at $x_3/h = 0.02$ are increased to -1570 MPa (-228 ksi). The change in location of high compressive stress from the upper layers near the tabs to the center of the specimen agrees with the experimental failure mode change at 589K (600°F) discussed earlier.

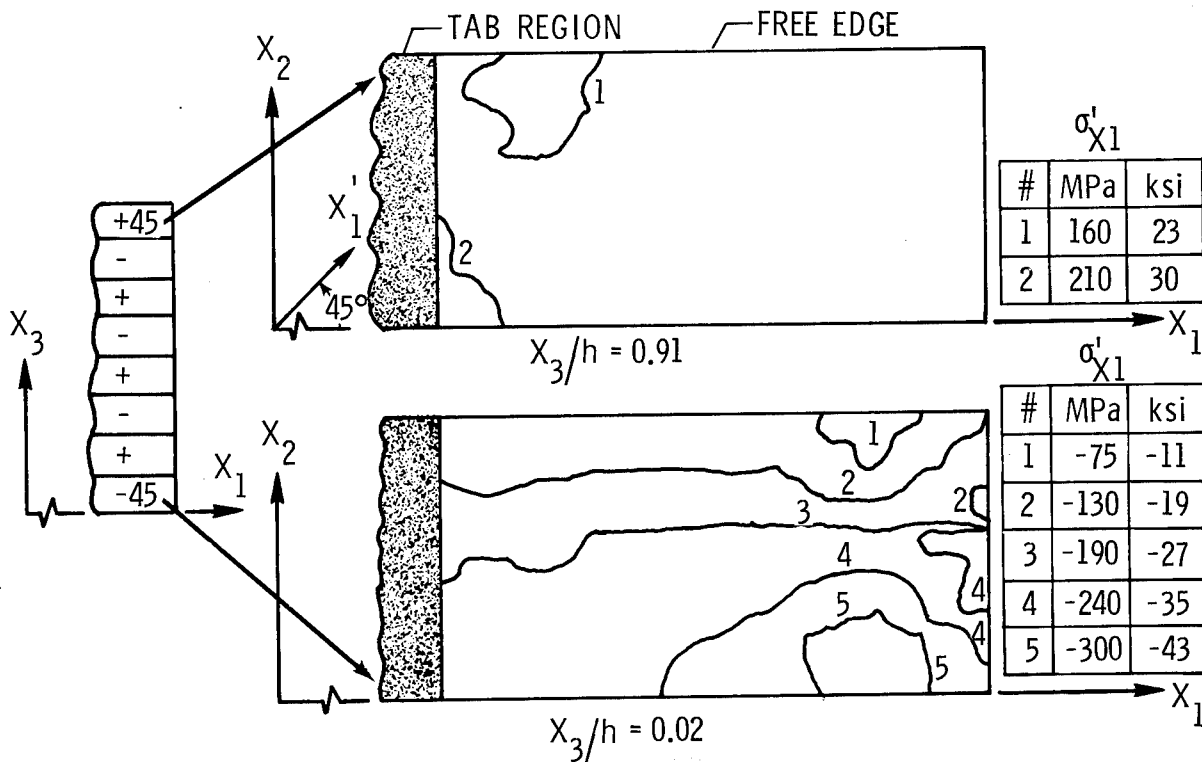


Figure 14

CONCLUSIONS

The IITRI test fixture was used in an experimental program to determine compressive material properties of HTS/PMR-15 graphite/polyimide material at elevated temperatures (589K (600°F)). A total of seventy-nine coupon specimens of various laminate orientations and widths were tested to verify feasibility of the IITRI technique at such temperatures, and to determine the effect of specimen width and temperature on modulus and ultimate strain values. The IITRI specimen was analyzed using three-dimensional finite elements to determine the magnitude and location of stress concentrations to assess their potential effects of measured moduli and ultimate strains.

The IITRI test fixture was found to be feasible for applications at temperatures up to 589K (600°F). The ultimate strain and modulus data obtained in the study indicate that graphite/polyimide is an attractive material for use at temperatures up to 589K (600°F). All laminates tested ($[0]$ (15 and 16 plies), $[90]_{20}$, $[\pm 45]_{4S}$, and $[0, \pm 45, 90]_{2S}$) exhibited nonlinear behavior. The variation of modulus values with strain was sufficiently large that design moduli should be based on operating strain levels.

Effects of variation in specimen width were the same order as the scatter in the data; average scatter for replicate tests was less than eight percent with minimum and maximum values of 0 and 18 percent, respectively.

Analytical results predicted areas of stress concentrations which probably result in conservative values of ultimate strength. However, calculated stresses in the strain gage region of the specimen were uniform and close to lamination theory; thus measured modulus values should be unaffected by stress concentrations. Insight into the failure modes of the specimens was obtained. In particular, a change in failure mode of the $[\pm 45]_{5S}$ laminate at elevated temperature which was observed experimentally correlated with changes in locations of peak stresses predicted analytically.

APPENDIX A. - MODULUS VARIATION WITH STRAIN

(a) Filament-Controlled Laminates

LAMINATE ORIENTATION	TEMPERATURE K(°F)	MODULUS GPa (psi x 10 ⁶)				
		STRAIN				
		0	0.002	0.004	0.006	0.008
[0] ₁₅	294 (70)	123 (17.8)	114 (16.6)	103 (15.0)	94 (13.6)	80 (11.6)
[0] ₁₆	589 (600)	145 (21.0)	142 (20.6)	127 (18.4)	-	-
[0,+45,90] 2s	294 (70)	54 (7.8)	44 (6.4)	41 (5.9)	36 (5.2)	30 (4.3)
	589 (600)	41 (6.0)	41 (6.0)	37 (5.4)	30 (4.4)	19 (2.7)

(b) Matrix-Controlled Laminates

LAMINATE ORIENTATION	TEMPERATURE K(°F)	MODULUS GPa (psi x 10 ⁶)				
		STRAIN				
		0	0.005	0.010	0.015	0.02
[+45] _{5s}	294 (70)	19 (2.8)	10 (1.5)	5 (0.7)	1 (0.2)	0
	589 (600)	7.4 (1.1)	4 (0.6)	2 (0.3)	0	-
[90] ₂₀	294 (70)	9.0 (1.3)	8.3 (1.2)	6.9 (1.0)	6 (0.9)	6 (0.9)
	589 (600)	6 (0.9)	5 (0.7)	3 (0.5)	1 (0.2)	-

APPENDIX B. - MATERIAL PROPERTIES ASSUMED IN FINITE-ELEMENT ANALYSIS

GRAPHITE/POLYIMIDE SPECIMEN:

$$\begin{aligned}E_{11} &= 140 \text{ GPa } (20 \times 10^6 \text{ psi}), \quad E_{22} = E_{33} = 14 \text{ GPa } (2.1 \times 10^6 \text{ psi}) \\G_{12} &= G_{13} = G_{23} = 5.9 \text{ GPa } (0.85 \times 10^6 \text{ psi}) \\v_{12} &= v_{13} = v_{23} = 0.21 \\\alpha_{11} &= 16 \times 10^{-8} \text{ m/m-K } (8.9 \times 10^{-8} \text{ in/in-}^\circ\text{F}) \\\alpha_{22} &= \alpha_{33} = 5 \times 10^{-5} \text{ m/m-K } (3 \times 10^{-5} \text{ in/in-}^\circ\text{F})\end{aligned}$$

GLASS/POLYIMIDE END TABS:

$$\begin{aligned}E_{11} &= 54 \text{ GPa } (7.8 \times 10^6 \text{ psi}), \quad E_{22} = E_{33} = 18 \text{ GPa } (2.6 \times 10^6 \text{ psi}) \\G_{12} &= G_{13} = G_{23} = 9.0 \text{ GPa } (1.3 \times 10^6 \text{ psi}) \\v_{12} &= v_{13} = v_{23} = 0.25 \\\alpha_{11} &= 9 \times 10^{-6} \text{ m/m-K } (5 \times 10^{-6} \text{ in/in-}^\circ\text{F}) \\\alpha_{22} &= \alpha_{33} = 5.8 \times 10^{-5} \text{ m/m-K } (3.2 \times 10^{-5} \text{ in/in-}^\circ\text{F})\end{aligned}$$

FM-34 ADHESIVE:

$$\begin{aligned}E_{11} &= 18 \text{ GPa } (2.6 \times 10^6 \text{ psi}), \quad E_{22} = E_{33} = 7 \text{ GPa } (1 \times 10^6 \text{ psi}) \\G_{12} &= G_{13} = G_{23} = 3.2 \text{ GPa } (0.46 \times 10^6 \text{ psi}) \\v_{12} &= 0.19, \quad v_{13} = v_{23} = 0.184 \\\alpha_{11} &= 12 \times 10^{-6} \text{ m/m-K } (6.7 \times 10^{-6} \text{ in/in-}^\circ\text{F}) \\\alpha_{22} &= \alpha_{33} = 2.9 \times 10^{-5} \text{ m/m-K } (1.6 \times 10^{-5} \text{ in/in-}^\circ\text{F})\end{aligned}$$

E is Young's modulus, G is the shear modulus, ν is Poisson's ratio, and α is the coefficient of thermal expansion. The subscripts 1, 2, and 3 refer to the longitudinal or fiber direction, transverse direction, and thickness direction, respectively.

REFERENCES

1. Composites for Advanced Space Transportation Systems (CASTS). Technical report for period July 1, 1975 through April 1, 1978. NASA TM-80038, 1979.
2. Hofer, Kenneth E.; and Rao, P. N.: A New Static Compression Fixture for Advanced Composite Materials. Journal of Testing and Evaluation, JTEVA, Vol. 5, No. 4, July 1977.
3. Hofer, Kenneth E.; Rao, P. N.; and Humphrey, V. E.: Development of Engineering Data on the Mechanical and Physical Properties of Advanced Composite Materials. Tech Report AFML-TR-72-205-Part I, Sept., 1975.
4. Shuart, Mark J.; and Herakovich, Carl T.: An Evaluation of the Sandwich Beam In Four-Point Bending as a Compressive Test Method of Composites. NASA TM-78783, Sept., 1978.
5. Verette, R. M.: Temperature/Humidity Effects on the Strength of Graphite/Epoxy Laminates. AIAA Paper 75-1011, Presented at the Aircraft System and Technology Meeting, Los Angeles, Aug. 4-7, 1975.
6. Ho, Tzu-Li: A Compressive Test Method for Composites. Proceedings of the Seventh National Technical Conference, Oct. 14-16, 1975, pp. 295-305.
7. Ewins, P. D.: A Compressive Test Specimen for Unidirectional Carbon Fibre Reinforced Plastics. ARC CP No. 1132, 1970.
8. Purslow, D.; and Collings, T. A.: A Test Specimen for the Compressive Strength and Modulus of Unidirectional Carbon Fibre Reinforced Plastic Laminates. R.A.E. Technical Report 72096, 1972.
9. Collings, T. A.: Transverse Compressive Behavior of the Unidirectional Carbon Fibre Reinforced Plastics. R.A.E. Technical Report 72237, 1973.
10. Collings, T. A.: Transverse Compressive Behavior of Unidirectional Carbon Fibre Reinforced Plastics. Composites, Vol. 5, May, 1974, pp. 108-116.
11. Ryder, J. T.; and Black, E. D.: Compression Testing of Large Gage Length Composite Coupons. Composite Materials: Testing and Design (Fourth Conference), ASTM STP 617, 1977, pp. 170-189.
12. Pagano, N. J.; and Halpin, J. C.: Influence of End Constraint in the Testing of Anisotropic Bodies. J. Composite Materials, Vol. 2, No. 1, Jan., 1968, pp. 18-31.

13. Lenoe, Edward: Testing and Design of Advanced Composite Materials. Journal of the Engineering Mechanics Division, Proceedings of the American Society of Civil Engineers, Dec., 1970, pp. 809-823.
14. Pipes, R. Bryon; and Pagan, N. J.: Interlaminar Stresses in Composite Laminates Under Axial Extension. J. Composite Materials, Vol. 4, Oct., 1970, pp. 538-548.
15. Pagano, J. J.; and Pipes, R. Bryon: Some Observations on the Interlaminar Strength of Composite Laminates, Int. J. Mech. Sci., Vol. 15 (1973), pp. 679.
16. Wang, A. S. D.; and Crossman, Frank W.: Some New Results of Edge Effect in Symmetric Composite Laminates. J. Composite Materials, Vol. 11, Jan. 1977, pp. 92-106.
17. Wang, A. S. D.; and Crossman, Frank W.: Edge Effects on Thermally Induced Stresses in Composite Laminates. J. Composite Materials, Vol. 11, Jan. 1977, pp. 300-312.
18. Herakovich, Carl T.: On Thermal Edge Effects in Composite Laminates. Int. J. Mech. Sci., Vol. 18, pp. 129-134, 1976.
19. Ewins, R. D.; and Ham, A. C.: The Nature of Compressive Failure in Unidirectional Carbon Fibre Reinforced Plastics. R.A.E. Tech. Report 73057, 1973.
20. Miller, Ralph E.: Structures and Technology and Impact of Computers. Proceedings of ASME Winter Annual Meeting, Integrated Design and Analysis of Aerospace Structures, Houston, Texas, Nov. 30-Dec. 5, 1977, pp. 57-70.

Ramon Garcia
Robert R. McWithey

NASA Langley Research Center

EXPANDED ABSTRACT

This report discusses the results of both an experimental test program and a finite element analysis of selected graphite/polyimide rail shear test specimens. The two-dimensional finite element analysis includes both mechanical and thermal loading (differential expansion) of the specimens and their elastic rails. Parameters in this analysis of unidirectional and symmetric, balanced angle-ply laminates include ply layup angles, the effect of flexible rails, the method of load introduction to the specimen and the effect of uniform heating of the specimen and rails. Two types of tensile rail shear fixtures were investigated experimentally: a uniform thickness, bolted-rail shear fixture loaded diagonally across the specimen test section; and a tapered thickness, bonded-rail shear fixture loaded axially along the centerline of the specimen test section. Test results include room-temperature and 589 K (600⁰F) strain data taken from the center of the specimen test section during loading.

RAIL SHEAR SPECIMENS

This test method consists of two metallic rails either bonded or bolted to a specimen of test material. An inplane shear load is transmitted to the test material by the differential displacement of the rails as shown in figure 1.

Ideally, a state of pure uniform shear can only be imposed on a rectangular specimen by loading all four boundaries. The presence of free edges in the rail shear test eliminates the possibility of a pure uniform shear state existing within the specimen test section. Coker (ref. 1), using photoelastic techniques on homogeneous glass, was able to demonstrate that a uniform state of shear existed in the central region of his isotropic specimens having large length-to-width ratios. Other investigators (ref. 2-7) have examined the rail shear test method as applied to composite materials.

The purpose of this investigation is to address some of the questions left unanswered by previous investigations. This investigation has two objectives: First, to analytically investigate the states of stress within the specimen due to mechanical and thermal loading where factors to be considered in the investigation include the influence of load introduction and rail configuration; and second, to compare the results from an experimental investigation of two types of shear fixtures where one rail shear fixture utilizes bolted rails of uniform cross-sectional area, while the other rail shear fixture utilizes bonded rails of tapered cross-sectional area. Shear stress-strain and shear modulus data are obtained at room temperature and 589 K.

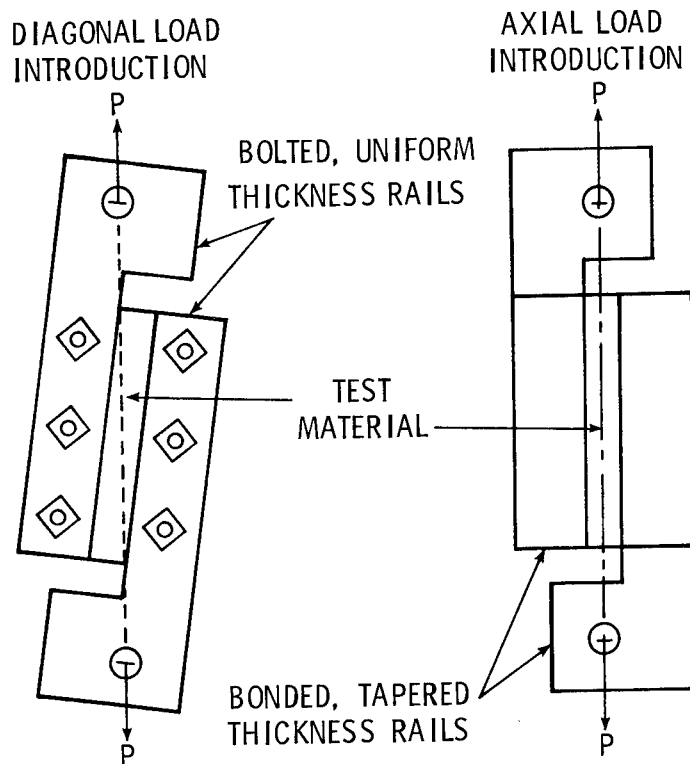


Figure 1

FINITE ELEMENT ANALYSIS

The SPAR structural analysis finite element computer code (ref. 8) was used to examine the rail shear test method. Finite element models were constructed using SPAR to investigate test parameters (Fig. 2).

Beam elements were used in the theoretical models of the rails. The material properties input to the beam rails were those of Ti-6Al-4V, which were obtained from reference 9 and are listed in the appendix.

Quadrilateral membrane/bending elements were used in the analytical models of the test specimen material. The quadrilateral elements were used to model four laminates having the following ply orientations: $[0]_{12}^T$, $[90]_{12}^T$, $[\pm 45]_2^s$ and $[90, \pm 45, 0]$. The material properties input to the quadrilateral elements were graphite/polyimide material properties obtained from reference 10 and listed in the appendix.

The finite element models were subjected to tension loading. Since a linear finite element analysis is used, the analytical data presented for a tensile rail shear model will also be valid with reverse sign for a compressive rail shear model.

Shear and normal stresses developed in the laminate due to mechanical loading were nondimensionalized with respect to the nominal value of the shear stress, computed as $\bar{\tau}_{xy} = P/bt$ (where P is the applied load, b is the length of the specimen and t is the thickness of the specimen).

Stress states as a result of a uniform rise in temperature were also examined. In addition, no attempt was made to model either bonded or bolted attachment behavior, and residual thermal stresses as a result of curing were not considered.

SPAR STRUCTURAL ANALYSIS PROGRAM

- LINEAR FINITE ELEMENT ANALYSIS
- QUADRILATERAL MEMBRANE/ BENDING ELEMENTS USED TO MODEL TEST MATERIAL
- RAILS MODELLED AS BEAM ELEMENTS

REFERENCE COORDINATES

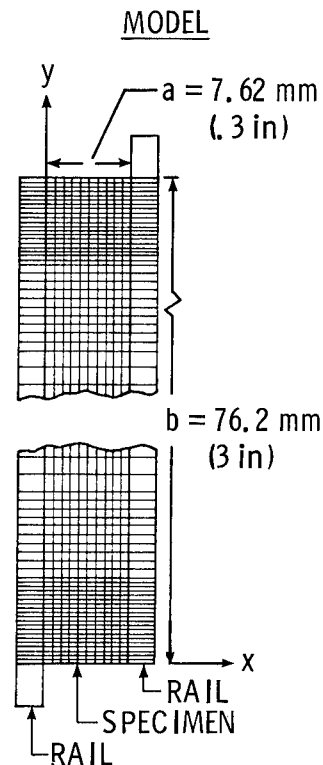
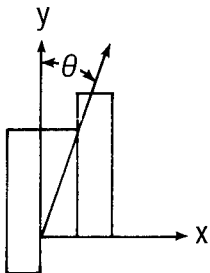


Figure 2

DIAGONAL AND AXIAL LOADING

Load can be introduced into the rail shear specimen in an axial or diagonal manner and is shown in figure 1. Both of these load introduction methods are commonly used in testing and merit investigation.

Tapered-rail and uniform-rail finite element models were subjected to both diagonal and axial loading. All four laminates previously cited were investigated. Nondimensionalized shear and normal stress distributions were investigated throughout the specimen test section.

A typical shear stress distribution $\tau_{xy}/\bar{\tau}_{xy}$ along the specimen center-line ($x = a/2$) is shown in figure 3. This shear stress distribution is for a $[\pm 45_2]_s$ rail shear specimen having rails of uniform cross-sectional area. Ideally, a state of uniform shear is desired throughout the entire specimen. This is not possible due to the presence of free edges. As can be seen, the shear stress rises from a value of zero to a peak value in less than one tenth of the specimen length. In the central region of the specimen, the shear stress has become uniform and is close to the nominal value. The difference in the shear stress distribution between the axial and diagonal load conditions is insignificant.

A comparison of shear and normal stress distributions throughout both the uniform rail specimen and the tapered-rail specimen for all four laminates indicates that no significant advantage is gained in using either axial or diagonal load introduction.

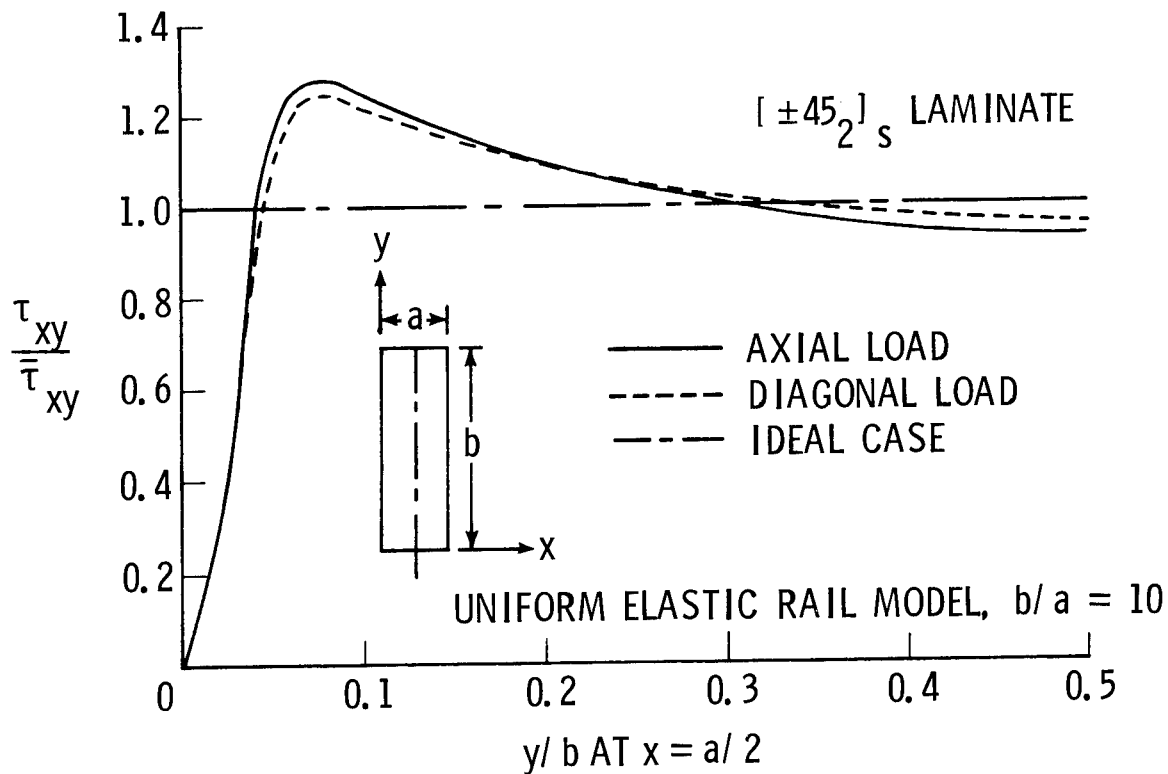


Figure 3

INFLUENCE OF UNIFORM AND TAPERED RAIL CONFIGURATION

One major difference to be found among the various rail configurations presently in use is that some specimens utilize rails of uniform cross-section while others utilize rails of tapered cross-section. Since no significant difference in stress states were evident due to axial or diagonal loading, the following discussion and associated figure will be limited to diagonal load introduction.

A typical normal stress distribution $\sigma_y/\bar{\tau}_{xy}$ across (x-direction) the specimen is shown in figure 4. This is the normal stress distribution for the $[0_{12}]_T$ laminate loaded diagonally. Ideally, normal stress values of zero are desired throughout the specimen. However, the presence of the free edges causes normal stresses to develop in the specimen to insure equilibrium. In figure 4, the uniform rail produces lower normal stress levels than the tapered rail. In all cases investigated, the uniform rail produces significantly smaller normal stress (σ_x and σ_y) values than those values produced by the tapered rail.

Comparisons of shear stress distributions throughout the specimen indicate that no significant advantage is gained by using either a tapered or uniform rail.

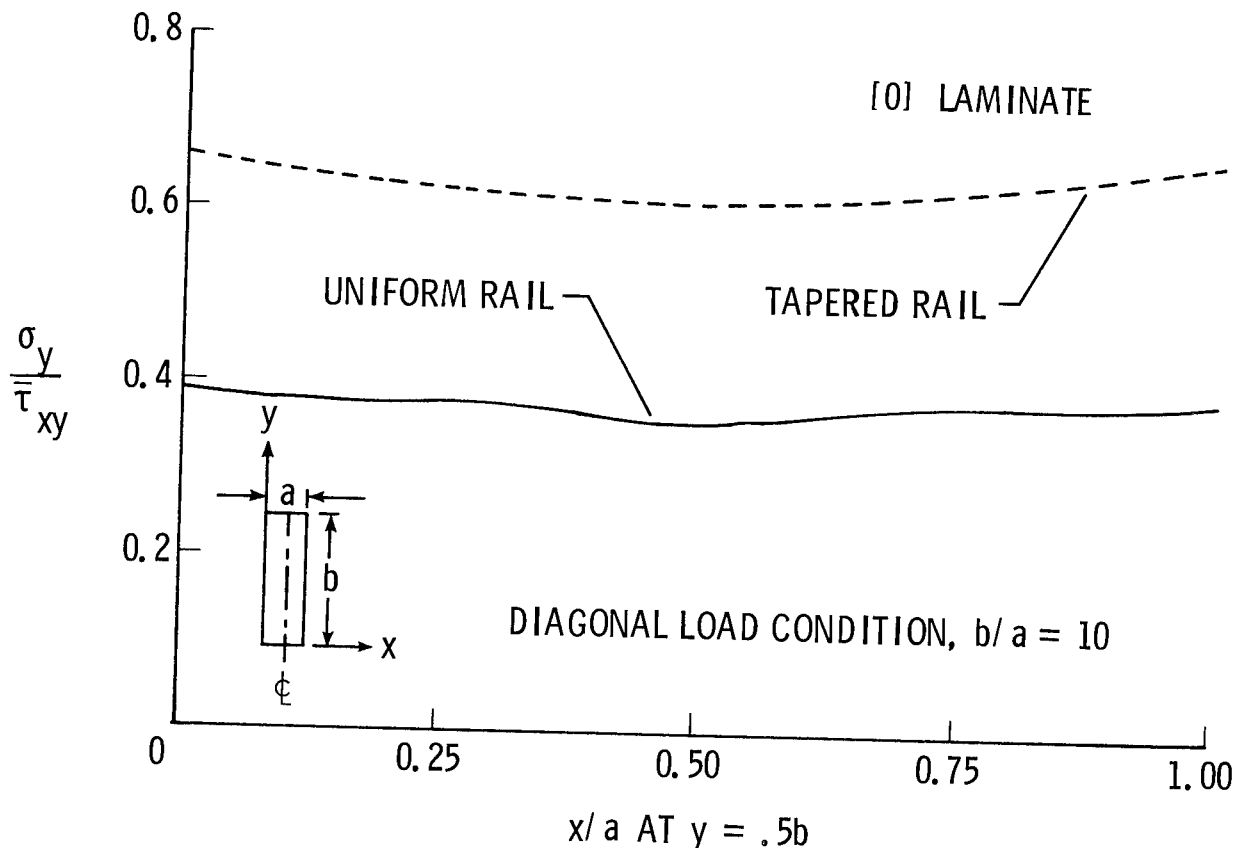


Figure 4

THERMAL STRESS DISTRIBUTION

A stress field will develop in a rail shear specimen that has been assembled at room temperature and then exposed to an elevated temperature. This stress field is due to differential expansion between the rail and test material. The thermal stresses discussed here are the result of applying a uniform temperature condition of 589 K (600°F) to the finite element models, while under no mechanical loading. The rails were assumed unconstrained laterally in the x-direction.

Both tapered-rail and uniform-rail finite element models were investigated for the [0] and [90] laminates. The thermal coefficients of expansion of the rail and laminates assumed are listed in the appendix.

The net effect of raising a [0] rail shear specimen to 589 K is that the test material is in tension in the y-direction. The net effect of raising a [90] rail shear specimen to 589 K is that the test material is in compression in the y-direction.

Shear stresses along the vertical and horizontal centerlines of the test section were zero for both the [0] and [90] laminates (for both tapered- and uniform-rail models) due to symmetry. Normal stresses were nondimensionalized with respect to material ultimate strengths listed in the appendix. The normal stress distribution σ_y/σ_{ult} along the specimen centerline ($x = a/2$) is shown in figure 5. As can be seen, normal stresses of the order of 50% of the ultimate stress (parallel to the rails) can develop in the test material as a result of thermal loading alone.

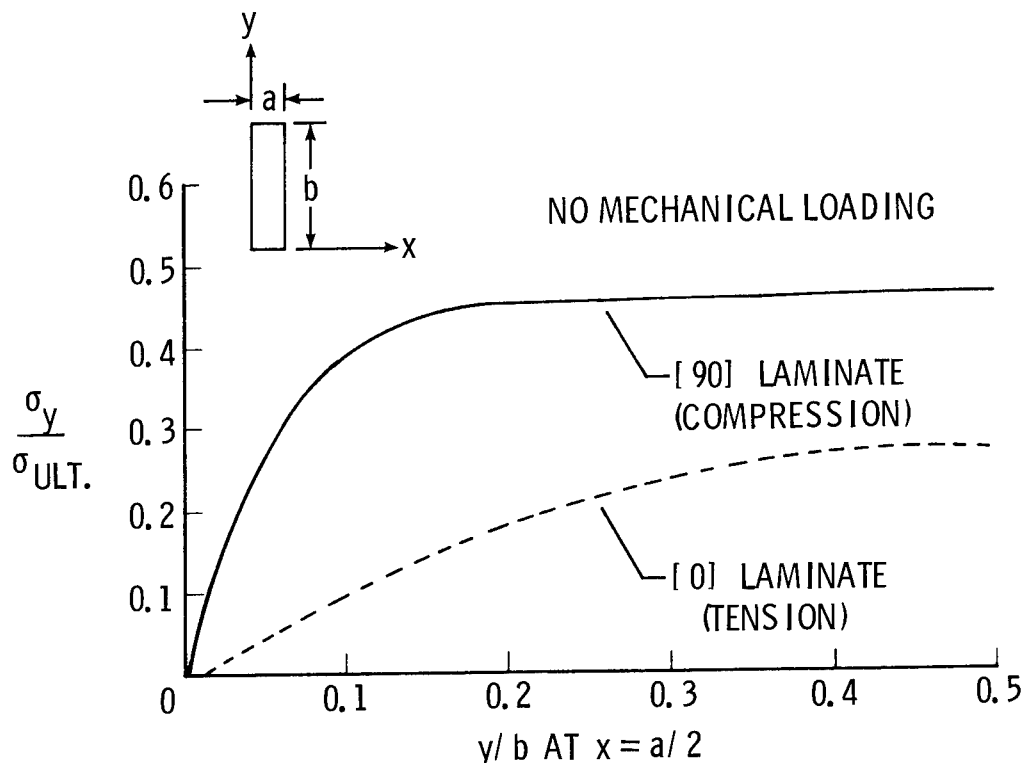


Figure 5

EXPERIMENTAL PROGRAM

An experimental program was designed to investigate and to compare the shear stress-strain behavior of the two rail shear specimens pictured in figure 6. One specimen introduces tensile load diagonally with rails of uniform cross-sectional area bolted to the test material. This specimen has oversized bolt holes in the test material and load is introduced by clamping action and not by bolt bearing forces. The other specimen introduces a tensile load axially along tapered rails which are bonded to the test material.

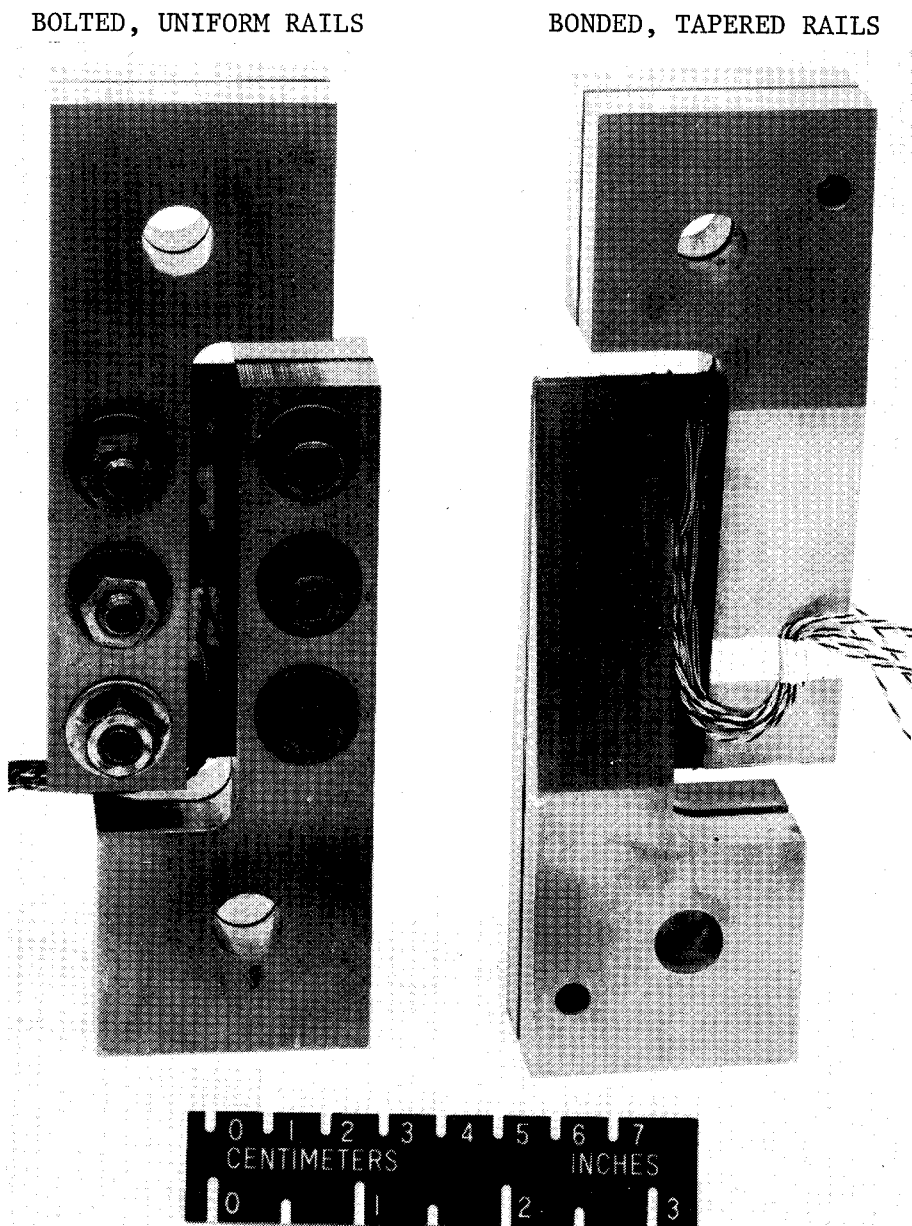


Figure 6

TEST MATRIX

The test program considered four laminates having the ply orientations: $[0]_{12}^T$, $[90]_{12}^T$, $[\pm 45]_2^S$ and $[90, \pm 45, 0]_S$. Laminates were fabricated from HTS-1/PMR-15 graphite/polyimide prepreg tape. The rails were machined from a block of Ti-6Al-4V, a titanium alloy.

A 0° - 45° - 90° , three-element, stacked-rosette strain gage was used for specimen instrumentation. Two rosettes were placed on each side of the specimen in the center of the test section. In addition, two iron-constantan thermocouples were placed on opposite sides at opposite ends of the 589 K test specimens to monitor test temperature.

Specimens were tested on a .53-MN (120 KIP) capacity mechanical test machine. Load was applied to the specimen at a cross-head motion rate of 1.27 mm (0.05 inches) per minute. Elevated temperature tests were conducted by mounting an oven on the test machine and allowing the test specimen to "soak" at 589 K for at least one-half hour before testing.

In summary, the parameters investigated included four laminate orientations, two test temperatures and two rail configurations. The various parameters and the number of tests conducted are listed in figure 7.

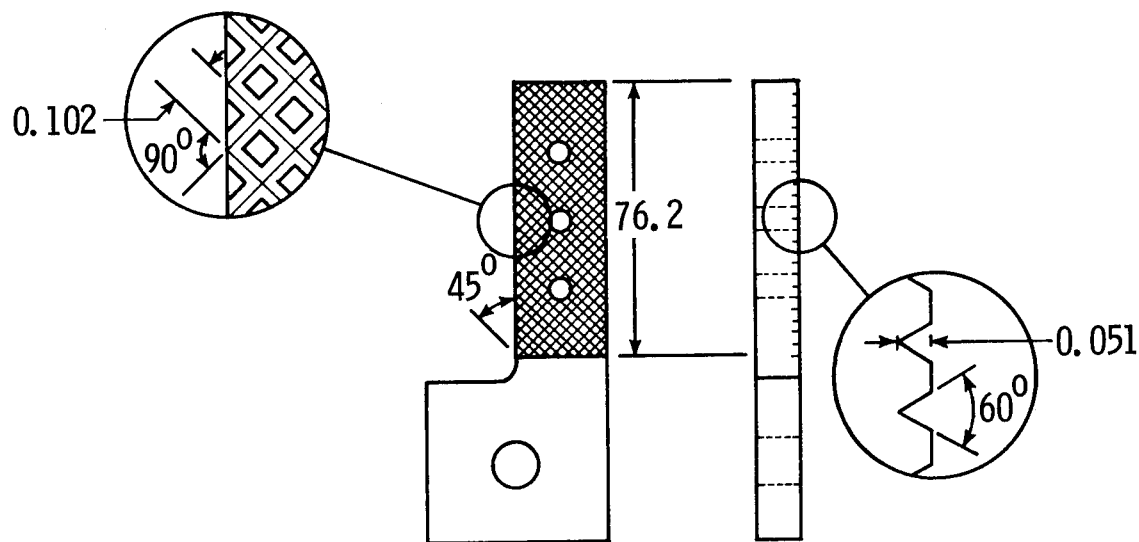
LAMINATE ORIENTATION	RAIL CONFIGURATION		TEST TEMPERATURE		NUMBER OF SPECIMENS TESTED
	BOLTED, UNIFORM	BONDED, TAPERED	ROOM TEMP.	589 K (600°F)	
$[0]_{12}^T$	X		X		4
$[90]_{12}^T$	X		X		3
$[\pm 45]_2^S$		X	X		5
$[\pm 45]_2^S$	X		X		5
$[\pm 45]_2^S$	X			X	2
$[90, \pm 45, 0]_S$		X	X		5
$[90, \pm 45, 0]_S$	X		X		6
$[90, \pm 45, 0]_S$	X			X	5

Figure 7

CONSIDERATIONS OF THE BOLTED AND BONDED RAIL

The standard procedure for testing bolted-rail shear specimens calls for a fine grit emery paper to be placed between the rail and test material to provide a sufficient friction force when clamped so that slippage does not occur. This method of preventing slippage at the rail/test material interface was ruled out for testing at 589 K because the emery paper burns at this temperature. Blasting of the rail surface with a fine abrasive powder was first used in an attempt to roughen the surface and thus increase the frictional force at the rail/test material interface. The abrasive blasting of the rail surface did increase the friction between the rail and test material, but slippage still occurred at higher loads. A second method based on roughening the rail contact surface using an electric discharge machining technique as illustrated in figure 8 was more successful. This process eliminated overall slippage for room temperature and 589 K test specimens without damaging the test material.

Bonded-rail specimens to be tested at room temperature were fabricated with a room-temperature curing adhesive. Room-temperature bonded specimens had sufficient bond strength to provide test material failure. Attempts to test bonded-rail shear specimens at 589 K were abandoned because of problems associated with rail surface preparation and adhesive curing. It is doubtful, however, that at present a bonded-rail shear specimen tested at 589 K would exhibit specimen failure and not adhesive failure since even the best elevated temperature bonding agents now available begin to degrade at temperatures below 589 K.



DIMENSIONS IN mm

Figure 8

DATA REDUCTION

A Hewlett-Packard data acquisition and processing system was used to record load and strain data at specified time intervals. A data reduction program converted the load-strain data to shear stress-strain data and then averaged the shear stress-strain data of the back-to-back gages for the individual tests. The data obtained from each series of replicate tests was then input to a regression analysis program. Coefficients of a second or third order polynomial equation which exhibited a best fit, in a least squares sense, to all the data in a series of replicate tests were then determined. A typical shear stress-strain curve generated in this manner is illustrated in figure 9. The shaded areas adjacent to the curve are an indication of experimental data scatter.

Tangent modulus-versus-strain curves were calculated by differentiating the resulting polynomial equations. Tangent modulus-versus-strain curves are given in the appendix for the shear stress-strain data presented in figures 10, 11 and 12.

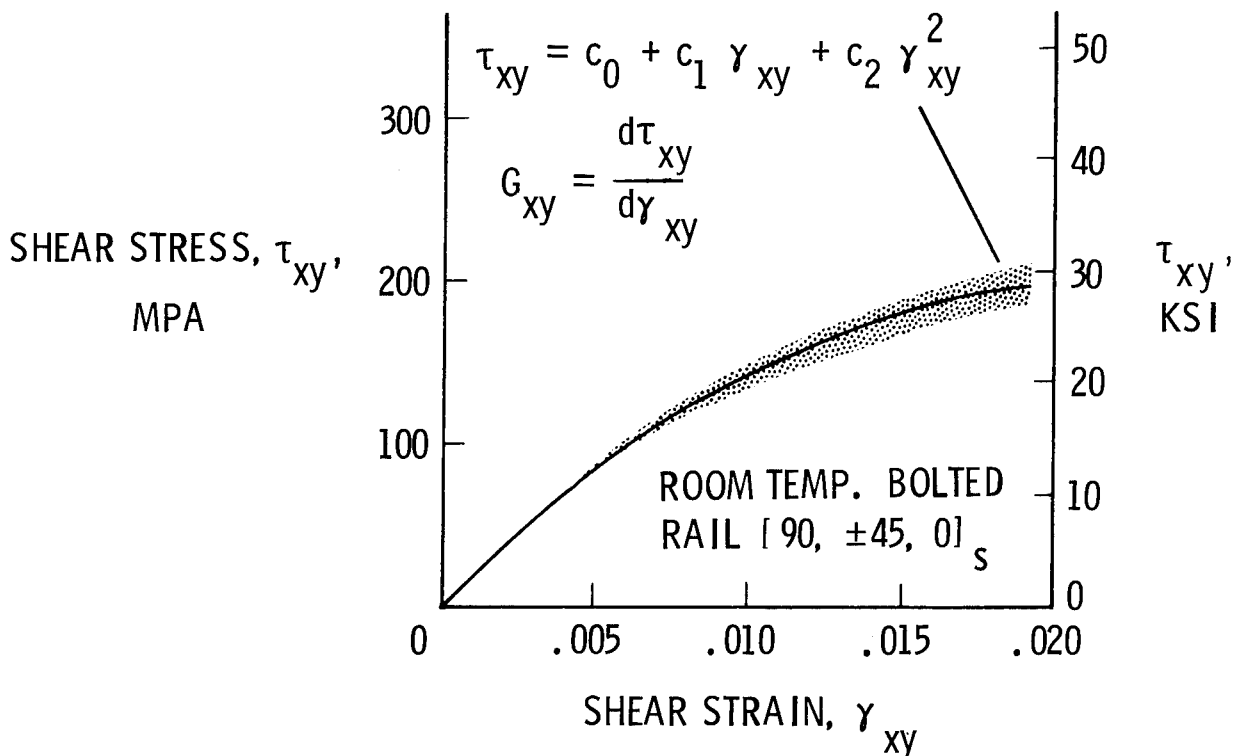


Figure 9

BEHAVIOR OF [0] AND [90] LAMINATES

The results of the finite element analysis performed at room temperature on the [0] and [90] laminates indicate that: A) the shear stress responses of the two laminates are essentially the same; B) the [0] laminate will have a large normal stress concentration, transverse to the fibers, in the vicinity of the free edge, and; C) the [90] laminate will have a large normal stress concentration, parallel to the fibers, in the vicinity of the free edge. The normal stress concentration for the [0] laminate occurs in a weak material direction, as opposed to the [90] laminate in which the normal stress concentration occurs in a strong material direction. Despite the fact that both laminates exhibit essentially the same shear behavior, the [0] laminate is expected to fail at a load and strain level considerably lower than the maximum level attained by the [90] laminate.

Illustrated in figure 10 is the shear stress-strain behavior, at room temperature, of the [0] and [90] laminates. This data was obtained by using bolted, uniform-rail shear specimens. The experimental data indicate that the [90] laminate should be used instead of the [0] laminate for determining the shear modulus and ultimate shear strain for unidirectional material.

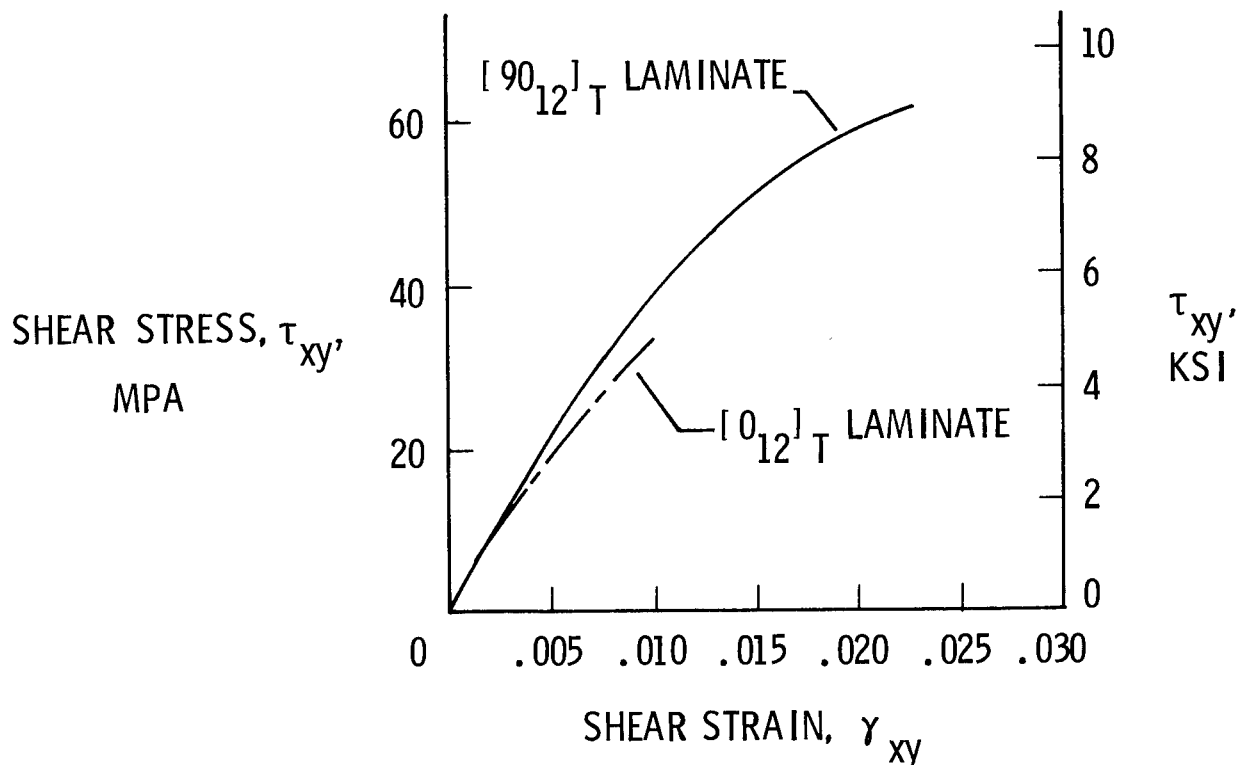


Figure 10

EFFECT OF RAIL CONFIGURATION ON SHEAR STRESS-STRAIN BEHAVIOR

The effect on shear behavior caused by the method of rail attachment to the test material, i.e. bonding or bolting, was not examined analytically. However, the method of rail attachment was examined experimentally at room temperature. Figure 11 illustrates the shear stress-strain responses for the $[\pm 45]_s$ and $[90, \pm 45, 0]_s$ laminates tested at room temperature. As can be seen, the shear stress-strain response of the bolted and bonded specimens is significantly different.

The bonded specimen utilizes tapered rails and axial load introduction, while the bolted specimen utilizes uniform rails and diagonal load introduction. The effect of load introduction path upon the stress states within the test material was found to be insignificant as a result of the finite element analysis. Analytical results also indicated that uniform rails produced more satisfactory normal stress states within the test material than tapered rails. The improvement in stress states caused by the uniform rail over the tapered rail cannot account for the magnitude of difference between the two specimens exhibited by the experimental data. Thus, the method of rail attachment to the test material has a significant effect on shear stress-strain response of the specimen. The bonded specimen exhibits a more effective load transfer to the test material than the bolted specimen and therefore should be used instead of the bolted specimen where possible.

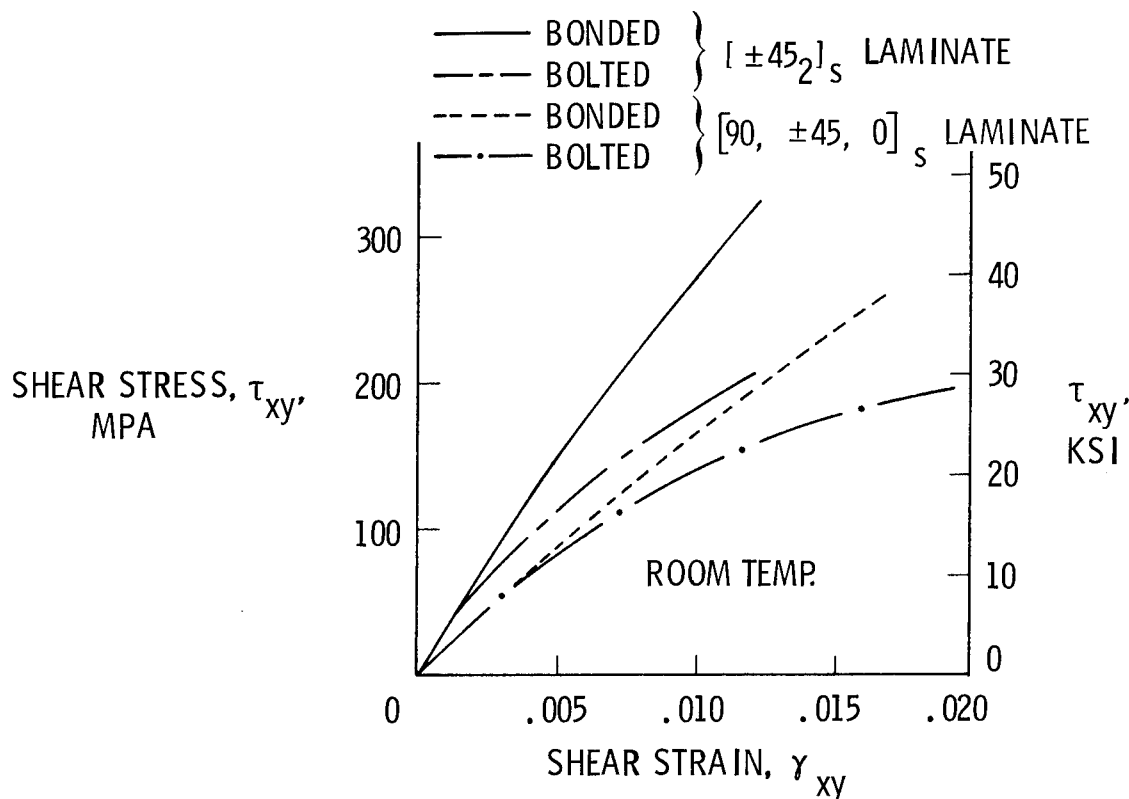


Figure 11

BEHAVIOR OF BOLTED SPECIMENS TESTED AT 589 K (600°F)

Analytical results indicate that large normal stresses parallel to the rails can develop due to thermal loading. The coefficient of thermal expansion of the rail is $9 \times 10^{-6}/\text{K}$ and that of the $[90, \pm 45, 0]_s$ laminate in the direction parallel to the rails, is $1.6 \times 10^{-6}/\text{K}$. Therefore, large normal stresses parallel to rails will occur in a $[90, \pm 45, 0]_s$ specimen if it is assembled at room temperature and then raised to a temperature of 589 K.

Two groups of $[90, \pm 45, 0]_s$ bolted-rail shear specimens were tested. One group of specimens was tested at room temperature, while the other group of specimens was tested at 589 K. The shear stress-strain data obtained from the two groups of specimens appear in figure 12. The specimens which were tested at 589 K exhibit a slightly lower shear stress at failure than the specimens tested at room temperature. An examination of both shear stress-strain curves over their entire length indicates that the determination of shear modulus should not be affected by thermal stresses as a result of differential expansion.

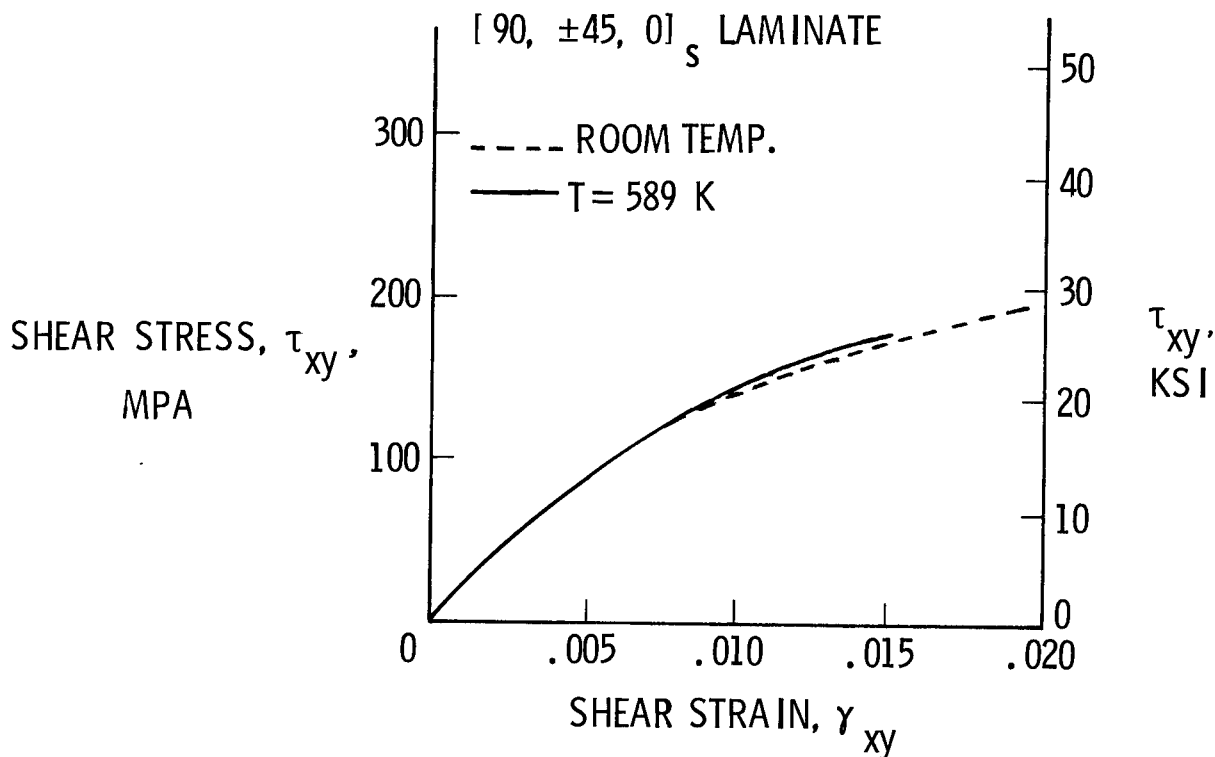


Figure 12

SUMMARY AND CONCLUSIONS

An analytical and experimental study has been presented that provides information about the mechanical behavior of laminated composite, rail shear test specimens. Analytical results indicate that:

No significant advantage is gained in using either axial or diagonal load introduction.

The uniform rail produces significantly smaller normal stress (σ_x and σ_y) values than those values produced by the tapered rail. Comparisons of shear stress distributions throughout the specimen indicate that no significant advantage is gained by using either a tapered or uniform rail.

Large normal stresses parallel to the rails can develop in the test material as a result of differential expansion between the rails and test material caused by thermal loading.

Experimental results indicate that:

The [90] laminate should be used to determine the unidirectional shear modulus and ultimate shear stress instead of the [0] laminate.

Bonded rails provide better load transfer to the test material than bolted rails at ambient temperature.

The overall conclusion to be drawn from this study and previous investigations is that the rail shear test method is good for determining inplane shear modulus but because of high stress concentrations near the free edges can be poor for determining ultimate shear stress values.

APPENDIX

A. Graphite/Polyimide

$$E_1 = 149.6 \text{ GPa } (21.7 \times 10^6 \text{ psi})$$

$$E_2 = 8.273 \text{ GPa } (1.2 \times 10^6 \text{ psi})$$

$$G_{12} = 4.137 \text{ GPa } (0.6 \times 10^6 \text{ psi})$$

$$\nu_{12} = 0.27$$

$$\nu_{21} = 0.015$$

$$\alpha_1 = 0$$

$$\alpha_2 = 26.1 \times 10^{-6} \text{ m/m/ K}$$

$$a = 7.62 \text{ mm } (0.30 \text{ inches})$$

$$t = 0.1016 \text{ mm/ply } (0.004 \text{ inches/ply})$$

B. Titanium

$$E = 113.8 \text{ GPa}$$

$$\nu = 0.342$$

$$\alpha = 9 \times 10^{-6} \text{ m/m/ K}$$

$$\text{Rail width} = 2.54 \text{ cm } (1 \text{ inch})$$

$$\text{Rail width} = 2.54 \text{ cm } (1 \text{ inch})$$

C. Ultimate stress values at 589 K

$$[90] \text{ (in compression): } \sigma_{\text{ult}} = -103.4 \text{ MPa}$$

$$[0] \text{ (in tension): } \sigma_{\text{ult}} = 1.289 \text{ GPa}$$

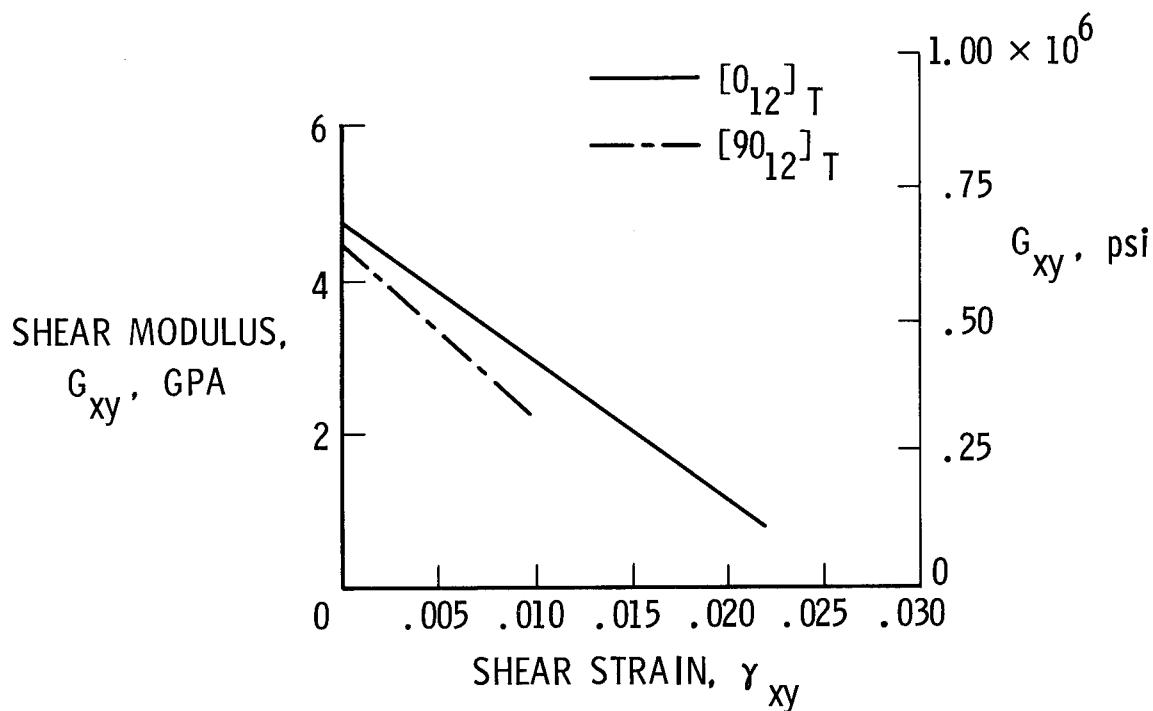


Figure A1.- Unidirectional shear modulus behavior at room temperature.
(See fig. 10.)

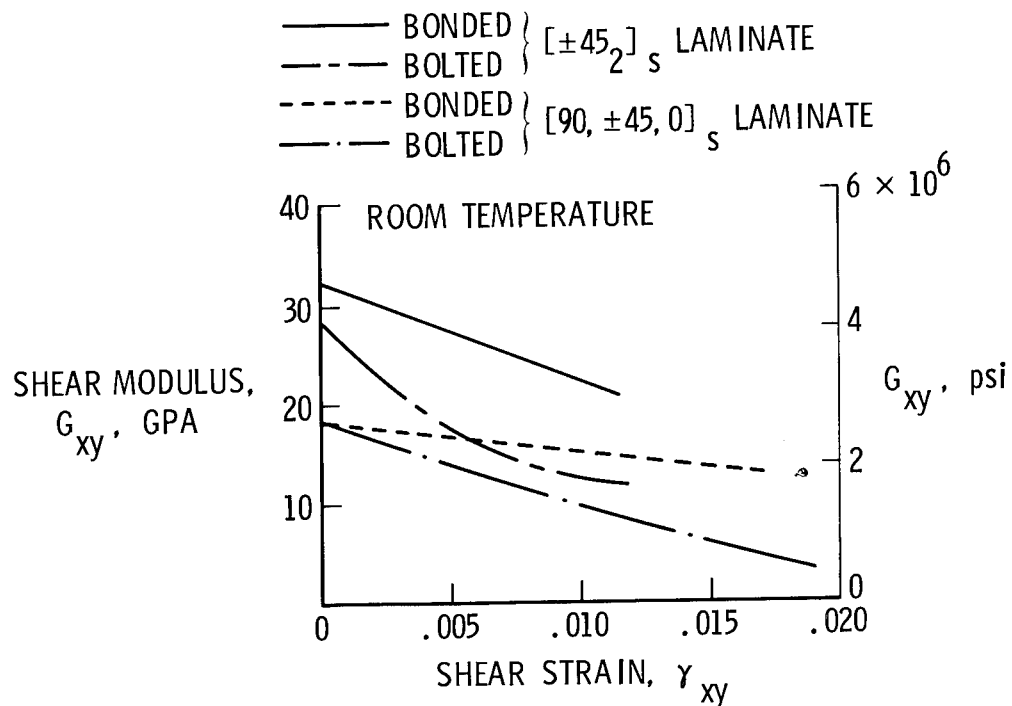


Figure A2.- Effect of rail configuration on shear modulus behavior.
(See fig. 11.)

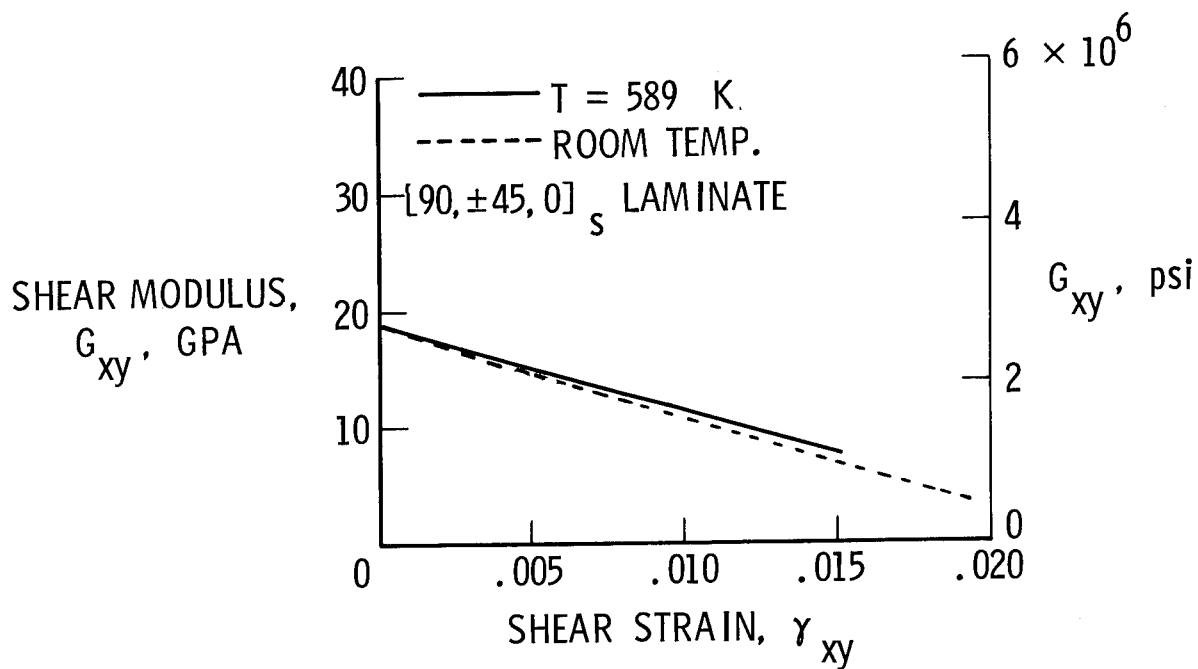


Figure A3.- Effect of temperature on shear modulus behavior.
(See fig. 12.)

REFERENCES

1. Coker, E. G.: An Optical Determination of the Variation of Stress in a Thin Rectangular Plate Subjected to Shear. Proceedings of the Royal Society of London (Series A), Vol. 86, 1912, p. 291.
2. Whitney, J. M.; Stansbarger, D. L.; and Howell, H. B.: Analysis of the Rail Shear Test - Applications and Limitations. J. of Composite Materials, Vol. 5, Jan. 1971, p. 24.
3. Bergner, H. W., Jr.; Davis, J. G., Jr.; and Herkovich, C. T.: Analysis of Shear Test Methods for Composite Laminates. Report No. VPI-E-77-14. Virginia Polytechnic Institute and State University, April 1977.
4. Sims, D. F.: In-Plane Shear Stress-Strain Response of Unidirectional Composite Materials. J. of Composite Materials, Vol. 7, Jan. 1973, p. 124.
5. Post, P. W.: Test Method and Manufacturing Process Effect on Shear Properties of Plywood. American Plywood Association Product Research Dept., April 1968.
6. Boller, K. H.: A Method to Measure Intralaminar Shear Properties of Composite Laminates. AFML-TR-69-31, December 1969.
7. Hughes, E. J.; and Rutherford, J. L.: Composite Tubes for Structural Use. Report No. KD-75-59, The Singer Company, July 1975.
8. Whetstone, W. D.: SPAR Structural Analysis System Reference Manual - System Level 11. Volume 1 - Program Execution. NASA CR-145098-1, 1977.
9. Metal Progress Databook 1976, American Society for Metals, 1976.
10. Hanson, M. P.; and Chamis, C. C.: Experimental and Theoretical Investigation of HT-S/PMR-PI Composites for Application to Advanced Aircraft Engines. Proceedings of 29th Annual Technical Conference, Reinforced Plastics/Composites Institute, The Society of Plastics Industry Inc., 1974, Section 16-C, p. 1.

EFFECTS OF LOW-VELOCITY IMPACT ON Gr/Pi COMPRESSION LAMINATES

Ramon Garcia and Marvin D. Rhodes
NASA Langley Research Center

EXPANDED ABSTRACT

Several investigations have recently been conducted to evaluate the effect of **low-velocity** impact in graphite-epoxy composites (refs. 1, 2 and 3). These investigations have shown that low-velocity impact can create internal damage with no apparent surface damage. This damage may result in significant reductions to both the tension and compression strength of the graphite-epoxy laminates. The results of reference 3 indicate that impact damage failures may be more dependent on the matrix than on the fiber in the composite material. The investigations cited have all been conducted on composite materials having epoxy matrices, and there is little information available on similar damage in composites having polyimide matrices.

This paper presents the results of low-velocity impact tests conducted on a graphite-polyimide laminate. The 48-ply orthotropic laminate tested during this investigation is typical of laminates being proposed for heavily loaded aircraft wing skins. The nature of the damage is described as well as the effect of that damage on the compression strength of the 48-ply orthotropic laminate. The results obtained for the graphite-polyimide laminate are compared to existing results of similar tests conducted on a graphite-epoxy laminate reported in reference 4.

EXPOSURE OF COMPOSITES TO IMPACT

Low-velocity impact is a potential source of damage to aircraft and some typical examples are shown in figure 1. The list of potential impact threats is not intended to be all-inclusive--only some of those threats which fall into the category of simulation by this investigation are listed.

The test specimens were fabricated from preimpregnated tape consisting of Celion graphite fibers in LARC-160 polyimide resin (ref. 5). The tape has a nominal cured thickness of 0.14 mm per ply and was laid to form a $(\pm 45/0_2/\pm 45/0_2/\pm 45/0/90)_{2s}$ laminate with 48 plies. Following autoclave cure, the laminates were ultrasonically inspected to evaluate specimen quality.

The impact projectile was a 12.7 mm diameter aluminum ball. Aluminum was chosen for the projectile because it has about the same density as most common rock materials. The velocities ranged from that necessary to initiate damage within the laminate to values high enough to create obvious physical damage on the specimen surface.

POTENTIAL THREAT

- A. RUNWAY STONES
- B. HAIL STONES
- C. DROPPED HAND TOOLS
- D. MAINTENANCE ABUSE

EXPERIMENTAL EVALUATION

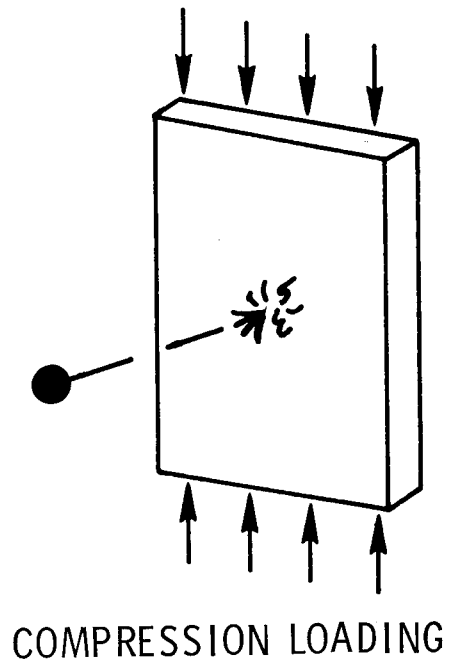


Figure 1

IMPACT DAMAGE CHARACTERIZATION

To characterize the nature and extent of impact damage, each specimen was inspected ultrasonically and then cross-sectioned through the damage region. Typical damage in a specimen impacted at 90 m/s is shown in figure 2. The extent of the damage as determined by ultrasonic inspection was about 30 mm wide by about 41 mm long. Photomicrographs of the cross section indicated that the extent of the damage was essentially the same as determined by ultrasonic inspection. From the photomicrograph shown in the figure, it is apparent that the interior damage is a complex pattern of intraply cracking and multi-layer delamination. The size of the damage region and the nature of the damage observed in the cross section is similar to that observed in specimens fabricated from graphite-epoxy (ref. 4).

Several specimens were damaged by impact to determine the lowest velocity required to initiate damage in the laminate interior and the lowest velocity required to initiate visible damage on the laminate exterior. These values were in the range of 30 to 40 m/s and 65 to 90 m/s, respectively. Laminate exterior damage was always more severe on the side of the specimen opposite the impact location and could seldom be detected on the contact surface. The fact that significant internal laminate damage may be caused by impact at velocities well below that necessary to cause visible damage is of special concern. Visual inspection is the primary source of defect and damage detection in current aircraft structures. Imposing routine inspection procedures that exceed visual requirements may be economically unfeasible.

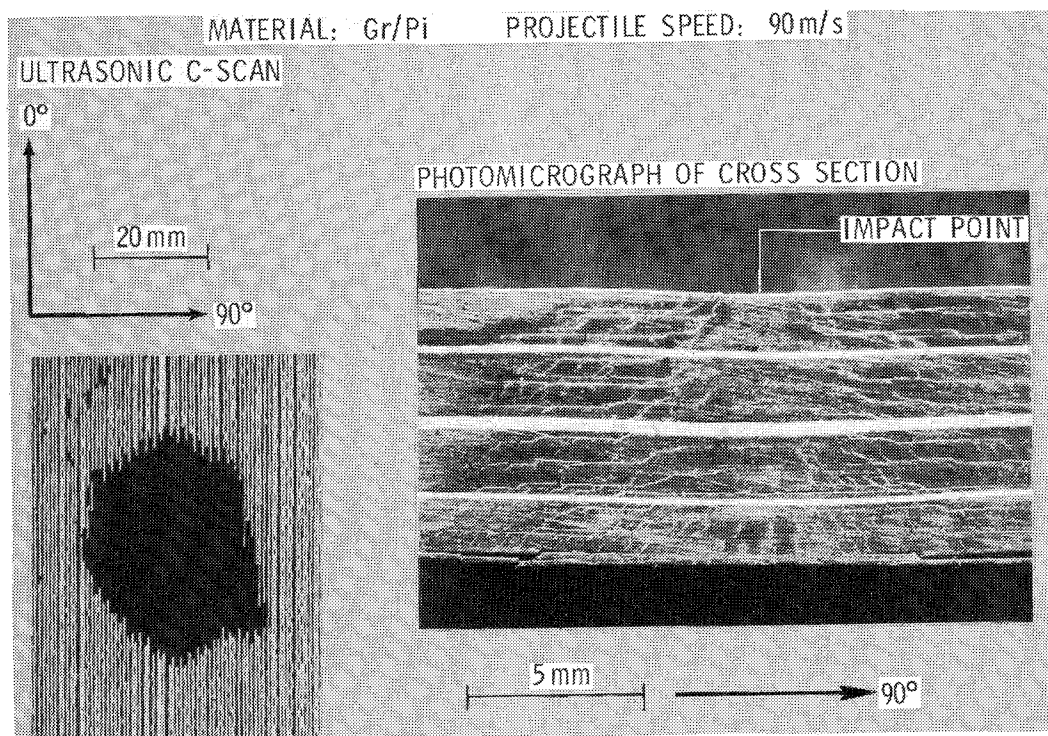


Figure 2

TEST SPECIMEN AND APPARATUS

To evaluate the effect of impact on static compression strength, specimens with impact damage were tested. Also, specimens were damaged by impact while under a static compression load. The test specimen and fixture used for these tests is shown in figure 3. The test specimens were 11.4 cm wide by 24.8 cm long. The width of the specimen was selected so that the local damaged region created by impact would not be close to the specimen edge. The width and length were sized so the panel buckling strain would be well above the expected failure strain of panels with impact damage. The specimen ends were ground flat and parallel to permit uniform compression loading. The specimen and fixture were placed between the platens of a 1.33 MN hydraulic testing machine which was used to apply the compression load. All impacts were at normal incidence to the specimen surface.

To monitor applied axial strain and bending strains caused by out-of-plane deformations, four electrical resistance strain gages were bonded to each specimen. The gages were placed at locations away from the impact region where local effects would not influence the measured values.

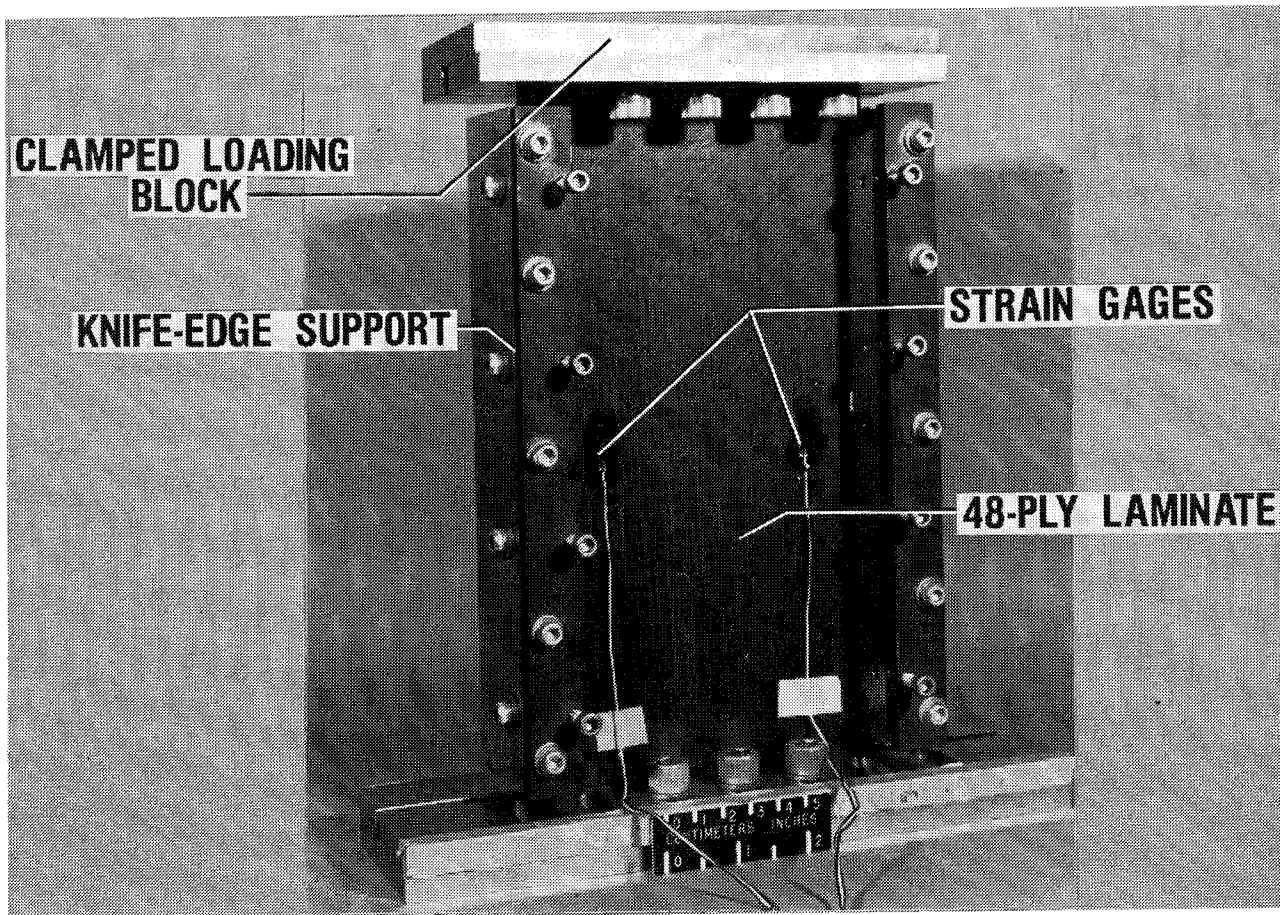


Figure 3

EFFECT OF IMPACT ON Gr/Pi COMPRESSION LAMINATES

The effect of low-velocity projectile impact on the compression strength of the Celion/LARC-160 graphite-polyimide test laminate is shown in figure 4. The ordinate is the axial compression strain in the specimen due to applied compression load when impact occurred and the abscissa is the projectile impact speed. The projectile kinetic energy is also shown on the abscissa for reference. The filled circles represent specimens that failed catastrophically on impact. The open triangles represent specimens that did not fail catastrophically on impact, even though they may have incurred some local damage. The open circles of the ordinate represent the failure strain of undamaged control specimens. These tests indicate that reductions in static compression strength of greater than 60% may occur due to small projectile impacts at velocities of 75 m/s or above. These results are similar to those obtained for graphite-epoxy test specimens reported in reference 4.

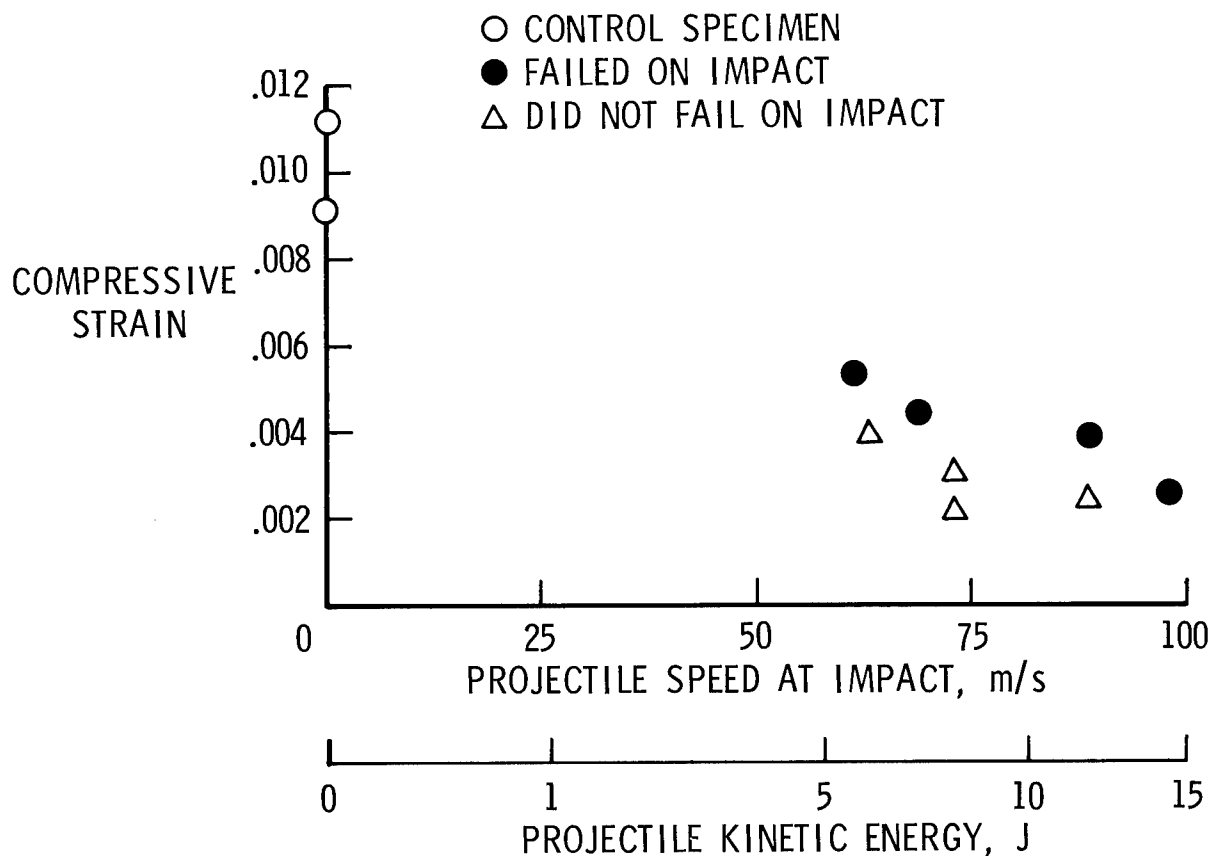


Figure 4

EFFECT OF IMPACT ON Gr/E COMPRESSION LAMINATES

For purposes of comparison, the effect of projectile impact on the compression strength of graphite-epoxy specimens reported in ref. 4 is shown in figure 5. These data were obtained from similar tests on specimens of the same laminate orientation and stacking sequence as the graphite-polyimide specimens tested in this investigation. The plot parameters and symbols are similar to those shown in figure 4. Also shown in figure 5 is a curve labeled catastrophic failure threshold. This curve was faired between those specimens which failed catastrophically on impact and those which did not. Well defined catastrophic failure threshold curves have been determined experimentally for several graphite-epoxy laminates tested in both tension and compression. The failure threshold indicates that a sharply defined region of safe loading exists for compression loaded structures subjected to impact at low velocities. The reductions in compression strength for the graphite-epoxy laminate are similar to those shown on the previous figure for the graphite-polyimide.

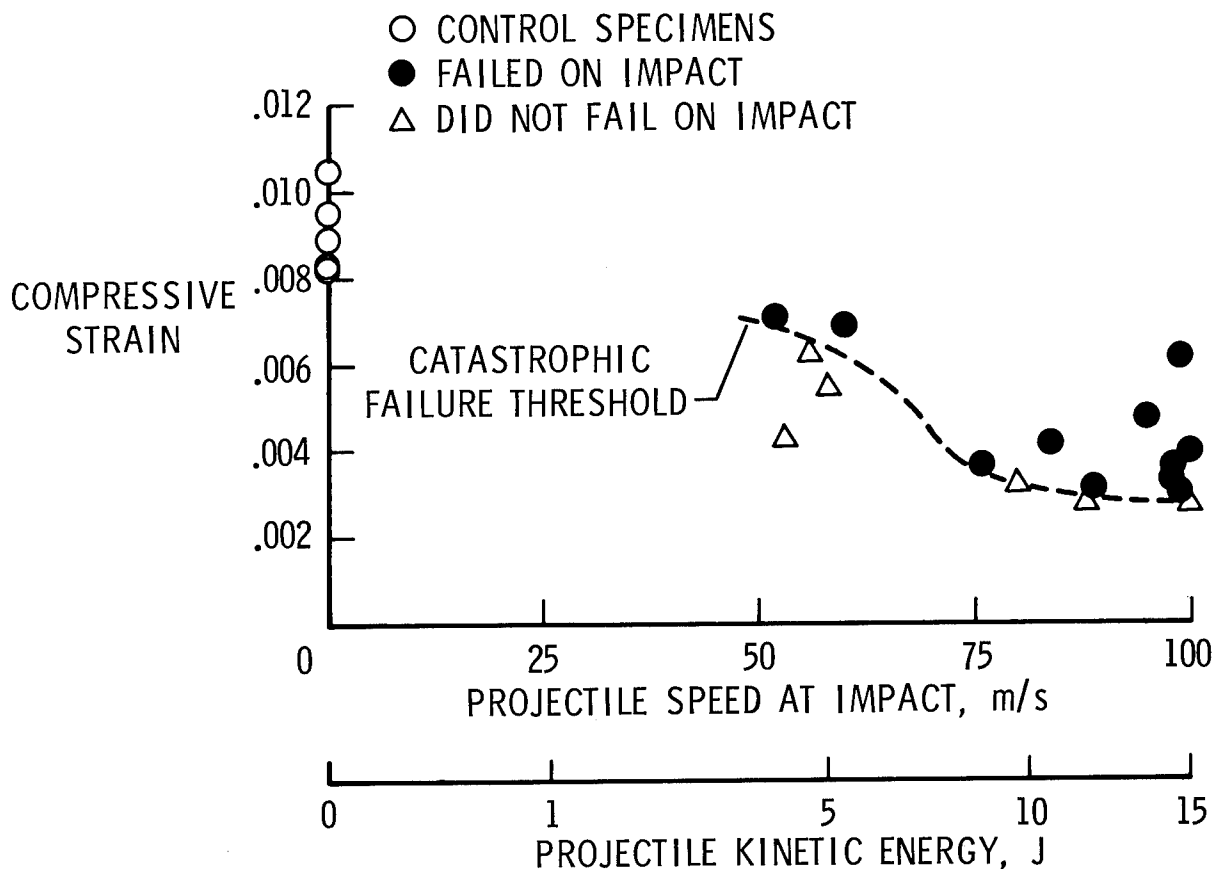


Figure 5

COMPARISON OF Gr/Pi AND Gr/E TEST DATA

The graphite-polyimide specimens that did not fail catastrophically due to impact were subsequently tested to determine their residual compression strength by measuring the applied static strain at failure. Other specimens were also damaged by impact with no applied compression load to determine their residual compression strength. Results of both tests are shown in figure 6. As on figures 4 and 5, the compressive strain has been plotted as a function of projectile velocity. The open symbols represent the axial static strain applied to the specimen when impact occurred and the filled symbols represent the strain at failure measured during the residual strength tests. Each open symbol has a corresponding filled symbol above it. Also shown on figure 6 is the catastrophic failure threshold curve for the graphite-epoxy data shown in figure 5. Comparison of the graphite-epoxy failure threshold curve with the results for the graphite-polyimide suggests that the failure threshold curve may be used to predict a lower bound for the residual static compression strain of graphite-polyimide laminates damaged by low-velocity impact. The difference in loaded and unloaded impact test results in the 60 to 65 m/s range indicates that there is an interaction or coupling between the applied inplane load and the local deformations associated with impact. This same behavior was exhibited by the graphite-epoxy laminates previously discussed.

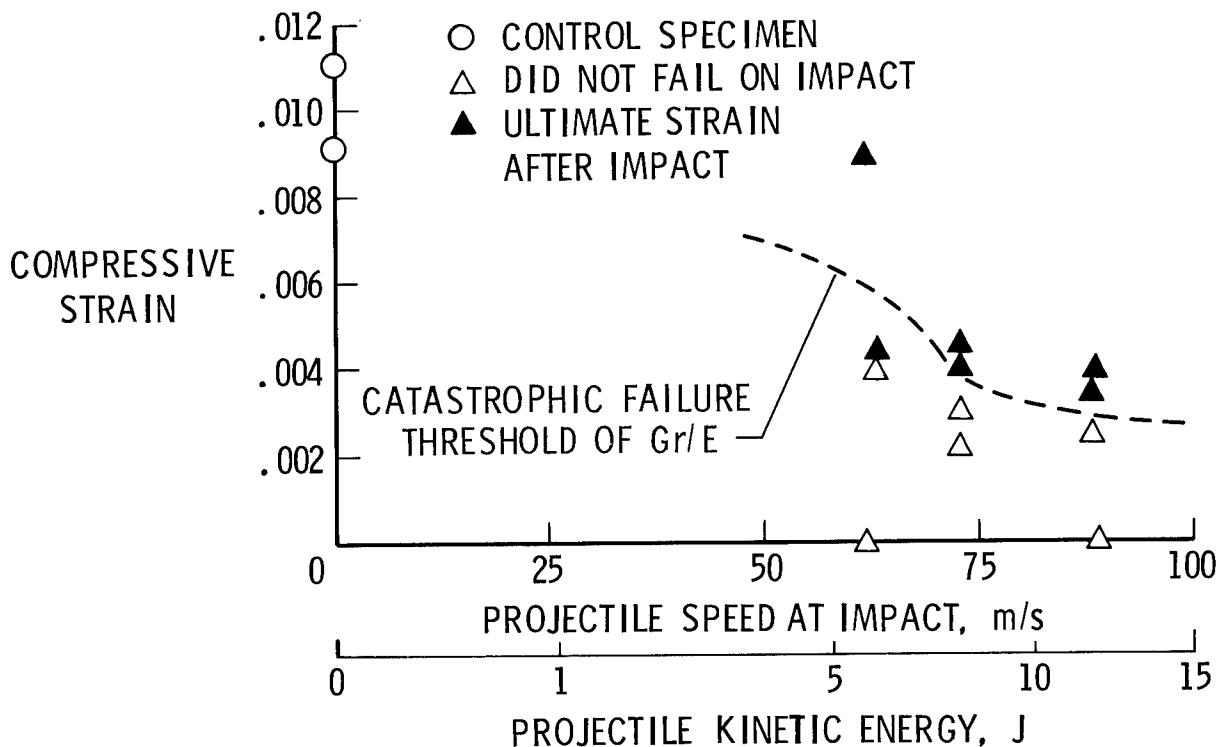


Figure 6

DAMAGE GROWTH IN Gr/Pi

The sequence of events leading to failure in a specimen damaged by impact appears in figure 7. This specimen was damaged by an 88 m/s projectile while at an applied strain of 0.0024. The panel incurred local internal damage but did not fail catastrophically. The panel was subsequently loaded to determine residual compressive strength. Prior to the test, the panel was painted white to reflect light and a moire grid was placed in front of the specimen to monitor out-of-plane deformations. The side of the panel opposite the impact site was chosen for observation because the damage, determined by inspection of the cross section of other test specimens, was always greater on this side. Photographs of the moire-fringe patterns during the residual strength test are shown in figure 7. These fringe patterns represent local out-of-plane deformations that developed due to delaminations caused by impact. The delamination was near the surface and the sublaminates buckled locally causing high stresses at the boundary of the delaminated region. These high local stresses cause the delamination to propagate. Delamination is one of several failure propagation modes identified in tests of compression loaded graphite-epoxy panels reported in reference 6.

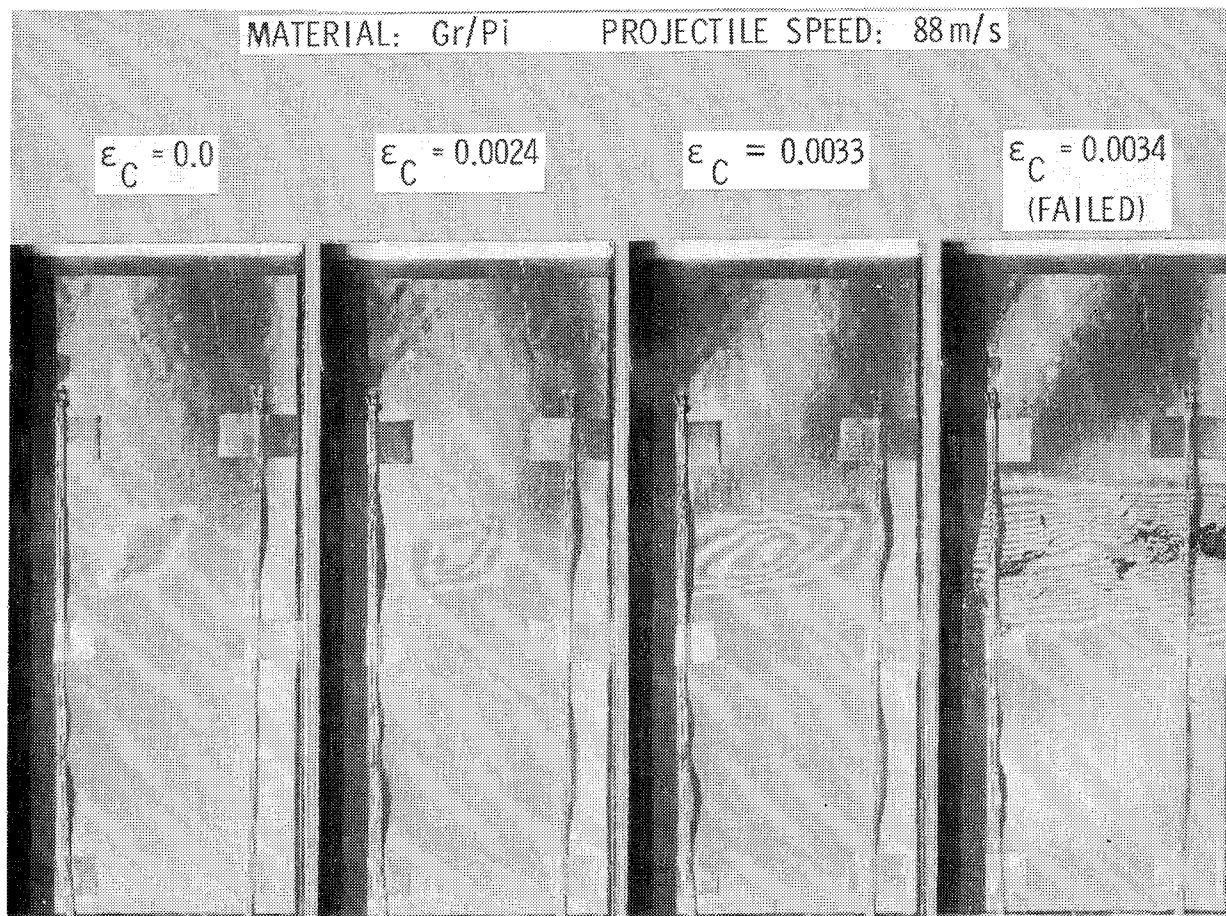


Figure 7

COMPRESSION LOAD-STRAIN RESPONSE

The compression load-strain response of two test specimens appears in figure 8. The dashed curve represents the average load-strain response to failure of an undamaged control specimen. The solid curve represents the average load-strain response to failure of an impact damaged specimen. This specimen was damaged by an 88 m/s projectile while under an applied compressive strain of 0.0024. As mentioned in the previous section, this specimen did not fail on impact and was subsequently loaded to failure.

The undamaged control specimen failed in the gap between the clamped loading block and the knife-edge restraints in a buckling mode. The impact damaged specimen failed laterally across the impact damaged region as illustrated in figure 7. The data indicates that the maximum load carrying capability of the impact damaged specimen is reduced by 65 percent.

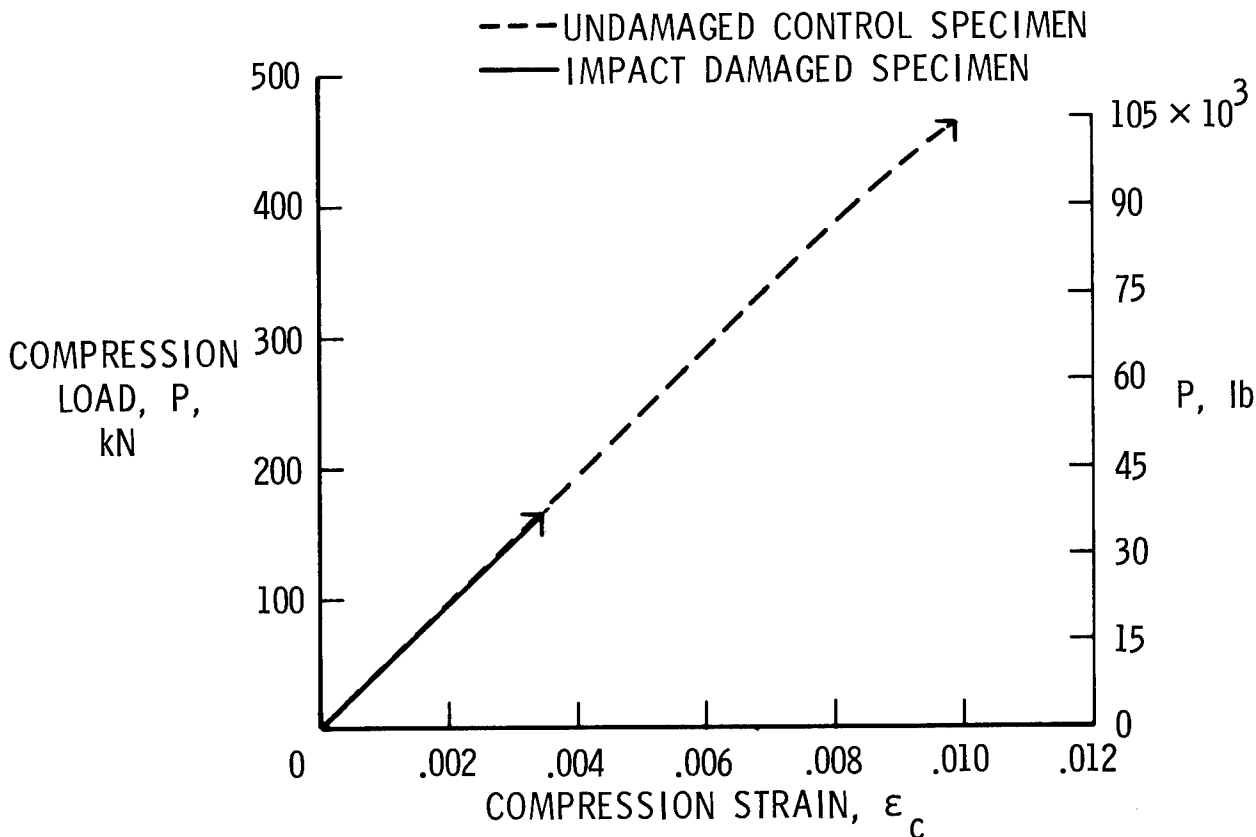


Figure 8

CONCLUDING REMARKS

An experimental investigation has been conducted to evaluate the effects of low-velocity impact damage on a 48-ply orthotropic graphite-polyimide laminate. Test results indicate that significant delamination and intraply cracking can be created in the graphite-polyimide laminate with no surface damage. This may have serious implications since visual inspection is the primary source of damage detection in aircraft structures.

Reductions in compression strength of up to 60 percent were caused by impact in specimens that had a compressive load applied when impact occurred. A comparison of the data for the graphite-polyimide with the data for a graphite-epoxy laminate with the same orientation and stacking sequence (ref. 4) indicates that similar results were obtained for both of these material systems.

REFERENCES

1. Rhodes, Marvin D.: Impact Tests on Fibrous Composite Sandwich Structures. NASA TM-78719, 1978.
2. Gause, Lee W.: Low Speed, Hard Object Impact on Thick Graphite/Epoxy Plates. Report No. NADC-78051-60, U.S. Navy, 1978.
3. Rhodes, Marvin D.; Williams, Jerry G.; and Starnes, James H. Jr.: Effect of Impact Damage on the Compression Strength of Filamentary-Composite Hat-Stiffened Panels. Volume 23 of National SAMPE Symposium and Exhibition, Soc. Advance. Mater. & Process Eng., 1978, pp. 300-319.
4. Starnes, James H., Jr.; Rhodes, Marvin D.; and Williams, Jerry G.: The Effect of Impact Damage and Circular Holes on the Compression Strength of a Graphite-Epoxy Laminate. NASA TM-78796, 1978.
5. Leahy, J.D.: LARC-160 Fabrication Development. Graphite-Polyimide Composites, NASA CP-2079, 1979. (Paper no. 6 of this compilation.)
6. Rhodes, Marvin D.; Williams, Jerry G.; and Starnes, James H., Jr.: Low-Velocity Impact Damage in Graphite-Fiber Reinforced Epoxy Laminates. 34th Annual Conference, Reinforced Plastics/Composite Institute, The Society of the Plastics Industry, Inc., New Orleans, Louisiana, January 29 - February 2, 1979.

Gregory R. Wichorek
NASA Langley Research Center

EXPANDED ABSTRACT

The lack of test data for the graphite/polyimide composite materials is evident, particularly for fiber-matrix combinations most likely to be used in attachment areas. The load-carrying capabilities of joint geometries and the associated failure modes need to be determined for bolted-joint design.

An experimental program to determine bolted-joint strength and failure modes for advanced graphite/polyimide composite laminates at 116 K (-250°F), room temperature, and 589 K (600°F) is being conducted to provide preliminary design data. The bolted-joint test set-up for the low and elevated temperature tests is described. Test results are reported on a quasi-isotropic laminate of Celion 6000/PMR-15. Single bolt, double-lap shear specimens were tested to obtain maximum joint strength and failure mode. The effect of joint geometry and temperature on joint strength and failure mode is also presented.

TEST PARAMETERS

The composite laminate, fastener and test variables selected for evaluation are shown in figure 1. Test specimens were fabricated from a single sheet of Celion 6000/PMR-15, 1.3 meters (50 inches) long by 0.66 meters (26 inches) wide, with a (0,+45,90) fiber orientation. Double-lap shear specimens with a single 4.93 mm (.194 in.) diameter bolt were tested in tension to obtain maximum joint stresses and failure modes. The test bolt was torqued to 1.7 N-m (15 in.-lbf) at room temperature. The joint ratios of W/D (specimen width/hole diameter) and e/D (center of hole to edge distance/hole diameter) were varied from 4 to 6 and 2 to 4 respectively. Test temperatures were 116 K (-250°F), room temperature and 589 K (600°F).

MATERIAL: CELION 6000/PMR-15

ORIENTATION: [0, 45, 90, -45, 0, 45, 90, -45]_S 16 PLY

FASTENER: BOLT 4.93 mm (.194 in.) D

BOLT TORQUE: 1.7 N-m (15 in.-lbf)

JOINT VARIABLES: W/D = 4 TO 6
e/D = 2 TO 4

TEMPERATURE: 116 K (-250 °F)
297 K (75 °F)
589 K (600 °F)

Figure 1

BASELINE TENSILE STRENGTH SPECIMENS

Baseline tensile properties were obtained at room temperature from tensile and open-hole specimens shown in figure 2. The Celion 6000/PMR-15 laminate had a tensile strength of 477.8 MPa (69.3 ksi) and a tensile modulus of 45.5 GPa (6.6×10^6 psi). The 16-ply laminate had a fiber volume fraction of 55 percent. The effect of the 4.95 mm (.195 in.) diameter bolt hole on the net tensile strength of the composite laminate was determined from open-hole specimens with W/D ratios of 4, 5 and 6. The open-hole specimens failed at an average net tensile stress of 363.4 MPa (52.7 ksi). This stress value translates into a 24 percent reduction in laminate strength due to the stress concentration around the unloaded bolt hole.

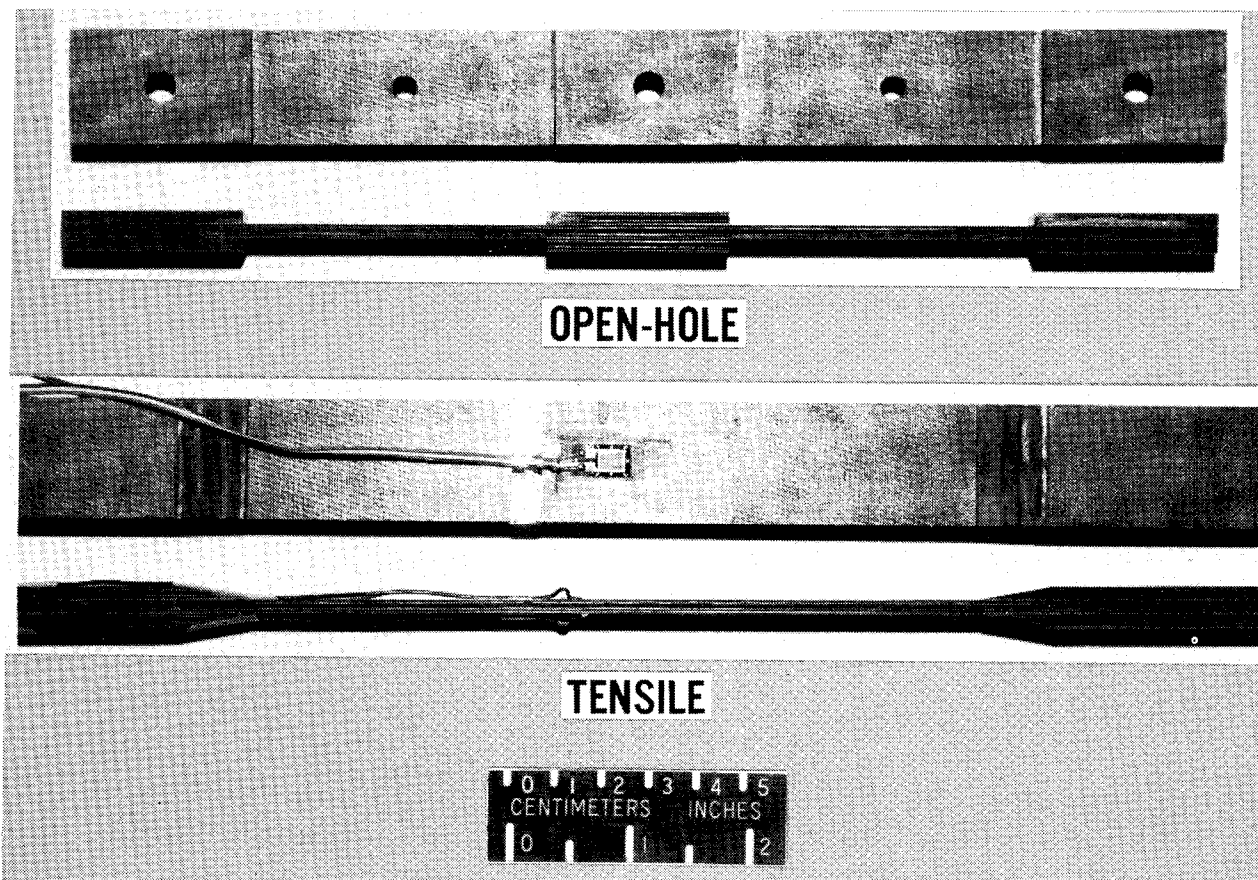


Figure 2

BOLTED-JOINT TEST SPECIMEN CONFIGURATIONS

Typical bolted-joint specimen configurations are shown in figure 3. Specimen width (W) and center of hole to edge distance (e) were varied for the room, low and elevated temperature specimens to obtain the desired test ratios of W/D and e/D . The room temperature specimens had 4 test holes of diameter (D) with a larger reinforced center hole for load transfer. After the two outer holes were tested, the specimens were cut to another edge distance (e) for the two inner holes as shown in the figure. The inner holes were five hole diameters from the reinforcing doublers. Specimens tested at 116 K (-250°F) and 589 K (600°F) had only one test hole. The length of these specimens was sized so that the doubler or load transfer end was outside the test chamber.

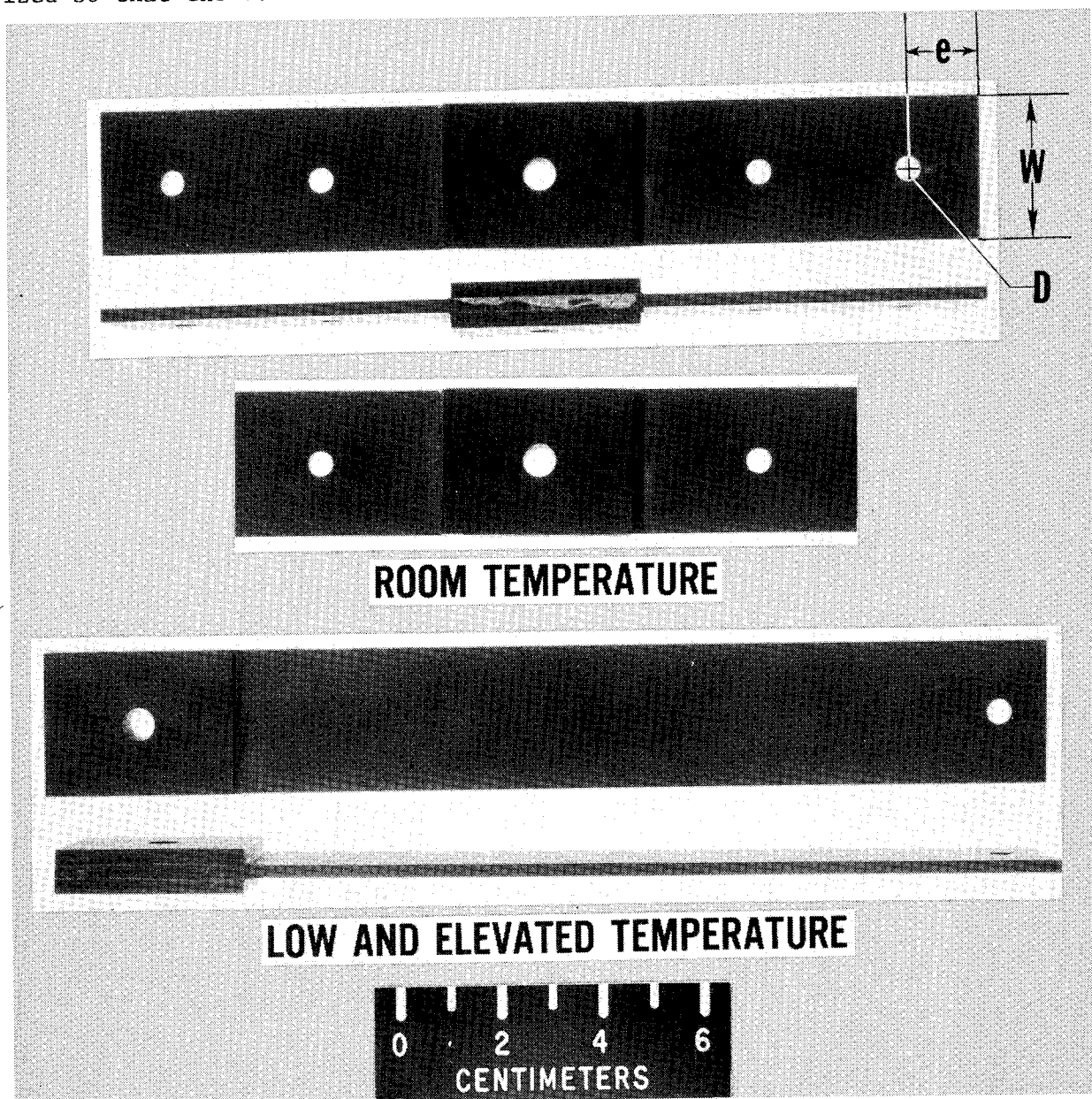


Figure 3

BOLTED-JOINT TEST APPARATUS

The bolted-joint test set-up for the low and elevated temperature tests is shown in figure 4. The test joint is located in the center of a split test chamber. The chamber can be rotated away from the load train and closed to minimize temperature losses in the chamber during specimen changes. Preliminary test runs were conducted to establish uniform test conditions and to determine uniformity of test joint temperatures. A temperature difference of 1 K (2°F) at 589 K (600°F) and 0 K (0°F) at 116 K (-250°F) was measured across the double-lap test joint. A single thermocouple clamped to the composite specimen 6.35 mm (.25 in.) below the double-lap area was used to monitor test temperature during the actual test runs. The joint area was held at test temperature 10 minutes before loading the joint to failure. Specimens were tested in a hydraulic test machine. A load rate of 2670 N/min (600 lbf/min) was set within the linear load-deflection response of the specimen and this constant head-motion was maintained until specimen failure.

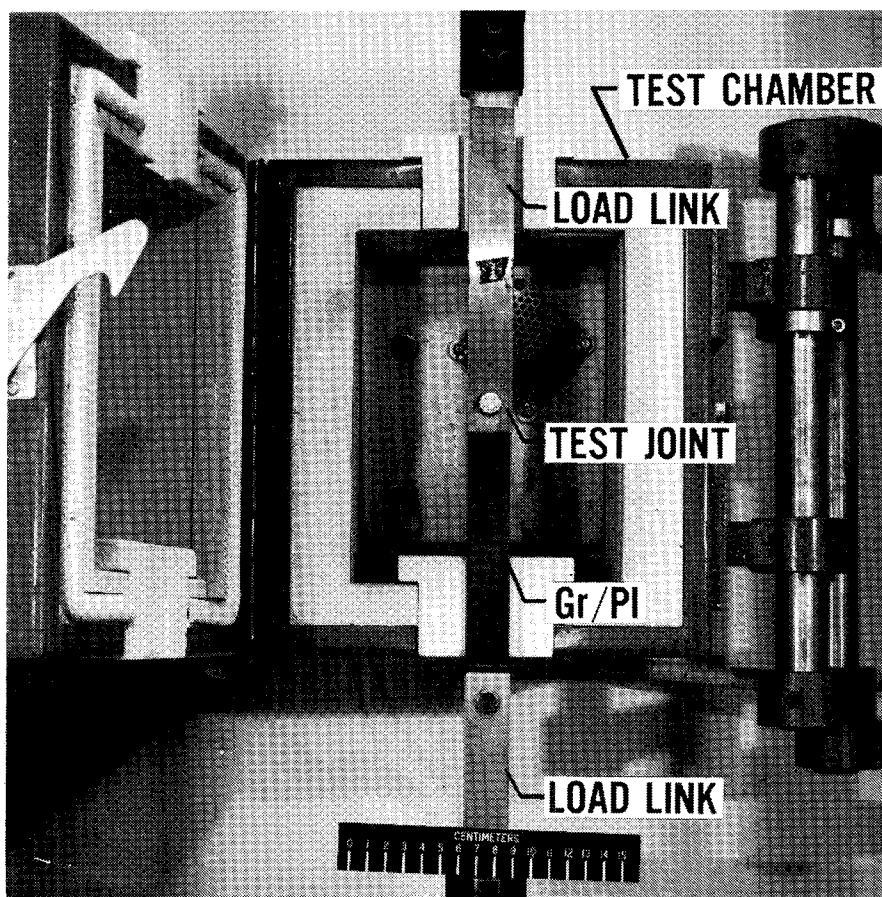


Figure 4

BOLTED-JOINT FAILURE MODES

Five bolted-joint failure modes were observed and they are shown in figure 5. The five failure modes are shear out, net tension, bearing, combination and multiple. The shear out, net-tension and bearing failures in the composite laminate are similar in appearance to the corresponding failure in metals. The main difference in failure mode between the two materials is the **occurrence** of interlaminar shear in the composite laminate which can be seen in the photo of a net tension failure. The combination failure **appears to be** a combination of shear out or cleavage and net-tension failure on one side of the bolt hole. The major difference between the combination and multiple failure modes is that in the multiple mode net-tension failure **occurs on** both sides of the bolt hole.

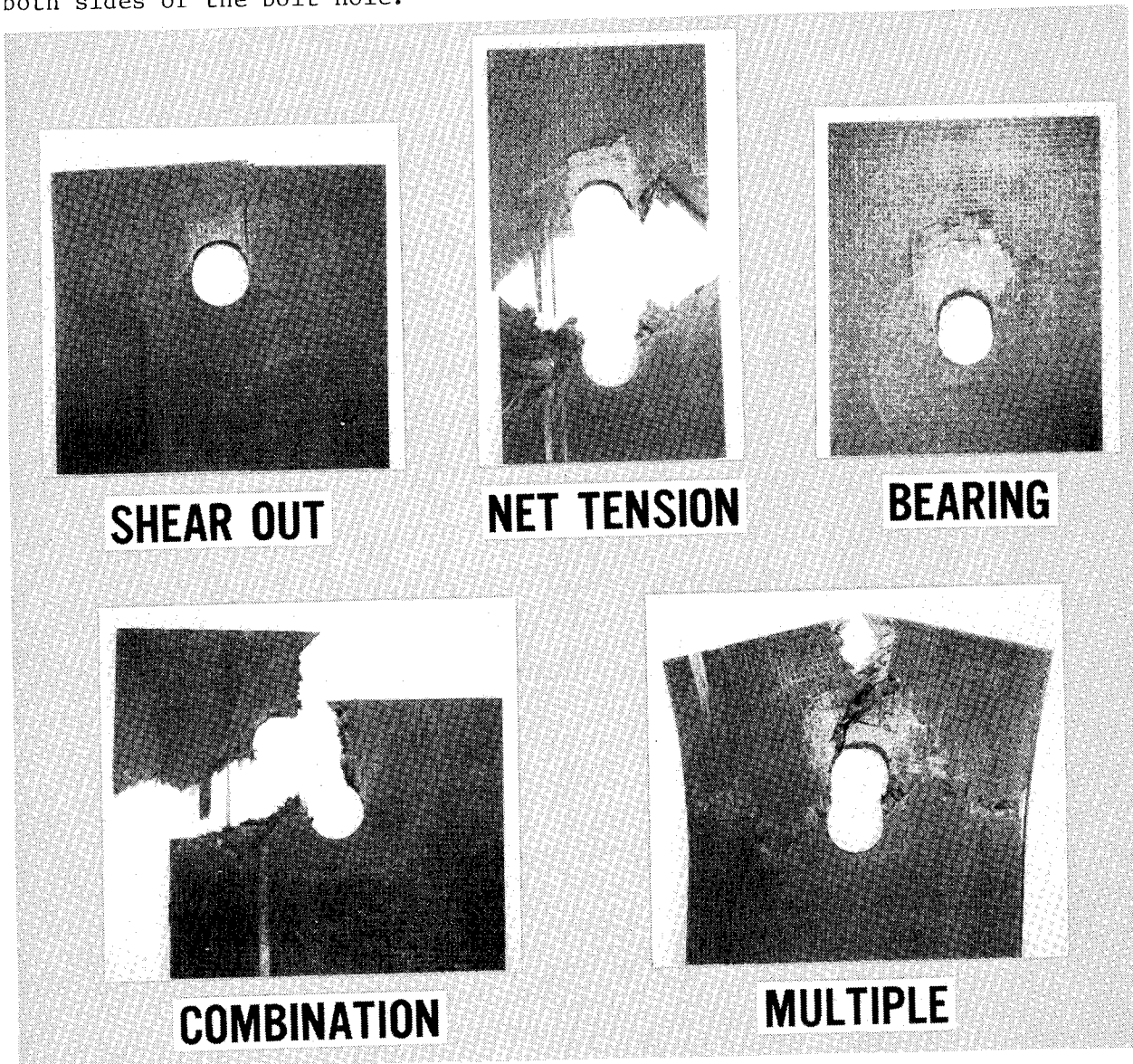


Figure 5

EFFECT OF GEOMETRY AND TEMPERATURE ON FAILURE MODE

The effect of joint geometry as well as temperature on the failure mode of the quasi-isotropic laminate is shown in figure 6. The test matrix of W/D and e/D ratios and temperatures are tabulated. Symbols denoting the failure modes are listed below the table. With a joint geometry of W/D=5.8 and e/D=2.0, shear-out failures occurred at room temperature and 589 K (600°F). The average maximum shear stress was 244.8MPa (35.5 ksi) at room temperature and 172.4MPa (25.0 ksi) at 589 K (600°F). These and all other stress values reported herein are maximum values which were achieved sometime after laminate damage had occurred and they should not be interpreted as usable joint strength. For W/D=3.9 and e/D=2.9, the bolted-joint specimens failed in net tension at all test temperatures; whereas for W/D=5.8 and e/D=3.9, the specimens failed in bearing at all test temperatures. The maximum net-tension and bearing stresses for these two joint geometries are shown in the next two figures for comparison with the other joint geometries.

W/D	TEST TEMPERATURE K (°F)	e/D									
		2.0		2.9				3.9			
3.9	116 (-250)			T	T	T		T	T	T	
	297 (75)			T	T	T	T	T	T	T	T
	589 (600)			T	T	T		B-T	B-T	B-T	
4.9	116 (-250)			T	T	T		T	T	T	
	297 (75)			M	M	M	M	B-T	B	B	B
	589 (600)			B-S	B-S	B-S		B-T	B-T	B-T	
5.8	116 (-250)	C	C	M				C	M	M	
	297 (75)	S	S	S	S			S	M	M	M
	589 (600)	S	S	S				B-S	B-S	B-S	

FAILURE MODE

T NET-TENSION C COMBINATION
 B BEARING M MULTIPLE
 S SHEAR-OUT

Figure 6

EFFECT OF GEOMETRY AND TEMPERATURE ON NET-TENSION STRESS

The effect of joint geometry and temperature on net-tension stress is shown in figure 7. The symbol key identifies failure mode. Net-tension stress data which are the average of four tests at room temperature and of three tests at 116 K (-250°F) and 589 K (600°F) are plotted against temperature. The effect of W/D on maximum net-tension stress is shown for e/D ratios of 2.9 and 3.9. For any W/D and e/D shown, net-tension stress decreases with increasing temperature from 116 K (-250°F) to 589 K (600°F). Also, net-tension stress decreases with increasing W/D from 3.9 to 5.8 for any constant e/D and temperature. Maximum joint strength in net tension is indicated for a joint geometry of W/D=3.9 and e/D=3.9. However for joint design, a bearing failure mode at 589 K (600°F) would have to be taken into account with this bolted-joint geometry. Bearing stresses corresponding to these net-tension stresses are given in figure 8.

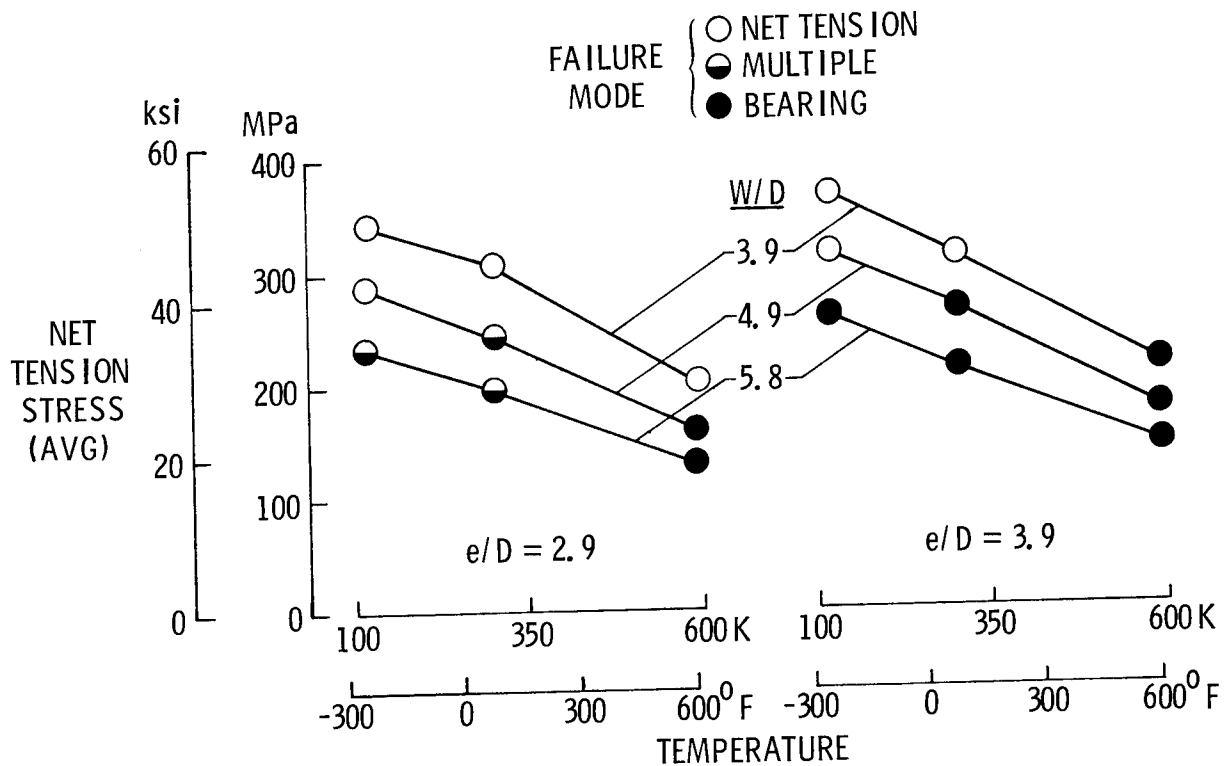


Figure 7

EFFECT OF GEOMETRY AND TEMPERATURE ON BEARING STRESS

The effect of joint geometry and temperature on bearing stress is shown in figure 8. For any W/D and e/D shown, bearing stress decreases with increasing temperature from 116 K (-250°F) to 589 K (600°F). For any constant e/D and temperature, bearing stress generally increases from $W/D=3.9$ to 4.9 with no significant increase in value from $W/D=4.9$ to 5.8. Maximum joint strength in bearing is indicated for a joint geometry of $W/D=5.8$ and $e/D=3.9$. The failure mode was bearing at all test temperatures for this bolted-joint geometry.

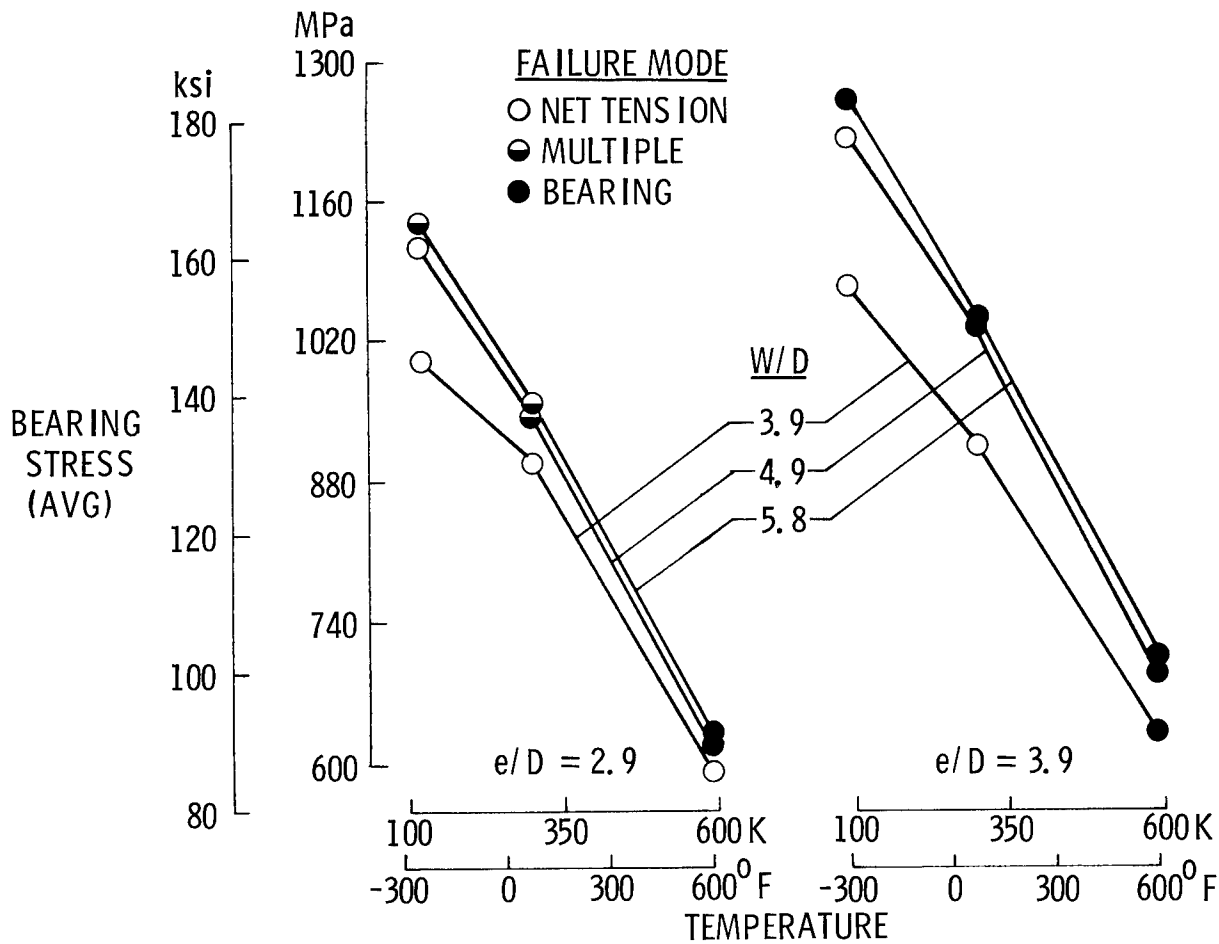


Figure 8

CONCLUDING REMARKS

Preliminary bolted-joint data has been presented for a 16-ply quasi-isotropic laminate of Celion 6000/PMR-15. A bolted-joint test capability was established and demonstrated for temperatures from 116 K (-250°F) to 589 K (600°F). Baseline tensile tests showed that the stress concentration around an open bolt hole reduced laminate strength 24 percent. The five bolted-joint failure modes observed were shear out, net tension, bearing, combination and multiple. Bolted-joint strength decreased with increasing temperature from 116 K (-250°F) to 589 K (600°F). Maximum joint strength was developed in net tension for $W/D=3.9$ and $e/D=3.9$ and in bearing for $W/D=5.8$ and $e/D=3.9$.

Walter Illg
NASA Langley Research Center

and

Richard A. Everett, Jr.
Structures Laboratory
U.S. Army Research and Technology Laboratories

EXPANDED ABSTRACT

Graphite composite materials have demonstrated superior fatigue properties at room temperature and to a limited extent at elevated and cryogenic temperatures. But the environment of the body-flap presents potential temperature extremes that have not been studied in a deliberate sense. The loading conditions are peculiar to the Shuttle structure; acoustic loading due to booster engine noise is expected to be the maximum loading with only minor actual flight-induced loads. In this study, the effects of the load/temperature environment on the fatigue life of the body-flap will be investigated by conducting real-time and accelerated flight-by-flight tests up to 500 flights on coupons containing holes.

On the fracture side, much is known about the sensitivity of the tensile strengths of composites to holes and other flaws, predominantly at room temperature. In this study, the effects of notches will be assessed for graphite/polyimides at the expected temperature extremes of the body-flap: 117 K (-250° F) to 589 K (600° F).

The two composite materials to be used for the majority of tests are Celion graphite fiber in matrices of PMR-15 and NR 150-B2. Only preliminary results are presented here with a description of specially-developed testing equipment.

FATIGUE AND FRACTURE PROGRAM OBJECTIVES

The major objectives are shown on this figure. In addition to determining potential limitations in fatigue performance, the effects of test acceleration on life will also be investigated. For fracture, the major emphasis is on assessing the effects of holes on tensile strength. Minor emphasis shall be on effects of slots. The materials of interest are Celion graphite fibers in two polyimide matrices (PMR-15 and NR 150-B2). Because specimens and test equipment were delayed, only preliminary test results are available; but program plans are also discussed. The program includes both constant-amplitude fatigue and real-time flight-by-flight behavior.

OBJECTIVES

FATIGUE :

TO DETERMINE POTENTIAL LIMITATIONS IN FATIGUE PERFORMANCE
OF GRAPHITE/POLYIMIDES IN THE SHUTTLE LOAD/TEMPERATURE
ENVIRONMENT

FRACTURE :

TO ASSESS THE EFFECTS OF NOTCHES ON THE TENSILE STRENGTHS
OF GRAPHITE/POLYIMIDES

Figure 1

PRELIMINARY FATIGUE RESULTS FOR HTS/PMR-15

This figure shows S-N curves for HTS/PMR-15 specimens. These specimens were 305 X 38 mm (12 by 1-1/2 inches) and contained a 6.4 mm (1/4-inch) central hole. If this material were homogeneous, the stress-concentration factor would be 2.5. The three test temperatures cover the maximum expected range for the body-flap. The trends shown here are similar to those found for other graphite composites, such as graphite/epoxy. These data show that this HTS/PMR-15 material is relatively insensitive to fatigue loading at the low temperature of 117 K (-250° F), but at room temperature and at 589 K (600° F) the curves have definite slopes. Lives are much shorter at the higher temperatures for a given stress level. At room temperature, the fatigue strength at 1 million cycles is about 60 percent of the tensile strength of notched specimens. These trends are quite different than for metals. S-N curves for metals are much more steeply sloped at all temperatures and fatigue limits are usually much below 50 percent of the tensile strengths. Subsequent tests will be on specimens made using Celion fibers in PMR-15 and NR 150-B2 polyimide matrices.

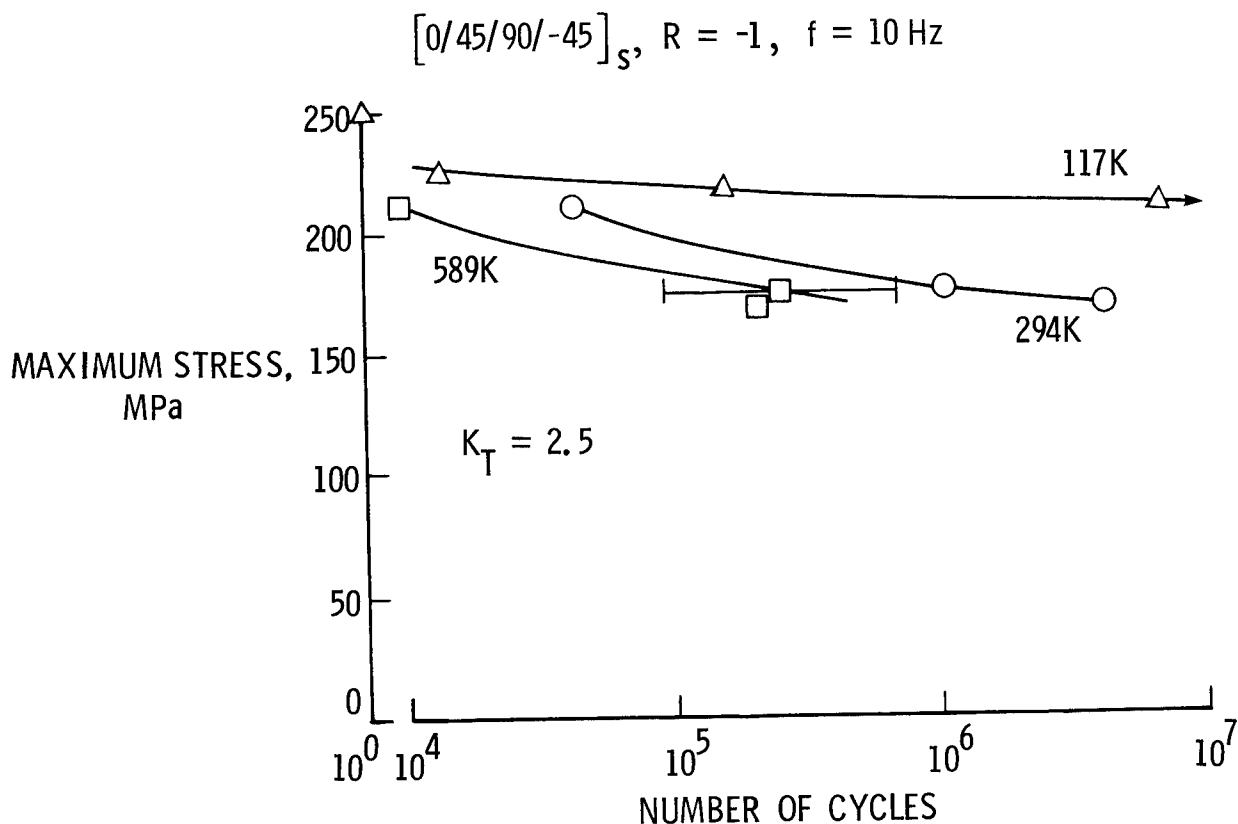


Figure 2

TYPICAL STRESS/TEMPERATURE PROFILE USED TO SIMULATE SHUTTLE BODY-FLAP ENVIRONMENT

Flight-by-flight real-time tests will be conducted in special machines, described later, that can be programed to reproduce a mission profile like the one shown in this figure. This profile represents the predicted stresses and temperatures for the flap. This basic mission profile was established from numbers generated for the aluminum flap. At launch, a severe acoustic environment excites the body-flap for 5 seconds. The aluminum flap responds mainly at 450 Hz, which translates into 2300 acoustic cycles for each launch. Because these composites have vibratory properties similar to those for aluminum, we assume a similar response. At 450 Hz, internal heating is expected. The temperature increases will be determined by cyclically bending samples at 450 Hz for a few thousand cycles at various stress levels. These temperature rises will be simulated in the real-time tests. The mission will be repeated for 4 times design life or up to 500 simulated flights, during which a bit over 1 million cycles of acoustic loading shall have transpired. Surviving specimens will be pulled to failure for residual strengths. Some of the test parameters to be varied are stress levels, maximum and minimum temperatures, and hold times in orbit. The specimens will be 8-ply plates of quasi-isotropic layup, containing a central hole to localize damage. One mission like this can be duplicated in the testing machines in as little as 60 minutes.

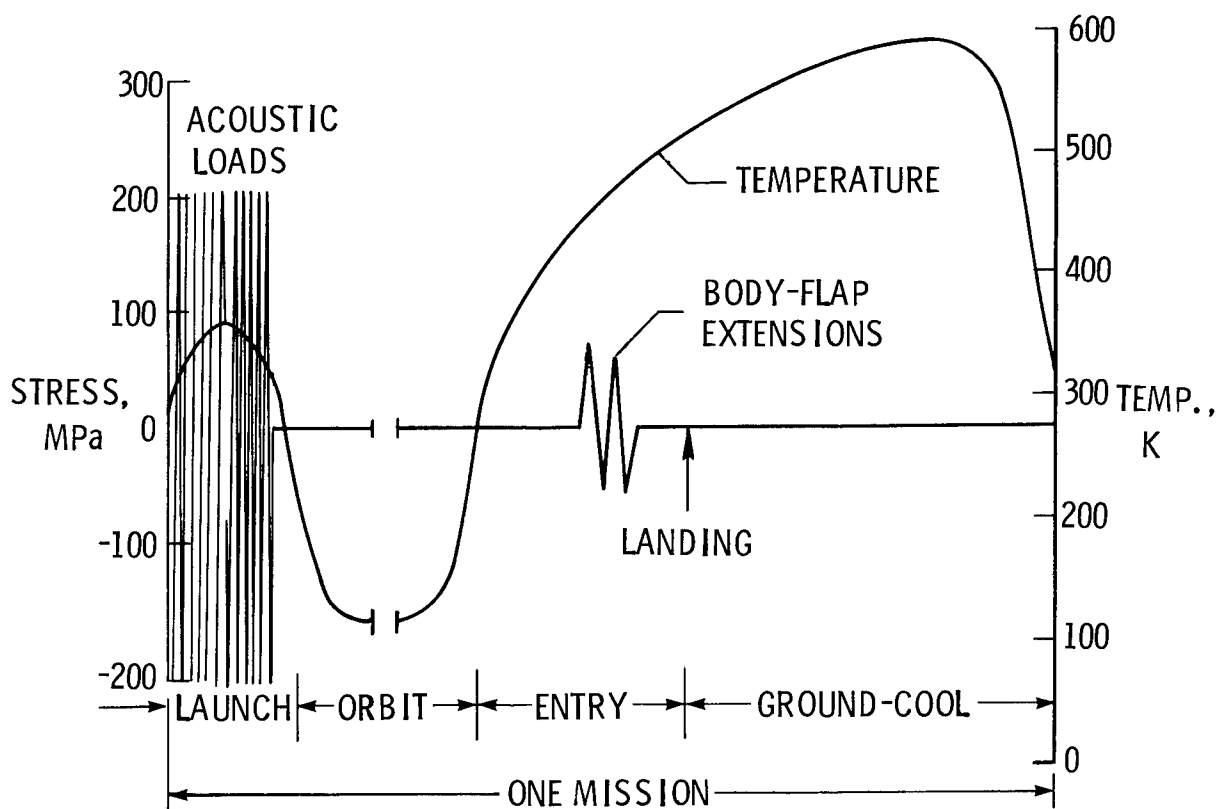


Figure 3

REAL-TIME FATIGUE TESTING MACHINES

The real-time testing machines that will utilize this profile are shown in this figure. On either side are five stands, each capable of independently testing a chain of five or six specimens. The control room, where the computerized controller is housed, can be seen through the window in the rear.

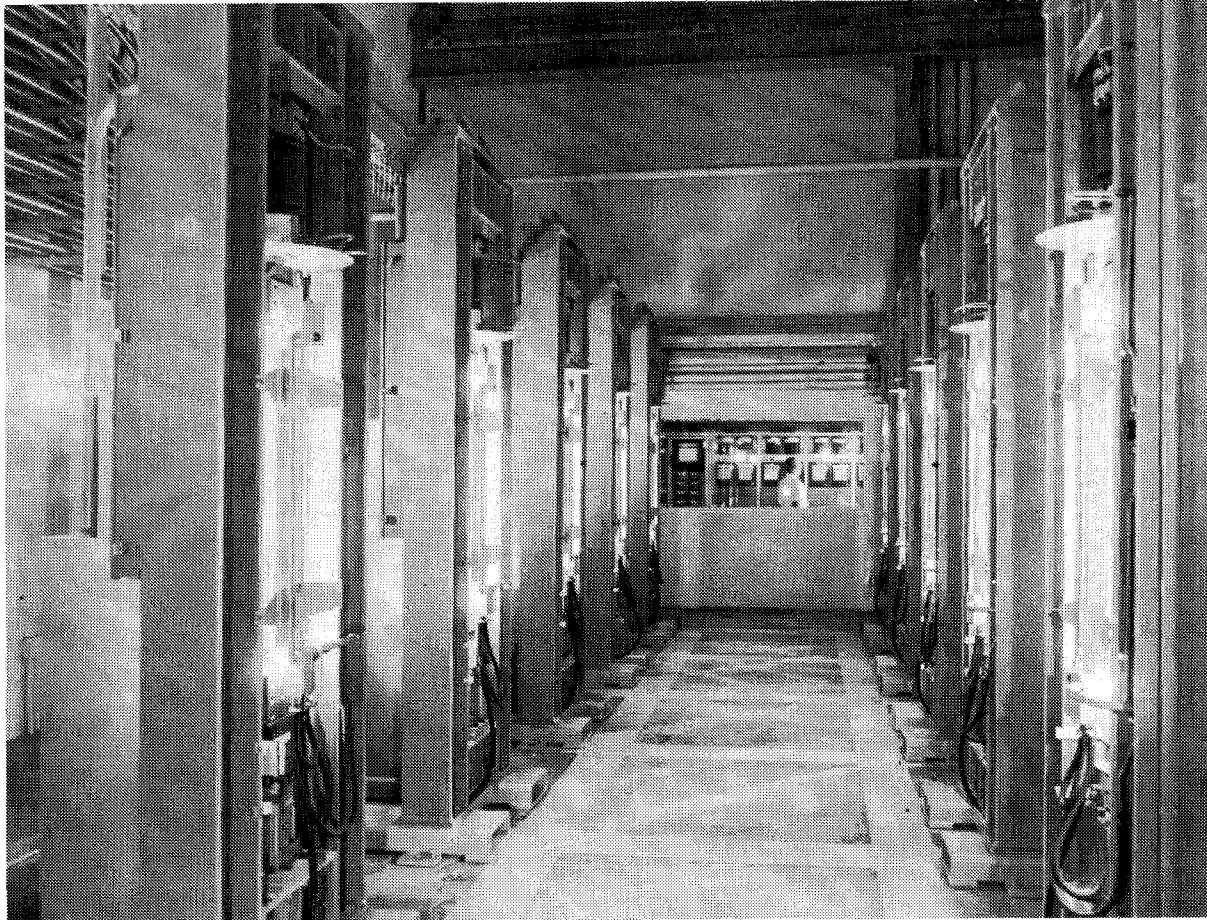


Figure 4

REAL-TIME MACHINE TEST STAND

This figure is a view of one entire chain of five specimens with heating and cooling systems installed. Each specimen is sandwiched between two furnace blocks that also act as coolers. The coolant is liquid nitrogen that is supplied through the lines covered by black and white insulation. In the collection of plumbing on the left are gages, manual valves, cryogenic solenoids, and rupture discs. The rupture discs guard against over-pressures that could rupture the copper lines.

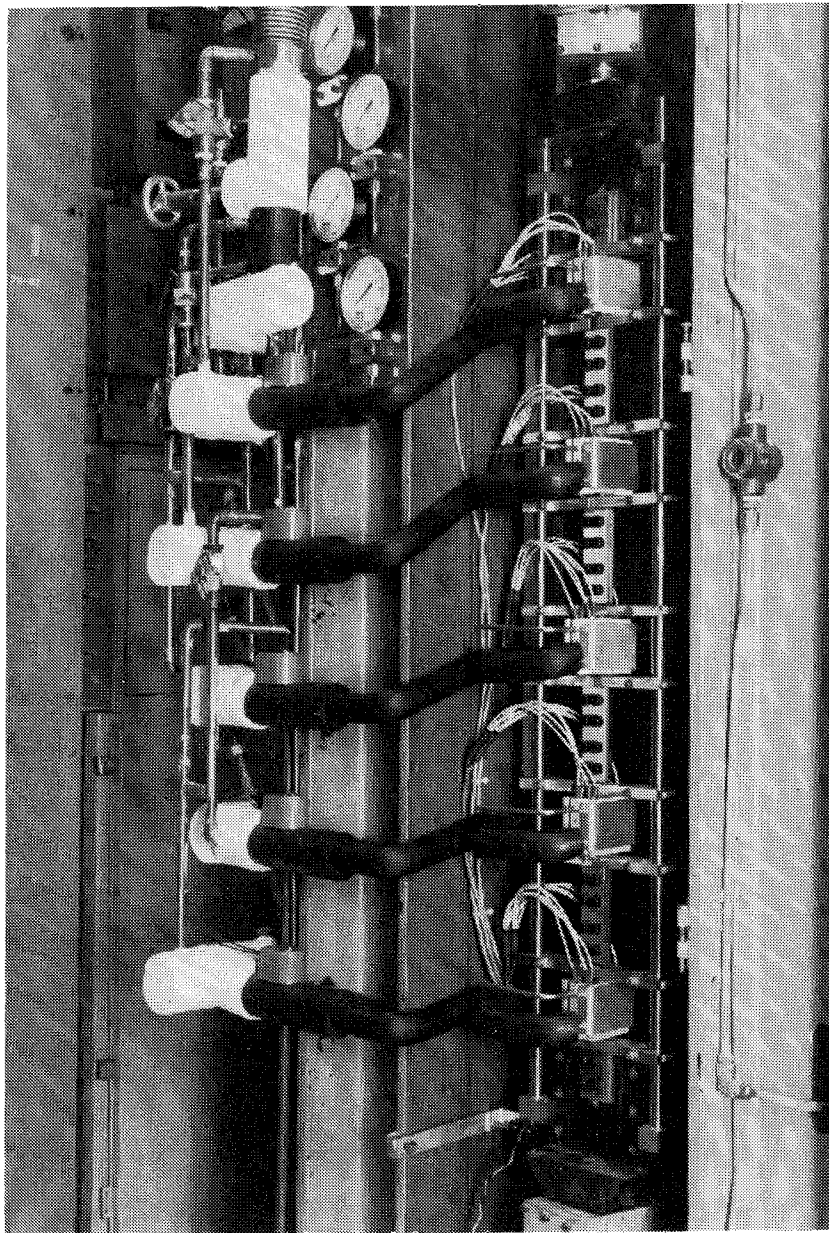


Figure 5

GUIDE FOR SPECIMEN IN REAL-TIME TEST STAND

This figure shows a closeup of a composite specimen with the furnace removed. The specimen is 38 mm (1-1/2 inches) wide. An anti-buckling guide supports the vertical edges of the specimen during compressive loading. The frame rides up and down on guideposts during cycling. These posts run the full length of a test stand. Above and below the specimen can be seen the bolts that connect specimens to each other to form a chain. The opening in the frame accepts a special furnace that was developed to heat and cool rapidly.

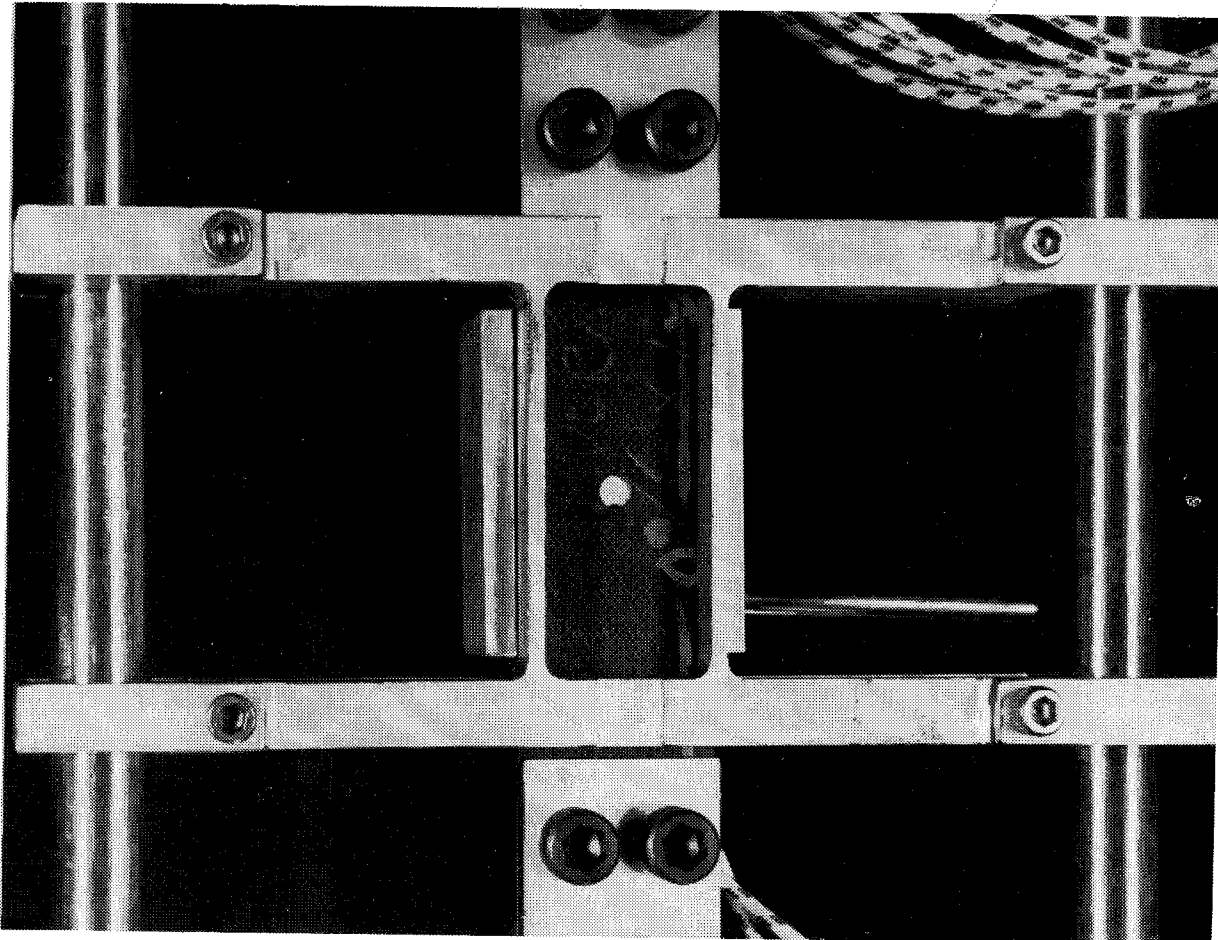


Figure 6

ASSEMBLED COMPACT HEATER/COOLER

This figure shows the special heater/cooler and associated parts. Two furnace blocks are shown clamped across a specimen. Heat is generated by two cartridges in each block and nitrogen is forced through cavities in the blocks when cooling is required. Specimen temperatures are sensed by the thermocouple probes that are passed through small apertures in the center of each block. Clips hold the blocks against the specimen. Shown on the left is a remotely-located cooling-temperature controller and a cryogenic solenoid. Liquid nitrogen is drawn from a 6.8 m³ (1800-gallon) tank.

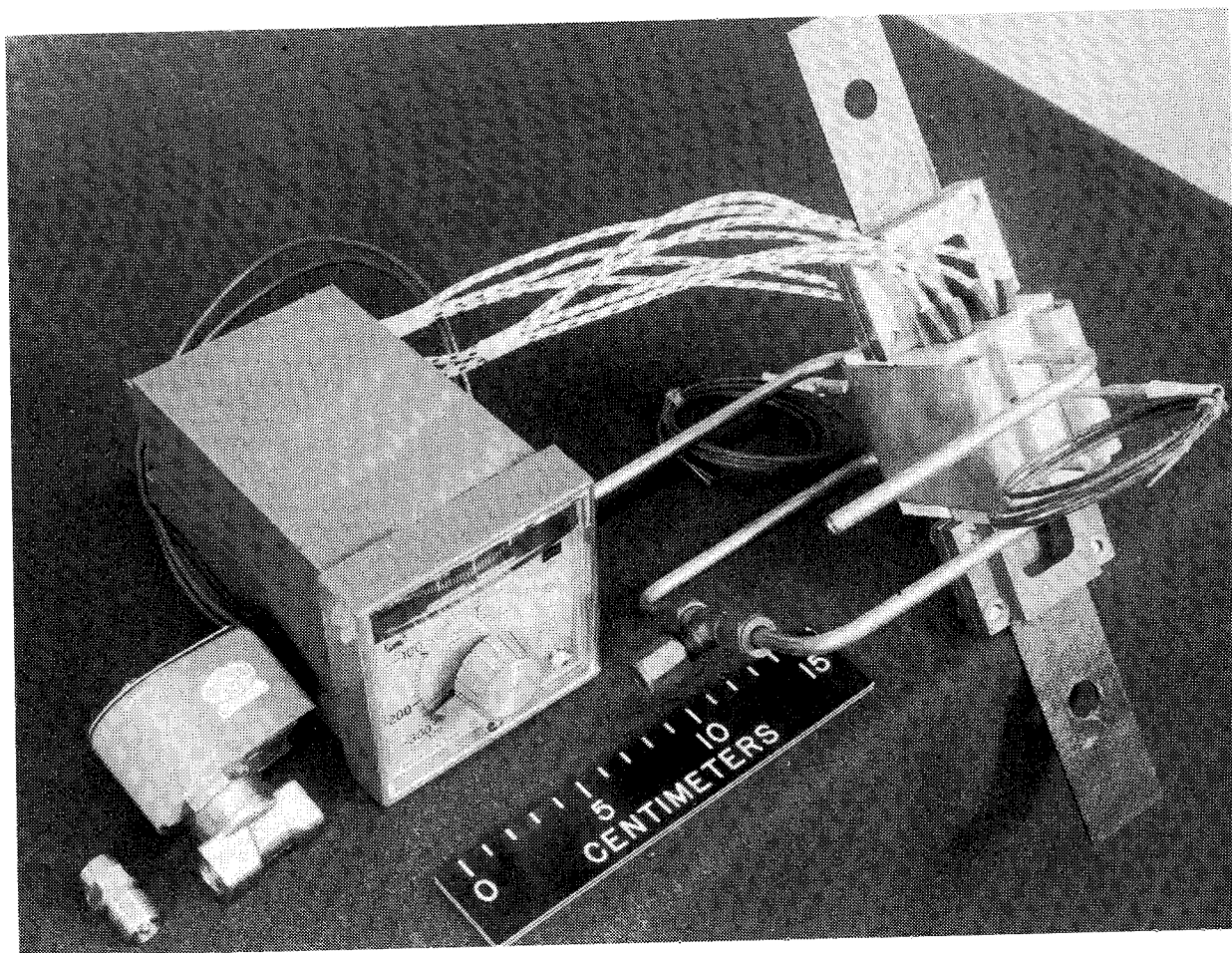


Figure 7

FRACTURE SPECIMEN CONFIGURATIONS

This figure shows the two types of specimens to be used: one with a hole and one with a slot. These are all 267 mm (10.5 in.) between grips and of various widths. Emphasis will be on specimens with holes because holes are more likely to occur in structures.

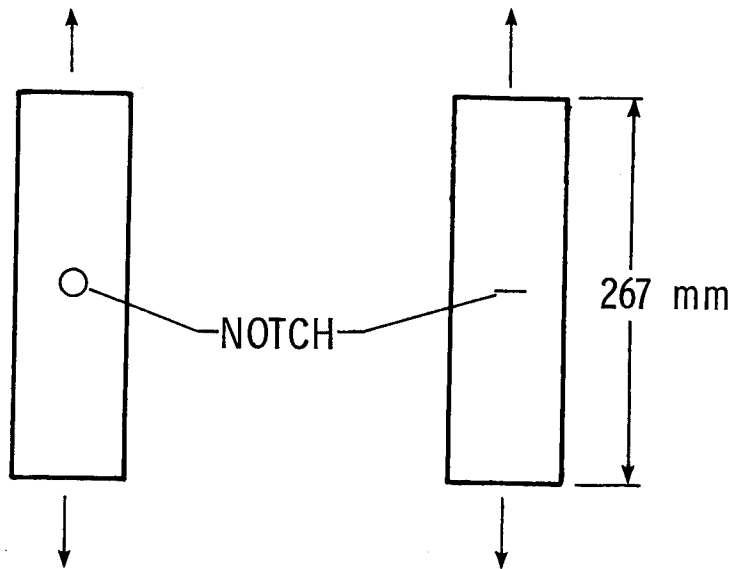
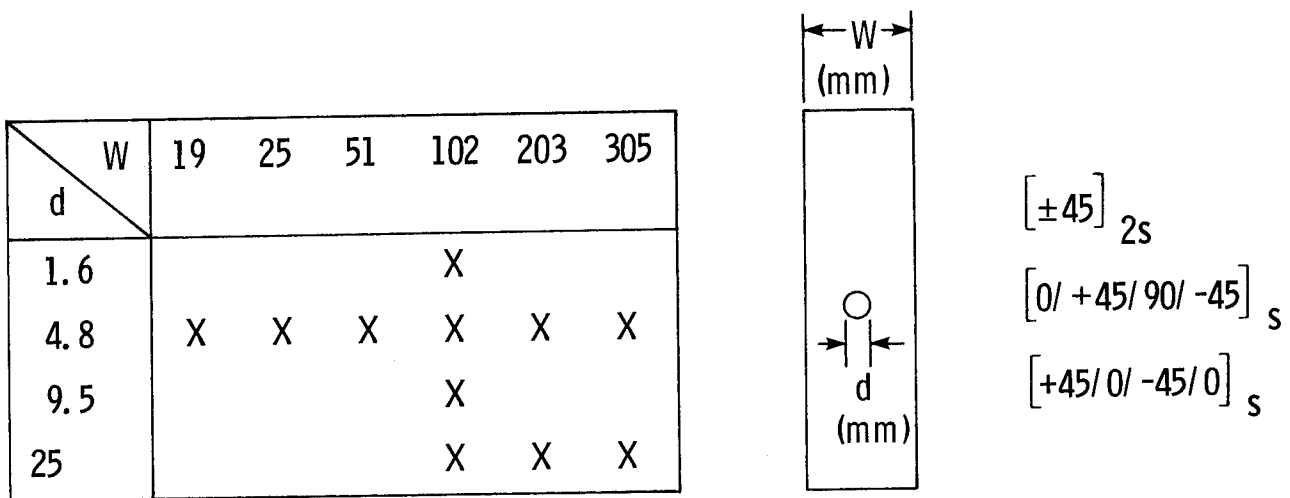


Figure 8

TEST VARIABLES FOR SPECIMENS WITH HOLES

This figure presents the test variables for specimens with holes. Widths range from 19 to 305 mm (3/4 to 12 inches) and holes range from 1.6 to 25 mm (.063 to 1 inch) in diameter. Three layups are to be studied: $[\pm 45]_{2s}$, $[0/+45/90/-45]_s$ and $[+45/0/-45/0]_s$. Tests will be at three temperatures: 117 K (-250° F), room temperature, and 589 K (600° F). In addition, the tensile strengths will be determined for as-fabricated specimens and for specimens after fatigue cycling. The X's indicate those combinations of width and hole diameter to be tested in this program.



TEST TEMPERATURES : 116K , RT , AND 589K

TENSILE STRENGTH : UNDAMAGED AND AFTER FATIGUE

Figure 9

EFFECT OF TEMPERATURE ON NOTCH STRENGTH

This figure shows the effect of temperature on the tensile strength of 102 mm (4-in.) wide specimens containing 6.4 mm (1/4-in.) holes. Two materials are shown: Celion and HTS graphite fibers in a PMR-15 matrix. For these layups, the strengths of both materials appear to be insensitive to these temperature changes.

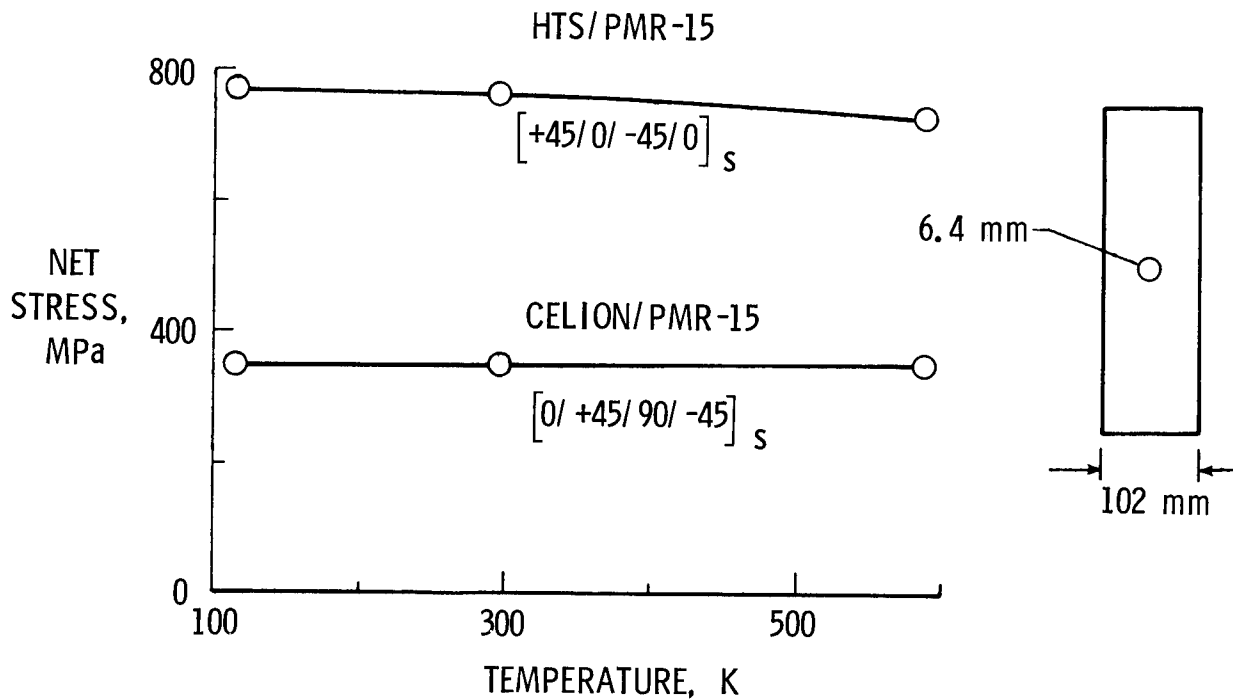


Figure 10

TENSILE STRENGTH FOR NOTCHED SPECIMENS

Much data have been published indicating that the effects of holes and slots on tensile strength of graphite/epoxy are equal. In metals, slots reduce strength much more severely than holes. This figure compares the strengths of specimens with 6.4 mm (1/4-inch) slots and holes for HTS/PMR-15 in two layups: quasi-isotropic at room temperature, and ± 45 at three temperatures. The data show no differences between strengths for 6.4 mm (1/4-inch) slots and holes. This finding is consistent with the behavior of graphite/epoxy.

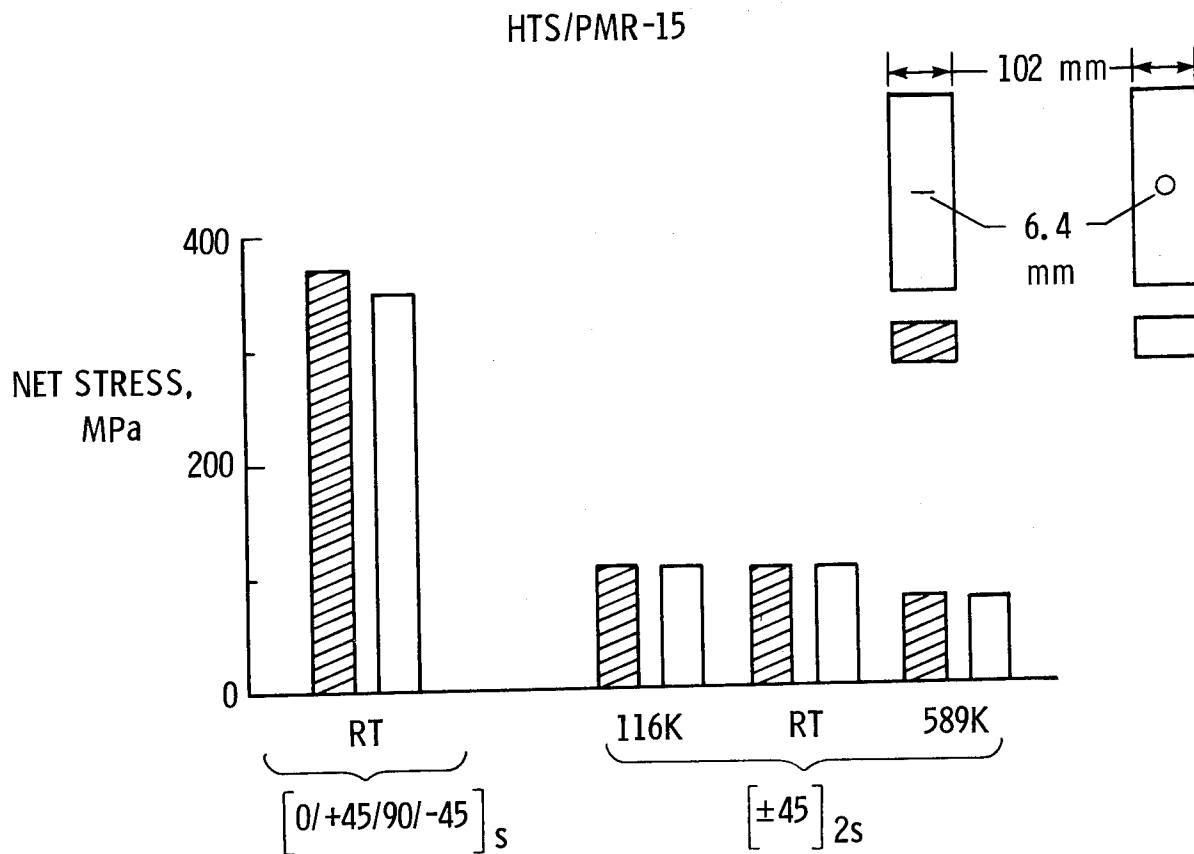


Figure 11

PRELIMINARY RESULTS FOR GRAPHITE/POLYIMIDES

The early results of constant-amplitude fatigue tests of HTS/PMR-15 at 117 K, 294 K, and 589 K indicate that the Shuttle temperature extremes may affect the fatigue properties. Fracture test results for the same material and for Celion/PMR-15, using specimens containing a round hole show no significant effect of the same three temperatures on tensile strength. For HTS/PMR-15, quasi-isotropic specimens at room temperature and $[\pm 45]_2$ specimens at the three aforementioned temperatures, tensile tests showed that round holes reduce strength equally with narrow slots.

- SHUTTLE TEMPERATURE EXTREMES MAY AFFECT FATIGUE PROPERTIES OF HTS/PMR-15
- NO SIGNIFICANT EFFECT OF TEMPERATURE ON NOTCH-STRENGTH
- TENSILE STRENGTHS FOR SPECIMENS WITH HOLES AND SLOTS ARE EQUAL

Figure 12

MECHANICAL PROPERTY DEGRADATION
OF GRAPHITE/POLYIMIDE COMPOSITES AFTER
EXPOSURE TO MOISTURE OR SHUTTLE ORBITER FLUIDS

20

W. Barry Lisagor
NASA Langley Research Center

EXPANDED ABSTRACT

Composite materials consisting of graphite fibers in a polyimide resin matrix offer potential for considerable weight savings in structural applications requiring high temperature service. The space shuttle orbiter vehicle aft body flap is a prime candidate for possible application, where operating temperatures will be too high for graphite epoxy consideration and considerable weight savings may be possible compared to conventional aluminum structure. However, the characterization of graphite polyimide materials with respect to mechanical property degradation by environmental effects has not yet been adequately accomplished.

The degradation of mechanical properties in graphite epoxy composite structural laminates by moisture absorption has been well recognized and investigated by many researchers over the past several years. Work has been conducted both on analytical moisture level predictions and on degree of degradation at specific moisture levels and temperatures. These results, however, may not be applicable to the broad general class of resin matrix materials, particularly the polyimides with their higher temperature curing characteristics and service capabilities. Little work has been reported on moisture absorption characteristics of polyimide matrix systems or the effect of moisture on mechanical properties of graphite polyimide composites. In order to commit the polyimide matrix composites to high temperature application such as the aft body flap of the space shuttle orbiter vehicle, full characterization of the materials with respect to potential degradation by moisture exposure or exposure to other expected service fluids must be accomplished.

This paper presents the initial results of a continuing study to investigate the effects of moisture exposure on the mechanical properties of graphite polyimide systems. The study includes efforts to investigate both the mechanism of the degradation and the magnitude of the effect associated with specific mechanical properties. The basic approach includes an experimental effort involving exposure to selected environmental variables and subsequent mechanical property testing and analysis.

MATERIAL AND ENVIRONMENTAL VARIABLES INVESTIGATED

The experimental program includes a large matrix of both material and environmental variables. The matrix shown should not be considered all inclusive, as the study is continuing, and emphasis may be changed based on interim results. Another material system, namely Celion 6000/LARC-160, may be added to the program based on recent development of that system. Laminate orientations of ± 45 and 90 may also be investigated to a lesser extent than the unidirectional and quasi-isotropic orientations which have received the greatest attention. The moisture conditioning treatments and temperatures were selected on the basis that they provided the extreme service boundary conditions associated with the space shuttle orbiter aft body flap application. Service liquids were included based on possibility of inadvertent contact with the graphite/polyimide structure, and which have been known to cause degradation of structural materials by chemical reaction.

Although the mechanical property variables include tension, rail shear, and flexure, initial attention has been focused on compressive and interlaminar behavior as those properties might be expected to be most significantly affected by environmental effects. The results reported herein will be limited to the compressive and the interlaminar shear behavior of the composite systems. Conventional short beam shear fixturing was employed using an environmental chamber for testing at other than ambient temperatures. Special fixturing was employed for the compression testing in order to minimize the time between removal from the environmental conditioning chambers and completion of the test. This will be discussed in further detail.

<u>MATERIAL</u>	HTS2/PMR 15, CELION/PMR 15
<u>ORIENTATION</u>	$(0, \pm 45, 90)_2, (0)_8$
<u>MOISTURE CONDITION</u>	AS PROCESSED, VACUUM DRIED, SATURATED, SATURATED AND THERMALLY CYCLED
<u>TEMPERATURE</u>	117, 294, 589 K (-250, 70, 600°F)
<u>PROPERTY</u>	TENSION, COMPRESSION, INTERLAMINAR SHEAR, RAIL SHEAR, FLEXURE
<u>SERVICE LIQUIDS</u>	HYDRAULIC FLUID, N_2H_4 , MMH, N_2O_4

Figure 1

SCHEMATIC DIAGRAM OF FACE SUPPORTED COMPRESSION TEST FIXTURE

In order to accomplish the compression testing of specimens after environmental conditioning a fixture was utilized which provided constraint for the specimen and also allowed for heating and cooling using cartridge heaters or liquid nitrogen manifolding. In addition, axial strain was monitored using mechanical extensometers. This test scheme provided for a minimum of time between removal of the specimens from the conditioning chambers and completion of the test. The test specimen was 300 mm (12 in.) long and 25 mm (1 in.) wide with 75 mm (3 in.) long aluminum tabs tacked on just prior to compression testing. The inner platens were split to allow for axial extension while the outer platens provided primary constraint. The outer platens were also channeled to allow for insertion of cartridge heaters or attachment of liquid nitrogen manifolding for heating and cooling. Cut-outs were made through both platens on each side to allow for attachment of mechanical extensometers on both sides of the specimen. The entire fixture was then contained in the plane of the specimen with the aid of large bolts attached to the hydraulic grips. The hydraulic grips were utilized to transfer load to the specimen by frictional forces between grips and tabs and between the tabs and the specimen. In this manner extensive adhesive bonding was avoided and specimens could be tested usually within one hour from removal from the controlled environment.

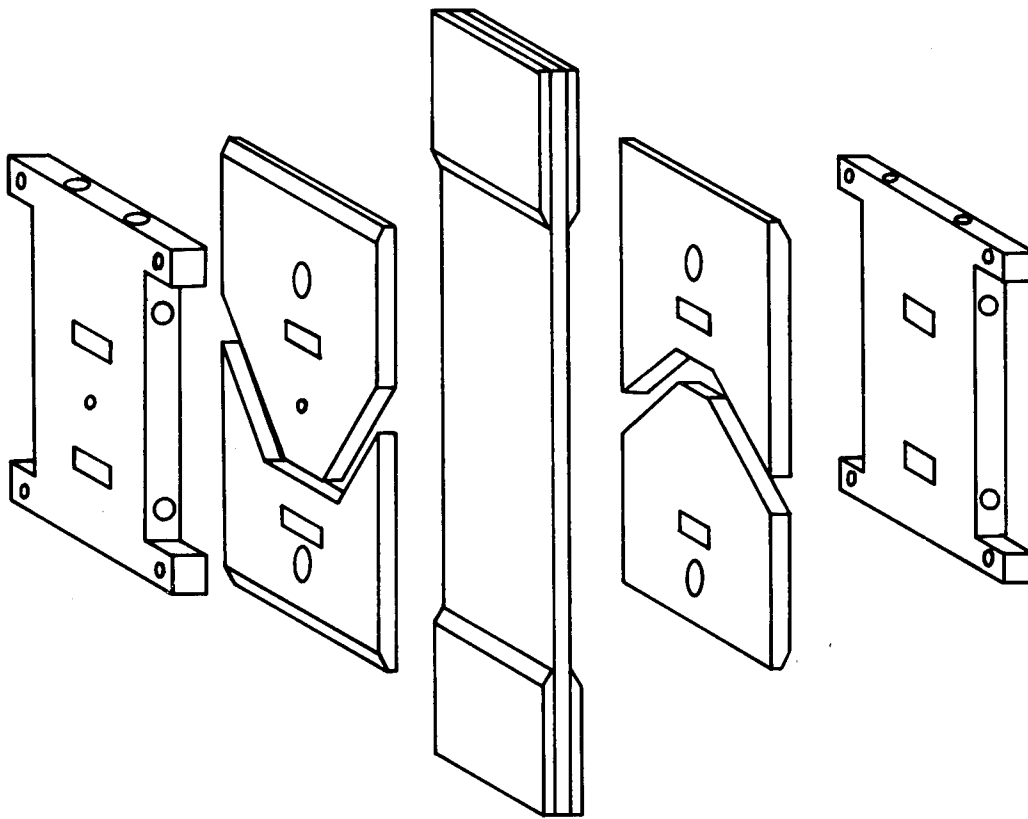


Figure 2

COMPRESSION TEST FIXTURE WITH LIQUID NITROGEN MANIFOLDING FOR LOW TEMPERATURE TESTING

The test fixture is shown located in the test position with manifolding for liquid nitrogen circulation through the platens in place. The hydraulic grips can be seen at the top and bottom of the figure. For this test the extensometer and strain gage wires are visible. Tests were conducted at 117 K (-250°F) and 294 K (70°F) with both strain gages and extensometers to compare strain values obtained. Generally, the values agreed within two percent.

Temperature control at 117 K (-250°F) was accomplished using an off/on controller, and control temperature could generally be maintained within three degrees of desired test temperature. Temperature uniformity over a 25 mm (1 in.) gage section in the center of the specimen was within a 6 K (10°F) range of desired test temperature. In this figure the bolts which hold the entire assembly in the plane of the specimen have been removed to show details of the fixture.

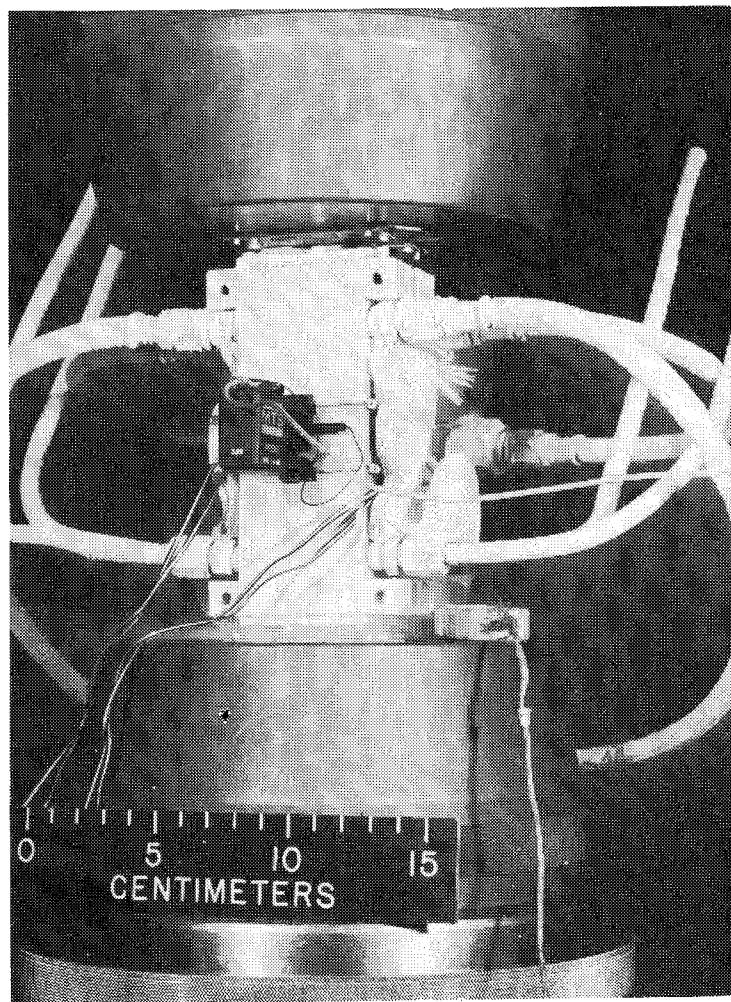


Figure 3

COMPRESSION TEST FIXTURE WITH CARTRIDGE HEATERS FOR HIGH TEMPERATURE TESTING

This figure shows the compression test fixture with the restraining bolts in place to hold the assembly in the plane of the specimen. Power leads to the cartridge heaters inserted in the outer platens are also visible. Temperature control was accomplished in the same manner as for the low temperature testing (off/on controller), and control temperature could be maintained within 3 K (5°F) of desired test temperature. Temperature uniformity over a 25 mm (1 in.) gage section in the center of the test specimen was also within a 6 K (10°F) range of desired test temperature.

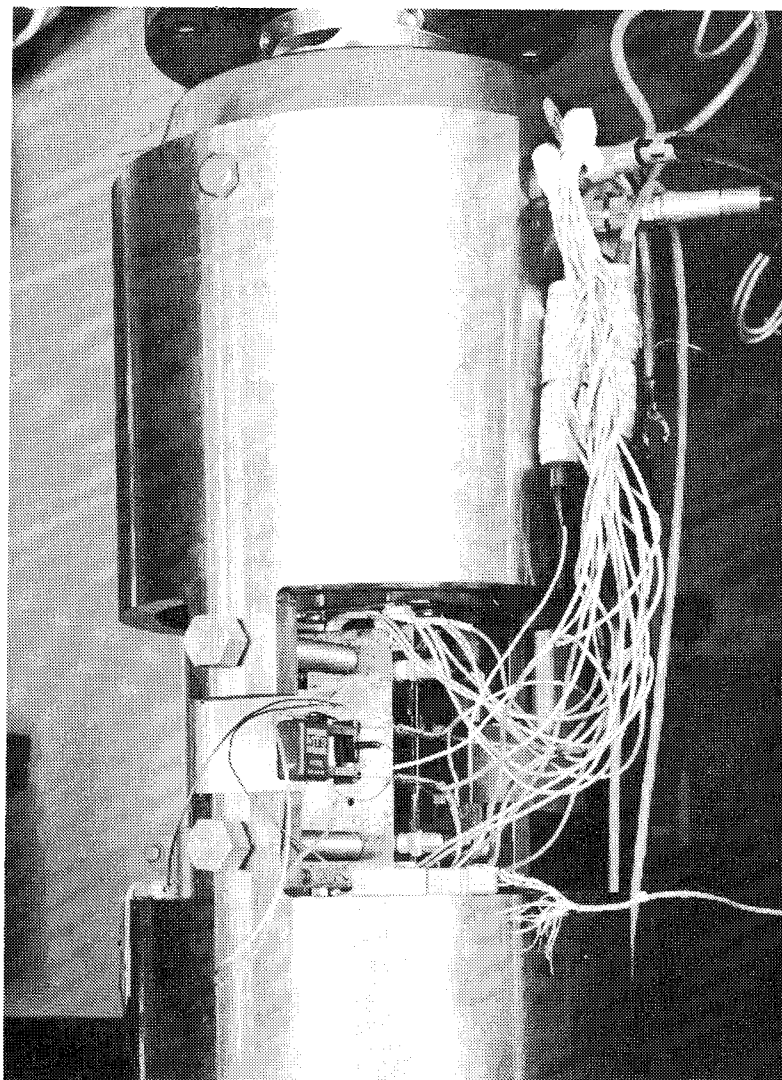


Figure 4

MOISTURE ABSORPTION AND DESORPTION CHARACTERISTICS
OF GRAPHITE/POLYIMIDE COMPOSITES

Moisture absorption of the graphite/polyimide systems studied was determined by exposing as-processed laminates in test specimen configuration (short beam shear, or compression) to condensing humidity environment at 355 K (180°F) and atmospheric pressure for times up to three months. The percent weight change (absorption) is shown for times to 180 hours and the bracketed intervals represent the range of weight gains observed for HTS2/PMR15, and Celion 6000/PMR15, in both quasi-isotropic and unidirectional laminates, and in the short beam shear and compression specimen configuration. The specimen thicknesses ranged from eight to 20 ply depending on the type of specimen. Average percent weight gain was from .8% to 1% compared to as-processed specimens.

Moisture desorption was determined by exposing as-processed specimens at 365 K (200°F) under vacuum below 10^{-3} torr. The average weight loss of all specimen combinations was .5% to .6%. The total moisture content, assuming the weight loss upon vacuum drying was attributable to residual moisture in the as-processed condition, from totally dry to fully saturated was approximately 1.5% based on total composite weight. This is essentially comparable to the epoxy matrix systems.

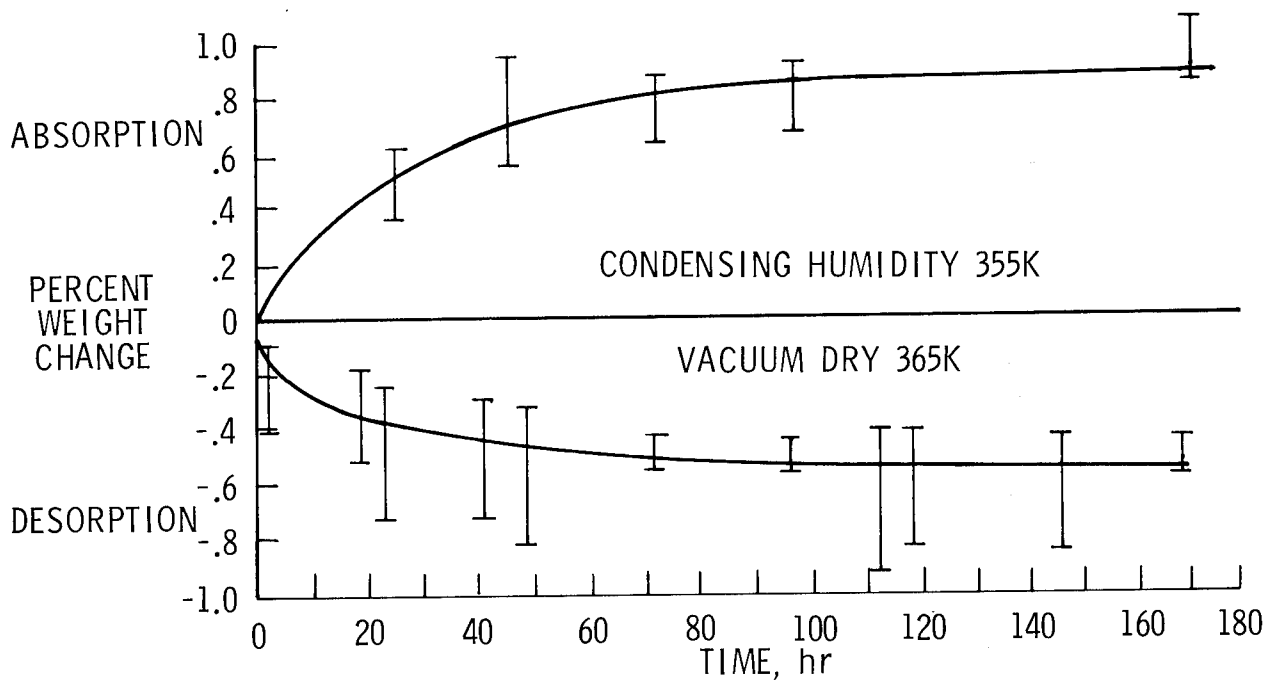


Figure 5

EFFECT OF TEMPERATURE ON INTERLAMINAR SHEAR STRENGTH OF AS-PROCESSED HTS2/PMR15

Values of interlaminar shear strength are shown for three test temperatures normalized to the average value determined for as-processed material tested at room temperature. In all cases where symbols are bracketed, the symbol represents an average value of five replicate tests for each test condition and the brackets represent one standard deviation from the mean value. There was little change in interlaminar shear strength at 117 K (-250°F) for either laminate compared to room temperature tests. Tests at 589 K (600°F) showed little effect of temperature for the quasi-isotropic specimens, but a substantial reduction was observed for unidirectional specimens. In addition, the failure mode for these specimens was not interlaminar shear, but rather yielding as a result of apparent matrix softening.

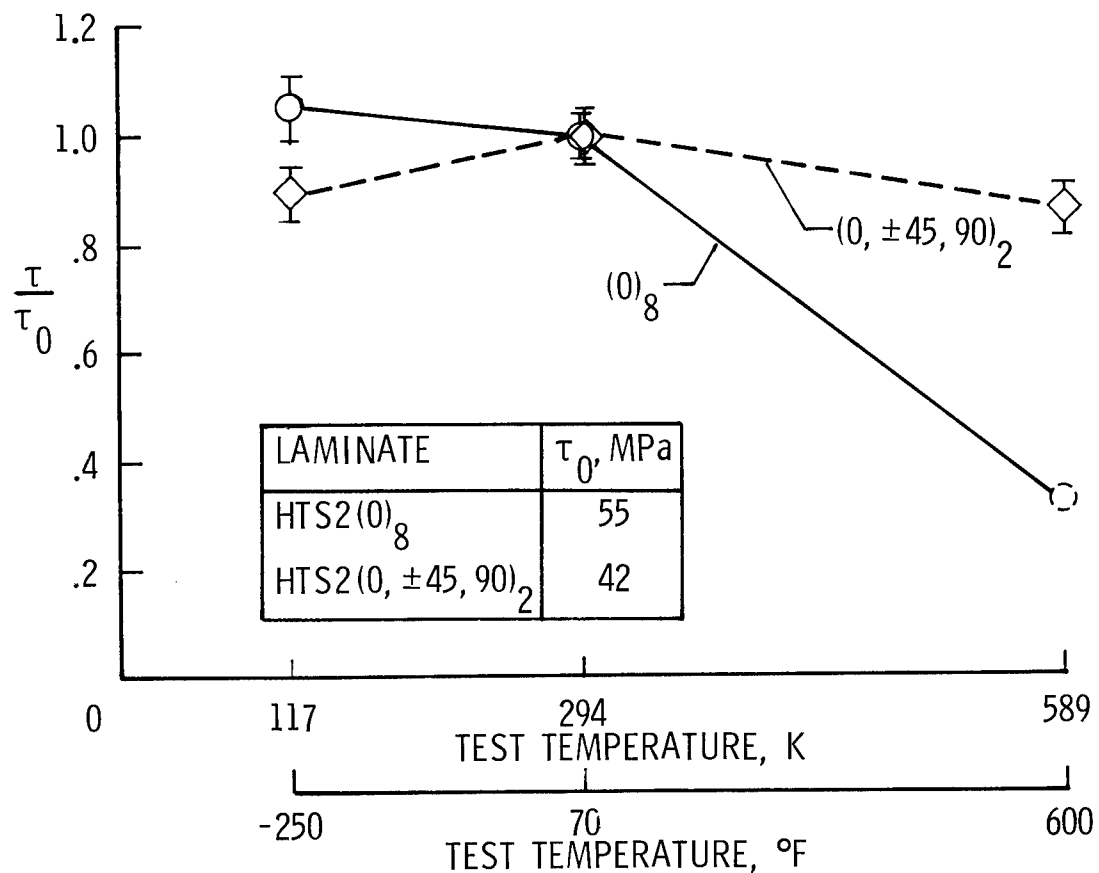


Figure 6

EFFECT OF VACUUM DRYING ON INTERLAMINAR SHEAR STRENGTH OF HTS2/PMR15

Results of short beam shear tests on specimens after vacuum drying are shown normalized to as-processed room temperature values for the three test temperatures. Vacuum drying had little effect on interlaminar shear strengths at 117 K (-250°F) and 294 K (70°F) compared to as-processed tests at comparable temperatures. At 589 K (600°F) vacuum drying resulted in a slight increase in the interlaminar shear strength of the quasi-isotropic laminate and in a substantial increase in the unidirectional laminate. This increase must likely be attributed to removal of residual moisture in the unidirectional laminate. The unidirectional material from which interlaminar shear specimens were obtained underwent an average weight decrease of nearly one percent upon vacuum drying, somewhat greater than was observed for the other laminate-specimen combinations investigated. The vacuum drying temperature (365 K (200°F)) must be assumed too low to affect curing behavior subsequent to processing. This increase in interlaminar shear strength as a result of vacuum drying also suggests that the observed low strengths at 589 K (600°F) for as-processed unidirectional material were a result of residual moisture remaining after laminate fabrication.

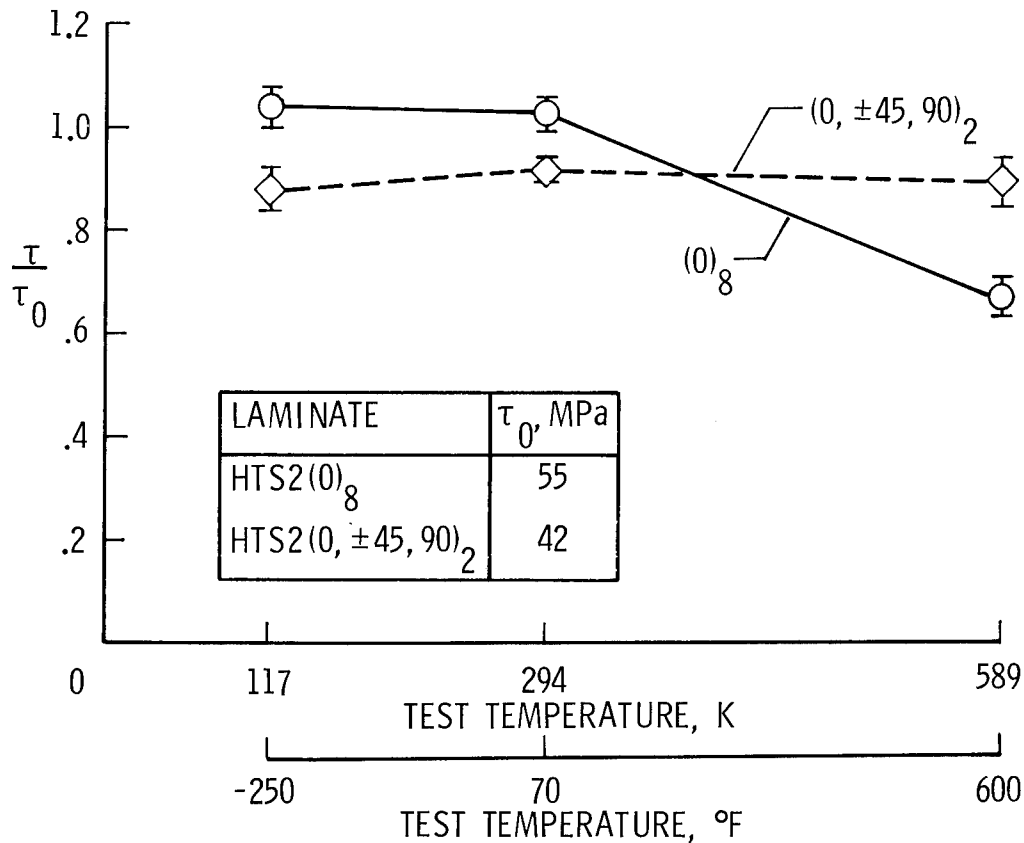


Figure 7

EFFECT OF MOISTURE ON INTERLAMINAR SHEAR STRENGTH OF HTS2/PMR15

Results of interlaminar shear tests on specimens moisture conditioned to a level of at least 90% of saturation are shown for both unidirectional and quasi-isotropic laminates. Tests at 117 K (-250°F) and 294 K (70°F) showed little significant effect on either laminate orientation. Tests at 589 K (600°F) resulted in reductions in interlaminar shear strength to approximately 60% of as-processed room temperature values. This corresponds to a 40% decrease for the quasi-isotropic laminate compared to as-processed or vacuum dried material tested at 589 K (600°F). Results on the unidirectional material were not conclusive when compared to material tested as processed because of the very low values observed for the as-processed material. Tests of moisture conditioned unidirectional specimens showed a reduction of 15-20% in interlaminar shear strength compared to vacuum dried specimens.

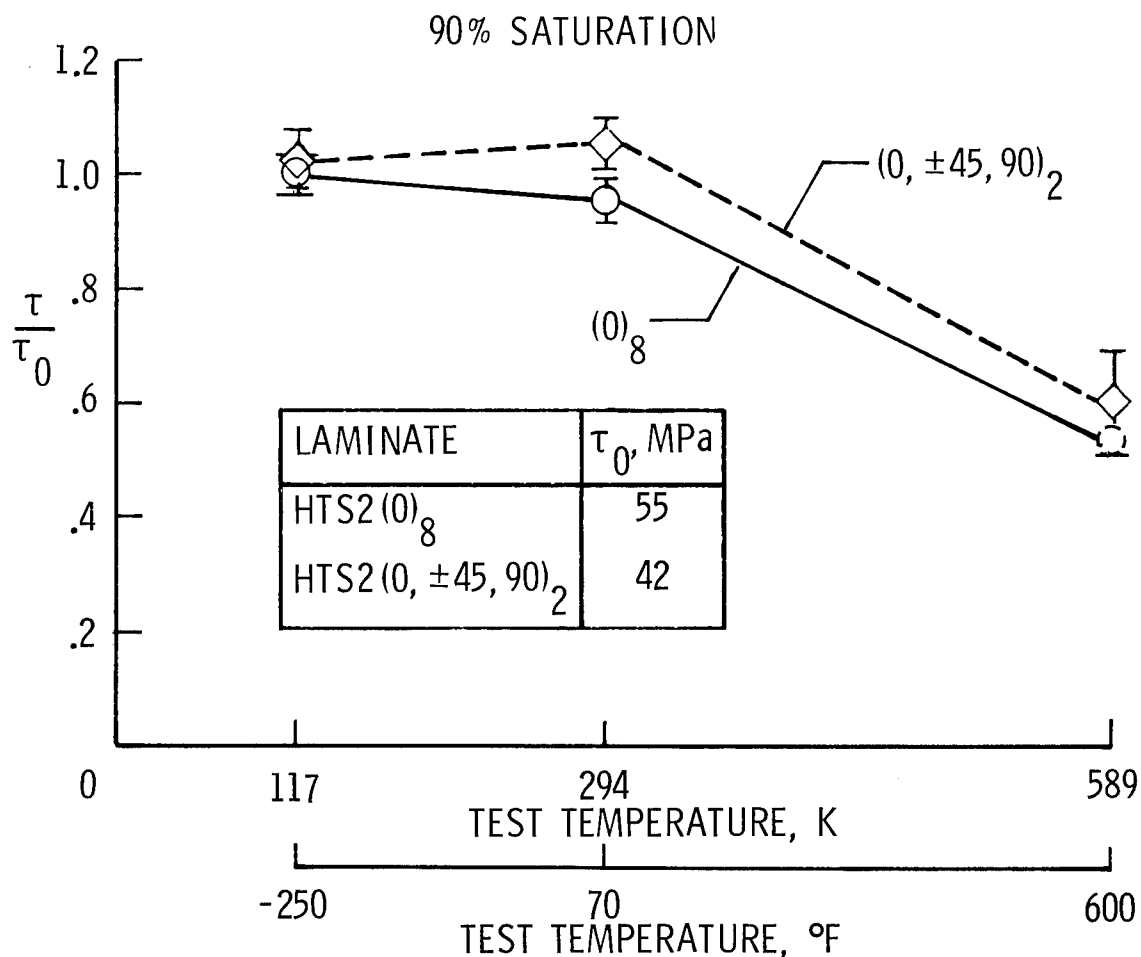


Figure 8

EFFECT OF TEMPERATURE ON COMPRESSIVE STRENGTH OF AS PROCESSED GR/PMR15

The results of compression testing of Gr/PMR15 are shown for both Celion 6000 and HTS2 fibers in a PMR15 matrix, and for both unidirectional and quasi-isotropic laminate orientations. The as processed, room temperature baseline values showed about the same compressive strength for both Celion 6000/PMR15 and HTS2/PMR15 in the unidirectional orientation. However, the Celion 6000/PMR15 material in the quasi-isotropic orientation had nearly twice the compressive strength as the HTS2/PMR15 quasi-isotropic material. This suggests some possible processing problem for the HTS2/PMR15 which affected the room temperature and low temperature properties significantly, but had little or no effect on tests at 589 K (600°F). This is also supported by the results of interlaminar shear tests which showed less than expected reductions in strength at the high test temperature. Testing at 117 K (-250°F) showed no effect on any of the specimens tested, while tests at 589 K (600°F) resulted in compressive strength values of 50 to 60% of the room temperature values for both Celion/PMR15 orientations and the HTS2/PMR15 unidirectional specimens. The quasi-isotropic HTS2/PMR15 specimens actually showed a slight increase in compressive strength at 589 K (600°F), but it should be noted that room temperature values were low for this material and a relative comparison based on those values would be expected to be high. The actual absolute strength values at 589 K (600°F) were nearly the same for both Celion/PMR15 and HTS2/PMR15 quasi-isotropic materials.

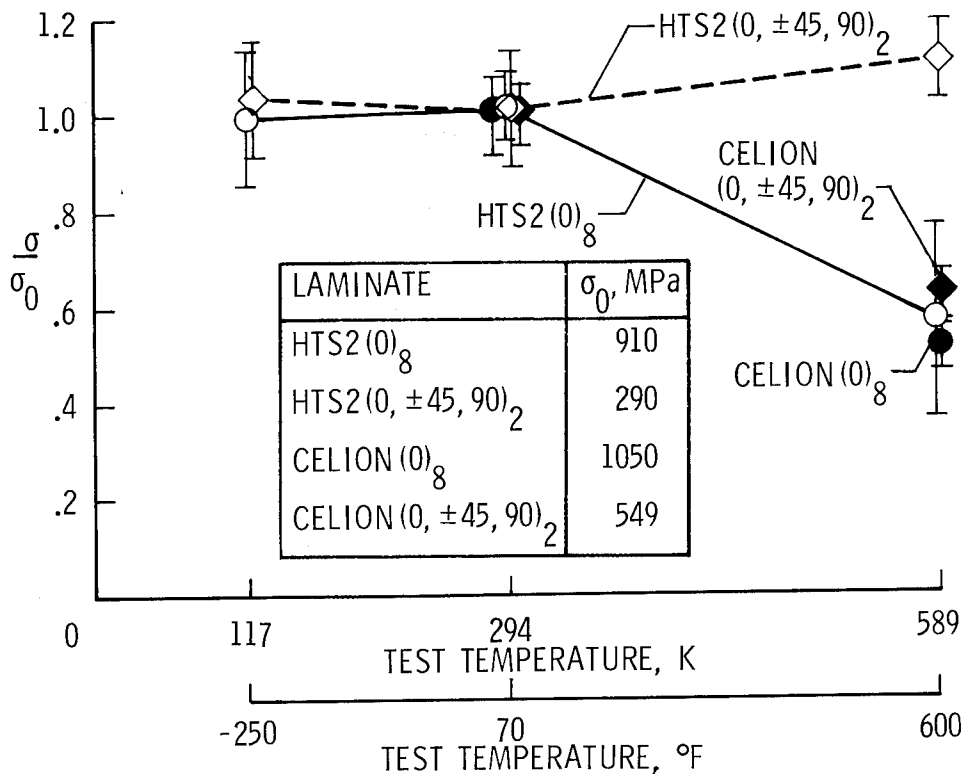


Figure 9

EFFECT OF VACUUM DRYING ON COMPRESSIVE STRENGTH OF GR/PMR15

Compression tests on specimens which had been vacuum dried showed the same general trend of increased strength values as was observed for the interlaminar shear tests. The increase in compressive strength was more significant and the results were conclusive for both Celion orientations and the HTS2 unidirectional material. The HTS2/PMR15 quasi-isotropic material showed essentially unchanged values compared to as-processed material.

Vacuum drying resulted in a 20-30% increase in compressive strength compared to as-processed material tested at 589 K (600°F) for the Celion and HTS2 unidirectional material. This increase is significant enough to suggest that final processing by such a treatment might be worthwhile if the improved properties were not sacrificed by environmental degradation in service.

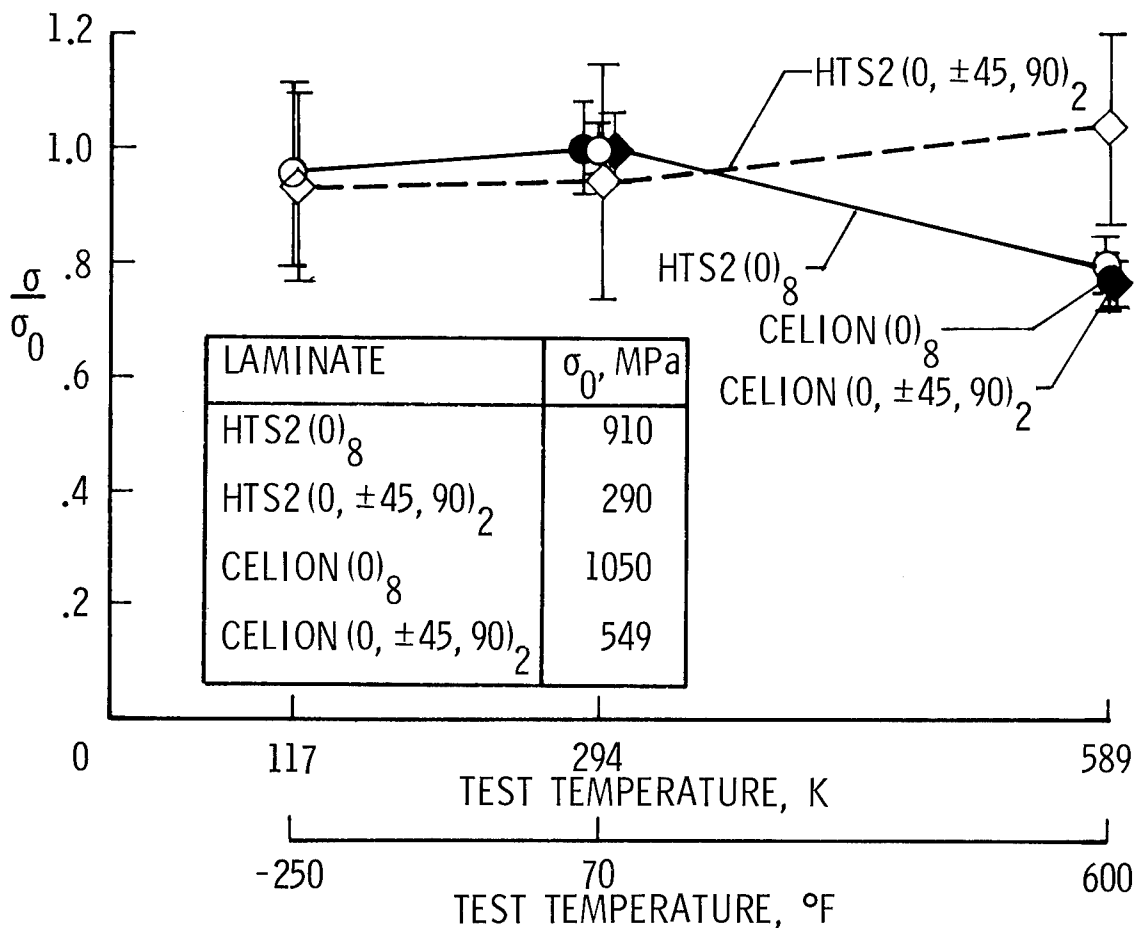


Figure 10

EFFECT OF MOISTURE ON COMPRESSIVE STRENGTH OF GR/PMR15

Results of tests on laminates fabricated with Celion 6000 and HTS2 fibers and PMR15 matrix are shown for both unidirectional and quasi-isotropic orientations after moisture conditioning. The HTS2 fiber laminates were conditioned to a moisture level of at least 90% saturation, and the Celion fiber laminates were conditioned to at least 70% saturation. There was no effect of moisture conditioning on the room temperature compressive strength observed for any of the laminates investigated. Compressive strength values obtained on specimens tested at 117 K (-250°F) showed minor differences compared to as-processed room temperature values. However, specimens tested at 589 K (600°F) showed severe strength reductions as a result of the moisture conditioning for both of the Celion laminate orientations and for the HTS2 unidirectional laminate. There was a moderate reduction in the HTS2 quasi-isotropic laminate compared to as-processed room temperature values. Those as-processed values however, were considered abnormally low, and the absolute compressive strengths for the HTS2 quasi-isotropic specimens were comparable to those observed for the Celion specimens of the same orientation. Strength values for the Celion and HTS2 unidirectional specimens were only 20% of the as-processed room temperature values, and only one-third of the value obtained on tests at 589 K (600°F). The effect of moisture conditioning appeared considerably more severe on the compressive strength property than on the interlaminar shear strength of specimens conditioned in the same manner.

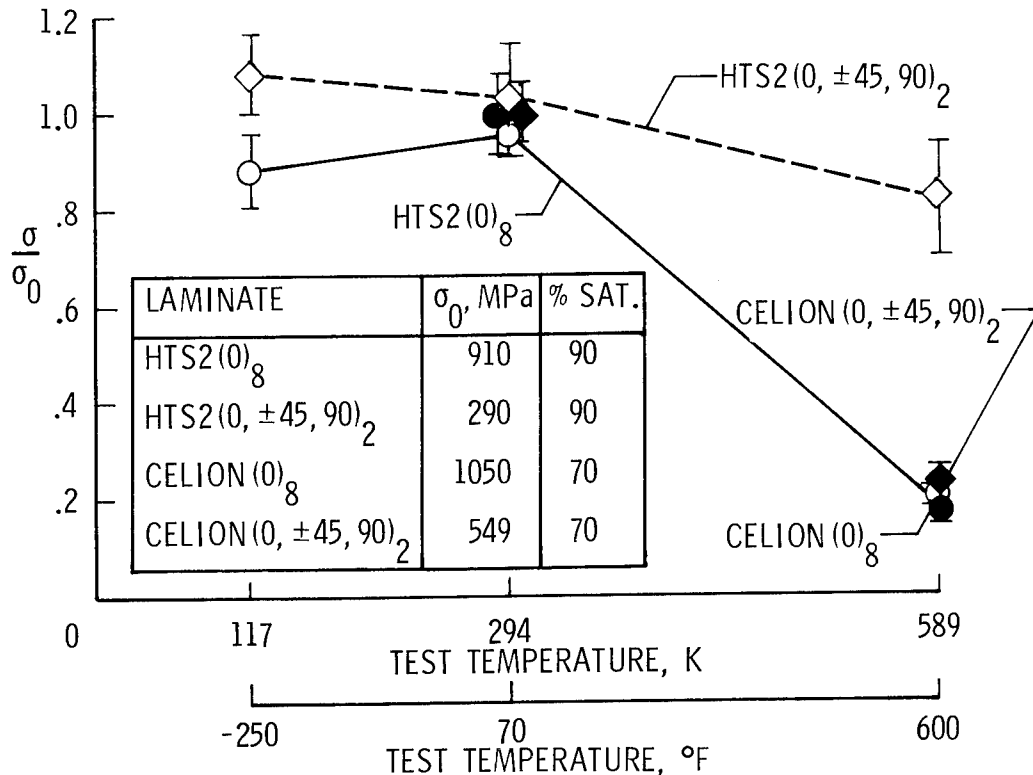


Figure 11

EFFECT OF MOISTURE ON THE GLASS TRANSITION TEMPERATURE OF GR/PMR15 COMPOSITES

The glass transition temperature was measured for laminates of both HTS2 and Celion fibers and for both unidirectional and quasi-isotropic laminate orientations. Measurements were made after processing, and after various treatments following processing of the laminate panels. The glass transition temperature of the HTS2/PMR15 unidirectional material was found to be approximately 540 K (513°F), considerably lower than should be expected for normal processing. This likely could account for the low interlaminar shear strength observed for this material. The other orientations exhibited glass transition temperatures around 589 K (600°F), and a four hour postcure at 602 K (625°F) had little effect on the measured glass transition temperature.

Moisture conditioning to saturation levels greater than 70% reduced the measured glass transition temperature on the order of 55 K (100°F), and more importantly, to values considerably below the maximum test temperature of 589 K (600°F). It was at this temperature that essentially all of the degradation resulting from moisture conditioning was observed. The degradation was considered caused by softening of the matrix material as a result of the lower glass transition temperature. This might be expected to affect the compressive strength property more severely by allowing microbuckling more readily.

T_G , K (°F)

MOISTURE CONDITION LAMINATE	AS PROCESSED	POST CURED	70% SATURATED	90% SATURATED
HTS2/PMR 15 (0) ₈	540 (513)	---	---	538 (509)
HTS2/PMR 15 (0, ±45, 90) ₂	599 (619)	---	---	528 (491)
CELION/PMR 15 (0) ₈	593 (608)	620 (657)	569 (565)	---
CELION/PMR 15 (0, ±45, 90) ₂	596 (613)	579 (583)	513 (464)	---

Figure 12

EFFECT OF EXPOSURE TO SHUTTLE ORBITER FLUIDS ON GR/PI FLEXURE PROPERTIES

The effects of short time exposure of GR/PI materials to shuttle orbiter service fluids were investigated by Rockwell International under contract to Johnson Space Center. These tests were meant to simulate the type of exposure which would be expected from an undetected, inadvertent spill. The tests included a ten minute total immersion in hydraulic fluid, nitrogen tetroxide, monomethyl hydrazine, or unsymmetrical dimethyl hydrazine at ambient temperature.

After immersion in one of the test liquids, specimens were tested in flexure and compared to baseline values obtained for unexposed specimens. The results indicated no significant change in the flexure property for either Celion/PMR15 or Celion/LARC 160 unidirectional material as a result of the short time immersion at ambient temperature.

Specimens were also exposed to hot vapors of hydrazine for one hour duration. Exposure to this severe chemical environment rendered the specimens too damaged to test mechanically.

10 MINUTE TOTAL IMMERSION

	CELION/PMR 15 (0) ₁₃		CELION/LARC 160 (0) ₁₃	
	FLEXURE STRENGTH, MPa (ksi)	FLEXURE MODULUS, GPa (ksi)	FLEXURE STRENGTH, MPa (ksi)	FLEXURE MODULUS, GPa (ksi)
BASELINE VALUES	1450 (210)	112 (1.63 x 10 ⁴)	1690 (245)	130 (1.89 x 10 ⁴)
HYDRAULIC FLUID	NO EFFECT		NO EFFECT	10% DECREASE
N ₂ H ₄ LIQUID	20% INCREASE	10% INCREASE	SLIGHT INCREASE	10% INCREASE
MMH LIQUID	SLIGHT INCREASE	7% INCREASE	SLIGHT INCREASE	10% INCREASE
N ₂ O ₄ LIQUID	SLIGHT INCREASE	SLIGHT INCREASE	SLIGHT INCREASE	10% INCREASE

Figure 13

CONCLUDING REMARKS

The general conclusions resulting from the on-going study to date are shown. Moisture conditioning produced moderate to severe reduction in compressive and interlaminar shear properties at 589 K (600°F). No reduction was observed in tests at room temperature or at 117 K (-250°F). The compressive property appeared to be affected more than the interlaminar shear property. Vacuum drying, on the other hand, appeared to improve both properties at elevated temperatures and might be considered for final processing if it can be shown that increases would not be lost by environmental degradation in service.

The degradation by moisture conditioning appears to be associated with the lowering of the glass transition temperature, and this can occur after only a few weeks exposure to condensing humidity conditions at 355 K (180°F).

Short time exposure to shuttle orbiter service liquids at ambient temperature had negligible effect on flexure properties of unidirectional material. However, exposure to hot vapors of hydrazine produced such severe damage that specimens could not be mechanically tested.

- MOISTURE CONDITIONING OF Gr/PMR 15 COMPOSITES PRODUCED MODERATE TO SEVERE REDUCTION IN COMPRESSIVE AND INTERLAMINAR SHEAR PROPERTIES AT 589K (600°F)
- THE DEGRADATION APPEARS TO BE ASSOCIATED WITH THE LOWERING OF THE GLASS TRANSITION TEMPERATURE OF THE MATRIX
- VACUUM DRYING OF AS PROCESSED SPECIMENS GENERALLY INCREASED THE ELEVATED TEMPERATURE COMPRESSIVE AND INTERLAMINAR SHEAR STRENGTHS
- SHORT TIME EXPOSURE TO SHUTTLE ORBITER FLUIDS HAD NEGLIGIBLE EFFECT ON FLEXURE PROPERTIES OF UNIDIRECTIONAL COMPOSITE

Figure 14

MECHANICAL AND THERMOPHYSICAL PROPERTIES OF
GRAPHITE/POLYIMIDE COMPOSITE MATERIALS

Donald R. Rummler and Ronald K. Clark
NASA Langley Research Center

EXPANDED ABSTRACT

An on-going program to characterize advanced composites for up to 50,000 hours of exposure to simulated supersonic cruise environments is summarized. Results are presented for up to 25,000 hours of thermal exposure and 10,000 hours of flight simulation at temperatures up to 560 K (550°F) with emphasis on HTS/710 graphite/polyimide composite material. Results to date indicate that the maximum use temperature for HTS/710 may be reduced to 505 K (450°F) for long-time (>1000 hours) application such as the supersonic transport.

Preliminary thermophysical properties data for HTS/PMR15 graphite/polyimide have been generated. These data include thermal conductivity, thermal expansion, and specific heat from 115 K (-252°F) to 590 K (600°F) and emittance at room temperature and 590 K (600°F). The purpose in generating these data was to validate use of state-of-the-art property measurement methods for advanced graphite fiber reinforced resin matrix composites. Based on results to this point, thermal expansion measurements for composites are most difficult to perform. A high degree of caution in conducting thermal expansion tests and analyzing results is required to produce reliable data.

TIME-TEMPERATURE-STRESS CAPABILITIES OF COMPOSITE MATERIALS

The goal of this program is to characterize advanced composite systems before and after exposures to a simulated supersonic cruise environment for real times up to 50,000 hours (ref. 1). Figure 1 outlines the content of the program which began in 1973 and is scheduled for completion in 1984. A single fiber/matrix was chosen for each of the materials classes shown. They were: B/Ep (B/5505), Gr/Ep (AS/3501), B/Al (B/6061), Gr/Pi (HTS/710), and B/Pi (B/P105A). Changes in baseline tensile, notched tensile, compression, shear, fatigue, and fracture properties that occur with exposure times up to 50,000 hours are being measured for ambient and continuous thermal aging conditions as well as random cyclic loading with cyclic temperature variations. These latter tests are intended to simulate the conditions experienced during supersonic flight.

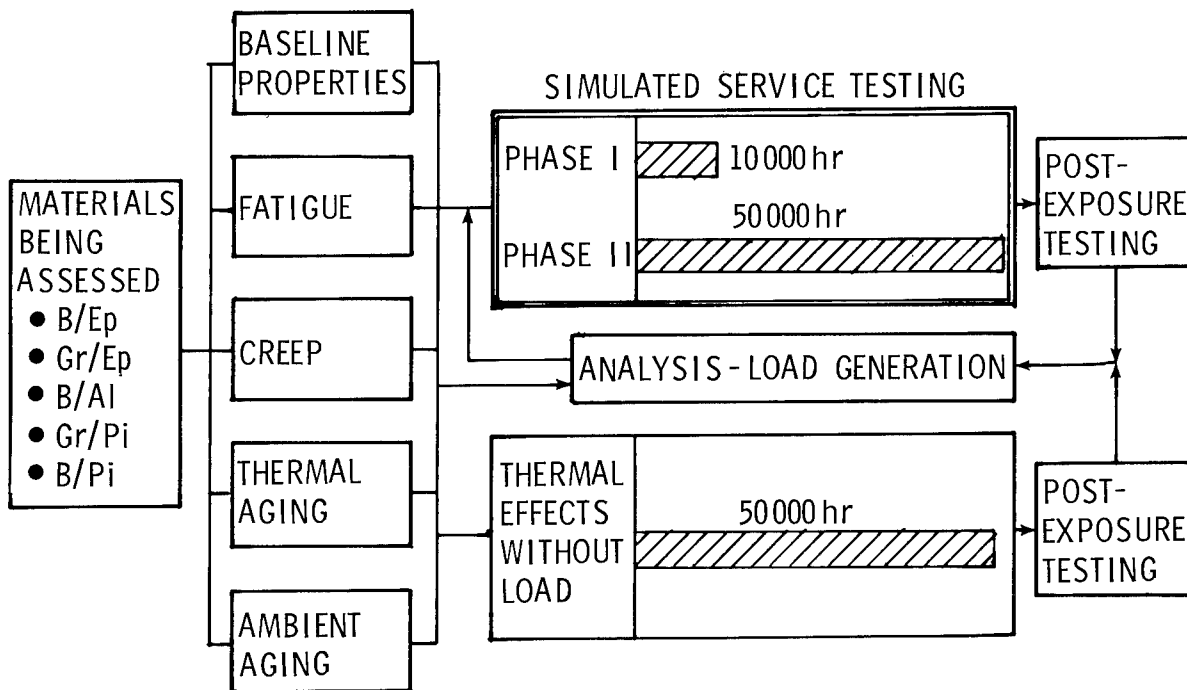


Figure 1

LOADING AND HEATING SIMULATORS FOR SUPERSONIC FLIGHT

The flight simulation equipment is shown in figure 2. There are 10 load frames, five of which are facing forward, and five more directly behind the front five (ref. 2). Each frame loads ten exposure specimens by a whiffle-tree arrangement using a single servo-controlled hydraulic cylinder and load cell. The flight simulation apparatus contains quartz heat lamps positioned so that the 50 mm (2 in.) center portion of each residual-property specimen is heated as required during flight simulation.

The exposure specimens, which are pin loaded to insure uniform loading, consist of 76 mm (3 in.) wide and 559 mm (22 in.) long blanks of composite material with 50 mm (2 in.) long titanium doublers bonded to each end. Half of the exposure specimens are for center-notched specimens and have 6.4 mm (0.25 in.) holes machined in the gage length such that at the conclusion of the flight simulation, each exposure specimen may be machined into six, 25 mm (1 in.) by 229 mm (9 in.), residual-property center-notched specimens. The remainder of the exposure specimens are unnotched and at the conclusion of the flight simulation each is machined into twelve, 13 mm (0.5 in.) by 229 mm (9 in.), residual-property specimens. Thus when all ten load frames are full, there are 100 exposure specimens undergoing flight simulation. These exposure specimens yield a total of 300 center-notched and 600 unnotched residual-property specimens.

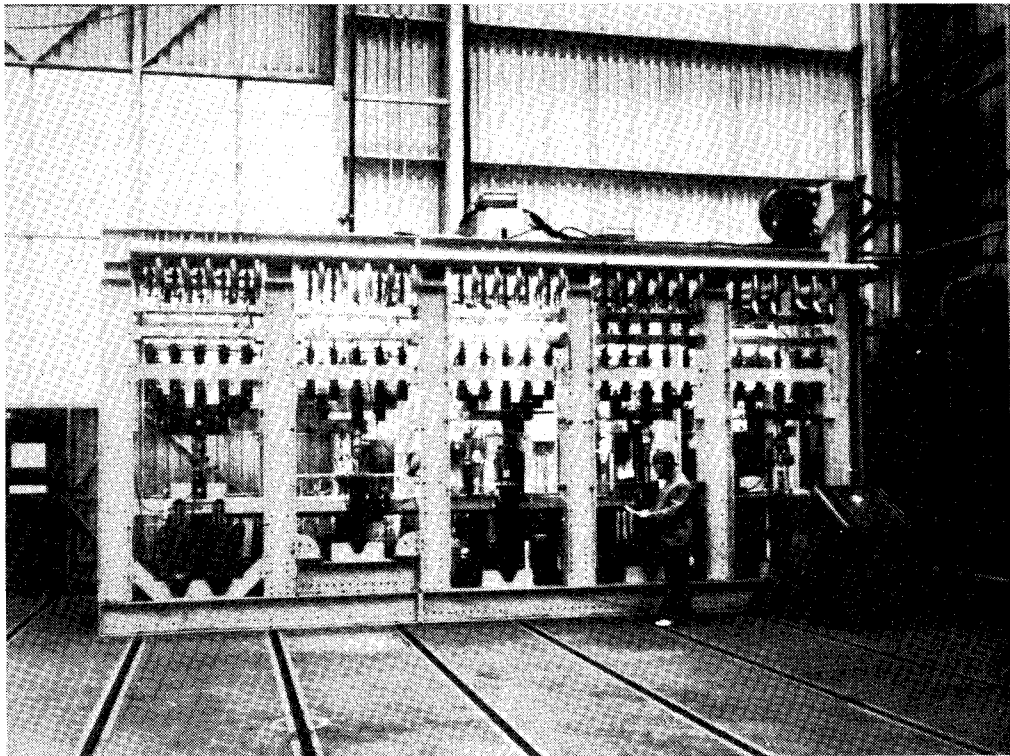


Figure 2

FLIGHT SIMULATION MISSION PROFILE

In this simulation, the life of a supersonic airplane is assumed to consist of 25,000 flights of 2 hours duration. Each flight consists of a 10-minute climb, a 90-minute cruise, a 20-minute descent, and a single landing.

The upper portion of figure 3 shows the temperature profile used for each of the 2-hour simulated flights. The temperature shown is for the Gr/Pi tests. The lower portion of figure 3 shows a typical load history produced by a random load program. The 1-g stress used for the Gr/Pi specimens is noted. The random load program insures that no two flights during the simulation testing will be the same as far as loads are concerned. The figure shows the relative frequency of the loads during climb, cruise, and descent. Note that the load during cruise is constant except for nine gust loads during a 2-minute period. The landing or compression load is applied at the beginning of the simulated flight for convenience in testing.

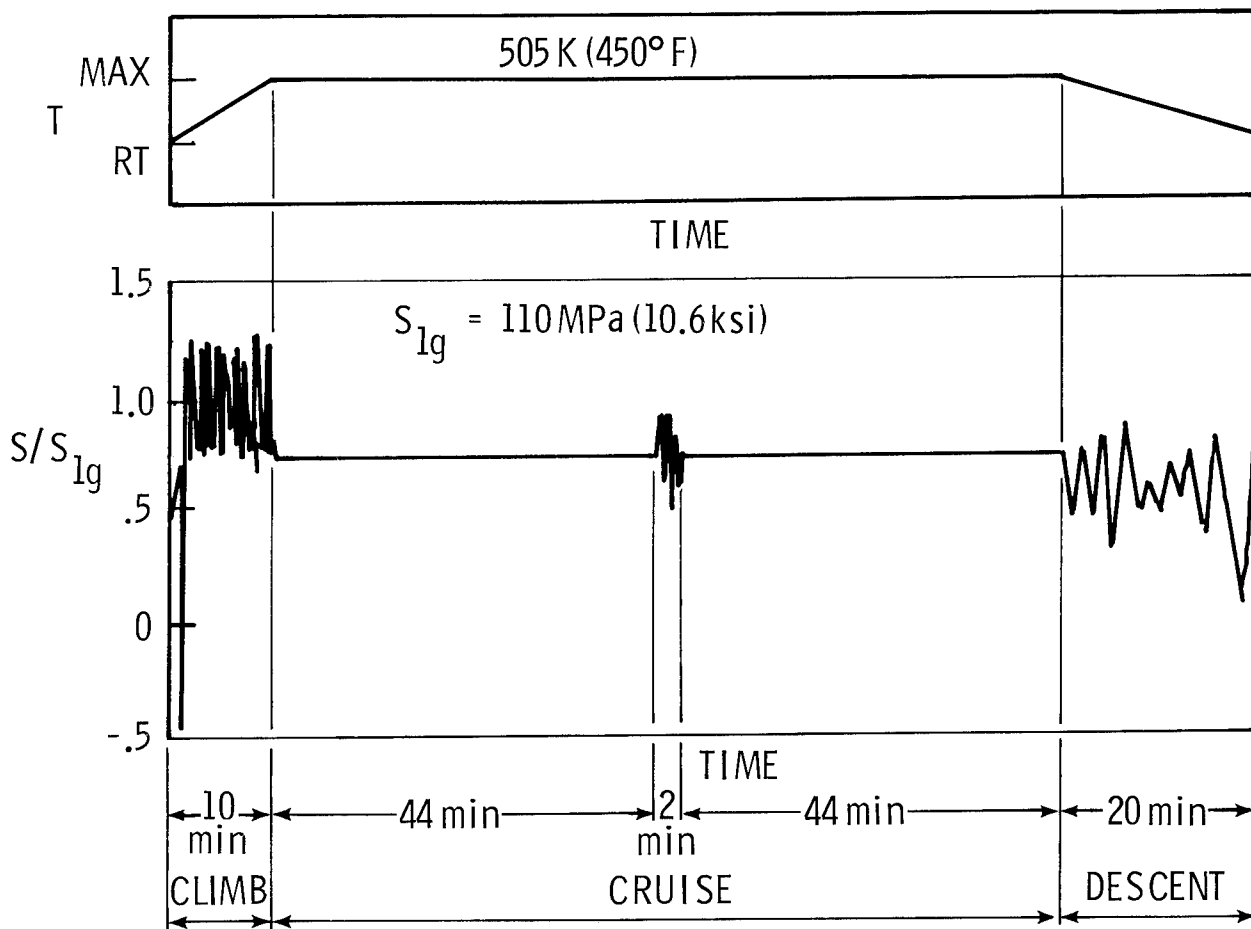


Figure 3

RESIDUAL PROPERTIES AFTER 10,000 HOURS FLIGHT SIMULATION TESTING

The results of room temperature residual strength tests of HTS/710 Gr/Pi specimens after 10,000 hours of flight simulation are summarized in figure 4. The specimens are six-ply (0/+45). All properties were reduced from their baseline values as a result of the 10,000-hour exposure. Unnotched specimens were more severely affected than were notched specimens. Although matrix degradation is suggested by the severe reduction in interlaminar shear strength, no completely satisfactory explanation has been developed to explain why properties of unnotched specimens are more severely degraded than properties of notched specimens. Similar differences in properties of notched and unnotched specimens of AS/3501 Gr/Ep composite material were also observed after 10,000 hours of flight simulation.

HTS/SKYBOND 710 [0 ± 45]₂

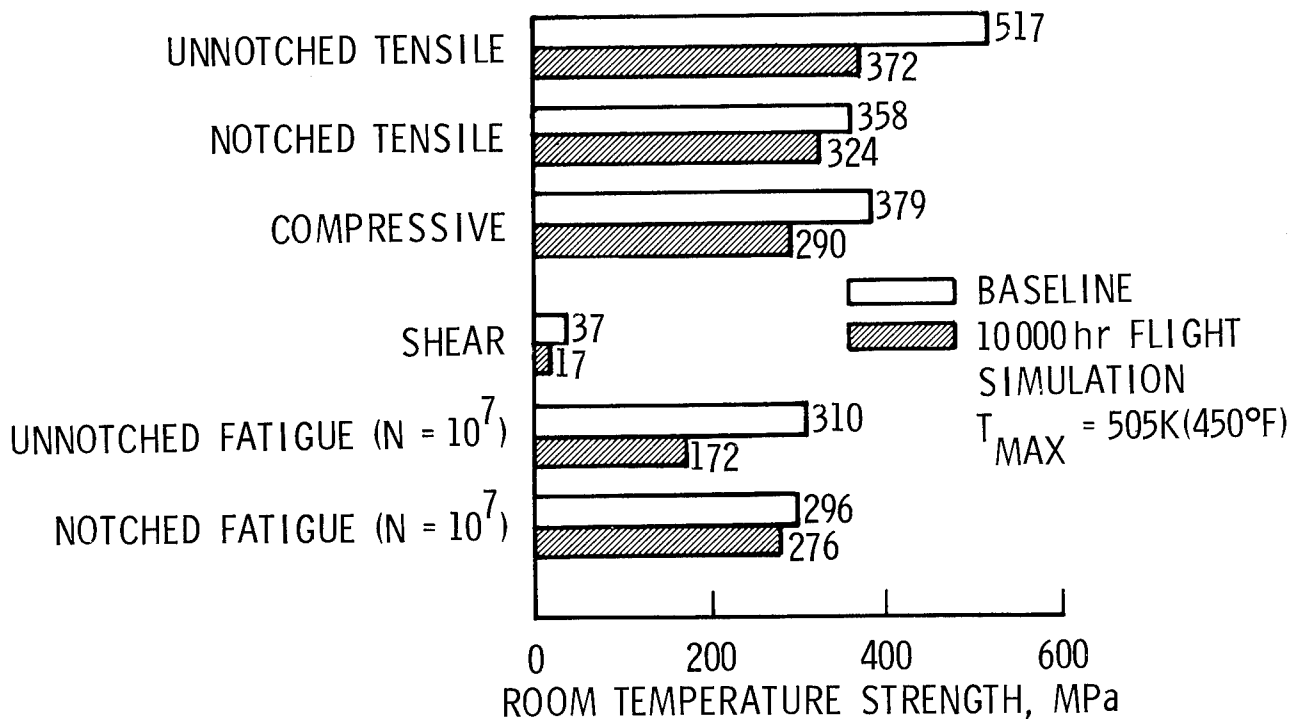


Figure 4

TENSILE STRENGTH OF HTS/710 AT TEMPERATURE (AFTER THERMAL AGING AT SAME TEMPERATURE)

Figure 5 shows the effect of thermally aging HTS/710 Gr/Pi for up to 25,000 hours in air at atmospheric pressure on the tensile strength at temperature. These specimens were aged at constant temperature with no applied load in circulating air ovens and were tested in tension at the aging temperature. Data are shown for 6-ply unidirectional and $[0/\pm 45]_S$ laminates. The data show no significant reduction in tensile properties for either lay-up at 505 K (450°F). This is in contrast to tests on $[0/\pm 45]_S$ specimens exposed to 10,000 hours of flight simulation (cyclic exposure to temperature and load) with a 505 K (450°F) maximum exposure temperature which suffered a 33 percent reduction in tensile strength.

After 10,000 hours of thermal aging at 560 K (550°F), the tensile strength of the unidirectional specimens began to decrease and after 10,000 hours exposure, the tensile strength of both types of specimens was severely degraded. Tensile properties of unidirectional specimens aged in low pressure air $[0.014 \text{ MN/m}^2 \text{ (2 psi)}]$ for 10,000 hours at 560 K (550°F) were reduced approximately the same amount (20%) as those tested in air at ambient pressure. Similar reductions in residual strength have been observed in epoxy matrix composites after aging at 450 K (350°F) and atmospheric pressure.

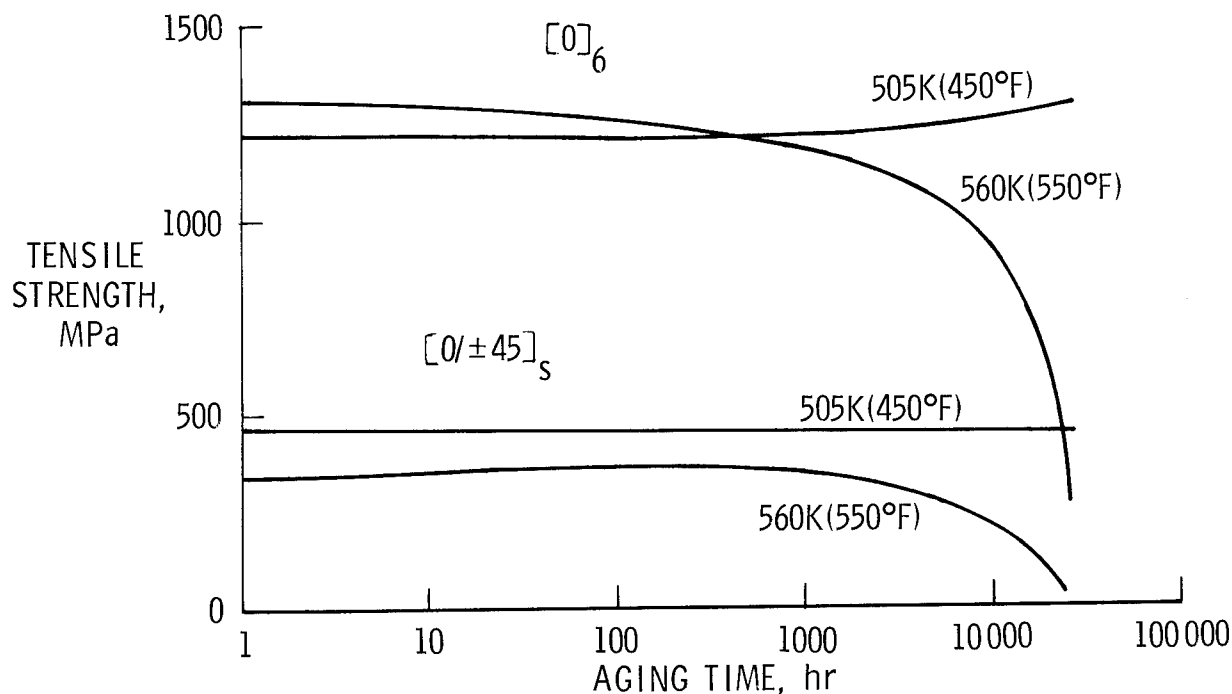


Figure 5

EFFECT OF THERMAL AGING

The Scanning Electron Microscope (SEM) photomicrographs of sectioned specimens (fig. 6) show the effects of thermal aging for both Gr/Ep (AS/3501) and Gr/Pi (HTS/710) composite materials. The photomicrograph of the as-received Gr/Ep specimen shows few voids as contrasted with photomicrograph of the 10,000-hour, 450 K (350°F) specimen which shows extensive loss of matrix material by oxidation. The effects of aging Gr/Pi at 560 K (550°F) are less obvious from viewing the photomicrographs. There is some evidence of initial porosity in the as-received material. The amount of porosity in the aged material is greater than in the as-received material. In addition, the photomicrographs indicate an increase in the amount of fibers which are not attached to the matrix material.

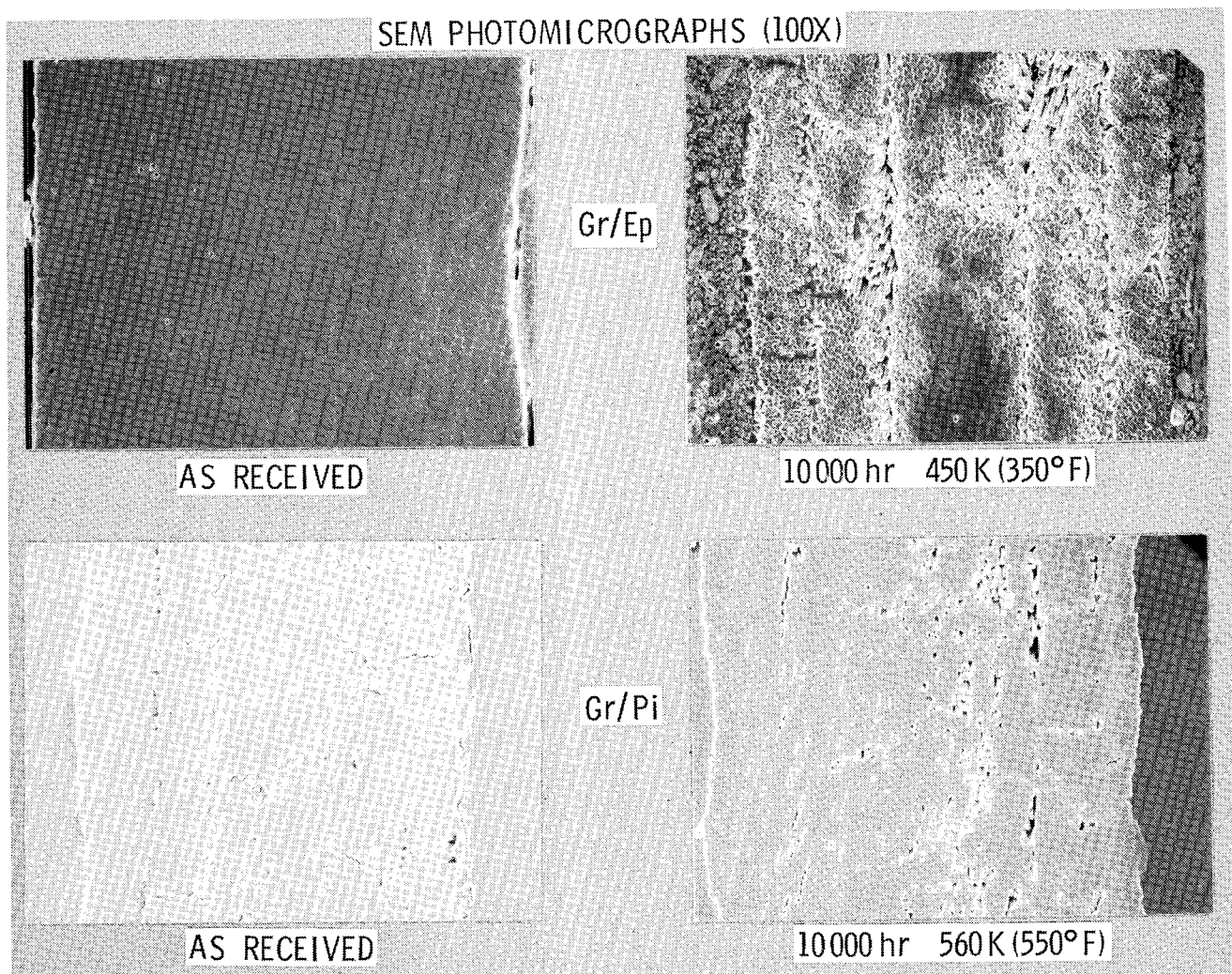


Figure 6

TIME-TEMPERATURE-STRESS CAPABILITIES OF COMPOSITES

The results of the long-time exposure program at the 10,000-hour point for all of the composite materials systems being evaluated are summarized in figure 7. For the resin matrix composites the maximum test temperature shown was the maximum temperature considered for long-time application when the program began. For the B/Al system 505K (450°F) was considered a reasonable maximum operating temperature for long-time application.

For all of the materials systems there has been a reduction in the estimated maximum temperature for a 10,000-hour design life (ref. 3). Matrix oxidation has been identified as a primary degradation mechanism in the resin systems. In contrast, reductions in the maximum use temperature for B/Al for long-time applications are attributed to both fiber degradation and matrix oxidation.

This summary of results clearly points out that the maximum use temperature of composite materials for long-time (>1000 hours) applications is significantly lower than for short-time uses. The maximum use temperature appears lower for those applications which require cyclic exposures to load and temperature.

10000 hr RESULTS

MATERIAL	MAXIMUM TEMPERATURE TESTED	MAXIMUM TEMPERATURE FOR 10000 hr DESIGN LIFE	REMARKS
Gr/Ep (A-S/3501)	450 K (350°F)	394 K (250°F)	MATRIX DEGRADATION
B/Ep (B/5505)	450 K (350°F)	394 K (250°F)	MATRIX DEGRADATION
B/Al (B/6061)	728 K (850°F)	450 K (350°F)	FIBER DEGRADATION MATRIX OXIDATION
Gr/Pi (HT-S/710)	561 K (550°F)	505 K (450°F)	MATRIX DEGRADATION
B/Pi (B/P105A)	561 K (550°F)	DROPPED FROM PROGRAM	SEVERE MATRIX DEGRADATION

Figure 7

COMPARISON OF THERMOPHYSICAL PROPERTIES OF GR/PI-GR/EP-TITANIUM

Figure 8 shows a comparison of room temperature properties for Gr/Pi, Gr/Ep, and titanium. Data are shown for thermal conductivity, thermal expansion, specific heat, and emittance. A comparative cut-strip method (ref. 4) was used to determine conductivity in the fiber direction and a guarded hot-plate (ref. 5) was used to determine conductivity in the cross-fiber direction. Thermal expansion was determined using a modified Leitz Dilatometer (ref. 4) and specific heat was measured using a differential scanning calorimeter. Emittance was determined using a spectral reflectometer (ref. 6). The GY70 fibers in the Gr/Ep material are high modulus fibers which have significantly higher thermal-conduction and lower thermal-expansion characteristics than the HTS fibers in the Gr/Pi material. These differences in fiber properties result in pronounced differences in thermal-conductivity and thermal-expansion characteristics of the respective composite materials. The specific heats and emittances of HTS/PMR15 and GY70/X30 are about the same. The thermal conductivity of titanium is near that for HTS/PMR15 and the specific heat of titanium is about half that for the composite materials. The thermal expansion of titanium is nearly one order higher than that for quasi-isotropic HTS/PMR15. The emittance of oxidized titanium (ref. 7) is about 0.6 compared with 0.85 for both composite materials. The emittance of titanium varies widely with mechanical finish and oxidation history.

ROOM TEMPERATURE

PROPERTY	HTS/PMR15 [0, ±45, 90] _s	GY70/X30 [0, ±45, 90] _s	Ti - 6Al - 4V
THERMAL CONDUCTIVITY (k_x), W/m-K	10	55	7
THERMAL EXPANSION COEF. (α_x), $\mu\text{m/m-K}$	1	-0.04	8.8
SPECIFIC HEAT (C_p), J/kg-K	800	880	420
EMITTANCE (ϵ)	0.84	0.86	0.60*

* OXIDIZED, VARIES WITH MECHANICAL FINISH AND OXIDATION HISTORY

Figure 8

EFFECT OF TEMPERATURE ON THERMOPHYSICAL PROPERTIES OF HTS/PMR15

Figure 9 presents tabular thermophysical properties data as a function of temperature for unidirectional and quasi-isotropic laminates of HTS/PMR15. Thermal conductivity, dimensional change with temperature (the slope of $\Delta L/L$ vs temperature is the thermal expansion coefficient), specific heat, and emittance data are included. Thermal conductivity and thermal expansion measurements were made for in-plane and through-the-thickness directions of both laminates. Specifically measurements were made in the fiber direction (x-direction) and across the fiber direction (y-direction) for the unidirectional laminate and in the x-direction and in the thickness direction (z-direction) for the quasi-isotropic laminate. The trends in the data are predictable in that the directional properties show the influence of the graphite fibers and the thermal conductivity and specific heat increase with temperature.

PROPERTY	TEMPERATURE, K		
	120	300	590
<u>THERMAL CONDUCTIVITY, W/m-K</u>			
UNI-DIR: k_x	8.3	22	41
k_y	0.5	0.9	1.4
QUASI-ISO: k_x	3.8	10	15
k_z	0.1	0.4	1.7
<u>THERMAL EXPANSION FROM</u>			
<u>300K, 10^{-4} m/m</u>			
UNI-DIR: $\Delta L/L_x$	0.5	0	-0.4
$\Delta L/L_y$	-36	0	79
QUASI-ISO: $\Delta L/L_x$	-1.6	0	2.7
$\Delta L/L_z$	-40	0	100
<u>SPECIFIC HEAT, J/kg-K</u>			
C_p	290	800	1360
<u>EMITTANCE</u>			
ϵ	-	0.84	0.86

x DIRECTION PARALLEL TO
0° FIBERS
y DIRECTION PERPENDICULAR
TO 0° FIBERS
z THROUGH THICKNESS

Figure 9

VARIATION IN THERMOPHYSICAL PROPERTIES WITH TEMPERATURE

Figure 10 is a graphical presentation of thermal conductivity and thermal expansion data for HTS/PMR15 and Ti-6Al-4V (ref. 7). The high-conductivity influence of the fibers is exhibited by the higher values for conductivity in the fiber direction compared to the cross-fiber direction. Also the low-expansion influence of the fibers is exhibited by the lower values for thermal expansion in the fiber direction compared to expansion across the fibers.

Thermal expansion is much more difficult to characterize for fiber reinforced composites than for conventional materials. The difficulty arises in part from the inhomogeneity of composites and, in some cases, variations in the quality of the composite material caused by factors such as cure gradients, resin gradients, fiber wetting, and minor variations in ply orientation which produce an imbalance in the laminate. Additionally, thermal expansion of composites is affected by presence of moisture in the material and rate sensitive processes like microcracking which may also occur. Dimensional changes for a 50 mm gage length (2 in.) can be as low as ten microns from room temperature to 590 K (600°F). The combined factors dictate that caution be exercised in collecting and analyzing thermal expansion data for composites.

HTS/PMR15 AND Ti-6Al-4V

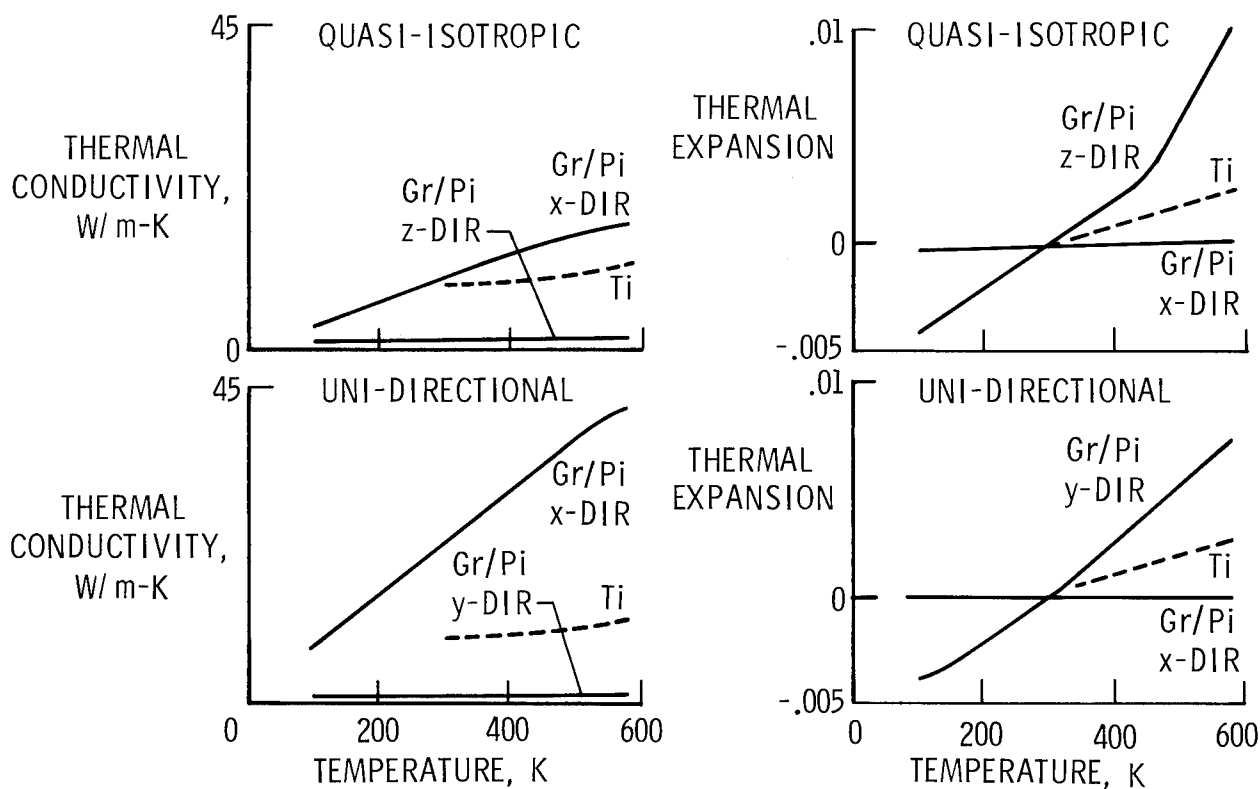


Figure 10

CONCLUDING REMARKS

The results of the long-time exposure program to date indicate that maximum service temperature of a composite material system for long-time applications such as the supersonic transport may be significantly reduced from the levels permitted for short-time use. In addition, there is some evidence that composite materials (including HTS/710 Gr/Pi) subjected to a real-time simulation of mission profiles with cyclic application of stress and temperature will experience mechanical property degradation in excess of that which would be observed if the materials were subjected to constant temperature aging for the same length of time.

Thermophysical properties data obtained to date indicate that reliable thermal conductivity, specific heat, and emittance measurements can be performed using existing property measurement methods. Thermal expansion measurements are much more difficult to perform because of the high sensitivities of that parameter to material properties, test techniques, and analysis of results. However, adequate data may be obtained with current methods by exercising extreme caution in preparing specimens, conducting tests, and analyzing results.

- MATRIX DEGRADATION MAY SIGNIFICANTLY REDUCE MAXIMUM USE TEMPERATURE FOR LONG-TIME APPLICATIONS.
- EXISTING METHODS ARE ADEQUATE TO DETERMINE THERMAL CONDUCTIVITY, SPECIFIC HEAT, AND EMITTANCE OF Gr/Pi.

THERMAL EXPANSION MEASUREMENTS REQUIRE PARTICULAR ATTENTION.

Figure 11

REFERENCES

1. Kerr, J. R.; Haskins, J. F.; and Stein, B. A.: Program Definition and Preliminary Results of a Long-Term Evaluation Program of Advanced Composites for Supersonic Cruise Aircraft Application. ASTM Special Technical Publication 602, 1976.
2. Haskins, J. F.; Wilkins, D. J.; and Stein, B. A.: Flight Simulation Testing Equipment for Composite Materials Systems. IBID.
3. Haskins, J. F.; Kerr, J. R.; and Stein, B. A.: Flight Simulation Testing of Advanced Composites for Supersonic Cruise Aircraft Applications. AIAA Paper 77-401, American Institute of Aeronautics and Astronautics, 1977.
4. Advanced Composites Design Data for Spacecraft Structural Applications. Second Quarterly Progress Report, Contract F33615-77C-5279 GDC, Report No. CASD-AFS-78-006, Oct. 1978.
5. Haskins, J. F.: A Flat-Plate Thermal Conductivity Apparatus for Measuring Low Conductivity Materials at Cryogenic Temperature. ASTM STP 411, 1967.
6. Use of Polished Fused Silica to Standardize Directional Emittance and Reflectance Measurements in the Infrared. SAMSO TR-74-202, Aug. 1974.
7. Aerospace Structural Metals Handbook, Vol. II. AFML-TR-68-115, 1969.

C. L. Blackburn
University of Tennessee at Nashville
and
J. C. Robinson
NASA Langley Research Center

EXPANDED ABSTRACT

An in-house preliminary design study of the shuttle orbiter body flap is being conducted to define loads and temperatures and to assess various structural concepts. The design study required laminated-structure analysis capability. An appraisal of the available structural analysis programs, NASTRAN (Ref. 1) and SPAR (Ref. 2), indicates that neither had all the capabilities required. The thermal analysis program, MITAS (Ref. 3), would solve the problem once a model was generated but model generation and verification was laborious and transfer of temperatures to the structural program usually required interpolation. Therefore it was decided to incorporate both capabilities in the SPAR finite element program.

Preliminary results obtained using the analysis capabilities and a description of the efforts to date on the preliminary design study are presented.

ANALYSIS METHODS FOR IN-HOUSE STUDY

SPAR was selected as the program to be modified to meet the analysis needs of the study based on in-house experience. The code is modular, which makes modification and addition of new capability relatively easy. It is efficient in the use of central processor time, memory space, and secondary storage. Perhaps the most important feature from the standpoint of an in-house study is that the program can be used in an interactive mode. This permits an analyst to run a problem directly from an interactive computer terminal. This is most desirable in the model generation and check-out process where actual computation is relatively small but manual effort, and, unfortunately, the number of errors is usually large. Interaction with the program during execution allows detection and correction of multiple modeling errors per run. This greatly reduces the calendar time required to generate and verify a model.

● SPAR ANALYSIS PROGRAM SELECTED

MODULAR
EFFICIENT
INTERACTIVE
EASILY MODIFIED

● ANALYSIS NEEDS

COMPOSITE ELEMENT

LAMINATED MATERIAL DESCRIPTION
THERMAL STRESS RECOVERY

WARPED QUADRILATERAL ELEMENT
THERMAL ANALYSIS

INPUT AUTOMATION
THERMAL/STRUCTURAL COMPATIBILITY

Figure 1

CONFIGURATION OF SPAR

The figure shows some of the functions performed by SPAR. Each box represents a module or processor that communicates only with the data base. The data base contains all the information required to solve the problem and supports extensive data manipulation capabilities. The two thermal processors for steady-state and transient thermal analysis were developed under the CASTS project. Incorporation of the thermal analysis capability in SPAR permits thermal model development and check-out using the structural processors for that purpose. Also, using a finite element approach for thermal analysis tends to make data transfer between the thermal and structural analyses easier. If a common finite element model can be used, data transfer is automatic.

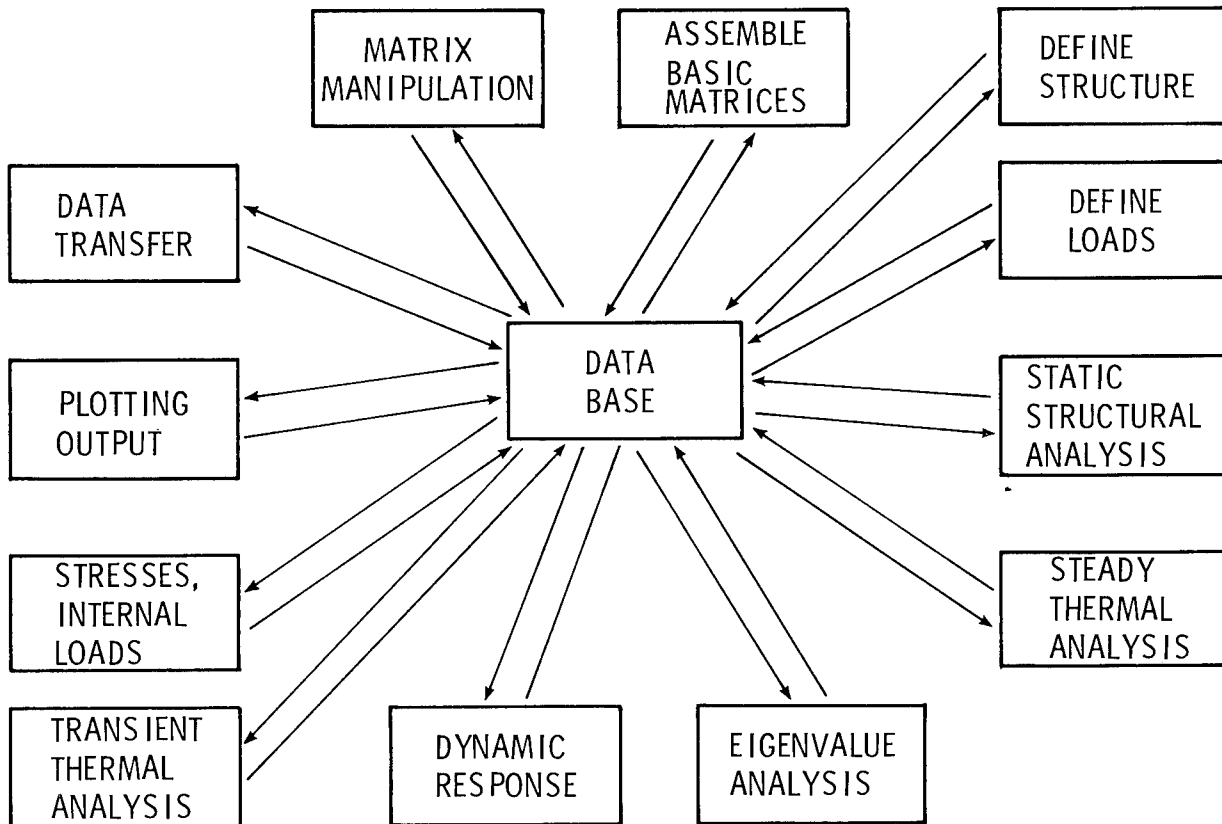


Figure 2

THERMAL ANALYSIS CAPABILITIES IN SPAR

Capability is required to determine both steady state and transient temperature distributions in structures subjected to thermal loads that vary with time. Material conduction properties vary with location, direction, temperature, and time. Six terms are required to describe variations of conductivity with direction. Individual lamina, for instance, have much larger conductivity in the fiber direction as compared to the direction across the fibers. The time dependence of properties is used to describe the change in conductivity caused by local aerodynamic pressure due to gas conductivity in the porous Reusable Surface Insulation (RSI) material, when the pressure is known as a function of time. Convection and radiation properties vary with location, temperature, and time. Time dependence is used to describe the trajectory dependent parameters. Applied heating loads and view factors are not calculated internally.

- CONDUCTION

 - ORTHOTROPIC PROPERTIES

 - TEMPERATURE AND TIME (PRESSURE) DEPENDENT

- CONVECTION

 - TEMPERATURE AND TIME DEPENDENT

- RADIATION

 - EXTERNAL VIEW FACTOR CALCULATION

- COMPATIBILITY WITH STRUCTURAL ANALYSIS

- MODEL GENERATION CAPABILITY

 - PLOTTING

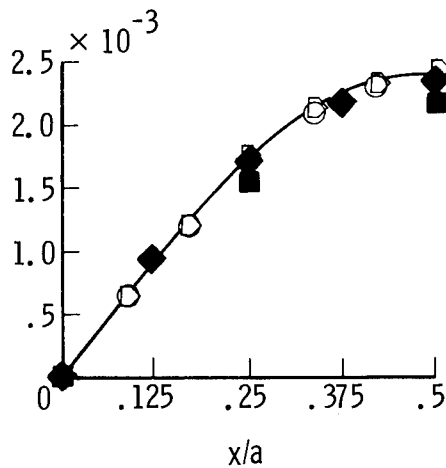
Figure 3

SIMPLY-SUPPORTED NINE-LAYERED PLATE

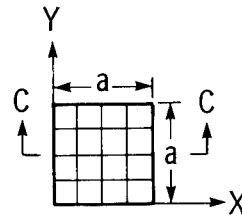
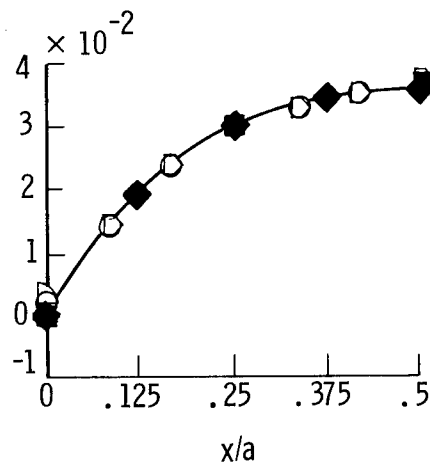
Analysis of a simply-supported nine-layered plate subjected to a normal pressure load provides an example of the SPAR laminated element property capability to determine displacements and stresses for comparison with those presented in reference 3. The laminated material capability permits description of individual layers by thickness, stiffness, orientation, and offset from structural joint locations. A description of this element and comparative studies are presented in reference 4. Reference 3 used higher-order elements with more degrees of freedom per element and transverse shear flexibility. For the case shown with the thickness to length ratio of .01, the SPAR results compare well with the reference results.

[45/ -45/ 45/ -45/ 45/ -45/ 45/ -45/ 45]

NONDIMENSIONAL
BENDING



NONDIMENSIONAL
DISPLACEMENT



$t/a = 0.01$

— CONVERGED
 ◇ SQH } 4 × 4 NOOR & MATHERS
 ○ SQ12 }
 ■ 4 × 4 } PRESENT ELEMENT
 ◆ 8 × 8 }

Figure 4

THERMAL CURING STRESSES IN Gr/Ep PANEL

Evaluation of thermal stresses in a laminated composite material requires that individual lamina thermal stresses be determined. This requires description of individual lamina orientation and thermal coefficients of expansion. The example shown, from reference 5, uses a $[0/90_{10}/0]$ lay-up subjected to a 111 K cool down from the curing temperature. The Gr/Ep material is assumed to be elastic. The maximum stresses occur in the thinner lamina. The SPAR results compare well with the results from reference 5 which are shown in parentheses.

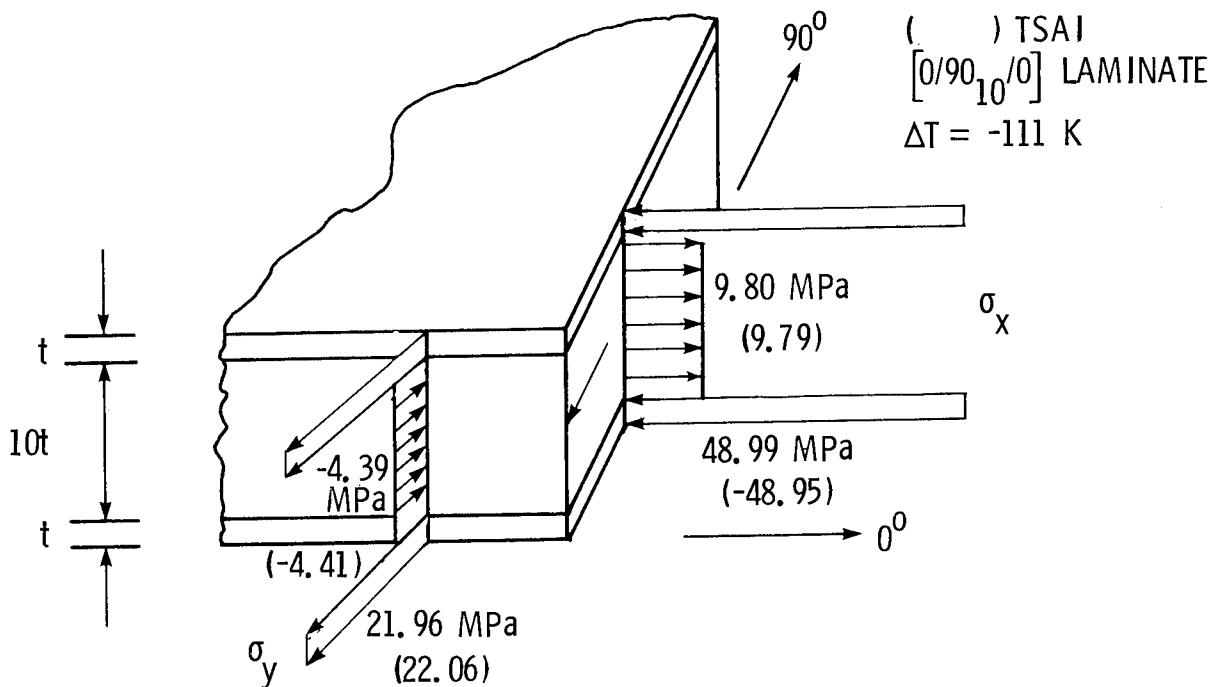


Figure 5

ALUMINUM BASELINE BODY FLAP

The overall dimensions of the aluminum baseline body flap shown in the figure are approximately 6.4m long by 2.1m wide. It is supported (connected to the shuttle fuselage) at four locations along the length. The mass breakdown in the lower right table shows that the Thermal Protection System (TPS) mass is approximately twice that of the aluminum structure. On the lower surface the TPS thickness is from 6.1 to 8.9 cm; the upper surface TPS is much thinner. The typical sandwich skin, as shown in the upper left, is constructed of thin skins (0.30 mm) and a relatively low density honeycomb core. Due to the low mass of the baseline structure, the largest mass savings will probably be in the TPS system where the higher operating temperature of the Gr/Pi allows greater heat sink capability which reduces the TPS thickness required.

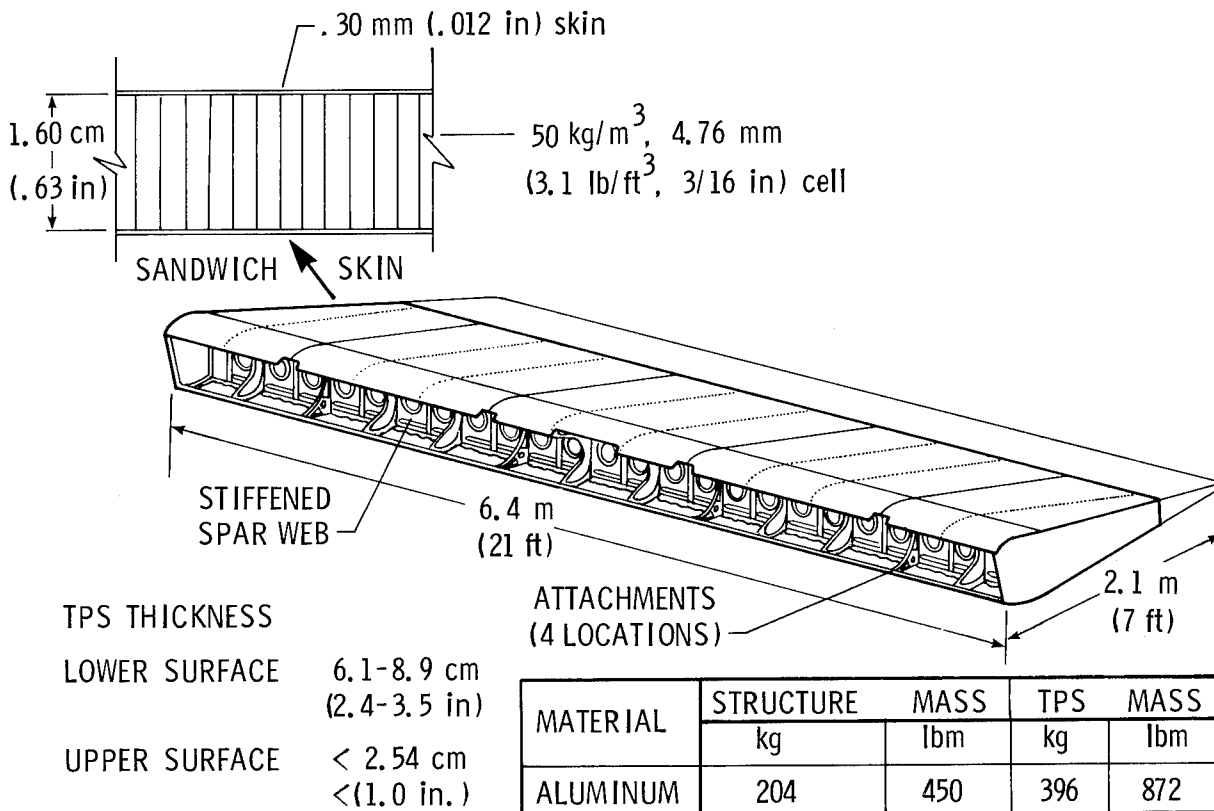


Figure 6

COARSE FINITE ELEMENT MODEL

The coarse finite element model of one-half of the body flap is shown in the figure. The applied loads shown in the lower left emphasize the importance of acoustics (165 dB overall sound pressure level) and heating (0.45 MW/m^2). The model was used to make a rough check of mechanical loads on the baseline body flap.

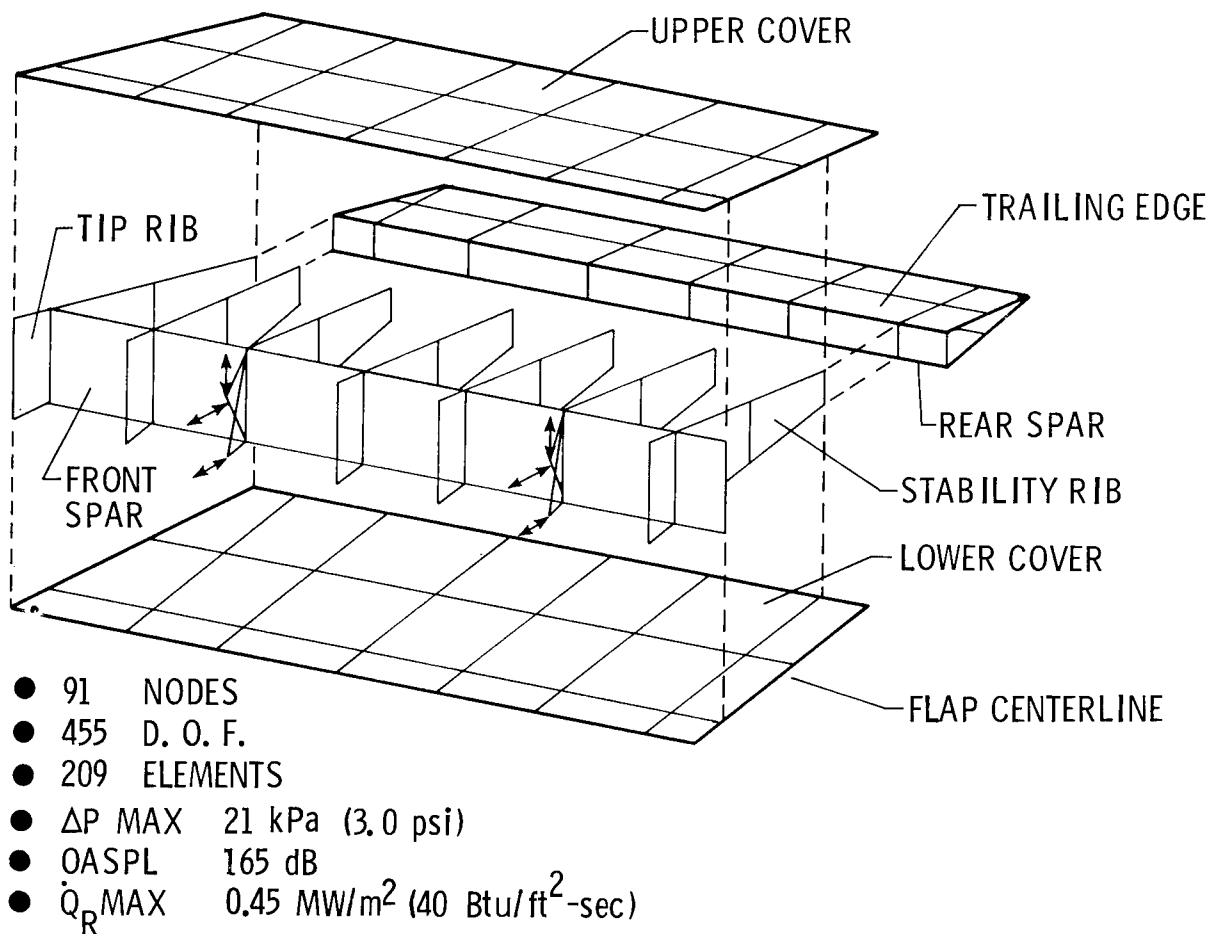
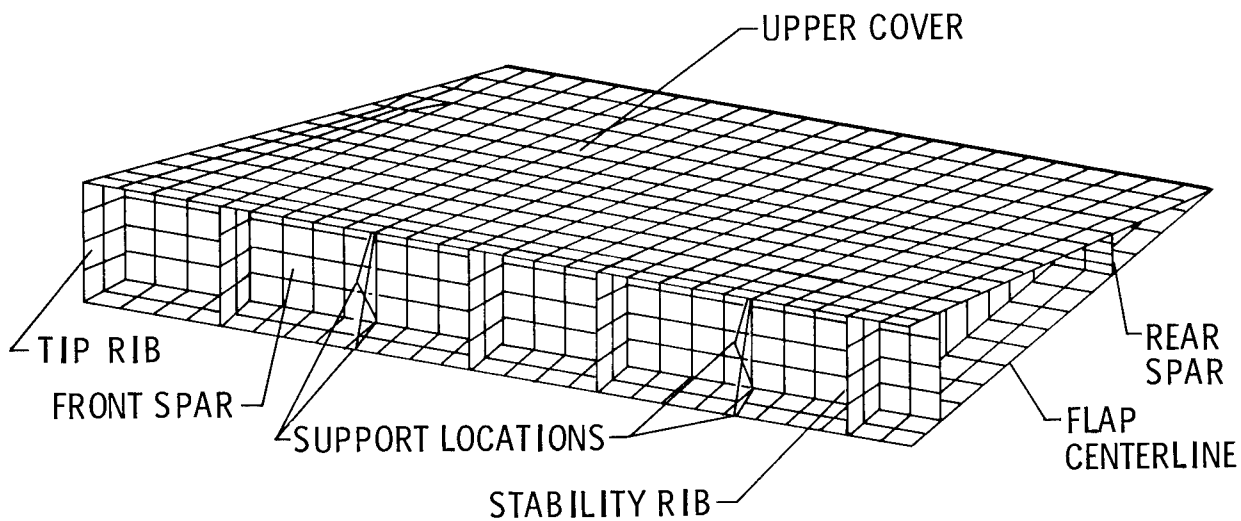


Figure 7

DETAILED FINITE ELEMENT MODEL

The detailed finite element model of half of the body flap has 5800 degrees of freedom. The model is used to study the interaction between cover panel bending and inplane stresses. Displacements calculated with this model will be used as boundary conditions on a local model of the front of the actuator rib (labeled support location in figure). Examination of results to date indicates that there are generally low internal loads in the structure. Considering the requirements of the reusable surface insulation for uniform support and the high sound pressure levels shown on the previous figure, sandwich construction appears to be the best concept for the body flap.



- 1120 NODES
- 5800 D. O. F.
- 1580 ELEMENTS

Figure 8

INTRA-CELL BUCKLING OF Gr/Pi SANDWICH SKIN

Early in the CASTS project Gr/Pi honeycomb core material of 10mm (3/8 in.) cell size was considered to be the minimum practical cell size. For the minimum gage facesheets required for a minimum weight design it appeared that intra-cell buckling might be a design limitation. Furthermore, the minimum gage face sheets require only four lamina, assuming pseudo isotropic, fiber-controlled properties, and the lack of symmetry about the midplane of the sheet causes extensional-bending coupling. SPAR finite element models of the facesheet over one core cell were developed, as shown in the lower right in figure, to analyze intra-cell buckling. The analysis was checked by using isotropic properties and comparing with commonly accepted values as shown by the buckling coefficients on the right. Buckling calculations for 6.4 mm (1/4 in.) cells and both 4 and 5 lamina lay-ups are shown on the left. The slopes of the curves were obtained from a classical flat plate buckling equation using the single calculated value from SPAR, and show what variation in buckling load is expected for various cell sizes. For the 0.08 mm (0.003 in.) lamina (assumed to be the minimum thickness available at that time), the analyses shows that the 10 mm (3/8 in.) cell is too large and therefore a 6.4mm cell is required.

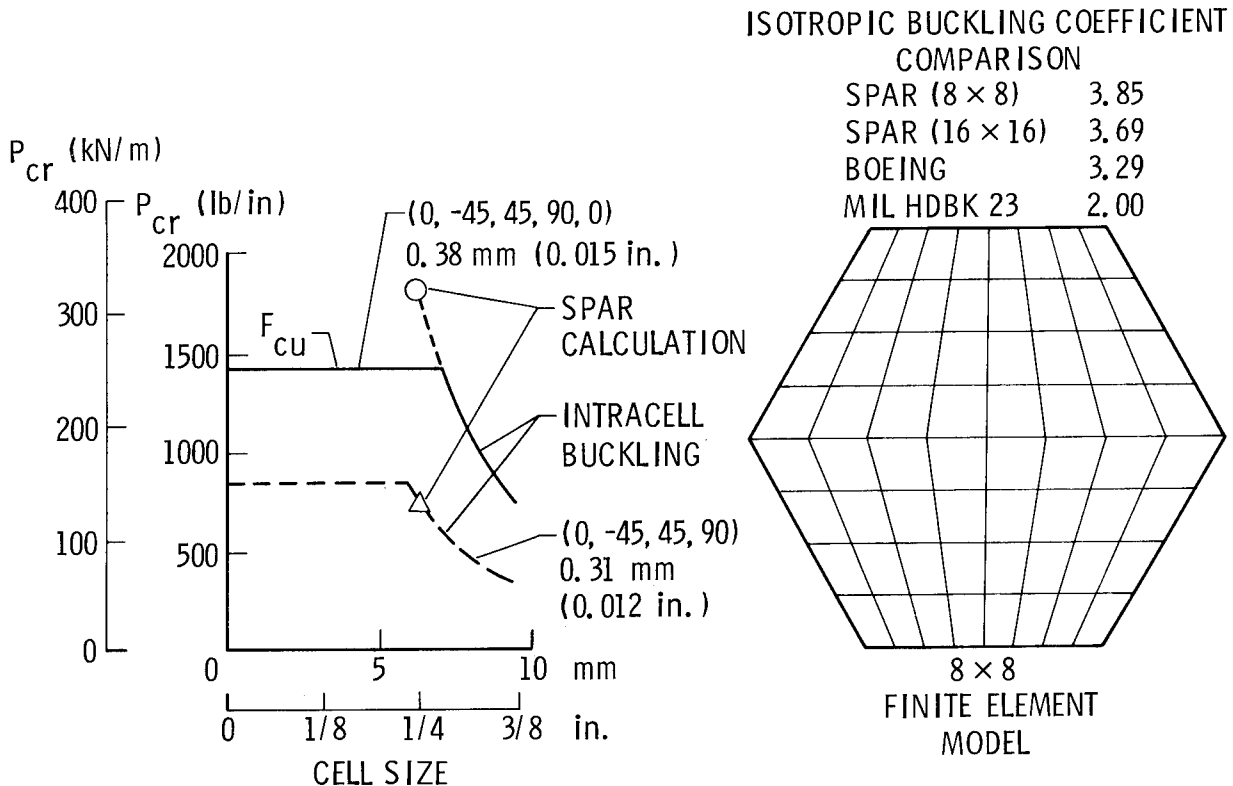


Figure 9

PRELIMINARY THERMAL MODEL

A preliminary one-dimensional thermal model of a "plug" through the body flap is shown in the figure. The components modeled are shown to the right of the model. The number of elements used in the model was required to adequately represent heat transfer through the RSI material. The RSI thicknesses shown represent an initial estimate of the RSI thickness necessary to limit structural temperatures to 589K (600°F). An entry heating-rate time-history, obtained from Rockwell International, is applied to the lower surface. Ascent heating data has been received from Johnson Space Center and will be used to complete the overall analysis.

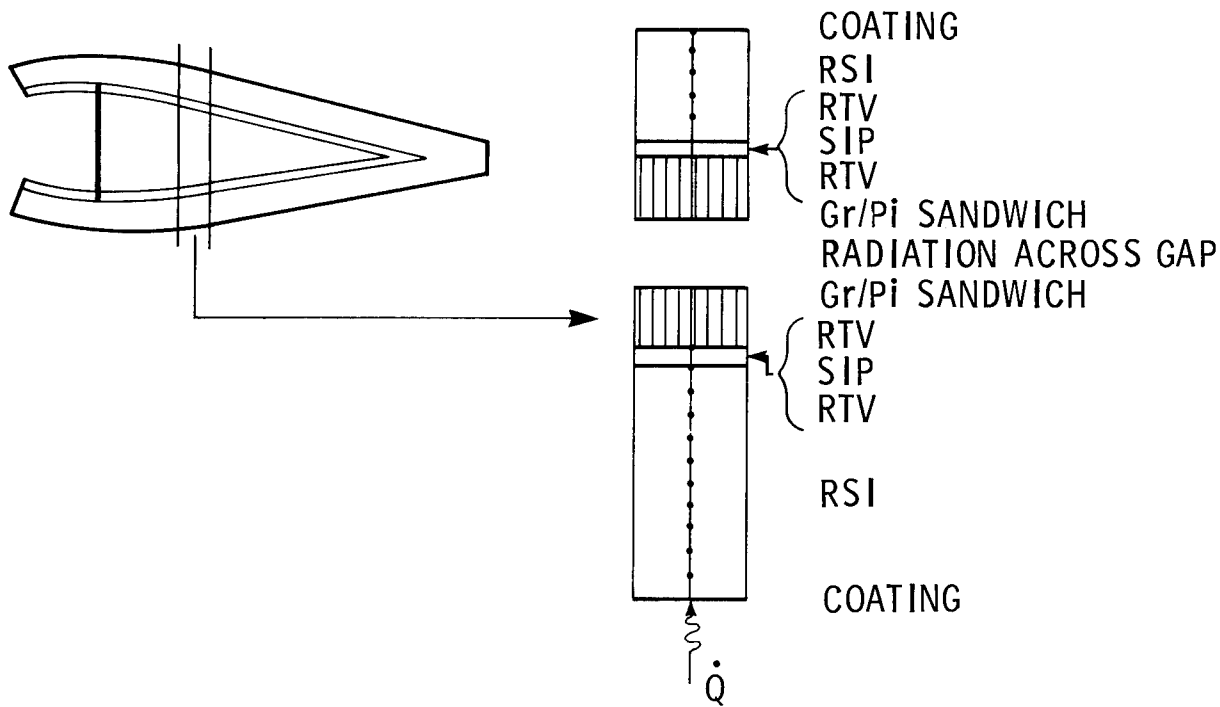


Figure 10

MAXIMUM TPS AND STRUCTURAL TEMPERATURES

The figure shows the maximum TPS and structural surface temperatures for the entry heating conditions for an assumed uniform temperature of 407K (275°F) at the beginning of entry. Inclusion of the ascent heating on the model and solution for the full trajectory (lift-off to maximum structural temperature) will provide a better estimate of the structural temperatures. Although the temperature differences through the strain isolator pad (SIP) can be as large as 67K (121°F) early in the trajectory, the difference between the maximum SIP temperature and the maximum structural temperature is only 38 K (68°F).

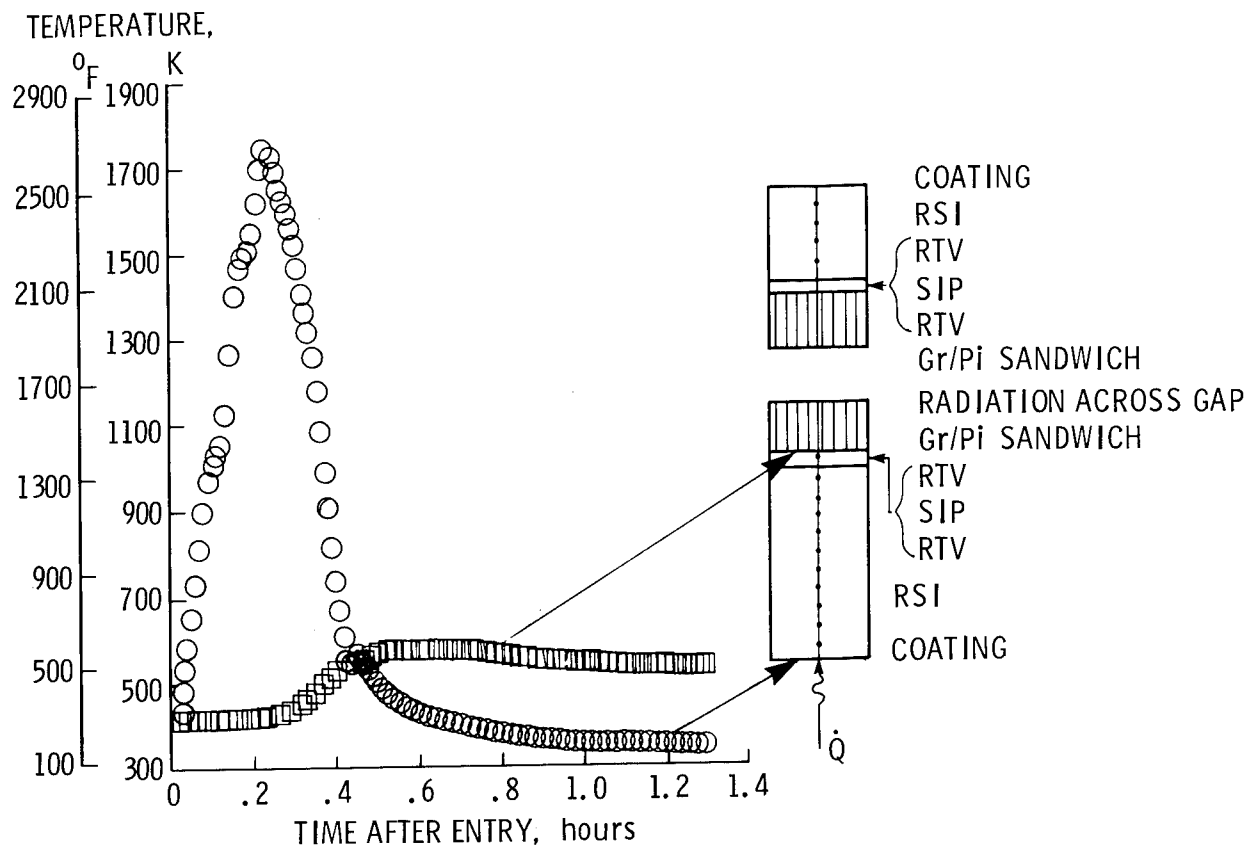


Figure 11

STRUCTURAL TEMPERATURES

The two curves in the figure show the maximum temperatures for the outer surface of the lower structural panel and the inner surface of the upper structural panel. The difference in the maxima of the two curves is approximately 40 K (70°F). This relatively small difference between the two panels is due to the radiation across the interior of the body flap and indicates that the structure away from the heat source is effective as a heat sink. The maximum structural temperature shown is below the limiting temperature of 589K (600°F); thus additional calculations with reduced RSI thickness are required to define the minimum mass design.

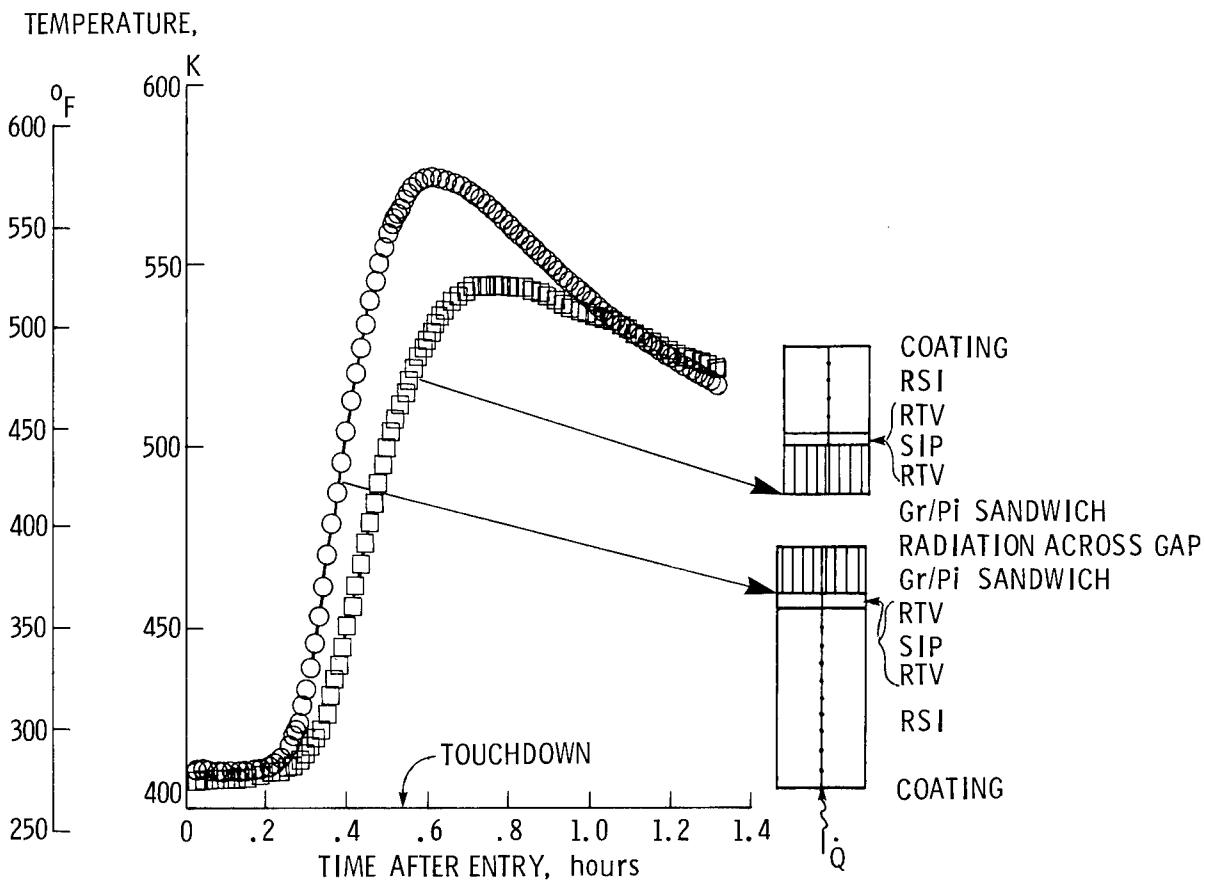


Figure 12

REMAINING EFFORT

Several tasks remain in the preliminary design study. An acoustic analyses of a typical body flap cover panel will be made. A more detailed stress analyses of the area surrounding the attachment points will be made to ensure that attachment loads can be transmitted to the structure. The preliminary one-dimensional thermal analysis will be completed and a two-dimensional model of a slice of one half of one bay will be made. Finally, the preliminary design structural concepts will be sized to withstand all imposed loads.

- ACOUSTIC ANALYSIS
- DETAILED STRESS ANALYSIS-ATTACHMENTS
- 2-D THERMAL ANALYSIS
- COMPLETE SIZING P. D. CONCEPTS

Figure 13

CONCLUDING REMARKS

An efficient analytical computer program, SPAR, has been modified to provide thermal and structural analyses capability for high-temperature advanced-composite structures. A preliminary design study of a composite body flap for the space shuttle orbiter is underway. Results to date indicate that a very light sandwich construction is necessary to support the loads consisting of small mechanical loads but severe acoustic and thermal loadings.

- SPAR MODIFIED FOR THERMAL AND STRUCTURAL ANALYSIS OF ADVANCED COMPOSITE STRUCTURES
- P. D. OF BODY FLAP UNDERWAY
- LOW LOAD LEVEL AND ACOUSTICS SUGGESTS SANDWICH CONSTRUCTION

Figure 14

REFERENCES

1. MacNeal, Richard H., ed.: The NASTRAN Theoretical Manual. NASA SP-221, 1970.
2. Whetstone, W. D.: SPAR Structural Analysis System Reference Manual - System Level 11. Volume 1 - Program Execution. NASA CR-145098-1, 1977.
3. Noor, Ahmed K.; and Mathers, Michael D.: Shear-Flexible Finite-Element Models of Laminated Composite Plates and Shells. NASA TN D-8044, 1975.
4. Robinson, James C.; and Blackburn, Charles B.: Evaluation of a Hybrid Anisotropic, Multilayered, Quadrilateral Finite Element. NASA TP-1236, 1978.
5. Tsai, Stephen W.: Strength Characteristics of Composite Materials. NASA CR-224, 1965.

DESIGN CONSIDERATIONS FOR COMPRESSION
PANELS AT ELEVATED TEMPERATURE

Robert R. McWithey and Charles J. Camarda
NASA Langley Research Center

Gerald G. Weaver
Graduate Student, University of Delaware

EXPANDED ABSTRACT

Design studies have indicated significant reductions in compression panel mass may be attained by using composite material in place of conventional metal panels. In addition, Gr/Pi composite materials provide structural composite laminates usable at elevated temperatures. To assess the potential of Gr/Pi, studies are being conducted on Gr/Pi honeycomb sandwich panels and stiffened panel concepts to develop lightweight panels for use at elevated temperatures. In the process of this development, the main technical objectives are to attain the capability to correctly predict panel buckling behavior and panel strength at elevated temperatures. This paper presents the interim results of this study and discusses the design, analysis and test techniques used in the study.

DESIGN CONSIDERATIONS FOR COMPRESSION PANELS AT ELEVATED TEMPERATURE

Studies are being conducted on Gr/Pi honeycomb sandwich panels and stiffened panel concepts to develop lightweight panels for use at elevated temperatures. In the process of this development, the main technical objectives are to attain the capability to correctly predict panel buckling behavior and panel strength at elevated temperature.

Different procedures are used in the design, analysis and test of the two types of panels. Preliminary results presented in reference 1 indicate that a honeycomb sandwich panel best meets the design requirements for the shuttle orbiter body flap design, the component focus of the CASTS project. Therefore, the emphasis in the honeycomb sandwich panel study has been directed specifically to this application. The stiffened panel study is focused on both supersonic cruise and space transportation system vehicles and, therefore, a wider range of loads and structural temperatures are under investigation. Because of these differences in design requirements, and because of inherent differences in panel compressive behavior between sandwich and stiffened panels; different design, analysis, and test techniques are used in these studies. This paper will present these techniques and discuss results obtained to date from these studies.

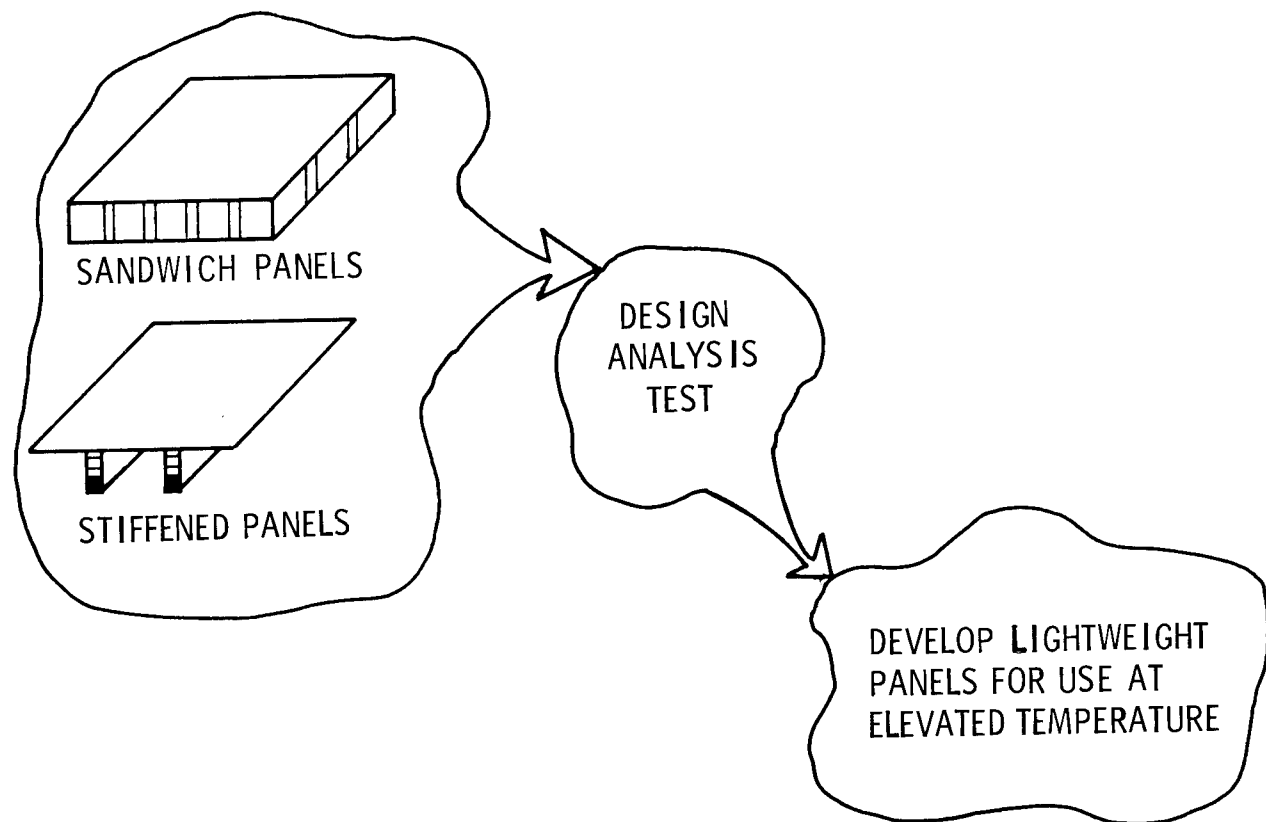


Figure 1

SANDWICH PANEL PROGRAM OUTLINE

An analytical and experimental program leading to the understanding of panel behavior was initiated as shown in the figure. Adhesive bonding studies were conducted to improve in-house bonding capability using FM-34 tape adhesive and to evaluate BR-34 primer as a cell-edge adhesive. Sandwich beam flexure tests will be conducted at 116K (-250°F), room temperature, and 589K (600°F) to obtain tensile and compressive material property data. Panel strength tests, at room temperature and elevated temperature, of square, simply supported panels with varying core thickness will qualify existing analysis methods in predicting panel strength and give performance characteristics at temperature.

- CONDUCT ADHESIVE BONDING STUDY
- CONDUCT MATERIAL PROPERTY TESTS
- PERFORM PANEL STRENGTH ANALYSIS AND TESTS

Figure 2

ADHESIVE BONDING STUDY
FAILED FLATWISE TENSILE SPECIMEN

A total of forty flatwise tensile specimens were tested at room temperature, 116K (-250°F) and 589K (600°F) to evaluate FM-34 tape adhesive. Two additional tests were conducted at room temperature to evaluate the use of BR-34 primer as a cell-edge adhesive.

The specimens were fabricated using precured, quasi-isotropic, 8 ply face sheets; glass/Pi core; and the desired adhesive. Steel load blocks were also adhesively bonded to the face sheets during the fabrication process. Each steel block has a blind tapped hole for attaching a loading rod. The assembled specimens were tested in tension in a universal testing machine. The temperatures other than room temperature were obtained using an environmental chamber positioned within the crossheads and posts of the testing machine. Specimen failures occurred either by face sheet delamination as shown in the figure or by failure of the bond line.

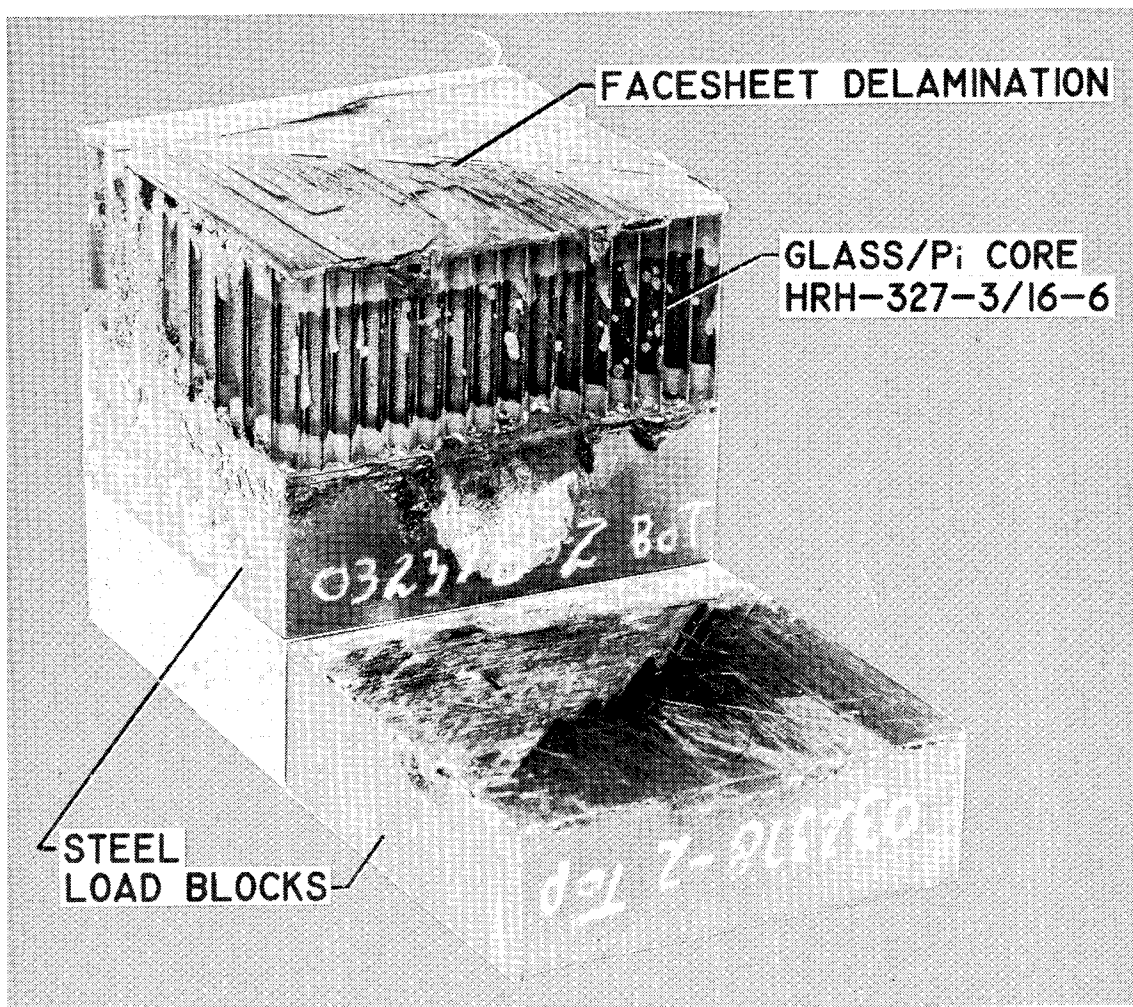


Figure 3

ADHESIVE BONDING STUDY RESULTS

This figure presents the important results of the adhesive bonding study. During the study, room temperature flatwise tensile strengths of specimens fabricated using FM-34 adhesive were increased from 1.6 MPa (230 psi) to strengths over 3.4 MPa (500 psi). This increase results primarily from improvements in priming techniques. Strengths over 3.4 MPa (500 psi) were also obtained at a test temperature of 116K (-250°F). Failures at this stress level were laminate failures. Flatwise tensile strengths at 589K (600°F) using FM-34 were greater than 1.4 MPa (200 psi) and failures occurred in the bond line.

Preliminary flatwise tension tests at room temperature of two specimens that were bonded in-house using BR-34 as a cell-edge adhesive indicated strengths similar to the strength obtained using FM-34. This strength was obtained using only half the mass of adhesive used with the FM-34. This is a mass savings equivalent to 10 percent of the panel mass for a panel consisting of 8 ply face sheets and a 12.7 mm (0.50 in.) thick core of 64 kg/m³ (4 lbm/ft³) density material. Although the initial results were encouraging, no further use was made of BR-34 as a cell-edge adhesive in this program because of manpower limitations.

FM-34

- $\sigma_{MAX} > 3.4 \text{ MPa (500 psi)}$
AT R.T. AND 116 K (-250°F)
LAMINATE FAILURES
- $\sigma_{MAX} \cong 1.4 \text{ MPa (200 psi)}$
AT 589 K (600°F)
BOND FAILURES

BR-34

- $\sigma_{MAX} > 3.4 \text{ MPa (500 psi)}$
AT R.T. 50 % REDUCTION IN
ADHESIVE MASS OVER FM-34
10 % REDUCTION IN PANEL MASS

Figure 4

MATERIAL PROPERTY TESTS

Material property tests will be conducted on 30 sandwich beam flexure specimens in a 4 point loading rig to obtain tensile and compression material properties at 116K (-250°F), room temperature, and 589K (600°F). Preliminary tests were conducted using the flexure beam method to determine adhesive and core strength capabilities. The test face sheet is an 8 ply quasi-isotropic laminate $([0,+45,-45,90]_s)$ and the opposite face sheet is a balanced, symmetric laminate containing several additional 0° laminae $([0_2,+45,90,-45]_s)$. The precured Celion 6000/PMR-15 face sheets are adhesively bonded to the 128 kg/m^3 (8 lbm/ft^3) glass/Pi core using FM-34 adhesive. The finished specimens are 559 mm (22 in.) long, 25.4 mm (1 in.) wide, and 31.8 mm (1.25 in.) deep.

Preliminary tests on flexure specimens indicated that the 128 kg/m^3 (8 lbm/ft^3) core and FM-34 adhesive possessed adequate strength for room temperature tensile and compressive tests. Adhesive failures occurred, however, at 589K (600°F) and thus the core cells in the shear loaded regions of all beams were filled with BR-34 to strengthen the adhesive bond between the core and face sheets. The test beams are fabricated but have not been instrumented. In addition, the test beams and test apparatus are similar to those described in reference 2. The beams differ from those in reference 2 because of differences in graphite fibers and core material.

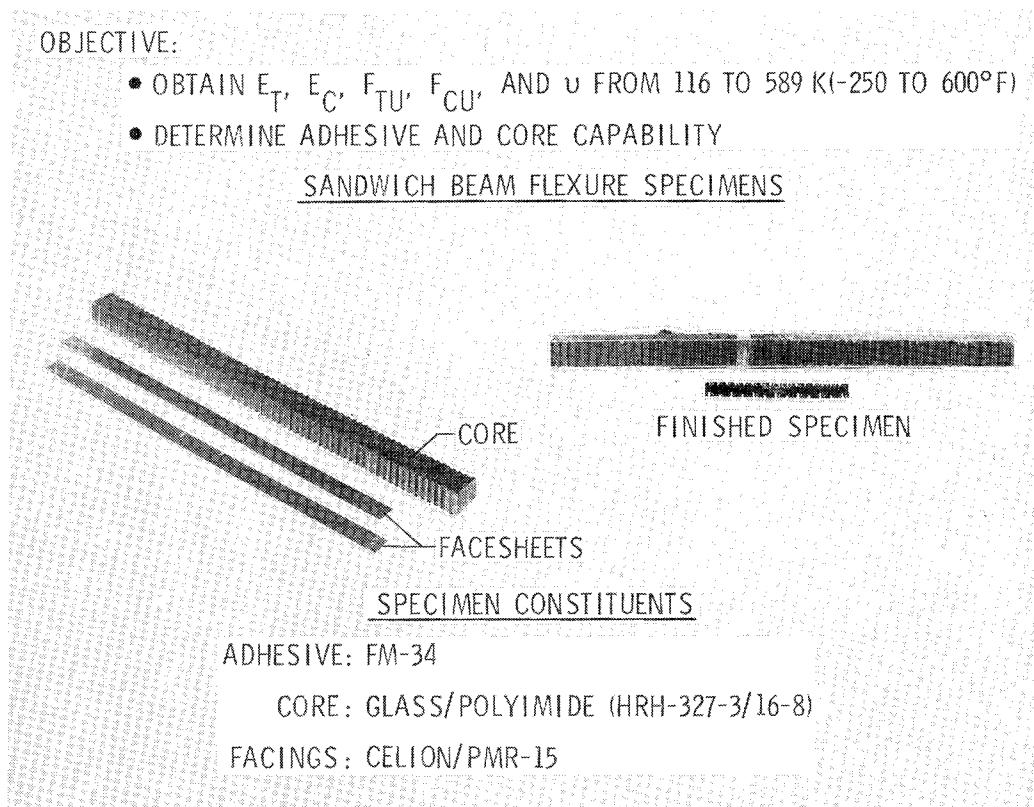


Figure 5

ANALYSIS PARAMETERS

Panel strength specimens were designed to evaluate available analytical methods for predicting wrinkling, dimpling, and shear-crimping failure modes. Practical considerations such as loading, minimum gages, and manufacturing methods resulted in the selection of a simply-supported panel configuration that is 305 mm (12 in.) square. Similarly, a nominal ply thickness of .076 mm (.003 in.) was used in the Celion 3000/Pi quasi-isotropic face sheet laminate $[0, +45, -45, 90]_s$. Glass/Pi honeycomb core with a density of 64 kg/m^3 (4 lbm/ft^3) (Hexcel HRH-327-3/8-4) was chosen as the core material because it was the lightest, commercially available composite core that maintained sufficient stiffness and strength at elevated temperature. The variable parameter in the analysis is the core height, t_c , which was varied from 6.4 mm (.25 in.) to 30.5 mm (1.2 in.).

● PANEL SIMPLY SUPPORTED ON ALL EDGES

- $B = 305 \text{ mm (12.0 in.)}$

- PLY THICKNESS
0.076 mm (0.003 in.)

- FACESHEET: $[0, \pm 45, 90]_s$, CELION/PI

- CORE: GLASS/PI, HRH-327-3/8-4

- CORE DEPTH 6.4 - 30.5 mm (0.25 - 1.20 in.)

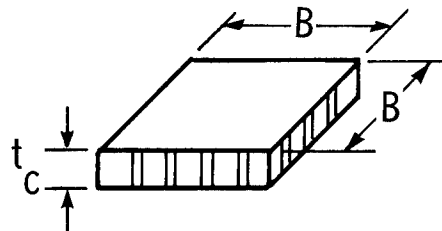


Figure 6

ANALYSIS RESULTS

The figure shows results from panel strength analyses of a simply-supported 305 x 305 mm (12 x 12 in.) panel where failure stress and strain are plotted as a function of core height for the various failure modes. Where two curves are shown for a failure mode, the curves represent the upper and lower bounds of different analysis methods. The analysis methods are presented in references 3-7. The curves indicate that the selected minimum gage face sheets and core eliminate shear crimping and dimpling as possible failure modes because these failure modes occur at stress levels above the ultimate compressive stress of the face sheets. The analyses indicate, however, that the core height variation will allow the experimental investigation of overall buckling, panel strength, and panel wrinkling. It should be noted that the strains associated with these failure modes are above the maximum permissible strains suggested for 48 ply lamina in reference 8 for impact damage tolerance.

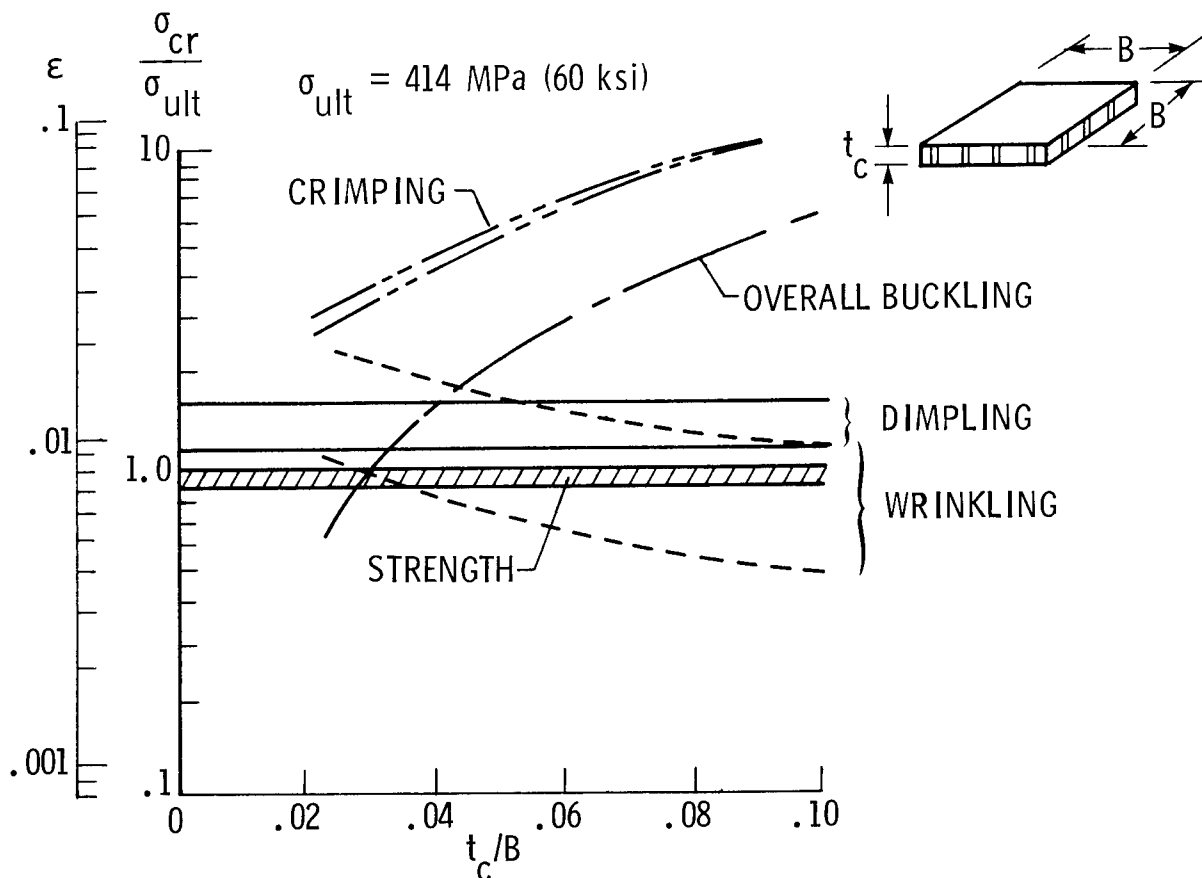


Figure 7

TEST MATRIX

The test matrix consists of twenty-four sandwich panels that will be fabricated with variation in core height from 6.4 mm (.25 in.) to 25.4 mm (1.0 in.). These values of core height correspond to values of t_c/B of approximately .02, .04, .06, and .08. Three panels of each core height will be tested at room temperature and at 589K (600°F).

t_c mm (in.)	$\frac{t_c}{B}$	NO. OF SPECIMENS	
		R. T.	589 K (600°F)
25.4 (1.00)	0.083	3	3
19.1 (0.75)	0.063	3	3
12.7 (0.50)	0.042	3	3
6.4 (0.25)	0.021	3	3

Figure 8

TEST PANEL CONFIGURATION

A sketch of the panel configuration is shown in the figure. The ends of the panel that will be loaded are reinforced by adding glass/Pi end tabs, glass/Pi scalloped doublers, and by filling the honeycomb core cells under the end tabs with BR-34 adhesive as shown in section sketch AA. All panel components such as the core, face sheets, tabs, and doublers are adhesively bonded together using FM-34 tape adhesive. Either the alignment pins shown or metal sheets will be bonded into the potted ends to position the panel ends in the knife edge slot.

The test fixture, which is not shown, is similar to those used in references 4 and 9 and will approximate simply-supported boundary conditions on the 4 edges of the panel. In addition, the test fixture will allow initial, room temperature adjustment along the loaded edges to obtain a uniform compressive strain over the panel width prior to testing. Elevated temperature tests will be conducted using an oven that is heated with electric finstrip heaters. Instrumentation will include strain gages and thermocouples attached to the panel, and linear variable differential transformers to determine mode shape. These panels are being fabricated by Rockwell International Corporation.

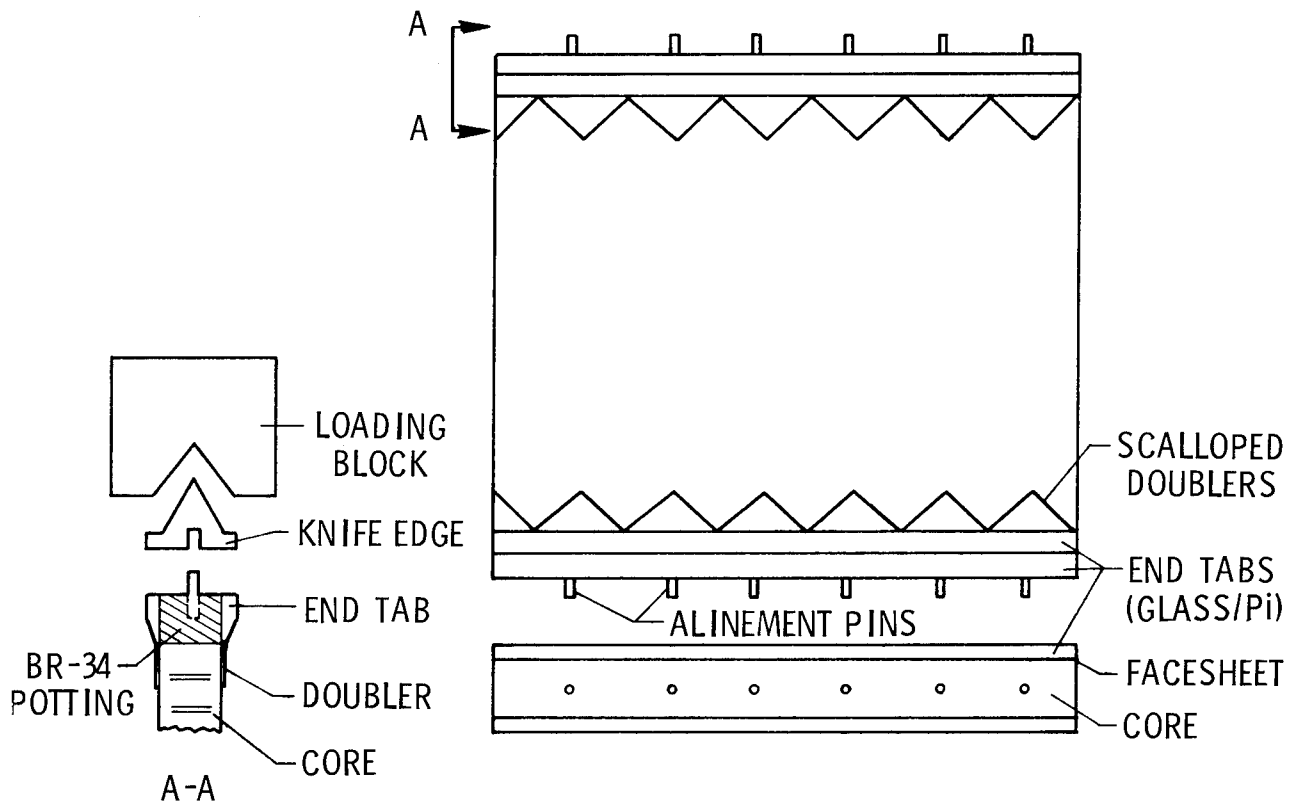


Figure 9

STIFFENED PANEL PROGRAM OUTLINE

An analytical and experimental program leading to the understanding of panel behavior was also initiated for stiffened panels as shown in the figure. This program focuses on both supersonic cruise and space transportation system vehicles. Consequently, a wide range of loads is considered and an elevated temperature of only 505K (450°F) is considered for some of the panels. The program outline includes design, fabrication and tests of local buckling specimens and is similar to the program for the honeycomb panels.

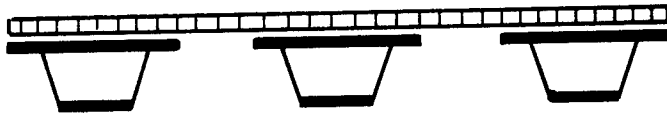
- SELECT PANEL CONFIGURATIONS
- DESIGN MINIMUM MASS PANELS
- FABRICATE AND TEST LOCAL BUCKLING SPECIMENS

Figure 10

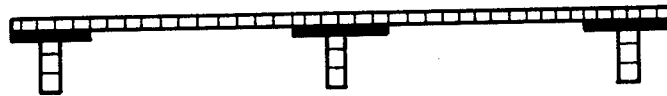
SELECTED PANEL CONFIGURATIONS

The panel configurations selected for evaluation in the stiffened panel program are shown in the figure. These types of stiffened panels have high structural efficiency (refs. 10, 11, & 12) and are structurally well understood in that previous studies have indicated good agreement between analytical predictions and experimental results for these general types of stiffened panels. In addition, the panel components for these configurations, which are the stiffeners, core, and skin, are relatively easy to fabricate using existing fabrication techniques for Gr/Pi. Similarly, final panel assembly is possible using existing adhesive bonding techniques for FM-34 adhesive.

HAT STIFFENED HONEYCOMB SANDWICH



BLADE STIFFENED HONEYCOMB SANDWICH



BLADE STIFFENED SKIN

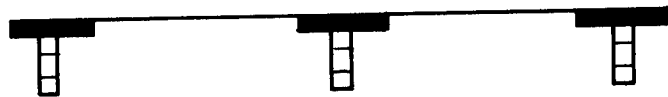


Figure 11

DESIGN PROCEDURE FOR STIFFENED PANELS

The procedure used for stiffened panel design utilized the Panel Analysis and Sizing Code PASCO discussed in reference 13. This code utilizes nonlinear mathematical programming techniques and a rigorous buckling analysis to obtain dimensions of minimum mass composite compression panels. An analytical model of the panel cross-section is input to the code along with the design conditions of load; panel bow, which is defined as the out-of-plane imperfection of the panel center divided by the panel length; and material property data. Variables in the present analysis include laminae thicknesses, stiffener spacing, and stiffener size. Ply orientation angles may also be treated as variables but, for the results to be shown, the orientations of the various plies were limited to 0° , $\pm 45^\circ$ and 90° ply orientations.

Constraints imposed on the panel variables during the design procedure insure that Euler and local buckling loads in the final panel design are equal to or greater than the design load. In addition, minimum gage constraints limit laminae thicknesses for lightly loaded panels, and the Tsai-Wu failure criterion (ref. 14), with the F_{12} term set equal to zero, constrains the designs for heavily loaded panels. Maximum gage constraints were also imposed in the analysis that reflect current Gr/Pi fabrication limitations.

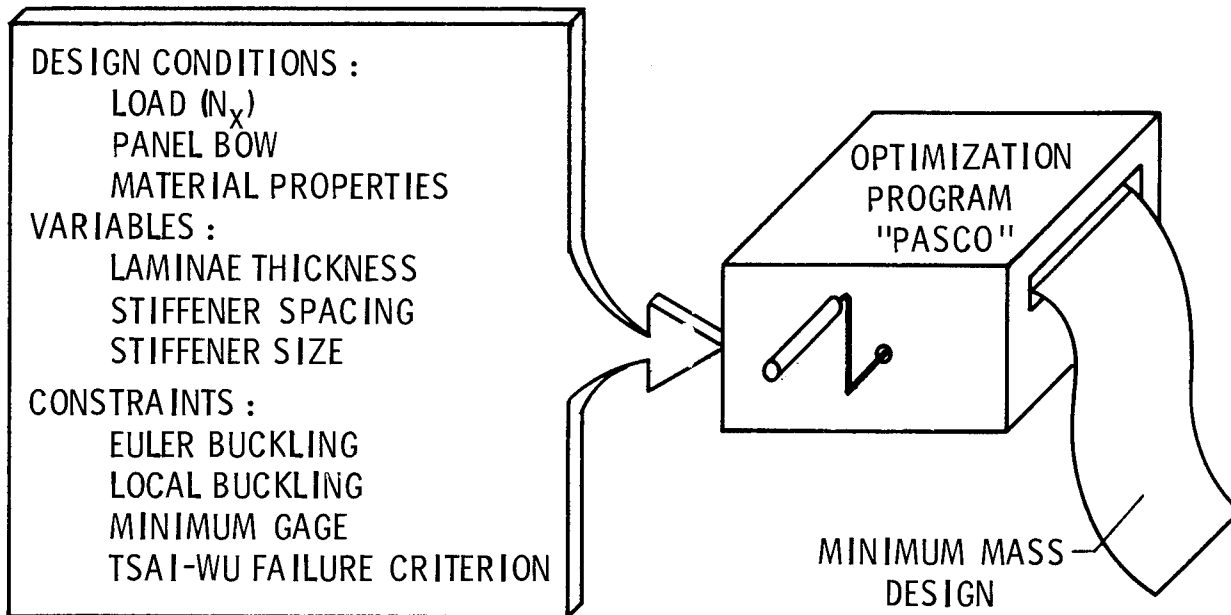


Figure 12

STRUCTURAL EFFICIENCY OF STIFFENED PANELS

Some results of the design procedure are shown in the figure in terms of mass index, which is mass per unit planform area, w , divided by the panel length L , versus the load index N_x/L . The Gr/Pi curves are from the present analysis. For the range of loading index shown, the titanium and aluminum hat stiffened panel designs are not influenced by minimum gage or material strength constraints. Portions of the Gr/Pi panels, however, are constrained by minimum gage constraints over the lower range of load index, and are constrained by the Tsai-Wu failure criterion over the higher range of load index. For a panel length of 762 mm (30 in.), a typical value of the load index for a supersonic transport wing would be 2.3 MPa (333 psi), which corresponds to a 1750 kN/m (10000 lbf/in.) compressive load and a compressive strain slightly less than .004. For the shuttle orbiter body flap, a typical load index is .07 MPa (10 psi), which corresponds to a 53 kN/m (300 lbf/in.) compressive load and a compressive strain of approximately .0006. The Tsai-Wu failure criterion limits panel longitudinal strains for all the Gr/Pi designs to less than .004. This value of strain may be in excess of the allowable strain determined by impact criteria as discussed in reference 8. However, when an impact sensitivity criterion is established, it can easily be incorporated into the design procedure.

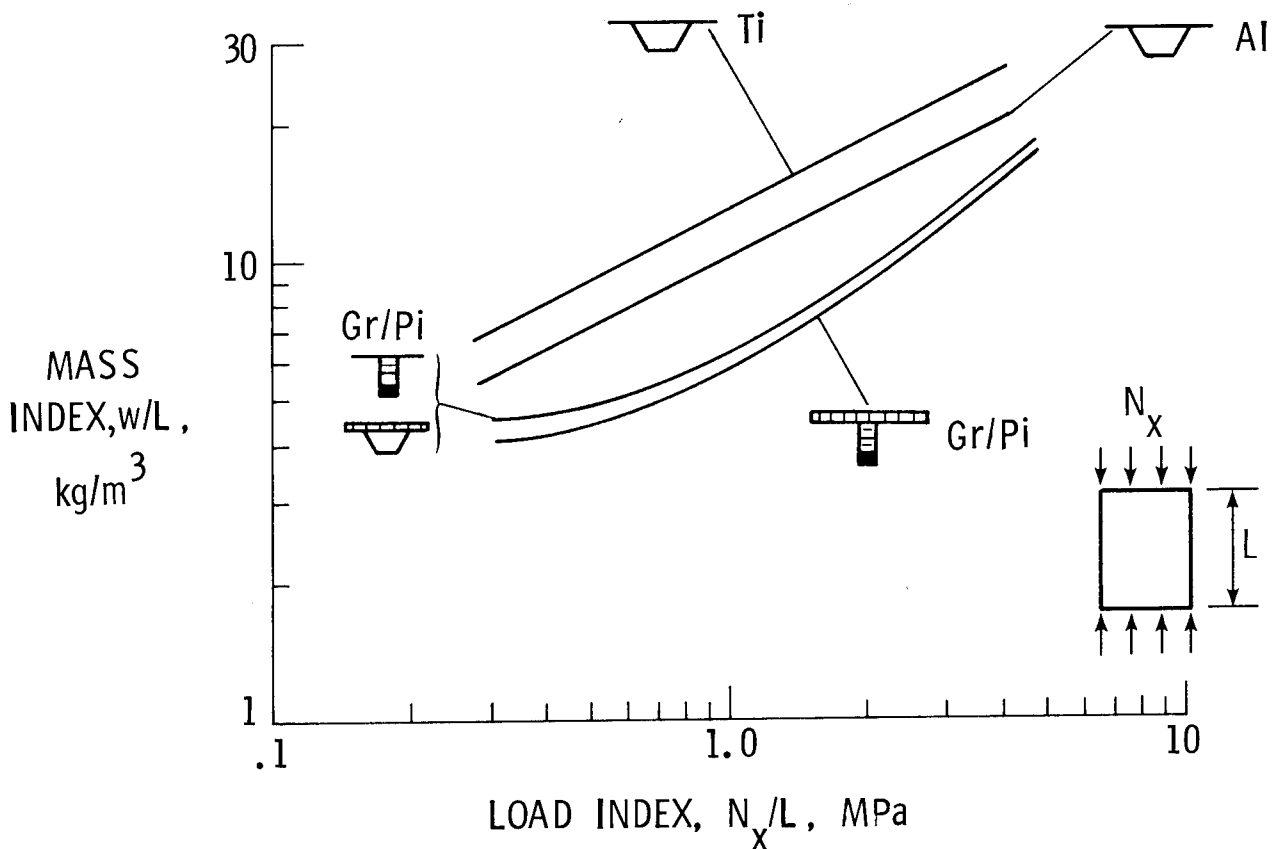


Figure 13

STIFFENED PANEL TEST MATRIX
LOCAL BUCKLING

Twenty-four stiffened panels will be tested to study local buckling characteristics. The general panel configurations are indicated in the figure. The dimension L is panel length, and the dimension W is panel width. Panel designs for the three basic panel configurations will be examined for a supersonic cruise load condition and temperature. The blade stiffened skin configuration will also be examined for the shuttle orbiter body flap load condition and temperature. These panels are presently being fabricated by Rockwell International Corporation.

CONFIGURATION	LOAD INDEX MPa (psi)	L mm (in.)	W mm (in.)	NO. OF SPECIMENS	
				R. T.	505 K (450 ⁰ F)
HAT-STIFFENED HONEYCOMB SANDWICH	2.3 (333)	760 (30)	610 (24)	3	3
BLADE-STIFFENED HONEYCOMB SANDWICH	2.3 (333)	760 (30)	410 (16.1)	3	3
BLADE-STIFFENED SKIN	0.07 (10)	760 (30)	430 (16.8)	3	3*
BLADE-STIFFENED SKIN	2.3 (333)	410 (16)	270 (10.6)	3	3

* TEST TEMPERATURE 589 K (600⁰F)

Figure 14

STATUS OF COMPRESSION PANELS PROGRAM

The status of the panel programs is shown in the figure. The flatwise tensile tests are completed and indicate that the use of a cell-edge adhesive in place of a tape adhesive has a potential of reducing sandwich panel mass. The sandwich beam flexure specimens are being instrumented and will be tested within the next few months. Several sandwich-panel specimens were successfully fabricated and fabrication of the remaining panels is scheduled for completion by April 1979. Design of the Gr/Pi stiffened panel specimens is completed and the results indicate mass savings of up to 50% over titanium panels. Fabrication of stiffened-panel, local-buckling specimens is scheduled for completion September 1979. The goal is to have the panels tested and results documented by June 1980.

SANDWICH PANELS

- FLATWISE TENSILE TESTS COMPLETED
- SANDWICH BEAM FLEXURE SPECIMENS FABRICATED
- DESIGN OF TEST PANELS COMPLETED;
SPECIMENS BEING FABRICATED

STIFFENED PANELS

- DESIGN OF LOCAL BUCKLING SPECIMENS COMPLETED;
SPECIMENS BEING FABRICATED

Figure 15

CONCLUSIONS

Although the compression panel program is not complete, the following conclusions may be made from the present results of this study:

1. Flatwise tensile strengths in the Gr/Pi laminates greater than 3.4 MPa (500 psi) were obtained at room temperature and 116K (-250°F).
2. Preliminary flatwise tensile tests indicate that the use of a cell-edge adhesive in place of a tape adhesive has a potential of reducing panel mass.
3. Analysis of sandwich panels indicates that use of minimum gage Celion 3000/Pi quasi-isotropic face sheets and minimum gage composite core material eliminates shear crimping and dimpling as possible failure modes.
4. Analysis of Gr/Pi stiffened panels indicates mass savings up to 50 percent over comparable stiffened titanium panels.
5. Strains developed in the sandwich panels and stiffened panels under design loads may be in excess of developing impact sensitivity criterion.

REFERENCES

1. Blackburn, C. L.; and Robinson, J. C.: Analysis Methods and Preliminary Design Study. Graphite/Polyimide Composites, NASA CP-2079, 1979. (Paper no. 22 of this compilation.)
2. Shuart, Mark J.: Sandwich Beam Compressive Test Method. Graphite/Polyimide Composites, NASA CP-2079, 1979. (Paper no. 14 of this compilation.)
3. Sullins, R. T.; Smith, G. W.; and Spier, E. E.: Manual For Structural Stability Analysis of Sandwich Plates and Shells. NASA CR-1457, Dec., 1969.
4. Pearce, T.R.A.: The Stability of Simply-Supported Sandwich Panels with Fiber Reinforced Faceplates. University of Bristol, Thesis Submitted for Degree of Ph.D., Sept., 1973.
5. Plantema, F. J.: Sandwich Construction. John Wiley & Sons Inc., 1966.
6. U.S. Department of Defense: Structural Sandwich Composites, MIL-HDBK-23, 30 Dec., 1968.
7. Peterson, James P.: Plastic Buckling of Plates and Shells Under Biaxial Loading. NASA TN D-4706, Aug., 1968.
8. Garcia, Ramon; and Rhodes, Marvin D.: Effects of Low-Velocity Impact on Gr/Pi Compression Laminates. Graphite/Polyimide Composites, NASA CP-2079, 1979. (Paper no. 17 of this compilation.)
9. Hoff, N. J.; Boley, Bruno A.; and Coun, John M.: The Development of a Technique for Testing Stiff Panels in Edgewise Compression. Experimental Stress Analysis, Vol. 5, No. 2, p. 14, 1948
10. Williams, Jerry G.; and Mikulas, Martin M., Jr.: Analytical and Experimental Study of Structurally Efficient Composite Hat-Stiffened Panels Loaded in Axial Compression. AIAA Paper No. 75-754, May 1975.
11. McWithey, Robert R.: Analytical Structural Efficiency Studies of Borsic/Aluminum Compression Panels. NASA TN D-8333. December 1976.
12. Stein, Manuel; and Williams, Jerry G.: Buckling and Structural Efficiency of Sandwich-Blade Stiffened Composite Compression Panels. NASA TP-1269. September 1978.
13. Anderson, Melvin S.; and Stroud, W. Jefferson: A General Panel Sizing Computer Code and Its Application to Composite Structural Panels. Proceedings of the AIAA/ASME 19th Structures, Structural Dynamics and Materials Conference, Bethesda, Maryland, April 3-5, 1978.

14. Tsai, Stephen W.; and Wu, Edward M.: A General Theory of Strength for Anisotropic Materials. Journal of Composite Materials, Vol. 5, (1971) p. 58.

GLASS POLYIMIDE HONEYCOMB CORES FOR ADVANCED
SPACE TRANSPORTATION SYSTEMS

Jay Brentjes
Hexcel Corporation

EXPANDED ABSTRACT

The use of a glass fiber reinforced polyimide honeycomb has been considered for various applications requiring lightweight stiff structures which may experience temperatures up to 600K. Currently available core types are made with the older condensation reaction polyimide resins. A NASA contract, NAS1-15356, was awarded to fabricate and test several honeycombs using woven E glass treated with LARC 160, PMR 15 and NR 150 and to compare mechanical properties with the older core type HRH[®] 327 at ambient temperature and 589K.

This paper reports the experiences and results of fabricating these core types. The process parameters and most desirable characteristics are noted. In particular, the differences in considering resins for making laminates versus their use in surface coatings are stressed. This comparison is made to explain the problems encountered in using the three new resin types for dipping honeycomb to the desired density.

In addition, some properties and the effect of post cure, forming and ventilating techniques for the condensation polyimide core types are presented.

HONEYCOMB TYPES

Polyimide honeycomb reinforced with woven fiberglass was first developed during the late 1960's for predominate use on the first U.S. SST aircraft designed by the Boeing Company. Several years of internally funded development efforts at Hexcel resulted in a honeycomb which not only utilizes polyimide resin for the impregnation and dip coating but also for the node bond adhesive. In addition, techniques were developed for orienting the glass fibers at $+45^{\circ}$ to the cell axis. This yielded higher shear modulus and subsequently a stiffer sandwich structure.

Although the SST was never built, many cubic feet of honeycomb were made and tested by Boeing, Rockwell International and other subcontractors for the SST. At the same time other applications were found at Boeing, Grumman, G.E. and other aerospace companies. Some were radomes; some were for high temperature uses. As a result the HRH 327 product line remained in existence and several core types are now available as a standard material.

With the advent of other polyimide resins such as NR 150, LARC 160 and PMR 15 and their easier processing parameters for making laminates, it was deemed important to evaluate these as resin candidates for honeycomb and compare these honeycomb cores with HRH 327.

Figure 1 outlines a series of honeycomb types which were considered for a development and evaluation program.

LARC 160	-	3/16	-	5.0
		3/16	-	4.0
		1/4	-	3.0
PMR 15	-	3/16	-	5.0
		3/16	-	4.0
		1/4	-	3.0
NR 150	-	3/16	-	5.0
		3/16	-	4.0
		1/4	-	3.0
HRH 327	-	3/16	-	4.0

Figure 1

TEST PARAMETERS

A NASA Langley program was set up to fabricate and test several honeycombs using the same techniques used for making HRH 327 except for incorporating PMR 15, LARC 160 and NR 150 as the resin matrices. The mechanical properties to be evaluated and exposure conditions are listed in Figure 2. The same tests will be performed on HRH 327-3/16-4.0 for comparison. The intent of this program is to determine if any of these resins will yield a lower cost honeycomb with equal or better properties, particularly at 589K.

To date the various core types have been fabricated and the testing phase has been started.

PROPERTY	EXPOSURES	CORE TYPES
FLATWISE COMPRESS. STR. & MOD.	R.T. AS IS	ALL
L SHEAR STR. & MOD.	R.T. AFTER 125 HRS. AT 589 K.	HRH327, LARC, PMR.
W SHEAR STR. & MOD.	R.T. AFTER 500 HRS. AT 589 K.	NR 150
	589 K AS IS	ALL
	589 K AFTER 125 HRS. AT 589 K.	HRH327, LARC, PMR.
	589 K AFTER 500 HRS. AT 589 K.	NR 150

Figure 2

MANUFACTURING PROCESS FOR NON-METALLIC HONEYCOMB

Figure 3 shows the basic manufacturing steps for non-metallic honeycomb. The important steps in making fiberglass reinforced core are impregnation, adhesive application, and curing. Ideally the impregnation step forms a non-porous film to prevent the node adhesive from penetrating through the sheet. However, if too much resin is used for impregnation, the fabric can become so stiff during the node bond cure cycle as to make the expansion difficult or impossible. Hence carefully controlled resin and adhesive parameters such as quantity and flow control are necessary to prevent bleed-through or blocking. The object is not to make a laminate. The resin for honeycomb is used as a coating and film former. The need for applying pressure and the use of an autoclave or vacuum bag would be undesirable and expensive processing requirements.

The core is normally dipped in a resin solution and withdrawn at a slow rate. This should provide all cell walls with a uniform coating and no large build-ups in the corners. Each dip coat is then fully or partially cured in an air circulating oven. The actual time/temperature cycle depends on the type of resin and solvents used. If too much heat is applied too fast, the resin can bubble and blister.

This was generally the experience in working with the three new resin systems. In order to prevent blistering during cure, the solids content of the dip solutions had to be cut back to as low as 20% for LARC 160 and PMR 15 and to about 25% for the NR 150. Thus very small amounts of pick-up per dip had to be used. This, combined with slow cure cycles, made the dipping process long, tedious and expensive.

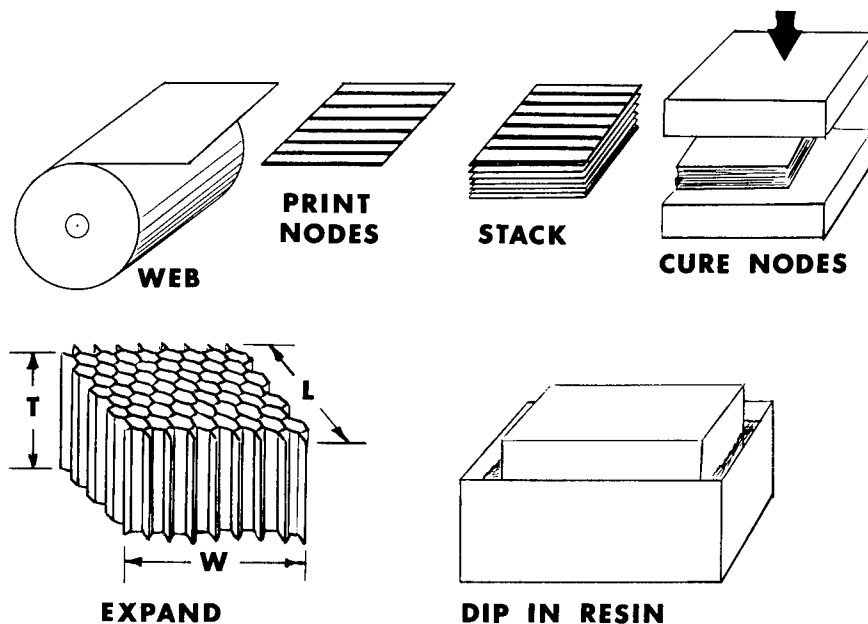


Figure 3

MECHANICAL PROPERTIES OF HRH327 HONEYCOMB

HRH 327 is based on condensation reaction polyimide resin. Prepregs with this resin are generally considered to be difficult to process when making laminates. However, again in the case of honeycomb, the resin is used very effectively as a coating without excessively long dip and cure cycles.

Figure 4 lists the mechanical properties of several combinations of cell size and density. This table is from Hexcel's publication TSB 120. Besides typical room temperature properties, some minimum acceptable values are listed for the more readily available core types.

Hexcel honeycomb designation	Compressive			Plate shear					
	Stabilized			"L" Direction			"W" Direction		
	Strength, kPa		Modulus, MPa	Strength, kPa		Modulus, MPa	Strength, kPa		Modulus, MPa
	typ	min	typ	typ	min	typ	typ	min	typ
HRH 327 - 3/16 - 4.0	3034	----	345	1930	----	200	0896	----	70
HRH 327 - 3/16 - 4.5	3585	2758	400	2206	1517	228	1034	758	76
HRH 327 - 3/16 - 5.0	4137	----	469	2551	----	255	1241	----	86
HRH 327 - 3/16 - 6.0	5378	4309	600	3172	2379	310	1586	1172	103
HRH 327 - 3/16 - 8.0	8963	6895	869	4482	3447	427	2827	2275	152
HRH 327 - 3/8 - 4.0	3034	2241	345	1930	1344	200	1034	689	83
HRH 327 - 3/8 - 5.5	4688	3723	538	2896	2068	283	1448	1103	93
HRH 327 - 3/8 - 7.0	6895 ^p	----	731 ^p	3792 ^p	----	365 ^p	2137 ^p	----	128 ^p

p - preliminary properties.

Figure 4

HRH 327-3/16-3.5 AT ELEVATED TEMPERATURES

Figure 5 shows some values for one block of HRH 327-3/16-3.5 at test temperatures up to 600K. Although the compressive strength was 20 percent lower at 500K than at room temperature, the shear strengths were essentially constant for this temperature range. All strengths were approximately 30 percent lower at 600K than at 500K. A major factor influencing this behavior was the post cure cycle of the core. A similar series of tests (not shown here) on core which had been given a much shorter post cure had strengths at 600K which were only about one half of the values shown. However, the room temperature values in that case were somewhat higher - about 12 percent. Thus, the strength properties can be somewhat manipulated depending on the service temperature requirements.

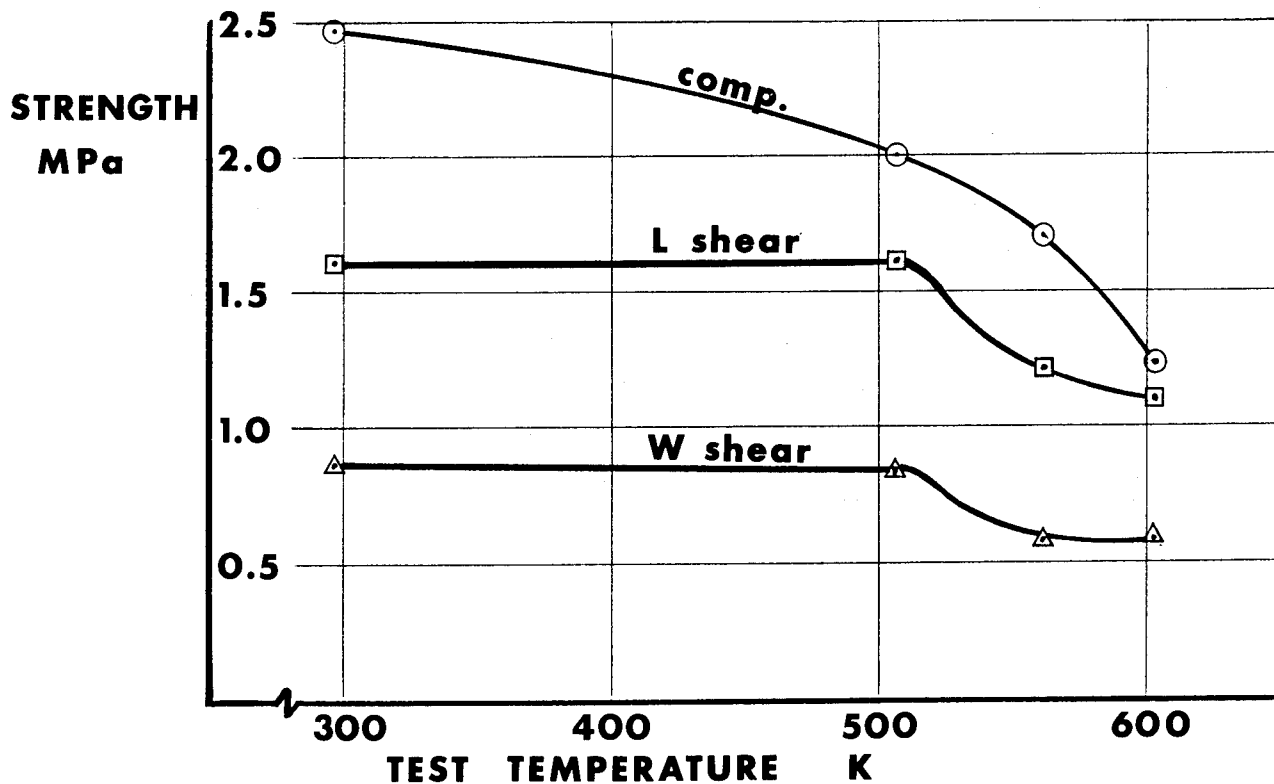


Figure 5

HRH 327 CAN BE HEAT FORMED TO COMPOUND CURVATURES

In some cases core is supplied which is not "fully" post cured. When the sandwich panel has a simple or compound curvature, the honeycomb has to be preformed. This is done by rapidly heating non-post cured core to temperatures up to 645K and immediately forcing it over a male tool of the desired contour. The details of this procedure depend a lot on the core type, shape and size. It is considered to be quite an art and requires experience and trial-and-error experimentation.

Figure 6 shows one of these contoured parts which can be made by this heat forming technique. The core should be post cured in the formed condition to get the elevated temperature properties. In order to prevent distortion of the shaped part, the post curing should be done with the honeycomb restrained over a tool.

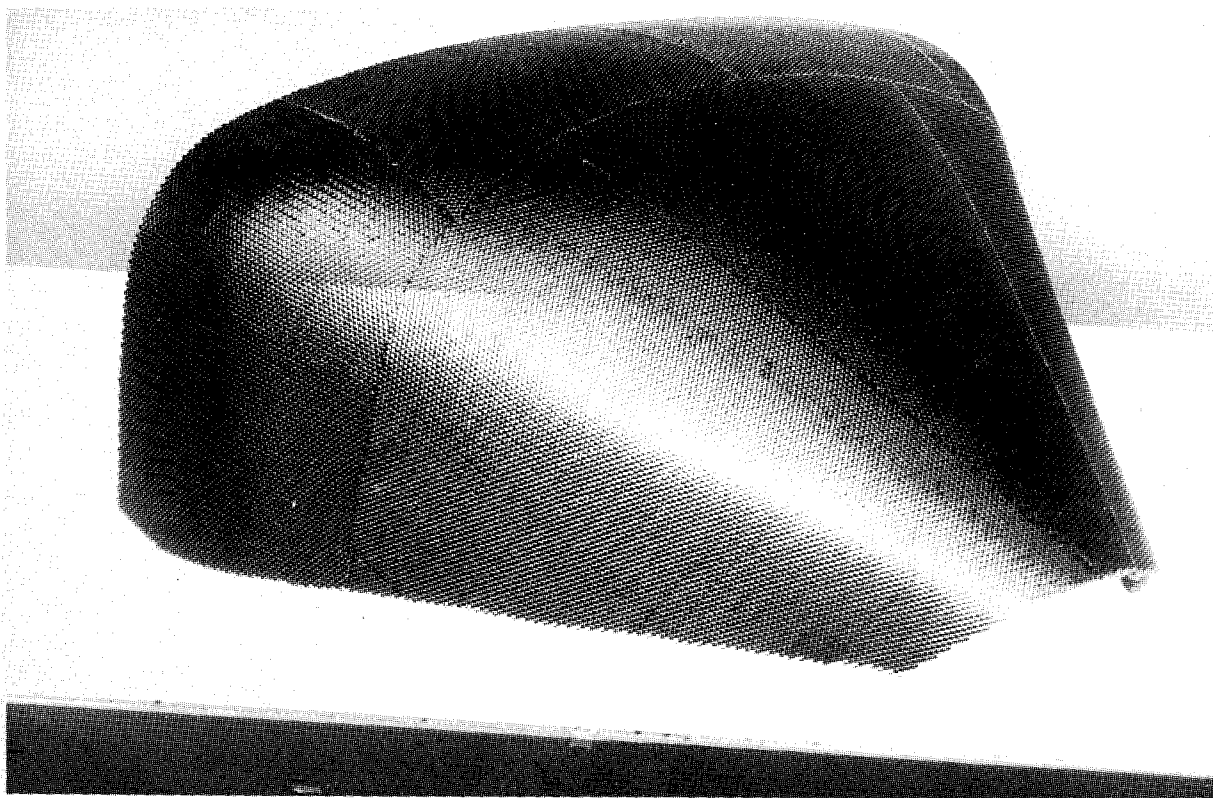


Figure 6

WAYS OF VENTILATING HONEYCOMB

In some applications it is considered important to have vented core. For example, polyimide film adhesives used for bonding the facings to core may give off condensation products and/or volatiles. When the top facing is a polyimide prepreg which is co-cured to the honeycomb, these volatiles can be bled off. However, it does require finely tuned cure cycles with proper timing of heat-up rate and temperature step function. If non-porous facings such as titanium are used, the cure can be inhibited unless a passageway is created through the core. This can be done for larger cell sizes (such as 6 or 10 mm) by slotting the cell walls on one side of the honeycomb sheet. These slots are typically 1.5 to 2 mm wide and 2.5 mm deep. They would be cut through every nodal cell wall so that every cell is vented to at least one edge of the panel.

Another way that completely random venting can be achieved is by bonding two sheets of honeycomb to each other at a center plane using a cell edge adhesive. By having the cells randomly located from one sheet to the next, a passageway is created from one cell to the next by moving up and down between the two layers. Of course, a film adhesive should not be used since it would block off all these passageways.

Precoating the cell edges with a roll-on or cell edge adhesive and precuring this before panel lay-up will also help in providing a larger bond surface for the core to face adhesive. Typical polyimide adhesives generally do not wet the cell walls well, and the filleting (which is so important in getting good bond strength) is not as good as what can be achieved with epoxy film adhesives. Thus a precoating of a polyimide paste adhesive can help this condition.

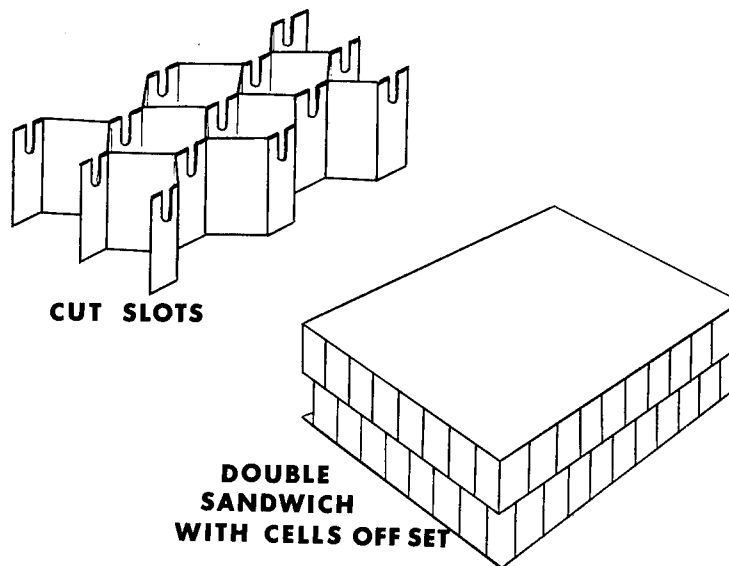


Figure 7

CONCLUSION

The fabrication phase of this program for glass reinforced honeycomb using LARC 160, PMR 15 and NR 150 has produced small quantities of core which will be used to evaluate mechanical properties at room temperature and 589K. However, the difficulties encountered will make these products very expensive to produce in quantity. The resins are used for coating the cell walls, which should not be confused with laminating requirements of prepreg systems. To prevent blistering, very small quantities had to be applied and cured with lengthy cycles.

HRH 327, polyimide honeycomb, which has been in production for several years has been tested previously and found to have good strength retention at high temperatures. Post cure cycles are important to achieve high values. HRH 327 can be heat-formed and slotted or double bonded to provide venting of a sandwich panel.

DEVELOPMENT OF HYBRID POLYIMIDE COMPOSITES

Milan G. Maximovich
SRI International

EXPANDED ABSTRACT

Graphite/polyimide composite materials exhibit high performance, low weight, and good thermal/oxidative stability, making them promising candidates for space shuttle applications. However, materials now being evaluated all have serious potential shortcomings; no single material is excellent in all respects: processability, thermal oxidative stability at 316°C, toughness, and mechanical properties.

This paper reports on the interim results in developing hybrid matrix composite laminates that combine attributes of two CASTS candidate resins, NR150B2 and LARC 160, while avoiding their drawbacks. Resin forms were selected, quality control techniques were evaluated and developed, high quality laminates were fabricated from both individual resin systems, and initial hybrid laminates were successfully co-cured.

Selection and Initial Tests

To avoid a series of problems associated with the standard NR150B2 with its mixed NMP/ethanol solvent system, three batches of NR150B2G were ordered from DuPont. NR150B2G is the designation for NR150B2 dissolved in pure NMP (approximately 49 wt% resin solids content).

LARC 160 A3 was initially selected over LARC 160 to avoid solvent-associated complications in processing. Three batches of LARC 160 A3 were synthesized according to the procedure published by T. L. St. Clair and R. A. Jewell (ref. 1). All LARC 160 A3 and NR150B2 batches were stored in a -27°C freezer.

Cured resin solids content tests were run on all batches with excellent reproducibility as shown in Table 1.

Table 1

<u>Sample</u>	<u>NR150B2G52</u>		
	<u>Batch 1</u>	<u>Batch 2</u>	<u>Batch 3</u>
a	49.1	48.9	48.9
b	49.0	48.8	48.9
c	<u>49.0</u>	<u>48.9</u>	<u>48.9</u>
Avg. $\pm \zeta$ (%)	49.0 \pm .1(.2)	48.9 \pm .1(.2)	48.8 \pm .1(.2)

	<u>LARC 160 A3</u>		
	<u>Batch 1</u>	<u>Batch 2</u>	<u>Batch 3</u>
a	77.2	77.2	77.3
b	76.8	77.1	77.4
c	<u>77.1</u>	<u>77.2</u>	<u>77.2</u>
Avg. $\pm \zeta$ (%)	77.0 \pm .2(.3)	77.2 \pm .1(.1)	77.3 \pm .1(.1)

Instrumental Analysis of Polyimide Matrices

Infrared analysis (IR) and high pressure liquid chromatography (HPLC) were applied to NR150B2 and to LARC 160 A3. The IR characterization was reproducible, but poorly correlated to processing characteristics. HPLC work was less reproducible, especially with NR150B2. Again, poor correlation with processing characteristics was observed. Additional developmental work is needed to develop HPLC into a truly quantitative tool. A more complete definition of the signal is required and real correlations must be made between HPLC traces and processing aromatics in various resin batches. Table 2 summarizes the results of this work.

Table 2

<u>Technique</u>	<u>Resin</u>	<u>Procedure</u>	<u>Efficiency</u>
IR	NR150B2G	As developed by General Dynamics, Convair Division (Ref. 2)	Reproducible, agrees well with literature, no correlation with processing.
	LARC 160 A3	Standard SRI Approach	As above
HPLC	NR150B2G	Per Du Pont recommendations, μ B C-18 Column, acetonitrile solvent.	Poor reproducibility, batch variations of as much as 22%, no correlation with processing.
	LARC 160 A3	Per NASA-Langley procedures, buffered (7.5 pH) NMP solvent.	Better reproducibility than for NR150B2G, poor correlation.

Acid and Amine Titrations

The procedure for acid titration developed by DuPont consists of weighing a sample of resin ($\pm .0001\text{g}$) and dissolving it in 50 ml of acetone. A potentiograph with a glass/Calomel combination electrode is used to titrate the sample with .1N tetrabutyl ammonium hydroxide (TBAH) in isopropanol. The acid titrations have been postponed due to the unavailability of TBAH.

The determination of the amine content is more difficult. DuPont did not have a satisfactory procedure for determining the amine content of NR150B2G. From a brief literature search for applicable conditions, acetonitrile as the solvent and HCl as the titrate were chosen.

A later modification was the substitution of tetrahydrofuran (THF) as the solvent for the NR150B2G and .1N HCl in Ac \equiv N as the titrant. This gave excellent reproducibility, with a variation on the order of 1%.

A similar investigation was undertaken for LARC 160 A3. Since both resins are monomeric mixtures of acids and amines, one would expect similarities in their behavior during titration. The final conditions for titrating the amines in LARC 160 A3 are essentially the same as those for NR150B2G; the sample is dissolved in THF and titrated with .1N HCl in acetonitrile.

Table 3 summarizes the data.

Table 3

A. LARC 160 A3

	Batch 1	Batch 2	Batch 3
a (g/meq) ⁺	454	342 [*]	399
b (g/meq) ⁺	467	401	397
c (g/meq) ⁺	462	391	400
Avg. $\pm \zeta$ (%)	461 \pm 7 (1.5)	396 \pm 7 (1.8) [#]	399 \pm 2 (.5)

B. NR150B2G

	Batch 1	Batch 2	Batch 3
First equivalence points (g/meq) ⁺			
a	1256	1237	1177
b	1251	1170	1136
c	<u>1232</u>	<u>1252</u>	<u>1139</u>
Avg. $\pm \zeta$ (%)	1246 \pm 13 (1)	1220 \pm 44 (4)	1151 \pm 23 (2)
a	644	637	611
b	637	630	492
c	<u>639</u>	<u>641</u>	<u>618</u>
Avg. $\pm \zeta$ (%)	640 \pm 4 (.6)	636 \pm 6 (.9)	607 \pm 13 (2)

^{*}Difficult, arbitrary analysis of titration curve.

[#]The average does not include the sample whose curve was difficult to analyze.

⁺g/meq = grams of raw resin divided by milliequivalents.

NR150B2 Process Development

Small laminates, nominally 10 cm square, were fabricated without much difficulty. Variations in prepreg staging were explored, as were hold times at various temperatures during cure. Volatiles and resin content were determined as a function of staging time. Dielectric measurements were taken on all runs using an Audrey II unit.

Good results were obtained on the small laminates and the properties of small laminates made from three batches of NR150B2G, all of which had similar processing and handling characteristics, are summarized in Table 4.

Scale-up problems were manifested in localized areas of delamination or blistering. In fabricating $[0^\circ]_{10}$, 19 cm x 20 cm laminates from the various batches of NR150B2G areas of individual laminates gave high properties, but major flaws were always found.

Most problems were tentatively attributed to incomplete solvent removal. A dense, low-void surface makes it very difficult to get additional volatiles out of the center of the laminate. Small laminates facilitate solvent removal and avoid the problem, while larger laminates exhibit localized delamination and voids. If solvent is not removed, plasticization is observed, resulting in poor elevated temperature performance.

Table 4

	52-1 (2675-19)	52-2 (2676-33)	52-3 (2675-35)	53-3* (2675-51)
Staging at 177°C	60 min	30 min	22 min	24 min
Appearance of surface	Smooth	Smooth	Smooth	Smooth
Resin solids content (%)	42.6	49.8	34.0	36.0
Density (g/cc)	1.59	1.48	1.60	1.57
C-scan	Clear	Slightly mottled	Clear	Dark
% of volatiles (based on resin content)	12.4	15.0	30.4	28.8
Ambient short-beam shear values, MPa	87.6	73.5	85.3	87.2
316°C short-beam shear values, MPa	51.6	34.1	36.7	38.1
Ambient flexure values, MPa	-	-	-	1,069
316°C flexure values, MPa	-	-	-	612

* A larger laminate made using the same processing used for 2675-35.

NR150B2GS6X Process Development

At the start of the program, a batch of NR150B2GS6X was included in all types of evaluations. This is the designation of NR150B2 solids dissolved in pure diglyme [bis(2-methoxyethyl)-ether] solvent. Diglyme proved far easier to remove during cure than did NMP, allowing successful fabrication of the larger laminates. The cure schedule developed for this material follows:

- (1) Apply full vacuum to be held until cool-down
- (2) Heat to 199°C under vacuum only, hold 60 min at 199°C
- (3) Apply 2.07 MPa, heat to 249°C, hold 60 min at 249°C
- (4) Heat to 352°C, release pressure at 352°C, heat under vacuum only to 399°C
- (5) Apply 2.07 MPa at 399°C, heat to 427°C, hold 1 hour under pressure and vacuum
- (6) Release pressure, cool slowly under contact pressure, releasing vacuum below 343°C.

Table 5 summarizes the laminate properties and compares them to contract goals.

As a result of this work, NR150B2GS6X was selected for hybrid composite development.

Table 5

<u>Property</u>	<u>Actual Results</u>	<u>Contract Goals</u>
Fiber Volume	55.0%	
Resin Content	39.5%	
Specific Gravity	1.62%	
Bleed (Based on laminate weight)	.2%	
T _g (TMA)	385°C	340°C
Average Ambient Short- Beam Shear Values	91.0 MPa	55.2 MPa
Average 316°C Short- Beam Shear Values	39.1 MPa	
Average Ambient Flexure Values (normalized to 60% fiber volume)	1300 MPa	1241 MPa
Average 316°C Flexure Values	596 MPa	
Calculated void content	0.4%	<4.0%

LARC 160 A3 Process Development

It was expected that the development of LARC 160 A3 would proceed more readily than the development of NR150B2. As with NR150B2, high quality small laminates (normally $[0^\circ]_{10}$ 10 cm square) were readily fabricated. Dielectric monitoring was used in all cures. A typical cure schedule for successful small laminates follows:

apply partial vacuum only (5 cm Hg)
heat 2-3°C/min to 163°C
hold 2 hours
heat to 260°C
apply full vacuum and 1.4 MPa
heat to 274°C
hold 1 hour
heat to 316°C
hold 4 hours

Table 6 summarize the properties of laminate made from LARC 160 A3.

However, localized cracks and defects developed in $[0^\circ]_{10}$, 19 cm by 20 cm laminates, suggesting that LARC 160 A3 be replaced in this study by LARC 160 resin.

Table 6

	Batch 1 2675-36	Batch 2 2675-41	Batch 3 2675-44	Batch 1* 2675-56
Resin solids content (%)	26.6	22.0	24.6	35.0
Density (g/cc)	1.58	1.55	1.61	1.58
Average ambient short-beam shear (MPa)	81.2	75.8	79.3	92.9
Prepreg volatile content (%)	0.9	13.76	12.3	12.9
% of flow	11.2	25.9	27.1	21.7
Average ambient flexure strength values (MPa)	-	-	-	1338
Average 288°C short- beam shear values (MPa)	38.3	48.8	42.4	38.5
Average 288°C flexure strength values (MPa)	-	-	-	641

*Larger laminate based on 2675-36

LARC 160 Process Development

In a series of process studies the scale-up problem for LARC 160 A3 was not resolved. Therefore, LARC 160 was used as an alternate system and high quality laminates were successfully produced. A typical cure schedule follows:

- o Applied partial vacuum (~ 1 cm Hg)
- o Heated $2.5^{\circ}\text{C}/\text{min}$ to 163°C , held 2 hours
- o Heated to 260°C , and applied full vacuum to 1.4 MPa
- o Heated to 274°C , held for 1 hour
- o Heated to 316°C , held 4 hours
- o Cooled slowly with contact pressure and full vacuum

Table 7 summarizes the laminate properties and contract goals.

Table 7

<u>Property</u>	<u>Actual Results</u>	<u>Contract Goals</u>
Resin Content	24.4%	
Specific Gravity	1.61%	
T _g (TMA)	345°C	340°C
Average Ambient Short-Beam Shear Strength	104.5 MPa	82.7 MPa
Average 316°C Short-Beam Shear	50.5 MPa	-
Average Ambient Flexural Strength	1,482 MPa	1,379 MPa
Average 316°C Flexural Strength	938 MPa	-
Calculated Void Content	<2%	<2%

Hybrid Laminate Fabrication Development

After successfully completing characterization and process development of the component resin system, a co-curing schedule for the hybrid NR150B2GS6X/LARC 160 (NR/LARC) system was developed. Work in this phase of the contract is limited to investigating a LARC-160 laminate covered with NR150 surface plies. The first small laminates were of $[0^\circ]_{12}$, with $[\text{NR}_3/\text{LARC}_6/\text{NR}_3]$ configuration.

Early work at Langley had indicated that the nadic anhydride (NA) component of LARC may migrate into the NR surface and prevent long chain NR molecules from forming. This can manifest itself through blistering and debonding at the NR/LARC interface.

A cure schedule designed to tie up the NA during precompaction successfully avoided the problem in a small laminate. This schedule was applied to a $[0^\circ]_{12}$, 19 cm x 20 cm panel, also $[\text{NR}_3/\text{LARC}_6/\text{NR}_3]$ in configuration.

The resulting laminate showed excellent compatibility between LARC and NR plies as shown in Figure 1. The LARC core was excessively rich, however, resulting in cracking of the core and premature failure of flexure specimens.

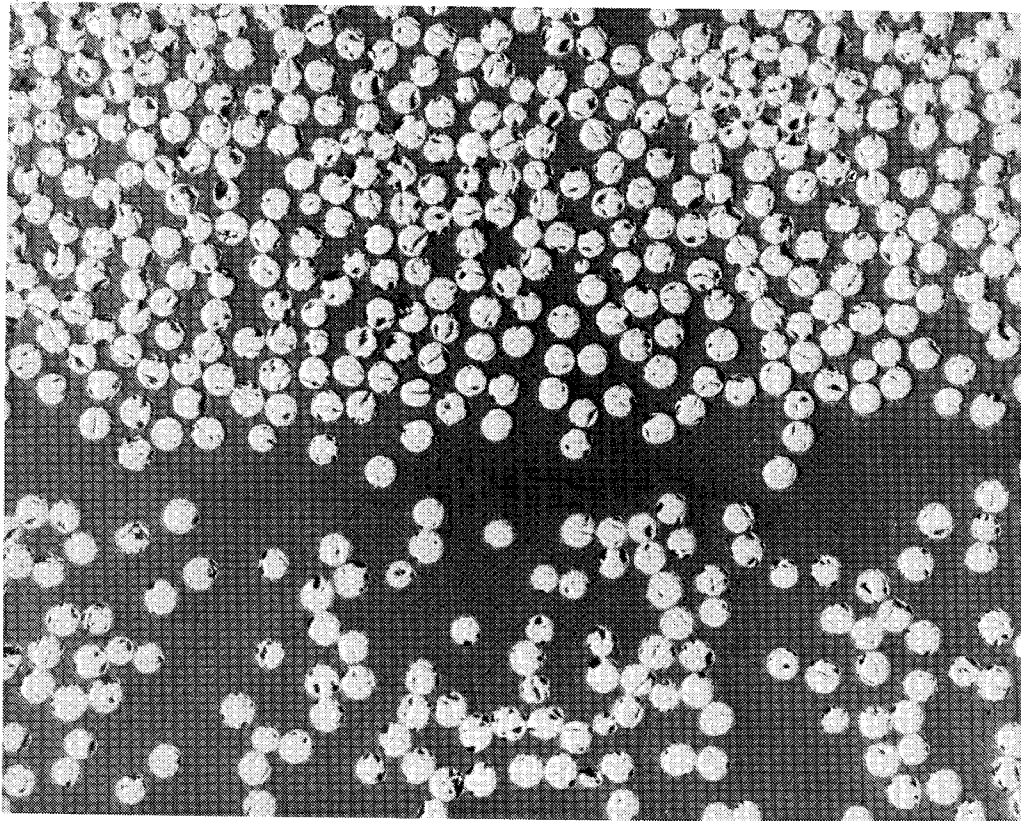


Figure 1

Hybrid Laminate Properties

A laminate $[0^\circ]_{12}, [NR_2/LARC_8/NR_2]$, with separate bleeding of the LARC core during precomposition, and then cured as described below, produced a high quality hybrid laminate. Properties of the two laminates are summarized in Table 8. This concludes the work to date on this contract.

Precompaction Cycle

- 1) Place the 8 ply LARC 160 assembly in vacuum bag.
- 2) Applied full vacuum, with caul plate pressure only, and shims to prevent contact pressure from the press.
- 3) Heat at $2.5^\circ\text{C}/\text{min}$ to 163° , held 2 hours.
- 4) Fast-cooled (Calculated resin 25.7%).

Cure Cycle

- 5) Applied 2 plys NR150B2S6X prepreg to each side of the LARC lay-up (above).
- 6) Place in vacuum bag with bleeder assembly.
- 7) Applied full vacuum and heated to 199°C at $2.5^\circ\text{C}/\text{min}$. Held 1 hour.
- 8) Applied 2.07 MPa and heated to 260°C at $2.5^\circ\text{C}/\text{min}$. Held 1 hour.
- 9) Heated to 399°C at $2.5^\circ\text{C}/\text{min}$. Held 2 hours.
- 10) Cooled slowly under vacuum and contact pressure.

Table 8

<u>Property</u>	<u>Hybrid 1</u>	<u>Hybrid 2</u>
Thickness	2.7 mm	2.0 mm
wt% Resin Content	43.7%	31.5%
Specific Gravity	1.52	1.59
T _g (TMA)	340°C	354°C
Ambient Short-Beam Shear	76.9 MPa	78.9 MPa
316°C Short-Beam Shear Strength	44.0 MPa	43.5 MPa
Ambient Flexural Strength	1158 MPa	1420 MPa
316°C Flexural Strength	620 MPa	820 MPa
Calculated Voids	3.4%	0.6%

REFERENCES

1. T. L. St. Clair and R. A. Jewell, "Solventless LARC 160 Polyimide Matrix Resins, " 23rd National SAMPE Symposium, Anaheim, CA, May 1978.
2. V. A. Chase, "Development of GR/PI Composite Structural Elements" Contract NAS1-14784, Quarterly Report No. 1, June 1977.

HPLC FOR QUALITY CONTROL OF POLYIMIDES

Philip R. Young and George F. Sykes
NASA Langley Research Center

EXPANDED ABSTRACT

The quality control of high-performance polymer matrix resins and pre-pregs is an area vitally important not only to the CASTS Project but also to the aerospace community in general. Simple, reliable, and acceptable techniques to insure that incoming resins and prepregs are of consistent quality must be available if the timely introduction of these advanced materials into aircraft and spacecraft structures is to be successful.

The objectives of the present study are to evaluate High Pressure Liquid Chromatography (HPLC) as a quality control tool for polyimide resins and pre-pregs and to develop a data base to help establish accept/reject criteria for these materials. This work is intended to supplement, not replace, standard quality control tests normally conducted on incoming resins and prepregs. To help achieve these objectives, the HPLC separation of LARC-160 polyimide precursor resin was characterized in detail. Room temperature resin aging effects were also studied. Graphite reinforced composites made from fresh and aged resin were then fabricated and tested to determine if changes observed by HPLC were significant. A discussion of future research in this area is also presented.

HIGH PRESSURE LIQUID CHROMATOGRAPHY

Chromatography is a separation technique. It is used to separate the individual components in a complex mixture so that further analysis and interpretation are possible. A schematic of the liquid chromatograph used to make this study is shown in figure 1. All forms of chromatography require a mobile and a stationary phase. In HPLC, a carrier liquid serves as the mobile phase and small particle silica gel-like material packed into a narrow bore column serves as the stationary phase. Due to these column conditions, a pump is required to force the liquid through the chromatograph. Pressures up to 41.3 MPa (6000 psi) may be used. The sample to be separated is introduced just prior to the column through an injector. Separation occurs in the column due to interactions between the various sample components and the column packing material. The stronger the interaction, the longer the component is retained in the column. A UV detector monitors the carrier liquid and signals a recorder when a component exits the column. The permanent record is called a chromatogram. A separated component can be collected at the detector for identification by some other technique. Fifteen minute analyses on a few micrograms of material are typical.

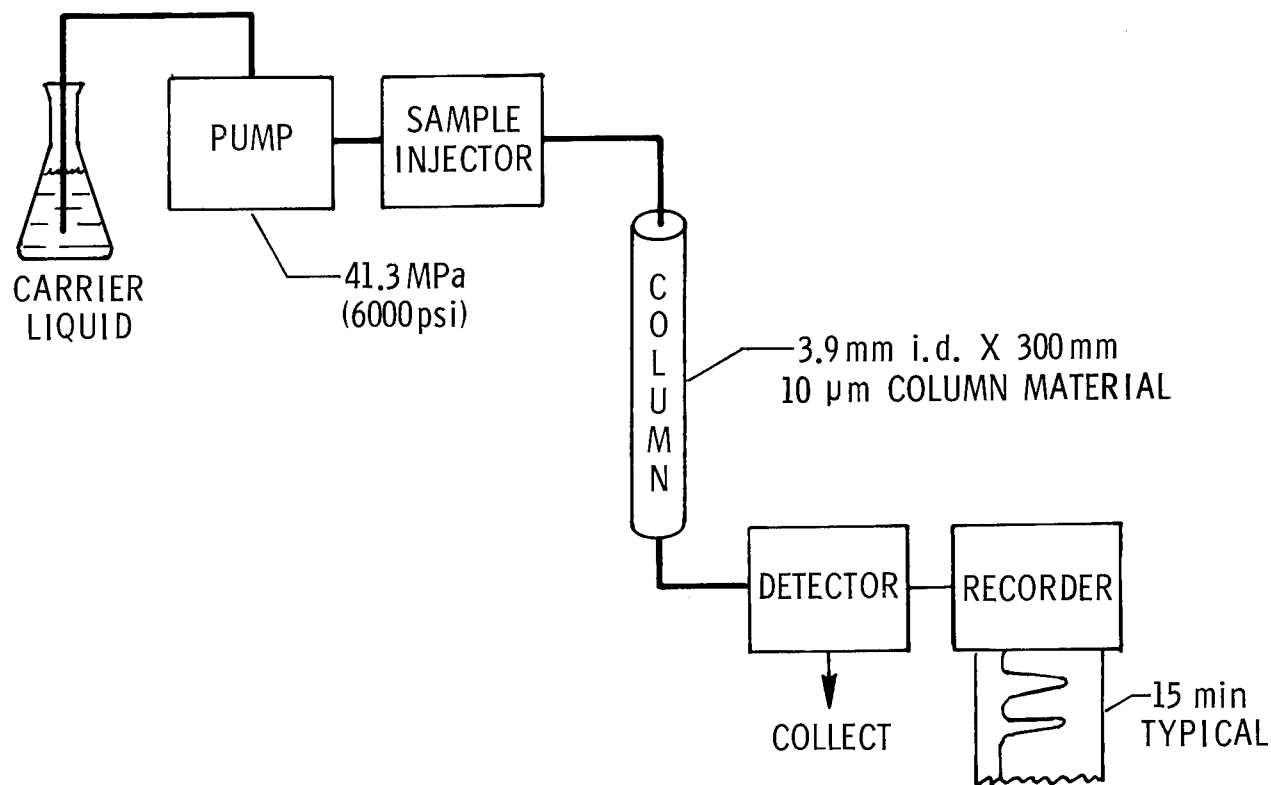


Figure 1

PARAMETERS DETECTABLE WITH HPLC

Some pertinent resin and prepreg quality control parameters detectable with high pressure liquid chromatography are given in figure 2. A fingerprint of the soluble constituents is contained in the chromatogram. However, other techniques such as infrared spectroscopy or mass spectrometry must be used to identify a particular component. A quantitative analysis yielding component purity and stoichiometry is possible by calibrating the detector response using standards. Molecular weight distributions can also be determined by selecting a column which separates components on the basis of size or molecular volume. Finally, resin and prepreg aging can be studied in cases where aging leads to a fingerprint which differs from the fingerprint obtained for a fresh material. Standard quality control tests, such as determinations of areal density, volatile content, and percent resin and fiber, normally run on incoming materials, will not yield this kind of information.

- CONSTITUENTS
- PURITY
- STOICHIOMETRY
- MOLECULAR WEIGHT DISTRIBUTION
- AGING PRODUCTS

Figure 2

CHANGE IN COLUMN PERFORMANCE

The performance of the chromatographic column used to make this study was observed to degrade with use. In figure 3, the number N of theoretical plates, an empirical value related to column efficiency and calculated by injecting a standard, decreases substantially with the number of samples analyzed. This demonstrates that the deterioration in column performance must be carefully monitored when using HPLC for quality control purposes. Otherwise, different investigators using columns of varying chromatographic histories may be unable to duplicate the findings of others or obtain the HPLC separation required for adequate quality control. Column plate count is specified for all separations made during this study. The minimum number of theoretical plates required for a satisfactory separation has not yet been established.

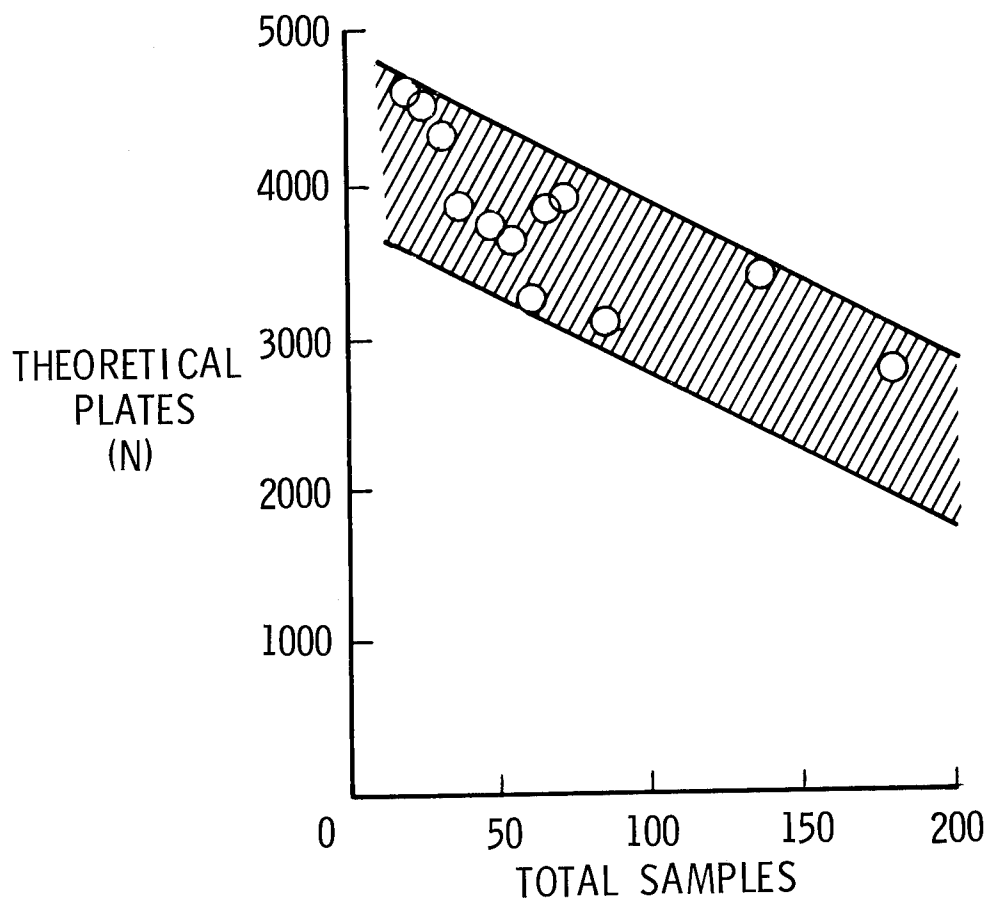


Figure 3

HPLC OF LARC-160 RESIN ON THREE DIFFERENT COLUMNS

Low column efficiency ($N < 1000$) may lead to a misinterpretation of the HPLC resin fingerprint. For example, figure 4 gives the chromatograms obtained for the same resin sample run on a column having 650 theoretical plates and on a column having only 100 theoretical plates. A chromatogram of the same sample run on a very good column ($N = 4600$) is included for comparison. The chromatographic conditions for the separation are also given in the figure. The poor resolution exhibited by the 650 and 100 plate columns is characteristic of low efficiency columns. Figure 4 suggests that an incoming resin or prepreg might be rejected because its HPLC fingerprint was unsatisfactory when, in fact, the material was of a consistent and acceptable level of quality. The unsatisfactory fingerprint might be the result of normal degradation in column performance with use.

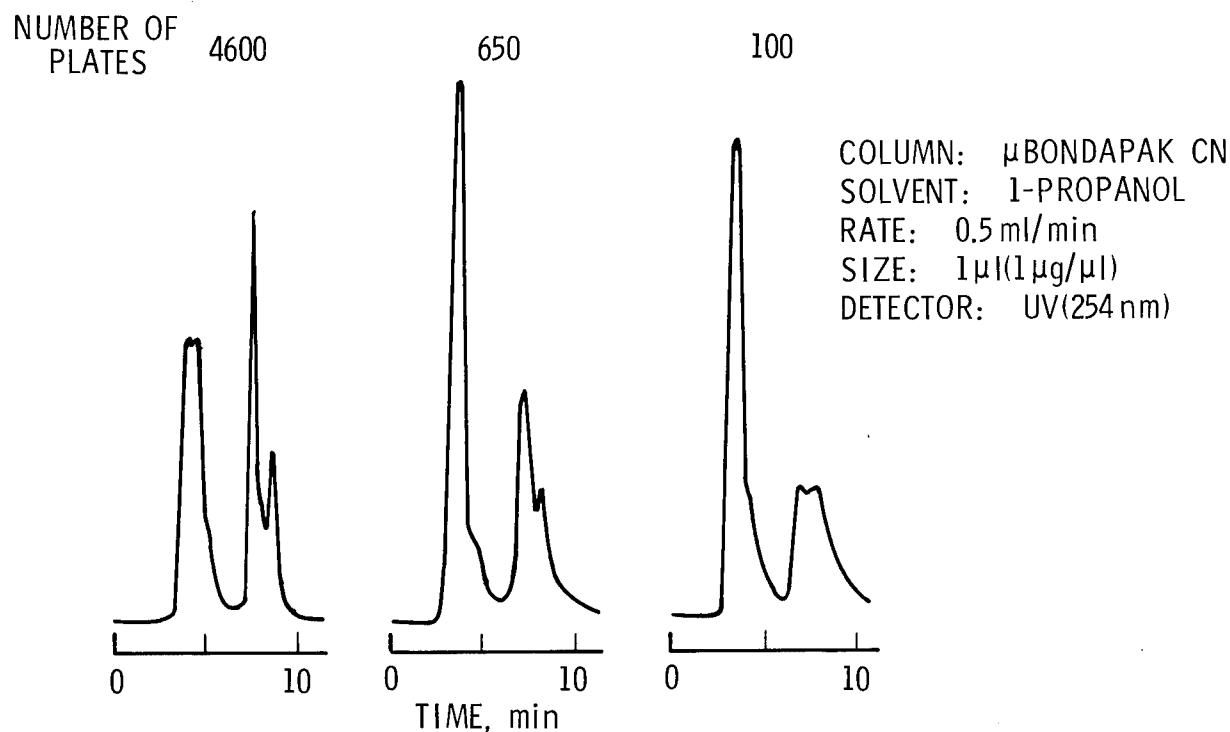


Figure 4

CHARACTERIZATION OF AGED LARC-160 RESIN

Figure 5 gives a chromatogram of room temperature aged (103 days) LARC-160 resin, the chromatographic conditions, and the identification of most of the peaks. The identification was made by collecting the fractions at the detector, evaporating the mobile phase, and transferring the residue to a mass spectrometer where spectra were obtained. The ester of nadic anhydride was not detected in the free state because the compound does not exhibit a UV chromophore at 254 nm.

Compounds I and II were present during preparation of the resin. The other three compounds (III, IV, and V) formed during aging. These three compounds could also be formed during the prepregging and molding operations. The bis-nadimide, IV, is an undesirable product regardless of how or when it is formed, since its formation upsets the designed LARC-160 chemistry. Fresh resin is formulated to yield an average imidized molecular weight of 1600. These 1600-molecular-weight-segments crosslink during cure. The cure of resin containing compound IV may yield more than the normal amount of lower molecular weight, highly crosslinked segments. Linear polyimide must then form to maintain stoichiometry.

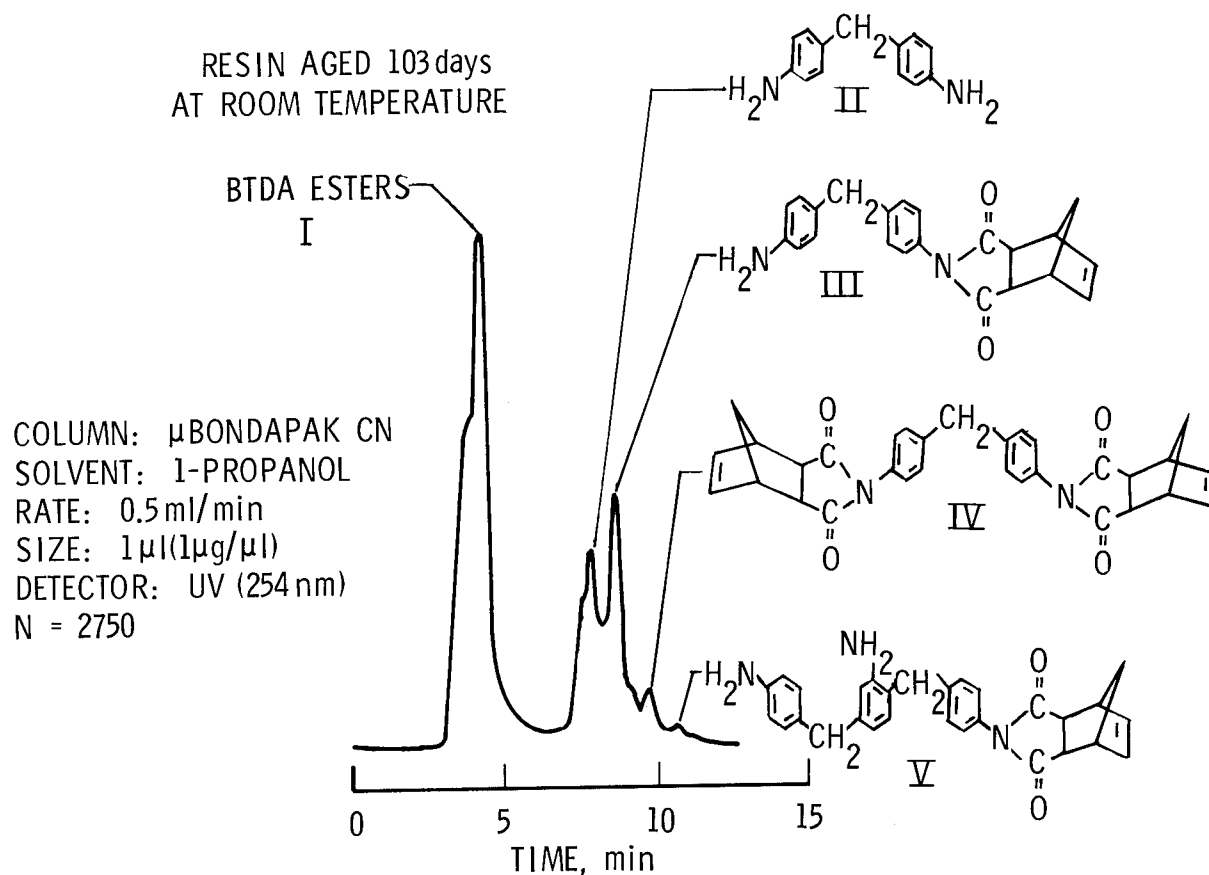


Figure 5

EFFECT OF ROOM TEMPERATURE AGING ON HPLC OF LARC-160 RESIN

After an acceptable HPLC analysis was obtained with confidence and the major peaks identified, the next step of this study was to determine if the observed changes markedly affected either processing or composite properties. Thus, a batch of LARC-160 resin was prepared and stored at room temperature. Periodically, samples were withdrawn and analyzed. Figure 6 shows how the HPLC fingerprint of this batch changed with time. A comparison with figure 5 shows that the amount of compound II decreased with aging while the amounts of III, IV, and V increased.

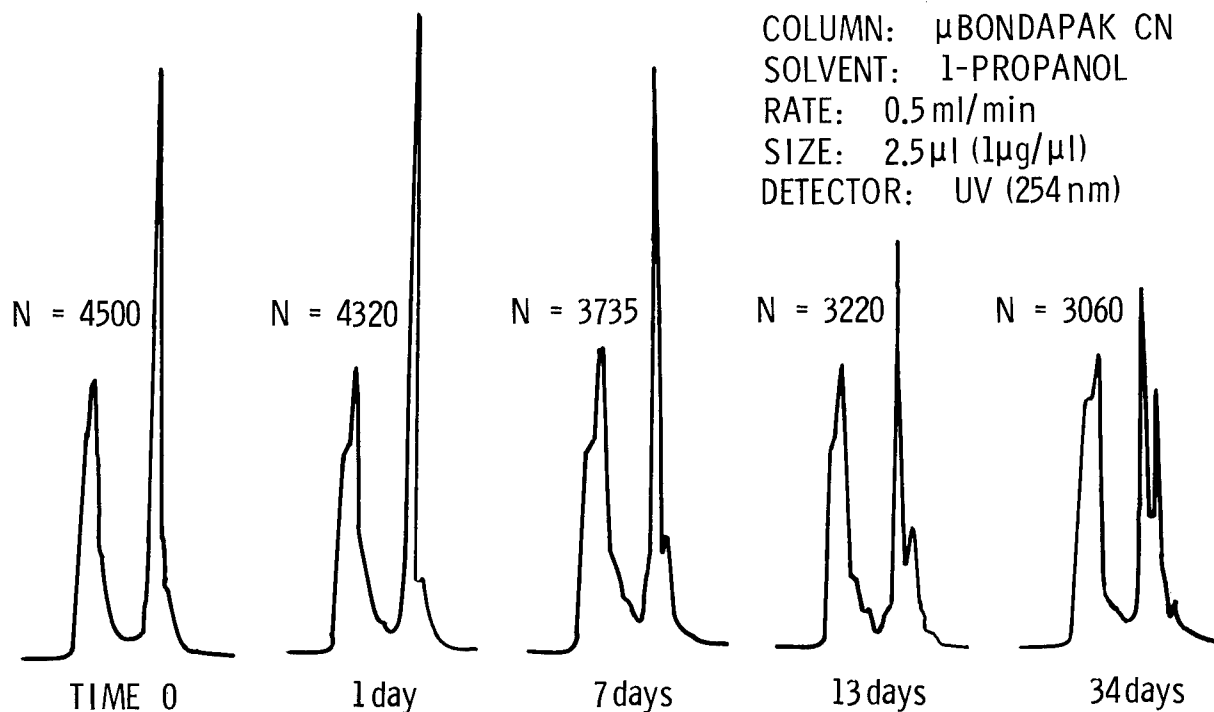


Figure 6

ROOM TEMPERATURE MECHANICAL PROPERTIES OF HTS1/LARC-160 COMPOSITES

Eight and 16-ply HTS1 graphite composites were prepared from a fresh batch of resin and from a batch of resin aged for 45 days at room temperature. Prepregging, laying-up, B-staging, and molding were conducted under identical conditions for each batch. Figure 7 shows the relative performance of the composites made from fresh and aged resins as determined from flexural strength, flexural modulus, and short-beam-shear measurements. For the aged resin composites, these values were 2100 MPa (305 Ksi), 151,000 MPa (21,700 Ksi), and 82 MPa (11.9 Ksi), respectively. The room temperature mechanical properties of composites made from fresh and aged resin appear to be about the same. Therefore, changes in resin chemistry with time, as fingerprinted in figure 6, may not be reflected in the room temperature mechanical properties, at least not those measured during this study.

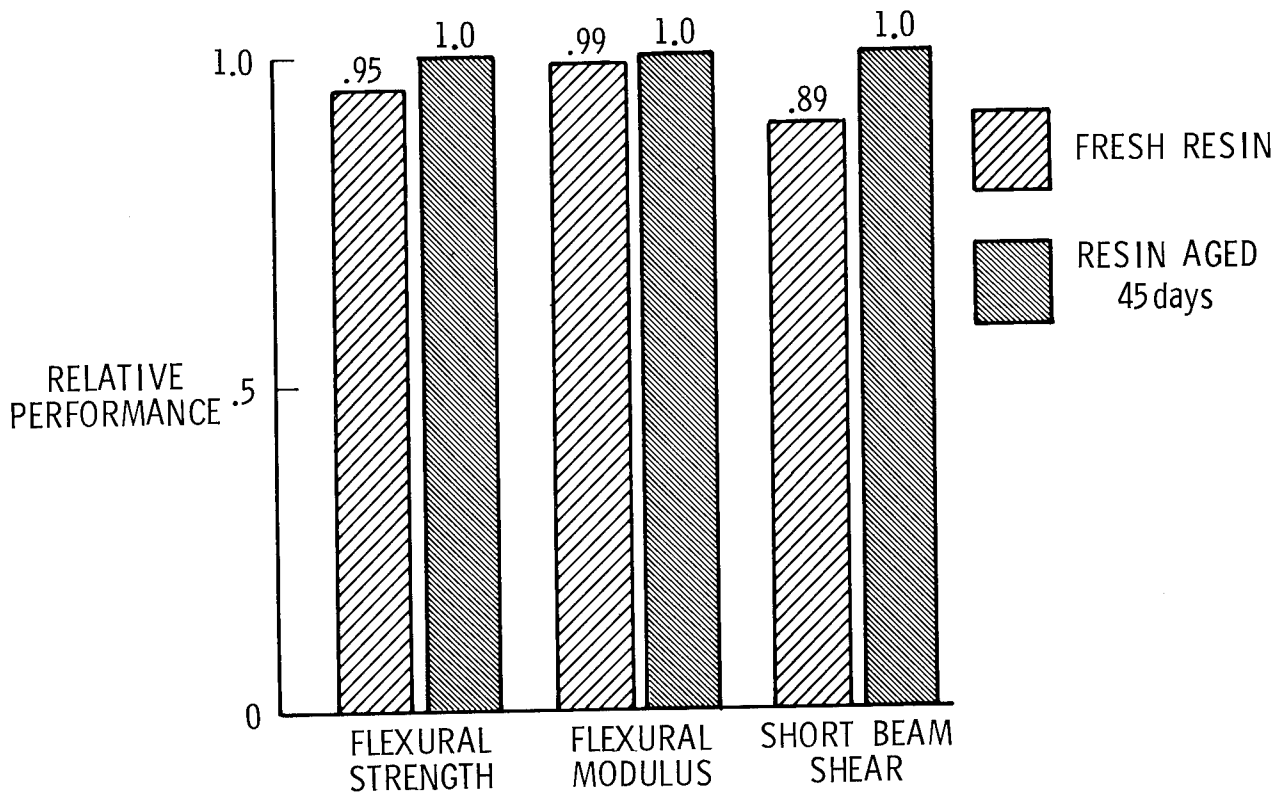


Figure 7

EFFECT OF AGING ON VISCOSITY OF LARC-160

The flow characteristics of thermally staged fresh and aged resin were also studied to determine if resin aging could affect the molding of composites. A sample of fresh resin was heated to 463 K (374° F) for 30 minutes in nitrogen, cooled to room temperature, ground up, and stored in a desiccator until tested. A second sample of the resin aged for 35 days was similarly treated. The difference in viscosity for the thermally staged fresh and aged resin was significant. Figure 8 shows at least an order-of-magnitude difference between the viscosity/temperature curves over most of the temperature range tested. The fact that aged resin had a lower viscosity when thermally treated indicated that its ability to be processed could be affected. Indeed, greater flow was visually observed in this study during molding of aged-resin/graphite composites than was observed during molding of fresh-resin/graphite composites. Some of the changes in resin chemistry fingerprinted in figure 6 play a role in resin viscosity.

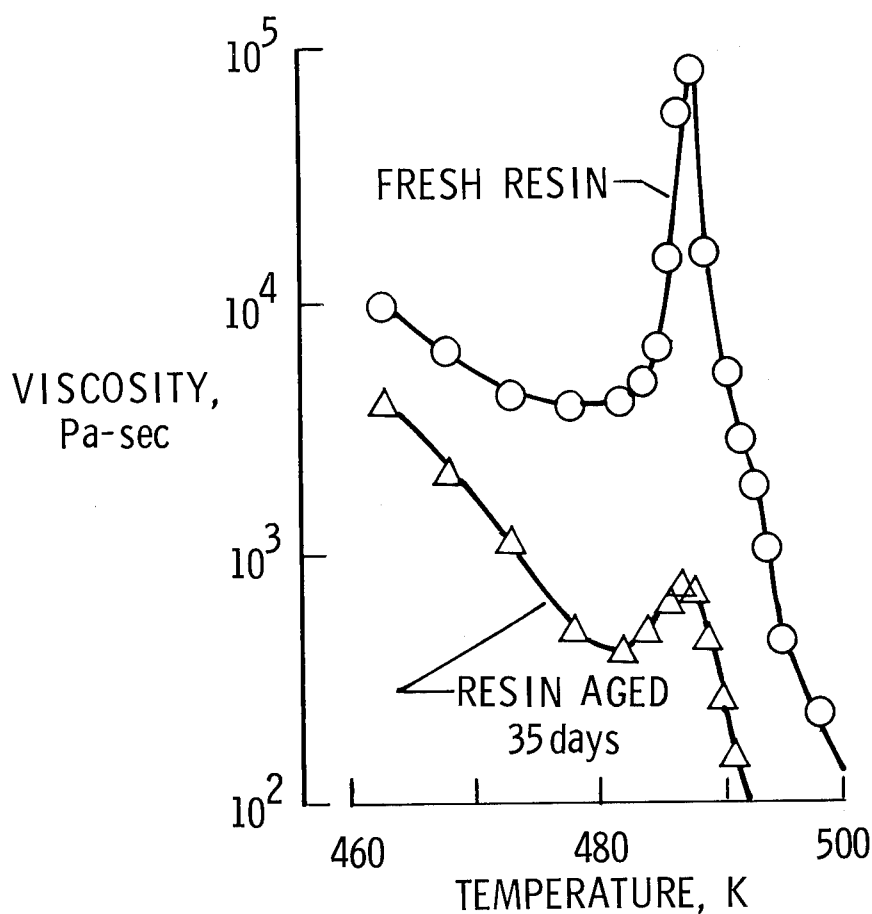


Figure 8

ISOTHERMAL WEIGHT LOSS AT 589 K (600° F) FOR HTS1/LARC-160 COMPOSITES

Short beam shear specimens were thermally aged at 589 K (600° F) and their weight loss measured periodically. These data are presented in figure 9 where each point represents the average weight loss of three specimens. The greater weight loss of the aged-resin composites was significant. The data suggest that if mechanical property measurements were made after periodic isothermal aging at 589 K, greater differences than those noted in figure 7 for composites made from fresh and aged resin on HTS1 would be observed. In a practical sense, a composite cannot tolerate much weight loss and maintain acceptable mechanical properties. Once again, resin changes fingerprinted by HPLC appear to be influencing results in a pertinent area, isothermal stability.

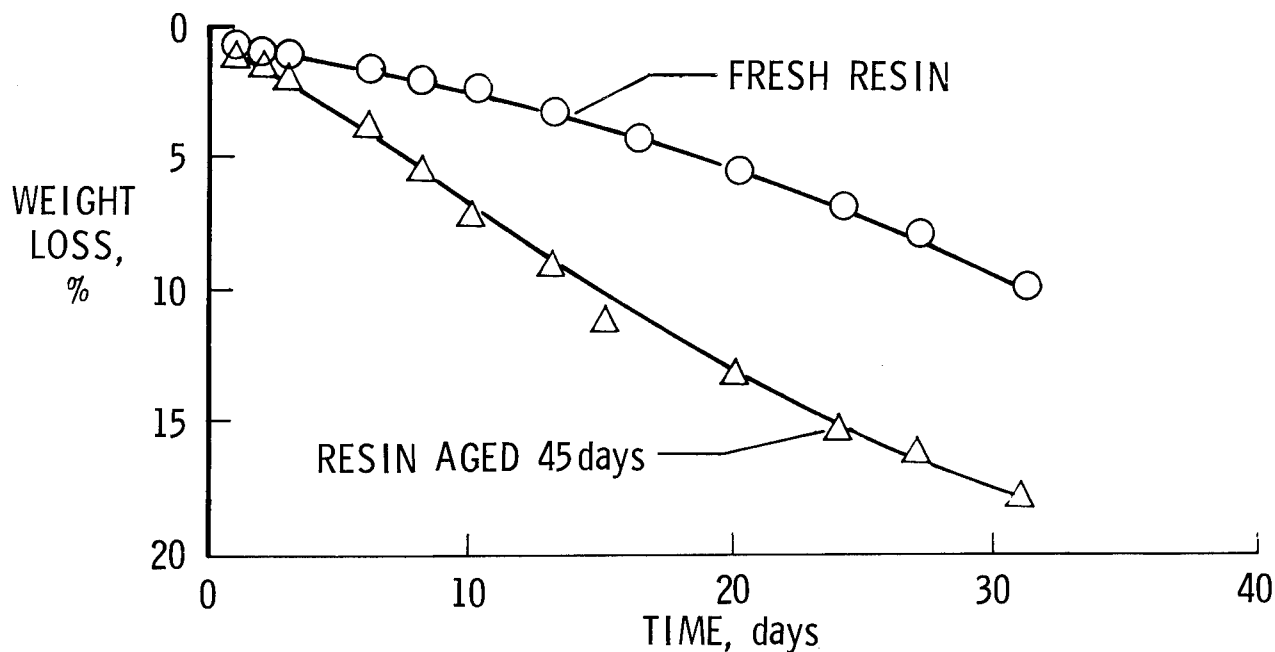
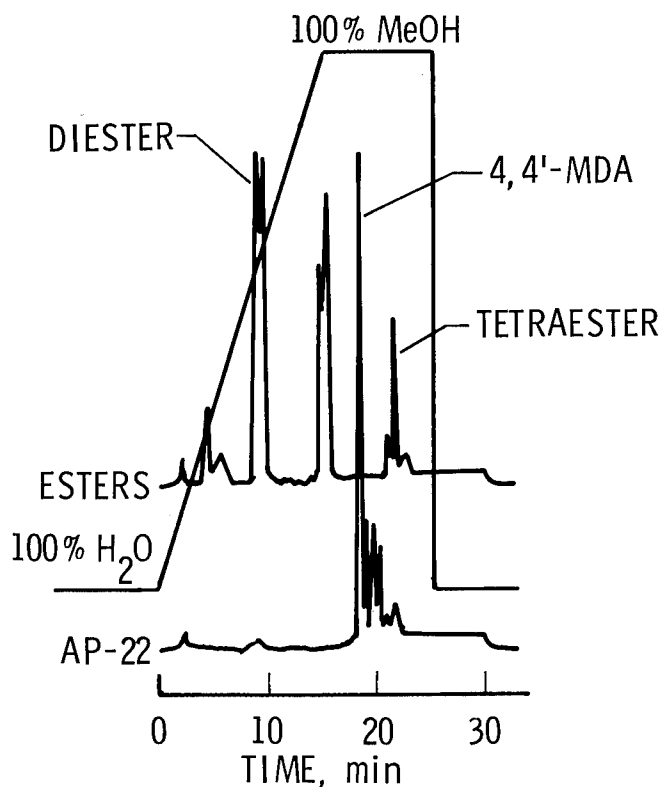


Figure 9

GRADIENT ELUTION HPLC OF LARC-160 STARTING MATERIALS

Although initial efforts to develop HPLC as a quality control tool for polyimides were satisfactory, future efforts will probably involve a chromatographic technique known as gradient elution. With this technique, the composition or polarity of the liquid phase is changed during the analysis. This requires an additional pump and a solvent programmer not shown in figure 1. Gradient elution in liquid chromatography is somewhat analogous to temperature programming in gas chromatography. Besides being able to separate a wider polarity range of sample components, the technique tends to regenerate the column each time the solvent program is run. Figure 10 shows the gradient elution HPLC of the starting materials used to formulate LARC-160 resin. The linear solvent program from 100% water to 100% methanol in 15 minutes is also included along with other pertinent chromatographic informations. The various esters and amines are easily resolved using this technique.



COLUMN: WHATMAN-10 ODS-2
PRECOLUMN: C₁₈-CORASIL
GRADIENT: H₂O → MeOH IN 15 min
FLOW RATE: 1.0 ml/min
SIZE: 10 μl (2 μg/μl)
DETECTOR: UV (254 nm)

Figure 10

GRADIENT ELUTION HPLC OF FRESH AND AGED LARC-160 RESINS

Gradient elution separations of fresh and aged LARC-160 resins are given in figure 11. The individual starting materials can be identified by comparing the chromatogram of the fresh resin with chromatograms of the starting materials given in figure 10. Resin changes due to aging are also easily detected. For example, the peak for 4, 4'-methylenedianiline which dominates the chromatogram of the fresh resin is a minor peak in the chromatogram of the aged resin. Compound III in figure 5, an aging product, is the dominant peak in the chromatogram of the aged resin. Other aging products have not been identified. Attempts will be made to correlate the information contained in these chromatograms with processing and mechanical properties. The improved resolution of constituents shown in figures 10 and 11 should enable a more detailed quantitative analysis to be made. Perhaps the greatest hope of establishing an HPLC criterion for either accepting or rejecting polyimide resins and prepreps lies in this type of separation.

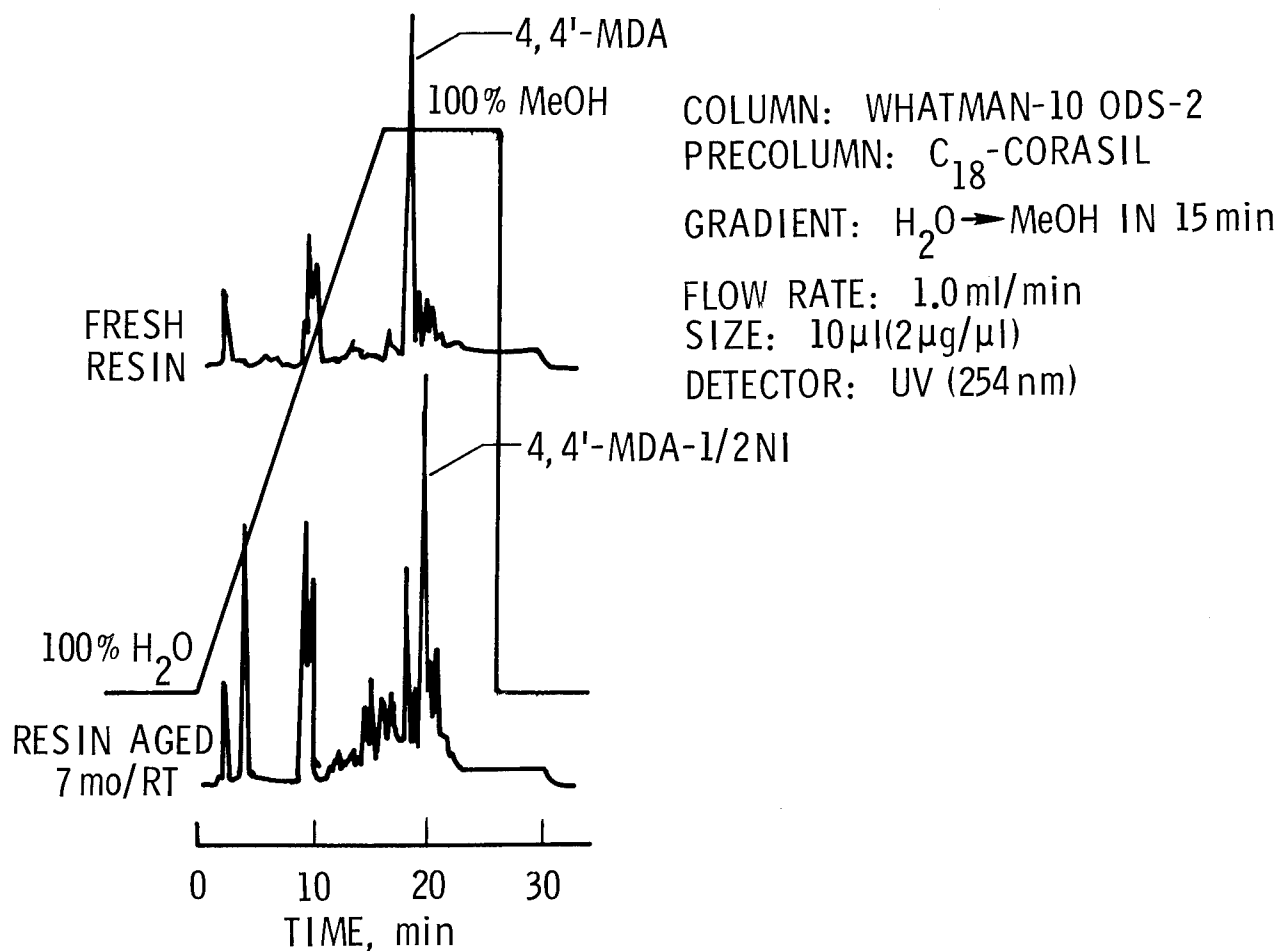


Figure 11

CONCLUDING REMARKS

Figure 12 summarizes the concluding remarks. High pressure liquid chromatography proved to be a valuable tool for fingerprinting changes in LARC-160 chemistry as the resin aged. Major aging products were identified. Graphite composites made from aged resin exhibited greater flow during processing and poorer isothermal stability as measured by isothermal weight loss at 589 K (600° F). However, changes in resin chemistry due to room-temperature storage did not affect room-temperature flexural or short-beam-shear strengths.

Future work will concern optimizing and quantifying a gradient elution separation of LARC-160 resin components. Efforts to correlate HPLC results with composite properties will continue.

- HPLC IS A VALUABLE TOOL FOR FINGERPRINTING RESIN CHANGES
- FINGERPRINTED CHANGES WERE CORRELATED WITH COMPOSITE BEHAVIOR

FUTURE WORK

- OPTIMIZE GRADIENT ELUTION SEPARATION
- CONTINUE EFFORTS TO CORRELATE HPLC RESULTS WITH COMPOSITE PROPERTIES

Figure 12

QUALITY ASSURANCE OF PMR-15

A. B. Hunter
Boeing Aerospace Company

EXPANDED ABSTRACT

The potential use of Graphite/PMR-15 polyimide in space transportation systems requires satisfactory method development for Quality Assurance.

This task of the program was devoted to establishing controls on the PMR-15 resin and/or prepreg to ensure a solid base for the subsequent process development task. The effort was divided into subtasks which included evaluation of commercially available graphite/PMR-15 polyimide preregs, detailed evaluation of materials and selection of chemical test procedures. During the initial phase of the program a variability problem was detected in the PMR-15 resin. The preliminary work accomplished to date identified the manufacturing and/or storage of the PMR-15 resin/esters as the chief cause for the variability with additional evaluations presently being conducted to confirm this conclusion.

PLAN FOR CHEMICAL CHARACTERIZATION OF PMR-15 GRAPHITE MATERIAL

Initial samples of PMR-15 material were submitted to an extensive analysis as indicated in Figure 1. The testing consisted of working through a chemical characterization schematic, reviewing the analysis methods and selecting those chemical tests that could adequately characterize the PMR-15 system.

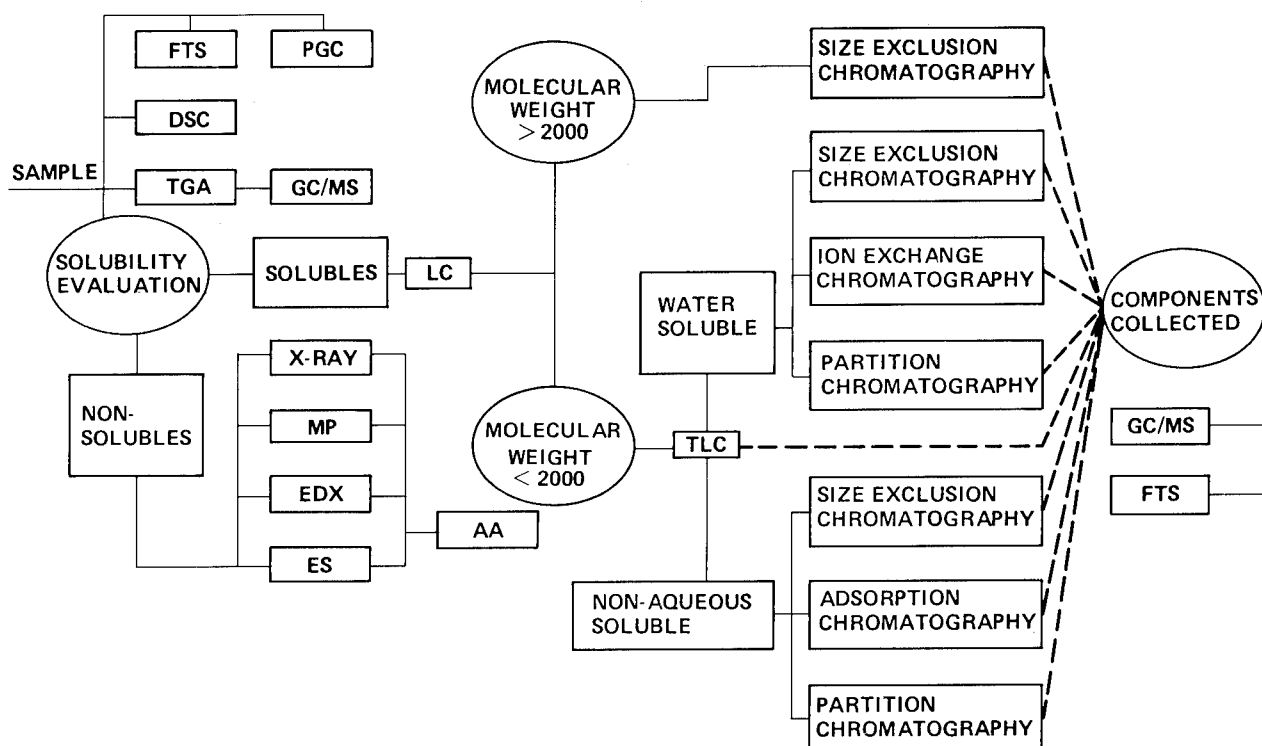


Figure 1

INFRARED ANALYSIS

The first method selected for characterizing the PMR-15 system was Infrared Spectroscopy. Using Fourier Transform Infrared Spectroscopy (FTS), imidization shows up readily at 1770 cm^{-1} . Also, the method is very useful in following the polymerization reaction of PMR-15 as noted by Figure 2.

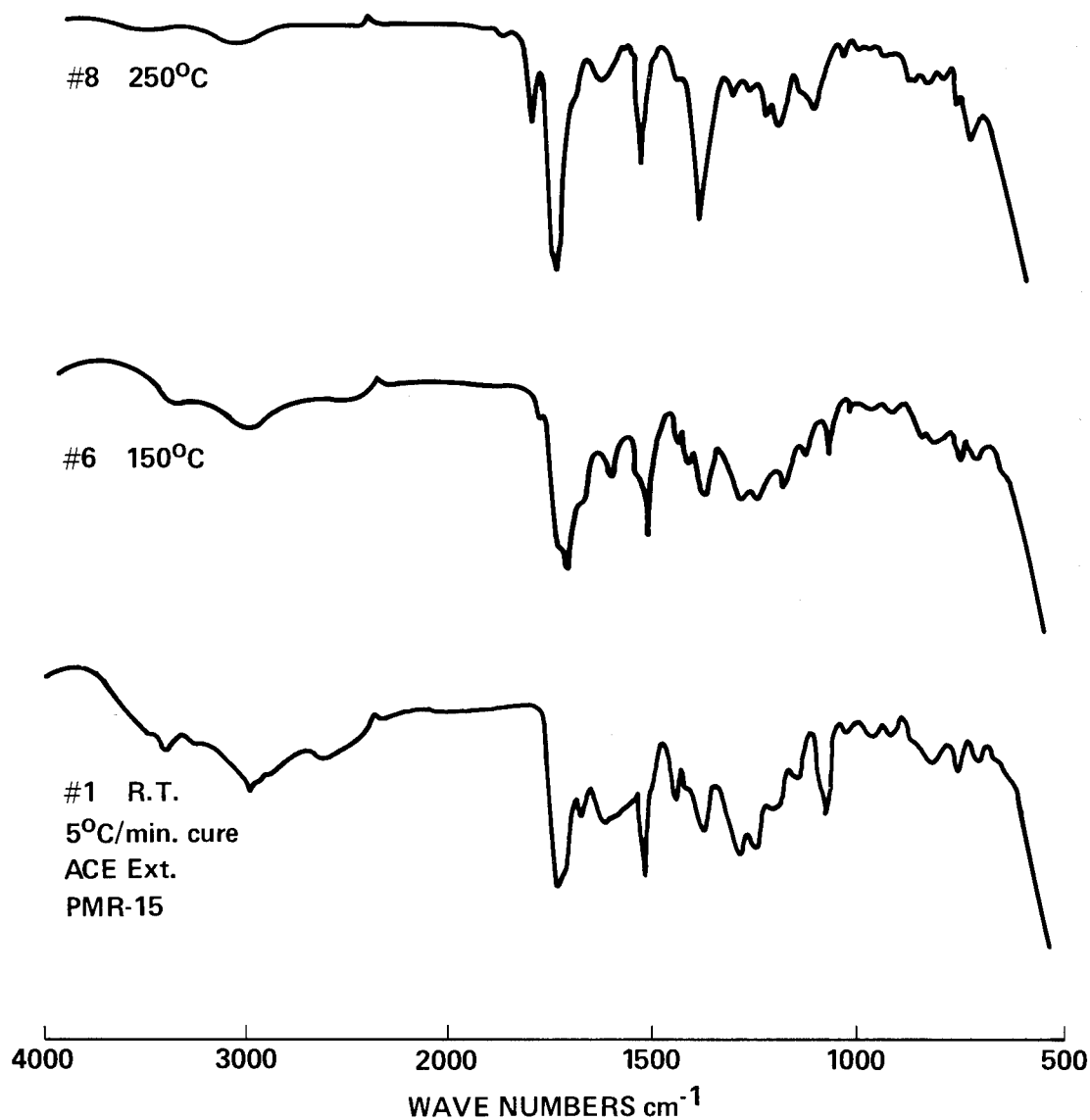


Figure 2

MASS CHROMATOGRAM

The next method used to characterize the PMR-15 resin was Gas Chromatography/Mass Spectrometry. This analysis identifies the thermal breakdown products of PMR-15 and also, the solvents used in its preparation. Using the Mass Spectrometer, unwanted solvents can be detected. Using this technique, figure 3 identifies methanol used with the batch analyzed. Other solvents have been used and identified with other batches.

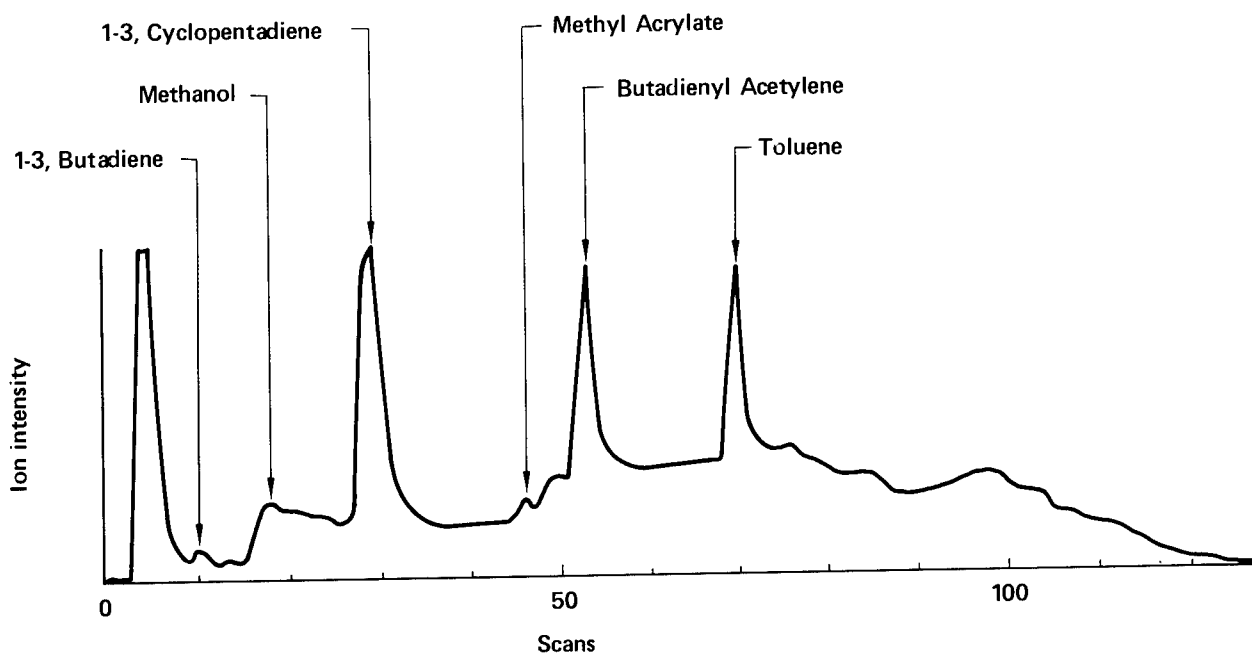


Figure 3

THERMAL GRAVIMETRIC ANALYSIS

The third technique selected for chemically characterizing the PMR-15 system was Thermal Gravimetric Analysis (Figure 4). This figure shows volatilization occurring during the initial reaction and finally the decomposition of the sample.

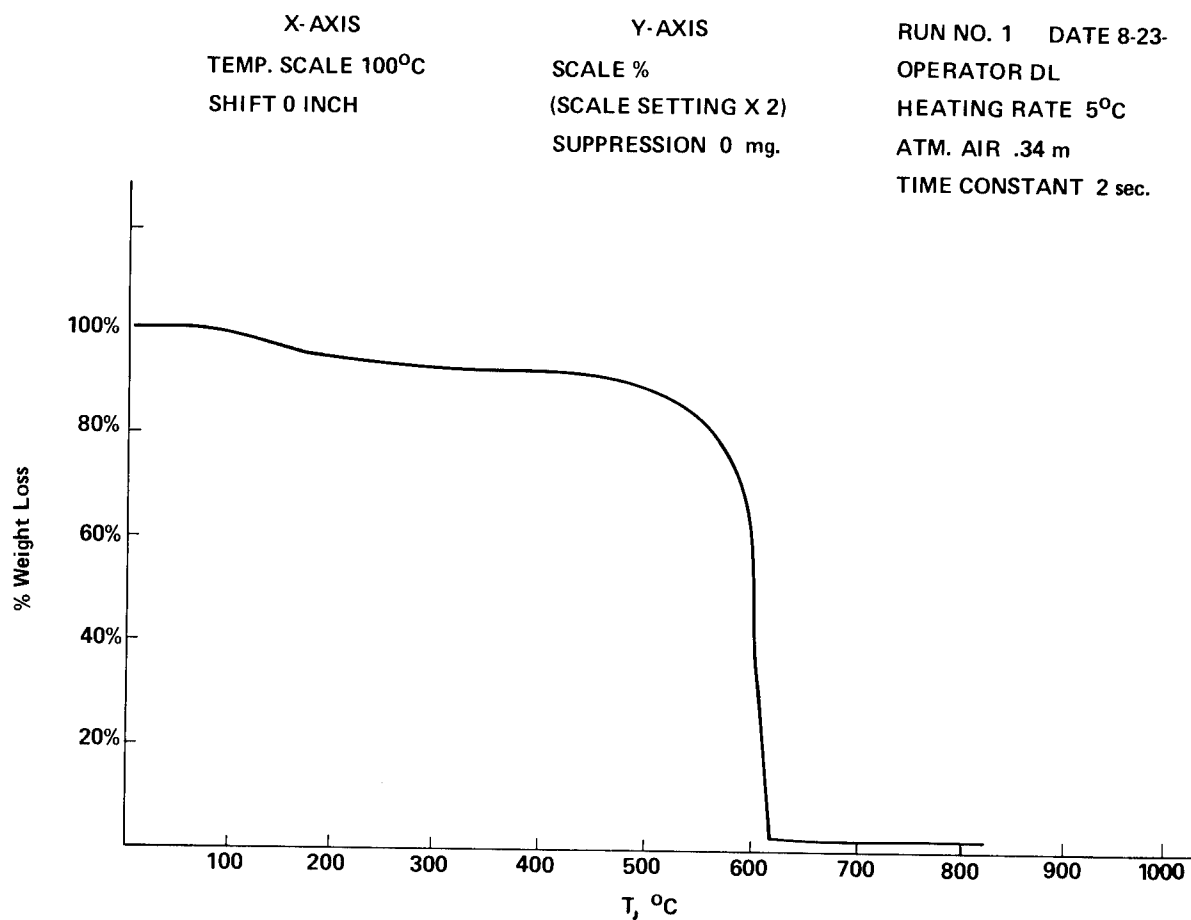


Figure 4

REVERSE PHASE CHROMATOGRAPHY

The last method selected for characterizing the PMR-15 resin was Liquid Chromatography. Much effort was spent in developing LC methods. This included a preliminary evaluation of mobile phases and packing material by Thin Layer Chromatography. Various modes were then evaluated on the Liquid Chromatograph. An isocratic reverse phase method (Figure 5) gave good separation with considerable detail. The analysis was done with 45% H₂O: THF mobile phase using a UV detector at 254 nm.

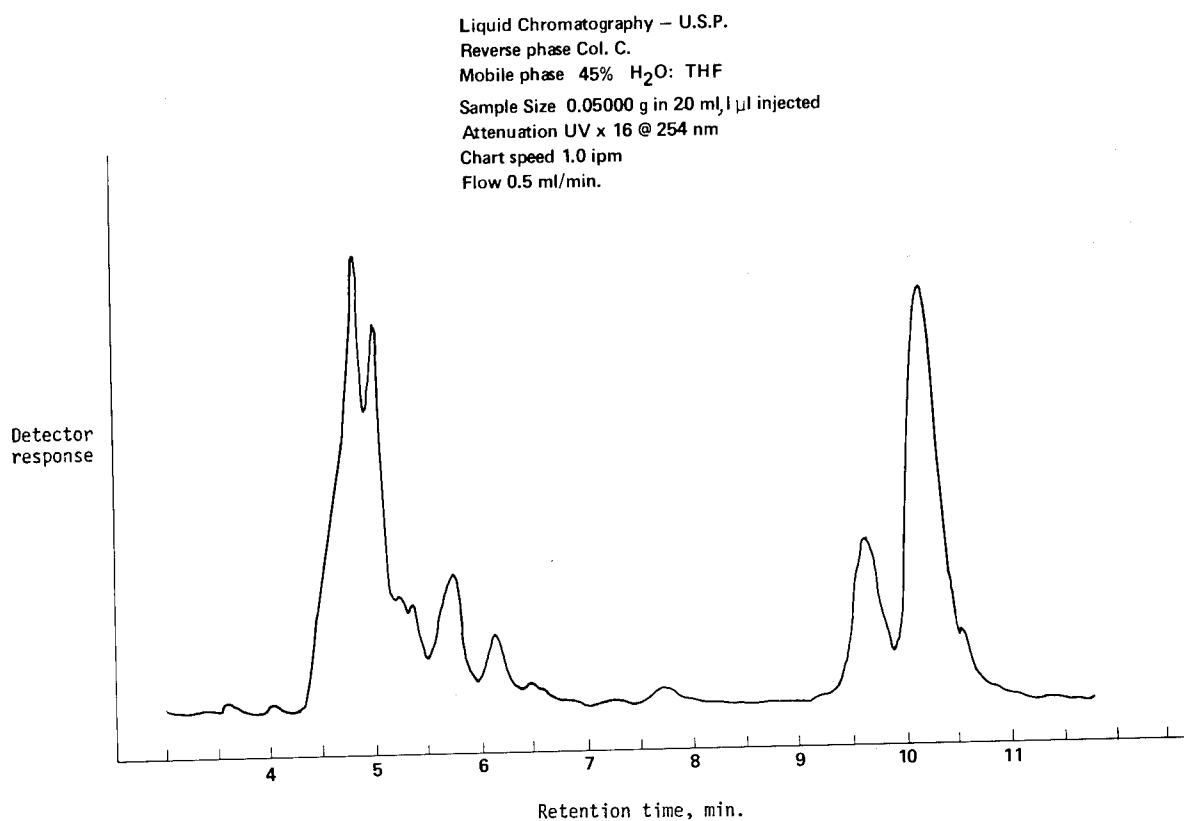


Figure 5

ADSORPTION CHROMATOGRAPHY

Another separation method was used with a microporosil column and tetrahydrofuran as the mobile phase, (Figure 6). The detector was UV at 254 nm. This method did not show the detail observed with reverse phase.

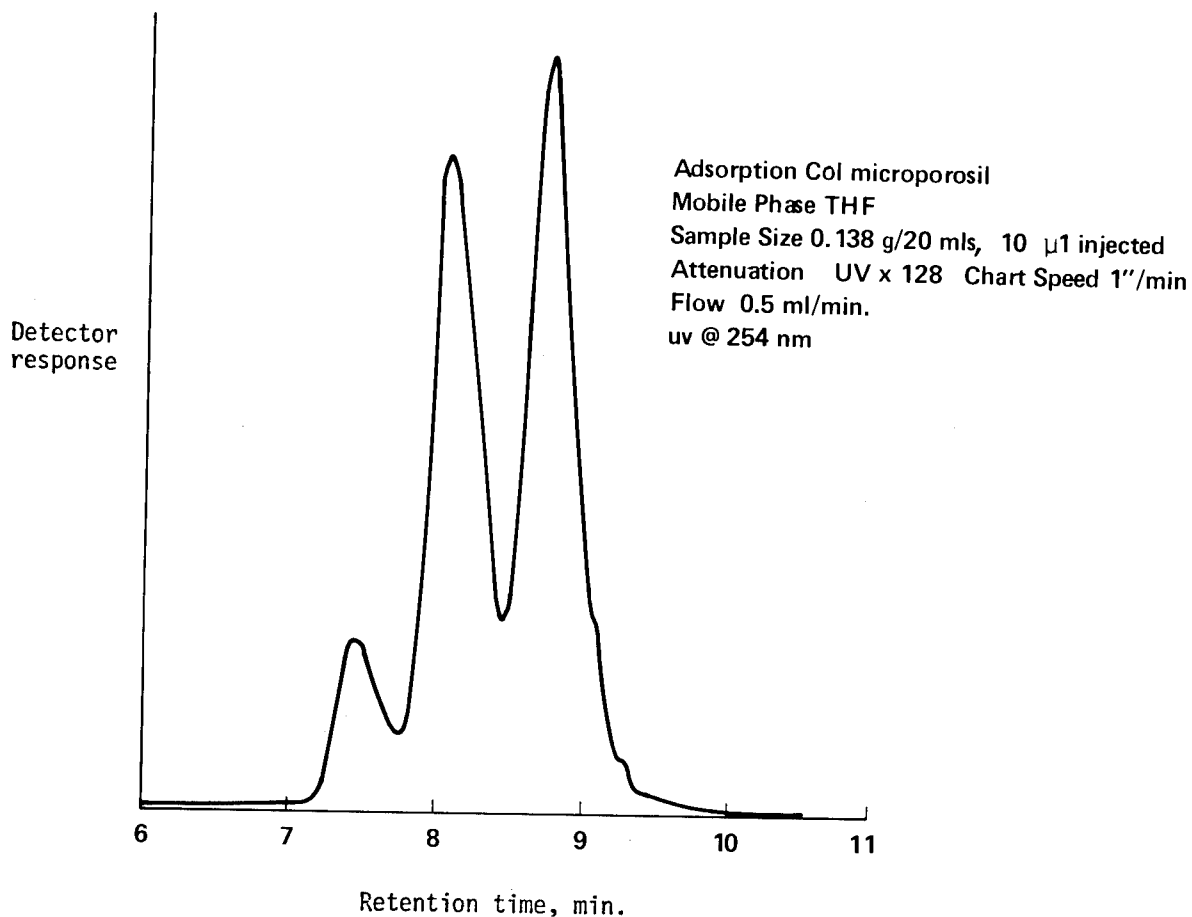


Figure 6

SIZE EXCLUSION CHROMATOGRAPHY

A determination was made to use size exclusion chromatography using silanized silica columns with methanol as a mobile phase and the UV detector at 254 nm (Figure 7). It was observed that this method did not provide adequate resolution.

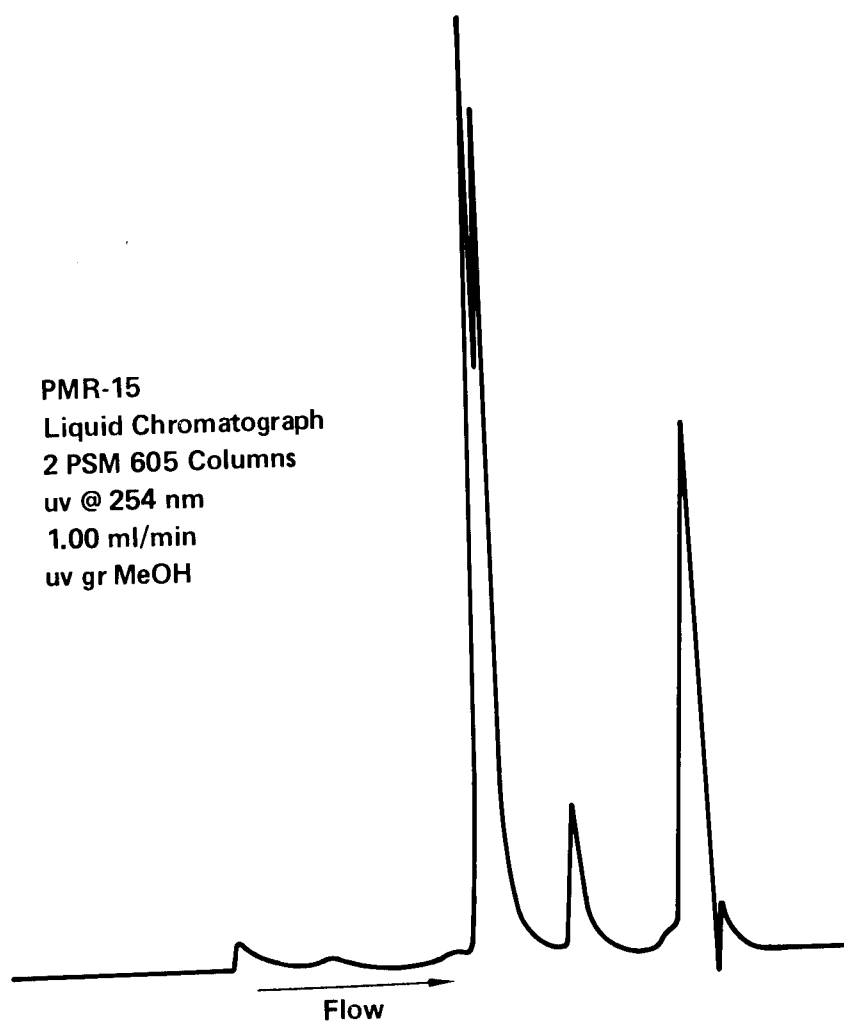


Figure 7

GEL PERMEATION CHROMATOGRAPHY

Based on test results obtained with different LC separation methods, the LC method selected for inclusion in the material specification was Gel Permeation Chromatography. The PMR-15 resin was evaluated by μ Styragel columns using a mobile phase of THF and the UV detector at 254 nm, (Figure 8). This separation seemed to give a good fingerprint of the material. The molecular size distribution is clearly shown. Also, batch to batch variation was easily noted in the component ratios. A problem developed with this method in that column life was short. The replacement cost was \$2500 for all five columns. The high cost of the columns and their short life seemed to prohibit their use for receiving inspection. Because of the success in noting batch to batch variation it seemed desirable to continue monitoring molecular size distribution.

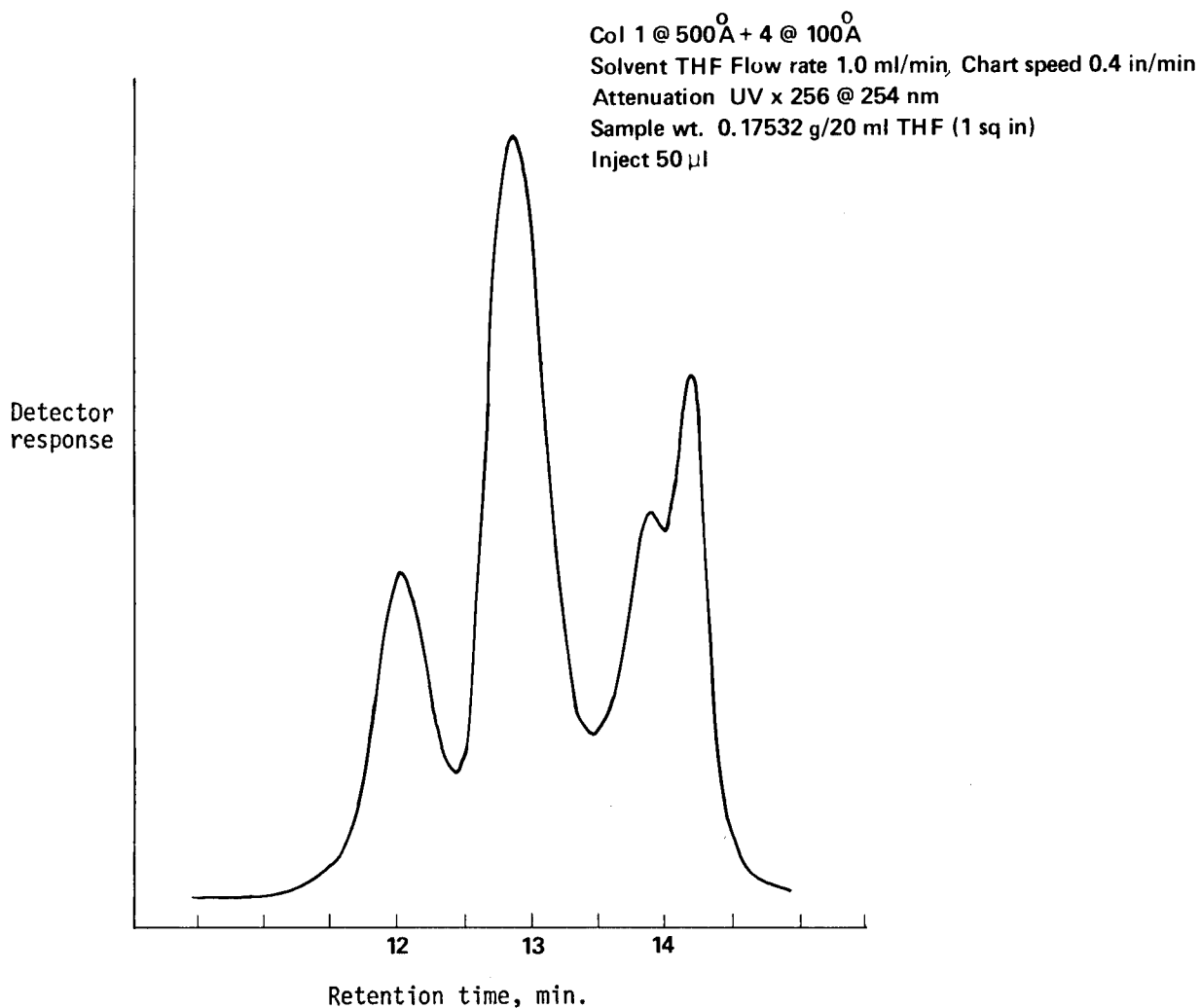


Figure 8

SIZE/ADSORPTION CHROMATOGRAPHY

The evaluation continued using SE 60 columns and various mobile phases, (Figure 9). These columns give an unusual separation in that up to 9.5 minutes is a size exclusion separation and the rest of the chromatogram is adsorption chromatography. This separation showed batch to batch variation. Also, the columns could be rejuvenated and the cost of the two columns is \$800. This method was a reasonable alternate to the μ Styragel method. The method consists of 2 SE 60 columns, a mobile phase of 2:1 H₂O: THF with 0.1% Acetic Acid and a UV detector at 254 nm. The method was then used to study prepreg variability.

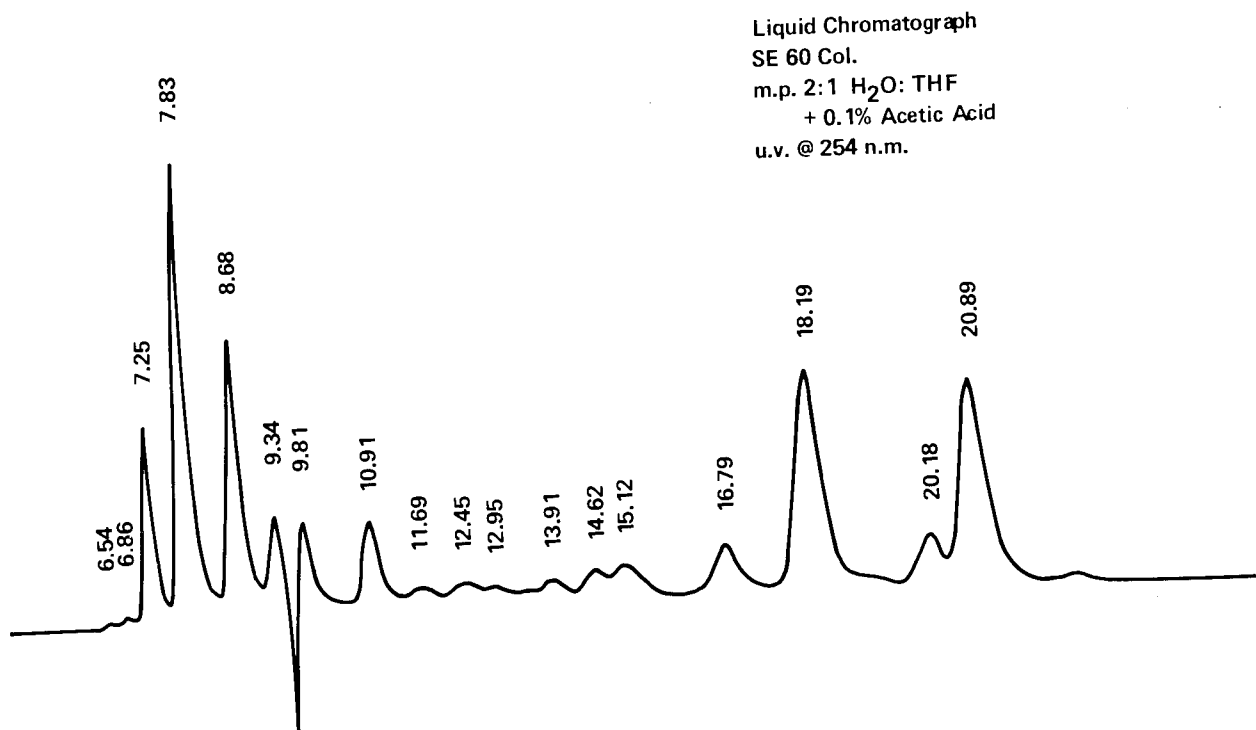


Figure 9

TASK J
LIQUID CHROMATOGRAPHY OF NE VARIATION

In the course of evaluating manufacturing methods for NE, samples of the ester were obtained and tested using the previously discussed size exclusion/adsorption method. Figure 10 clearly demonstrates that the preparation procedure of the NE is critical.

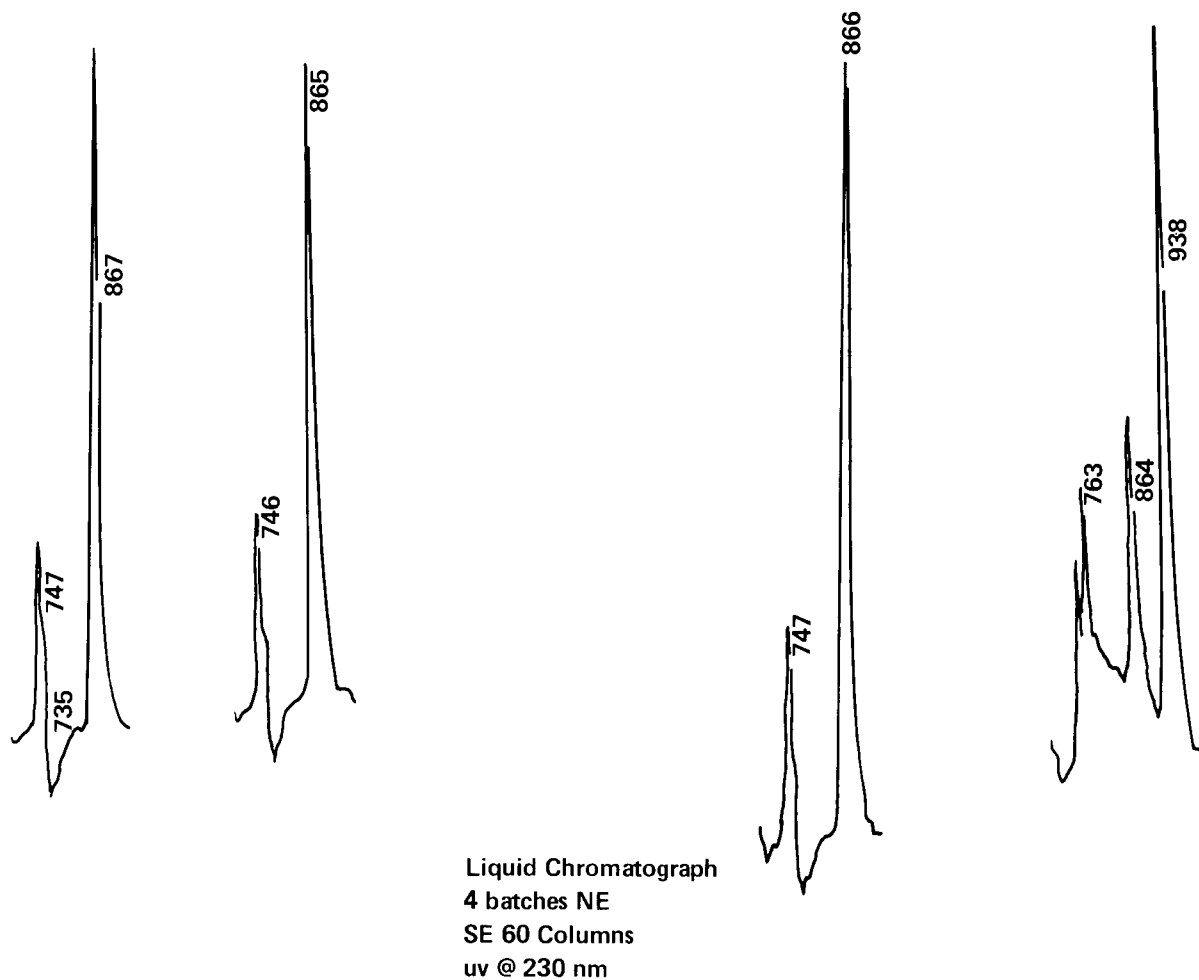


Figure 10

TASK J
LIQUID CHROMATOGRAPH OF BTDE VARIATION

Part of the analysis of monomer manufacture samples of BTDE were also tested using the Size Exclusion/Adsorption Method. Figure 11 clearly indicates that the BTDE is also sensitive to manufacturing conditions.

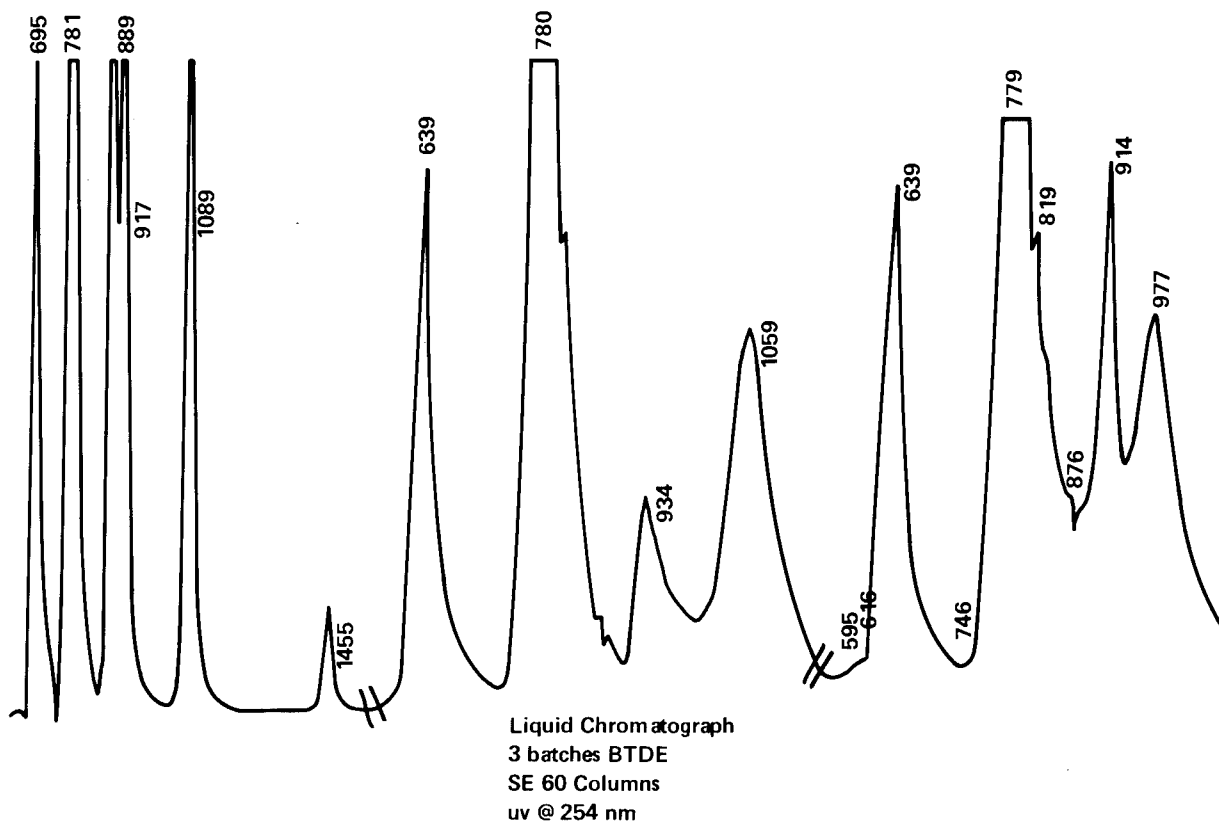


Figure 11

LIQUID CHROMATOGRAPH OF BTDE

As part of the variability study, aging characteristics of the BTDE monomer were evaluated. Figure 12 clearly indicates the monomer to be stable at both aging temperatures.

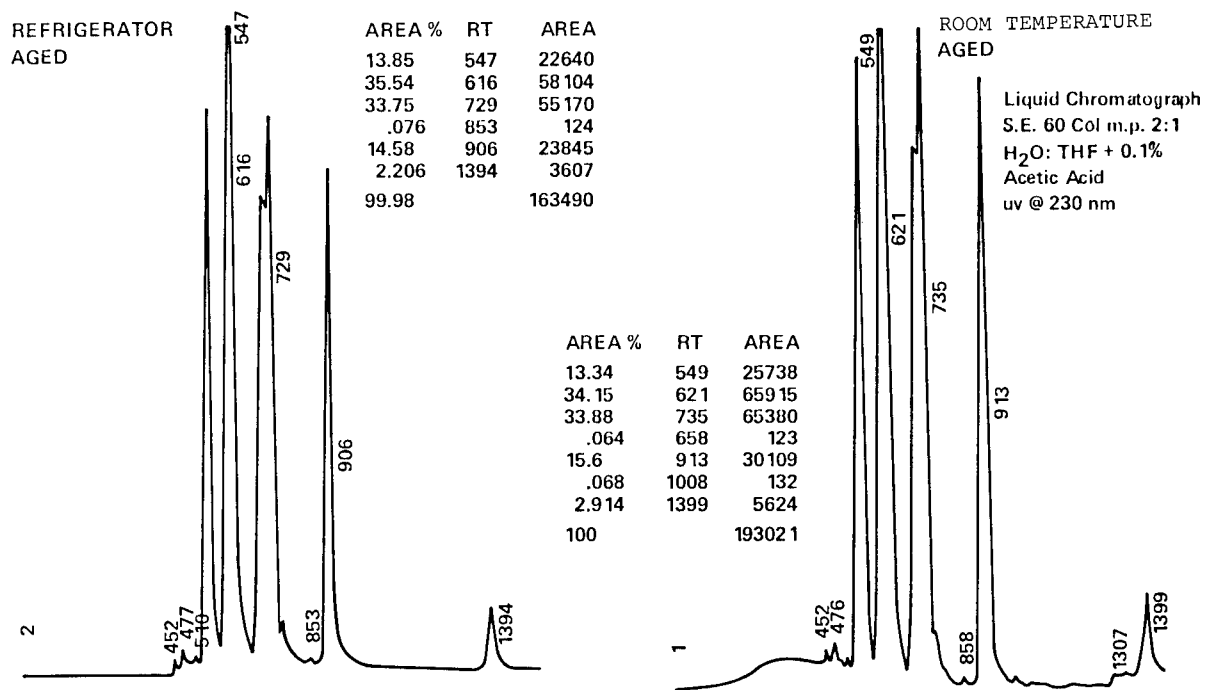


Figure 12

LIQUID CHROMATOGRAPHY

The data previously shown indicates extensive variability in the esters depending on cook time and solvent ratio.

Also, since the NE does not absorb at 254 nm but readily absorbs at 210 nm the method was changed accordingly. In addition, aging of the esters and resin was followed by the L C. However, extensive differences were noted in the resin itself with aging (Figure 13). The LC Method adopted seems to be sensitive to variations and aging characteristic, of the resin. Also, with a UV detector operating at 210 nm all components can be seen on one scan as well as certain reaction products.

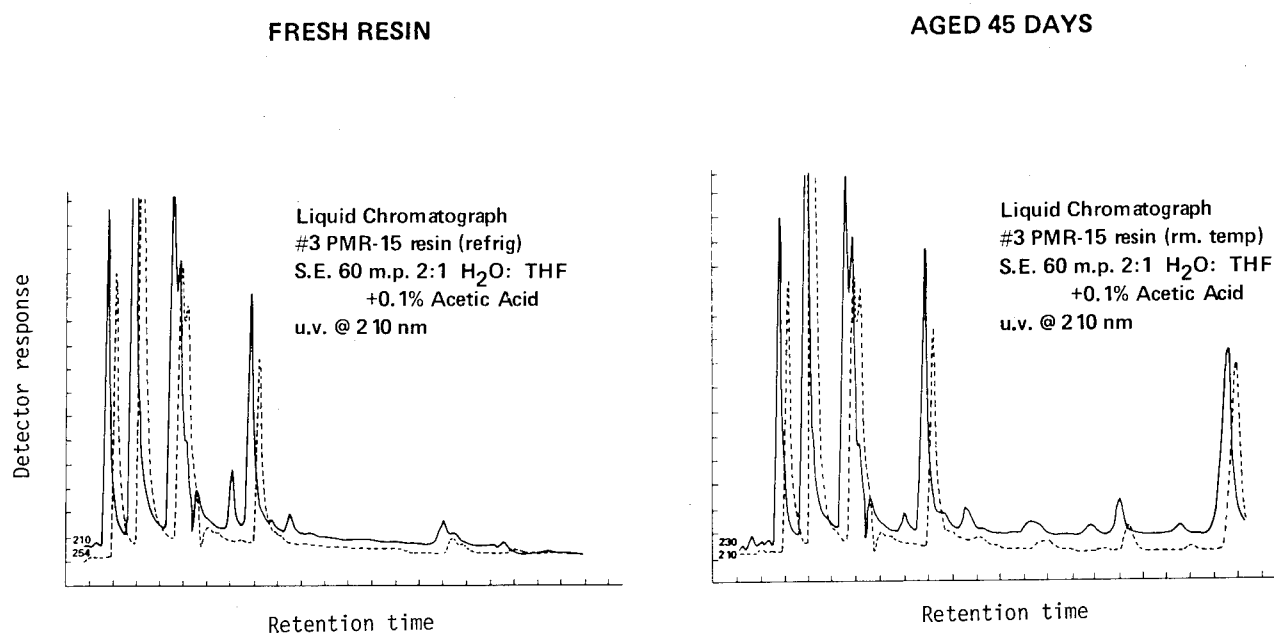


Figure 13

TASK J SE 60
COLUMN DEGRADATION

Some precautions must be observed with the use of the SE 60 columns. Not only the plate count must be controlled but also the adsorption characteristics must be monitored. The plate count can be monitored with toluene in tetrahydrofuran. The adsorption characteristics can be controlled by using Benzanilid and 4-Bromoacetanilide in a mobile phase of 98.9% methylene chloride, 0.1% water and 1% methanol.

In addition, ultrapure water and solvents must be used. Also, the mobile phase should not be used if it is more than two days old. If these precautions are followed, the above described LC method seems very suitable for Quality Control of PMR-15.

Figure 14 shows that the SE 60 column maintains an acceptable plate count level through at least 40 injections of PMR-15 samples.

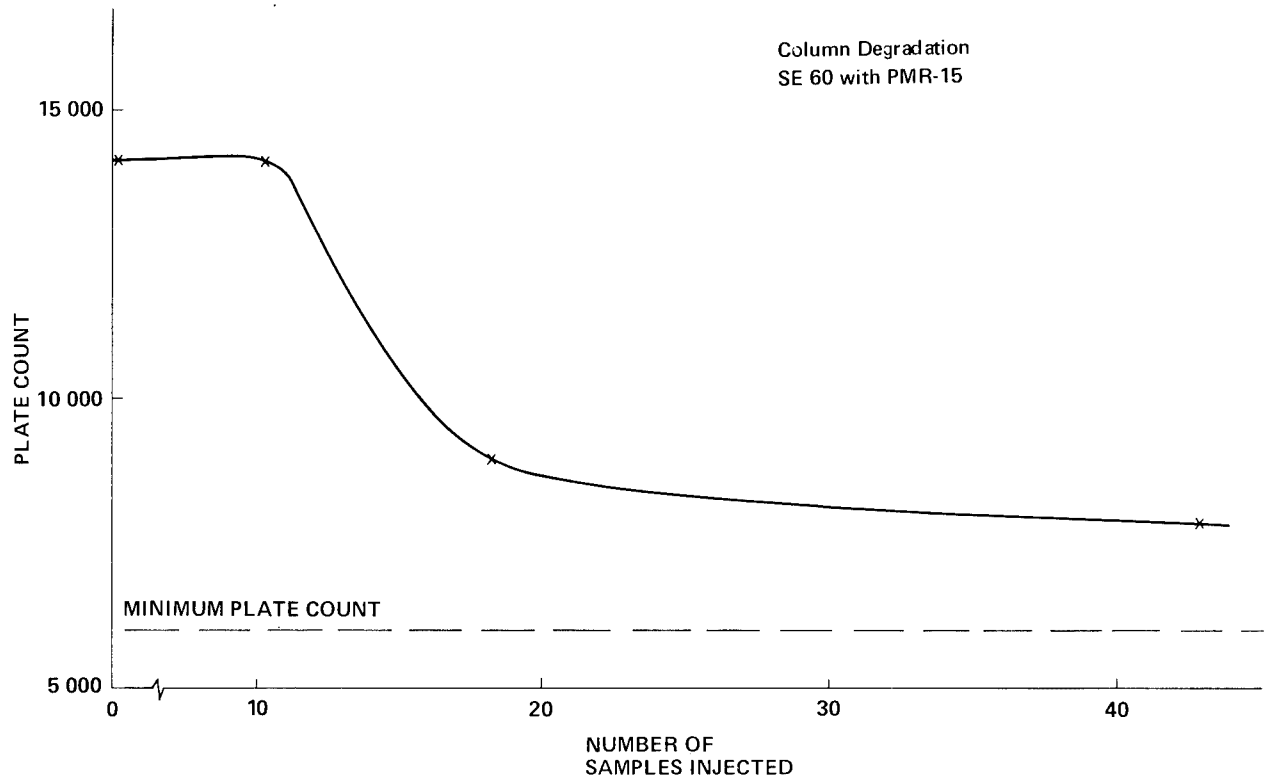


Figure 14

RECENT DEVELOPMENTS IN PMR POLYIMIDES
AT NASA LEWIS

T. T. Serafini
NASA Lewis Research Center

EXPANDED ABSTRACT

Studies conducted at the NASA Lewis Research Center led to the development of the class of polyimides known as PMR (for in situ polymerization of monomer reactants) polyimides (ref. 1-2). In the PMR approach, the reinforcing fibers are impregnated with a solution containing a mixture of monomers dissolved in a low boiling point alkyl alcohol. The monomers are essentially unreactive at room temperature, but react in situ at elevated temperatures to form a thermo-oxidatively stable polyimide matrix. These highly processable addition-type polyimides are now making it possible to realize much of the potential of high temperature polymer matrix composites.

The purpose of this paper is to review some of the recent PMR polyimide research studies conducted at Lewis in the following areas: (1) prepreg tack and drape; (2) cure temperature; (3) solution characterization; and (4) elevated temperature composite properties. Recent hardware applications of PMR-15 by various fabricators are also reviewed.

MONOMERS USED FOR PMR-15 POLYIMIDE

The structures of the monomers used in PMR-15 are shown in figure 1. The use of norbornenyl groups to achieve addition curing polyimides was developed by investigators at TRW Systems (ref. 3). The number of moles of each monomer reactant is governed by the following ratio: $n:(n+1):2$, where n , $(n+1)$ and 2 are the number of moles of BTDE, MDA and NE, respectively. In PMR-15 the value of n is 2.087. This PMR composition was found to provide the best overall balance of processing characteristics and thermo-oxidative stability at 316°C (600°F). Prepreg materials based on PMR-15 are commercially available from the major prepreg suppliers.

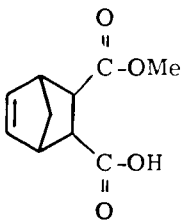
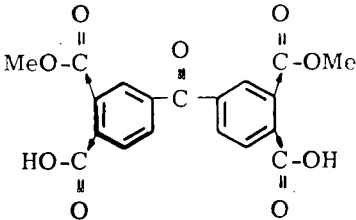
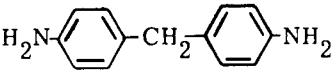
STRUCTURE	NAME	ABBREVIATION
	MONOMETHYL ESTER OF 5-NORBORNENE-2,3-DICARBOXYLIC ACID	NE
	DIMETHYL ESTER OF 3,3',4,4'-BENZOPHENONETETRACARBOXYLIC ACID	BTDE
	4,4'-METHYLENEDIANILINE	MDA

Figure 1

RESIN FLOW OF PMR POLYIMIDES

The early studies (refs. 1 and 4) conducted at Lewis clearly demonstrated the efficiency and versatility of the PMR approach. By varying the chemical nature of either the dialkyl ester-acid or aromatic diamine, or both, and the monomer reactant stoichiometry, PMR matrices having a broad range of processing characteristics and properties could easily be synthesized. A modified PMR-15, called LARC-160, has been developed by substituting an aromatic polyamine for MDA (ref. 5). Other studies (ref. 6) demonstrated the feasibility of using the PMR approach to "tailor make" matrix resins. For example, as shown in figure 2, the resin flow characteristics of PMR polyimides can be varied, or "tailored", over a broad range simply by varying the formulated molecular weight.

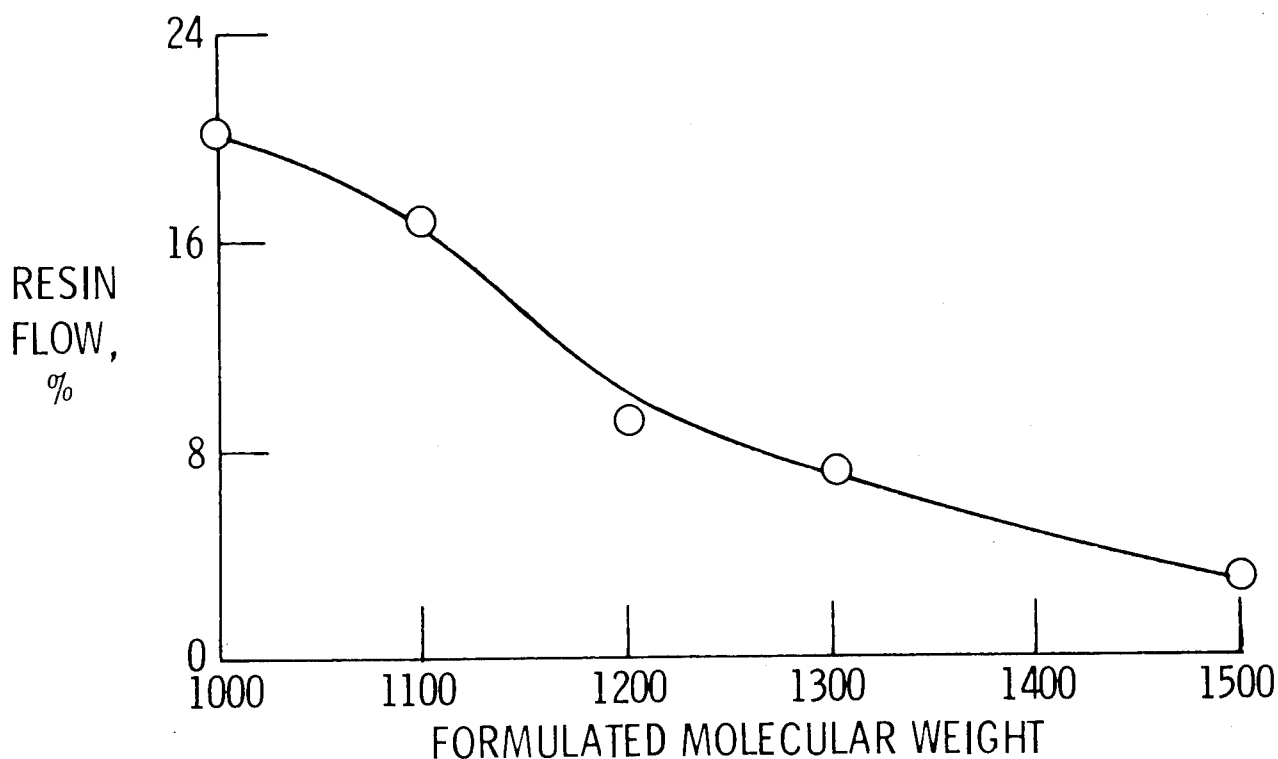


Figure 2

MONOMERS USED FOR SECOND GENERATION PMR POLYIMIDES

Our continuing research with PMR polyimides has identified a monomer reactant system which provides PMR polyimides with improved thermo-oxidative stability (ref. 7). These PMR polyimides are referred to as "second generation" materials, or PMR-II, to differentiate them from the earlier developed materials. The structures of the monomers used in the second generation polyimides are shown in figure 3. Prepreg materials based on the second generation monomer reactants are not commercially available. However, the monomers can be obtained from E. I. duPont de Nemours and Co., Inc.

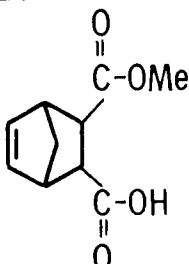
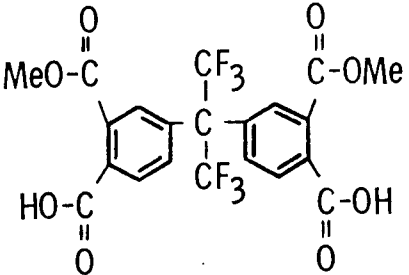
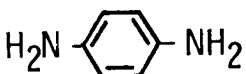
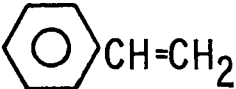

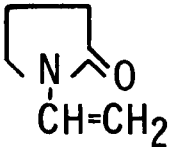
STRUCTURE	NAME	ABBREVIATION
	MONOMETHYL ESTER OF 5-NORBORNENE-2, 3-DICARBOXYLIC ACID	NE
	DIMETHYL ESTER OF 4, 4'- (HEXAFLUOROISOPROPYLIDENE) - BIS(PHTHALIC ACID)	HFDE
	p-PHENYLENEDIAMINE	PPDA

Figure 3

REACTIVE DILUENTS

Current PMR polyimide prepreg technology utilizes methanol or ethanol solvents for the preparation of the prepreg solutions. The volatility of these solvents limits the tack and drape retention characteristics of unprotected prepreg exposed to ambient conditions. Studies to achieve PMR-15 prepreg with improved tack and drape are reported in reference 8. The approach consisted of adding a fourth monomer, or reactive diluent, containing an olefinic double bond which could possibly enter into the final addition curing reaction. The molecular structure of the reactive diluents studied are shown in figure 4.

STRUCTURE	NAME	BOILING POINT		ABBREVIATION
		°C	°F	
 <chem>c1ccccc1C=C</chem>	STYRENE	145	293	STY
 <chem>C1=CC2C(C1)C=CC2</chem>	BICYCLO[2.2.1]HEPTA- 2,5-DIENE	89	192	BHD
 <chem>C1CC(=O)N1C=C</chem>	1-VINYL-2-PYRROLIDINONE	a		NVP

^aPOLYMERIZES ABOVE 135° C (275° F).

Figure 4

QUALITATIVE OBSERVATIONS OF PREPREG TACK AND DRAPE RETENTION CHARACTERISTICS

Figure 5 summarizes the qualitative observations of the tack and drape retention characteristics of prepreg from PMR-15 E (E for ethanol) and PMR-15 M (M for methanol) solutions containing the various types and amounts of reactive diluents. The reactive diluent which provided the most marked improvement of prepreg tack and drape retention characteristics was styrene.

MONOMER / REACTIVE SYSTEM / DILUENT	DILUENT LEVEL, w/o	TIME TO TACK LOSS, DAYS	TIME TO DRAPE LOSS, DAYS
PMR 15E/NONE	--	2	3-4
PMR 15E/STYRENE	1	2	3-4
PMR 15E/STYRENE	2	2-3	4-5
PMR 15E/STYRENE	5	4	5-6
PMR 15M/NONE	--	1	1
PMR 15M/STYRENE	5	1	1
PMR 15M/STYRENE	10	1-2	1-2
PMR 15M/STYRENE	20	2	2-3
PMR 15M/BHD	5	1	1
PMR 15M/BHD	10	1	1
PMR 15M/BHD	20	1-2	1-2
PMR 15M/NVP	5	1	1
PMR 15M/NVP	10	1	1
PMR 15M/NVP	20	1-2	2

Figure 5

WEIGHT LOSS OF PMR-15E/HTS-2 GRAPHITE FIBER COMPOSITES

Improvements in prepreg tack and drape retention characteristics would be of no practical value if the composite thermal and mechanical properties were adversely affected. Weight loss data for PMR-15E composites exposed in air at 316°C (600°F) are shown in figure 6. The figure shows that additions of styrene to the PMR prepreg solutions in the range of 1 to 5 weight percent did not appreciably lower the composite thermo-oxidative stability.

EXPOSED IN AIR AT 316°C (600°F)

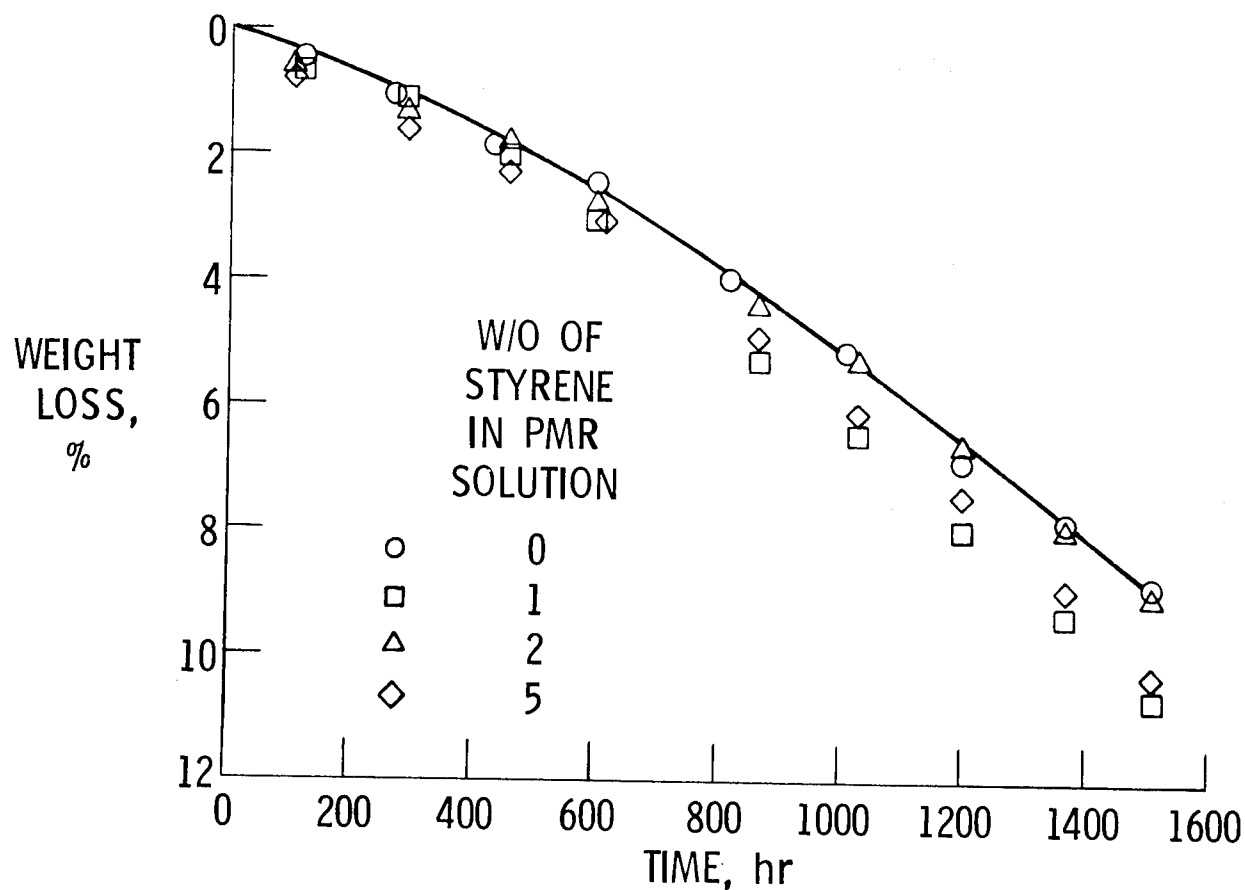


Figure 6

INTERLAMINAR SHEAR STRENGTH OF PMR-15E/HTS-2 GRAPHITE FIBER COMPOSITES

Figure 7 shows the retention of interlaminar shear strength for the PMR-15E composites after exposure in air at 316°C (600°F). It can be seen in the figure that the data for the composites prepared from prepreg solutions containing styrene follow the same general trend as the data for the control (zero styrene).

It needs to be emphasized that the data presented in figures 6 and 7 are very preliminary. Considerably more work needs to be performed to identify and evaluate other potential reactive diluents.

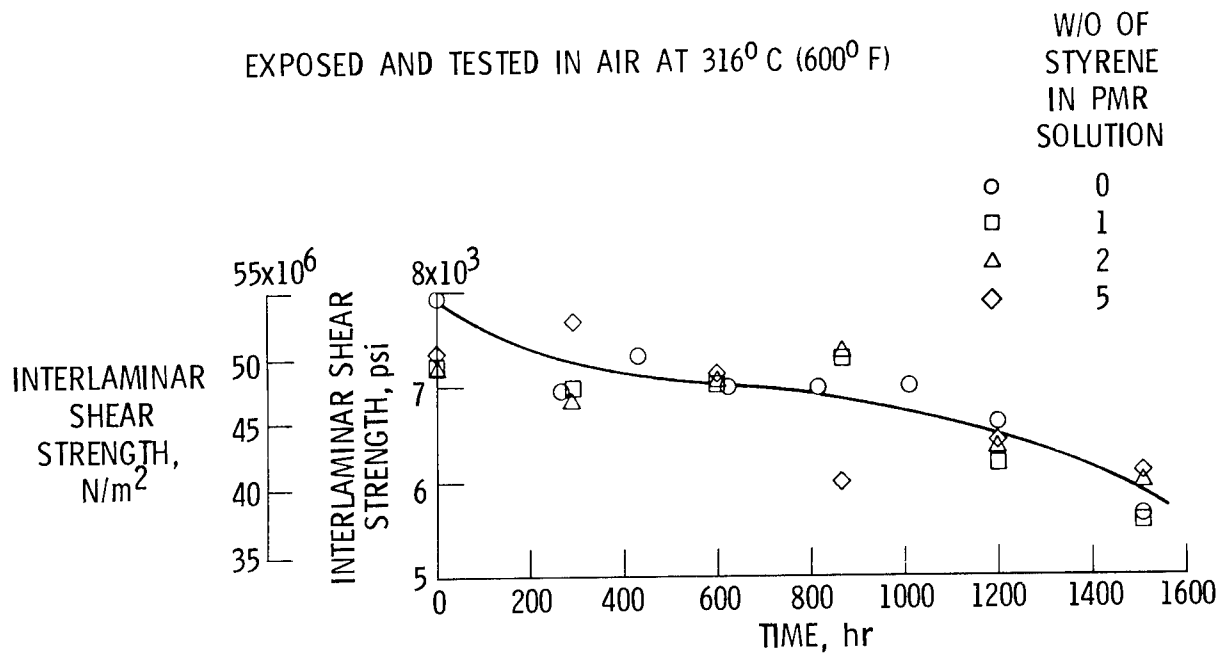


Figure 7

PMR CURE TEMPERATURES

The recommended cure temperature for curing of PMR-15 and PMR-II is 316°C (600°F). This temperature exceeds the temperature capabilities of many autoclave facilities which were originally acquired for curing of epoxy matrix composites. Therefore, studies were conducted to achieve a lower temperature curing PMR type polyimide. The approach consisted of replacing the NE with m-aminostyrene. Figure 8 compares the cure temperatures of PMR-VC (based on m-aminostyrene) and the state-of-the-art PMR materials. It can be seen that the use of m-aminostyrene lowered the cure temperature by 56°C (100°F).

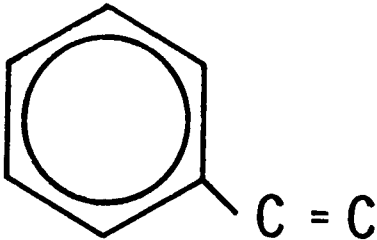
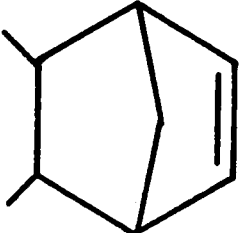
SYSTEM	END-CAP	CURE TEMP, °C (°F)
PMR-VC		260 (500)
PMR 15 } PMR II }		316 (600)

Figure 8

PROPERTIES OF PMR-VC AND PMR-15

The glass transition temperatures and elevated weight loss characteristics of PMR-VC and PMR-15 neat resins are compared in figure 9. The 2 MAS/3 BTDE/2 MDA and 2 MAS/3 HFDE/2 PDA formulations are PMR-VC analogs of PMR-15 and PMR-II, respectively. Although the PMR-VC resins exhibited good thermo-oxidative stability at 288°C (550°F), the value of their respective glass transition temperatures limits their upper use temperature to about 260°C (500°F).

RESIN	T _g °C (°F)	% WEIGHT LOSS
2MAS/3BTDE/2MDA	270 (518)	6.9 ^a
2MAS/3HFDE/2PDA	275 (527)	2.4 ^a
PMR 15	332 (630)	6.0 ^b

^aEXPOSED IN AIR AT 288° C (550° F) FOR 1000 hr.

^bEXPOSED IN AIR AT 316° C (600° F) FOR 1000 hr.

Figure 9

PROPERTIES OF PMR-VC/HTS-2 COMPOSITES

The thermo-oxidative stability and mechanical properties of PMR-VC/HTS-2 graphite fiber composites are summarized in figure 10. It can be seen that both PMR-VC composites exhibited excellent thermo-oxidative stability at 260°C (550°F). However, the mechanical properties of both composites are lower than similar properties of composites made with their PMR-15 and PMR-II analogs. It is apparent that additional studies with m-aminostyrene need to be performed.

RESIN	FIBER V/O	COMPOSITE WT. LOSS, ^a % 260 ⁰ C (550 ⁰ F)	INTERLAMINAR SHEAR STRENGTH, MPa (ksi)		FLEXURAL STRENGTH, MPa (ksi)		FLEXURAL MODULUS, GPa	
			24 ⁰ C (75 ⁰ F)	260 ⁰ C (500 ⁰ F)	24 ⁰ C (75 ⁰ F)	260 ⁰ C (500 ⁰ F)	24 ⁰ C (75 ⁰ F)	260 ⁰ C (500 ⁰ F)
2MAS/3BTDE/2MDA	60.4	2.4	42.7 (6.2)	31.0 (4.5)	944.6 (137)	786 (114)	110 (16)	103 (15)
2MAS/3HFDE/2MDA	58.0	2.6	90.3 (13.1)	36.5 (5.3)	1510 (219)	724 (105)	117 (17)	96.5 (14)

^aEXPOSED IN AIR FOR 1500 hr.

Figure 10

NMR SPECTRA OF PMR-15 MONOMER SOLUTIONS

The development of chemical quality control (QC) methodology for polymer matrix materials is currently being pursued by many investigators. Various experimental approaches are being used in our laboratories to develop a better understanding of PMR solution and prepreg chemistry. The stability of PMR-15 and PMR-II solutions stored at ambient temperature, 5°C (41°F) and -18°C (0°F) has been studied using nuclear magnetic resonance spectroscopy (ref. 9). Proton magnetic resonance spectra of a freshly prepared PMR-15 solution and a solution stored at ambient temperature for 17 days (time to initial precipitation) are shown in figure 11. The appearance of a new peak in the spectrum of the aged solution at 1.7 ppm and the changes in the MDA peaks have been attributed to the formation of nadimide (reaction product of NE + MDA).

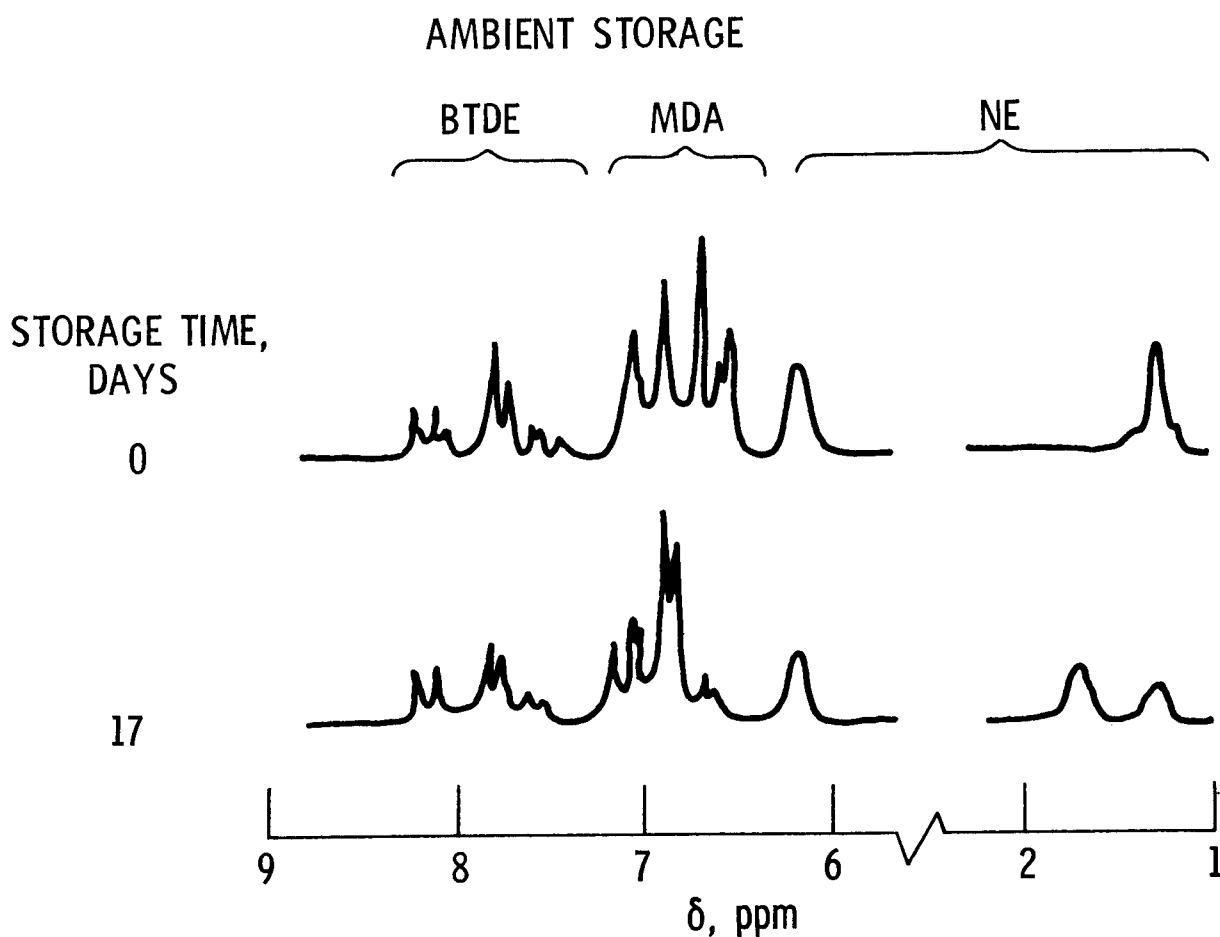


Figure 11

NMR SPECTRA OF PMR-15

The undesirable effect of higher BTDE esters (tri and tetra-esters) on composite quality has been discussed (ref. 10). Proton magnetic resonance spectra of the spectral region in which methyl ester peaks occur are shown in figure 12 for solutions stored at -18°C (0°F). Comparison of the integral data for the freshly prepared and aged solutions did not show any significant change in BTDE content.

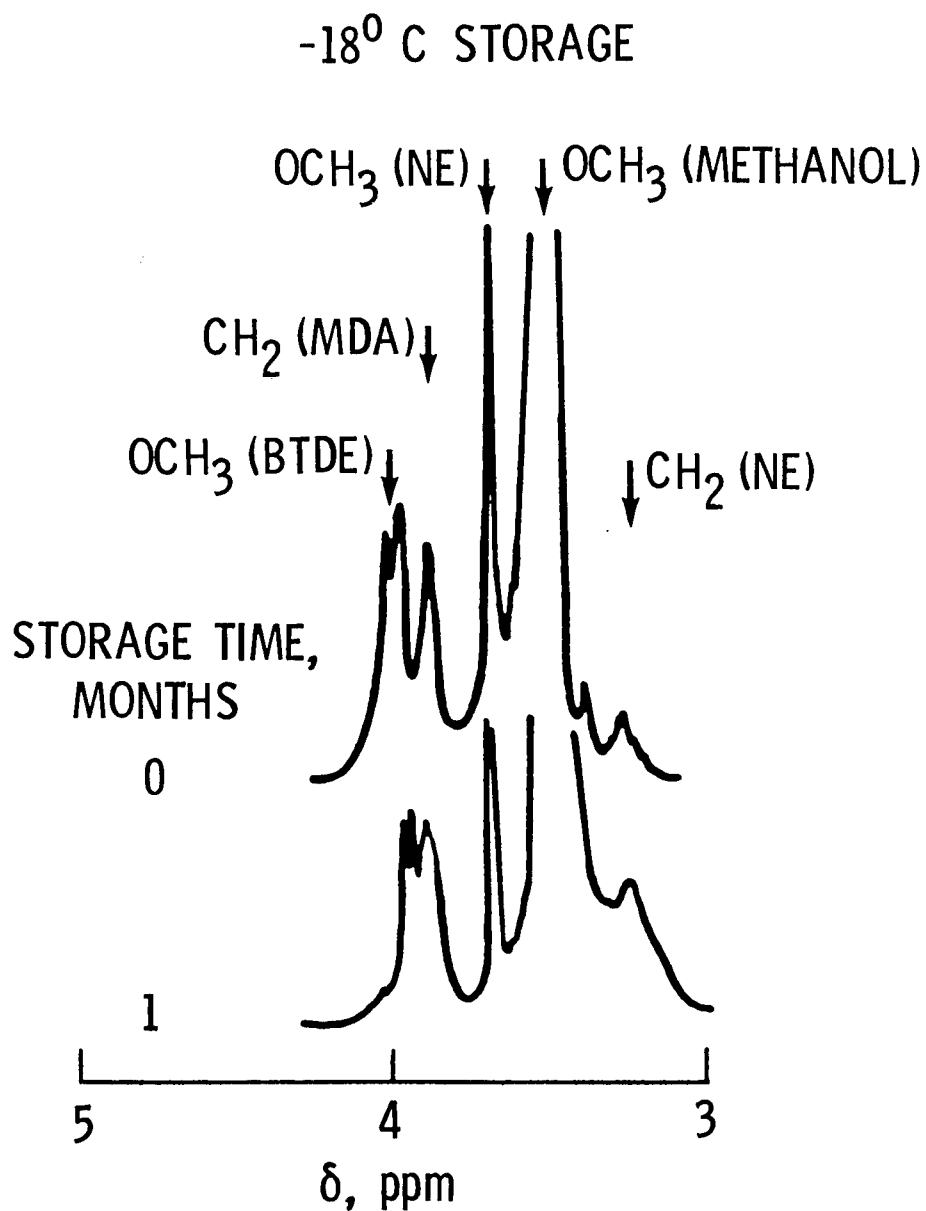


Figure 12

FLEXURAL STRENGTH AND INTERLAMINAR SHEAR STRENGTH OF PMR-15/GRAPHITE COMPOSITES

Graphite fiber prepreg and unidirectional composites were fabricated from the aged solutions. Although the aged solutions exhibited slightly poorer fiber wetting and the resulting prepreg exhibited less resin flow during composite processing, the overall quality of the composites, as assessed by ultrasonic transmission, was not significantly affected. Figure 13 shows the variation of flexural and interlaminar shear strengths as a function of monomer solution storage time. It can be seen in the figure that solution storage time did not have any effect on composite properties until 4 months of storage time had elapsed.

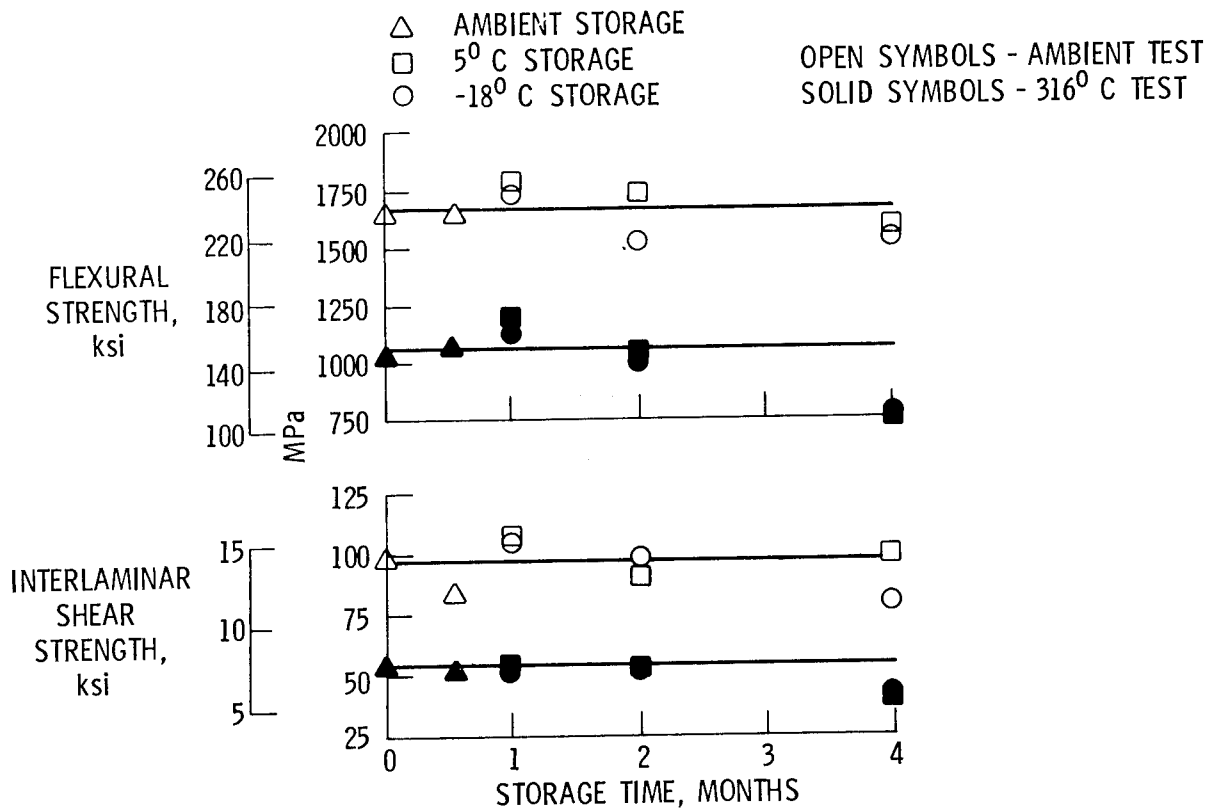


Figure 13

PMR-15/GRAPHITE FIBER COMPOSITE WEIGHT LOSS

Further improvement in the performance of PMR polyimides at elevated temperatures has been made possible by the recent development of graphite fibers with improved thermo-oxidative stability. Figure 14 compares the weight loss characteristics of PMR-15 composites made with HTS-1, HTS-2, and Celion 6000 graphite fibers after isothermal exposure in air at 316°C (600°F). The HTS-1 composite data are from reference 4 and the HTS-2 and Celion 6000 composite are from reference 11. The data presented in the figure clearly show the significantly improved elevated temperature stability of the HTS-2 and Celion 6000 composites compared to the HTS-1 composites.

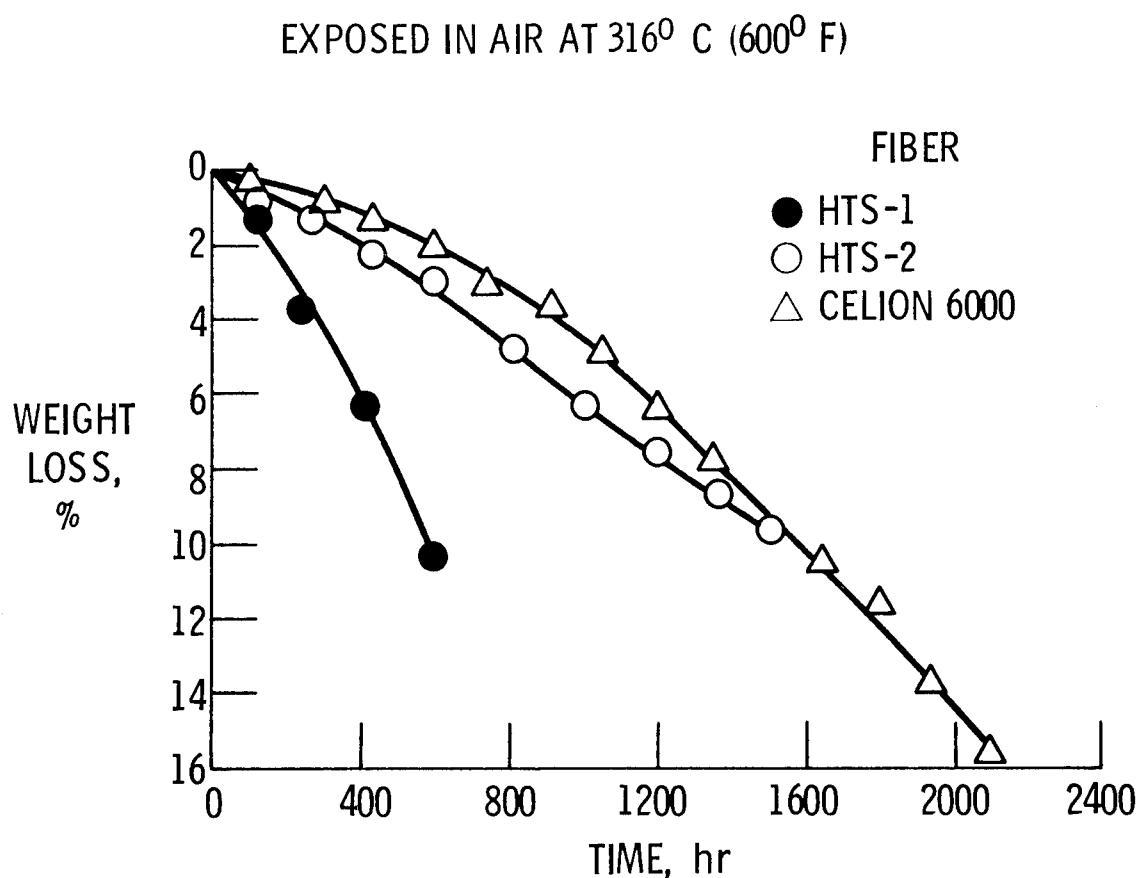


Figure 14

INTERLAMINAR SHEAR STRENGTH OF PMR-15/GRAPHITE

Figure 15 compares the interlaminar shear strength retention after exposure in air at 316°C (600°F) of PMR-15/HTS-1, PMR-15/HTS-2 and PMR-15/Celion 6000 composites. It can be seen that both the HTS-2 and Celion 6000 composites exhibited 100 percent retention of their initial 316°C (600°F) interlaminar shear strength during the first 1000 hours of exposure. The shear strength then slowly decreased with further exposure. These mechanical property data and the composite weight loss data shown in the previous figure clearly show that the useful life of PMR-15 composites at 316°C (600°F) made with high strength, intermediate modulus graphite fibers such as HTS-2 and Celion 6000 is at least 1000 hours.

EXPOSED AND TESTED IN AIR AT 316°C (600°F)

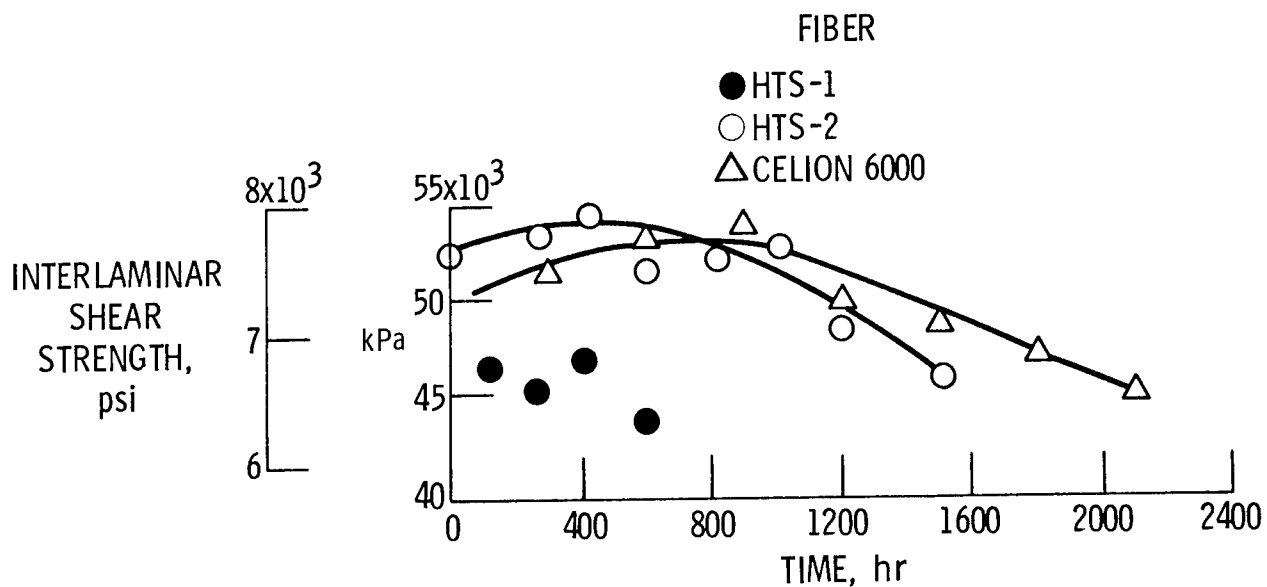


Figure 15

WEIGHT LOSS OF PMR-15/GRAPHITE FIBER COMPOSITES

The PMR-15/Celion 6000 composite data presented in figures 14 and 15 are for composites fabricated with unsized Celion 6000 fibers. Figure 16 compares the 316°C (600°F) composite weight loss behavior of PMR-15 composites made with unsized Celion 6000 fibers, NR-150B sized Celion 6000 fibers and Thornel 300 Exp. B fibers. Comparison of the data for the Celion 6000 composites shows that the rate of composite weight loss for the composites made with the NR-150B sized Celion fibers was significantly higher than the weight loss rate for the composites made with unsized Celion fibers. The excellent thermo-oxidative stability of the PMR-15 composites made with the Thornel 300 Exp. B fibers is clearly evident in figure 16.

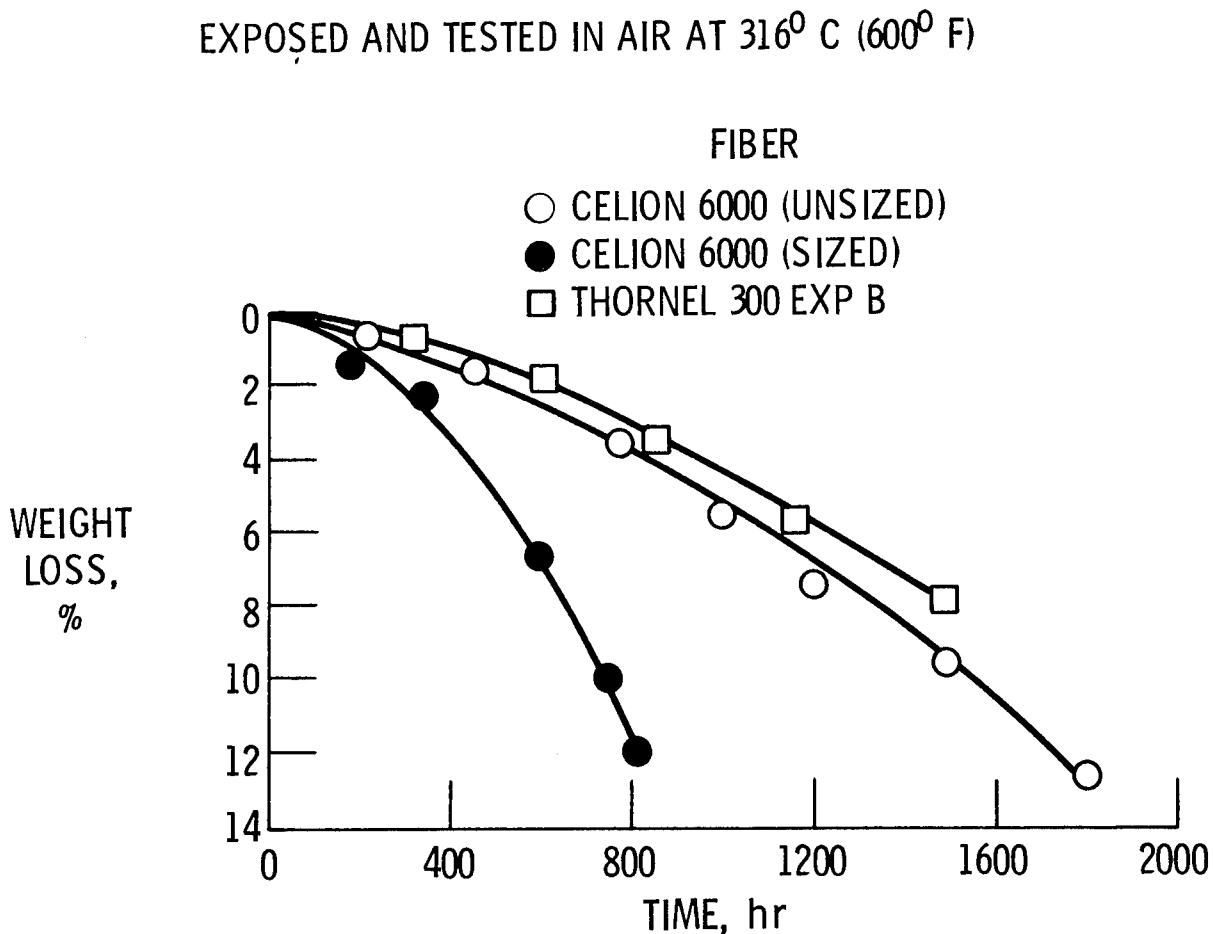


Figure 16

INTERLAMINAR SHEAR STRENGTH OF PMR-15/GRAPHITE FIBER COMPOSITES

Figure 17 compares the interlaminar shear strength retention behavior at 316°C (600°F) of PMR-15 composites made with unsized and NR-150B sized Celion fibers after isothermal exposure in air at 316°C (600°F). The composites made with the sized fibers exhibited lower initial properties and an increased rate of property loss compared to the composites made with the unsized fibers. Based on the data presented in figures 16 and 17, it is apparent that the NR-150B size has a deleterious effect on composite performance and should not be employed.

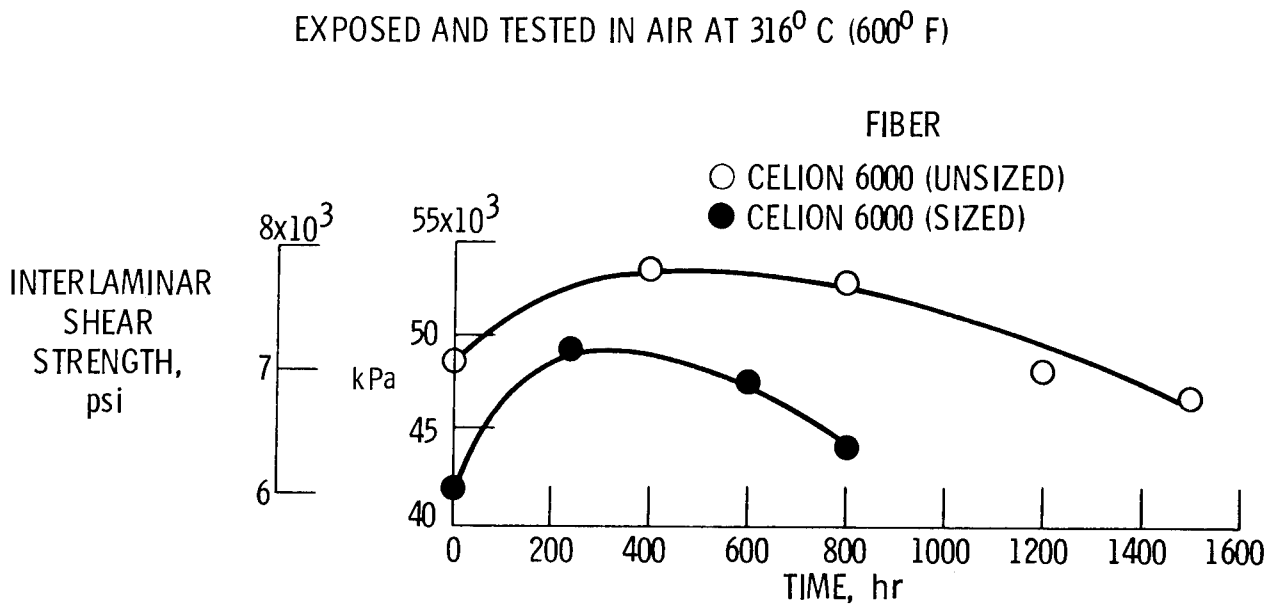


Figure 17

APPLICATIONS OF PMR TECHNOLOGY

Because of their excellent processing characteristics, elevated temperature properties and commercial availability, PMR-15 polyimide composites have been or are being used in a number of diverse structural components (ref. 12). Some of these components, the sponsoring agency and the contractor are listed in figure 18.

COMPONENT	AGENCY	CONTRACTOR
JT8D REVERSER STANG FAIRING	NASA-LeRC	McDONNELL-DOUGLAS
F404 DUCT	NASA-LeRC/NAVY	GENERAL ELECTRIC
ION ENGINE BEAM SHIELD	NASA-LeRC	HUGHES
AEDC SUPERSONIC WIND TUNNEL COMPRESSOR BLADES	AIR FORCE	HAMILTON STANDARD
QCSEE INNER COWL	NASA-LeRC	GENERAL ELECTRIC
SHUTTLE ORBITER AFT BODY FLAP	NASA-LaRC	BOEING
P&W F-100 AUGMENTOR DUCT	AIR FORCE	COMPOSITES HORIZONS

Figure 18

PMR-15 QCSEE INNER COWL

Figure 19 shows the inner cowl for an experimental engine, called QCSEE (for Quiet Clean Short-Haul Experimental Engine), autoclave fabricated with PMR-15 by General Electric (ref. 13). The cowl has a maximum diameter of about 90 cm (~ 36 in.) and is primarily of honeycomb sandwich construction. The cowl has successfully undergone more than 100 hours of ground engine testing.

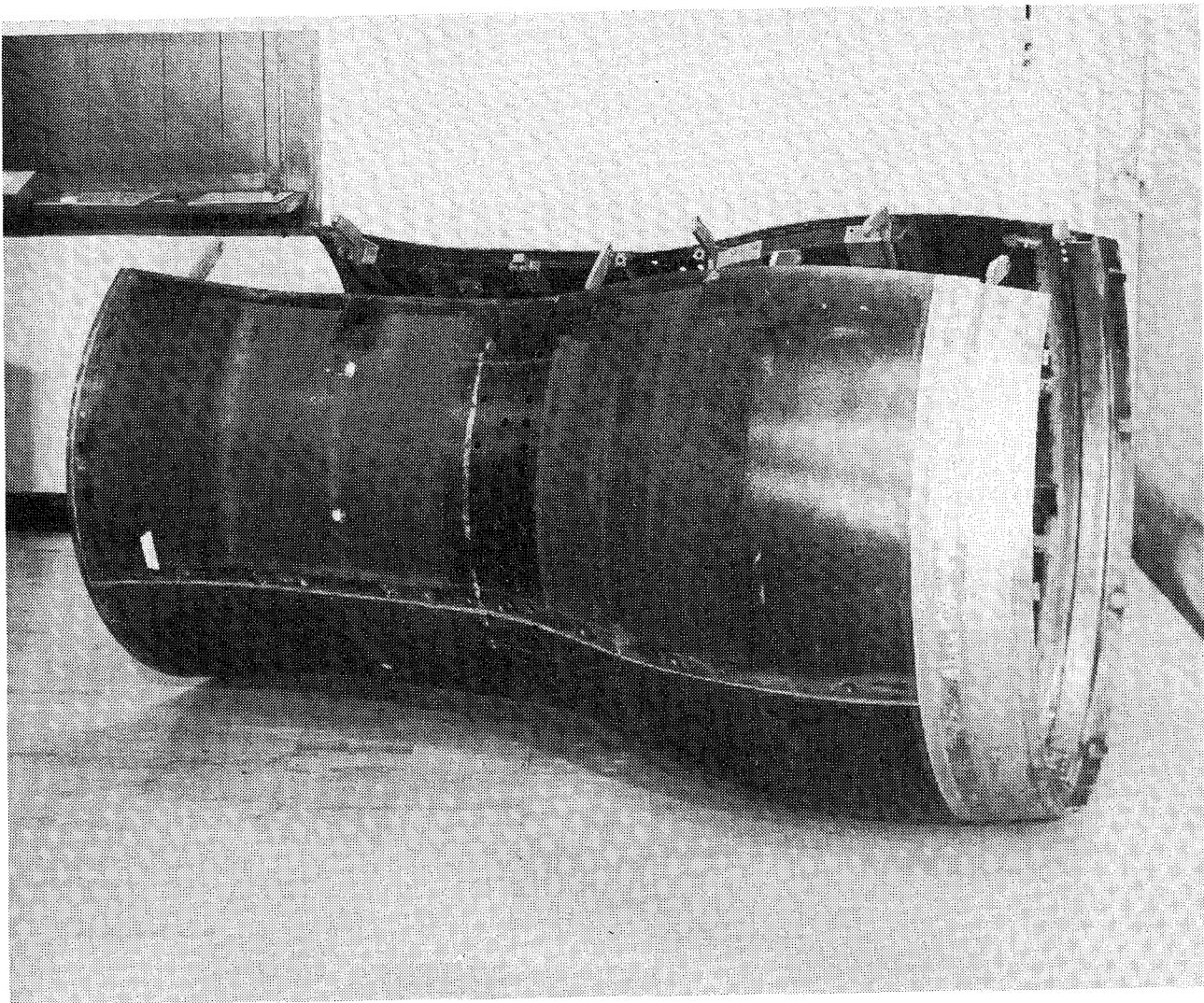


Figure 19

DC-9 DRAG REDUCTION

Figure 20 shows a photograph of a DC-9. The inserts schematically show the design of the presently used metal fairing and the re-designed composite fairing currently being developed by the Douglas Aircraft Company (Contract NAS3-21763) under the NASA-LeRC ECI (Engine Component Improvement) program. Studies have shown that a re-designed fairing provides an opportunity to reduce baseline drag and reduce fuel consumption. A composite fairing made from PMR-15 and Kevlar fabric has been autoclave fabricated and recently flight tested. The flight test data are presently being analyzed.

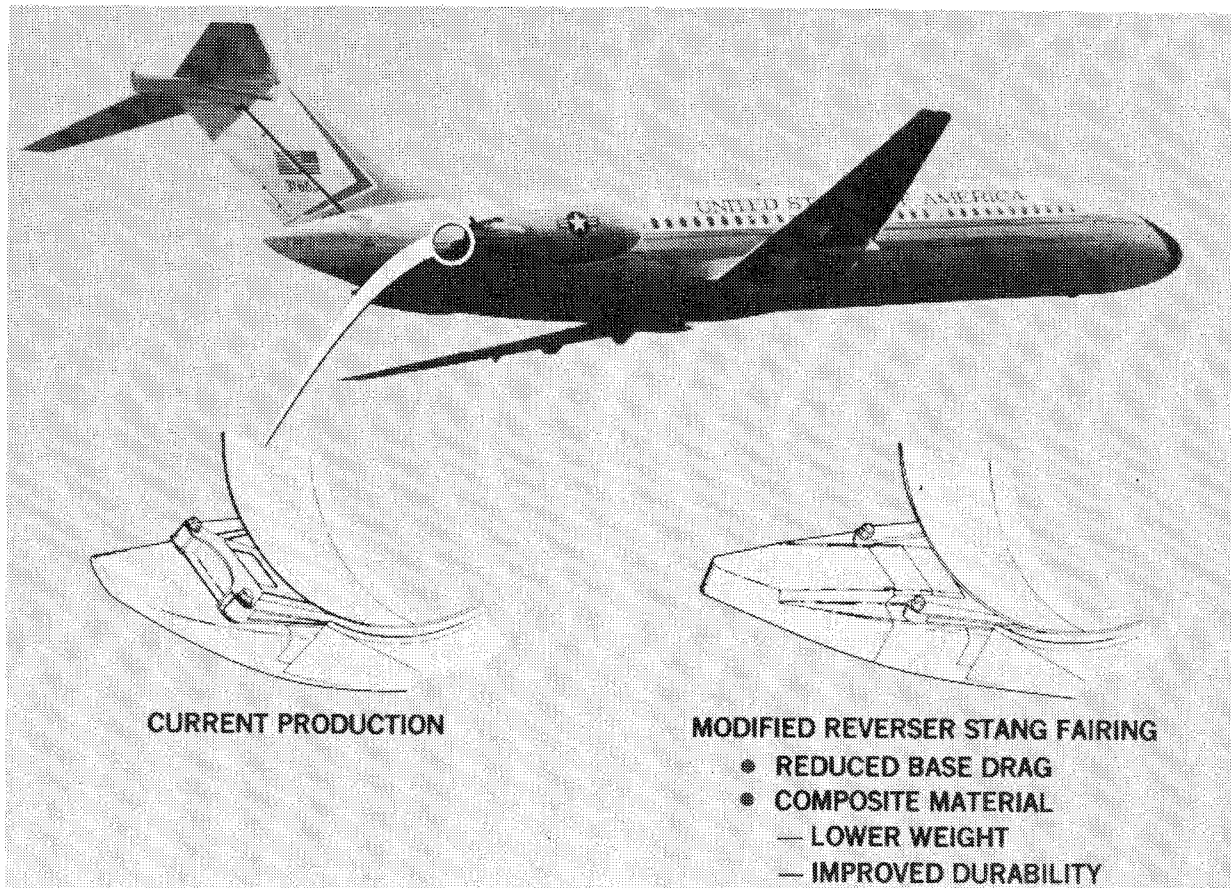


Figure 20

REFERENCES

1. Serafini, T. T.; Delvigs, P.; and Lightsey, G. R.: Thermally Stable Polyimides from Solutions of Monomeric Reactants. *J. Appl. Polym. Sci.*, Vol. 16, No. 4, April 1972, pp. 905-916.
2. Serafini, T. T.; Delvigs, P.; and Lightsey, G. R.: Preparation of Polyimides from Mixtures of Monomeric Diamines and Esters of Polycarboxylic Acids. U.S. Patent 3,745,149, July 10, 1973.
3. Burns, E. A.; Lubowitz, H. R.; and Jones, J. F.: Investigation of Resin Systems for Improved Ablative Materials. NASA CR-72460, 1968.
4. Delvigs, P.; Serafini, T. T.; and Lightsey, G. R.: Addition-Type Polyimides from Solutions of Monomeric Reactants. NASA TN D-6877, 1972.
5. St. Clair, T. L.; and Jewell, R. A.: Solventless LARC-160 Polyimide Matrix Resin. Proc. of the 23rd National SAMPE Symposium, 1978.
6. Serafini, T. T.; and Vannucci, R. D.: Tailor Making High Performance Graphite Fiber Reinforced Polyimides. Proc. of the 30th SPI Reinforced Plastics Conf., 1975, Paper 14E.
7. Serafini, T. T.; Vannucci, R. D.; and Alston, W. B.: Second Generation PMR Polyimides. NASA TM X-71894, 1976.
8. Serafini, T. T.; and Delvigs, P.: PMR Polyimides with Improved Tack Characteristics. NASA TM-73898, 1978.
9. Lauver, R. W.; Alston, W. B.; and Vannucci, R. D.: Stability of PMR Polyimide Monomer Solutions. Proc. of the 34th SPI Reinforced Plastics Conference, 1979, Paper 23A.
10. Lauver, R. W.: Effect of Ester Impurities in PMR Polyimide Resin. NASA TM X-73444, 1976.
11. Delvigs, P.; Alston, W. B.; and Vannucci, R. D.: Effect of Graphite Fiber Stability on the Properties of PMR Polyimide Composites. Proc. of the 24th National SAMPE Symposium, 1979.
12. Serafini, T. T.: Status Review of PMR Polyimides. NASA TM-79039, 1979.
13. Ruggles, C. L.: Quiet Clean Short-Haul Experimental Engine, Under-the-Wing (UTW) Graphite/PMR Cowl Development. NASA CR-135279, 1978.

HIGH TEMPERATURE POLYMER RESEARCH AT NASA LANGLEY

Terry L. St. Clair
NASA Langley Research Center

EXPANDED ABSTRACT

A number of approaches have been undertaken at NASA-Langley to improve polymeric materials for use as adhesives and matrix resins. The effort includes a continuing program of synthesis of monomers and polymers aimed at better understanding the structure-property relationships of polymers for adhesive and matrix resin applications. Of particular interest are the toughness properties of existing and modified resins for these two applications.

Current activities of interest are novel crosslinking systems which are potentially inexpensive and can cure with no volatile evolution, adhesive scale-up and screening, and the stability and processability of Langley matrix resins.

POLYMER SYNTHESIS

Past activities in polymer synthesis at Langley have been directed towards the incorporation of novel amines and anhydrides into polyimides in an effort to develop adhesives and/or matrix resins for NASA applications. This same type of structure-property study has also been carried on for other high temperature systems such as quinoxalines and asymmetric triazines.

Currently investigations are under way to determine the utility of incorporating crosslinking agents such as acetylenes, propargyls, and cyanates into polymers either as end caps for addition systems or as latent crosslinkers. The problem of toughening matrix resins and adhesives is also being examined.

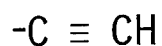
PAST ACTIVITY

- NOVEL DIAMINES AND DIANHYDRIDES - LARC-160 AND LARC-13
- NEW POLYQUINOXALINES AND POLY-AS-TRIAZINES

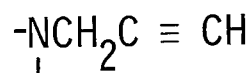
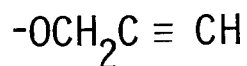
CURRENT ACTIVITY

- CROSSLINKING AGENTS

ACETYLENE



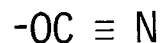
PROPARGYL



|

R

CYANATE



- POLYIMIDE TOUGHENING

Figure 1

THE PROPARGYL GROUP

The need for a high temperature resin system which cures via an addition mechanism is well known. The use of the norbornene endcap has yielded systems which can be cured under pressure to yield excellent matrix resins and adhesives (refs. 1-3), but they still lack the properties that made the epoxides so popular - no volatile generation and very low pressure cure. The problems with the norbornene systems are the necessity for a "B"-stage where condensation volatiles are eliminated and the generation of cyclopentadiene via a reverse Diels-Alder which may lead to microporosity. The incorporation of terminal acetylene groups as in the work at Hughes (ref. 4) has led to polymers with excellent thermal stability, but they remain difficult to fabricate.

The propargyl group is now under investigation at NASA-Langley and it appears to cure to a thermally stable system. The systems investigated to date have been either liquid-like epoxides or low-melting with excellent flow properties. These systems are also commercially attractive because of the potential low cost and ease associated with their syntheses.

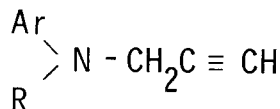
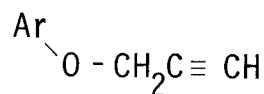
ADVANTAGES

- NO-VOLATILE ADDITION CURE
- LOW COST
- VERSATILE X-LINKER

END CAPPER
PENDENT ATTACHMENT

- POTENTIAL LOW TEMPERATURE CURE

CHEMICAL STRUCTURE



DIFFERENTIAL SCANNING CALORIMETRY

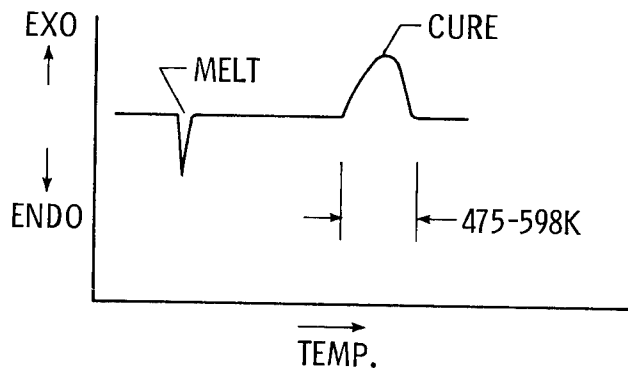


Figure 2

POLYIMIDE TOUGHENING

The addition of thermoset polyimide systems all lack the toughness associated with linear or thermoplastic systems. In an effort to alleviate this shortcoming NASA-Langley is modifying LARC-160 and LARC-13 (matrix resin and adhesive respectively) with elastomers just as has been done with 398K (250°F) epoxide systems. The approach has been to either pre-react elastomer blocks into the addition systems or to physically blend the elastomers into the resin system. The latter systems always incorporate a functional unit which can react with the norbornene moiety during the cure of the resin.

The results of these modifications are being measured in the case of adhesives by a "T"-peel test, the Naval Research Labs (NRL) double-cantilever beam method (ref. 5), or by the use of an autographic falling weight impact tester which has been developed at VPI&SU on grant to NASA-Langley (ref. 6). This impact tester can also be used for matrix resin evaluation. Laminates from the matrix resins are being tested by NRL using the width-tapered beam and in-plane loader techniques (ref. 7).

APPROACH :

USE TWO-PHASE SYSTEMS

VINYLFLUOROSILICONE

VINYLSILICONE

SILICONE-IMIDE BLOCK COPOLYMER

AMINE-TERMINATED POLYBUTADIENE-ACRYLONITRILE

EVALUATION METHODS :

T-PEEL (ADHESIVE)

NRL DOUBLE-CANTILEVER BEAM (ADHESIVE)

NRL WIDTH-TAPERED BEAM (MATRIX)

NRL IN-PLANE LOADER (MATRIX)

VPI AND SU IMPACT TESTER (ADHESIVE AND MATRIX)

Figure 3

EFFECT OF ELASTOMERS ON RESIN TOUGHNESS

The results obtained to date for toughening both the LARC-13 and LARC-160 are encouraging. The incorporation of a block elastomer into the adhesive oligomer has afforded a five-fold increase in peel strength. The use of a physical blend of a vinyl capped silicone has yielded the most promising results.

Crossplied graphite/LARC-160 laminates with and without a vinyl capped silicone have been fabricated at Langley and tested at NRL in the width-tapered beam mode. The LARC-160 without elastomer had a fracture energy of 100 J/m^2 which is approximately the same as a 450K (350°F) epoxide (85 J/m^2). The laminate with 15 percent elastomer had a fracture energy of 185 J/m^2 . These initial results are encouraging and work is continuing.

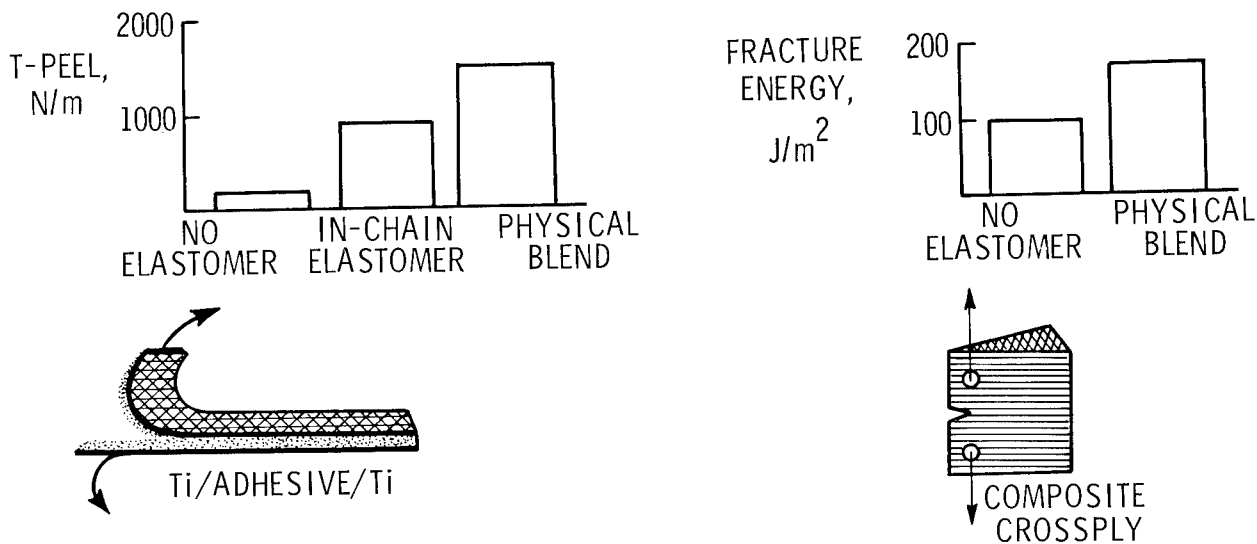


Figure 4

ADHESIVES

The adhesives effort at NASA-Langley has been quite varied due to program requirements. LARC-13, which is being used on the Supersonic Cruise Research (SCR) and the CASTS programs, contains a diamine that is being made by a specialty chemical producer. Two alternate commercial sources are being investigated.

A polyphenylquinoxaline developed for the CASTS program has yielded promising results which will subsequently be discussed in more detail as will a contractual effort with Boeing on the evaluation of adhesives for SCR applications.

Two other adhesive applications that will be covered are the bonding of polyimide films, an outgrowth of the Solar Sail Program, and the incorporation of metal ions into polyimide adhesives.

- LARC-13 MONOMER AVAILABILITY (COMMERCIAL SCALE-UP)
- POLYPHENYLQUINOXALINE TEST RESULTS
- EVALUATION OF ADHESIVES FOR SCR APPLICATIONS
- POLYIMIDE FILM BONDING
- POLYIMIDES CONTAINING METAL IONS

Figure 5

LARC-13 MONOMER AVAILABILITY

The monomer 3,3'-methylenedianiline (3,3'-MDA) which is used in the preparation of LARC-13 (ref. 8) is presently being made on special order in 4-10 kg batches by Ash Stevens, Carleton, Michigan. Both DuPont and Gulf have expressed interest in the commercialization of this monomer. DuPont has made a lab-scale and a large batch of this material which has been analyzed by NASA-Langley and shown to be of high purity.

Gulf Chemical has prepared an alternate material which by liquid chromatographic analysis assays to be 70 percent 3,3'-MDA with the remaining 30 percent being isomers. Data on a LARC-13 made from this material is presented in figure 7.

DuPONT

- PREPARED 3, 3' - MDA OF HIGH PURITY ON LAB-SCALE
- PREPARED LARGER QUANTITY WITH SAME PURITY
- CONSIDERING COMMERCIAL PRODUCTION OF MONOMER
AND / OR LARC-13

GULF

- PREPARED A MIXTURE OF ISOMERIC METHYLENEDIANILINES
- CONSIDERING COMMERCIAL PRODUCTION OF THE MONOMER

Figure 6

LAP SHEAR STRENGTH OF LARC-13

The LARC-13 prepared with the monomer mixture from Gulf was used as an adhesive for bonding crossplied Celion/PMR-15 laminates. This work was done in order to determine how this adhesive formulation would compare to standard LARC-13. The adhesive utilizing the Gulf monomer yielded results before aging 5-9% lower than LARC-13 and 5-6% lower when compared after aging. These results are probably within experimental accuracy, so before pursuing this monomer source more testing will be done with composite and titanium adherends.

MONOMER SOURCE	EXPOSURE CONDITION	TEST TEMPERATURE	STRENGTH, MPa (ksi)
LANGLEY	AS FABRICATED	RT	13.5 (1.96)
LANGLEY	AS FABRICATED	589K (600°F)	10.4 (1.51)
GULF	AS FABRICATED	RT	12.9 (1.81)
GULF	AS FABRICATED	589K	9.4 (1.37)
LANGLEY	125 hr AT 589K	RT	8.5 (1.23)
LANGLEY	125 hr AT 589K	589K	7.9 (1.15)
GULF	125 hr AT 589K	RT	8.0 (1.16)
GULF	125 hr AT 589K	589K	7.5 (1.09)

Figure 7

PPQ LAP SHEAR STRENGTH

An attractive high-temperature adhesive system is the polyphenylquinoxaline (ref. 9). This material offers distinct advantages over most polyimides for production applications because it is a thermoplastic which allows for rapid no-volatile bonding. This adhesive is also very tough which would allow use in structures where peel forces may be encountered. Results obtained from a titanium bonding study showed the PPQ to have an exceptional room temperature lap shear strength of 31.1 MPa (4500 psi), but at 589K (600°F) the strength was poor. This low elevated-temperature strength was shown to be due to thermoplastic failure, possibly due to a slight amount of plasticization by solvent. When HTS/NR150B2 was bonded this effect was not encountered with the PPQ affording excellent room temperature and 589K strengths. Because of the need to process this adhesive at temperatures near 673K (750°F), it could not be used with PMR-15 because of severe blistering.

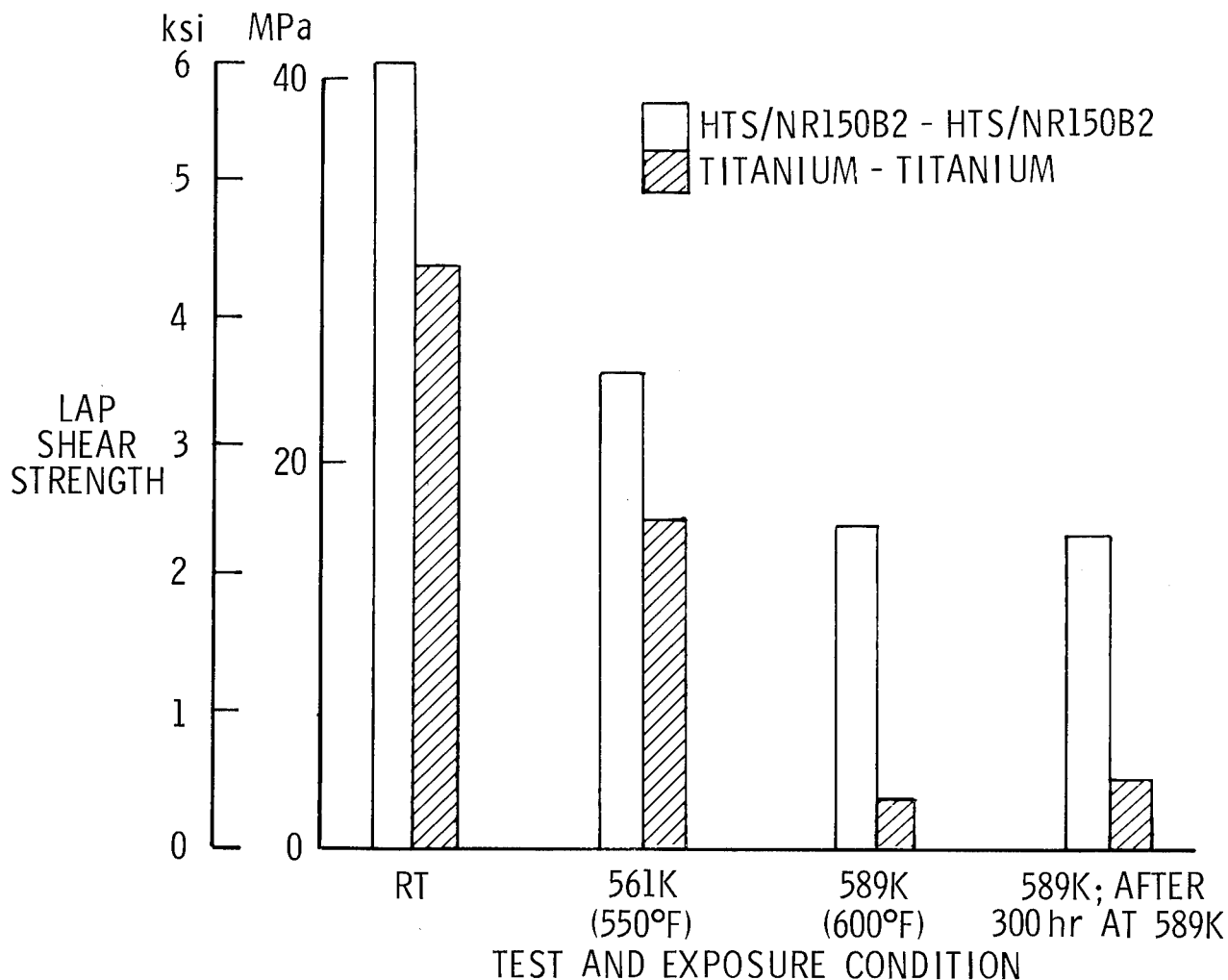


Figure 8

SCR Ti-Ti BONDING PROGRAM

In an effort to develop Supersonic Cruise Research (SCR) technology in adhesive bonding NASA-Langley has funded Boeing Aerospace Company for a three-phase program to advance the state of the art of titanium bonding for 505K (450°F) long-term use. The program will involve the screening of 10 adhesives and 8 surface treatments followed by the optimization of two systems. These two systems in the third phase of the program will be subjected to environmental exposure which will include thermal aging, humidity, and hydraulic fluid exposure with an aim of ultimately obtaining 50 000 hour data. An adhesively bonded subcomponent will also be fabricated. The data generated on this program should prove valuable in future composite bonding efforts.

OBJECTIVE : ADVANCE STATE-OF-THE-ART OF Ti BONDING FOR SCR STRUCTURES

FY-79	FY-80	FY-81
-------	-------	-------

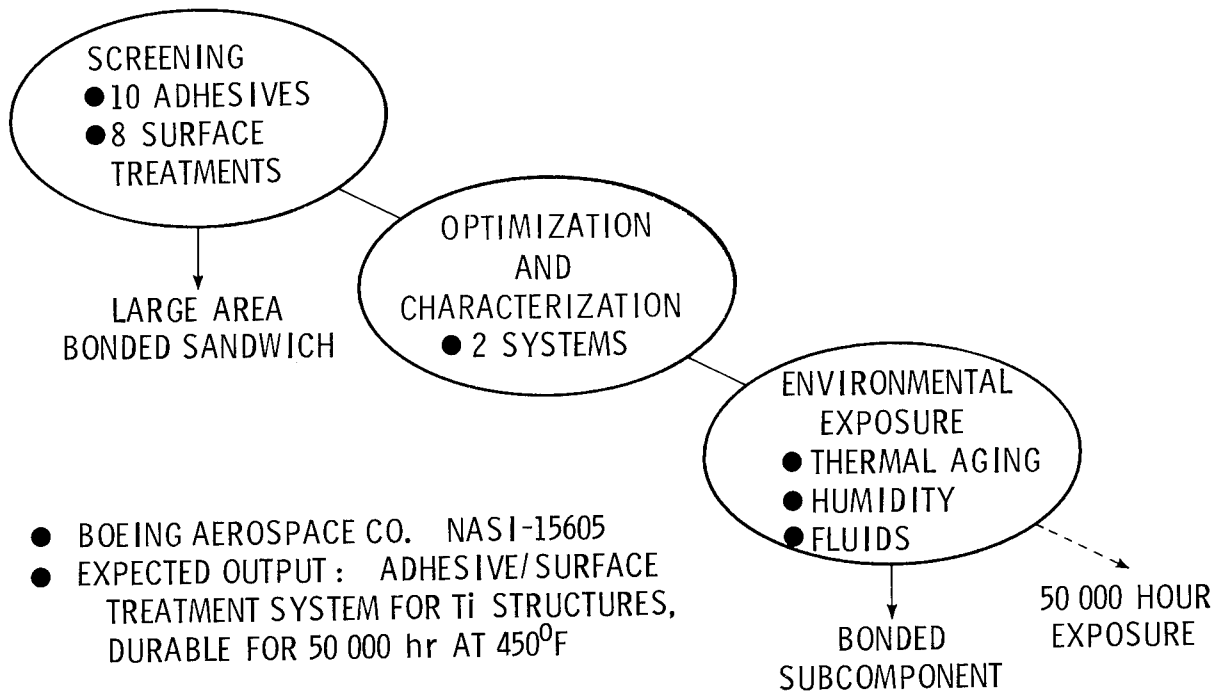


Figure 9

SCR Ti-Ti BONDING PROGRAM
-CANDIDATE ADHESIVE RESINS-

The adhesives to be screened in the SCR program are listed in figure 10. The first six materials will be screened first with the last four materials being anticipated improvements which will result from experience gained in the initial screening effort. The choice of the final two adhesives will be made from the entire list and not from just the last four materials. Both of these adhesives will be carried through the third phase and one or both may be used for the fabrication of the subcomponent which will include a 1.22x1.22m (4x4 ft.) titanium-to-titanium bond.

<u>ADHESIVE</u>	<u>SOURCE</u>
1. LARC-13 POLYIMIDE	NASA-LaRC
2. NR 150 B2 POLYIMIDE	DuPONT
3. NR 150 A2 POLYIMIDE	DuPONT
4. POLYPHENYLQUINOXALINE	NASA-LaRC
5. FM-34 POLYIMIDE	AMERICAN CYANAMID
6. HR 602 POLYIMIDE	HUGHES
7. LARC-13-MOD I	NASA-LaRC/ BOEING
8. LARC-13-MOD II	NASA-LaRC/ BOEING
9. NR 150 A2-MOD I	DuPONT/ BOEING
10. POLYPHENYLQUINOXALINE-MOD I	NASA-LaRC/ BOEING

Figure 10

BONDING OF POLYIMIDE FILM

This work was the outgrowth of the Solar Sail Program where an adhesive was needed for bonding thin Kapton® film. Langley developed three adhesives for this program with the most promising system being LARC-4, a linear polyimide with a glass transition temperature in excess of 575K (575°F) (ref. 10).

The films were bonded under approximately 70 kPa (10 psi) for twenty seconds at 598-625K (615-660°F). The adhesive was strong enough to fail the adherends that were to be used for the solar sail. The data presented is for Kapton that was thick enough to fail in the adhesive or the film at the bondline. Strength retention for samples aged in vacuum at 575K (575°F) for 6000 hours was excellent.

- LARC-4 POLYIMIDE ADHESIVE DEVELOPED
- FACILE 20 sec/LOW PRESSURE BONDING
- ADHESIVE/BONDING TECHNOLOGY SHOWS POTENTIAL FOR USE ON FUTURE LARGE SPACE STRUCTURES

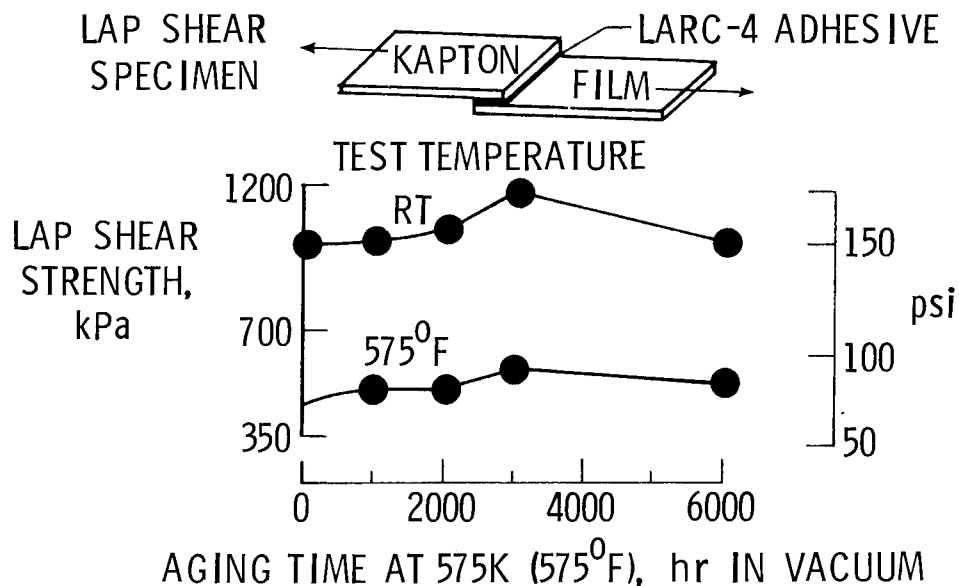


Figure 11

POLYIMIDES CONTAINING METAL IONS

The objectives of this program were to increase the electrical conductivity of polyimides, to improve high temperature adhesive properties, and to investigate the anti-oxidant nature of these materials in the bonding of metals.

The initial approach was to incorporate transition-metal ions into Langley polyimide adhesives. This was accomplished both by physically blending these materials and by chemically reacting them into the polymer. The table shows some initial results where an aluminum complex was mixed with a linear polyimide adhesive which had low strength at elevated temperature (ref. 11). The 548K (527°F) strength was over three times higher with the incorporation of these metal ions. Electrical conductivity has also been increased by this technique.

OBJECTIVE :

- INCREASE ELECTRICAL CONDUCTIVITY OF POLYIMIDES
- IMPROVE HIGH TEMPERATURE ADHESIVE PROPERTIES
- INCREASE ANTI-OXIDANT CAPABILITY FOR BONDING METALS

APPROACH :

INCORPORATION OF TRANSITION METAL IONS INTO LANGLEY POLYIMIDE RESINS

- BLENDED AS FILLERS
- CHEMICALLY REACTED

	Ti/Ti LAP SHEAR STRENGTH, MPa (ksi)	
	RT	548K (527°F)
NO METAL	20.4 (3.0)	3.1 (0.5)
ALUMINUM IONS	16.5 (2.4)	11.4 (1.7)

Figure 12

EFFECT OF THERMAL EXPOSURE ON CELION/LARC-160

Figure 13 shows the thermal stability of Celion/LARC-160 panels made at Langley from commercial prepreg. The data is impressive in that there is excellent retention of initial strengths both for the room temperature and 589K (600°F) samples after aging at 589K. This data is considerably better than the initial data that was published on HTS/LARC-160 (ref. 12). This difference is probably due to the quality of prepregging and the change in fiber.

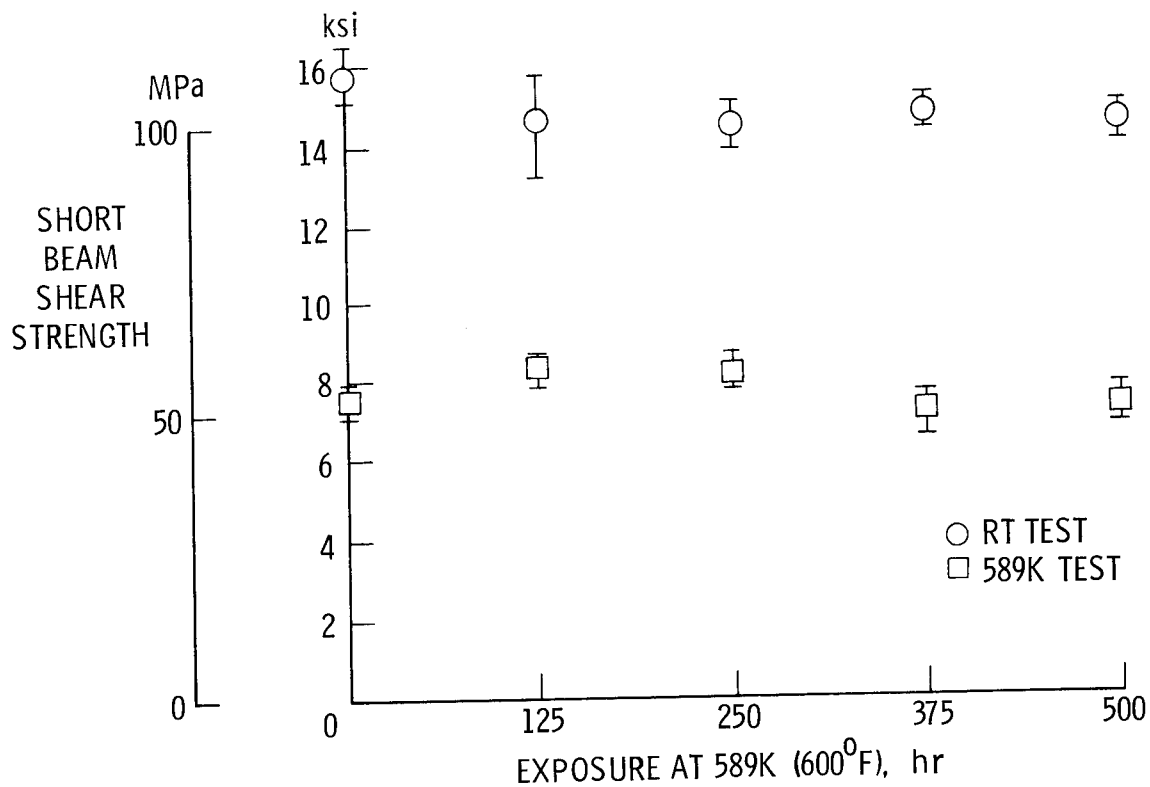


Figure 13

MONOETHYLPHTHALATE
-ADDITION-POLYIMIDE TACKIFIER-

The components of the liquid LARC-160 system are two solids and a viscous liquid. When these three materials are mixed they tend to form a eutectic which is a liquid. After prepregging, this mixture tends to convert to a glass on standing. This conversion results in the loss of tack and drape for the system, but this can be averted by using a reactive plasticizer, monoethylphthalate (MEP), in lieu of some of either the BTDE or NE.

RESIN FORMULATION :

ALIPHATIC CROSSLINKER	- NADIC ESTER-ACID (SOLID)
ANHYDRIDE CHAIN EXTENDER	- BTDA ESTER-ACID (SOLID)
AMINE CHAIN EXTENDER	- MDA MIXTURE (VICOUS LIQUID)
REACTIVE TACKIFIER	- MONOETHYLPHTHALATE (LIQUID) (MEP)

Figure 14

EFFECT OF MEP ON TACK LIFE AND SHORT BEAM SHEAR STRENGTH
-CELION/LARC-160-

The use of monoethylphthalate (MEP) at a three percent level resulted in a LARC-160 resin with considerably better tack and drape life, 2 to 4 days versus eight months (ref. 13). This formulation involved substituting phthalic anhydride (PA) for ten percent of the BTDA used in a LARC-160 resin preparation. When the PA is refluxed in ethyl alcohol along with BTDA and NA, the resulting mixture consists of MEP, BTDE and NE (ethyl esters). These materials are mixed with the liquid amine constituent to form LARC-160.

The short beam shear strengths as tested at room temperature and 589K (600°F) both before and after aging at 589K show no significant differences. The low shear strength levels for both systems is attributed to the quality of the Langley-prepared prepreg.

% MEP	TACK LIFE	EXPOSURE	TEST TEMPERATURE	SBS STRENGTH, MPa (ksi)
0	2-4 days	AS FABRICATED	RT	80 (11.6)
0	2-4 days	AS FABRICATED	589K (600°F)	37 (5.4)
3	8 months	AS FABRICATED	RT	76 (11.0)
3	8 months	AS FABRICATED	589K	37 (5.4)
0	2-4 days	500 hr AT 589K	RT	65 (9.4)
0	2-4 days	500 hr AT 589K	589K	36 (5.2)
3	8 months	500 hr AT 589K	RT	65 (9.4)
3	8 months	500 hr AT 589K	589K	36 (5.2)

Figure 15

FUTURE ACTIVITIES

Future programs at NASA-Langley will involve programs on the long-term aging of composites and adhesives at 505K (450⁰F) for SCR applications. A considerable amount of work is also foreseen in the development and characterization of tougher resin systems for high temperature as well as lower temperature (CTOL) applications. A comprehensive synthetic program will be continued in an effort to develop better adhesives and matrix resins. The characterization of titanium surfaces for adhesive bonding will also be a continuing program.

- LONG-TERM AGING STUDIES ON COMPOSITES AND ADHESIVES
505K (450⁰F)
- IMPROVED TOUGHNESS PROPERTIES
- SYNTHESIS
- TITANIUM SURFACE STUDIES

Figure 16

REFERENCES

1. Lubowitz, H. R.: U. S. Patent 3,528,950, Sept. 1970.
2. St. Clair, A. K.; and St. Clair, T. L.: Polymer Eng. and Sci., vol. 16, no. 5, 1976, pp. 314-317.
3. Serafini, T. T.; Delvigs, P.; and Lightsey, G. R.: J. Appl. Polym. Sci., vol. 16, no. 4, 1972, p. 905.
4. Bilow, N.; and Landis, A. L.: U. S. Patent 3,845,018, Oct. 1974.
5. Bascom, W. D.; Cottingham, R. L.; Jones, R. L.; and Peyser, P.: J. Appl. Polym. Sci., vol. 19, 1975, pp. 2545-2562.
6. Wnuk, A. J.; Ward, T. C.; and McGrath, J. E.: Autographic Impact Tester. Presented at Southeastern Am. Chem. Soc. Meeting, 1978.
7. Beaubien, L. A.; Clifford, M. F.; Mast, P. W.; Mulville, D. R.; Sutton, S. A.; Thomas, R. W.; Tirosh, J.; and Wolock, I.: Failure Criteria for Composite Structures. NRL Memorandum Report 3721, 1978, pp. 103-131.
8. St. Clair, T. L.; and Progar, D. J.: LARC-13 Polyimide Adhesive Bonding. SAMPE, vol. 24, 1979, in press.
9. Hergenrother, P. M.; and Progar, D. J.: High-Temperature Composite Bonding with PPQ. Adhesives Age, Dec. 1977, pp. 38-43.
10. St. Clair, A. K.; Slempe, W. S.; and St. Clair, T. L.: High-Temperature Adhesives for Bonding Polyimide Film. Adhesives Age, Jan. 1979, pp. 35-39.
11. St. Clair, A. K.; Carver, V. C.; and Taylor, L. T.: The Incorporation of Metal Ions Into Polyimides. Presented at Southeastern Am. Chem. Soc. Meeting, 1978.
12. St. Clair, T. L.; and Jewell, R. A.: LARC-160: A New 550°F Polyimide Laminating Resin. SAMPE, vol. 8, 1976, pp. 82-93.
13. St. Clair, T. L.; and Butler, J. M.: Tackifier for Addition Polyimides. Presented at Southeastern Am. Chem. Soc. Meeting, 1978.

GRAPHITE/POLYIMIDE STATE-OF-THE-ART

PANEL DISCUSSION

William G. Scheck
General Dynamics Convair

EXPANDED ABSTRACT

This paper presents a brief overview of potential applications and problems associated with graphite/polyimide composites. Graphite/polyimides have potential applications on advanced high performance missile structures, aircraft structures, large space structures and space shuttle.

The major roadblock to the application of graphite/polyimides is consistent resin and prepreg materials which process the same each time.

UTILIZATION OF GRAPHITE/POLYIMIDE

We see the use of graphite/polyimide composites on advanced high performance offensive missile structure as well as aircraft structure where graphite/epoxy will not meet the design and temperature requirements. Space Shuttle applications such as the body flap, elevons, and vertical tail fall within potential applications of graphite/polyimide in which General Dynamics is interested. Some of the proposed large space structures will require graphite/polyimide composites since the temperature will exceed the capabilities of graphite/epoxy or graphite/polysulfone composites.

- High performance missile structure
- Military large space structures
- Space shuttle applications
- Aircraft structure
- NASA large space structures

Figure 1

USE FOR HEAT RESISTANT POLYMERS

A recent Convair survey developed this list of potential applications for graphite polyimide composites. Not all of these fall within the General Dynamics product line but do represent potential applications for graphite/polyimide composites.

Electrical components (circuit boards, moldings, insulation)
Gaskets, sealants & tubing
Binding system in brake shoes & abrasive wheels
Geothermal energy conversion systems (casings & nozzles)
Advanced aircraft, space vehicles & missiles (composites & adhesives)
Engine components (fan blades, flaps & ducting)
Nuclear reactors (coolants & insulation)
Conveyor belts (drying of materials)
Filters (exhaust stacks)
Pipes (chemical processing)
Flame resistant materials (flight suits & parachutes)
Reinforcement (high modulus structural material)
Ablators

Figure 2

TECHNICAL ROADBLOCKS TO INCREASED APPLICATIONS

Various problem areas have been identified that prevent the widespread use of graphite/polyimide applications. The Casts efforts and similar programs are aimed at satisfying the problem area. Cooperation from not only within the aerospace industry but from the resin formulators and prepreg manufacturers will be required to overcome these problems. The problem areas are listed in the priority that they should be solved in as seen by General Dynamics.

- Consistent resin matrix which is fully characterized and made in large quantities
- Consistent prepreg materials which process the same each time
- Lack of adequate design data
- Commercially available characterized high temperature adhesive (low volatiles)
- Inspection criteria
- Damage tolerance and repair techniques
- Cost

Figure 3

PANEL DISCUSSION

Morton Kushner
Boeing Aerospace Company

EXPANDED ABSTRACT

This brief paper presents The Boeing Company current assessment of the use of graphite/polyimide composite technology at Boeing. Although the author is associated with the Boeing Aerospace Company, the comments herein cover the Boeing Corporate assessment.

Boeing plans no immediate use of graphite/polyimide composites on Boeing-designed and fabricated program hardware. However, due to probable use in the future as a cost-effective alternative to more common materials and design, an extensive IR&D and R&D effort is being pursued at Boeing. Work in reducing material variability, developing a broader design data base and scale-up details is required for the future.

UTILIZATION OF GRAPHITE/POLYIMIDE

As shown by the chart below, Boeing has no immediate program application. Our present activity is concentrated in IR&D and R&D. Future utilization is contemplated for those areas where high temperature, high modulus, high strength and light weight would be cost advantageous or would have performance capabilities not attainable by more common, less costly materials. This hardware would include satellite and space transportation applications, tactical missile applications, structure for high performance fighters and bombers, supersonic transport aircraft and laser and nuclear hardening.

- CURRENT
 - NO IMMEDIATE PROGRAM APPLICATION
 - PRESENT ACTIVITY CONCENTRATED IN IR&D/R&D
- FUTURE
 - HIGH TEMPERATURE STABLE SYSTEM FOR SATELLITE AND SPACE TRANSPORTATION APPLICATIONS
 - TACTICAL MISSILE SYSTEMS
 - HIGH PERFORMANCE FIGHTER AND BOMBER APPLICATIONS
 - SST, IF DEVELOPED
 - LASER AND NUCLEAR HARDENING

Figure 1

TECHNICAL ROADBLOCKS TO INCREASED APPLICATION

The chart below indicates there are no known unsolvable problems associated with the use of graphite/polyimide composites. However, there are some items that deserve attention. The material system is currently immature. Different investigators report varying processing problems and resultant mechanical properties. This has led to only a limited design data base which will require significant expansion. The graphite/polyimide system requires high temperature - high pressure curing cycles which limit capabilities to existing high temperature processing facilities. This is especially true of large facilities capable of handling large parts. There just aren't too many of these facilities available today. In addition to the above, material variability, lot-to-lot, has been a problem to-date. Raw material processing controls must be developed and strengthened to assure lot-to-lot repeatability. Boeing is currently studying this phenomenon on graphite/PMR-15 polyimide material under NASA Langley Contract NAS1-15009.

- NO UNSOLVABLE PROBLEMS
- TECHNICAL ROADBLOCKS TO INCREASED APPLICATIONS
 - RELATIVELY IMMATURE MATERIAL SYSTEM
 - LIMITED DESIGN DATA BASE
 - LIMITED PROCESSING FACILITIES (LARGE SCALE)
(600°/500 PSI AUTOCLAVE)
 - MATERIAL VARIABILITY
(BEING RESOLVED BY NASI 15009)

Figure 2

PRIORITY OF TECHNICAL PROBLEMS NEEDING NEAR-TERM SOLUTIONS

We feel that first priority must be assigned to reducing lot-to-lot material variability. This may be accomplished by increased chemical and mechanical controls during processing. Once material variability has been licked, the design data base must be broadened. More structural/mechanical, thermal and thermo-physical data must be obtained to present a range of values to the designer. In addition, environmental effects must be ascertained before complete design utilization can be realized. However, from a practical standpoint, none of these developments will result in increased usage unless scale-up processes and facilities are developed.

- **REDUCTION IN MATERIAL VARIABILITY**
 - **IMPROVED CHEMICAL/MECHANICAL CONTROL**
- **DATA BASE INCREASE**
- **ENVIRONMENTAL EFFECTS STUDIES**
- **SCALE UP OF MANUFACTURING PROCESSES & FACILITIES**

Figure 3

SUMMARY

In summary, although there is no immediate use of graphite/polyimide composites contemplated on current Boeing-designed and fabricated program hardware, the future could be bright for this material. Its use, however, will be dependent on hardware performance needs and cost effectiveness, including full life cycle costing. We feel there are no unsolvable problems foreseen in the full development of this material as a design alternative to more common high temperature materials. However, we require more work to solve the problems of material variability, an expanded data base for design utilization, and scale-up details.

- NO IMMEDIATE USE OF GRAPHITE/POLYIMIDE COMPOSITES CURRENTLY AT BOEING
- USE DEPENDENT ON FUTURE HARDWARE NEEDS
- NO UNSOLVABLE PROBLEMS IN USE THEREOF
- NEED ADDITIONAL WORK ON
 - MATERIAL VARIABILITY
 - DATA BASE
 - SCALE UP

Figure 4

GRAPHITE/POLYIMIDE STATE-OF-THE-ART

PANEL DISCUSSION

William H. Morita

SHUTTLE ORBITER DIVISION

ROCKWELL INTERNATIONAL

Expanded Abstract

Utilization of advanced composite materials for the Shuttle Orbiter was identified from early weight savings studies on the Shuttle Program. As a result, advanced composites such as GR/EP payload bay doors were incorporated into the baseline design. However, structural components located in areas of high thermal loads did not show significant weight savings unless a high temperature composite such as GR/PI was utilized. Initial effort on the retrofittable Orbiter components were based on 533 K polyimide system. Later, however, 589 K polyimide systems were used as the basis and showed weight saving of 25% to 30%. Utilization of 589 K GR/PI systems on satellites showed weight savings of 17% to 30% in structural components where laser survivability and high temperature capability were required. At the present time, a funded planned utilization of GR/PI does not exist in the Space Systems Group of Rockwell.

State-of-the-Art of GR/PI composites is presented under two related subject areas; technical roadblocks to increased application and priority of technical problems. Technical roadblocks are the maturity of the 589 K GR/PI material system and GR/PI structure fabrication technology. Substantial progress toward the development of the 589 K PI systems has been made under the CASTS Program since 1976. However, a need to better understand the process and its sensitivity persists. Priority of the GR/PI technical problems involves the selection of a primary polyimide resin system to reduce the scope of development problems. The GR/PI structure first priority problem is the selection and development of high temperature adhesive systems.

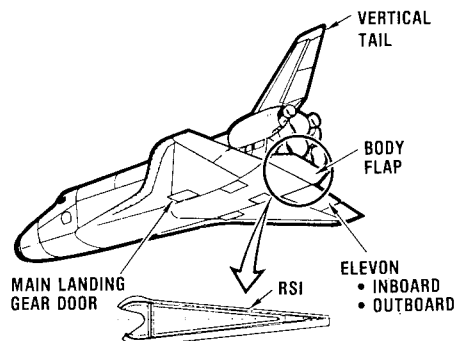
UTILIZATION OF GRAPHITE/POLYIMIDE COMPOSITES

Shuttle Orbiter studies as early as 1973 showed that use of advanced composites on the vertical tail, elevon, and aft body flap would achieve significant orbiter weight savings, particularly if constructed with high temperature graphite/polyimide (GR/PI). As a result, the use of graphite/polyimide on the orbiter has been studied since that time.

Graphite/Polyimide utilization on the Shuttle Orbiter falls into two categories; near-term retrofittable structural components, figure 1, and far-term non-retrofittable structure. Near-term potential weight savings is 910 kg whereas far-term potential weight savings is 4080 kg. Over half of the weight savings is due to reduced Reusable Surface Insulation requirements (RSI) that result from the high temperature 589 K capability of GR/PI.

In 1978, data developed in support of CASTS was used as the primary source of information to prepare a response to a NASA Orbiter Project request for planning information on the use of GR/PI Body Flap and Elevons.

Graphite/Polyimide utilization on satellites, predicated upon studies by the Satellite Systems Division, showed weight savings on structural components from 17% to 30%. Satellites that required structure for laser survivability and higher temperatures showed the highest weight savings. Systems considered in the study included Global Positioning System (GPS), P80-1 Spacecraft, Teal Ruby Sensor System, ADOPT System, HALO Focal Plan Assembly and Large Space Structure.



SPACE SHUTTLE ORBITER

- NEAR TERM-RETROFITTABLE STRUCTURE
 - 25% TO 30% WT SAVINGS
- FAR TERM-NONRETROFITTABLE STRUCTURE
 - 25% TO 30% WT SAVINGS

SATELLITES

- STRUCTURAL COMPONENT
 - 17% TO 30% WT SAVINGS (LASER SURVIVABILITY)

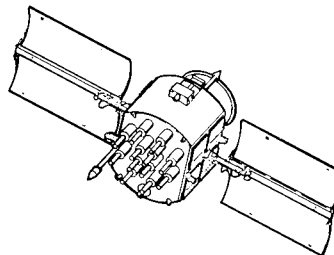
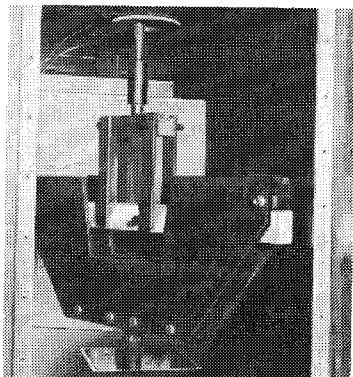


Figure 1

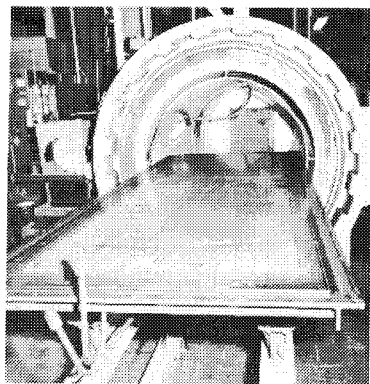
TECHNICAL ROADBLOCKS TO INCREASED APPLICATION

Technical roadblocks to increased application of graphite/polyimide composites are the maturity of: 1) the GR/PI material system and 2) the GR/PI structure fabrication technology of large and complex components as illustrated in Figure 2. Although substantial progress toward GR/PI material system maturity under the CASTS Program has been made, areas identified as problems that must be resolved are: (1) establishment of prepreg material control and reproducibility, (2) confirming material receiving and inspection techniques, (3) demonstrating process procedures and reproducibility to reduce the process to practice, and (4) establishing design allowables. GR/PI structure fabrication technology maturity requires additional effort in the following: (1) high temperature adhesives must be more fully developed and characterized for surface to surface bonds, honeycomb sandwich bonds, and laminate to metal bonds, (2) typical structural joints and attachments must be more fully developed and characterized, and (3) large component process procedures and tooling concepts must be demonstrated such as large area panel fabrication, co-cure and secondary bonding of long joint sections and assembly closeout procedures.



GR/PI MATERIAL SYSTEM MATURITY —REDUCE PROCESS TO PRACTICE

- PREPREG MATERIAL CONTROL & REPRODUCIBILITY
- MATERIAL RECEIVING INSPECTION TECHNIQUE
- PROCESS PROCEDURES & REPRODUCIBILITY
- DESIGN ALLOWABLES



GR/PI STRUCTURE FABRICATION TECHNOLOGY MATURITY—LARGE COMPLEX COMPONENTS

- HIGH TEMP ADHESIVE DEVELOPMENT & CHARACTERIZATION
- JOINT & ATTACHMENT DEVELOPMENT & CHARACTERIZATION
- LARGE COMPONENT PROCESS PROCEDURES & TOOLING

Figure 2

PRIORITY OF TECHNICAL PROBLEMS

Priority of technical problems for graphite/polyimide composites include those of the material system and those of the structure as illustrated in Figure 3. The first problem is the selection of a primary GR/PI material system which impacts all the problems directly or indirectly. Under the CASTS program, four polyimide resin systems are under development namely; NR150-B2, PMR-15, LARC160, and Thermid 600. NR-150-B2 is classified as a condensation-type polyimide system. Water is split off as a condensation product throughout its cure. The PMR-15, LARC-160 and Thermid 600 systems are classified as addition-type polyimides. These materials cure by addition reactions, after a prepolymer, an imide, is first formed by staging at a low temperature such as 450 K. One of these resin systems should be selected to reduce the scope of the problems. The second problem, prepreg material control and reproducible supply requires a better understanding of the process and its sensitivity. The third and fourth problems are associated with GR/PI structure and are the selection and development of high temperature adhesives. Adhesive systems under evaluation for use at 589 K include FM-34, NR-150 and LARC-13. The FM-34 and NR-150 materials are condensation-type systems releasing volatile products during cure. However, LARC-13 is an addition-type system such as PMR-15 and LARC-160, capable of forming large area void-free bonds. The fifth problem is the development of design allowable data in sufficient depth to permit design studies and is predicated upon resolution of problems 1 and 2. The sixth problem, joint and attachment design data, is a major design concern and the highest weight penalty in the use of composites. The seventh problem is the fabrication of large and complex GR/PI structures.

GR/PI MATERIAL SYSTEM

- ① • SELECTION OF PRIMARY SYSTEM
- ② • PREPREG MATERIAL CONTROL & REPRODUCIBLE SUPPLY
 - MATERIAL RECEIVING & INSPECTION TECHNIQUES
- ⑤ • DESIGN ALLOWABLES

GR/PI STRUCTURE

- ③ • SELECTION OF HIGH TEMPERATURE ADHESIVE SYSTEMS
 - SURFACE TO SURFACE
 - HONEYCOMB SANDWICH
 - LAMINATE TO METAL
- ④ • ADHESIVE PROCESS PROCEDURES & DESIGN ALLOWABLES
- ⑥ • JOINT & ATTACHMENT DESIGN DATA
- ⑦ • LARGE & COMPLEX COMPONENT PROCESS PROCEDURES & TOOLING

Figure 3

GRAPHITE/POLYIMIDE STATE-OF-THE-ART

PANEL DISCUSSION

Robert C. Curley
McDonnell Douglas Astronautics Company
Huntington Beach, California

EXPANDED ABSTRACT

This paper provides a brief overview of current and planned applications of graphite/polyimide composites at McDonnell Douglas Astronautics Company (MDAC). A short discussion of technical problems delaying the application of graphite polyimide composites in aerospace structures and near-term solutions to these problems are also included.

UTILIZATION OF GRAPHITE POLYIMIDE

MDAC's uses for graphite polyimide composites all relate to structures for missiles and space applications. For convenience the applications can be divided into four categories:

Missile Structures - this category consists of bodies and aerodynamic surfaces (wings and control fins) for small missiles having flight trajectories within the earth's atmosphere. These missiles are usually on the order of three meters long and .15 to .30 meters in diameter.

Reentry Vehicle (RV) Structures - this category consists of structures for vehicles which are boosted out of the earth's atmosphere and then reenter.

Booster Structures - this category consists of the structure of the large rockets used to lift payloads out of the earth's atmosphere.

Space Structures - this category consists of lightly loaded stiffness critical structures used in space.

The criteria governing the application of graphite/polyimide materials vary slightly from category to category. At the present time MDAC activities with graphite/polyimide consist of development programs in each of the above categories. The earliest anticipated production use of graphite/polyimide is 1982.

• CURRENT

DEVELOPMENT PROGRAMS

• FUTURE

MISSILE STRUCTURE

REENTRY VEHICLE STRUCTURE

BOOSTER STRUCTURE

SPACE STRUCTURE

Figure 1

POLYIMIDE RESIN SELECTION

Since the structures in all of the categories listed in figure 1 are buckling critical, the retention of compression modulus at elevated temperature is a critical consideration for each application. The graphite/polyimide structure must show a performance gain over competitive metal or composite structures in all applications. Additional considerations for missile applications are cost vs. weight, and ablation behavior. MDAC studies to date show that composites are not cost effective for missile structures unless the cost reduction that can be achieved by elimination of a separate TPS can be realized. Therefore property retention at elevated temperature and ablation/insulation performance of the composite are significant selection factors. The temperature range of interest for most missile applications is between 670 K on the body and 925 K on fin leading edges with a steep thermal gradient through the thickness of the structure. For RV's and Boosters the trade-offs between weight, cost and performance become more complex because a TPS is still required even if polyimides are used. The gains realized in these applications stem primarily from the reductions in TPS weight allowed by the increased structure operating temperature made possible by the use of polyimides. In space structures graphite/polyimide is useful when its application allows the substitution of composites for less efficient metal structure where the service temperature is above that of epoxies but below the maximum for polyimides.

APPLICATION	SELECTION FACTORS	SOURCE OF PAYOFF
MISSILE STRUCTURE	COMPRESSION MODULUS RETENTION COST VS WEIGHT ABLATION	ELIMINATION OF TPS
REENTRY VEHICLE STRUCTURE	COMPRESSION MODULUS RETENTION WEIGHT	REDUCED TPS
BOOSTER STRUCTURE	COMPRESSION MODULUS RETENTION INTERLAMINAR SHEAR STRENGTH RESIN TOUGHNESS COST VS WEIGHT	REDUCED TPS
SPACE STRUCTURE	COMPRESSION MODULUS RETENTION LIFE IN SPACE ENVIRONMENT	MATERIAL SUBSTITUTION

Figure 2

TYPICAL REENTRY VEHICLE STRUCTURE

Figure 3 shows a graphite polyimide reentry vehicle structure typical of those being developed by MDAC under USAF contracts. The structure consists of a conical skin approximately .5 meter long and .5 meter in diameter having a thickness of 2.5×10^{-3} meters, two graphite polyimide intermediate frames and two aluminum end frames. Five of these structures are being built for static and flight tests.

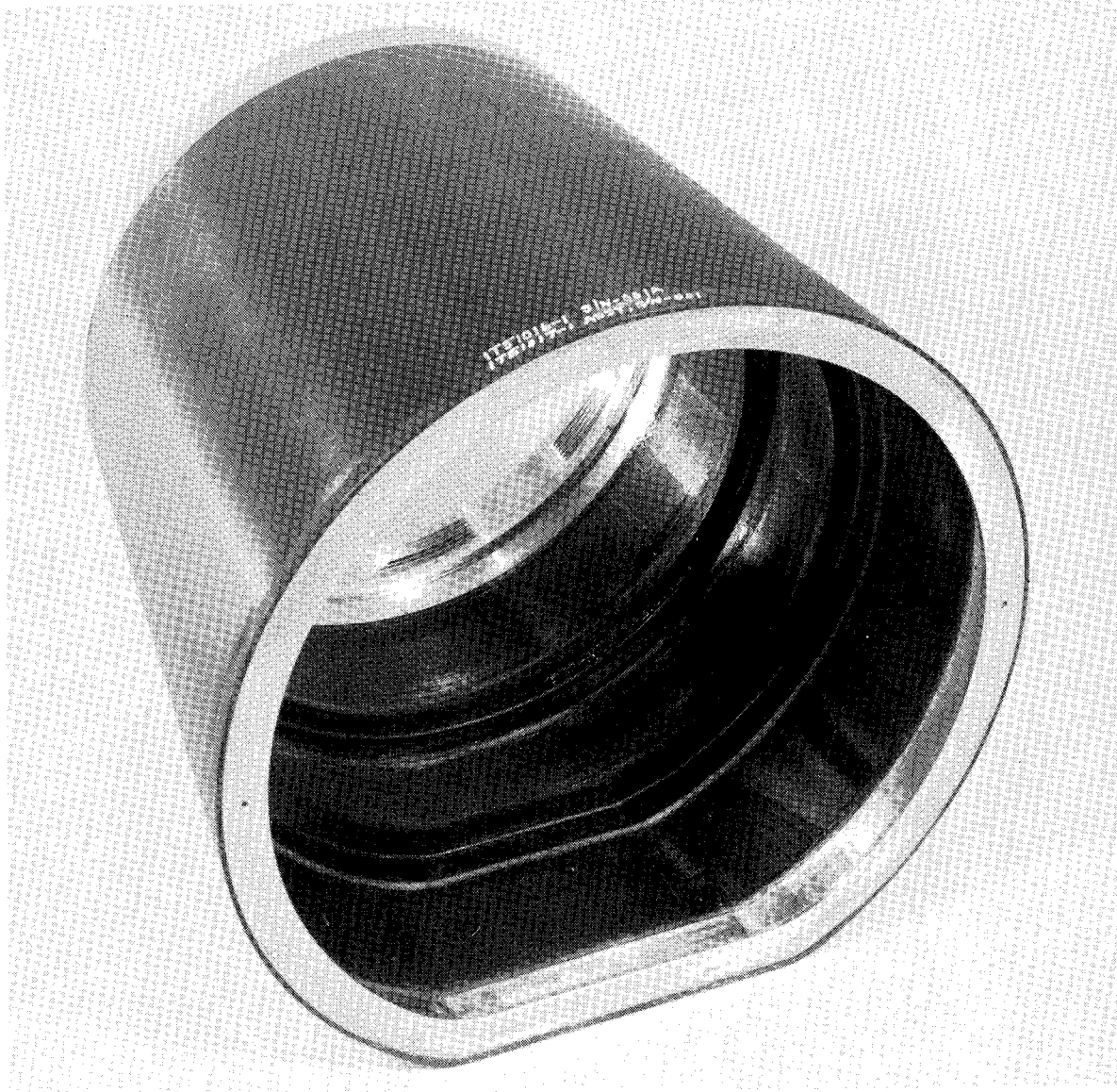


Figure 3

TECHNICAL ROADBLOCKS TO INCREASED APPLICATIONS

The two items listed are really symptoms of interactions between several technical problems. Unfortunately time does not permit discussion of the individual problems. Erratic composite quality is identified as a technical roadblock because of the frequent production of poor quality graphite/polyimide composites even though materials and production processes thought to be proven and controlled are used. Processing conditions and techniques required to produce graphite/polyimide composites is identified as the second technical roadblock because the materials and processes which produce the best graphite/polyimide composites are very different than those that are desirable for a production environment. Graphite/polyimide composites are most reliably produced using dry board materials having low volatile content and curing at high temperatures and pressures, while in a production situation tacky drapable materials that can be cured under relatively mild conditions and will tolerate a variety of cure conditions are desired.

INCREASED APPLICATION OF GRAPHITE/POLYIMIDE COMPOSITES IN AEROSPACE STRUCTURES IS BEING IMPEDED BY:

- ERRATIC COMPOSITE QUALITY
- PROCESSING CONDITIONS/TECHNIQUES REQUIRED

Figure 4

TECHNICAL PROBLEMS NEEDING NEAR TERM SOLUTIONS

The technical problems needing near term solution are directly related to the roadblocks identified on the previous figure. Much of the erratic processing behavior of polyimide resins appears to be attributable to changes in the resin during storage. Typical changes that have been identified and are known to change processing behavior are increases in resin molecular weight, variations in ester content or composition and water absorption from the atmosphere. Elimination or reduction of changes during storage should result in materials with a more consistent response to a given set of cure conditions. Even if polyimide resins were perfectly stable in storage, variations in composition which affect processing behavior will occur because of unavoidable variations in the resin manufacturing process. Methods are needed to identify these variations and correlate them with processing response. In-process cure monitoring is probably the best long term solution to the problem of variable quality in polyimide composites. By in-process cure monitoring is meant a means of measuring resin condition during cure and controlling the cure cycle on the basis of resin condition rather than using preselected temperatures and pressures. This mode of controlling curing should allow compensation for variations in the starting materials.

- RESIN/ PREPREG STORAGE STABILITY
- RESIN/ PREPREG CHARACTERIZATION METHODS
- IN-PROCESS CURE MONITORING

Figure 5

GRAPHITE/POLYIMIDE STATE-OF-THE-ART

PANEL DISCUSSION

Clayton A. May
Lockheed Missiles & Space Company, Inc.

EXPANDED ABSTRACT

Based on current knowledge, graphite/polyimide composites have a definite place in the aerospace industry providing certain problems can be solved. Foremost among these are material uniformity and it's control and more exacting controls on the curing process. The tools required for solution are available but their application to these problems remains to be accomplished.

UTILIZATION OF GRAPHITE/POLYIMIDES

Currently, LMSC uses for graphite polyimide composites are essentially nonexistent. However, the potential for missile applications is excellent. The Trident I Missile contains approximately 160 graphite/epoxy composite (GR/EP) parts. These range in size from a 1.8 m diameter honeycomb core conical structure to numerous small brackets for instrumentation support. Elevated temperature performance of the composite structure is a key factor in the vehicle performance. Current Gr/Ep parts require considerable insulation to permit their use in the high temperature regimes needed for a successful mission. Polyimides can substantially reduce the required insulation. This means a weight savings and increased range. Future generation launch vehicles will undoubtedly involve more composite structure.

In space applications, the potential for graphite/polyimide utilization is much more difficult to assess. The types of structure are much more varied. Predictions of the potential for graphite/polyimide are further complicated by the fact that many of the space programs are classified. From the standpoint of moisture absorption influencing the glass transition temperature (T_g), polyimides would appear on the surface to be superior to the epoxies. This is primarily due to the absorbed moisture diffusing out of the structure before the T_g is reached. The true influence of moisture is thus camouflaged. Of greater concern is how moisture absorption influences dimensional stability. It is known that polyimides, because of their polar nature, can absorb considerable quantities of moisture. The utility of polyimides in space hardware requires further definition.

MISSILES SYSTEM DIVISION

- CURRENTLY 160 Gr/Ep PARTS IN TRIDENT I
- MORE PARTS, ALL Gr/Pi IN FUTURE

SPACE SYSTEMS DIVISION

- SOLAR PANELS
- LENTICULAR BOOMS
- ANTENNA STRUCTURES
- MISCELLANEOUS HARDWARE

Figure 1

TECHNICAL ROADBLOCKS TO INCREASED APPLICATION

Our opinion is that the technical road blocks to the application of polyimide composites in missile and space applications are solvable. Material uniformity is a major problem. Current evidence indicates that workable prepregs can be manufactured but consistency has not been adequately demonstrated. Manufacturing procedures in all probability, will have to be more exacting. Other major factors key to the successful application of these materials are our abilities to properly assess the elevated temperature performance of polyimide composites and to solve the problems associated with adhesive bonding.

There also exist a number of minor problems associated with the handling and processing of polyimides. High temperature ancillary materials such as bagging, sealants, bleeders, etc. are more difficult to handle but are required because of the higher temperatures employed during cure. Much of this difficulty can be avoided through the reactive monomer approach using materials such as PMR-15 and/or LARC-160 as matrix resins which are readily processible. Evidence to date indicates, however, that cure cycles will be more exacting. Progress in the definitive monitoring of cure cycle events through a combination of dielectric and rheological measurements should result in the additional required controls. Shop life problems, such as maintenance of tack during part lay up, also appear to have viable solutions.

MAJOR

- MATERIAL UNIFORMITY
- ELEVATED TEMPERATURE TESTING CAPABILITIES
- ADHESIVE BONDING

MINOR

- ANCILLARY MATERIALS
- MORE EXACTING CURE
- SHOP LIFE

Figure 2

PRIORITY OF TECHNICAL PROBLEMS

There are a number of technical problems which must be solved in order to insure successful use of graphite/polyimide composite structures. Our opinion is that material uniformity is currently the most important road block. This will require measurement techniques which not only define the chemical structure of the materials but also their processing behavior. Since the graphite/polyimide laminations will have to be joined to form useful structures, adhesive bonding continues to be a high priority, yet not totally solved, problem. It has already been indicated that curing of these materials is more exacting than the conventional epoxies, thus cure monitoring and controls will be needed to verify proper processing. Elevated temperature testing in the higher temperature regimes has always been a problem and this will most probably impact design allowable studies. Finally, the more exacting processing requirement will undoubtedly cause tooling problems such as more accurate and uniform temperature control during the composite cure.

- MATERIAL UNIFORMITY & CHARACTERIZATION
- ADHESIVE BONDING
- CURE MONITORING & CONTROL
- ELEVATED TEMPERATURE TESTING & DESIGN ALLOWABLES
- TOOLING

Figure 3

1. Report No. NASA CP-2079		2. Government Accession No.		3. Recipient's Catalog No.	
4. Title and Subtitle GRAPHITE/POLYIMIDE COMPOSITES				5. Report Date August 1979	
				6. Performing Organization Code	
7. Author(s) H. Benson Dexter and John G. Davis, Jr., editors				8. Performing Organization Report No. L-12953	
9. Performing Organization Name and Address NASA Langley Research Center Hampton, VA 23665				10. Work Unit No. 524-71-03-01	
				11. Contract or Grant No.	
12. Sponsoring Agency Name and Address National Aeronautics and Space Administration Washington, DC 20546				13. Type of Report and Period Covered Conference Publication	
				14. Sponsoring Agency Code	
15. Supplementary Notes					
16. Abstract <p>This document is a compilation of papers presented at the CASTS Project Technical Symposium on Graphite/Polyimide Composites held at the NASA Langley Research Center, February 28 - March 1, 1979. Papers were presented by NASA and industry personnel on technology that was developed primarily under sponsorship of the CASTS Project. Topics covered fabrication, adhesives, test methods, structural integrity, design and analysis, advanced technology developments, recent high-temperature polymer research at NASA, and a panel discussion on the state-of-the-art of graphite/polyimide composites.</p>					
17. Key Words (Suggested by Author(s)) Composites Composite structures			18. Distribution Statement Unclassified - Unlimited Subject Category 24		
19. Security Classif. (of this report) Unclassified	20. Security Classif. (of this page) Unclassified	21. No. of Pages 458	22. Price* \$14.50		

National Aeronautics and
Space Administration

Washington, D.C.
20546

SPECIAL FOURTH CLASS MAIL
BOOK

Postage and Fees Paid
National Aeronautics and
Space Administration
NASA-451



Official Business

Penalty for Private Use, \$300

Joseph A. Maciejczyk
Plastec
ARRADCOM
Dover, NJ 07801

2427

NASA

POSTMASTER: If Undeliverable (Section 158
Postal Manual) Do Not Return